Combined Theoretical and Experimental Investigation of N-Heterocyclic Carbenes as Lewis Base Catalysts and as Ancillary Ligands in Ru-Catalyzed Olefin Metathesis. Mechanistic Investigation of Fluxional Behavior of Ru-Based Olefin Metathesis Catalysts

Author: Adil R. Zhugralin

Boston College Electronic Thesis or Dissertation, 2011

Boston College

The Graduate School of Arts and Sciences

Department of Chemistry

COMBINED THEORETICAL AND EXPERIMENTAL INVESTIGATION OF N-HETEROCYCLIC CARBENES AS LEWIS BASE CATALYSTS AND AS ANCILLARY LIGANDS IN Ru-CATALYZED OLEFIN METATHESIS. MECHANISTIC INVESTIGATION OF FLUXIONAL BEHAVIOR OF Ru-BASED OLEFIN METATHESIS CATALYSTS

a dissertation

by

ADIL R. ZHUGRALIN

submitted in partial fulfillment of the requirements

for the degree of

Doctor of Philosophy

May, 2011

COMBINED THEORETICAL AND EXPERIMENTAL INVESTIGATION OF N-HETEROCYCLIC CARBENES AS LEWIS BASE CATALYSTS AND AS ANCILLARY LIGANDS IN Ru-CATALYZED OLEFIN METATHESIS. MECHANISTIC INVESTIGATION OF FLUXIONAL BEHAVIOR OF Ru-BASED OLEFIN METATHESIS CATALYSTS

Adil R Zhugralin

Thesis Advisor: Professor Amir H. Hoveyda

Abstract

Chapter 1. Through the use of quantum theory of atoms in molecules (QTAIM) the similarities and differences between transition metal complexes ligated by phosphines and *N*-heterocyclic carbenes (NHC) were elucidated. Among the key findings, the phosphines were identified as stronger charge donors than NHCs; however, the latter class of ligands exhibits a weaker π-accepting character than the former. Furthermore, Tolman electronic parameter (TEP) was determined to be an inadequate gauge for the total electron donating ability of phosphines and NHCs; rather TEP can serve as a measurement of population of d_π set of orbitals of a metal center in question. Computational and experimental studies of the mechanism of NHC-catalyzed boron and silicon addition to α,β-unsaturated carbonyls reactions were carried out. Through the use of radical traps the mechanisms involving homolytic cleavage of B-B or B-Si bonds were ruled out. Computational (DFT) studies of the mechanism identified two pathways: (1) direct activation of diboron or borosilyl reagents through coordination of NHC to the B atom, (2) net oxidative addition of the diboron or borosilyl reagents to the carbon (II) of the NHC. The insights gained from the aforementioned studies were employed to

rationalize the observed lack of reactivity of NHC-activated diboron complexes in the presence of aldehydes.

Chapter 2. New C_1-symmetric chiral monodentate *N*-heterocyclic carbenes were prepared, and corresponding chiral Ru-carbene complexes were synthesized. These complexes were employed to gain empirical understanding of factors that govern stereoselectivity in Ru-catalyzed enantioselective olefin ring-closing metathesis. The data thus obtained was employed to infer that *syn*-to-NHC reaction pathways are competitive and non-selective. One plausible mechanism, through which *syn*-to-NHC pathways can be accessed, involves Berry pseudorotations. Through the use of stereogenic-at-Ru complexes diastereomeric Ru-carbenes were isolated (silica gel chromatography) and spectroscopically characterized in solution phase. The diastereomeric Ru-carbenes were found to undergo non-metathesis stereomutations at Ru center, thereby providing additional support for the above hypothesis regarding accessibility of *syn*-to-NHC olefin metathesis pathways. Non-metathesis stereomutation at Ru was found to be accelerated in the presence of protic additives, suggesting the plausibility of hydrogen bonding between the acidic proton and the X-type ligands on Ru. Occurrence of hydrogen bonding was corroborated through the use of chiral allylic alcohols in Ru-catalyzed diastereoselective ring-opening/cross metathesis, which was developed into a versatile method for highly diastereoselective functionalization of terminal olefins.

Table of Contents

Chapter 1. *N*-Heterocyclic Carbenes as Ancillary Ligands for Transition Metals and Main Group Elements

Chapter 2. Development of New Catalysts and Methods for Stereoselective Ru-Catalyzed Olefin Metathesis. Mechanistic Investigation of Action of the Stereogenic-at-Ru Olefin Metathesis Catalysts through Isolation of Key Reactive Intermediates

ACKNOWLEDGEMENTS

In Russian language there are two words for a diamond: “алмаз” stands for a raw diamond, and “бриллиант” defines a cut diamond. Throughout my doctoral studies in Hoveyda group I observed that from the intellectual standpoint arriving new graduate students resemble the former, while those graduating are akin to the latter. The person responsible for such a transformation is Prof. Amir H. Hoveyda. It is Amir’s care for the intellectual development of the group members that allows the latter to develop a refined critical mind – an essential attribute of a scientist. Amir welcomes scientific arguments with and between students; although, rarely does either side changes its mind, neither side leaves an argument with the exact same opinion as the one that each side possessed prior to the said discourse. Through these arguments and discussions hypotheses are generated, refined, and usually discarded. The multi-hour discussions that are a part of any Hoveyda group meeting, which Amir encourages, thus, give the necessary nourishment to the minds of the group members. I like to think that I benefited from the aforementioned environment of intellectual discourse, and I am most grateful to Amir for letting me be a part of this intellectual powerhouse. Thank you, Amir.

The graduate school experience was challenging but overall enriching. It is the support of my peers that helped me overcome the challenges and/or contribute to my graduate experience: Prof. Dennis G. Gillingham, Dr. Kang-Sand Lee, Dr. Yunmi Lee, Tricia L. May, Dr. Steven J. Malcolmson, Dr. Simon J. Meek, Prof. Elizabeth S. Sattely, Erika Vieira, and many others. I am most grateful to the group members, with whom I had a distinct pleasure of collaborating on Ru-catalyzed olefin metathesis projects: Dr. Pamela J. Lombardi, Robert O’Brien, III, and R. Kashif Khan.

To my parents, Mr. Ruslan G. Zhugralin and Mrs. Marzhan K. Zhugralina for being at the right place at the right time and immeasurable support throughout my academic pursuits.

Chapter 1

N-Heterocyclic Carbenes as Ancillary Ligands for Transition Metals and Main Group Elements

1.1. Introduction

Over the past century chemistry has transitioned from the realm of fundamental exploration to that of design, largely due to the remarkable diversity of imaginable chemical compounds within the chemical space.[1] Thus, navigation through the chemical space necessitates a more targeted rather than an exclusivelyexhaustive approach. More so than the latter, the former approach requires significant reflection upon an experiment and the resulting data, yielding hypotheses to be tested and reformulated until a robust theory emerges. Indeed, the quotation by Henri Poincaré is apropos:[2]

> *Cannot we be content with experiment alone? No, that is impossible; that would be a complete misunderstanding of the true character of science. The man of science must work with method. Science is built up of facts, as a house is built of stones; but an accumulation of facts is no more a science than a heap of stones is a house...*

In the chapters of the present dissertation I will attempt to put forward models and rationalizations for observations made in the course of my experimental and theoretical studies of *N*-heterocyclic carbene-catalyzed conjugate additions of borylsilane and diborane reagents to activated olefins and Ru-catalyzed olefin metathesis.

---

(1) For example, the number of possible *constitutional* isomers for *n*-hectane ($C_{100}H_{202}$) is $5.92107 \cdot 10^{39}$ (not counting stereoisomers). Preparation of an appreciable amount (1 µmol, 1.4 mg) of each constitutional isomer of *n*-hectane would require a total of $1 \cdot 10^{69}$ atoms, far exceeding the total number of atoms, estimated to constitute the planet Earth ($1.3 \cdot 10^{50}$ atoms). Gverdsiteli, M. I.; Gamziani, G. A. *J. Struct. Chem.* **1987**, *28*, 768-770.

(2) Poincare, H. *Science and Hypothesis*; The Walter Scott Publishing Co., LTD: New York, 1905.

1.1.1. Electronic Structure Theory: Description of Bonding in Molecules

The advances in the field of organic chemistry are significantly indebted to predictive and descriptive power of the electronic structure theory, which provided chemists – theoreticians and experimentalists alike – with the necessary thought framework to understand experimental data and utilize it for the purpose of guided design of further experiments.

The beginnings of the electronic structure theory can be traced back to the pioneering work of G. N. Lewis, who introduced the central concept to the field of chemistry: an electron pair.[3] His idea of bringing two negative charges together was revolutionary at the time, as quantum theory had yet to be developed[4] and applied to describe bonding in molecules[5]. Indeed, the concept of an electron pair led Lewis to question the validity of Coulomb's law at small distances.[3] However, the development of quantum mechanics and its application to the description of chemical bonding provided the necessary foundation for the development of a rigorous theory of electronic structure. It is the purpose of the current section of the thesis to outline the theories and tools developed within the area of modern electronic structure theory, as the concepts and methods discussed herein will be employed throughout the subsequent sections of the present dissertation.[6]

1.1.1.1. Quantum Theory of Atoms in Molecules (QTAIM)

One of the major problems of modern theoretical chemistry lies in the fact that a wavefunction[7] does not provide detailed information for a chemical bond. Indeed, there is no mathematical operator for a chemical bond, a partial atomic charge, or even for an

---

(3) Lewis, G. N. *J. Am. Chem. Soc.* **1916**, *38*, 762-785.

(4) Schrodinger, E. *Phys. Rev.* **1926**, *28*, 1049-1070.

(5) Heitler, W.; London, F. *Z. Phys.* **1927**, *44*, 455-472.

(6) For the purpose of brevity the discussion of electronic structure will focus on the chemical interpretation of the theory, for a more technical discussion see Ref 7.

(7) There is a wealth of methods available for obtaining wavefunctions within wavefunction theory (WFT) or density functional theory (DFT). Depending on the method and basis sets employed wavefunctions of varying qualities can be obtained. For an introductory discussion on DFT and important basic concepts such as exchange and correlation interactions see: (a) Perdew, J. P.; Ruzsinsky, A.; Constantin, L. A.; Sun, J.; Csonka, G. I. *J. Chem. Theory. Comput.* **2009**, *5*, 902-908. For the introductory text to theoretical and computational chemistry see: (b) Cramer, C. J. *Essentials of Computational Chemistry: Theory and Models*, 2nd Ed.; John Wiley & Sons Ltd.: England, 2004.

atom within a molecule (*i.e.*, it is not clear whether the concepts that chemists use in their daily language are even physical observables). Although, the definition of a molecular geometry of a chemical compound is easily defined as a set of nuclei in 3-dimensional (3D) space,[8] graph theoretic view[9] of a molecule is not evident from this definition. Bader and co-workers answered rigorously a number of vital questions regarding the existence of atoms in molecules and their properties through quantitative analysis of electron density distribution (ρ),[10] which is a physical observable and can be obtained easily computationally or experimentally.[11] Analysis of the electron density distribution (ρ) of a molecule yields the electronic properties as a number of descriptors that are outlined below.

One of the major features of molecular electron density (ρ) is the presence of critical points, which are defined as points in space where electron density reaches a local maximum or minimum. There are four types of critical points: nuclear atomic critical point (NACP), bond critical point (BCP), ring critical point (RCP), cage critical point (CCP).[10]

As illustrated in Figure 1.1, electron density along the H-H bond of the H_2 molecule reaches a maximum at the location of nuclei and a minimum halfway between H nuclei. The maxima (nuclei) are maxima in electron density in all directions; *i.e.*, movement away from a nucleus in any direction results in the decrease of the observable electron density. Thus a maximum in all possible directions in electron density defines

---

[8] Similarly, the concept of stability of a molecular geometry can be incorporated into the definition. Without resorting to arbitrary cut-offs a stable molecular geometry of a chemical compound can be defined as: a set of atomic nuclei in 3-dimensional (3D) space, for which there exists a variationally optimized non-time dependent Born-Oppenheimer wavefunction $\boldsymbol{\Psi}(\mathbf{r})$, and the following criteria are fulfilled: $d\langle\boldsymbol{\Psi}(\mathbf{r})|\hat{\boldsymbol{H}}|\boldsymbol{\Psi}(\mathbf{r})\rangle/d\mathbf{R}_\mathbf{n}=0$ and $d^2\langle\boldsymbol{\Psi}(\mathbf{r})|\hat{\boldsymbol{H}}|\boldsymbol{\Psi}(\mathbf{r})\rangle/d\mathbf{R}_\mathbf{n}^2>0$, where $\mathbf{R}_\mathbf{n}$ is an internal coordinate of the system and $\mathbf{r}$ is a coordinate of an electron.

[9] Graph theoretic view is the familiar representation of molecules, where bonds represented by lines (edges) connect atoms represented by points (nodes). For a discussion on representation in chemistry, see: Hoffmann, R.; Laszlo, P. *Angew. Chem. Int. Ed. Engl.* **1991**, *30*, 1-16.

[10] For the rigorous account of the foundations of quantum theory of atoms in molecules, see: (a) Bader, R. F. W. *Atoms in Molecules: A Quantum Theory*; Oxford University Press: New York, NY, 1990. For the review of application of QTAIM see: (b) *The Quantum Theory of Atoms in Molecules: From Solid State to DNA and Drug Design*; Matta, C. F.; Boyd, R. J., Eds.; WILEY-VCH Verlag GmbH & Co. KGaA: Weinheim, 2007.

[11] For a detailed discussion on the QTAIM analysis of experimental electron densities that are accessible by X-ray, γ-ray, or synchrotron radiation crystallography, see: Ref. 10b.

location of a nucleus and is called a nuclear atomic critical point (NACP). The halfway point between the two NACPs is a minimum in electron density; however, when viewed in the plane orthogonal with respect to the H-H bond it is a maximum. Similarly, ring critical points (RCP) can be found inside the ring of a cyclic compound, in which case RCPs are minima in electron density in two dimensions but they remain a maximum in one dimension. Cage critical points (CCPs) are minima in all three dimensions and can be found inside cage compounds such as cubane. As suggested by their names, the critical points define the presence of certain structural elements within a compound.

Figure 1.1. Electron Density of H_2 Molecule

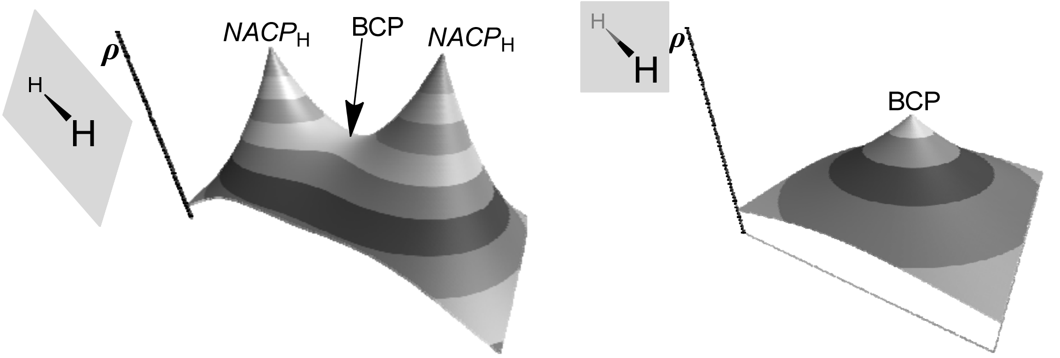
(a) Density in the plane of H-H bond

(b) Density in the plane bisecting H-H bond

Further analysis of the electron density distribution shows that between two nuclei connected by a bond there exists a path of maximum electron density, on which the BCP resides. This path of maximum electron density is called a *bonding path* and can be used to define a *bond*. Indeed, bonding paths represent the notion of bonding that is most intuitive to chemists and reproduce the concepts that were previously inferred for bonds. For example, ring strain of cyclopropanes is smaller than would be expected for sp^3-hybridized carbon atom that is forced to bear a 60^o bond angle. This unusual thermodynamic stability was attributed to banana bonds that occur due to the overlap of sp^3-hybridized orbitals of two carbon atoms at an angle that is less than the ideal 180^o. An electron density map of cyclopropane shows that C-C bonding paths are not straight and instead curve outward as would be expected of a banana bond. The electron density map of the cross-section of the C-C double bond exhibits ellipticity as would be expected of a combination of a single σ-bond and a single π-bond.

Figure 1.2. Analysis of Electron Density of *bis*-glycolatodiboron

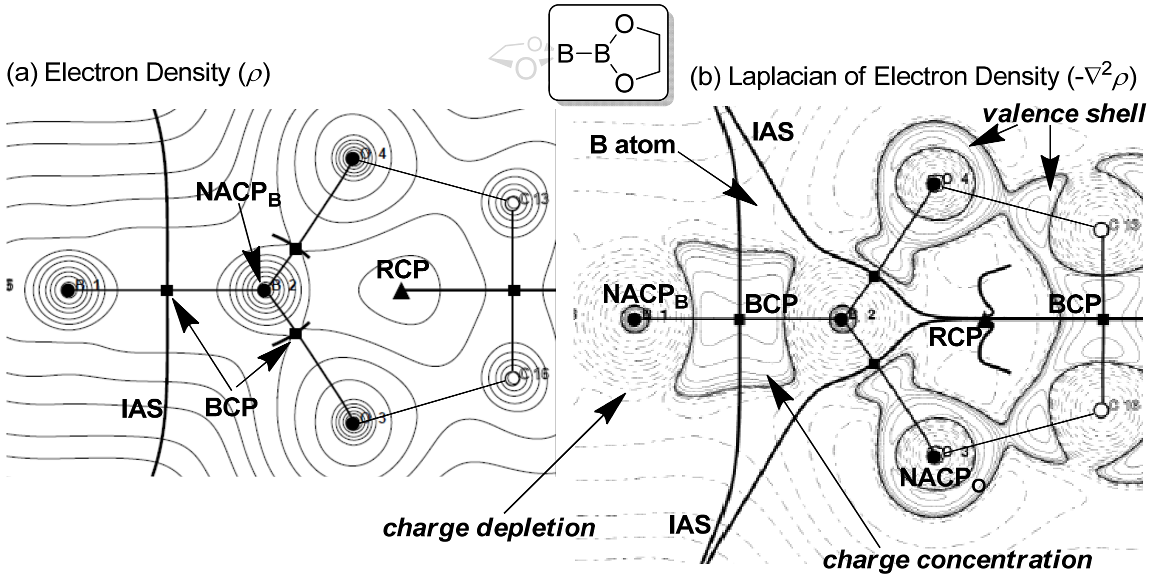
(a) Electron Density (ρ)

(b) Laplacian of Electron Density ($-\nabla^2\rho$)

As the BCP is a minimum observed along the bonding path, there are points of minimum electron density in a single direction between two bonded atoms that are neither mimima nor maxima in other directions; the combination of these points forms an interatomic surface (IAS). The interatomic surface is most conveniently defined as a surface of zero flux of electron density. The combination of all interatomic surfaces around a single NACP forms an atom. Thus, the fundamental difference between quantum theory of atoms in molecules (QTAIM) and the “chemical intuition” is the assumption of the latter that a molecule results from overlapping spherical atoms. Within QTAIM, atoms do not overlap but change their shape so as to match the shape of other atoms, to which the atom in question is bonded. For example, as shown in Figure 1.2a the space of the molecule of *bis*-glycolatodiboron can be divided into atoms, which are bounded by the interatomic surfaces (for example, boron atom), within which reside bond critical points (BCP). At the confluence of interatomic surfaces (IAS) inside the glycolatoboron ring there is a ring critical point (RCP).[12]

---

(12) Note that not all interatomic surfaces are rendered on the images. In (a) both B-O IASs and both C-O IASs are not rendered; in (b) both C-O IASs are not shown.

A particularly informative view of electron density (ρ) is that of its second derivative: laplacian of electron density ($\nabla^2\rho$). As shown in Figure 1.2b, $\nabla^2\rho$ can take on either negative or positive values (solid vs dashed contours in Figure 1.2b, respectively), where negative values imply areas of relative depletion of electron density, while positive values point to the areas of relative concentration of electron density. For small main group elements that are not bonded to elements that are significantly more electronegative, a spherical region of charge concentration can be located; it corresponds to the valence shell of the atom, and deformation of the valence shell can be indicative of either the presence of a lone pair (or valence shell charge concentration: VSCC) or a polarizing interaction. For example, in Figure 1.2b, the negatively charged oxygen atoms are strongly polarized towards the positively charged boron atom.

The properties of chemical bonds can be inferred from a number of numerical descriptors at the bond critical point (BCP). Based on the values of these descriptors the bonding interaction can be classified as either *shared interactions* or *closed-shell interactions*. The concentration of electronic charge in the internuclear region leads to a large and negative $\nabla^2\rho$ value, while ρ is also large. Such interactions fall into the category of covalent or polar covalent and are called *shared interactions*. *Closed-shell interactions* such as hydrogen bonds, Lewis acid/base adducts, etc. are characterized by a small positive $\nabla^2\rho$ value at the BCP, and ρ is also small. Complete interatomic charge transfer leads to formation of ionic bonds, which are characterized as *closed-shell interactions*.

Another important descriptor is that of ellipticity (ε), which measures the degree of the departure of the bond from the cylindrical symmetry. For example, a single bond in ethane or a triple bond in acetylene exhibit $\varepsilon = 0$ at the BCP, whereas C-C bond in benzene has ε=0.23, and the C-C bond of ethylene (a formal double bond) shows ellipticity of 0.45.[10b]

The important consequence of the division of molecular real space into atoms with IASs of zero flux of electron density is the fact that the resulting atoms are well-defined open quantum systems and obey the virial ratio, $-V(\Omega)/T(\Omega)=2$, *i.e.*, the ratio of potential energy of an atom to kinetic energy of an atom is equal to 2.[10] As a result, a number of atomic properties can be defined for the atom in a molecule, most notably, the electronic kinetic energy $T(\Omega)$, the total energy $E(\Omega)$, electronic population $N(\Omega)$, and the resulting partial atomic charge $q(\Omega)$.

It should also be noted that quantum theory of atoms in molecules (QTAIM) has been utilized to provide the physical basis for VSEPR theory.[10] As mentioned above, the valence shell charge concentrations (VSCCs) are analogous to lone pairs and thus QTAIM can be utilized to localize them in space.

1.1.1.2. Energy Decomposition Analysis and Charge Decomposition Analysis

Energy decomposition analysis (EDA) was developed independently by Morokuma,[13a] and Ziegler and Rauk.[13b-c] The underlying principle for energy decomposition analysis (EDA) is that of energy being a state function, *i.e.* the path connecting two points is inconsequential to the value of energy, which is determined only by the starting and the end points. Thus, a bond forming process between two fragments can be envisioned to be occurring in well-defined steps even though changes to all parameters assessed in the process of EDA occur simultaneously during the actual reaction (Figure 1.3).

The bond forming process for an A-B bond can be viewed to occur in 3 main steps. First, the separated-to-infinity, relaxed geometries of fragments A and B in their electronic ground states are prepared by changing their geometries (nuclear coordinates) to the ones found in compound A-B. During this process, the fragments are also promoted to their excited electronic states if necessary. Overall the preparation process results in an increase in the total energy of the system ($\Delta E_{\text{Prep}} > 0$). The second step entails bringing the two prepared fragments together to form the compound A-B in its final geometry; however, the electron densities of fragments A and B are kept constant; the resulting ΔE^0 (Figure 1.3) can take on either positive or negative values and can be further divided into ΔE_{el} (electrostatic component) and ΔE_{er} (exchange repulsion). The former is best thought of as the electrostatic interaction of the nuclei of A-B at its final

---

(13) (a) Morokuma, K. *J. Chem. Phys.* **1971**, *55*, 1236-1244; (b) Ziegler, T.; Rauk, A. *Theor. Chim. Acta.* **1977**, *46*, 1-10; (c) Ziegler, T.; Rauk, A. *Inorg. Chem.* **1979**, *18*, 1558-1565.

Figure 1.3. Energy Decomposition Analysis Scheme

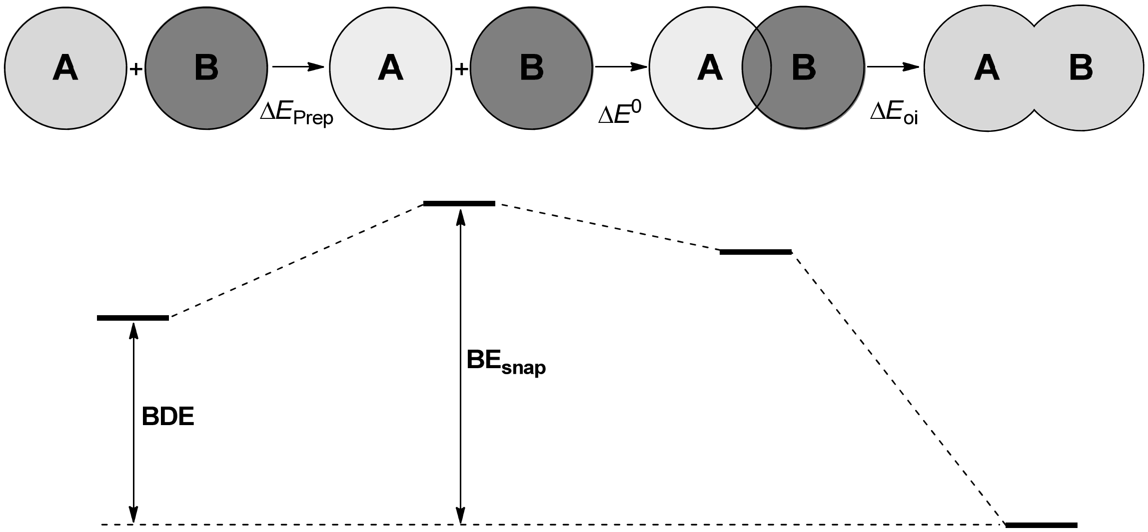

geometry with unperturbed electron densities of A and B. The exchange repulsion (ΔE_{er}) is often referred to as Pauli repulsion and corresponds to the intuitive concept of steric repulsion. Pauli repulsion is due to the electron-electron repulsive interactions between the two unrelaxed electron densities of fragments A and B. The final step of the bond-forming process is relaxation of electron densities of A and B fragments to afford the electron density of A-B molecule in its ground electronic state. The resulting term is ΔE_{oi} (orbital overlap energy) is negative as relaxation of electron densities allows for the bonding interactions to occur between the fragments A and B through overlap between appropriate orbitals. Orbital overlap energy can be partitioned further to account for contributing interactions of appropriate symmetry (each orbital interaction is within the irreducible representation Γ of the overall symmetry of A-B).[14]

The sum of all the energies derived from energy decomposition analysis (EDA) gives the bond dissociation energy (BDE) – an experimental observable. However, BE_{snap} (bond snapping energy) constitutes the bond forming process, whereas ΔE_{Prep} accounts for the independent preparation of each fragment prior to the bond formation.

Charge decomposition analysis (CDA) was introduced by Frenking and co-workers to address some of the problems associated with the existing population

---

(14) The overall interaction can be summarized as: $BDE = \Delta E + \Delta E_{Prep}$; $BE_{snap} = \Delta E^0 + \Delta E_{oi}$; $\Delta E^0 = \Delta E_{el} + \Delta E_{er}$

analyses.[15,16] The basic principle behind CDA is the same as that behind EDA, *i.e.*, the bond forming process is considered in steps; however, instead of monitoring changes in the overall energy of the system, changes in orbital contributions to the overall bonding scheme are monitored.

One of the main criticisms of EDA and CDA lies in the fact that the intermediate states that are generated in the process of bond formation are unphysical and thus are not physically observable. However, EDA and CDA can be seen as a *gedanken* experiment that does not attempt to reproduce the physical bond-forming process and instead seeks to provide information about each factor that contributes to bonding.

1.1.1.3. Natural Bond Orbitals (NBO)

The concept of molecular orbitals, as used by most chemists, differs significantly from that used computationally (standard atomic orbital basis functions). The concept of "natural" orbitals was introduced by Löwdin to describe the orbitals that are singled out as the most "natural" representation of electrons within a wavefunction (from a computational standpoint) to reproduce the electron density.[17] The natural orbitals, however, are *symmetry adapted* and thus appear as strongly delocalized and unique to a specific geometry. This uniqueness renders the orbitals non-transferable, for example, the concept of a σ-bond or a π-bond is lost, as the diffuse natural orbitals may mix them throughout the molecule. Furthermore, the representation of bonding within a molecule in terms of natural orbitals does not provide a physical basis for a Lewis structure, even for simple closed-shell organic molecules. Thus, Weinhold introduced the concept of natural bond orbitals and various other types of natural orbitals as intermediate steps within the

---

(15) Dapprich, S.; Frenking, G. *J. Phys. Chem.* **1995**, *9352-9362*.

(16) Other common population analysis schemes are: Mulliken Population Analysis (a) Mulliken, R. S. *J. Chem. Phys.* **1955**, *23*, 1833-1840; (b) Mulliken, R. S. *J. Chem. Phys.* **1955**, *23*, 1841-1846; (c) Mulliken, R. S. *J. Chem. Phys.* **1955**, *23*, 2338-2342; Löwdin Population Analysis (d) Löwdin, P. –O. *Adv. Quantum Chem.* **1970**, *5*, 185-199, Roby Population Analysis (e) Roby, K. R. *Mol. Phys.* **1974**, *27*, 81-104; Mayer (f) Mayer, I. *Chem. Phys. Lett.* **1984**, *110*, 440-444; Cioslowski's Atomic Polar Tensor (g) Cislowski, J. *J. Am. Chem. Soc.* **1989**, *111*, 8333-8336. These population analysis schemes generally suffer from high dependence upon the basis sets employed, and, in the case of Mulliken and to a lesser extent of Löwdin population analyses, there is no convergence with increased flexibility of the basis set with the same electronic structure model (for example, Hartree-Fock).

(17) Löwdin, P. –O. *Phys. Rev.* **1955**, *97*, 1474-1489.

NBO analysis.[18] The mathematical foundation of NBO is beyond the scope of the current discussion; however, an NBO procedure is essentially a localization operation in terms of natural orbitals yielding natural bond orbitals that are sufficiently localized to provide a picture that is intuitive to most chemists. Furthermore, NBO provides a measure of accuracy for Lewis structures in describing the electronic structure of a molecule (for common organic molecules it is not unusual to observe >99% accuracy). The remaining non-Lewis character of a molecule is due to interactions (delocalization effects) that are not representable by a Lewis structure, for example, hyperconjugation (donations from an occupied natural localized molecular orbital into the unoccupied one, provided there is sufficient overlap[19]). The delocalization effects are quantifiable within NBO. As the polarization effects within localized orbitals and the delocalization effects are accounted for, it is possible to calculate atomic populations – natural population analysis (NPA).[20]

1.1.1.4. Conclusion

The purpose of this section was to provide a brief overview of theoretical methods that will be utilized to rationalize experimental observations described in this manuscript; any finer points will be explicated, as necessary, in the course of the discussion. The discussion of the theories was not exhaustive neither in terms of the applications available within each theoretical method nor in terms of covering all available theoretical methods. For example, many partitioning schemes for atoms in molecules have been developed; however, QTAIM was the method of choice due to non-arbitrariness in its derivation and the focus on physical observables. Other variational partitioning schemes for interpenetrating atoms in molecules include but are not limited to: Hirshfeld,[21] Li and

---

(18) (a) Foster, J. P.; Weinhold, F. *J. Am. Chem. Soc.* **1980**, *102*, 7211-7218; (b) Reed, A. E.; Curtiss, L. A.; Weinhold, F. *Chem. Rev.* **1988**, *88*, 899-926; (c) Weinhold, F.; Landis, C. R. *Chem. Educ. Res. Pract. Eur.* **2001**, *2*, 91-104.

(19) It should be noted that one of the common misconceptions is that a bonding occurs due to geometric orbital overlap in real 3D-space; the orbital overlap refers to the overlap between matrix elements within the system's Hamiltonian.

(20) Reed, A. E.; Weinstock, R. B.; Weinhold, F. *J. Chem. Phys.* **1984**, *83*, 735-746.

(21) Hirshfeld, F. L. *Theor. Chim. Acta* **1977**, *44*, 129-138.

Parr,[22] and Fernández Rico;[23] non-variational non-interpenetrating atoms in molecules scheme: Voronoi Deformation Density (VDD).[24] An alternative to NBO electron localization scheme was developed by Becke – Electron Localization Function (ELF); unlike NBO, ELF localizes electrons not in orbitals but in real 3D-space.[25]

1.1.2. N-Heterocyclic Carbenes: Properties of Free Carbenes, their Transition-Metal and Main Group Element Complexes

Although the first *N*-heterocyclic carbene-metal complexes (NHC-metal complexes) were prepared in 1968,[26] their potential in catalysis had not been realized until three decades later. Following the demonstration of thermodynamic stability of sterically hindered free *N*-heterocyclic carbenes by Arduengo and co-workers,[27] the field of metal-catalyzed transformations was significantly impacted by the reintroduction of NHC-metal complexes.[28] Initially, NHC ligands were viewed largely as an alternative to phosphines; however, it is now clear that NHC ligands present a class of ancillary ligands of their own with electronic and steric attributes that are difficult to replicate in

---

(22) Bader's partitioning scheme for QTAIM can be considered as a special case of Li-Parr partitioning scheme: Li, L.; Parr, R. G. *J. Chem. Phys.* **1986**, *84*, 1704-1711.

(23) Fernández Rico, J.; López, R.; Ramírez, G.; Ema, I.; Ludeña, E. V. *J. Comput. Chem.* **2004**, *25*, 1355-1363.

(24) Fonseca Guerra, C.; Handgraaf, J. –W.; Baerends, E. J.; Bickelhaupt, F. M. *J. Comput. Chem.* **2004**, *25*, 189-210.

(25) Becke, A. D.; Edgecombe, K. E. *J. Chem. Phys.* **1990**, *92*, 5397-5403.

(26) (a) Öfele, K. *J. Organomet. Chem.***1968**, *12*, P42-P43; (b) Wanzlick, H. –W.; Schonherr, H. –J. *Angew. Chem., Int. Ed. Engl.* **1968**, *7*, 141-142.

(27) (a) Arduengo, A. J. III; Harlow, R. L.; Kline, M. *J. Am. Chem. Soc.* **1991**, *113*, 361-363; (b) Arduengo, A. J. III; Dias, H. V. R.; Harlow, R. L.; Kline, M. *J. Am. Chem. Soc.* **1992**, *114*, 5530-5534; (c) Arduengo, A. J. III *Acc. Chem. Res.* **1999**, *32*, 913-921.

(28) For reviews on applications of *N*-heterocyclic carbenes as ancillary ligands for transition metals in catalysis see: (a) Herrmann, W. A.; Kocher, C. *Angew. Chem. Int. Ed.* **1997**, *36*, 2162-2187; (b) Herrmann, W. A. *Angew. Chem. Int. Ed.* **2002**, *41*, 1290-1309; (c) Cesar, V.; Bellemin-Laponaz, S.; Gade, L. H. *Chem. Soc. Rev.* **2004**, *33*, 619-636; (d) Glorius, F. *Top. Organomet. Chem.* **2007**, *21*, 1-20; (e) Rogers, M. M.; Stahl, S. S. *Top. Organomet. Chem.* **2007**, *21*, 21-46; (f) Diez-Gonzalez, S.; Nolan, S. P. *Top. Organomet. Chem.* **2007**, *21*, 47-82; (g) Gade, L. H.; Bellemin-Laponaz, S. *Top. Organomet. Chem.* **2007**, *21*, 117-157; (h) Tekavec, T. N.; Louie, J. *Top. Organomet. Chem.* **2007**, *21*, 159-192; (i) Despagnet-Ayoub, E.; Ritter, T. *Top. Organomet. Chem.* **2007**, *21*, 193-218; (j) Diez-Gonzalez, S.; Marion, N.; Nolan, S. P. *Chem. Rev.* **2009**, *109*, 3612-3676; (k) Alcaide, B.; Almendros, P.; Luna, A. *Chem. Rev.* **2009**, *109*, 3817-3858; (l) Payatos, M.; Mata, J. A.; Peris, E. *Chem. Rev.* **2009**, *109*, 3677-3707; (m) Samojlowicz, C.; Bieniek, M.; Grela, K. *Chem. Rev.* **2009**, *109*, 3708-3742; (n) Vougioukalakis, G. C.; Grubbs, R. H. *Chem. Rev.* **2010**, *110*, 1746-1787. For a review on the methods of preparation of NHC-metal complexes see: (o) Peris, E. *Top. Organomet. Chem.* **2007**, *21*, 83-116.

phosphines and thus NHC-metal complexes exhibit unique reactivity profiles in catalytic reactions.

1.1.2.1. Electronic States of Carbenes

In order to analyze the stereoelectronic properties of NHCs, properties of carbenes should be evaluated. The simplest carbene molecule is that of methylene ($:CH_2$); there are four electronic configurations of methylene carbene that need to be considered (Figure 1.4). The $^1A_1$ state, which results from population of the *p*-orbital of the carbene carbon atom with an e^--pair that is much higher in energy for methylene and thus its contribution to the wavefunction of methylene is minimal (in the case of methods accounting for configurational interaction). The contribution of the remaining states to the wavefunction of the methylene would determine the observable state (singlet *vs.* triplet). The energetic difference between electronic states constituting the singlet state and the triplet state for methylene is ~11 kcal/mol in favor of the latter, *i.e.* the ground electronic state of methylene is triplet (a mixture of the triplet $^3B_1$ and the open-shell singlet $^1B_1$ states).[29,30]

Figure 1.4. Electronic Configurations of Methylene

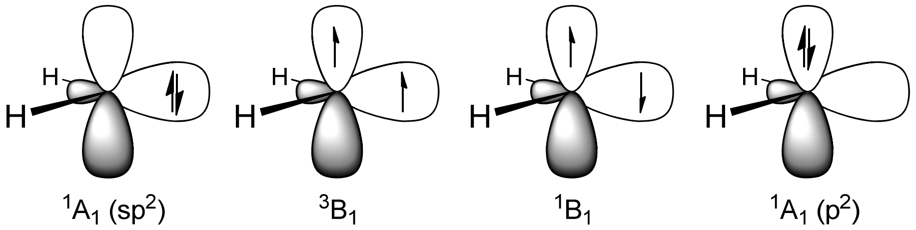

In 1962, partly drawing on Breslow's pioneering work on the mechanism of thiamine action,[31] Wanzlick suggested that the introduction of π-donating substituents at the methylene carbene may lead to the enhanced stability and the switch in the electronic nature of carbenes from electrophilic to nucleophilic.[32] Experimental results in the same manuscript indicated that Wanzlick prepared *N*,*N*-diphenylimidazolinylidene, which was isolated as a dimer. The dimerization reaction, however, proved reversible in the solution

---

[29] Skell, P.S.; Woodworth, R. C. *J. Am. Chem. Soc.* **1958**, *78*, 4496-4497.

[30] For a review on electronic properties of stable carbenes, see: Bourissou, D.; Guerret, O.; Gabbai, F. P.; Bertrand, G. *Chem. Rev.* **2000**, *100*, 39-91.

[31] Breslow, R. *J. Am. Chem. Soc.* **1958**, *80*, 3719-3726.

[32] Wanzlick, H. W. *Angew. Chem. Int. Ed. Engl.* **1962**, *1*, 75-80.

and thus the presence of the carbene in the solution phase was established indirectly through observed reactivity with various small molecules such as oxygen, methanol, furfural, and tetracyanoethylene. The reactivity profile of diphenylimidazolinylidene is suggestive of the closed-shell singlet character of the carbene, *i.e.* the major contributing electronic configuration can be assigned to $^1A_1$ (sp^2). In light of the dichotomy between the ground electronic states of the two carbenes presented so far, it is necessary to establish the location, within the chemical space, where the singlet and triplet potential energy surfaces cross.

For a singlet state to constitute a ground state for a molecule, the HOMO-LUMO gap must be ~40 kcal/mol due to the necessity to account for the energy of restricting two negatively charged particles to the same three quantum numbers (n, l, and m_l).[33] Thus presence of only a single π-donor at the divalent carbon affords sufficient stabilization to a singlet state carbene [$^1A_1(sp^2)$], which was confirmed experimentally for hydroxymethylene carbene[34] and cyclic alkylaminocarbenes (CAAC)[35]. The presence of the second π-donor at the divalent carbon increases the gap between singlet and triplet states (S-T gap) to 65-85 kcal/mol.[36] Thus, for the purpose of designing a Lewis basic ancillary ligand, a single π-donor substituent at the divalent carbon suffices to ascertain the multiplicity of the ligand in question.

1.1.2.2. Dimerization of Carbenes as an Indication of their Electronic and Steric Properties

The electronic structure of a carbene can be modulated by means of the incorporation of appropriate substituents at the carbene, such that a singlet state is preferred. However, the thermodynamic and kinetic stabilities of a carbene are not necessarily guaranteed by reducing the diradical character of the carbon atom. The S-T

---

(33) Hoffmann, R. *J. Am. Chem. Soc.* **1968**, *90*, 1475-1485.

(34) The gap between singlet and triplet states (S-T gap) of hydroxymethylene was determined to be ~28 kcal/mol: Schreiner, P. R.; Reisenauer, H. P.; Pickard, F. C. IV; Simmonett, A. C.; Allen, W. D.; Matyus, E.; Csaszar, A. G. *Nature* **2008**, *453*, 906-911.

(35) The S-T gap for CAAC ligands was determined to be 46 kcal/mol: (a) Melaimi, M; Soleilhavoup, M.; Bertrand, G. *Angew. Chem. Int. Ed.* **2010**, *49*, 8810-8849; (b) Lavallo, V.; Canac, Y.; Prasang, C.; Donnadieu, B.; Bertrand, G. *Angew. Chem. Int. Ed.* **2005**, *44*, 5705-5709.

(36) Heinemann, C.; Thiel, W. *Chem. Phys. Lett.* **1994**, *217*, 11-16.

gaps of NHCs are still not sufficiently large to ensure complete inaccessibility of the triplet state. For example, as mentioned above, free *N*-heterocyclic carbenes can undergo a facile dimerization in the solution phase (eq 1, Table 1.1).[37] The monomeric fragment within the carbene dimer can be viewed as being in a triplet state (*i.e.*, combination of $^1B_1$ and $^3B_1$ configurations); that dimers are thermodynamic minima for some NHCs point to the accessibility of the triplet state.

Table 1.1. Thermodynamic Stability towards Dimerization of NHCs in the solution phase

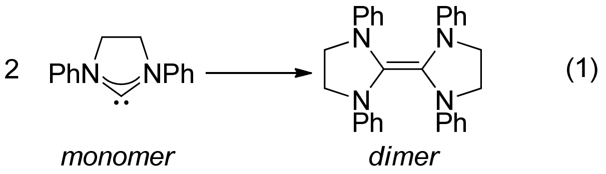

(1)

R / scaffold	-⌇-t-Bu	-⌇-Mes	-⌇-Cy	-⌇-Ph	-⌇-Me
	monomer (12.6)	monomer (7.8)	dimer[1] (-13.9)	dimer (-16.6)	dimer (-18.7)
	monomer (34.4)	monomer (26.7)	monomer[1] (14.0)	equilibrium[1] (-1.3)	monomer (4.3)
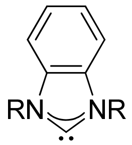	monomer (20.4)	monomer[1] (12.5)	monomer[1] (1.5)	equilibrium[1] (-8.8)	equilibrium (-9.0)

Calculated dimerization energies ($E^{DFT}{}_{dim}$) in kcal/mol for the reaction in eq 1 with the corresponding free carbenes are given in parantheses.The numeric data was obtained from Ref. 37.

[1] No experimental data available. Prediction is based on the linear regression fit described in the text

The wealth of experimental and theoretical data[37] on the dimerization of NHCs in the solution phase indicate that the carbenes can be modified sterically *and* electronically in favor of a monomeric form. As expected, larger *N*-substituents within the structure of the NHC destabilizes the dimeric form. As for the electronic modification of the NHCs, the degree of aromaticity within the NHC ring correlates with the S-T gap and the preference for the monomeric form. For example, NHCs bearing a saturated C-C

---

(37) Poater, A.; Ragone, F.; Giudice, S.; Costabile, C.; Dorta, R.; Nolan, S. P.; Cavallo, L. *Organometallics* **2008**, *27*, 2679-2681.

backbone (saturated NHCs), thus lacking in aromatic stabilization, exhibit thermodynamic preference for dimeric forms, compared to their unsaturated counterparts (see Table 1.1). The benzo-NHCs (benzimidazolylidenes) lie in between the saturated and unsaturated NHCs with respect to the thermodynamic stability of their monomers.[37] The degree of aromaticity accounts for the latter observation, as the aromatic stabilization of the *N*-heterocyclic ring of the benzo-NHCs is lower than that of the unsaturated NHCs but higher than that of the saturated NHCs. Indeed, based on such trends and observations, Cavallo and co-workers correlated the calculated dimerization energies ($E_{\text{dim}}^{\text{DFT}}$) to experimental dimerization energies (E_{dim}), and separated the steric and electronic properties of NHCs within a linear regression fit (eq 2).[37] Following the analysis of fitted dimerization energies ($E_{\text{dim}}^{\text{fit}}$) of various NHCs and correlation of these energies to experimental observations, Cavallo and co-workers concluded that NHCs are likely to be thermodynamically stable as monomers with respect to dimerization if $E_{\text{dim}}^{\text{fit}} >$ -3 kcal/mol and as dimers if $E_{\text{dim}}^{\text{fit}} <$ -22 kcal/mol. In eq 2, the $\text{NHC}_{\text{Steric}}$ is $\%V_{\text{Bur}}$ (*vide infra*) and the $\text{NHC}_{\text{Electronic}}$ is the S-T gap.

$$E_{\text{dim}} = A \cdot \text{NHC}_{\text{Steric}} + B \cdot \text{NHC}_{\text{Electronic}} + C \qquad (2)$$

The discussion above points to NHCs as viable Lewis bases that can be modified to ascertain their thermodynamic stability towards dimerization, allowing for their use as catalysts in their own right or as adducts with other elements. However, for consideration of practical utility, the stereoelectronic properties of NHCs and their complexes with transition metals and main group elements need to be discussed.

1.1.2.3. A Steric Metric for N-Heterocyclic Carbenes

Despite the similarity in Lewis basic nature of phosphines and NHCs, the two exhibit different electronic and steric properties. For example, consider a spherical environment around the metal center, bearing a single Lewis basic donor ligand that is either an NHC or a phosphine (Figure 1.5). As illustrated in Figure 1.5, the substitution pattern of the divalent carbon allows for division of space around the metal center into *four* sectors,[38] whereas the substitution pattern of the trivalent phosphorus allows for the division of space into *three* sectors. Through ligand modification it is possible to effect steric blocking of various sectors; however, for NHC the division of space into 2n sectors can be achieved in principle. Similarly, the three-fold symmetry of phosphines is conducive to ligand designs, wherein the space is divided into 3n sectors.[39] Thus, the divalent carbon lends itself to 2n-fold symmetry, and trivalent phosphorus lends itself to 3n-fold symmetry; therefore, the steric metrics applicable to phosphines are not necessarily extendable to NHCs. For example, approximation of a tertiary phosphine as a cone allows for the corresponding cone angle (Tolman cone angle) to serve as a sterics scale for various phosphines.[40] Unfortunately, attempts to extend the concept of Tolman cone angle to *N*-heterocyclic carbenes proved fraught with difficulties due to the fact that the ray originating at the metal center and tangent to the surface of the outermost atoms of the *N*-substituents (~80° for *p*-methyl groups of the *N*-substituents on SIMes ligand)

Figure 1.5. Steric Environment around the Metal Nucleus, Bearing (a) NHC or (b) phosphine ligand

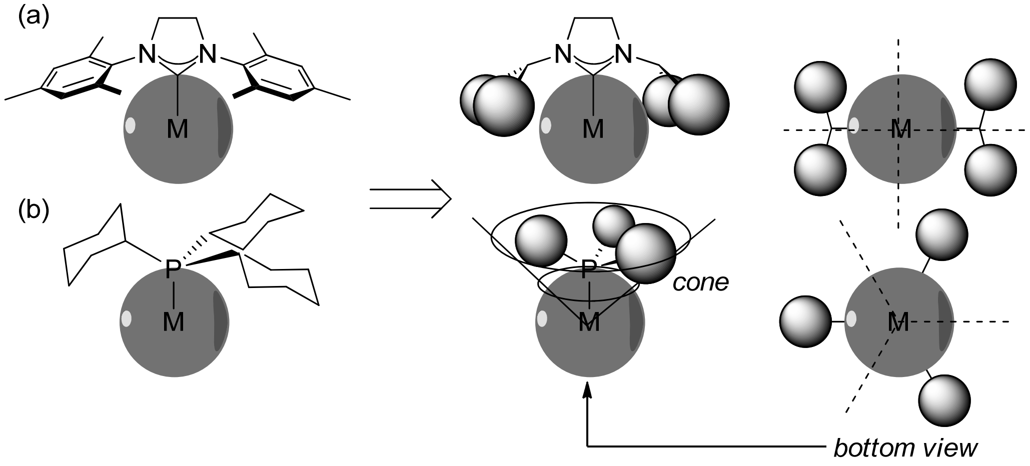

---

[38] Although, NHC can be viewed as having a 2-fold symmetry and thus only two sectors, which can be either sterically occupied or free, appropriate modifications to the ligand scaffold allow for finer control of space around the metal center in a 4-fold manner. The NHC scaffolds that allow for steric control of 4 quadrants will be discussed in Chapter 2.

[39] In principle, an NHC structure can be modified to afford a 3n-fold divided space around the metal center, and similarly a phosphine structure can be conceived such that the space around the metal is divisible into 2n number of sectors. However, given the natural predisposition of each scaffold for a particular symmetry and in absence of electronic requirement of a particular reaction for NHC or phosphine ligand, it may be advisable to start ligand structure optimization with the ligand scaffold that best matches the symmetry of the reactive metal center.

[40] Tolman, C. A. *Chem. Rev.* **1977**, *77*, 313-348.

and the ray that lies in the plane bisecting the imidazolinylidene ring (essentially 0°) have drastically varying values.[41]

Figure 1.6. $\%V_{Bur}$ as a sterics metric for NHCs

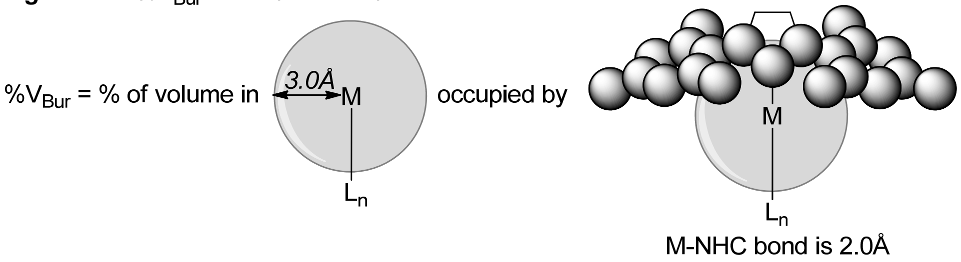

Cavallo, Nolan, and co-workers have proposed a different metric for measuring sterics in NHCs: $\%V_{Bur}$.[41] This steric descriptor can be accessed easily from either X-ray crystallographic or computational studies. As shown in Figure 1.6, $\%V_{Bur}$ is simply the percentage of the volume of the sphere (radius = 3Å), centered on the metal nucleus, which is occupied by the van der Waals volumes of atoms of the ligand in question. For the purposes of comparison, the metal-ligand bond is assumed to be equal to 2Å. The descriptor $\%V_{Bur}$ has proved sufficiently flexible to provide similarly accurate metric of sterics for phosphines.

It was found that $\%V_{Bur}$ provides reverse linear correlation with experimental bond decomposition energies (BDE) of the corresponding metal-NHC complexes, indicating the importance of steric interactions between bulky NHCs or phosphines with the metal center for the stability of ancillary ligand-metal bonds. The values of $\%V_{Bur}$ for NHCs under investigation were found to vary between 23 and 37; for comparison, the values of $\%V_{Bur}$ of PPh_3 and PCy_3 are 27 and 32, respectively (Figure 1.7).[42]

Figure 1.7. $\%V_{Bur}$ Values for Common NHCs and Phosphines

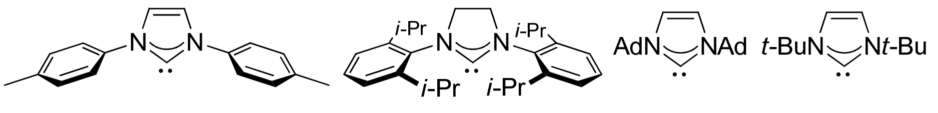

	ITol	SIPr	IAd	I*t*-Bu
$\%V_{Bur}$ =	23	30	37	37

---

(41) Cavallo, L.; Correa, A.; Costabile, C.; Jacobsen, H. *J. Organomet. Chem.* **2005**, *690*, 5407-5413.

(42) The naming of NHCs follows the following nomenclatural scheme: the ring of the NHC is defined by the descriptor "I" (for imidazolylidene), which in the case of the saturated version (imidazolinylidene) is called "SI". This descriptor is then followed by an abbreviation for the *N*-substituents (Tol for *p*-tolyl, Pr for di-*iso*-propyl phenyl, Ad for adamantyl, *t*-Bu for *t*-butyl).

Although, the steric descriptor %V_{Bur} fits well for measuring the intrinsic steric properties of the metal-NHC complexes, the application of this descriptor to account for trends observed in reactions should be exercised with care, as steric pressure points vary for different reactions.[43] However, %V_{Bur} algorithm could be used as a model to develop sterics metrics specific to a particular class of reactions under investigation.

1.1.2.4. Electronic Structure of Carbenes

Understanding the electronic properties of NHCs requires accounting of many contributing interactions, which become evident upon consideration of the electronic properties of carbenes in general. The pioneering work, analyzing metal-carbon double bonds, was carried out by Taylor and Hill in 1984;[44] in their seminal publication they provided the electronic rationale for distinct behavior of nucleophilic (Schrock-type alkylidenes) and electrophilic carbenes (Fischer-type carbenes),[45] which is briefly summarized below.[46]

A carbene-metal complex can be envisioned as a combination of two fragments: a carbene and a metal in their ground electronic states (Figure 1.8). For example, the coordination of methylene in its ground electronic state[47] (triplet) to a high-spin metal results in summation of the atomic orbitals of appropriate symmetries to afford a singlet organometallic complex (provided that the only unpaired electrons are the ones shown in

---

(43) The steric pressure points refer to the locations in space surrounding a metal center, to which reactants a limited by virtue of the coordination sphere (square planar, trigonal bipyramidal, etc.) of the metal center in question. For example of different steric requirements (*i.e.*, different pressure points) in Cu-catalyzed hydroboration of alkynes, see: Jang, H.; Zhugralin, A. R.; Lee, Y.; Hoveyda, A. H. *Unpublished Results.*

(44) Taylor, T. E.; Hall, M. B. *J. Am. Chem. Soc.* **1984**, *106*, 1576-1584.

(45) The philicity of a carbene is largely determined by the metal center and *not the carbene ligand*: (a) Ref. 20; (b) Cundari, T. R.; Gordon, M. S. *J. Am. Chem. Soc.* **1991**, *113*, 5231-5243; (c) Cundari, T. R.; Gordon, M. S. *J. Am. Chem. Soc.* **1992**, *114*, 539-548; (d) Cundari, T. R.; Gordon, M. S. *Organometallics* **1991**, *11*, 55-63.

(46) Note that terms Fischer carbene and Schrock alkylidene are used in the present manuscript to describe electronic states of the metal and ligand fragments and do not follow conventional definitions for the two classes of carbenes (*vide infra*).

(47) $\Delta E(AO_2\text{-}AO_1)$ < electron-pairing energies (*vide supra*). Note that the S-T gap is not equal to $\Delta E(AO_2\text{-}AO_1)$, as the latter is the difference in the energies of atomic orbitals within either a singlet or a triplet wavefunction, whereas the former is the difference between electronic energies of single and triplet wavefunctions at the same geometry, corresponding to a vertical excitation.

Figure 1.8). Such combination of electrons of two triplet centers affords a Schrock-type alkylidene.[48] Schrock-type alkylidenes were observed to exhibit nucleophilic properties in the presence of electrophiles such as acidic protons or carbonyl groups; however, *the philicity of a metal-carbon double bond does not necessarily define it as a Schrock-type alkylidene.*

On the other hand, the combination of a carbene in a singlet state due to the π-donating nature of the substituents at the carbon (for example, if R_1 = OMe) with a singlet metal center, results in the formation of a Fischer carbene complex,[49] which can be viewed as a Lewis acid/base complex. However, both the carbene and the metal center act simultaneously as Lewis acids and bases;[50] effectively, the metal-carbon bond for singlet carbene/singlet metal complex in Figure 1.8 can be viewed as comprising two Lewis acid/base interactions: AO_1(carbene)→AO_2(metal) (the carbene is a Lewis base and the metal is a Lewis acid), and AO_1(metal)→AO_2(carbene) (the metal is a Lewis base and the carbene is a Lewis acid).[51] The latter interaction is often referred to as metal to ligand π-back donation.

The combination of metal and ligand fragments affects the energies of the atomic orbitals (AOs) of the fragments, thus resulting in excited states of the fragments becoming the ground states and *vice versa*. The perturbations due to bond-formations have been addressed by means of energy decomposition analysis (EDA).[13] For example, perturbations may cause a metal center in the ground high-spin state to undergo a transition into an excited low-spin state due to the external field of a ligand (high field ligands in ligand-field theory), and thus the resulting metal-carbene could be viewed as a Fischer carbene complex with some character of a Schrock alkylidene. The reverse is also

---

(48) For a review on metal alkylidenes see: (a) Schrock, R. R. *Chem. Rev.* **2002**, *102*, 145-179. The first example of an isolated metal alkylidene: (b) Schrock, R. R. *J. Am. Chem. Soc.* **1975**, *97*, 6577-6578.

(49) Fischer, E. O.; Maasbol, A. *Angew. Chem. Int. Ed. Engl.* **1964**, *8*, 580-581.

(50) The simultaneous involvement of Lewis acidity and basicity in metal-ligand bonds is explained by Dewar-Chatt-Duncanson model: (a) Dewar, M. J. S. *Bull. Soc. Chim. Fr.* **1951**, *18*, C71-C79; (b) Chatt, J.; Duncanson, L. A. *J. Chem. Soc.* **1953**, 2939-2947.

(51) The view of bonding in Fischer carbenes as σ/π dative interaction has been supported by extensive theoretical studies involving high-level CASSCF calculations and was found to be accurate even for methylene Fischer carbenes: Marquez, A.; Fernandez Sanz, J. *J. Am. Chem. Soc.***1992**, *114*, 2903-2909.

Figure 1.8. Metal-Carbene Bond Formation

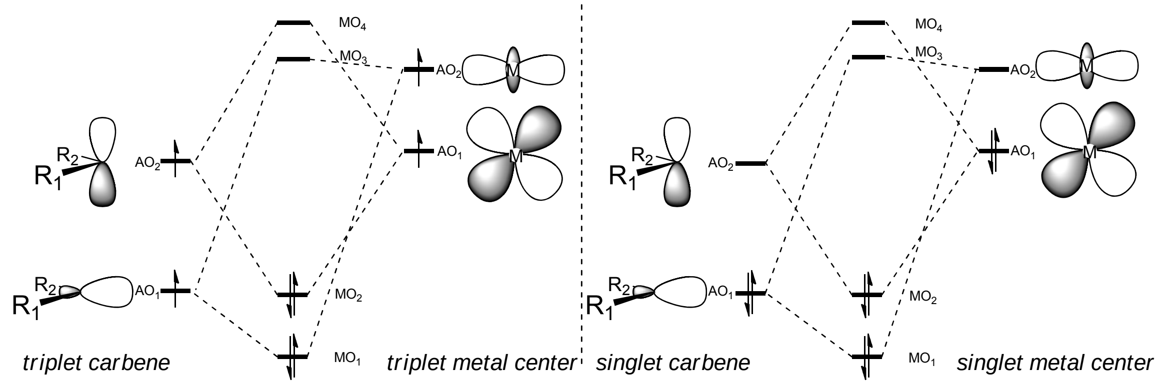
(a) *Schrock-type Alkylidene*

(b) *Fischer Carbene*

possible: the field of a low-spin transition metal center may cause an increase in $\Delta E(AO_2\text{-}AO_1)$ of the carbene such that the carbene would be viewed best as being in a singlet state within the complex.[52] The latter case is exemplified by Grubbs' olefin metathesis catalyst **GII**, which upon treatment with ethylene gas undergoes olefin metathesis to afford the corresponding Ru-methylene that due to the electrophilic character of the carbon atom traps PCy_3 (Scheme 1.1).[53]

Electrophilic character of a metal carbene is characteristic of a Fischer carbene; however, the ground electronic state of free methylene is triplet (*i.e.*, methylene would be expected to engage in bonding with a metal center to form a Schrock-type alkylidene). Thus, Ru-methylene carbene can be viewed as a combination of a low-spin Ru center and a triplet carbene, in which $\Delta E(AO_2\text{-}AO_1)$ was enhanced by the field of the singlet Ru

Scheme 1.1. Grubbs' Olefin Metathesis Catalysts as Fischer Carbenes

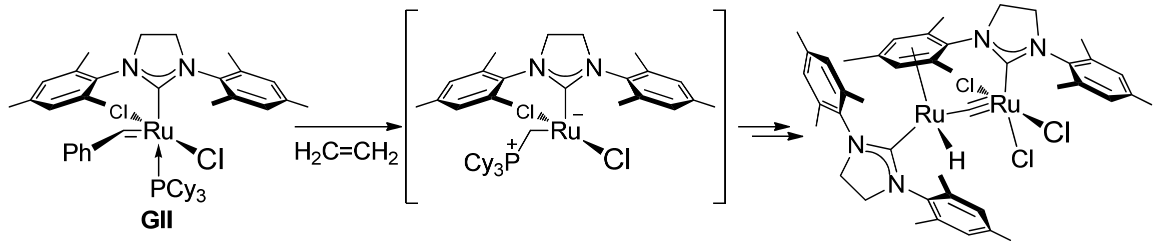

GII

---

(52) $\Delta E(AO_2\text{-}AO_1)$ of a singlet carbene can be referred to as a HOMO-LUMO gap and will be referred to as such henceforth; however, a HOMO and a LUMO should refer to local frontier MOs that have the largest coefficients on the NCN framework of the NHC, as either coefficients of the true HOMO or true LUMO may not be greatest for AOs of NCN framework in a global sense. For example, a NHC with a pendant carbanion is unlikely to have the greatest HOMO coefficients at the carbon atom of the NHC.

(53) Hong, S. H.; Wenzel, A. G.; Salguero, T. T.; Day, M. W.; Grubbs, R. H. *J. Am. Chem. Soc.* **2007**, *127*, 7961-7968.

center, thereby leading to the switch in methylene's ground state from triplet to singlet. Thus, it is appropriate to view Ru carbenes of olefin metathesis catalysts as Fischer carbenes with a minor contribution from the Schrock alkylidene character.

From the above discussion it is clear that the presence of π-electron donating substituents at the carbon center is not necessary to form Fischer carbenes, as the electronic structure of a carbene can be modulated by the metal itself, provided the $\Delta E(AO_2\text{-}AO_1)$ of the carbene is sufficiently small as is the case for methylene. In other words, the chemical space of metal carbenes is continuous between Fischer carbenes and Schrock alkylidenes rather than discrete with separate subspaces corresponding to the former and the latter. It should be noted that in most organometallic textbooks[54] the term Fischer carbene is used to describe a low oxidation state transition metal carbene complex with a heteroatom substituent at the carbon center, which exhibits electrophilic character, whereas the term Schrock alkylidene is used to describe a high oxidation state transition metal complex with alkyl groups or hydrogen atoms as substituents at the carbene center, which exhibits nucleophilic character. However, the oxidation state is a poor predictive criterion for the nature of a carbene, for example, the low oxidation state Os(II) complex $Os(=CH_2)(NO)(PPh_3)_2Cl$ exhibits nucleophilic character at the carbon center.[55] Thus, classification of metal carbenes as Fischer-type carbenes or Schrock-type alkylidenes should reflect the particular electronic character of a M=C bond in question.[56] The defining electronic properties of Schrock alkylidenes and Fischer carbenes are outlined in the discussion above. The unconventional classification of metal carbenes, based solely on the electronic states of the fragments presents advantages over the conventional scheme, which involves oxidation states and carbene substitution patterns, as it is more consistent with experimental and theoretical data.

As depicted in Scheme 1.1, **GII** contains two different carbenes: a NHC, which does not undergo olefin metathesis and remains coordinated to the metal center

---

(54) For example, see: Crabtree, R. H. *The Organometallic Chemistry of the Transition Metals*, 4th ed.; John Wiley & Sons, Inc.: Hoboken, NJ, 2005, pp. 310-311.

(55) Hill, A. F.; Roper, W. R.; Waters, J. M.; Wright, A. H. *J. Am. Chem. Soc.* **1983**, *105*, 5940-5942.

(56) Vyboischikov, S. F.; Frenking, G. *Chem. Eur. J.* **1998**, *4*, 1428-1438.

throughout the reaction, and a Fischer carbene with minor Schrock alkylidene character, which participates in the olefin metathesis process. Lack of the reactivity of the NHC in this case can be accounted for by the geometry of the reacting metal complex, but the electronic structure of this ligand plays a role in its lack of reactivity. The metal-NHC complex is of the Fischer carbene variety,[57] where, due to the large S-T gap of NHCs, an interaction between the singlet carbene and the singlet metal center is effectively the only bonding character that needs to be considered. For a detailed description of the electronic structure of NHC-metal bond, it is best that the π-system due to nitrogen atoms is explicitly included within the molecular orbital diagram rather than its effects are treated as perturbative interactions with the substituents (Figure 1.9).

Figure 1.9. NHC-Metal Bond Molecular Orbital Diagram

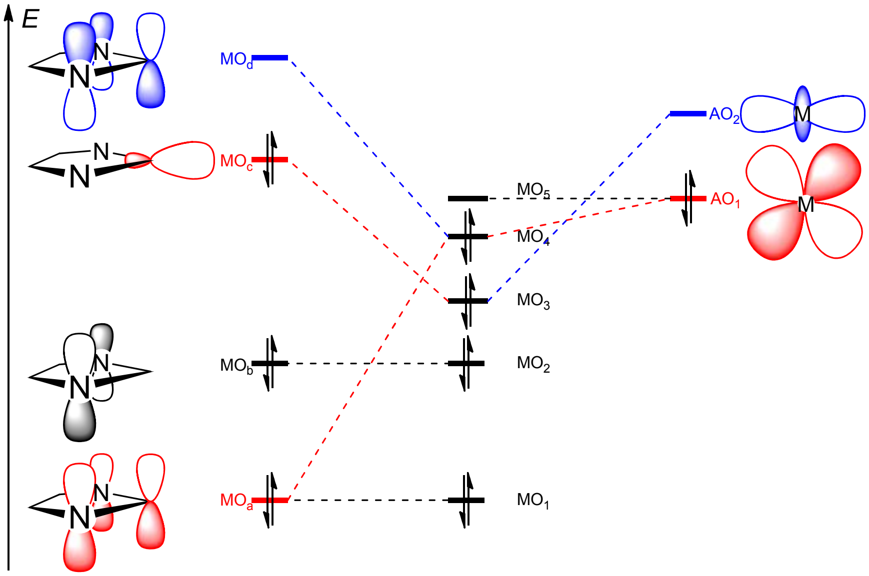

There are four main molecular orbitals (MO) to be considered for NCN fragment of the NHC (Figure 1.9); three of these MOs (MO$_a$, MO$_b$, and MO$_d$) correspond to the NCN π-system and MO$_c$ is the populated sp^2-hybrid orbital on the carbon atom (lone pair of the carbene). The possible donor orbitals are shown in red, the acceptor orbitals are shown in blue, and non-bonding orbitals are in black (Figure 1.9). Among these orbitals

---

(57) Heteroatom-substituted Ru-based Fischer carbenes are known to exhibit poor reactivity in olefin metathesis. Thus, it is reasonable to expect the doubly heteroatom-substituted Ru carbene to be unreactive in olefin metathesis, see: Adlhart, C.; Chen, P. *J. Am. Chem. Soc.* **2004**, *126*, 3496-3510.

MO_b does not match the symmetry of any proximal AO of the metal center and thus it does not contribute to metal-carbene bonding. Of the remaining MOs of the NHC fragment MO_a and MO_d are of appropriate symmetry to contribute to bonding with the metal center, provided the gap with AO_1 of the metal is sufficiently small. Thus, from the MO diagram three major interactions can be seen: (1) σ-donation from the NHC (MO_c) into the empty AO_2 of the metal to give MO_3; (2) π-donation from AO_1 of the metal into the empty MO_d to give MO_4; (3) if the gap between *empty* AO_1 and MO_a is sufficiently small MO_4 could result from the π-donation from NHC's MO_a into metal's AO_1.

The possible bonding scenarios for NHC-metal complexes are varied, as summarized in Figure 1.10.[58] If the gap between MO_a, MO_d and AO_1 is sufficiently large, MO_a and AO_1 become MO_1 and MO_5, respectively, *i.e.*, MO_1 and MO_5 do not contribute either productively or destructively towards the NHC-metal bond. Thus, within the interactions outlines in Figure 1.10, only σ-donation become significant. Indeed, NHCs have been argued to be pure σ-donors with no or negligible π-accepting ability. [28b] The above argument was largely justified by the fact that NHCs form relatively strong bonds with d^0 transition metals, as well as alkali, alkali-earth, and main group elements; in

Figure 1.10. Bonding Scenarios for NHC-Metal Complexes

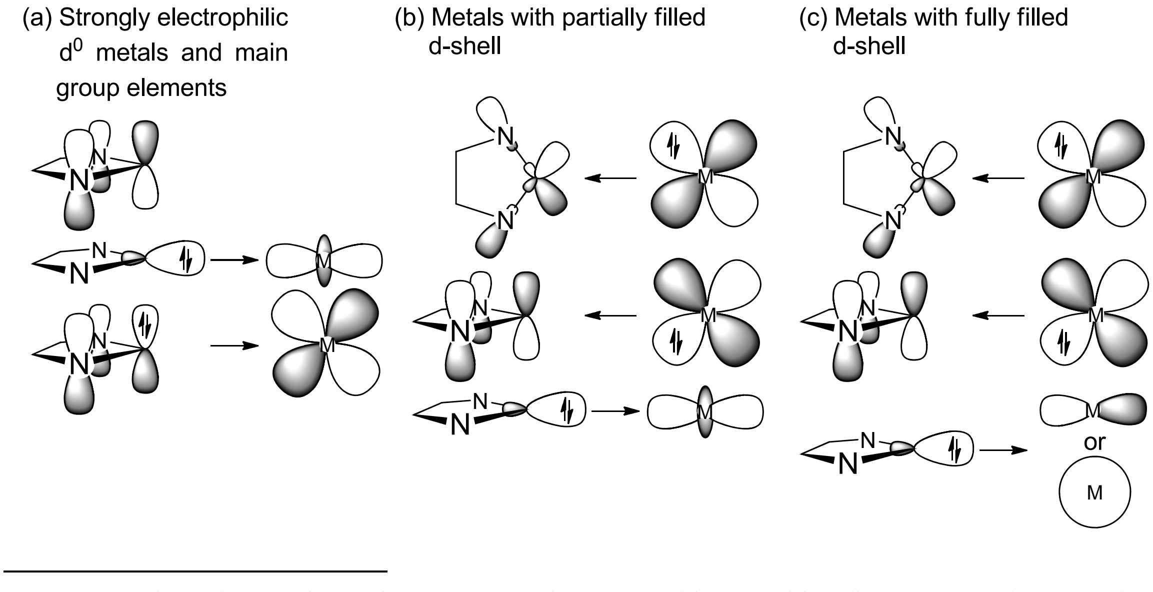
(a) Strongly electrophilic d^0 metals and main group elements

(b) Metals with partially filled d-shell

(c) Metals with fully filled d-shell

---

[58] For a review of stereoelectronic parameters of NHC-transition metal bonding, see: (a) Diéz-González, S.; Nolan, S. P. *Coord. Chem. Rev.* **2007**, *251*, 874-883; (b) Jacobsen, H.; Correa, A.; Poater, A.; Costabille, C.; Cavallo, L. *Coord. Chem. Rev.* **2009**, *253*, 687-703.

contrast phosphines, which are known for their relative π-accepting ability, do not form such complexes.[59] However, as early as 1994, Arduengo and co-workers invoked M→NHC π-donation to rationalize unusually short M-NHC bonds observed in X-ray crystal structures of the 14 electron Ni(0) and Pd(0) complexes and the chemical shifts of carbene carbons in ^{13}C NMR.[60] The significance of π-back donation had not been fully appreciated until a series of combined theoretical/experimental studies pointed out that π-back donation is qualitatively significant;[61] however, no attempts at quantification of this interaction were made.

Combined experimental and theoretical studies of relatively electron-poor complexes of Rh(III) and Ir(III), bearing NHC ligands, led Nolan and co-workers to propose π-donation from the NCN π-orbitals into the relevant *d*-orbitals of the metal centers (scenario (a) in Figure 1.10). The next section (1.1.2.5) summarizes attempts at distinguishing quantitatively between various bonding schemes that are illustrated in Figure 1.10.

---

(59) For examples of NHC complexes involving main group elements, see: (a) Arduengo, A. J. III; Rasika Dias, H. V.; Calabrese, J. C.; Davidson, F. *J. Am. Chem. Soc.* **1992**, *114*, 97259726; (b) Kuhn, N.; Henkel, G.; Kratz, T.; Kreutzberg, J.; Boese, R.; Maulitz, A. H. *Chem. Ber.* **1993**, *126*, 2041-2045; (c) Kuhn, N.; Kratz, T.; Bläser, Boese, R. *Chem. Ber.* **1995**, *128*, 245-250; (d) Li, X. W.; Su, J.; Robinson, G. H. *Chem. Commun.* **1996**, 2683-2684; (e) Nakai, H.; Tang, Y.; Gantzel, P.; Meyer, K. *Chem. Commun.* **2003**, 24-25; (d) Lee, Y.; Li, B.; Hoveyda, A. H. *J. Am. Chem. Soc.* **2009**, *131*, 11625-11633. For examples of alkali metal-NHC complex see: (f) Alder, R. W.; Blake, M. E.; Bortolotti, C.; Bufali, S.; Butts, C. P.; Linehan, E.; Oliva, J. M.; Orpen, A. G.; Quayle, M. J. *Chem. Commun.* **1999**, 241-242; (g) Wang, Y.; Xie, Y.; Abraham, M. Y.; Wei, P.; Schaefer, H. F. III; Schleyer, P. v. R.; Robinson, G. H. *J. Am. Chem. Soc.* **2010**, *132*, 14370-14372. For examples of alkali-earth metal-NHC complexes see: (h) Arduengo, A. J. III; Rasika Dias, H. V.; Davidson, F.; Harlow, R. W. *J. Organomet. Chem.* **1993**, *462*, 13-18; (i) Herrmann, W. A.; Runte, O.; Artus, G. *J. Organomet. Chem.* **1995**, *501*, C1-C4; (j) Arduengo, A. J. III; Davidson, F.; Krafczyk, R.; Marshall, W. J.; Tamm, M. *Organometallics* **1998**, *17*, 3375-3382; (k) Schumann, H.; Gottfriedsen, J.; Glanz, M.; Dechert, S.; Demtschuk, J. *J. Organomet. Chem.* **2001**, *617*, 588-600. For examples of NHC complexes of lanthanides see: (l) Arduengo, A. J. III; Tamm, M.; McLain, S. J.; Calabrese, J. C.; Davidson, F.; Marshall, W. J. *J. Am. Chem. Soc.* **1994**, *116*, 7927-7928; (m) Schumann, H.; Glanz, M.; Winterfeld, J.; Hemling, H.; Kuhn, N.; Kratz, T. *Angew. Chem. Int. Ed. Engl.* **1994**, *33*, 1733-1734. For examples of d^0 transition metal-NHC complexes see: (n) Niehues, M.; Erker, G.; Kehr, G.; Schwab, P.; Frohlich, R. *Organometallics* **2002**, *21*, 2905-2911; (o) Abernethy, C. D.; Codd, G. M.; Spicer, M. D.; Taylor, M. K. *J. Am. Chem. Soc.* **2003**, *125*, 1128-1129.

(60) Arduengo, A. J. III; Gamper, S. F.; Calabrese, J. C.; Davidson, F. *J. Am. Chem. Soc.* **1994**, *116*, 4391-4394.

(61) (a) Tulloch, A. A. D.; Danopoulos, A. A.; Kleinhenz, S.; Light, M. E.; Hursthouse, M. B.; Eastham, G. *Organometallics* **2001**, *20*, 2027-2031; (b) Garrison, J. C.; Simons, R. S.; Kofron, W. G.; Tessier, C. A.; Youngs, W. J. *Chem. Commun.* **2001**, 1780-1781; (c) ; (d) Hu, X.; Tang, Y.; Gantzel, P.; Meyer, K. *Organometallics* **2003**, *22*, 612-614.

1.1.2.5. Carbenes as π-Acceptors and Donors

To date all the attempts at quantifying the contributions of σ,π-interactions in metal-NHC complexes have been focused on application of energy decomposition analysis (EDA) to the problem. As the orbital interaction ΔE_{oi} can be divided into contributions due to each irreducible representation Γ within the overall symmetry of the molecule, contributions due to σ-donation, π-donation, and π-back donation can be obtained.

Among the first attempts at a quantitative analysis of σ,π-interactions in transition metal-NHC complexes was that of Pyykkö and Runeberg.[62] Comparison of L-AuCl systems demonstrated that the interaction between PMe_3 and AuCl fragments is qualitatively similar to that between IMe and AuCl; in both cases, electrostatic interactions (ΔE_{el}) accounted for 72-75% of the attractive interaction energies. The remaining orbital interaction energies (ΔE_{oi}) were further divided into σ- and π-contributions for model systems, where Me groups were replaced with H atoms. It was found that π-contribution for PH_3 is slightly larger than that for imidazolylidene (33% for PH_3 vs. 28% for imidazolylidene). It should be noted, however, that the charge of AuCl fragment (from Hirshfeld population analysis[21]) is more negative for imidazolylidene-AuCl than for H_3PAuCl (-0.1041 *vs*. -0.0864) in the systems where σ,π-contributions were evaluated. In contrast, AuCl fragment charge in Me_3PAuCl is more negative than in IMe-AuCl (-0.1414 vs -0.1184). Thus, it is possible that the π-back donation from Au center into $\sigma^*_{\mathrm{P\text{-}H}}$ is more pronounced, resulting in an inflated value for π-contributions in H_3PAuCl.

Systematic analysis of the ligand effect on the electronic structure of the metal center was undertaken by Frenking and co-workers in 2006.[63] The study encompassed d^0 (L-MCl_4, M = Ti, Zr, Hf), d^6 (L-$M(CO)_5$, M = Cr, Mo, W), d^8 (L-$M(CO)_4$, M = Fe, Ru,

---

[62] Pyykkö, P.; Runeberg, N. *Chem. Asian J.* **2006**, *1*, 623-628.

[63] For the studies of NHC-transition metal complexes, see: (a) Tonner, R.; Heydenrych, G.; Frenking, G. *Chem. Asian. J.* **2007**, *2*, 1555-1567. For the studies of phosphine-transition metal complexes see: (b) Frenking, G.; Wichmann, K.; Fröhlich, N.; Grobe, J.; Golla, W.; Le Van, D.; Krebs, B.; Läge, M. *Organometallics* **2002**, *21*, 2921-2930.

Os), and d^{10} (L-MCl, M = Cu, Ag, Au) transition metals. Consistent with the studies outlined above, it was found the electrostatic interactions (ΔE_{el}) account for 66-78% of the attractive interactions. The importance of the electrostatic interactions was directly correlated to the d-electron count, increasing from Ti (66%) to Cu (77%), which is indicative of the more pronounced covalent character of the NHC-Ti bond than that of the NHC-Cu bond.[64] Within each triad the contribution of electrostatic interactions to bonding increases with the exception of Cu-Ag-Au triad, where due to the relativistic contraction of the Au atom the orbital interactions play a more important role than in the corresponding complexes of Ag.[65] Of the orbital interactions (ΔE_{oi}) π-contributions account for 13% (Ti) – 27% (Cu). However, the nature of π-interactions differs significantly between the transition metals of different d-electron counts. For d^0 metals $\pi_{M\rightarrow NHC}$ (-4.0 kcal/mol) are of the same magnitude as $\pi_{NHC\rightarrow M}$ (-3.5 kcal/mol). The former interaction is likely due to deformation of the core electron density of the metal, whereas the latter is due to the overlap between MO_a of NHC (Figure 1.9) and the corresponding empty d-orbital of the metal center. As the d-electron count increases the $\pi_{NHC\rightarrow M}$ diminishes in its magnitude, reaching a low of -0.9 kcal/mol for Ag. However, the $\pi_{M\rightarrow NHC}$ increases in its magnitude to a high of -11.5 kcal/mol for Cu – 91% of the π-interaction, which accounts for 27% of the orbital interaction energy (ΔE_{oi}). Due to C_{2v}-symmetry of d^{10} transition metal complexes L-M-Cl it was possible to separate the σ-contribution term into $\sigma(a_1)$ and $\pi_{||}(b_2)$ interactions, where the former term accounts for the $\sigma_{NHC\rightarrow M}$ donation, while the latter term accounts for the backbonding from d_π into $\sigma^*_{C\text{-}N(NHC)}$. It was found that the relative contribution of the $\pi_{||}$ interaction (11.0% of ΔE_{oi}) is significantly smaller than that of the $\sigma_{NHC\rightarrow M}$ interaction (62.3% of ΔE_{oi}). The results for d^{10} transition metal NHC complexes are summarized in Table 1.2. Thus, the total

---

(64) The interpretation of ΔE_{el} as contribution due to ionic character of the bond may not be entirely accurate, despite its popular use. Since ΔE_{el} is calculated from the frozen charge density distribution, the effects of charge polarization (and charge transfer, depending on the employed definition of an atom) are absorbed entirely by ΔE_{oi}, which, given the conditions above, is often employed to assess the percentage of the covalent character. It is entirely plausible that valence bond-theoretic wavefunctions offer a more accurate assessment of bond covalency.

(65) For a review on relativistic effects, see: Pyykkö, P. *Chem. Rev.* **1988**, *88*, 563-594.

contribution due to π-interactions is actually higher when $\pi_{||}$ contribution is separated from $\sigma_{\mathrm{NHC}\rightarrow\mathrm{M}}$.

Table 1.2. Results of EDA for IMe-M-Cl Complexes (M = Cu, Ag, Au)[a]

	IMe-CuCl	IMe-AgCl	IMe-AuCl
$\Delta E_{\mathrm{int}} = \mathrm{BE}_{\mathrm{snap}}$	-68.6	-53.9	-77.4
$\Delta E_{\mathrm{Pauli}}$	124.4	129.6	210.4
ΔE_{el}	-148.1 [76.7][b]	-143.0 [77.9][b]	-217.1 [75.4][b]
ΔE_{oi}	-44.9 [23.3][b]	-40.6 [22.1][b]	-70.7 [24.6][b]
ΔE_{σ} (a_1)	-28.0 (62.3)[c]	-29.1 (71.7)[c]	-50.9 (72.0)[c]
$\Delta E_{\pi\perp}$ (b_1)[d]	-11.9 (26.5)[c]	-7.5 (18.5)[c]	-13.0 (18.4)[c]
$\Delta E_{\pi\|\|}$ (b_2)	-5.0 (11.0)[c]	-3.8 (9.3)[c]	-6.5 (9.2)[c]
ΔE_{Prep}	0.7	0.5	1.0
ΔE = -*BDE*	-67.9	-53.4	-76.4

[a] Energies are in kcal/mol; [b] The values in square brackets are the percentage contribution to the total attractive interactions; [c] The values in parantheses are the percentage contribution to the orbital interactions energy ΔE_{oi}; [d] The $\pi_{\perp}$ contribution is the sum of $\pi_{\mathrm{M}\rightarrow\mathrm{NHC}}$ and $\pi_{\mathrm{NHC}\rightarrow\mathrm{M}}$ interactions.

Frenking and co-workers also compared the EDA data for NHC d^6-metal complexes to that for phosphine d^6-metal complexes (L-M(CO)$_5$, M = Cr, Mo, W, L = PMe$_3$, IMe) and found that orbital interaction contributions is higher (35-39%) for the phosphine-based complexes than those that carry NHC ligands (29-34%); that is, these researchers established that the P-metal bond might be more covalent than the C-metal bond.[63,64] Furthermore, π-contributions for the phosphine complexes (26-28%) were higher than for NHC complexes (17-19%). However, as stated above, the $\pi_{||}$ contributions for complexes that bear NHC ligands are absorbed in σ-interactions and cannot be separated; proper assessment of π- vs σ-contributions is therefore incomplete. On the basis of the discussion above and consistent with other reports, Frenking concluded that

NHCs are stronger σ-donors and weaker π-acceptors than phosphines.[28b,66] It is, nevertheless, noteworthy that for d^{10} NHC-metal complexes, where all π-contributions were separated from σ-contributions, the total withdrawing π-interactions account for *a third* of orbital interaction energies (34.5% of ΔE_{oi}).

The systematic study by Jacobsen and co-workers[67] of NHC-metal bonding preceded the work of Frenking and his team; nonetheless, the former study does not mention the in-plane $\pi_{||}$ interactions, and as a result π-interactions are included within the σ-contribution to ΔE_{oi}. Overall, the data of Frenking on π-contributions is similar to that of Jacobsen. The latter found that in some NHC-metal complexes π-contributions can be as high as 25% of ΔE_{oi} (for imidazolylidene-Ni(C_2H_4)$_2$). A systematic study involving imidazolinylidenes has not been disclosed to date; these saturated NHCs (imidazolinylidenes) have been implicated qualitatively as stronger π-acidic ligands than unsaturated variants (imidazolylidenes).[68]

A detailed analysis of NHC-metal and phosphine-metal complexes is outlined in the next section. The purpose of this investigation is to identify the similarities and differences in ligand-metal bonding by means of QTAIM. In particular, our aim is an understanding of the effect that an NHC can impart on a bound metal through electronic polarization and charge transfer and not by energies contributing to the stability of the NHC-metal complexes, which were accomplished previously[63,67] with all the caveats associated with EDA.[64]

---

(66) (a) Lappert, M. F. *J. Organomet. Chem.* **1988**, *358*, 185-214; (b) Öfele, K.; Herrmann, W. A.; Mihailos, D.; Elison, M.; Herdtweck, E.; Scherer, W.; Mink, J. *J. Organomet. Chem.* **1993**, *459*, 177-184. For a review comparing NHCs to phosphines see: (c) Crabtree, R. H. *J. Organomet. Chem.* **2005**, *690*, 5451-5457.

(67) Jacobsen, H.; Correa, A.; Costabille, C.; Cavallo, L. *J. Organomet. Chem.* **2006**, *691*, 4350-4358.

(68) Fantasia, S.; Petersen, J. L.; Jacobsen, H.; Cavallo, L.; Nolan, S. P. *Organometallics* **2007**, *26*, 5880-5889.

1.2. Electronic Effects in the Bonding of N-Heterocyclic Carbenes and Phosphines with Transition Metals: A Comparative Study

It is often assumed that *N*-heterocyclic carbenes are stronger electron donors than phosphines. To a large extent this assumption has been promulgated due to the comparison of the Tolman electronic parameter (TEP) of NHCs to that of phosphines.[69] Although – somewhat simple and crude in nature – the TEP electron donating ability metric has proved useful in rationalization of the behavior of several systems.[70] The origins of TEP can be traced back to the fact that "… phosphorus ligands can be ranked in a *π-acceptor strength* series which is generally valid for a wide variety of monosubstituted metal carbonyls".[40,71,72] Indeed, the π-acceptor strength of an ancillary ligand is assessed directly from the observed change in the experimental IR stretch of a carbonyl group bound to the metal center (Figure 1.11). However, σ-donating ability of an ancillary ligand *cannot be measured directly* from the IR stretching frequency of the carbonyl ligand, as the primary effect of a more electron-rich σ-framework does not have a direct effect on the strength of CO bond within the carbonyl ligand; the higher electron density at the metal center resulting in higher-lying populated *d*-orbitals of a metal center has a secondary effect on the IR stretch of the carbonyl group in a metal carbonyl complex. It should be noted, however, that TEP can be used for quantification of *a net electron donating ability of an ancillary ligand if the σ-donating ability remains constant* within a set of ligands under study, as π-donating/back donating effects due to the said ancillary ligand are varied. Although TEP can be viewed as a first-order approximation metric of the net electron donating ability of a ligand, characterization of the ligand-metal bonding and identification of various electronic factors contributing to bonding is a compelling objective, as these factors may play different roles in structure

---

(69) Kelly, R. A. III; Clavier, H.; Giudice, S.; Scott, N. M.; Stevens, E. D.; Bordner, J.; Samardjiev, I.; Hoff, C. D.; Cavallo, L.; Nolan, S. P. *Organometallics* **2008**, *27*, 202-210.

(70) For some of the early examples, see: (a) Collman, J. P. *Acc. Chem. Res.* **1968**, *1*, 136-143; (b) Montelatici, S.; van der Ent, A.; Osborn, J. A.; Wilkinson, G. *J. Chem. Soc. A* **1968**, 1054-1058.

(71) Strohmeier, W.; Müller, F. J. *Chem. Ber.* **1967**, *100*, 2812-2821.

(72) Tolman, C. *J. Am. Chem. Soc.* **1970**, *92*, 2953-2956.

Figure 1.11. Interactions of the Donor/Acceptor Ligand Orbitals with those of a Transition Metal Center affecting the IR Stretching Frequencies of Carbonyl Ligands

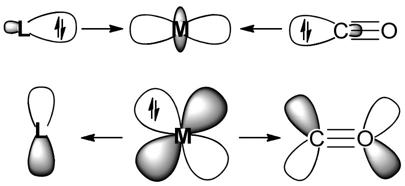

(a) σ-donation from L → weaker donation from CO
→ no effect on CO bond → ***no effect on IR(CO) stretching frequency***

(b) π-acidic L → weaker backdonation into π(CO)
→ weaker CO bond → ***lower IR(CO) stretching frequency***

activity/selectivity relationship studies, thereby leading to a more rational approach to ligand design.

Assessment of the electronic effects due to the ancillary ligand-metal bond, in principle, should be achieved by comparison of the electronic structure of the free ligand to that of the ligand-metal complex. Thus, the study presented herein was designed around the middle to late transition-metal complexes (Chart 1.1), the electronic structure of which is examined within the confines of the quantum theory of atoms in molecules (see section 1.1.1.1 for the brief introduction to QTAIM).

The complexes depicted in Chart 1.1 were selected for the study to represent low oxidation state medium to late transition metals. The model ligands IMe, SIMe, and PMe_3 were chosen as reasonable representatives of their respective classes. The inclusion of the metal carbonyl complexes is beneficial in two respects: (1) carbonyls are high field ligands[73] and thus the resulting metal complexes are expected to be in a *singlet* ground state (or in another accessible low-spin state), thereby allowing for direct comparison of the data across all of the complexes; (2) calculated IR stretching frequencies of carbonyl ligands can be compared to the QTAIM data, which might allow for determination of the physical basis for TEP. It should be noted that the 5d transition metals were excluded from the present study, due to the fact that relativistic effects become non-negligible and

---

(73) In ligand field theory, spectrochemical series provides an empirical method for ordering ligands according to their respective field strength, allowing for identification of high and low field ligands. Ligation of a ligand results in reduction of symmetry away from spherical symmetry, thereby leading to splitting of otherwise degenerate *d*-orbitals of a metal center. Thus, ligands, coordination of which to a metal center results in high splitting energy between the *d*-orbitals, are called high field ligands.

thus either explicit (relativistic Hamiltonian)[74] or implicit (relativistic effective core potential)[75] treatment of these effects is required.

Chart 1.1. The Transition Metal Complexes Investigated in the Current Study

				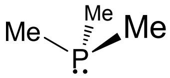
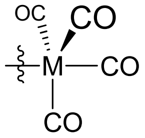	**M = Fe**	**1.1i**	**1.1s**	**1.1p**
	M = Ru	**1.4i**	**1.4s**	**1.4p**
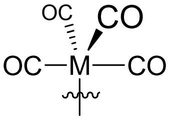	**M = Ru**	**1.5i**	**1.5s**	**1.5p**
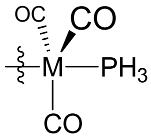	**M = Fe**	**1.2i**	**1.2s**	**1.2p**
	M = Ru	**1.6i**	**1.6s**	**1.6p**
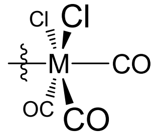	**M = Fe**	**1.3i**	**1.3s**	**1.3p**
	M = Ru	**1.7i**	**1.7s**	**1.7p**
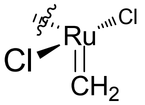		**1.8i**	**1.8s**	**1.8p**
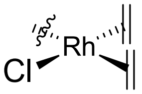		**1.9i**	**1.9s**	**1.9p**
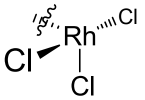		**1.10i**	**1.10s**	**1.10p**
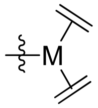	**M = Ni**	**1.11i**	**1.11s**	**1.11p**
	M = Pd	**1.12i**	**1.12s**	**1.12p**
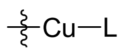	**L = H**	**1.13i**	**1.13s**	**1.13p**
	L = Me	**1.14i**	**1.14s**	**1.14p**
	L = CN	**1.15i**	**1.15s**	**1.15p**
	L = F	**1.16i**	**1.16s**	**1.16p**
	L = Cl	**1.17i**	**1.17s**	**1.17p**
	L = Br	**1.18i**	**1.18s**	**1.18p**
	L = I	**1.19i**	**1.19s**	**1.19p**

---

(74) Quantum theory of atoms in molecules (QTAIM) was only recently extended to analyze relativistic wavefunctions. See: Bader, R. F. W. *J. Phys. Chem. A* **2007**, *111*, 7966-7972.

(75) Wavefunctions including effective core potentials cannot be analyzed with the currently available software packages.

1.2.1. Analysis of the Geometries and Vibrational Frequencies of the Transition Metal Complexes

Comparison of experimental or calculated bond lengths in transition metal complexes is a useful technique for estimating the relative strengths of metal-ligand bonds. Thus, comparison of C_{NHC}-M bond lengths between **1.1i-1.19i** (1.980 ± 0.090Å)[76] and **1.1s-1.19s** (1.986 ± 0.088Å) reveals that the expected BDE(SIMe-M) is expected to be higher than BDE(IMe-M) in their respective complexes. Indeed, Nolan and co-workers found C_{NHC}-M bonds are shorter for imidazolinylidenes than that for imidazolylidenes, and in concert the experimental BDEs for imidazolinylidenes are higher than those for imidazolylidenes.[77] Although, comparison of M-L data from above to **1.1p-1.19p** is not possible, it should be noted that phosphines metal complexes exhibit relatively lower BDEs for phosphine dissociation than for NHC dissociation.[63]

Another key structural attribute of NHC ligands is the C_{NHC}-N bond length, which can be correlated to the degree of π-acidity of imidazolinylidenes; relatively short C_{NHC}-N bond lengths indicate a higher bond order and thus a less π-acidic NHC ligand. However, comparison between C_{NHC}-N bond lengths of imidazolylidenes and imidazolinylidenes to estimate their relative π-acidities is not consistent with both theoretical and experimental observations.[68]

Additional structural information can be gained from the analysis of calculated vibrational spectra; in particular, the C-O stretching frequencies may be utilized to determine Tolman electronic parameter (TEP) for ancillary ligands. Analysis of calculated vibrational spectra of complexes **1.1i-1.7i**, **1.1s-1.7s**, and **1.1p-1.7p** reveals that the average C-O stretching frequencies for IMe-bearing metal-carbonyl complexes (2123.9 ± 65.2 cm^{-1}) are indicative of a more pronounced back donation into π^*(CO) than

---

(76) The standard deviations provided along with the calculated values denote *the spread of the values of a particular metric* and not the uncertainty due to calculations.

(77) The systems investigated include Cp*Ru(L)Cl (a) and $LNi(CO)_2$ (b). See: (a) Hillier, A. C.; Sommer, W. J.; Yong, B. S.; Petersen, J. L.; Cavallo, L.; Nolan, S. P. *Organometallics* **2003**, *22*, 4322-4326; (b) Dorta, R.; Stevens, E. D.; Scott, N. M.; Costabile, C.; Cavallo, L.; Hoff, C. D. Nolan, S. P. *J. Am. Chem. Soc.* **2005**, *127*, 2485-2495.

in the case of SIMe-bearing (2125.4 ± 64.7 cm^{-1}) or PMe$_3$-bearing (2130.6 ± 63.8 cm^{-1}) variants.[76] This observation is in concert with the TEP values for the respective ligands.[78]

1.2.2. QTAIM Analysis of the Free Ligands

It is convenient first to consider the electronic structure of free ligands. The electronic structure data is summarized in Table 1.3.

Table 1.3. Results of QTAIM Analysis of Free Ligands[a]

	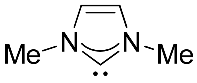 **IMe**	 **SIMe**		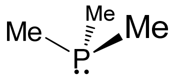 **PMe$_3$**
(a) Charges				
$q(C_{NHC})$	0.756	0.902	$q(P)$	1.660
$q(N)$	-1.299	-1.258		
$q(C_{NHC}\vert N)$	0.378	0.451	$q(P\vert C)$	0.554
(b) Localization and Delocalization Indices				
$\lambda(C_{NHC})$[b]	4.133	4.002	$\lambda(P)$[b]	12.161
$\lambda(N)$[b]	6.675	6.677	$\lambda(C)$[b]	4.876
$\Sigma\delta(C_{NHC},N)$[c]	1.9208	1.9401	$\Sigma\delta(P,C)$[c]	2.1178
$\Sigma\delta(C_{NHC},C_{backbone})$[c]	0.1291	0.0722		
(c) Bond Critical Point				
$\rho^{BCP}(C_{NHC}\vert N)$	0.3085	0.3242	$\rho^{BCP}(P\vert C)$	0.1559
$\nabla^2\rho^{BCP}(C_{NHC}\vert N)$	-0.5661	-0.6967	$\nabla^2\rho^{BCP}(P\vert C)$	-0.1263
$\vert\lambda_1\vert/\lambda_3\ (C_{NHC}\vert N)$[d]	0.926	1.055	$\vert\lambda_1\vert/\lambda_3\ (P\vert C)$[d]	0.784
$\varepsilon(C_{NHC}\vert N)$[e]	0.0151	0.107	$\varepsilon(P\vert C)$[e]	0.1333

[a] All values are in atomic units (a.u.). [b] $\lambda(\Omega)$ - atomic localization index: total number of electrons that are fully localized on the atom. [c] $\delta(\Omega,\Lambda)$ - delocalization index: total number of electrons shared between atoms Ω and Λ. The data shown in the table is the sum of all $\delta(\Omega,\Lambda)$ of the same class, for example $\delta(C_{NHC},N)_{IMe} = 0.9604$, there are two C_{NHC}-N bonds and thus $\Sigma\delta(C_{NHC},N) = 1.9208$. [d] $\vert\lambda_1\vert/\lambda_3$ measures the charge concentration in the plane bisecting the bond, $\vert\lambda_1\vert/\lambda_3 > 1$ for most shared interactions (covalent bonds). [e] ε - ellipticity.

---

(78) TEP values for SIMe and IMe are 2054.7 and 2054.1, respectively. See: (a) Gusev, D. G. *Organometallics* **2009**, *28*, 6458-6461. TEP value for PMe$_3$ is 2064.1, see: Ref. 70.

As shown in Table 1.3 the partial atomic charge of the carbene carbon q(C_{NHC}) in IMe is lower than that of SIMe, similarly the localization index λ(C_{NHC}) is higher for the carbene carbon atoms in IMe than in SIMe.[79] The localization index for carbene carbon atoms is consistent with the divalent carbon centers in the formal oxidation C(II). Comparison of the partial atomic charges of nitrogen atoms of IMe and SIMe (q(N)) reveals that IMe bears a relatively more electron rich NCN framework than SIMe. It is worth noting that the bond index δ(C_{NHC},N) is greater for SIMe than for IMe, and the contributions of the interatomic surface (C_{NHC}|N) to the net charge of C_{NHC} are greater for the former than the latter, *i.e.* $q(C_{NHC}|N)_{SIMe} > q(C_{NHC}|N)_{IMe}$. The combination of these values points to the fact that the C-N bond in SIMe is stronger and more polarized than in IMe, which is consistent with the observed C-N bond lengths ($r(\text{C-N})_{IMe}$ = 1.361Å, $r(\text{C-N})_{SIMe}$ = 1.343Å).

Among the sources of the electron density for the NCN framework, the backbone carbon atoms play an important role as evidenced by the greater values of the delocalization index between C_{NHC} and the backbone carbon atoms ($\Sigma\delta(C_{NHC},C_{backbone})$).[80] Within the IMe ligand C_{NHC} is capable of accepting electron density from backbone carbons through the π-system, whereas within the SIMe ligand only σ-framework is available for the delocalization of the electron density.

The phosphine ligand cannot be directly compared to the NHCs; however, a few relevant observations can be made regarding the electronic structure of PMe_3. The phosphorus center bears a significant positive charge as evidenced by q(P) = 1.660 a.u. The localization index λ(P) is consistent with P(III) oxidation state. Thus, PMe_3 despite its high positive charge at the P-center is still capable of acting as a Lewis base. Nonetheless, Lewis basicity of PMe_3 is likely to be limited by the necessity for the

---

(79) Localization index $\lambda(\Omega)$ for an atom Ω is defined as a number of electrons that can be fully localized within the atomic boundaries of the atom Ω. Higher values of the localization index $\lambda(\Omega)$ indicate that the atom Ω is electron rich and likely exists in a low oxidation state.

(80) Delocalization index $\delta(\Omega,\Lambda)$ is defined as a number of electrons that are shared between atoms Ω and Λ. Higher values of $\delta(\Omega,\Lambda)$ are indicative of a stronger shared interaction. In cases when the atoms Ω and Λ are connected by a bonding path $\delta(\Omega,\Lambda)$ is referred to as *bond index*, and *it is directly related to the bond order* and the degree of *covalency* of a bond.

Figure 1.12. Contour Maps of ρ and $\nabla^2\rho$ of the Ligands

(a) ρ of IMe (b) ρ of SIMe

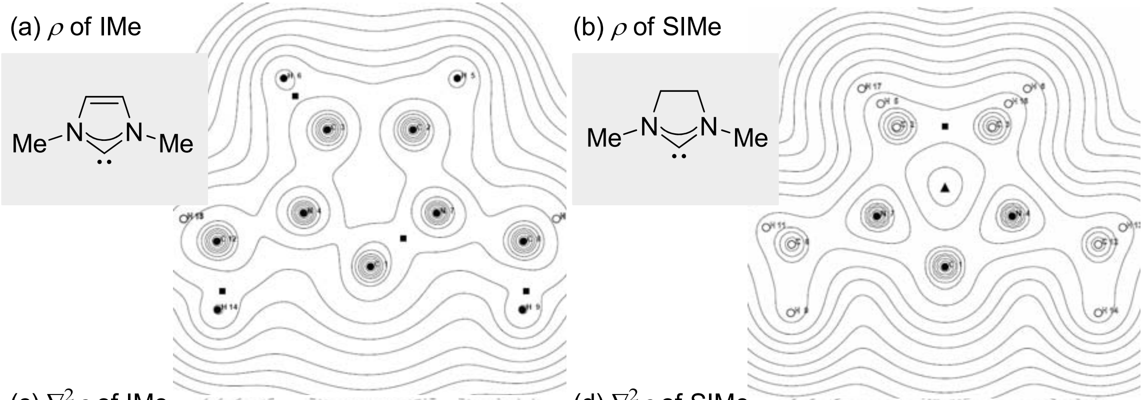

(c) $\nabla^2\rho$ of IMe (d) $\nabla^2\rho$ of SIMe

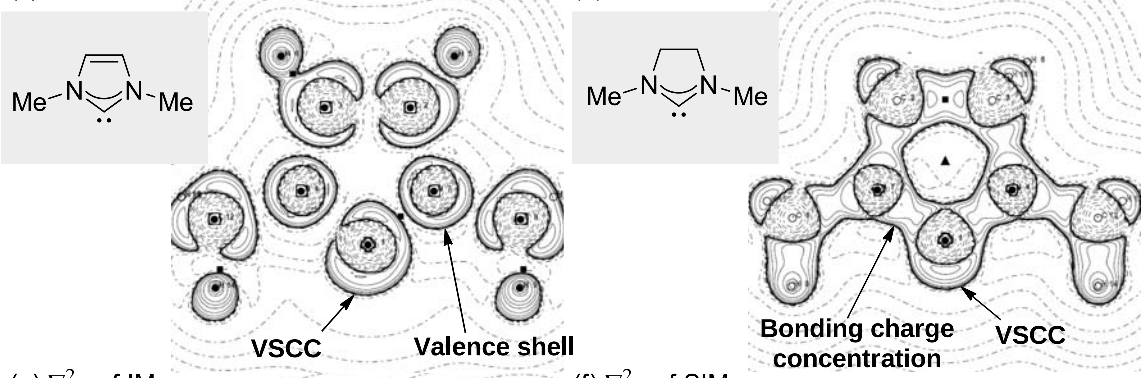

(e) $\nabla^2\rho$ of IMe (f) $\nabla^2\rho$ of SIMe

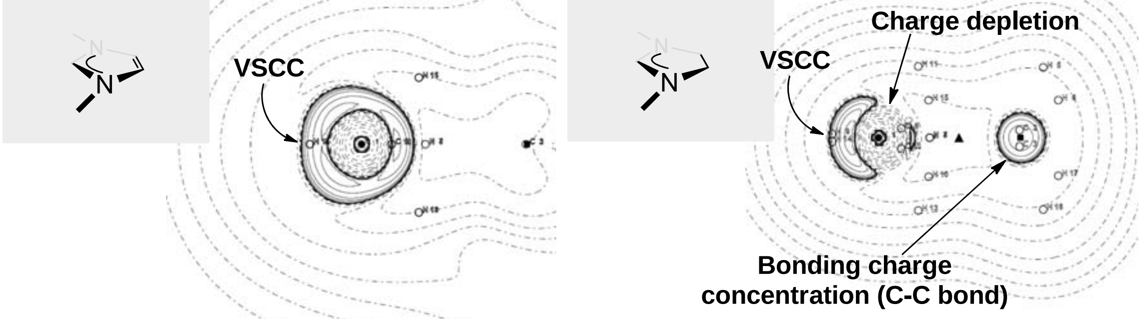

(g) $\nabla^2\rho$ of IMe (h) $\nabla^2\rho$ of SIMe

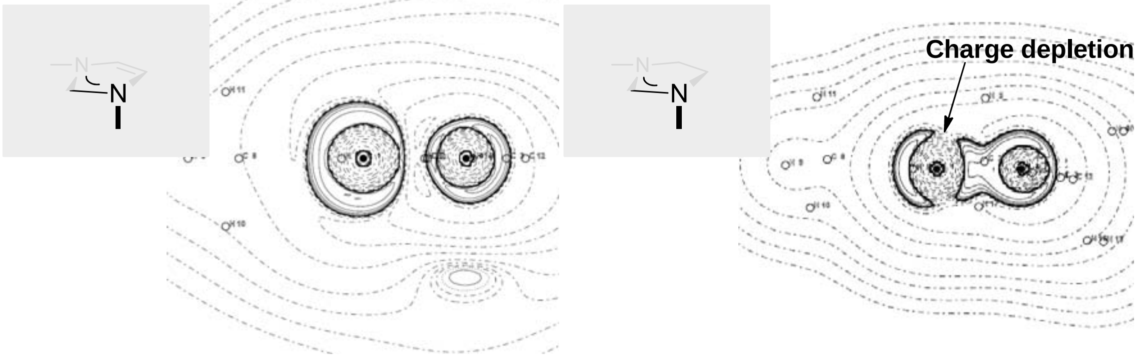

significant charge separation due to the donation from P-center into a metal.

The bonding patterns within NHCs differ significantly as shown in Figure 1.12. Particularly revealing are the contour maps of $\nabla^2\rho$ of IMe and SIMe. For example, the valence shells of the carbon and nitrogen atoms are isolated in IMe, whereas in SIMe they form a continuous ring with clear presence of areas of *bonding charge concentration* (cf. (c) and(d) in Figure 1.12). This observation is consistent with numeric data for *bond critical points* BCP($C_{NHC}|N$): as shown in Table 1.2 electron density $\rho^{BCP}(C_{NHC}|N)_{SIMe}$ is greater than $\rho^{BCP}(C_{NHC}|N)_{IMe}$ (0.3242 and 0.3085, respectively). Furthermore, $\nabla^2\rho^{BCP}(C_{NHC}|N)_{SIMe}$ is more negative than $\nabla^2\rho^{BCP}(C_{NHC}|N)_{IMe}$ (-0.6967 and -0.5661, respectively) indicating higher negative curvature in electron density at BCP of the former than of the latter; in other words charge accumulation at BCP$(C_{NHC}|N)_{SIMe}$ is greater than at BCP$(C_{NHC}|N)_{IMe}$. Thus, the electron density within 5-membered ring of IMe is more diffuse in π-direction, whereas that of SIMe is more concentrated within the σ-framework. Due to the benefit of higher charge density at C_{NHC} of IMe, it bears a larger region of *valence shell charge concentration* (VSCC) than C_{NHC} of SIMe, thereby leading to an expectation that IMe is a stronger σ-donor than SIMe. Furthermore, C_{NHC} of IMe is expected to be a weaker π-acceptor than SIMe as the valence shell of C_{NHC}(IMe) is continuous, whereas areas of *charge depletion* can be found on C_{NHC}(SIMe) (cf. (e) and (f) in Figure 1.12). The C_{NHC}-N bond of IMe bond does not exhibit strong polarization of the N atom towards C_{NHC}(IMe), whereas N is strongly polarized towards C_{NHC}(SIMe) (cf. (g) and (h) in Figure 1.12). Thus, the absence of areas of charge depletion on C_{NHC}(IMe) is due to the presence of the π-bond on the backbone, which allows for the formation of a cyclic π-system with 6 electrons. On the other hand, strong polarization of the N(SIMe) atoms towards C_{NHC}(SIMe) is indicative of the dominating $p_N \rightarrow p_{C(NHC)}$ interaction, which is not sufficient to eliminate the area of charge depletion.

Overall, solely based on the analysis of free NHC ligands IMe is expected to be a stronger σ-donor than SIMe, while the latter is expected to be a stronger π-acceptor. Because the π-effects have a more pronounced effect on carbonyl stretching frequencies as discussed above, TEP values for saturated NHCs are expected to be higher than for unsaturated NHCs. Indeed, the stronger σ-donation of unsaturated NHCs may not play a significant role in the observed differences in TEPs for unsaturated *vs* saturated NHCs.

The contour maps of the electron density and the laplacian of electron density for PMe_3 are shown in Figure 1.13. As expected the molecule of PMe_3 bears a valence shell charge concentration corresponding to the lone pair at the P atom. Additionally there's a bond charge concentration for each P-C bond; the charge concentrations of valence shells are not diffuse and thus the P-C bond is covalent despite significant charge transfer from P to each C atom (q(P|C) = 0.554). However, formation of the P-C bond requires the overlap between n=2 shell orbitals of the P atom and n=1 shell of carbon atoms and thus accumulation of the electron density at BCP(P|C) is smaller (ρ^{BCP}(P|C) = 0.1559 and $\nabla^2\rho^{BCP}$(P|C) = -0.1263) than what is observed for C-N bonds described above.

Figure 1.13. Contour Maps of ρ and $\nabla^2\rho$ of PMe_3

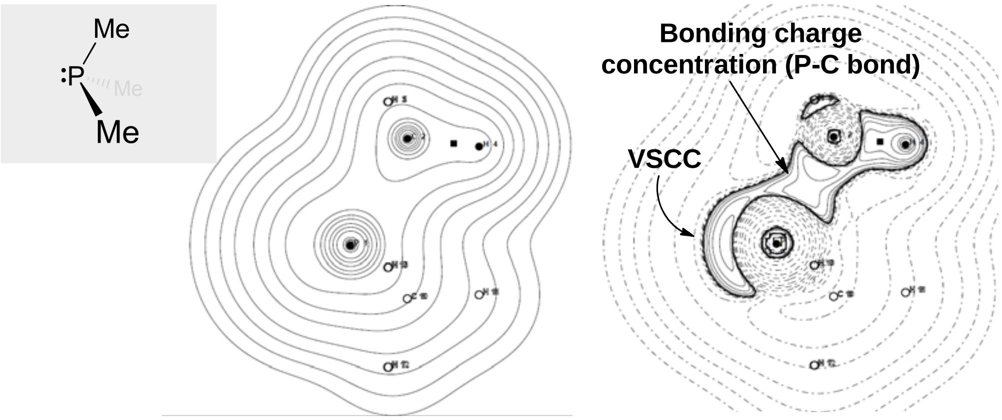
(a) ρ of PMe_3

(b) $\nabla^2\rho$ of PMe_3

1.2.3. QTAIM Analysis of the Transition Metal Complexes of N-Heterocyclic Carbenes and Trimethylphosphine

1.2.3.1. Multipoles and Electrostatic Interaction Energies

The multipolar expansion of charge allows for approximation of charge distribution by means of expansion into monopole, dipole, quadrupole, octapole, etc. moments. The monopole moment is commonly referred to as a net charge, and for an atom it is a partial atomic charge. Atomic monopoles or partial atomic charges can be utilized to gain understanding of net charge transfers within a molecule. For example, the sum of partial atomic charges of a ligand is necessarily equal to the negative of the sum of partial atomic charges of the metal center and the remaining ligands, thus the net charge transfer from a ligand to the metal can be estimated. The table 1.4 provides the charges of the donor ligands (IMe, SIMe, PMe_3) for all the transition metal complexes under investigation. As shown in Table 1.4 the most donating ligand is PMe_3, followed by SIMe and IMe, respectively, as judged by the q(Ligand) values; the mean q(Ligand)

Table 1.4. QTAIM Charges

							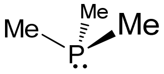		
	q(M)^a	q(IMe)^b	q(L_n)^c	q(M)^a	q(SIMe)^b	q(L_n)^c	q(M)^a	q(PMe_3)^b	q(L_n)^c
1.1	0.073	0.301	-0.375	0.052	0.298	-0.354	-0.135	0.466	-0.330
1.2	-0.068	0.281	-0.213	-0.085	0.274	-0.190	-0.321	0.471	-0.150
1.3	0.908	0.347	-1.257	0.895	0.380	-1.275	0.752	0.485	-1.238
1.4	0.758	0.273	-1.031	0.751	0.269	-1.021	0.625	0.389	-1.015
1.5	0.777	0.220	-0.997	0.773	0.216	-0.989	0.641	0.268	-0.908
1.6	0.562	0.269	-0.830	0.560	0.262	-0.822	0.420	0.393	-0.813
1.7	1.009	0.366	-1.375	0.992	0.378	-1.370	0.872	0.491	-1.363
1.8	0.818	0.428	-1.247	0.808	0.409	-1.216	0.599	0.630	-1.229
1.9	0.536	0.327	-0.863	0.531	0.328	-0.860	0.408	0.389	-0.796
1.10	0.748	0.451	-1.200	0.737	0.635	-1.373	0.561	0.830	-1.390
1.11	0.298	0.181	-0.476	0.235	0.180	-0.416	0.201	0.233	-0.433
1.12	0.304	0.162	-0.466	0.305	0.154	-0.458	0.215	0.193	-0.406
1.13	0.276	0.177	-0.451	0.282	0.169	-0.452	0.223	0.209	-0.432
1.14	0.330	0.171	-0.499	0.334	0.164	-0.499	0.266	0.206	-0.472
1.15	0.469	0.226	-0.694	0.472	0.222	-0.694	0.409	0.271	-0.680
1.16	0.576	0.216	-0.792	0.581	0.211	-0.792	0.509	0.274	-0.783
1.17	0.478	0.224	-0.702	0.481	0.220	-0.701	0.412	0.275	-0.686
1.18	0.432	0.227	-0.659	0.435	0.222	-0.658	0.365	0.275	-0.640
1.19	0.357	0.225	-0.582	0.360	0.221	-0.581	0.289	0.270	-0.559
Mean^d:	0.507	0.267	-0.774	0.500	0.274	-0.775	0.385	0.369	-0.754
Median^d:	0.478	0.227	-0.702	0.481	0.222	-0.701	0.409	0.227	-0.686
σ^e:	0.282	0.085	0.335	0.284	0.115	0.355	0.286	0.165	0.361
Skewness^f:	-0.107	0.780	-0.274	-0.184	1.703	-0.313	-0.725	1.262	-0.351

[a] q(M) - Charge of the metal center. [b] q(Ligand) - Total charge of the donor ligand (IMe, SIMe, or PMe_3) in the field of the molecule. [c] q(L_n) - Total charge of the ligands on the metal center, excluding the donor ligand (IMe, SIMe, PMe_3). [d] The average (mean and median) of all the values in the column for a given property of a given ligand. [e] The standard deviation of the set of values for a given property of a given ligand. [f] Skewness measures the degree of distortion of a normal distribution curve. Negative values of skewness are indicative of a larger tail of the response curve in the negative direction with respect to the mean along the input variable dimension.

values for IMe, SIMe, and PMe_3 are 0.369, 0.274, and 0.267, respectively. It is also necessary to examine the median values of q(Ligand), which indicate that PMe_3 and IMe are equally strong net electron donors; however, skewness of the sample reveals that the data for IMe is significantly less skewed in the positive direction than PMe_3. Thus, although PMe_3 and IMe are equally strong charge donors, the former is capable of higher charge donation in cases of electron-poor metals than the latter. Furthermore, positive skewness of SIMe is larger than that of either IMe of PMe_3, indicating the greater relative capability of SIMe for charge donation to electron-poor transition metals. Thus, it is possible to classify the three ligands as soft Lewis bases and order them according to their Lewis basic softness (SIMe>PMe_3>IMe).[81]

The standard deviations derived for each one of the average values allows for graphic comparison of the net charge donorability of the ligands. Assuming the complexes in Chart 1.1 represent a sample of a larger set of middle to late transition metal complexes, the averages and the standard deviations in Table 1.4 can be used to derive an analytical normal distribution (Gaussian curve).[82] As shown in Figure 1.14, such curves were derived for the current set of organometallic complexes to describe the relative net electron donorability of the ligands (a), total charge at the metal center (b), total charge of the ligands at the metal center (c), excluding the donor ligand (IMe, SIMe, PMe_3). Additionally, as a metric of polarization between the metal and the ligands the normal distributions of the magnitude of the difference between q(M) and $q(L_n)$[83] values is given in Figure 1.14(d).

---

[81] Although the commonly used term is nucleophilic softness, it implies kinetic aspect of the electron density availability. As the classification of the ligands presumes thermodynamic electron density availability (thermodynamic stability of a ligand with respect to withdrawal of charge density), and thus it is appropriate to introduce the term *Lewis basic softness*. The Lewis basic softness should be thought of within the confines of the thermodynamic counterpart to the Hard/Soft Acid/Base (HSAB) theory of Pearson: (a) Pearson, R. G. *J. Am. Chem. Soc.* **1963**, *85*, 3533-3539; (b) Pearson, R. G. *Science* **1966**, *151*, 172-177.

[82] Note that the curves provided are normal distributions, whereas the sample data indicates that the distribution is skew-normal (γ-distribution). Thus, the charts in Figures 1.14 and 1.15 provide average (mean) information but make no distinction between the relative propensities for increased/decreased donation as a function of the transition metal's electron deficiency outside the confines of the set examined herein.

[83] $q(L_n)$ is defined as the sum of atomic charges on ligands bound to the metal center with the exception of the donor ligands, electron donating abilities of which are being studied (IMe, SIMe, PMe_3).

Figure 1.14. Normal Distributions of Partial Atomic Charges

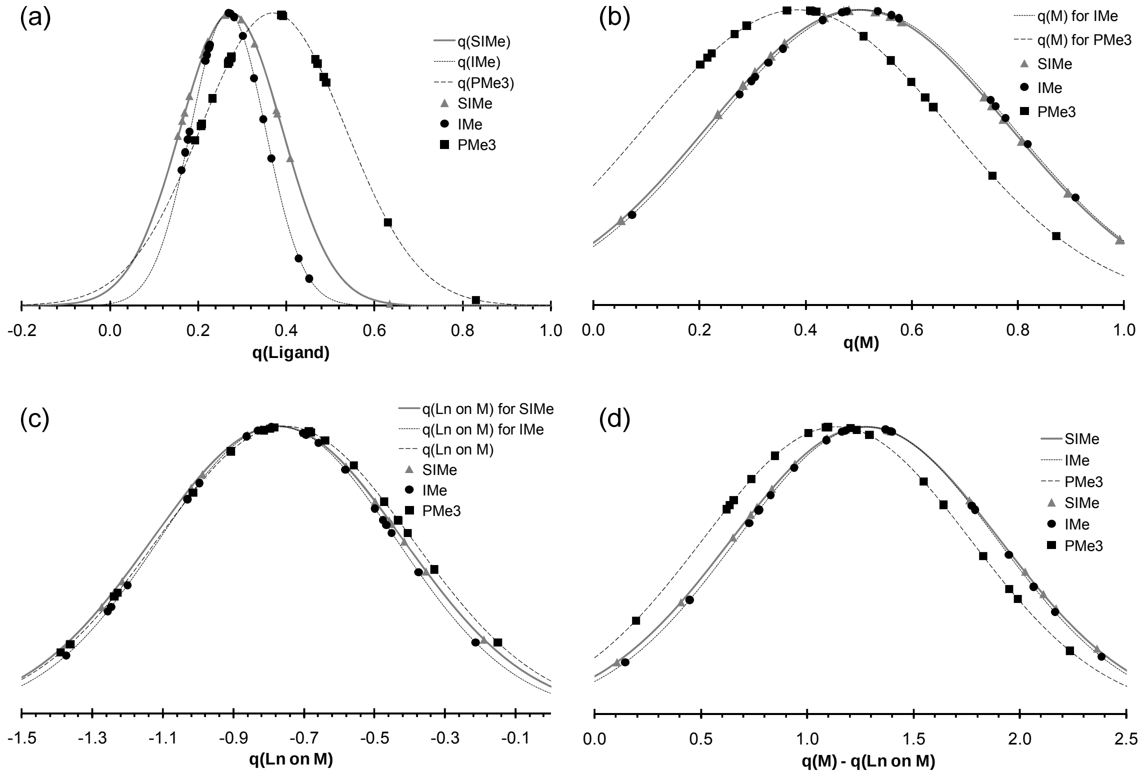

As mentioned above PMe_3 is a stronger net charge donor than the SIMe and IMe, which are very similar in their net average electron donating ability. However, the Gaussian curve for SIMe is wider than that for IMe, indicating the relatively softer nature of SIMe. On the other hand, PMe_3 is addition to exhibiting a superior electron donating ability is the softest ligand among the three shown above. Indeed, this observation holds with other population analyses (Mulliken Population Analysis (MPA)[16a], Atomic Polar Tensor (APT)[16g]), but is contested by Hirshfeld Population Analysis (HPA)[21] (Figure 1.15, the markers were removed for clarity). The results of MPA analysis are inconsistent with the observation that NHCs and phosphines are net electron donors, as the results put NHCs as net electron acceptors. Overall, the Hirshfeld scheme for partitioning molecules into atoms seems to be more consistent with Tolman electronic parameters; however, within Hirshfeld scheme the atoms are not open quantum systems and thus many electronic parameters are not accessible.

Figure 1.15. Normal Distributions of Partial Atomic Charges of Ligands

(a) QTAIM

(b) Atomic Polar Tensor

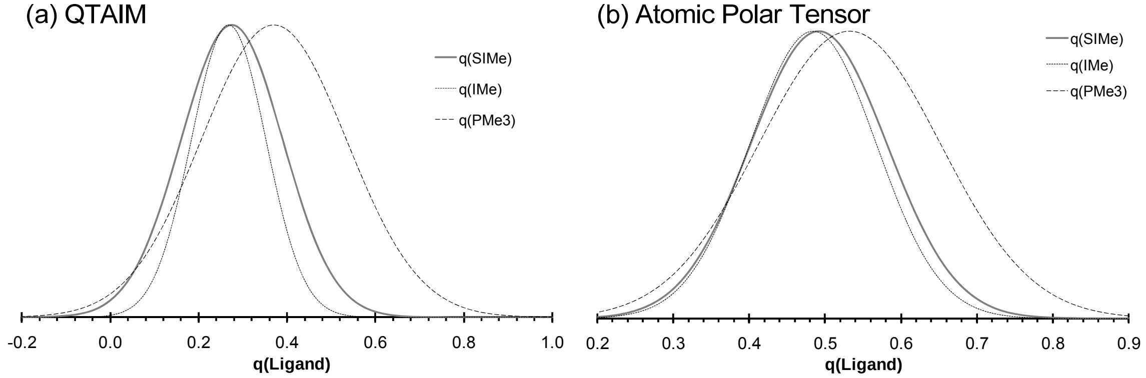

(c) Hirshfeld Population Analysis

(d) Mulliken Population Analysis

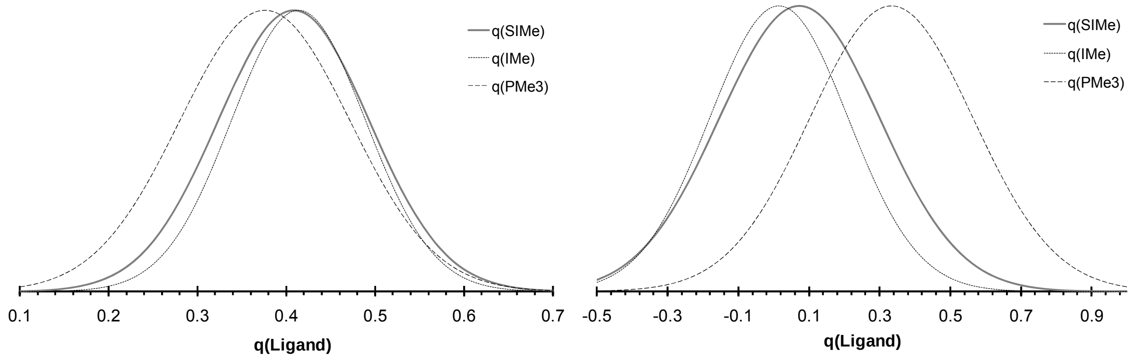

Further analysis of the QTAIM electron charge reveals that a metal center bearing PMe_3 bears a relatively smaller positive charge than the one bearing either SIMe or IMe (Figure 1.14(b)). However, despite the superior net electron donating ability of PMe_3 the sum of atomic charges on ligands $q(L_n)$ remains essentially unchanged; indeed, $q(L_n)$ is slightly more negative on average for SIMe (-0.775) and IMe (-0.774) (Figure 1.14(c)). In other words, the charge separation is greater in the NHC-transition metal complexes than in phosphine-transition metal complexes; the difference between q(M) and $q(L_n)$ for SIMe (1.275) and IMe (1.281) is greater than that for PMe_3 (1.139).

In order to understand the difference in polarization between phosphine-transition metal complexes and NHC-transition metal complexes the electrostatic interaction energies $V_{en}(\Omega,\Lambda)$[84] between the electron density of a metal atom and the nucleus of an atom that is directly bound to it were investigated. However, to compare the values for

---

(84) $V_{en}(\Omega,\Lambda)$ – electrostatic interaction energy between the electron density of the atom Ω and the nucleus of the atom Λ. The negative values of $V_{en}(\Omega,\Lambda)$ are indicative of attractive interactions.

$V_{en}(\Omega,\Lambda)$ across different metals (Ω = Fe, Ru, Rh, Ni, Pd, Cu) the values for $V_{en}(\Omega,\Lambda)$ were weighted by the respective atomic electronic populations of the metal centers.

As shown in Table 1.5, the electrostatic interaction energy per electron of the transition metal atom $V_{en}(\Omega,\Lambda)/N(\Omega)$ is almost twice as large for PMe_3 as that for IMe or SIMe. This interaction energy weighted per proton of the nucleus of the donor atom is lower in magnitude for PMe_3, albeit insignificantly. Thus, the electron density of the P atom is not sufficient for efficient shielding of the P nucleus. Indeed, the net average charge of the P atom within complexed PMe_3 is 1.964 ± 0.137, whereas the net average charges of the C atoms of IMe and SIMe within the same complexes are 0.832 ± 0.061 and 0.967 ± 0.137. Thus, the large excess positive charge of the P atom exerts a stronger attractive force on the electron density of the metal atom. The resulting intraatomic polarization can be assessed by means of the dipolar polarization of the metal atom.

Table 1.5. Mean Electrostatic Interaction Energies[a]

			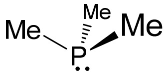
$V_{en}(\Omega,\Lambda)$	-54.149 ± 11.626	-54.902 ± 11.865	-114.159 ± 29.666
$V_{en}(\Omega,\Lambda)/ N(\Omega)$	-1.602 ± 0.064	-1.607 ± 0.065	-3.455 ± 0.463
$V_{en}(\Omega,\Lambda)/ [N(\Omega)\cdot Z(\Lambda)]$[b]	-0.268 ± 0.011	-0.267 ± 0.011	-0.230 ± 0.031

[a] All values are in a.u. Atoms Ω are those of the transition metals. Atoms Λ are those of the ligands directly attached to the transition metal (C_{NHC} of SIMe or IMe, P of PMe_3). The values are averages (mean) across the set of transition metal complexes with standard deviations, indicating the spread of single data points. [b] $V_{en}(\Omega,\Lambda)/[N(\Omega)\cdot Z(\Lambda)]$ - provides the measurement of the electrostatic interaction energy per electron of the atom Ω per proton of the nucleus of Λ.

1.2.3.2. Atomic Dipole and Quadrupole Moments of the Metal Atoms

Following the analysis of monopole moments (atomic charges) it is necessary to consider atomic dipole moments. The magnitude of the atomic dipole moment $|\boldsymbol{\mu}(\Omega)|$ provides the magnitude of a vector $\boldsymbol{\mu}(\Omega)$ that can be divided into its contributing parts $\boldsymbol{\mu}_x(\Omega)\mathbf{x} + \boldsymbol{\mu}_y(\Omega)\mathbf{y} + \boldsymbol{\mu}_z(\Omega)\mathbf{z}$ (**x**, **y**, and **z** are unit vectors along x, y, and z axes, respectively). For the purpose of the following discussion $\boldsymbol{\mu}_z(\Omega)$ will refer to the dipole moment vector along the M-L axis (L = IMe, SIMe, PMe_3) with negative values indicating polarization in the direction of the L ligand and positive value indicating polarization in the direction away from the L ligand. Within QTAIM atomic dipole moments $\boldsymbol{\mu}(\Omega)$ are further partitioned into the intraatomic dipolar polarization $\boldsymbol{\mu}_{\mathbf{intra}}(\Omega)$ and the polarization due to bonding $\boldsymbol{\mu}_{\mathbf{bond}}(\Omega)$.[85] The intraatomic dipole moment $\boldsymbol{\mu}_{\mathbf{intra}}(\Omega)$ provides the measurement of dipolar polarization of the electron density within the atom Ω. The bonding dipole moment $\boldsymbol{\mu}_{\mathbf{bond}}(\Omega)$ furnishes the metric for the dipolar polarization of the atom Ω due to charge transfer between Ω and other atoms bonded to it, as indicated by the presence of IASs and bond paths. The bonding dipole moment can be separated further into contributions from each bonding interaction between atoms Ω and Λ ($\boldsymbol{\mu}_{\mathbf{bond}}(\Omega|\Lambda)$).

The total atomic dipole moments of the metal atoms $|\boldsymbol{\mu}(\mathrm{M})|$ in complexes of $\mathrm{PMe_3}$ are very similar to those of SIMe and IMe. However, $|\boldsymbol{\mu}_{\mathbf{intra}}(\mathrm{M})|$ and $|\boldsymbol{\mu}_{\mathbf{bond}}(\mathrm{M})|$ values are greater for $\mathrm{PMe_3}$-metal complexes (see supporting information for details). As stated above the charge transfer from $\mathrm{PMe_3}$ ligand to the metal center is greater than that from NHC ligands, thus the $|\boldsymbol{\mu}_{\mathbf{bond}}(\mathrm{M})|$ values are also greater for $\mathrm{PMe_3}$-metal complexes; however, there's an opposing intraatomic polarization within the metal atom that results in a net $|\boldsymbol{\mu}(\mathrm{M})|$ being similar for all complexes within each triad (L-M, L = IMe, SIMe, $\mathrm{PMe_3}$). To assess the effect of the ligands on the dipolar polarization of the metal center along the M-L axis $\boldsymbol{\mu}_{\mathbf{z}}(\mathrm{M})$ values were examined (Table 1.6).[86]

As shown in Table 1.6 the total atomic dipolar polarizations along the z-axis $\boldsymbol{\mu}_{\mathbf{z}}(\mathrm{M})$ vary for all the metal complexes without a discernible pattern. The large positive values of $\boldsymbol{\mu}_{\mathbf{bond\_z}}(\mathrm{M})$ are indicative of a significant charge transfer from the donor ligand to the metal center; the magnitude of the values for the metal center decreases with respect to the ligands in the following order $\mathrm{PMe_3}$>IMe>SIMe. The magnitude of the

---

(85) The division of dipole moment $\boldsymbol{\mu}(\Omega)$ into intraatomic and bonding parts allowed for explanation of the seemingly counterintuitive dipole moment of carbon monoxide, wherein the vector is pointing from O atom to C atom, despite the fact that carbon is in low oxidation state C(II). Within QTAIM, there's a large $\boldsymbol{\mu}_{\mathbf{bond}}(\mathrm{C,O})$ pointing in the direction of O atom; however, there's a larger opposing intraatomic polarization due to significant accumulation of the positive charge on C atom. For the full explanation see: Ref. 10.

(86) The data for compound **1.5** was excluded from the study due to difficulties in calculating some interatomic surfaces, and as a result measures requiring integration of all atoms within a molecule are not available.

Table 1.6. Dipolar Polarization of the Metal Centers in Complexes of IMe, SIMe, and PMe_3[a]

	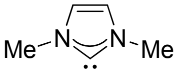						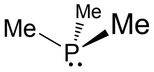		
	μ_z(M)	μ_{bond_z}(M)	μ_{intra_z}(M)	μ_z(M)	μ_{bond_z}(M)	μ_{intra_z}(M)	μ_z(M)	μ_{bond_z}(M)	μ_{intra_z}(M)
1.1	0.660	0.687	-0.027	0.729	0.758	-0.029	1.096	1.372	-0.276
1.2	-0.045	-0.294	0.249	0.004	-0.241	0.244	0.412	0.428	-0.016
1.3	0.132	0.168	-0.035	0.119	0.191	-0.071	0.302	0.508	-0.206
1.4	0.351	0.350	0.001	0.405	0.412	-0.007	0.905	1.131	-0.225
1.6	0.166	-0.426	0.260	-0.118	-0.364	0.246	0.393	0.393	0.000
1.7	0.099	0.101	-0.002	0.113	0.149	-0.036	0.331	0.534	-0.203
1.8	0.056	0.309	-0.253	0.203	0.539	-0.336	1.003	1.669	-0.665
1.9	0.638	0.597	0.042	0.608	0.571	0.037	0.532	0.768	-0.236
1.10	1.229	1.524	-0.295	0.319	0.559	-0.240	1.461	2.054	-0.593
1.11	0.676	0.638	0.039	0.651	0.592	0.058	0.513	0.731	-0.218
1.12	0.727	0.744	-0.017	0.696	0.721	-0.026	0.510	0.770	-0.261
1.13	1.336	1.127	0.209	1.312	1.118	0.194	1.226	1.184	0.042
1.14	1.212	1.202	0.010	1.188	1.191	-0.003	1.089	1.252	-0.163
1.15	1.560	1.613	-0.053	1.541	1.606	-0.065	1.476	1.714	-0.237
1.16	1.294	1.676	-0.382	1.269	1.664	-0.396	1.218	1.805	-0.588
1.17	1.468	1.661	-0.192	1.446	1.651	-0.205	1.383	1.765	-0.382
1.18	1.528	1.640	-0.113	1.506	1.631	-0.125	1.436	1.735	-0.299
1.19	1.573	1.558	0.016	1.551	1.548	0.003	1.472	1.633	-0.161

[a] All values are in atomic units. In all cases the dipolar polarization of electron density of a metal atom is measured with negative values indicating polarization towards to the ligand (IMe, SIMe, or PMe_3).

contribution of C_{NHC} or P atoms to the bonding dipolar polarization was obtained from $|\boldsymbol{\mu}_{\mathbf{bond}}(M|\Lambda)|$ values (where $\Lambda = C_{NHC}$ for IMe and SIMe, or Λ = P for PMe_3) and proved consistent with the statement above (see supporting information for details). The order of $\boldsymbol{\mu}_{\mathbf{bond\_z}}$(M) values was consistent with net charge transfer as assessed by q(M) and q(Ligand) (see section 1.2.3.1).

The intraatomic dipolar polarizations of the metal atoms are indicative of stronger polarization of the electron density of the metal atom towards the P atom of PMe_3 than towards then C_{NHC} atom of either IMe or SIMe. In fact the values of $\boldsymbol{\mu}_{\mathbf{intra\_z}}$(M) for PMe_3-bound metal centers are negative for all complexes with the exception of **1.6p** and **1.13p**. The former case the metal center is bound to the PH_3 ligand, which is in competition with PMe_3 in polarizing the electron density of Ru atom towards the P atom of PH_3. It is worth a note that complex **1.2p** is slightly polarized towards PMe_3 over PH_3, indicating that electronic properties of the phosphine ligands depend on the metal center in question.

Within the complex **1.13p** the electron density of the Cu atom is polarized towards H atom over P atom of PMe_3 as indicated by the small positive $\boldsymbol{\mu}_{\mathbf{intra\_z}}$(Cu) = 0.042. The charge transfer between Cu and H atoms is insufficient to insulate the electron density of the Cu atom from the strong attractive field due to the proton of H, which exceeds that due to the P nucleus.

Figure 1.16. Normal Distributions of $\mu_{\mathrm{intra\_z}}$(M)

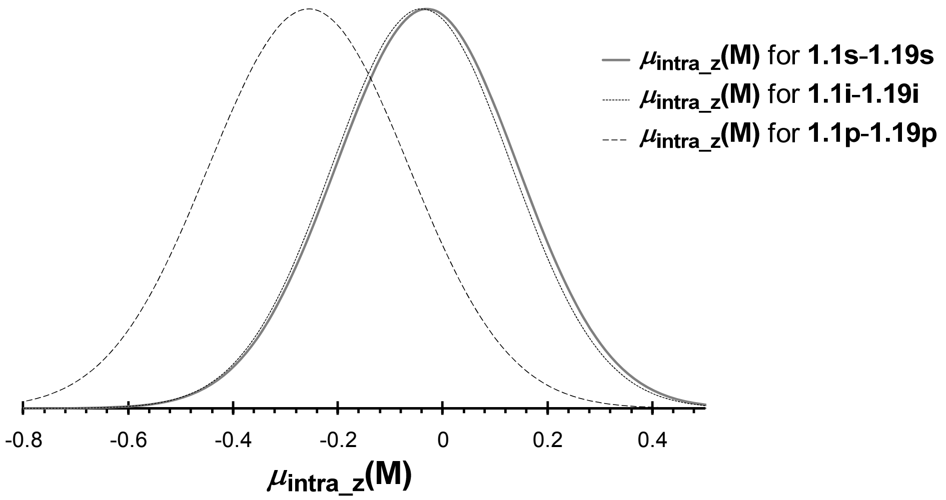

To appreciate fully the difference in the intraatomic dipolar polarizations of the metal atoms between the complexes of PMe_3 and those of NHCs, it is convenient to visualize $\boldsymbol{\mu}_{\mathbf{intra\_z}}$(M) as a Gaussian curve (Figure 1.16).[87] Indeed, the intraatomic dipolar polarization of a metal atom due to PMe_3 is significantly stronger than that of NHCs; the mean value for the latter is found more than a standard deviation to the right of the mean value for the former.

As hypothesized above, the strong intraatomic dipolar polarization of metal atoms of phosphine complexes can be explained within QTAIM by considering the attraction of electron density of the metal center towards the P nucleus, which is poorly shielded by the electron density of the P atom due to higher positive atomic charge. However, the origins of this polarization can be viewed in the framework of MO theory as resulting from stronger π-back donation in phosphines than in NHCs. Analysis of quadrupolar

---

(87) The Gaussian curves were constructed as described in section 1.2.3.1.

interactions allows recovering the π-back donation interactions observed in MO theoretic treatment of NHCs and phosphines.[88] Unfortunately, presence of ligands in the plane orthogonal to M-L bond does not allow for meaningful analysis of atomic quadrupolar moments for the metal centers; however, the complexes **1.13i-1.19i**, **1.13s-1.19s**, and **1.13p-1.19p** have linear divalent Cu atoms, and thus these complexes are analyzed further. The Table 1.7 summarizes all primary components ($\mathbf{Q_{XX}}$, $\mathbf{Q_{YY}}$, $\mathbf{Q_{ZZ}}$) of the quadrupole tensor $\mathbf{Q_{ij}}$ for the metal atoms of the aforementioned complexes. Other components ($\mathbf{Q_{XY}}$, $\mathbf{Q_{XZ}}$, $\mathbf{Q_{YZ}}$) of the quadrupole tensor are at least two orders of magnitude smaller than the primary components. The negative values of $\mathbf{Q_{NN}}$ are indicative of charge density enrichment along the **N** axis relative to the plane orthogonal to the **N** axis. On the other hand the positive values of $\mathbf{Q_{NN}}$ are indicative of charge density enrichment in the plane orthogonal to **N** axis. To visualize this type of polarization consider an isosphere of some value of electron density with the Cu nucleus embedded in the center. This isosphere is deformed from spherical symmetry by inflating a perfect sphere within the XY plane, while holding the points along the Z axis constant. In other words the isosphere of electron density with $\mathbf{Q_{ZZ}}(\mathrm{M})>0$ is an oblate spheroid with the equator orthogonal to the Z axis. The displacement of this oblate spheroid along the Z axis is measured by $\boldsymbol{\mu}_{\mathbf{intra\_z}}(\mathrm{M})$.

As shown in Table 1.7, the values of $\mathbf{Q_{ZZ}}(\mathrm{Cu})$ for all complexes are positive with magnitudes being largest for **1.13i-1.19i**, indicating enrichment in electron density within the XY plane relative to the Z axis. The π-backbonding interaction is expected to concentrate electron density within the XY plane as dictated by the spatial requirements for overlap between d_π electrons of a metal center with the partially populated $p(C_{NHC})$ and $\sigma^*(C_{NHC}N)$ for NHCs or σ^*(P-C) for phosphines. As distortion of the electron density along the Z axis is given by $\boldsymbol{\mu}_{\mathbf{intra\_z}}(\mathrm{M})$, it is possible to devise a theoretical descriptor for π-back donation by multiplying $\boldsymbol{\mu}_{\mathbf{intra\_z}}(\mathrm{M})$ by $\mathbf{Q_{ZZ}}(\mathrm{M})$ and weighting the

---

(88) For MO-theoretic and EDA analyses of π-back donation interactions in NHC-metal complexes see the section 1.1.2.5. For MO-theoretic analysis of π-back donation interactions in phosphine-metal complexes see: (a) Xiao, S. –X.; Trogler, W. C.; Ellis, D. E.; Berkovitch-Yellin, Z. *J. Am. Chem. Soc.* **1983**, *105*, 7033-7037; (b) Marynick, D. S. *J. Am. Chem. Soc.* **1984**, *106*, 4064-4065.

Table 1.7. Quadrupole Tensor Components[a]

							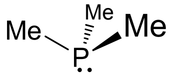		
	Q_{XX}	**Q_{YY}**	**Q_{ZZ}**	**Q_{XX}**	**Q_{YY}**	**Q_{ZZ}**	**Q_{XX}**	**Q_{YY}**	**Q_{ZZ}**
1.13	-3.35	-2.15	5.50	-3.39	-2.01	5.40	-2.63	-2.63	5.25
1.14	-3.60	-2.25	5.86	-3.64	-2.12	5.76	-2.84	-2.84	5.68
1.15	-3.03	-2.05	5.08	-3.05	-1.94	5.00	-2.39	-2.39	4.78
1.16	-3.42	-2.12	5.54	-3.46	-1.99	5.45	-2.61	-2.61	5.21
1.17	-3.14	-2.05	5.19	-3.19	-1.92	5.10	-2.44	-2.44	4.89
1.18	-3.05	-2.01	5.06	-3.09	-1.89	4.98	-2.39	-2.39	4.78
1.19	-2.99	-1.96	4.95	-3.05	-1.83	4.88	-2.36	-2.36	4.72
Mean[b]:	-3.23	-2.09	5.31	-3.27	-1.96	5.22	-2.52	-2.52	5.04
Median[b]:	-3.14	-2.05	5.19	-3.19	-1.94	5.10	-2.44	-2.44	4.89
σ[c]:	0.23	0.10	0.33	0.23	0.09	0.32	0.18	0.18	0.35
Skewness[d]:	-0.51	-0.54	0.54	-0.52	-0.40	0.56	-0.80	-0.80	0.81

[a] All values are in a.u. The Z axis is defined by M-C_{NHC} or M-P_{PMe3} bond; the plane of an *N*-heterocycle defines YZ plane; the 3-fold symmetry of PMe_3 renders it isotropic with respect to X and Y axes. [b] The average (mean or median) of all the values in the column for given property of a given ligand. [c] The standard deviation of the set of values for a given property of a given ligand. [d] The skewness of the sample set measures the degree of distortion of a normal distribution curve. Negative values of skewness are indicative of a larger tail of the response curve in the negative direction with respect to the mean along the input variable dimension.

resulting value by M-L bond length.[89] Thus, based on the data for **1.15i**-**1.18i**, **1.15s**-**1.18s**, and **1.15p**-**1.18p**, the descriptor $\boldsymbol{P}_\pi$ takes on the following values: -0.52 for IMe, -0.55 for SIMe, and -0.86 for PMe_3 (Table 1.8). Based on individual $\boldsymbol{P}_\pi$ values PMe_3 is a stronger π-acceptor than IMe by *119%* on average (*mean*), whereas SIMe ligand is a

---

(89) Suppose a descriptor $\boldsymbol{P}_\pi$ assesses the degree of π-interaction between a metal and a ligand. The dipolar charge polarization along M-L axis is given by $\boldsymbol{\mu}_{\mathbf{intra\_z}}$(M) and quadrupolar polarization is measured by a tensor $\overleftrightarrow{\boldsymbol{Q}}(M)$. The scalar product of vector $\boldsymbol{\mu}_{\mathbf{intra\_z}}$(M) and the tensor $\overleftrightarrow{\boldsymbol{Q}}(M)$ gives three scalar values $C_X = 0$, $C_Y = 0$, and $C_Z = \boldsymbol{\mu}_{\mathbf{intra\_z}}(M) \cdot \mathbf{Q_{ZZ}}(M)$. Thus, the value of C_Z can taken on either positive values {(a): $\boldsymbol{\mu}_{\mathbf{intra\_z}}(M)>0$, $\mathbf{Q_{ZZ}}(M)>0$ or (b): $\boldsymbol{\mu}_{\mathbf{intra\_z}}(M)<0$, $\mathbf{Q_{ZZ}}(M)<0$)} or negative values {(c): $\boldsymbol{\mu}_{\mathbf{intra\_z}}(M)<0$, $\mathbf{Q_{ZZ}}(M)>0$ or (d): $\boldsymbol{\mu}_{\mathbf{intra\_z}}(M)>0$, $\mathbf{Q_{ZZ}}(M)<0$}. Each one of the cases is unique and fully characterizes the ligand in question as π-donor (case a) or π-acceptor (case c). Cases (b) and (d) are likely to arise from *protonation* of the metal center that is in cases where π-interactions are absent. However, metal ligand bonds vary in their magnitude and thus the total value *C* needs to be weighted by the M-L bond length {r(M-L)}. It is appropriate to weight $\boldsymbol{\mu}_{\mathbf{intra\_z}}$(M) by r(M-L), because the Coulombic forces dissipate as simply linearly with respect to distance. Thus, for cases (a) and (c) $\boldsymbol{P}_\pi = C_Z$/r(M-L). The magnitude of $\boldsymbol{P}_\pi$ provides an estimate of the strength of the π-interaction and its sign defines whether the ligand in question is π-donor ($\boldsymbol{P}_\pi>0$) or π-acceptor ($\boldsymbol{P}_\pi<0$).

stronger π-acceptor than IMe by 9%. However, based on *median values* of $\boldsymbol{P}_{\pi}$, PMe_3 is a stronger π-acceptor than IMe by *91%*, while SIMe ligand is a stronger π-acceptor than IMe by 7%. The difference between *mean* and *median* relative values for PMe_3 provides an indication that the π-back donation plays a fundamentally different role in complexes of phosphines than those of NHCs. Consider the ratio of $\boldsymbol{P}_{\pi}$ for the stronger π-interaction over the weakest one for each ligand; the ratios thus obtained are 8.09, 6.78, and 2.78 for IMe, SIMe, and PMe_3, respectively. The ligand IMe is capable of adapting its π-acidity to the π-basicity of a metal atom to a greater extent than either SIMe or PMe_3.[90] In other words the *π-acidic softness of IMe is greatest, followed by SIMe and PMe_3.*[81a-b]

Table 1.8. Comparison of π-accepting Abilities of the Ligands

					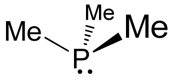	
	***P*π**	relative ***P*π**	***P*π**	relative ***P*π**	***P*π**	relative ***P*π**
1.15	-0.14	1.00	-0.17	1.21	-0.51	3.67
1.16	-1.13	1.00	-1.15	1.02	-1.43	1.26
1.17	-0.53	1.00	-0.55	1.05	-0.86	1.63
1.18	-0.30	1.00	-0.33	1.09	-0.65	2.18
Mean:	-0.52	1.00	-0.55	1.09	-0.86	2.19
Median:	-0.41	1.00	-0.44	1.07	-0.76	1.91
σ:	0.43		0.43		0.40	
Skewness:	-0.73		-0.73		-0.76	

Quadrupole moments also allow distinguishing the anisotropic π-back donation. Due to the symmetry of PMe_3 the back donation is isotropic as both d_{xz} and d_{yz} orbitals of Cu overlap identically with σ^*(P-C) orbitals. However, in the case of NHCs the relative π-acidities due to the partially populated $p(C_{NHC})$ and $\sigma^*(C_{NHC}\text{-N})$ orbitals can be estimated. The component $\mathbf{Q_{XX}}$ measures the quadrupolar polarization due to the $d_{xz}(Cu) \rightarrow p(C_{NHC})$ interaction, while $\mathbf{Q_{YY}}$ does the same for $d_{yz} \rightarrow \sigma^*(C_{NHC}\text{-N})$ interaction. As shown in Table 1.7, both $\mathbf{Q_{XX}}$ and $\mathbf{Q_{YY}}$ values are negative for all Cu complexes,

---

(90) The π-basicity of a Cu atom is determined by the X ligand bound to it. In complexes **1.15i**, **1.15s**, and **1.15p** the X ligand (F) is a strong π-donor thus resulting in higher availability of filled d_{π} orbitals of Cu. On the other hand the complexes **1.16i**, **1.16s**, and **1.16p** bear a π-acidic X ligand (CN) that is in competition with the other ligand (IMe, SIMe, or PMe_3) for the same set of d_{π} orbitals of Cu atom.

indicating the enrichment in electron density along the X and Y axes. However, for both SIMe and IMe **|Q_{XX}|>|Q_{YY}|**, indicating that $d_{xz}(Cu) \rightarrow p(C_{NHC})$ donation is more pronounced than $d_{yz} \rightarrow \sigma^*(C_{NHC}\text{-}N)$ interaction. The former interaction is more significant for SIMe-Cu than for IMe-Cu complexes (**Q_{XX}/Q_{YY}** = 1.67 ± 0.05 for SIMe and 1.55 ± 0.05 for IMe). The $d_{xz}(Cu) \rightarrow p(C_{NHC})$ interaction is somewhat softer than the $d_{yz} \rightarrow \sigma^*(C_{NHC}\text{-}N)$ as can be seen from the standard deviations for **Q_{XX}** and **Q_{YY}** values; **Q_{XX}** = -3.27 ± 7.0% for SIMe and -3.23 ± 7.2%, whereas **Q_{YY}** = -1.96 ± 4.8% for SIMe and -2.09 ± 4.7%.

1.2.3.3. Delocalization and Localization Indices

Further insight into the bonding with the organometallic complexes can be provided by delocalization and localization indices. The localization indices $\lambda(M)$, $\lambda(C_{NHC})$, and $\lambda(P_{PMe3})$ for the all complexes are listed in Table 1.9.

The localization indices for the metal atoms are consistent with the observation that the net electron donorability of PMe_3 into *the metal center* is greater than that of IMe or SIMe, as in all cases $\lambda(M)$ increases from IMe to SIMe to PMe_3 (consistent with q(M) discussed in 1.2.3.1). Positive values for $\Delta\lambda(M)$ demonstrate that the formal number of electrons for the transition metals in a certain oxidation state is higher than the actual number of localized electrons at the metal center $\lambda(M)$; the single exception to this statement is Rh(III) (**1.10i**, **1.10s**, and **1.10p**). Although in complexes **1.10i**, **1.10s**, and **1.10p** Rh bears a formal (III) charge, and in complexes **1.09i**, **1.09s**, and **1.09p** Rh is formally Rh(I), the localization indices $\lambda(Rh)$ are consistent with the Rh atom being more electron rich in the former complex rather than the latter.

The localization indices for the complexed C_{NHC} and P atoms – $\lambda(C_{NHC})$ and $\lambda(P_{PMe3})$, respectively – are smaller than those for the atoms in free ligands by 0.434 for IMe, 0.436 for SIMe, and 0.676 for PMe_3. Loss of electron density at C_{NHC} is partially compensated for by the small decrease in $\lambda(N_{NHC})$: 0.018 (range: 0.004-0.044) for SIMe, and 0.012 (range: 0.002-0.030) for IMe. The charge transfer between C_{NHC} and N atoms is also decreased as evidenced by the mean $q(C_{NHC}|N)$ which is equal to 0.378 and 0.451 for free IMe and SIMe, respectively, while mean $q(C_{NHC}|N)$ is 0.343 and 0.404 for

Table 1.9. Localization Indices of the Metal Atoms[a]

							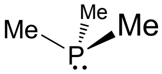		
	λ(M)[b]	$\lambda(C_{NHC})$[c]	$\Delta\lambda$(M)[d]	λ(M)[b]	$\lambda(C_{NHC})$[c]	$\Delta\lambda$(M)[d]	λ(M)[b]	λ(P)[e]	$\Delta\lambda$(M)[d]
1.1	24.306	3.658	1.694	24.325	3.539	1.675	24.658	11.362	1.342
1.2	24.344	3.652	1.656	24.364	3.544	1.636	24.785	11.344	1.215
1.3	22.911	3.691	1.089	22.921	3.562	1.079	23.041	11.437	0.959
1.4	40.590	3.681	3.410	40.595	3.551	3.405	40.694	11.425	3.306
1.5	40.584	3.722	3.416	40.585	3.593	3.415	40.723	11.541	3.277
1.6	40.729	3.643	3.271	40.730	3.522	3.270	40.847	11.380	3.153
1.7	40.298	3.665	1.702	40.310	3.530	1.690	40.406	11.404	1.594
1.8	41.180	3.503	0.820	41.164	3.400	0.836	41.366	11.183	0.634
1.9	42.398	3.581	1.602	42.394	3.461	1.606	42.553	11.451	1.447
1.10	42.963	3.568	-0.963	42.404	3.294	-0.404	42.599	11.113	-0.599
1.11	26.427	3.744	1.573	26.536	3.654	1.464	26.497	11.604	1.503
1.12	44.091	3.730	1.909	44.083	3.618	1.917	44.209	11.616	1.791
1.13	27.821	3.800	0.179	27.813	3.667	0.187	27.898	11.673	0.102
1.14	27.725	3.795	0.275	27.718	3.662	0.282	27.810	11.663	0.190
1.15	27.625	3.790	0.375	27.623	3.649	0.377	27.706	11.632	0.294
1.16	27.574	3.747	0.426	27.565	3.615	0.435	27.650	11.569	0.350
1.17	27.613	3.762	0.387	27.607	3.626	0.393	27.686	11.595	0.314
1.18	27.649	3.765	0.351	27.644	3.628	0.356	27.722	11.601	0.278
1.19	27.698	3.772	0.302	27.694	3.634	0.306	27.770	11.615	0.230

[a] All values are in a.u. [b] λ(M) - Number of electrons that are localized to the atomic basin of the metal center. [c] $\lambda(C_{NHC})$ - Number of electrons that are localized with the atomic basin of the C_{NHC} of IMe or SIMe. [d] $\Delta\lambda(M) = N^{formal}(M) - \lambda(M)$, where N^{formal}(M) is the number of electrons formally belonging to the metal center of the appropriate oxidation state, for example, N^{formal}(Cu(I)) = 28. [e] λ(P) - Number of electrons that are localized with the atomic basin of the P atom of PMe_3.

complexed IMe and SIMe, respectively. The decrease (0.049 for IMe and 0.040 for SIMe) in delocalization indices $\delta(C_{NHC},N)$ indicates that the C_{NHC} atom is primarily stabilized through the decrease in charge transfer ($q(C_{NHC}|N)$) and not due to enhanced covalent interaction between the N and C_{NHC} atoms relatively to the free NHC ligands (see Table 1.10 for the delocalization indices). The localization indices of C atoms of the complexed PMe_3 – $\lambda(C_{PMe3})$ *increase* relatively to those of the free PMe_3 by 0.065 (range: 0.033-0.116). The back donation $d_{\pi} \rightarrow \sigma^*$(P-C) could account for this observation. It is noteworthy that the largest increase of 0.116 in $\lambda(C_{PMe3})$ is found in the formally electron-poor complex 14-electron complex **1.10p**. However, the complex **1.10p** carries no π-

acidic ligands and thus it bears a fully occupied d_π set of orbitals which are capable of polarizing towards the phosphorus atom. Overall the P-C bond in PMe_3 is weakened as the sum of delocalization indices $\Sigma\delta(P,C)$ is lower for the bound ligand that for the free ligand ($\Sigma\delta(P,C)$ for free PMe_3 = 2.118).

As shown in table 1.10, the sum of delocalization indices $\delta(M,\Lambda)$, where $\Lambda = N_{NHC}$(IMe or SIMe) or $\Lambda = C(PMe_3)$ have considerably high values on the order of 0.1 a.u. The shared interaction between the metal and N_{NHC} or C_{PMe3} atoms may be related to either σ-framework or π-system interaction from the MO theoretic point of view. Because N_{NHC} and C_{PMe3} atoms are bound C_{NHC} and P_{PMe3} atoms, respectively, and not to the metal atom, the σ-interactions may be negligible and the dominant contributor to the metal-N_{NHC} or metal-$C_{phosphine}$ interaction is likely to involve d_π-electrons of the metal center. This hypothesis was confirmed in the context of $Cr(CO)_5$ Fischer carbene complexes through correlation of $\delta(Cr,\Lambda)$ (Λ = atom connected to the carbene atom) from QTAIM analysis to ΔE_π from Energy Decomposition Analysis.[91] Another way of corroborating the aforementioned hypothesis is through establishing correlations between π-interactions-sensitive observable such as stretching frequency of a carbonyl ligand on the metal center to an appropriate $\delta(M,\Lambda)$ such as $\delta(M,O_{CO})$. Thus, correlation between delocalization indices $\delta(M,O_{CO})$ and corresponding vibrational stretching values $\tilde{\upsilon}(CO)$ has to be established. It should be noted that a vibrational mode thus examined *must be separated from other vibrational modes*. From the set of calculated carbonyl stretching frequencies for metal carbonyl complexes in Chart 1.1 the isolated modes were selected and plotted against stretching frequencies $\tilde{\upsilon}(CO)$ (Figure 1.17). As expected there's an inverse linear correlation between $\tilde{\upsilon}(CO)$ of each specific CO vibrational mode and the corresponding $\delta(M,O_{CO})$, signifying that the higher number of electrons in a shared interaction between the metal atom and the O atom of the carbonyl ligand leads to a decrease in CO bond order, which results in the decrease of the magnitude of the

---

(91) Poater, J.; Cases, M.; Fradera, X.; Duran, M.; Solà, M. *Chem. Phys.* **2003**, *294*, 129-139.

vibrational stretching frequency $\tilde{\upsilon}$(CO). The observed high correlations ($0.99 < R^2 \leq 1.0$) confirm δ(M,Λ) as a metric of π-interactions.

Figure 1.17. Correlation of δ[M,O(CO)] to the Carbonyl Stretching Frequencies

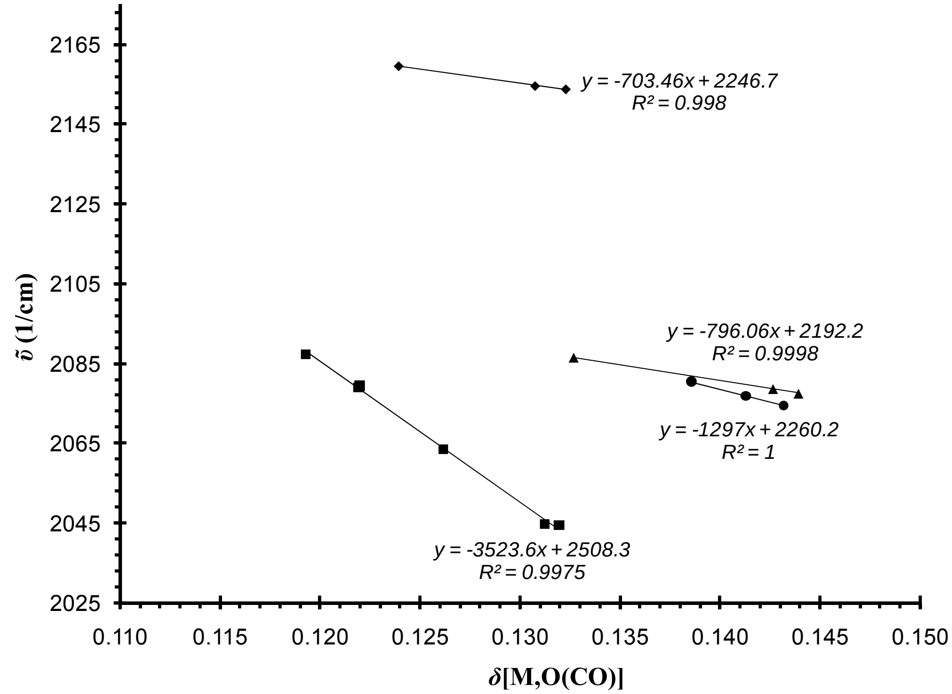

As shown in Figure 1.17, appropriate δ(M,Λ) can be employed to compare the strengths of π-interactions across different complexes and metals. As the metal-ligand π-interactions involve the 4-electron 3-center π-system NCN of a NHC or the σ*(P-C) orbitals of a phosphine the number of electrons that a metal center shares with either one of the systems reflects in delocalization indices δ(M,C_{NHC}), δ(M,N_{NHC}), δ(M,$P_{phosphine}$), and δ(M,$C_{phosphine}$), of which the first and the third also include σ-interactions (*i.e.* donation from C_{NHC} or P into the metal atom) and thus the π-interactions are inseparable. However, the second and the fourth indices include only negligible contributions due to the σ-donation into the metal center. Thus, δ(M,N_{NHC}) and δ(M,$C_{phosphine}$) provide a good estimate of π-interactions. Because there are two N atoms within a NHC and three C atoms within a phosphine in conjugation with a metal center, each delocalization index has to be counted towards a sum, for example, $\Sigma\delta$(M,N_{NHC}) which is equal to the total number of electrons participating in the metal-ligand π-interaction. Note, however, that $\Sigma\delta(\mathrm{M,N_{NHC}})$ does not distinguish between ligand-to-metal and metal-to-ligand π-donations; this point will be elaborated upon further below.

As shown in Table 1.10, $\Sigma\delta(\mathrm{M,N_{IMe}}) < \Sigma\delta(\mathrm{M,N_{SIMe}}) < \Sigma\delta(\mathrm{M,C_{PMe3}})$, which is in agreement with $\boldsymbol{P_\pi}$ descriptors for the IMe, SIMe, and PMe$_3$ ligands, indicating that for all metals in the current study the ligand-to-metal π-donations are negligible.[92] The

Table 1.10. Delocalization Indices[a]

							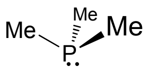		
	δ(M,C)[b]	$\Sigma\delta$(M,N)[c]	$\Sigma\delta$(C,N)[d]	δ(M,C)[b]	$\Sigma\delta$(M,N)[c]	$\Sigma\delta$(C,N)[d]	δ(M,P)[e]	$\Sigma\delta$(M,C)[f]	$\Sigma\delta$(P,C)[g]
1.1	0.632	0.093	1.838	0.638	0.098	1.859	0.675	0.128	1.940
1.2	0.672	0.104	1.824	0.681	0.109	1.840	0.713	0.135	1.917
1.3	0.600	0.076	1.885	0.605	0.081	1.919	0.617	0.096	2.010
1.4	0.673	0.089	1.885	0.679	0.097	1.916	0.729	0.125	1.997
1.5	0.634	0.083	1.885	0.638	0.092	1.917	0.714	0.112	1.998
1.6	0.732	0.103	1.870	0.743	0.113	1.898	0.789	0.139	1.973
1.7	0.660	0.078	1.896	0.663	0.086	1.936	0.681	0.103	2.027
1.8	0.978	0.161	1.841	1.023	0.181	1.863	0.990	0.197	1.943
1.9	0.751	0.099	1.864	0.770	0.110	1.888	0.784	0.123	1.998
1.11	0.674	0.087	1.838	0.683	0.094	1.848	0.762	0.115	1.966
1.12	0.655	0.084	1.861	0.667	0.093	1.877	0.745	0.110	1.993
1.13	0.708	0.092	1.884	0.705	0.101	1.916	0.744	0.114	2.047
1.14	0.721	0.095	1.880	0.720	0.104	1.911	0.762	0.118	2.039
1.15	0.719	0.092	1.896	0.713	0.100	1.933	0.759	0.118	2.060
1.16	0.805	0.112	1.876	0.808	0.123	1.907	0.866	0.142	2.025
1.17	0.763	0.102	1.886	0.760	0.110	1.920	0.813	0.129	2.042
1.18	0.753	0.099	1.889	0.749	0.108	1.924	0.800	0.126	2.047
1.19	0.736	0.096	1.891	0.732	0.104	1.927	0.779	0.121	2.052
Mean:	0.715	0.097	1.872	0.721	0.106	1.900	0.762	0.125	2.004
Median:	0.713	0.094	1.882	0.709	0.102	1.913	0.760	0.122	2.004
σ:	0.085	0.019	0.022	0.092	0.021	0.030	0.080	0.022	0.043
Skewness:	1.597	2.295	-0.861	1.979	2.503	-0.760	1.008	2.061	-0.522

[a] All values are in a.u. [b] δ(M,C) - delocalization index between the metal and the $\mathrm{C_{NHC}}$ atoms. The value is a number of electrons shared between the two atoms. [c] $\Sigma\delta$(M,N) - the sum of both δ(M,N) delocalization indices, which measure the number of electrons shared between the metal and the $\mathrm{N_{NHC}}$ atoms. [d] $\Sigma\delta$(C,N) - the sum of both δ(C,N) delocalization indices, which measure the number of electrons shared between the $\mathrm{C_{NHC}}$ and $\mathrm{N_{NHC}}$ atoms. [e] δ(M,P) - the number of electrons shared between the metal and $\mathrm{P_{PMe3}}$ atoms. [f] $\Sigma\delta$(M,C) - The sum of three δ(M,C), which measure the number of electrons shared between metal and $\mathrm{C_{PMe3}}$ atoms. [g] $\Sigma\delta$(P,C) - The sum of three δ(P,C), which measure the number of electrons shared between $\mathrm{P_{PMe3}}$ and $\mathrm{C_{PMe3}}$ atoms.

---

(92) This result is in accord with findings of EDA analysis that NHC-to-metal π-donations for middle to late transition metal complexes are negligible (see section 1.1.2.5).

descriptor $\boldsymbol{P}_{\pi}$ deserves another mention as it was not correlated to any other measure that is sensitive to π-interactions. As was demonstrated above the delocalization indices $\delta(\mathrm{M,O_{CO}})$ correlated well to frequencies $\tilde{\upsilon}(\mathrm{CO})$ of carbonyl stretching modes, and thus sums of delocalization indices $\Sigma\delta(\mathrm{M,N_{IMe}})$, $\Sigma\delta(\mathrm{M,N_{SIMe}})$, and $\Sigma\delta(\mathrm{M,C_{PMe3}})$ were related to π-populations at the metal center. Thus, it is possible to relate the latter three metrics to $\boldsymbol{P}_{\pi}$ values. As shown in Figure 1.18, the values of $\Sigma\delta(\mathrm{M},\Lambda)$ correlate well to those of $\boldsymbol{P}_{\pi}$, when they are correlated according to either a ligand or a metal salt. However, if all 12 datapoints are correlated together the coefficient of determination is low $R^2 = 0.677$. Thus, it is more convenient from both computational and generality standpoints to use $\Sigma\delta(\mathrm{M},\Lambda)$ values for estimation of π-interactions, albeit with a qualification that these values would not distinguish between ligand-to-metal and metal-to-ligand π-donations, and thus their use for high oxidation early transition metals with non-zero d-electron counts is unlikely to provide physically informative data.

Figure 1.18. Correlation of $\Sigma\delta(\mathrm{M},\Lambda)$ to $\boldsymbol{P}_{\pi}$

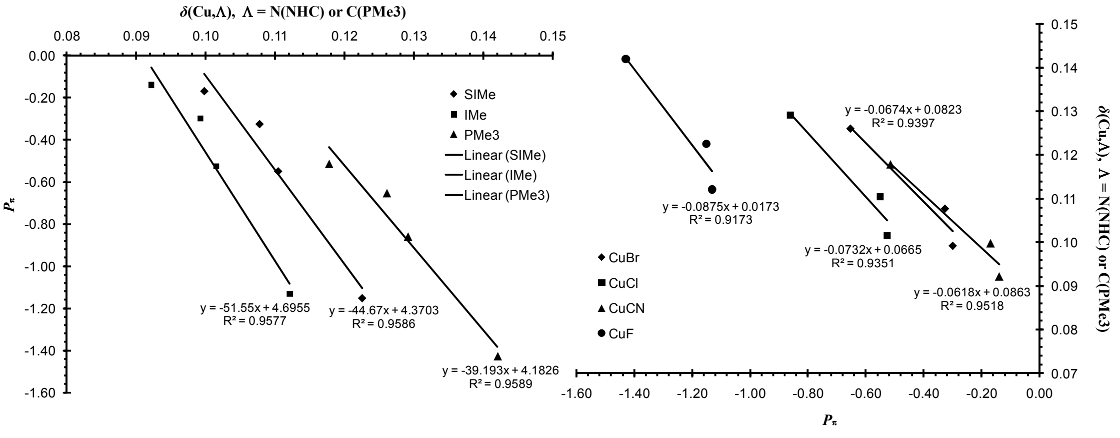

(a) $\Sigma\delta(\mathrm{M},\Lambda)$ to $\boldsymbol{P}_{\pi}$ grouped by ligand

(b) $\Sigma\delta(\mathrm{M},\Lambda)$ to $\boldsymbol{P}_{\pi}$ grouped by Cu salt

1.2.3.4. Tolman Electronic Parameter and the Electronic Structure of N-Heterocyclic Carbene Ligands and Phosphines

Because the vibrational modes are correlated to $\delta(\mathrm{M,O_{CO}})$ and thus to the π-population of a metal center, which is also correlated to other delocalization indices that provide a measurement of π-interactions of other ligands with a metal center, it is reasonable to raise a question whether any of the theoretical values could be used to predict Tolman electronic parameters (TEP) for NHCs and phosphines. Furthermore, it is important to consider the areas of application for TEP.

As mentioned above, the sum $\Sigma\delta$(M,Λ) (where, $\Lambda = N_{NHC}$ or C_{PMe3}) is capable of measurement of π-acidity of NHC and phosphine ligands. Thus, these values would be expected to correlate to carbonyl stretching frequencies $\tilde{\upsilon}$(CO), because the carbonyl ligands are in competition for the same π-electrons as NHCs and phosphines. In order to compare the carbonyl stretching frequencies $\tilde{\upsilon}$(CO) to $\Sigma\delta$(M,Λ) the modes are allowed to mix, so long as the relative contributions of difference carbonyl groups towards the same frequency does not change across the IMe/SIMe/PMe_3 series. Figure 1.19 demonstrates that in case of all 12 different carbonyl stretching modes that were examined there's a direct correlation between $\Sigma\delta$(M,Λ) and $\tilde{\upsilon}$(CO), signifying that enhanced π-interaction between the metal center and N_{NHC} or $C_{phosphine}$ atoms leads to strengthening of CO bond, as indicated by the corresponding increase in $\tilde{\upsilon}$(CO). Therefore, carbonyl stretching frequencies (TEP) provide an accurate measure of ancillary ligands' π-acidities.

Figure 1.19. Correlation of $\Sigma\delta$(M,Λ) to the Carbonyl Stretching Frequencies

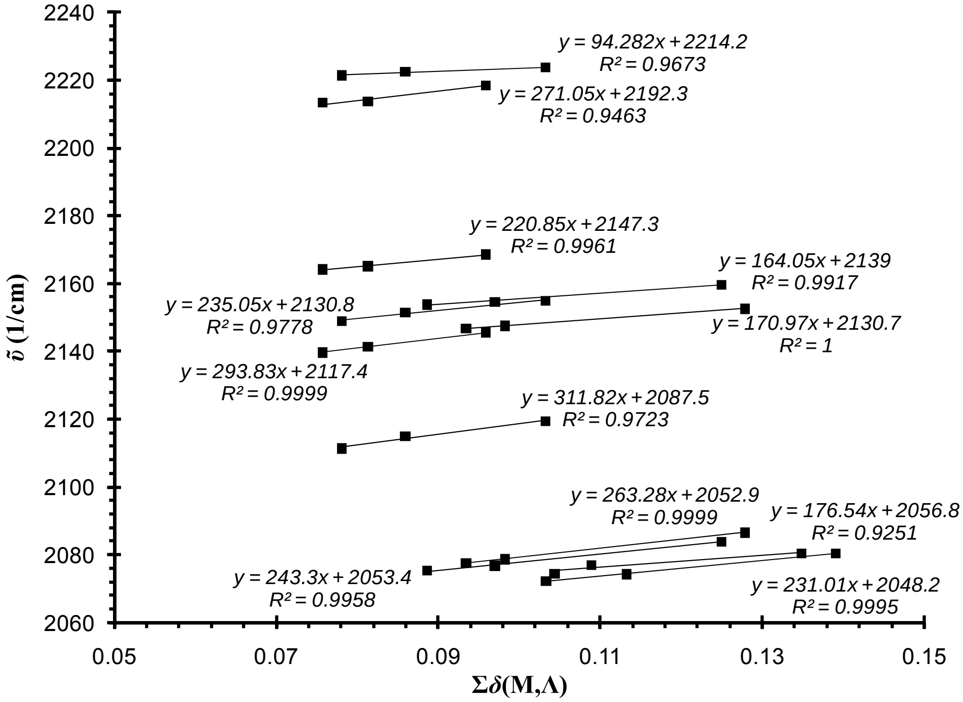

Although the π-acidities of ancillary ligands are well-described by the carbonyl stretching frequencies it is unclear whether the latter account for the net charge transfer between the ancillary ligand and the metal center in question. To assess the net electron donating abilities of NHC and phosphine ligands, the values of QTAIM charges – q(Ligand) (where Ligand = IMe, SIMe or PMe_3), q(M), and $q(L_n)$ – were compared to the same as above carbonyl stretching frequencies. Unexpectedly, direct correlations were found for q(Ligand) and $q(L_n)$, and inverse correlation was determined for q(M),[93] leading to a conclusion that as the ancillary ligand transfers more charge to a metal center the vibrational frequencies increase as well. At first sight QTAIM charges appear to be an inadequate metric for charge donating ability of NHCs and phosphines, and this apparent inadequacy will be discussed further later.

The reader should recall that Hirshfeld population analysis (HPA) appeared consistent with Tolman electronic parameters in ordering the ligands according to their charge donating ability as follows: IMe>SIMe>PMe_3 (see section 1.2.3.1). Indeed,

Figure 1.20. Correlation of HPA Charges to the Carbonyl Stretching Frequencies

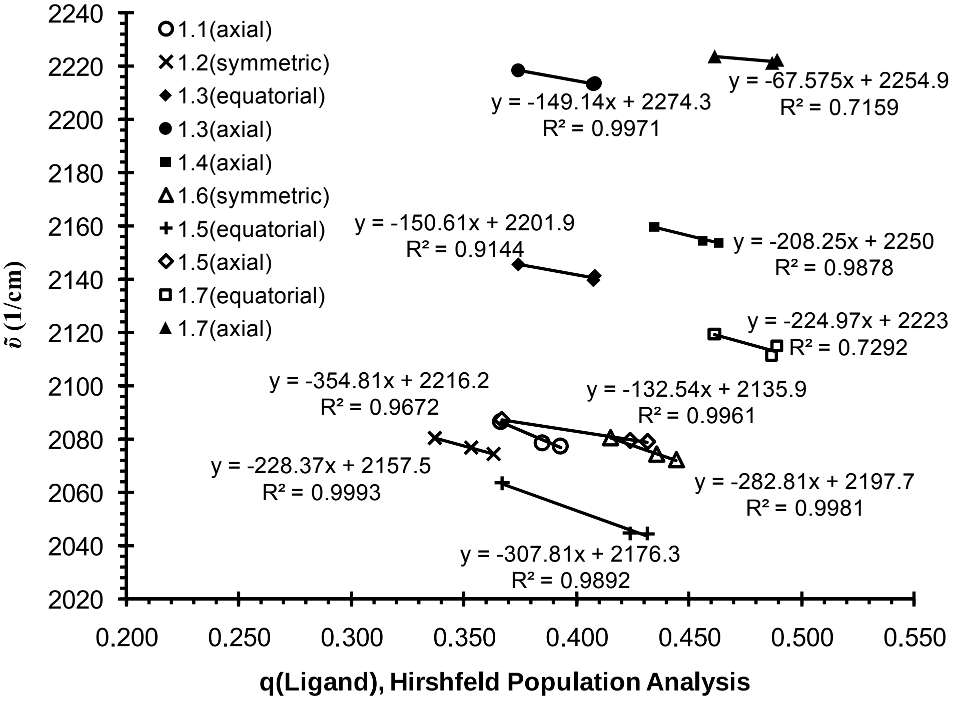

---

(93) See supporting information for details.

correlation of q_{HPA}(Ligand) to the carbonyl ligand stretching frequencies $\tilde{\upsilon}$(CO) gave the expected inverse correlations with high R^2 for ten of the twelve vibrational modes examined (Figure 1.20).

At first glance HPA charges seem to represent the physical observables $\tilde{\upsilon}$(CO), while QTAIM charges contradict the expected trends in carbonyl ligand stretching frequencies. The physical basis for QTAIM partition of real space into atoms and the resulting charges has been addressed previously.[94] The physical meaning of QTAIM charges, however, deserves a special explication. The charges within QTAIM are defined such that they measure *the net electron charge transfer* and polarization effects are addressed by means of higher order-moments within multipole expansion. However, other partitioning schemes may include varying degrees of atomic polarization in the corresponding charge transfer measures – atomic charges. With regard to the ancillary ligands QTAIM charges alone imply that *phosphines are more pronounced charge donors than NHCs*. This observation is consistent with observations where *charge transfer is a decisive factor*. For example, unlike phosphines NHCs could be utilized as ancillary ligands in oxidative processes, where phosphines are known to undergo rapid oxidation.[28e,95] Peroxo-Pd(II) and trioxo-Re(VII) complexes of NHCs have been isolated and characterized, indicating that *NHCs have a more negative oxidation potential than phosphines*.[96] These experimental observations are thus in contrast to the HPA charges.

Although phosphines were found to be more electron donating as stated in section 1.2.3.1, these ligands were also found to polarize the metal center toward the P_{PMe3} atom as described in section 1.2.3.2, which effectively is due to the higher π-acidity of the phosphine (section 1.2.3.3). The carbene ligands on the other hand are weaker charge

---

(94) Bader, R. F. W.; Matta, C. F. *J. Phys. Chem. A* **2004**, *108*, 8385-8394.

(95) (a) Muehlhofer, M.; Strassner, T.; Herrmann, W. A. *Angew. Chem. Int. Ed.* **2002**, *41*, 1745-1747; (b) Poyatos, M.; Mata, J. A.; Falomir, E.; Crabtree, R. H.; Peris, E. *Organometallics* **2003**, *22*, 1110-1114; (c) Muñiz, K. *Adv. Synth. Catal.* **2004**, *346*, 1425-1428; (d) Schultz, M. J.; Hamilton, S. S.; Jensen, D. R.; Sigman, M. S. *J. Org. Chem.* **2005**, *70*, 3343-3352.

(96) The phosphines are known to undergo rapid oxidation in the presence of $MeReO_3$, whereas NHCs form adducts that are stable up to -20 °C: (a) Herrmann, W. A.; Öfele, K.; Elison, M.; Kühn, F. E.; Roesky, P. W. *J. Organomet. Chem.* **1994**, *480*, C7-C9; (b) Konnick, M. M.; Guzei, I. A.; Stahl, S. S. *J. Am. Chem. Soc.* **2004**, *126*, 10212-10213; (c) Yamashita, M.; Goto, K.; Kawashima, T. *J. Am. Chem. Soc.* **2005**, *127*, 7294-7295.

transfer donor ligands, but they are also weaker π-acids, and thus $\tilde{\upsilon}$(CO) are lower for NHCs than phosphines. Therefore, *it is appropriate to consider TEP as a metric for π-acidity rather than net electron donating ability of a ligand.*

If TEP provides the measurement of π-acidity of Lewis bases, why has it been successful as a predictive and explanatory tool for reactivity patterns? The answer to this question can be found in the fact that phosphines have been utilized in transformations involving the soft middle to late transition-metals, as early transition metals do not complex phosphines readily. Therefore, the reactions that have been addressed to a large extent involve soft reactants, the bonding of which with metals is addressed by Dewar-Chatt-Duncanson model.[50] Thus, *correlation of efficiency of a reaction to TEP of ligands involved provides an important insight into the mechanism, as high values of correlation measures indicate the degree of metal's π-electrons contribution to the reaction in question.*

In conclusion, the herein presented study confirms the NHCs as *weaker net electron donors* and *weaker π-acids* than phosphines. The phosphines are the softer ligands in terms of the net charge transfer than NHCs, among which the saturated NHCs were found to be softer Lewis bases than the unsaturated NHCs; however, the latter are stronger charge donors than the former. The phosphines are stronger and harder π-acids, while the saturated NHCs are slightly stronger and softer π-acids than their unsaturated counterparts. Because the phosphine-bound transition metal atoms are polarized towards the P atom but bear a higher and more diffuse electron density than NHC-bound metal atoms, the phosphine ligands are expected to have less of a differentiation between *cis*- and *trans*-influenceas compared to NHCs.

From the theoretic standpoint, it was found that metal-ligand π-interactions are described well by $\Sigma\delta(\mathrm{M},\Lambda)$ (where, $\Lambda = \mathrm{N}_{\mathrm{NHC}}$ or α-$\mathrm{C}_{\mathrm{phosphine}}$). The overall charge density donation is assessed by the total charge taken on by a ligand within a complex – q(Ligand). The intraatomic dipolar and quadrupolar polarizations recover the MO-theoretic view of π-back donations. All these QTAIM descriptors were utilized to determine the physical interpretation of Tolman electronic parameters. It is important to stress that any single QTAIM descriptor is insufficient to account for all electronic effects due to metal ligation. Hirshfeld population analysis recovers TEP and thus can be utilized to predict d_π-population at the metal center; however, the use of HPA should be qualified upon analysis of a reaction in general and the metal center involved, in particular.

Involvement of ancillary ligands with $d_\pi = 0$ metals and main group elements to a large extent has been an uncharted territory for ligand/catalyst classification. In light of the discussion above, TEP is not expected be an adequate metric in these cases. The assessment of electronic aspects of NHCs that do not exhibit themselves in middle to late transition metal organometallic chemistry is undertaken in the next section and will take form of a case study in the area of NHC-catalyzed reactions of main-group elements.

1.3. Mechanistic Investigation of N-Heterocyclic Carbene-catalyzed Conjugate Addition of Boron and Silicon

1.3.1. Introduction: free N-Heterocyclic Carbenes as Catalysts and Activators

The use of *N*-heterocyclic carbenes as catalysts on their own right dates back to the pioneering work of Breslow.[31] In his seminal paper on the mechanism of thiamine-catalyzed decarboxylation of pyruvic acid Breslow investigated the behavior of various thiazolium salts as a model system for thiamine.[97] Following on previous observation that thiazolium salts catalyze benzoin condensation,[98] he extended the Lapworth mechanism[99] for cyanide-catalyzed benzoin condensation to include thiazolidenes as shown in Scheme 1.2. Breslow called the adduct of thiazolidene and benzaldehyde an “active aldehyde”, which is now known as Breslow intermediate.

Scheme 1.2. Breslow's Proposal for the Mechanism of Thiazolidene-catalyed Benzoin Condensation

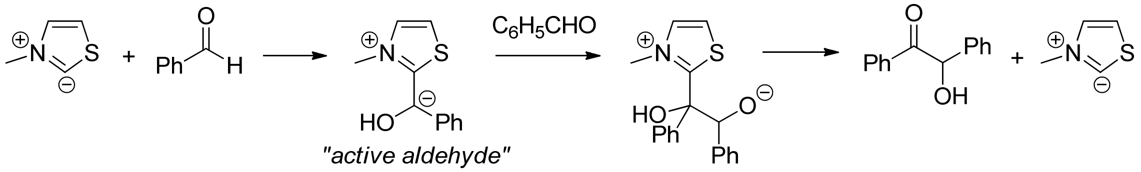

---

(97) For a review of functions of thiamine see: Jansen, B. *Vitamins and Hormones* **1949**, *7*, 83.

(98) Ugai, T.; Tanaka, S.; Dokawa, S. *J. Pharm. Soc. Japan* **1943**, *63*, 269.

(99) Lapworth, A. *J. Chem. Soc.* **1903**, *83*, 995-1005.

Following on Breslow's proposal, Sheehan and co-workers as a proof of principle demonstrated that the benzoin reaction of benzaldehyde can be carried out in the presence of catalytic amounts of chiral thiazolium salts to afford benzoin with 61:39 *er*.[100] The Breslow intermediate-related derivatives of *N*-heterocyclic carbenes proved to be versatile nucleophiles, and thus numerous catalytic protocols incorporating these intermediates were developed.[101] However, NHC-catalyzed organic transformations that do not involve reactions of NHCs with carbonyl groups and their vinylogous equivalents have only recently began to emerge.[102]

Recently, Curran and co-workers noted that B-H bonds in NHC complexes of borane are significantly weaker, as evidenced by the decrease in values for $BDE_{B\text{-}H}$ (free borane $BDE_{B\text{-}H}$ = 111.7 kcal/mol at UB3LYP/LACVP* level of theory, and NHC-borane $BDE_{B\text{-}H}$ = 74-80 kcal/mol at the same level of theory).[103] The $BDE_{B\text{-}H}$ of the NHC-borane complex is effectively the same as $BDE_{Sn\text{-}H}$ of *n*-Bu_3SnH, [104] rendering these complexes synthetically useful as H-radical donors. Thus, as a proof of principle NHC-BH_3 complexes were employed as stoichiometric reducing agents in Barton-McCombie deoxygenation reaction.[103,105] Further studies of various NHC-BH_3 complexes revealed that rate of H-atom abstraction of these complexes is higher than that for Et_3SiH but lower than that for Bu_3GeH and Bu_3SnH. Among the 19 NHC-BH_3 complexes the rates for H-atom abstraction were highest for ICy, IMe, and a sterically exposed *N,N*'-dimethyl-triazolidene.[106c]

---

(100) Sheehan, J. C.; Hunneman, D. H. *J. Am. Chem. Soc.* **1966**, *88*, 3666-3667.

(101) For reviews on carbene-catalyzed organic reactions see: (a) Enders, D.; Balensiefer, T. *Acc. Chem. Res.* **2004**, *37*, 534-541; (b) Enders, D.; Niemeier, O.; Henseler, A. *Chem. Rev.* **2007**, *107*, 5606-5655; (c) Moore, J. L.; Rovis, T. *Top. Curr. Chem.* **2010**, *291*, 77-144.

(102) (a) Movassaghi, M.; Schmidt, M. A. *Org. Lett.* **2005**, *7*, 2453-2456; (b) Phillips, E. M.; Riedrich, M.; Scheidt, K. *J. Am. Chem. Soc.* **2010**, *132*, 13179-13181.

(103) Ueng, S. –H.; Brahmi, M. M.' Derat, É.; Fensterbank, L.; Lacôte, E.; Malacria, M.; Curran, D. P. *J. Am. Chem. Soc.* **2008**, *130*, 10082-10083.

(104) Griller, D.; Wayner, D. D. M. *Pure. Appl. Chem.* **1989**, *61*, 717-724.

(105) Barton, D. H. R.; McCombie, S. W. *J. Chem. Soc., Perkin Trans. 1* **1975**, 1574-1585.

(106) For studies of NHC-borane radical formation and its intermediacy in deoxygenation reactions described in Ref. 100 see: (a) Ueng, S. –H.; Solovyev, A.; Yuan, X.; Geib, S. J.; Fensterbank, L.; Lacôte, E.; Malacria, M.; Newcomb, M.; Walton, J. C.; Curran, D. P. *J. Am. Chem. Soc.* **2009**, *131*, 11256-11262; (b) Walton, J. C.; Brahmi, M. M.; Fensterbank, L.; Lacôte, E.; Malacria, M.; Chu, Q.; Ueng, S. –H.; Solovyev, A.; Curran, D. P. *J. Am. Chem. Soc.* **2010**, *132*, 2350-2358; (c) Solovyev, A.; Ueng, S. –H.; Monot, J.; Fensterbank, L.; Malacria, M.; Lacôte, E.; Curran, D. P. *Org. Lett.* **2010**, *12*, 2998-3001.

Utility of NHC-BH_3 complexes as stoichiometric reducing agents as an alternative to tin hydrides was extended further to include Pd-catalyzed and non-catalytic dehalogenation and deoxygenation reactions, where NHC-BH_3 complexes serve as hydride and not H radical donors.[107] Thus, the studies of Curran and co-workers demonstrated the potential richness of NHC-borane chemistry.

1.3.2. N-Heterocyclic Carbene-catalyzed 1,4-Addition of Bis(pinacolato)diboron and Dimethylphenylsilyl-pinacolatoborane to α,β-Unsaturated Carbonyls

1.3.2.1. Reaction Design: Direct Activation of Diboron Compounds with NHC

Among the long-standing interests of our research group has been the activation of main group elements for the purpose of enhancing their reactivity towards bond-forming reactions that are important for organic synthesis.[59d,108] The bond that allows to access significant chemical diversity upon its elaboration is that between carbon and boron.[109] Thus, a great deal of research has been dedicated to the development of C-B bond forming reactions.[110]

---

[107] Chu, Q.; Brahmi, M. M.; Solovyev, A.; Ueng, S. –H.; Curran, D. P.; Malacria, M.; Fensterbank, L.; Lacôte, E. *Chem. Eur. J.* **2009**, *15*, 12937-12940.

[108] (a) Zhao, Y.; Rodrigo, J.; Hoveyda, A. H.; Snapper, M. L. *Nature* **2006**, *443*, 67-70; (b) Lee, Y.; Hoveyda, A. H. *J. Am. Chem. Soc.* **2006**, *128*, 15604-15605.

[109] For a review on derivatization of organoboron compounds through substitution reactions see: (a) Brown, H. C.; Singaram, B. *Pure Appl. Chem.* **1987**, *59*, 879-894. For a review on homologation of organoboranes see: (b) Thomas, S. P.; French, R. M.; Jheengut, V.; Aggarwal, V. K. *Chem. Rec.* **2009**, *9*, 24-39. For reviews on Suzuki-Miyaura reaction see: (c) Miyaura, N.; Suzuki, A. *Chem. Rev.* **1995**, *95*, 2457-2483; (d) Chemler, S. R.; Trauner, D.; Danishefsky, S. J. *Angew. Chem. Int. Ed.* **2001**, *40*, 4544-4568; (e) Nicolaou, K. C.; Bulger, P. G.; Sarlah, D. *Angew. Chem. Int. Ed.* **2005**, *44*, 2-49; (f) Corbet, J. –P.; Mignani, G. *Chem. Rev.* **2006**, *106*, 2651-2710; (g) Doucet, H. *Eur. J. Org. Chem.* **2008**, 2013-2030; (h) Martin, R.; Buchwald, S. L. *Acc. Chem. Res.* **2008**, *41*, 1461-1473; (i) Molander, G. A.; Canturk, B. *Angew. Chem. Int. Ed.* **2009**, *48*, 9240-9261; (j) Suzuki, A. *Pure App. Chem.* **2010**, *80*, 15-43.

[110] For reviews on hydroboration and diboration reactions see: (a) Brown, H. C. *Pure App. Chem.* **1976**, *47*, 49-60; (b) Brown, H. C.; Chandrasekharan, J.; Wang, K. K. *Pure App. Chem.* **1983**, *55*, 1387-1414; (c) Burgess, K.; Ohlmeyer, M. J. *Chem. Rev.* **1991**, *91*, 1179-1191; (d) Brown, H. C.; Ramachandran, P. V. *Pure App. Chem.* **1994**, *66*, 201-212; (e) Beletskaya, I.; Pelter, A. *Tetrahedron* **1997**, *53*, 4957-5026; (f) Marder, T. B.; Norman, N. C. *Top. Catal.* **1998**, *5*, 63-73; (g) Carroll, A. –M.; O'Sullivan, T. P.; Guiry, P. J. *Adv. Synth. Catal.* **2005**, *347*, 609-631; (h) Burks, H. E.; Morken, J. P. *Chem. Commun.* **2007**, 4717-4725; (i) Ramírez, J,; Lillo, V.; Segarra, A. M.; Fernández, E. *Compt. Rend. Chim.* **2007**, *10*, 138-151. For some recent examples of transition metal-catalyzed diboron additions to alkenes, alkynes, aldehydes, and imines see: (j) Mann, G.; John, K. D.; Baker, R. T. *Org. Lett.* **2000**, *2*, 2105-2108; (k) Morgan, J. B.; Miller, S. P.; Morken, J. P. *J. Am. Chem. Soc.* **2003**, *125*, 8702-8703; (l) Ramírez, J.; Segarra, A. M.; Fernández, E. *Tetrahedron: Asym.* **2005**, *16*, 1289-1294; (m) Ramírez, J.; Corberán, R.; Sanaú, M.; Peris, E.; Fernández, E. *Chem. Commun.* **2005**, 3056-3058; (n) Trudeau, S.; Morgan, J. B.; Shrestha, M.; Morken,

Addition of boron reagents to *α,β*-unsaturated carbonyls is particularly important, as this reaction allows for preparation of aldol addition and Mannich reaction products. Furthermore, the transformation that can be performed to give a product of 1,4-diboration of an *α,β*-unsaturated carbonyl allows for accessing a product that is a boron enolate, thereby allowing for additional *site-selective nucleophilic* reactivity on an aldol product (see Scheme 1.3).

Scheme 1.3. Conjugate Addition of Boron to an Enone

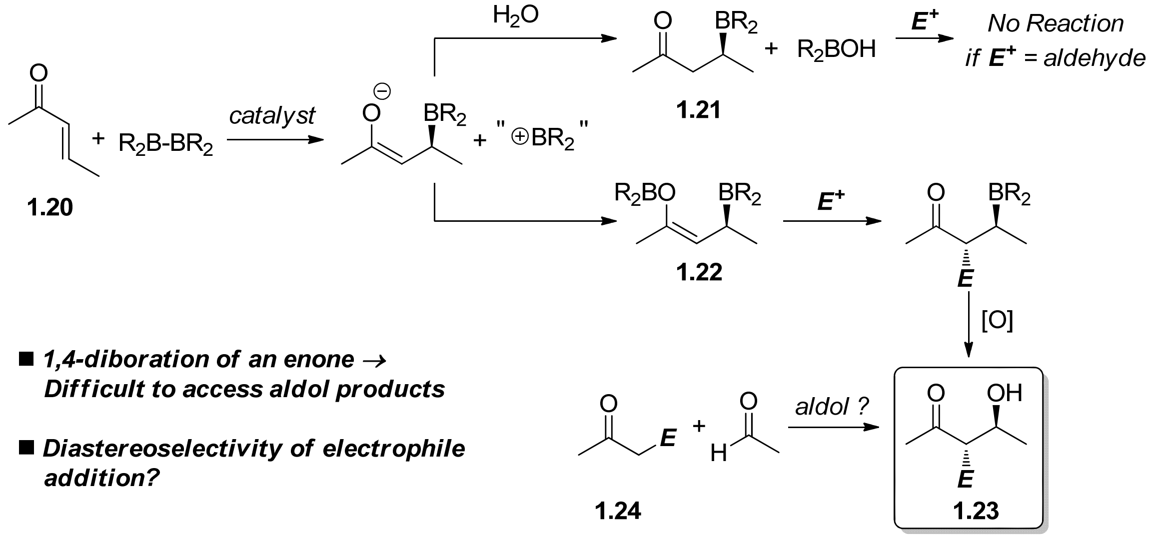

- ***1,4-diboration of an enone → Difficult to access aldol products***
- ***Diastereoselectivity of electrophile addition?***

Consider synthetic routes to the compound **1.23** in Scheme 1.3. The disconnection of C_{α}-C_{β} bond gives the compound **1.24** and acetaldehyde as retrons; such aldol addition reaction may prove difficult on many counts, most important of them being: (1) identity of ***E***-group – if **1.24** is itself a product of an aldol reaction, formation of an enolate on **1.24** will result in elimination of the hydroxyl substituent; (2) control of the diastereoselectivity of the enolate formation; (3) aldol reactions of acetaldehyde tend to

---

J. P. *J. Org. Chem.* **2005**, *70*, 9538-9544; (o) Laitar, D. S.; Tsui, E. Y.; Sadighi, J. P. *J. Am. Chem. Soc.* **2006**, *128*, 11036-11037; (p) Corberán, R.; Lillo, V.; Mata, J. A.; Fernández, E.; Peris, E. *Organometallics* **2007**, *26*, 4350-4353; (q) Penno, D.; Lillo, V.; Koshevoy, I. O.; Sanaú, M.; Ubeda, M. A.; Lahuerta, P.; Fernández, E. *Chem. Eur. J.* **2008**, *14*, 10648-10655; (r) Burks, H. E.; Kliman, L. T.; Morken, J. P. *J. Am. Chem. Soc.* **2009**, *131*, 9134-9135; (s) Kliman, L.; Mlynarski, S. N.; Morken, J. P. *J. Am. Chem. Soc.* **2009**, *131*, 13210-13211; (t) Lee, Y.; Jang, H.; Hoveyda, A. H. *J. Am. Chem. Soc.* **2009**, *131*, 18234-18235 (u) Iwadate, N.; Suginome, M. *J. Am. Chem. Soc.* **2010**, *132*, 2548-2549; (v) Pubill-Ulldemolins, C.; Bo, C.; Mata, J. A.; Fernández, E. *Chem. Asian J.* **2010**, *5*, 261-264; (w) McIntosh, M. L.; Moore, C. M.; Clark, T. B. *Org. Lett.* **2010**, *12*, 1996-1999; (x) Ely, R.; Morken, J. P. *Org. Lett.* **2010**, *12*, 4348-4351.

be inefficient due to its propensity to oligomerize and form self-aldol condensation products.[111] An alternative approach to synthesis of **1.23** is addition of a nucleophilic oxygen surrogate such that upon addition the resulting enolate undergoes addition to an electrophile, affording **1.23** after oxidative work up. Indeed, this approach has been utilized by our group previously in the context of Cu-catalyzed 1,4-diboration of α,β-unsaturated carbonyls with commercially available bis(pinacolato)diboron.[112] There are, however, limitations to this method, as Cu is also known to catalyze hydroboration reactions of alkynes[110t] and aldehydes.[110o] Thus, we considered the possibility of directly activating a diboron compound with a Lewis base such as NHC. It was hypothesized that formation of an adduct NHC-B_2R_n between NHC and a diboron compound should result in electronic reorganization, wherein due to rehybridization of one of the boron centers ($sp^2 \rightarrow sp^3$) the σ_{B-B} bond would polarize towards the sp^2-hybridized boron atom, thereby rendering it nucleophilic. We reasoned that the partially occupied p-orbital of the sp^2-hybridized boron atom should prevent reactivity between the NHC-B_2R_n and the strongly electrophilic carbonyl group, thereby preventing 1,2-additions (Scheme 1.4). Thus, the identity of substituents R on the boron atoms is important; the groups must be sufficiently π-donating so as to not inhibit the desired reaction, while the π-donations must be sufficiently weak so as to ensure that no competitive 1,2-addition to carbonyls occur. For these reasons and considerations of practicality of the overall transformation bis(pinacolato)diboron was chosen as the diboron reagent. Another effect of NHC coordination to a diboron species was expected to be the weakening of B-B bond as was observed in the case of B-H bonds of borane (Scheme 1.4).[103]

Consider the possible mechanisms for a hypothetic transformation involving the NHC-$B_2(pin)_2$ adduct **1.25** and cyclohexenone **1.26**. Concerted direct transfer of the pinacolatoboron moiety from **1.25** to **1.26** would result in formation of **1.27**. Although the main interaction between the sp^2-hybridized boron atom and the enone is expected to be $HOMO_{\mathbf{1.25}} \rightarrow LUMO_{\mathbf{1.26}}$, considerable mixing between $HOMO_{\mathbf{1.26}}$ and $LUMO_{\mathbf{1.25}}$

---

(111) Yang, J. W.; Chandler, C.; Stadler, M.; Kampen, D.; List, B. *Nature* **2008**, *452*, 453-455.
(112) O'Brien, J. M.; Lee, K.; Hoveyda, A. H. *J. Am. Chem. Soc.* **2010**, *132*, 10630-10633.

should occur. In the case of an aldehyde, however, mixing of $\mathrm{HOMO}_{\mathrm{aldehyde}}$ and $\mathrm{LUMO}_{\mathbf{1.25}}$ is unlikely, as $\mathrm{HOMO}_{\mathrm{aldehyde}}$ is significantly lower than that of an enone and thus LUMO-LUMO mixing would be expected to dominate, thereby destabilizing the transition state structure of addition of **1.25** to an aldehyde.

Scheme 1.4. Hypothesized Reactivity of NHC-$B_2(pin)_2$ Adduct

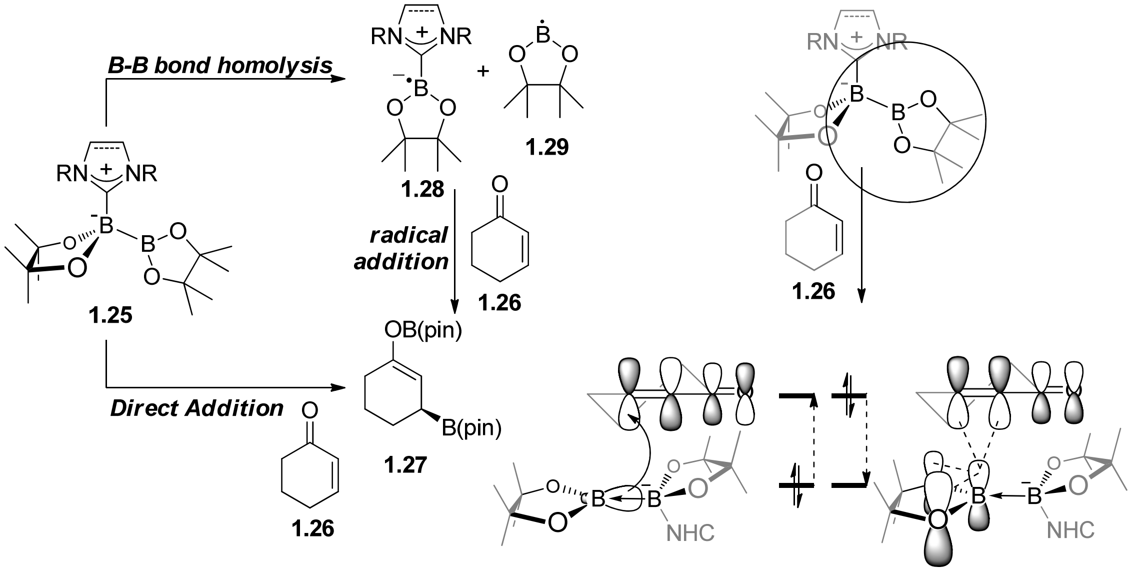

The alternative mechanism is the radical mechanism, wherein weakened B-B bond of **1.25** undergoes homolytic cleavage and to give radicals **1.28** and **1.29**, the former is expected to be nucleophilic, while the latter should be electrophilic. Thus, **1.28** should undergo conjugate addition to **1.26** to afford a radical intermediate, which is trapped by **1.29**. Alternatively, addition of electrophilic radical **1.29** precedes that of **1.28**; however, due to its electrophilicity the former would be expected to add to the O-atom of enone affording a π-allyl radical, which is then trapped by **1.28**.

In all aforementioned mechanistic manifolds the reaction is expected to be amenable to development of the corresponding enantioselective protocol, as the NHC ligand is directly involved in C-B bond-forming process.

1.3.2.2. *Experimental Confirmation of the Hypotherical Direct Activation of Diboron Compounds with N-Heterocyclic Carbenes*

To confirm our hypothesis we treated cyclohexenone to $B_2(pin)_2$ in the presence of various Lewis bases as shown in Table 1.11. In case of NHCs the Brønsted base was used to deprotonate an imidazolium or an imidazolinium salt to liberate the free Lewis basic carbene.

Table 1.11. Lewis Base-catalyzed Conjugate Addition of Boron to Cyclohexenone[a]

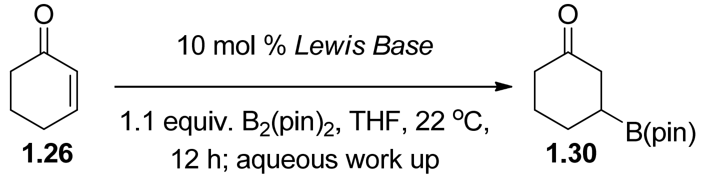

entry	*Lewis Base*[c]	*Brønsted Base* (mol %)	*conv* (%)[b]
1	SIMes·HCl	NaO*t*-Bu (10)	66
2	IMes·HCl	NaO*t*-Bu (10)	92
3	IPr·HCl	NaO*t*-Bu (10)	45
4	ICy·HBF_4	NaO*t*-Bu (10)	>98
5	*none*	NaO*t*-Bu (10)	<2
6	PPh_3	*none*	<2
7	PCy_3	*none*	<2
8	$OPPh_3$	*none*	50

[a] All reactions were performed under dry N_2 atmosphere. [b] Conversion to product was determined by analysis of 400 MHz ^1H NMR spectra of crude reaction mixtures. [c] For explanation of the nomenclature for naming simple NHCs see Ref 42.

As shown in Table 1.11, Brønsted bases such as NaO*t*-Bu are not adequate activators for $B_2(pin)_2$ (entry 5). However, the Lewis bases that are not strong π-acids are capable of catalyzing the reaction. As described in section 1.2, the phosphines are relatively stronger π-acids than imidazolylidenes, which in turn are stronger π-acids than imidazolinylidenes. The conversions are described well by the two main factors: π-acidity of Lewis bases and their steric bulk. The Lewis bases that require a significant contribution from π-back donation in order to form an adduct do not catalyze this reaction. For example, as shown in entries 6 and 7 (Table 1.11), PPh_3 and PCy_3 are unlikely to coordinate to $B_2(pin)_2$, as phosphines exhibit significant π-acidity in their complexes, and thus the sole π-basic orbital – the B-B bond – is insufficient to stabilize the phosphine-boron adduct. On the other hand the weaker π-acidity NHCs allows them to form complexes even when the frontier π-basic orbitals are lacking,[59] and thus complexation is possible for NHCs and boranes that are even mildly Lewis acidic. The reaction efficiency is dependent on the π-acidity of an NHC; for example, *N*,*N*'-dimesitylimidazolylidene (IMes) outperforms *N*,*N*'-dimesitylimidazolinylidene (SIMes) (entries 1 and 2), as the former is less π-acidic than the latter and thus the complexation to $B_2(pin)_2$ of the former is expected to be thermodynamically more favored that that of the latter. Indeed, π-acidity of IPr is comparable to that of SIMes as judged by the Tolman electronic parameters, which is 2051.5 for both of them,[69] and thus the reaction efficiencies are relatively similar with IPr exhibiting lower reactivity due to its relatively higher steric bulk (entries 1 and 3). Among the examined Lewis bases the best catalyst was ICy (entry 4), which is the least π-acidic ligand among the NHCs and phosphines in the current study. Imidazolinylidenes are better net charge donors than the corresponding imidazolylidenes (see section 1.2). The aforementioned polarization of B-B bond would be expected to be more pronounced for the imidazolinylidenes than for imidazolylidenes.

It is notable that phosphine oxides are sufficiently powerful donors for activation of $B_2(pin)_2$ towards conjugate addition to an enone (entry 8, Table 1.11). Hosomi and co-workers reported that n-Bu_3P is capable of catalyzing conjugate boron addition in the absence of Cu salts (7% yield after 12 h).[113] As a solvent in this reaction DMF was employed, purification of which did not include deoxygenation.[114] Thus, the possibility of phosphine oxide *in situ* formation should not be ruled out. Recently, Fernández and co-workers reported phosphine-catalyzed conjugate addition of boron ($B_2(pin)_2$) to enoates.[115] It was found that phosphines are capable of catalyzing this reaction in the

---

(113) Ito, H.; Yamanaka, H.; Tateiwa, J.; Hosomi, A. *Tetrahedron Lett.* **2000**, *41*, 6821-6825.

(114) Common purification procedure for DMF includes distillation from drying agents, and no deoxygenation procedure is involved: Burfield, D. R.; Smithers, R. H. *J. Org. Chem.* **1978**, *43*, 3966-3968.

(115) Bonet, A.; Gulyás,, H.; Fernández, E. *Angew. Chem. Int. Ed.* **2010**, *49*, 5130-5134.

presence of methanol and base such as Cs_2CO_3. To ascertain that the transformation is not catalyzed by metal impurities present in the Brønsted basic salt, they compared enantioselectivities of the reactions in the presence and absence of transition metal salts such as $Fe(acac)_2$, CuCl, and $NiCl_2$. The change in enantioselectivities between the reactions carried out either in the presence of the absence of the metal salts indicated that in the latter case the reactions were not catalyzed by transition metal impurities that are present in Cs_2CO_3. However, the conjugate boron addition reaction in table 1.11 is carried out with achiral ligands and thus approaches based on observing changes in stereoselectivities are not applicable. Although NaO*t*-Bu was found to be inactive as a catalyst for the reaction (*i.e.* the impurities present in it do not catalyze the reaction either), it is possible that one of the metal impurities in NaO*t*-Bu requires the presence of a Lewis basic ligand such as NHC to become an efficient catalyst for the reaction. Thus, we reasoned that the importance of transition metal impurities in NaO*t*-Bu could be tested by varying the amount of NaO*t*-Bu with respect to that of the imidazolium salt while maintaining the net amount of the resulting free carbene constant. As shown in Scheme 1.5, the reaction of conjugate addition of boron to isophorone showed no dependence on the excess amount of either NaO*t*-Bu or imidazolium salt.

Scheme 1.5. Dependence of the Efficiency of Conjugate Addition of Boron on the Excess of the Ligand or the Brønsted Base[a]

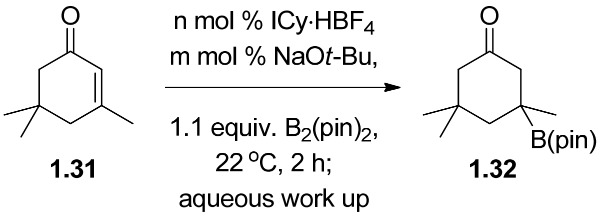

1.31 **1.32**

entry	*n*	*m*	*conv* (%)[b]
1	5	5	50
2	10	5	58
3	5	10	56

[a] All reactions were performed under dry N_2 atmosphere. [b] Conversion to product was determined by analysis of 400 MHz ^1H NMR spectra of crude reaction mixtures.

The synthetic utility of this reaction can be seen in the scope of the reaction as shown in Table 1.12. Conjugate addition of boron to various cyclic and acyclic enones, enoates, lactones, including sterically hindered substrates is readily promoted by ICy.

Table 1.12. Substrate Scope of Lewis Base-catalyzed Conjugate Addition of Boron to Enones and Enoates[a]

entry	*substrate*	*product*		*catalyst loading* (%)[b]	*time* (%)	*conv* (%)[c]
1	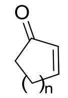	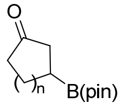	n = 1 (**1.33**)	2.5	1	>98 (93)
2			n = 2 (**1.34**)	2.5	1	>98 (91)
3			n = 3 (**1.35**)	2.5	1	>98 (93)
4			n = 4 (**1.36**)	2.5	1	>98 (89)
5	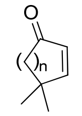	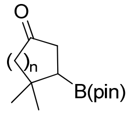	n = 1 (**1.37**)	2.5	1	>98 (97)
6			n = 2 (**1.38**)	2.5	1	>98 (98)
9[d]	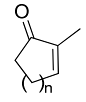	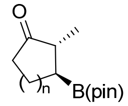	**1.39**	2.5	1	>98 (88)
10[e]	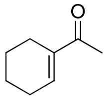	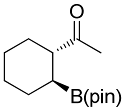	**1.40**	2.5	1	>98 (90)
11	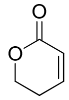	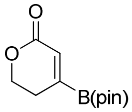	**1.41**	5.0	24	>98 (95)
12	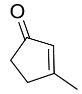	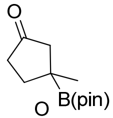	**1.42**	2.5	12	>98 (91)
13	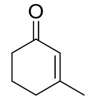	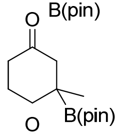	**1.43**	2.5	6	>98 (96)
14	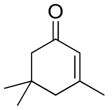	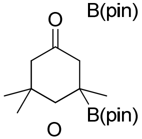	**1.32**	2.5	12	73 (69)
15	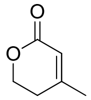	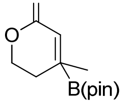	**1.44**	5.0	24	56 (44)
16[f]	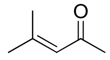	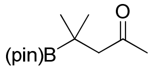	**1.45**	5.0	6	(92)
17	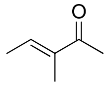	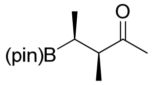	**1.46**	2.5	1	(>98)
18	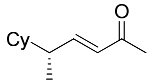	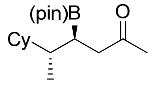	**1.47**	10.0	2	(70)
19	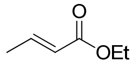	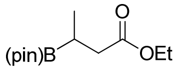	**1.48**	5.0	24	(93)

[a] All reactions were performed under dry N_2 atmosphere with dry, degassed THF as a solvent. [b] Catalyst loading is measured as the number of mol % of ICy, generated from ICy·HBF_4 and NaO*t*-Bu. [c] Conversion to product was determined by analysis of 400 MHz ^1H NMR spectra of crude reaction mixtures. Isolated yields are given in parantheses. [d] dr - 1.6:1. [e] dr = 7.1:1. [f] The reaction was performed at 0 °C.

As stated above the Cu-catalyzed protocol for conjugate addition of boron to α,β-unsaturated carbonyls suffers from limitations due to functional group compatibility. The present method was compared to the above mentioned protocol as shown in Scheme 1.6.

Scheme 1.6. Comparison of NHC-catalyzed Conjugate Addition of Boron to Enones to the Corresponding Cu-catalyzed protocol[a]

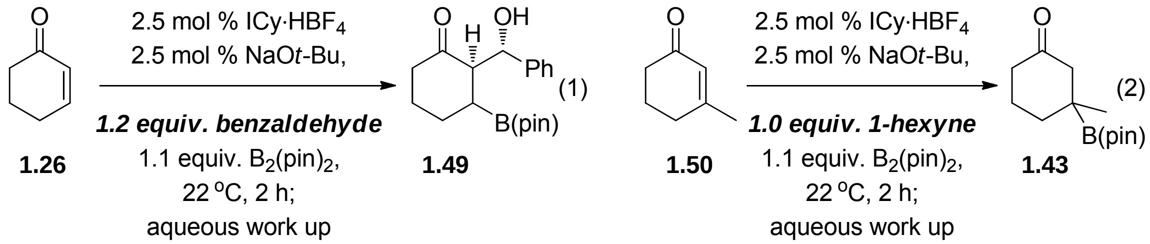

***with 2.5 mol % CuOt-Bu: 31% yield of 1.49**[b]*

without Cu salt: 85% yield (>98:2 dr)

with 2.5 mol % CuOt-Bu: <2% conv

without Cu salt: 85% conv, 81% yield

[a] All reactions were performed under dry N_2 atmosphere. [b] In addition to **1.49**, benzaldehyde diboration product (19%) and unidentified byproduct (26%) were isolated.

The reaction in eq 1 confirms that the Lewis base (NHC) catalyzed conjugate boron addition is compatible with aldehydes, as no diboration of benzaldehyde products are observed; however, the corresponding Cu-catalyzed protocol affords the desired product in a diminished yield with other byproducts including the product due to diboration of benzaldehyde. Similarly, eq 2 demonstrates that unlike Cu-catalyzed method ICy is not inhibited by the presence of alkynes.

The method presented herein, indeed, follows the expectation of enhanced functional group compatibility relative to the Cu-catalyzed protocol. However, the question that needs to be answered is which of the two mechanisms in Scheme 1.4 is active or is there another unaccounted for mechanism? Specifically, the question addresses the problem of the C-B bond forming process.

1.3.2.3. Experimental and Theoretical Investigation of the Mechanism of NHC-catalyzed Diboration of α,β-Unsaturated Carbonyls

Consideration of the abbreviated mechanisms given in Scheme 1.4 reveals that testing the radical mechanism can be achieved by means of radical traps;[116] however, the

---

[116] Newcomb, M. *Tetrahedron* **1993**, *49*, 1151-1176.

direction addition mechanism presents a challenge if it entails concerted addition of B-B bond across the enone. It is reasonable to rule out mechanisms involving heterolytic cleavage of the B-B bond to give pinacolatoboryl anion, as the latter would be expected to add to an aldehyde, the product of such a transformation is not observed. Also, boryl anions are known to exhibit poor nucleophilicity and instead tend to act as Brønstead bases towards cyclohexenone.[117] Note that boryl radical (as well as other radicals), on the other hand, does not add to aldehydes due to the fact that π(C-O) bond is strong, and addition of a radical to a carbonyl group at the carbon atom results in the formation of a high-energy oxygen radical.[118] As described above boryl radicals are accessible from NHC-BH_3. Rablen demonstrated that formation of Lewis base adducts of boron compounds tends to result in decreased BDEs of B-X bonds (X = substituent at the boron atom).[119] Renaud and co-workers demonstrated that Lewis bases such as DMPU could be employed to activate catecholatoboranes to effect radical conjugate additions including addition/aldol cascades – a process that is similar to the eq 1 in Scheme 1.6.[120]

Calculations at unrestricted M06L/6-31+G(d,p) level of theory[121] revealed that BDE for $B_2(pin)_2$ is 104.6 kcal/mol and for the corresponding NHC (IMe) adduct it is 62.6 kcal/mol – lower than BDE for B-H bond in NHC-BH_3 complex (*vide supra*) or Sn-H bond in *n*-Bu_3SnH. In light of the data and precedents described above the intermediacy of radicals is plausible. As mentioned above the radical traps are a useful way of confirming the presence of radicals in the reaction mixture. Investigation of the plausibility of a radical mechanism by means of theoretical methods is prohibitive in the

---

(117) Kajiwara, T.; Terabayashi, T.; Yamashita, M.; Nozaki, K. *Angew. Chem. Int. Ed.* **2008**, *47*, 6606-6610.

(118) Yamada, K.; Yamamoto, Y.; Tomioka, K. *Org. Lett.* **2003**, *5*, 1797-1799.

(119) Rablen, P. R. *J. Am. Chem. Soc.* **1997**, *119*, 8350-8360.

(120) (a) Kumli, E.; Montermini, F.; Renaud, P. *Org. Lett.* **2006**, *8*, 5861-5864; (b) Beauseigneur, A.; Ericsson, C.; Renaud, P.; Schenk, K. *Org. Lett.* **2009**, *11*, 3778-3781. For a review on organoboranes as a source of radicals see: (c) Ollivier, C.; Renaud, P. *Chem. Rev.* **2001**, *101*, 3415-3434; (d) Darmency, V.; Renaud, P. *Top. Curr. Chem.* **2006**, *263*, 71-106.

(121) The use of M06 suite of density functionals is advantageous with respect to other DFT methods due to the fact that M06L is corrected for medium range correlations. For the disclosures and a thorough standard benchmarking study of M06 suite of density functionals see: (a) Zhao, Y.; Truhlar, D. G. *J. Chem. Phys.* **2006**, *125*, 194101; (b) Zhao, Y.; Truhlar, D. G. *Theor. Chem. Acc.* **2008**, *120*, 215-241. For a review on M06 suite of density functionals see: (c) Zhao, Y.; Truhlar, D. G. *Acc. Chem. Res.* **2008**, *41*, 157-167.

present case, as theoretical treatment of allyl radicals requires explicit consideration of correlation energies by means of complete active space methods such as CASSCF and CASPT2.[122] These methods are prohibitively expensive from computational standpoint if the π-system of the dioxoborolane unit is included in the active space. Experimental evidence for the presence of radicals in the reaction mixture does not imply that the mechanism for the observed reaction involves radicals, and thus, in light of the impracticality of theoretical methods in treatment of allyl radicals, radical traps should be incorporated into the substrates. As shown in Scheme 1.7, the intermediacy of radicals could be ruled out safely.

Scheme 1.7. Test for Radical Intermediates in NHC-catalyzed Conjugate Addition of Boron to Enones

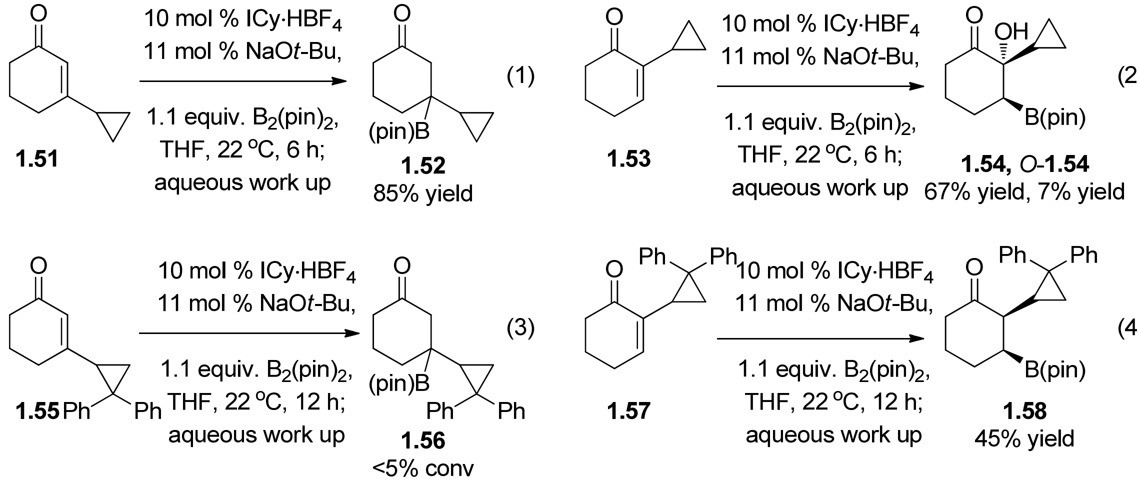

Initially cyclopropyl-cyclohexenones **1.51** and **1.53** were subjected to the reaction conditions shown above, and no cyclopropane ring-opening products were isolated. However, the rate of cyclopropyl-methyl radical rearrangement to butenyl radical is ~3 orders of magnitude below that of diffusion controlled reactions; if the rate of recombination of radical intermediates is at the diffusion limit the amount of ring-opened product is expected to be negligible. Thus, the (diphenyl)-cyclopropyl-cyclohexenones **1.55** and **1.57** were subjected to the same reaction conditions,[123] and similarly no cyclopropane ring-opening products due to the possible presence of boron radical

---

(122) Aquilante, F.; Jensen, K. P.; Roos, B. O. *Chem. Phys. Lett.* **2003**, *380*, 689-698.

(123) (Diphenyl)cyclopropyl-methyl radical rearrangement occurs with rate above that for diffusion-controlled reactions: see Ref. 113.

intermediates were observed. In the case of **1.55** <5% conversion was observed, indicating that β-substituent steric hindrance is detrimental to the reaction efficiency. *i.e.* C_β-B bond formation is crucial to the reaction mechanism. It should be noted that compound **1.58** is air-sensitive and was found to undergo oxidation on silica gel, thus its yields vary. The oxidation product of **1.58** was isolated and its structure (**1.59**) was established by 2D NMR studies and X-ray crystallography.

As radical mechanism was ruled out by the experiments above, the concerted mechanisms need to be considered. As shown in Scheme 1.8 there are two plausible mechanisms that involve concerted formation of C-B bond.

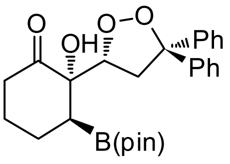

1.59

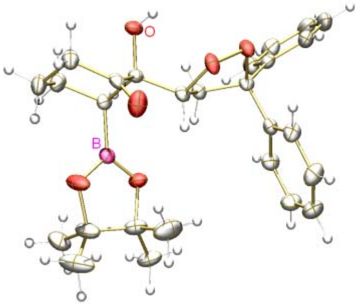

Scheme 1.8. Plausible Mechanisms, Involving Concerted Formation of C-B Bond

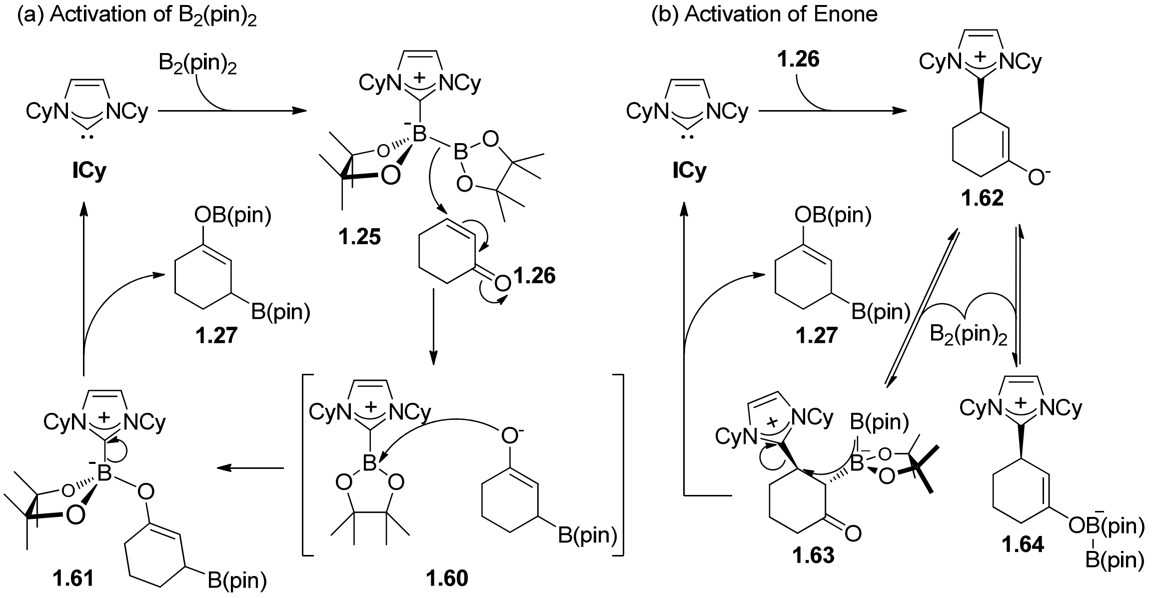
(a) Activation of $B_2(pin)_2$

(b) Activation of Enone

The mechanism (a) is consistent with the one briefly outlined above. Addition of ICy carbene to $B_2(pin)_2$ leads to the adduct **1.25**, which transfers the B(pin) moiety to the enone **1.26** in a concerted fashion, thereby generating the tight ion pair **1.60** that consists of the NHC-borenium ion and the enolate. Recombination of the tight ion pair **1.60** leads to the formation of **1.61**, wherein the B atom is less Lewis acidic than in $B_2(pin)_2$ due to the presence of three π-donors in the former. Thus, decoordination of NHC affords **1.27** and regenerates the free carbene. Within the intermediate **1.60** the NHC-borenium ion can be viewed as an imidazolium salt where the proton was displaced with a B(pin) moiety.[124]

The intermediate **1.60** can be reached through a different pathway (Scheme 1.9). If the bonding within the complex **1.25** is considered it becomes apparent that the sole source of stabilizing π-back donation is $\sigma_{B\text{-}B} \rightarrow p_{C(NHC)}$. If this donation is sufficiently strong the terminal B(pin) moiety may undergo a [1,2]-shift.[125] Bertrand and co-workers reported recently that NHCs and cyclic alkyl amino carbenes (CAAC) are capable to activate H-H, B-H, Si-H, P-H, and P-P bonds.[126] Formally, the reaction between ICy and $B_2(pin)_2$ constitutes an oxidative insertion of C(II), and depending on the mechanism of the reaction **1.60**→ICy+**1.27**, this transformation can be viewed as a reductive elimination.

The mechanism (b) (Scheme 1.8) is based on the proposal by Chenard and co-workers for the cyanide-catalyzed silastannylation of enones[127] and by Parrain and co-workers for NHC-catalyzed silastannylation of aldehydes.[128] Unlike mechanism (a) the mechanism (b) entails activation of the electrophile through conjugate addition of the ICy carbene to the enone **1.26**, the resulting enolate undergoes reversible coordination of

---

(124) For examples of a stable NHC-borenium ion see: (a) Matsumoto, T.; Gabbaï, F. P. *Organometallics* **2009**, *28*, 4252-4253; (b) Tsai, J. –H.; Lin, S. –T.; Yang, R. B. –G.; Yap, G. P. A.; Ong, T. –G. *Organometallics* **2010**, *29*, 4004-4006.

(125) For example, d^0-transition metals such as Zr(IV) were found to transfer alkyl groups to C_{NHC} affording zirconio-aminals, see: Romain, C.; Miqueu, K.; Sotiropoulos, J. –M.; Bellemin-Laponnaz, S.; Dagorne, S. *Angew. Chem. Int. Ed.* **2010**, *49*, 2198-2201.

(126) For the example of activation of H_2 by CAACs see: (a) Frey, G. D.; Lavallo, V.; Donnadieu, B.; Schoeller, W. W.; Bertrand, G. *Science* **2007**, *316*, 439-441. For examples of P-P bond activation by NHCs see: (b) Masuda, J. D.; Schoeller, W. W.; Donnadieu, B.; Bertrand, G. *J. Am. Chem. Soc.* **2007**, *129*, 14180-14181. For examples of activation of B-H, Si-H, and P-H bonds by NHCs see: (c) Frey, G. D.; Masuda, J. D.; Donnadieu, B.; Bertrand, G. *Angew. Chem. Int. Ed.* **2010**, *49*, 9444-9447.

(127) For cyanide-catalyzed silastannylation of enones see: (a) Chenard, B. L.; Laganis, E. D.; Davidson, F.; RajanBabu, T. V. *J. Org. Chem.* **1985**, *50*, 3667-3669. For conjugate addition of tin reagents in basic media to α,β-unsaturated carbonyls see: Schmidt, R. K.; Oestreich, M. *Synlett* **2008**, *11*, 1690-1692.

(128) For NHC-catalyzed silastannylation of aldehydes see: (a) Blanc, R.; Commeiras, L.; Parrain, J. –L. *Adv. Synth. Catal.* **2010**, *352*, 661-666. For cyanide-catalyzed silastannylation of aldehydes see: (b) Bhatt, R. K.; Ye, J.; Falck, J. R. *Tetrahedron Lett.* **1994**, *35*, 4081-4084.

Scheme 1.9. Oxidative Insertion of NHC to B-B Bond

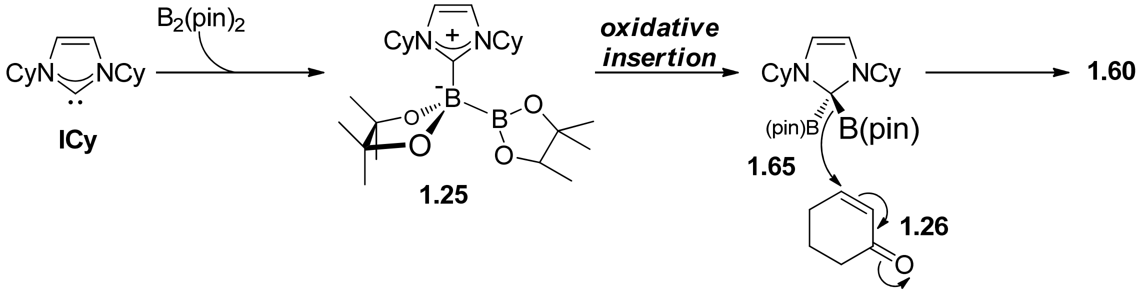

$B_2(pin)_2$ at either carbon atom (**1.63**) or oxygen atom (**1.64**). Although the latter is more stable thermodynamically, it cannot undergo the shift of the B(pin) moiety to the β-carbon, to which the NHC is bound. On the other hand the compound **1.63** is capable of undergoing the B(pin) moiety transfer to displace ICy in a reaction that constitutes an intramolecular S_N2 reaction. Note that *this transformation does not constitute a [1,3] shift – formally forbidden by Woodward-Hoffmann rules*, because these rules apply to rearrangements across π-systems where phasing of the wavefunction determines whether a shift is suprafacial or antarafacial. Nonetheless, the mechanism (b) was ruled out on the grounds that no transition state was located for the shift.

In order to confirm the assignment of the structure for NHC-$B_2(pin)_2$ adduct as **1.25** the calculated ^{11}B NMR spectra were correlated to the experimental ones.[129] As shown in Figure 1.21, the calculated ^{11}B NMR chemical shifts for **1.25** are almost equal to the experimental chemical shifts; this correlation provides theoretical support for the structure of **1.25**. The B-B bond elongation in $B_2(pin)_2$ upon coordination of ICy is indicative of the bond weakening, which is consistent with calculated BDE values (*vide supra*) and Rablen's observation that B-X bonds are weakened upon coordination of a Lewis base to the boron atom.[119] The electronic reorganization within the B-B bond is evident from the APT charges of boron atoms: significant charge transfer is observed from ICy to $B_2(pin)_2$, in which the sp^2-hybridized boron atom benefits from the inflow of the electron density more than the sp^3-boron atom. The latter observation can be

---

(129) ^{11}B NMR spectra were calculated at M06L/6-311++G(2df,2p)//M06L/6-31+G(d,p) level of theory including the correction due to solvation with tetrahydrofuran (polarized continuum model with united atom topological model scaled Kohn-Sham radii, $\alpha = 1.1$). For a review on polarizable continuum solvation models see: Tomasi, J.; Mennucci, B.; Cammi, R. *Chem. Rev.* **2005**, *105*, 2999-3093.

Figure 1.21. ^{11}B NMR and Geometric Data for $B_2(pin)_2$ and its Adduct with ICy

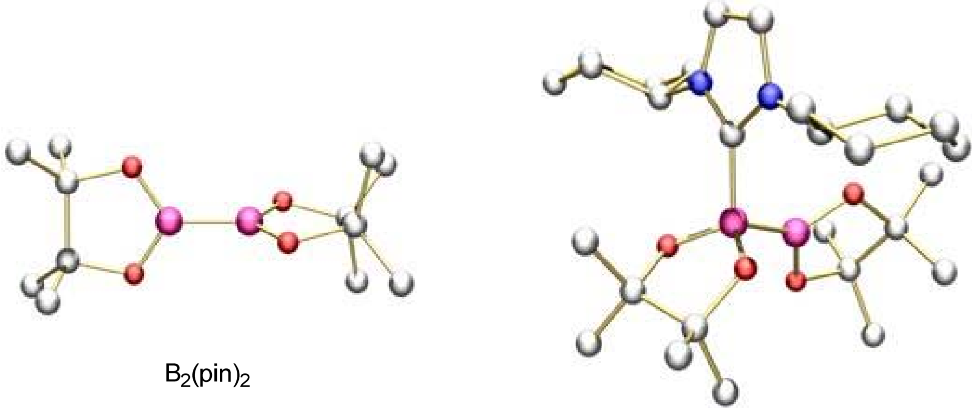

$B_2(pin)_2$

1.25

APT charge on B:	***+0.923***	***+0.848***	***+0.772***
B-B length (Å):	***1.688***	***1.738***	
Experimental ^{11}B NMR:	***30.1***	***36.3***	***1.8***
Calculated ^{11}B NMR:	***30.1^{a}***	***36.2***	***0.8***

^{a} The calculated chemical shifts for **1.25** are relative to the calculated chemical shifts for $B_2(pin)_2$, which were set to equal the experimental ^{11}B NMR chemical shift of $B_2(pin)_2$.

rationalized by the fact that sp^3-hybrid is less electronegative than the sp^2-hybrid, and thus B-B bond is polarized towards the sp^2-hybridized boron atom, as described above.

The plausible mechanism (a) in Scheme 1.8 including the pathway shown in Scheme 1.9 was analyzed computationally with focus on the C-B bond forming event. The calculated reaction energy diagram is shown in Figure 1.22.[130]

The calculations were carried out on a model system (see supporting information); thus, the structures shown in Figure 1.22 are shown to emphasize their relevance to the mechanistic discussion above. Coordination of ICy to $B_2(pin)_2$ is exoergic with ΔG^{o}_{298} = -5.4 kcal/mol, which is consistent with the observation that all $B_2(pin)_2$ is consumed in the stoichiometric reaction between the NHC and $B_2(pin)_2$. The insertion transition state **1.65TS** is lower in energy ($\Delta G^{\ddagger}_{298}$) than the transition state **1.60-TS1**; however, the enthalpies and ZPE-corrected energies indicate that **1.65TS** is higher in energy than either of the C-B bond-forming transition states **1.60TS-1** or **1.60TS-2**.

---

[130] All geometries and energies are at M06L/6-31+G(d,p) level of theory.

This difference in calculated Gibbs free energies and enthalpies is due to the fact that the C-B bond forming process is bimolecular and thus significant entropic contribution renders the transition states **1.60TS-1** and **1.60TS-2** higher in energy than **1.65TS**. The net process of C-B bond forming process is exoergic, as indicated by Gibbs free energies

Figure 1.22. Reaction Energy Diagram[a]

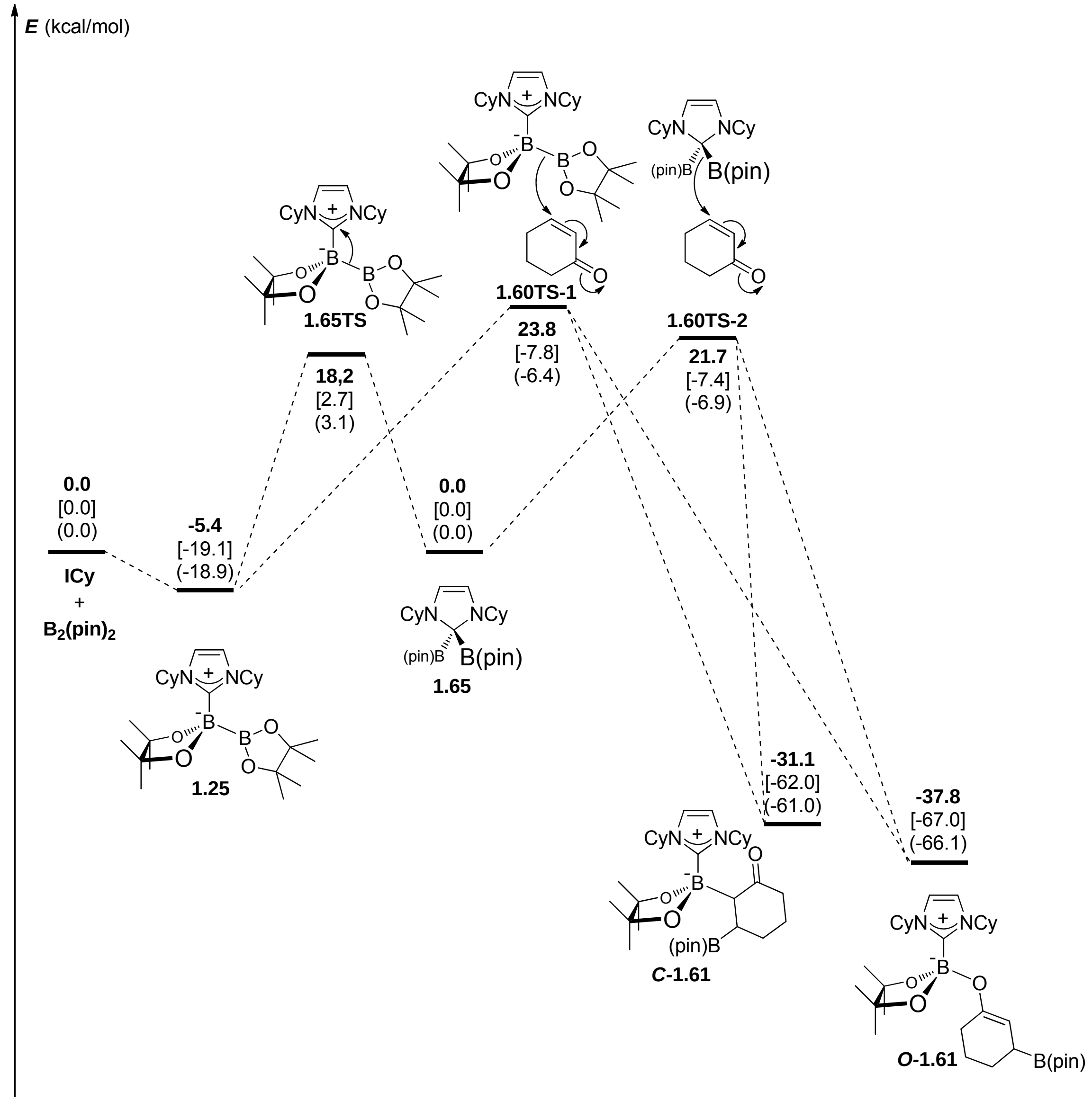

[a] All energies are in kcal/mol. The values in **bold** are relative Gibbs free energies, the values in brackets are enthalpies, the values in parantheses are ZPE-corrected electronic energies.

of ***C*-1.61** and ***O*-1.61**. Subsequent decoordination of ICy affords the *C*-bound boronate or **1.27**, where the latter can be obtained from the former by a [1,3]-borotropic shift.[131]

The attempts to account for solvation by means of the single point energy calculations including implicit solvation model (IEFPCM)[129] on gas-phase geometries gave unreasonably high Gibbs free energies for transition states **1.60TS-1** and **1.60TS-2** ($\Delta G^{\ddagger}_{298}$ values are 34.3 and 31.9 kcal/mol, respectively), even though the charge-separation in these transition states was expected to be stabilized relative to **1.25** by inclusion of solvation energies.

The reactions described herein were found to benefit from the presence of protic co-solvent.[132] It is likely that protic co-solvent (methanol) serves to relieve the developing negative charge at the oxygen atom of the carbonyl group through hydrogen bonding. Indeed, inclusion of a single water molecule (model for a molecule of methanol) resulted in a substantial decrease in enthalpy of activation $\Delta H^{\ddagger}$ for transition states **1.60TS-1** and **1.60TS-2**: -19.0 kcal/mol and -15.1 kcal/mol, respectively. Gibbs free energies, however, remained approximately the same (21.5 kcal/mol and 23.0 kcal/mol, respectively) due to higher entropic contribution.[133] Because methanol is a co-solvent the entropic contribution due to inclusion of a molecule of solvent in a transition state is not expected to be as large. Thus, enthalpies are likely to provide a better energy descriptor in this case.

The geometries of the transition states **1.60TS-1** and **1.60TS-2** deserve particular attention. As shown in Figure 1.23, the transition state structure **1.60TS-1** is more advanced than the transition state **1.60-TS2** as evidenced by the bond lengths in cyclohexenone that are more enolate-like for the former and the nascent C-B bond lengths (cf. $r_{C\text{-}B}$ in ***C*-1.61** and ***O*-1.61** is 1.564Å). Thus, due to its more advanced nature the transition state **1.60TS-1** is expected to be more sensitive to the sterics of the enone;

---

(131) (a) Brown, H. C.; Rogić, M M.; Rathke, M. W. *J. Am. Chem. Soc.* **1968**, *90*, 6218-6219; (b) Bai, J.; Burke, L. D.; Shea, K. J. *J. Am. Chem. Soc.* **2007**, *129*, 4981-4991. For a theoretical study of borotropic shifts see: (c) Ibrahim, M. R.; Bühl, M.; Knab, R.; Schleyer, P. V. R. *J. Comput. Chem.* **1992**, *13*, 423-428.

(132) Wu, H. *Unpublished Results*.

(133) Because calculations are carried out in the gas phase, the cost of bringing each additional molecule into a transition state results in a significant decrease in entropy.

orientation of the NHC in the transition state is also indicative of potentially significant steric interactions between the *N*-substituents of the NHC and the enone or enoate. Thus, overall contribution due to the transition state **1.60TS-2** is likely to be more pronounced in the case of the experimental systems such as the ones shown above.

Figure 1.23. Transition State Structures **1.60TS-1** (a) and **1.60TS-2** (b)[a,b]

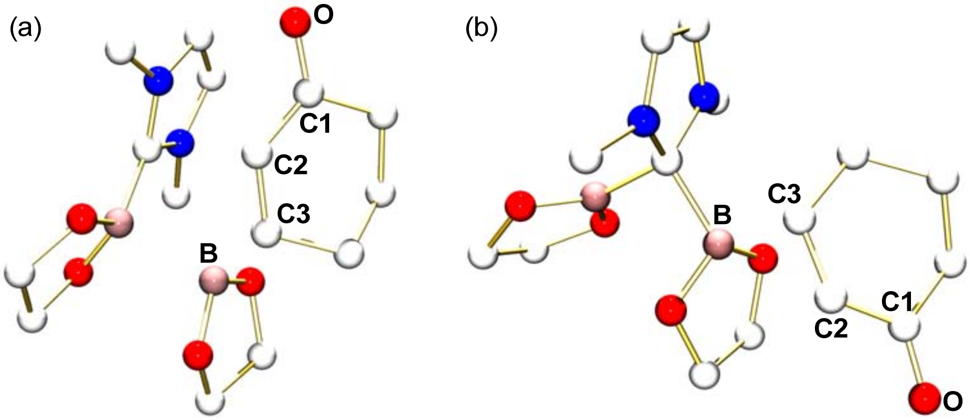

[a] Hydrogen atoms were eliminated for clarity. [b] Key bond lengths: (a) C1-O: 1.253Å; C1-C2: 1.426Å; C2-C3: 1.415Å; C3-B: 1.867Å; (b) C1-O: 1.237Å; C1-C2: 1.450Å; C2-C3: 1.384Å; C3-B: 2.034Å.

A particularly interesting experimental observation described above is that the ICy-$B_2(pin)_2$ adduct was found to be inert to aldehydes. The expectation of the inertness of these adducts to aldehydes was pinned on the proposal that secondary orbital interactions were expected to be responsible for the higher barrier of addition to strongly electrophilic carbonyl groups (Scheme 1.4). However, the resulting difference in energies is not evident *a priori*. Thus, transition states for 1,2-addition to cyclohexenone and to benzaldehyde were calculated (Figure 1.24). In both cases, the transition state energies are higher than the corresponding transition states for conjugate addition of boron. However, the Gibbs free energy of boron addition to benzaldehyde appears to be relatively close to that of conjugate boron addition to cyclohexenone (Figure 1.22). The energy difference is sufficient to ensure that no benzaldehyde diboration occurs under the reaction conditions in the presence of an enone. Note that no transition states were located for 1,2-additions to either cyclohexenone or benzaldehyde with **1.65**.

Relatively higher electrophilicity of the carbonyl of benzaldehyde is detrimental to the efficiency of the reaction with the activated $B_2(pin)_2$. However, as evidenced by the fact that the transition state energy remains reasonably low, it is possible that electronic modifications of an aldehyde or utilization of an imine as a substrate may result in an efficient reaction at ambient temperature. Future developments in this area may thus involve 1,2-additions of $B_2(pin)_2$ to imines.

Figure 1.24. Reaction Energy Diagram[a]

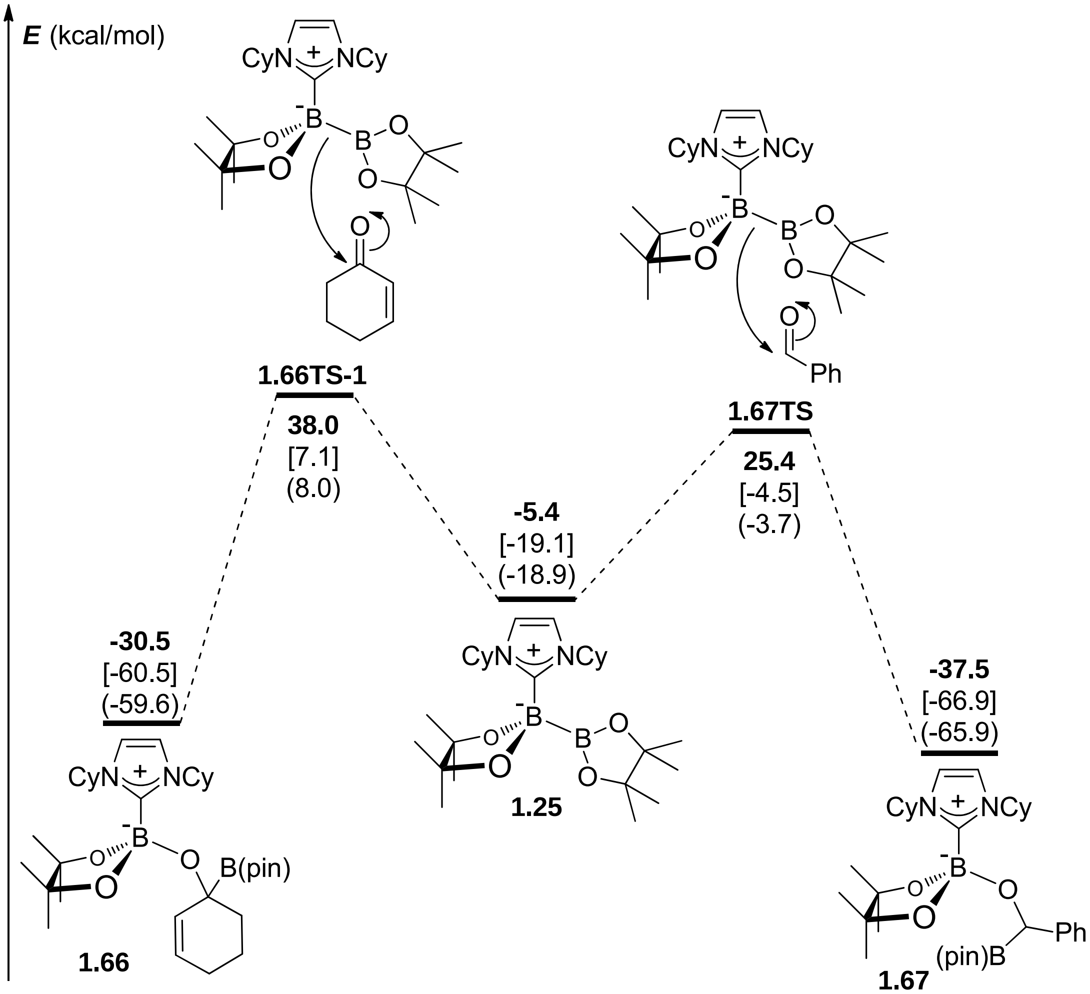

[a] All energies are in kcal/mol. The values in **bold** are relative Gibbs free energies, the values in brackets are enthalpies, the values in parantheses are ZPE-corrected electronic energies.

1.3.2.4. Experimental and Theoretical Investigation of the NHC-catalyzed Silaboration of α,β-Unsaturated Carbonyls

The method described in section 1.3.2.2. is not limited to activation of diboron compounds; the experimental studies in our group demonstrated that borosilane DMPS-Bpin is also capable of being activated for the purpose of addition to *α,β*-unsaturated carbonyls. Curiously, only products due to conjugate addition of Si were observed in all examined cases.[134]

Scheme 1.10. Activation of DMPS-Bpin with NHC

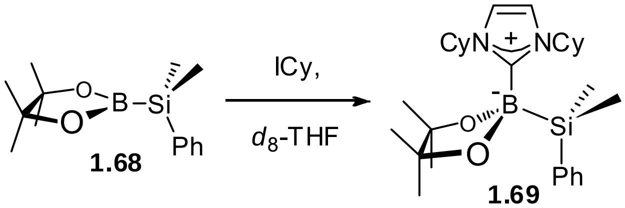

As was observed for **1.25**, the BDE$_{\text{B-Si}}$ for **1.69** (48.4 kcal/mol) was lower than for DMPS-Bpin **1.68** (88.6 kcal/mol). Given the small BDE$_{\text{B-Si}}$ value for **1.69**, the radical mechanism is plausible. Formation of **1.69** was observed by ^{11}B NMR (Scheme 1.10, see supporting information), indicating that this complex is a plausible intermediate. Thus, the presence of radical intermediates was ruled out by means of test reactions with substrates with embedded fast radical traps (Scheme 1.11). Similarly to conjugate boron addition reactions, the addition of Si is also sensitive to steric hindrance at C$_{\beta}$ atom, reaffirming the importance of C$_{\beta}$-Si bond formation to the overall transition state energy.

Scheme 1.11. Test for Radical Intermediates in NHC-catalyzed Conjugate Addition of Silicon to Enones

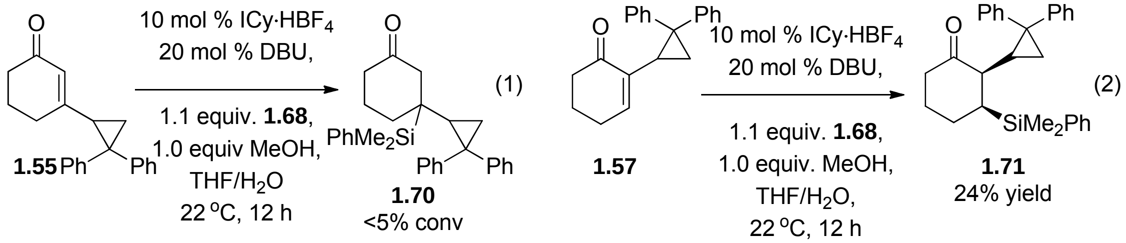

The plausible concerted mechanism for conjugate silicon addition was calculated (Figure 1.25). Note that all attempts at finding structures for NHC coordination to the Si-center of DMPS-Bpin **1.68** proved unsuccessful, as NHC was observed to migrate

---

[134] Lee, K. *PhD Thesis*, Boston College, 2011.

spontaneously from the Si center to the B center. Also, key C-Si bond forming transition state involving borosilane could not be located for mechanism (b) in Scheme 1.8.

As shown in Figure 1.25, formation of the complex **1.69** is exoergic both in the gas phase and in solution phase (with polarized continuum model of solvation). The silaboryl-aminal **1.72** is significantly higher in energy than **1.69**. However, the transition state **1.72TS** is significantly lower in energy than either one of the C-Si bond forming transition states **1.73TS-1** and **1.73TS-2**. Thus, the reaction is likely to be under Curtin-Hammett control. Unlike the case of the diboration reaction described above, where no stationary point was found for the tight ion pair, the silicon conjugate addition reaction boasts of a tight ion pair as a reaction intermediate – **1.73**. The barrier for the recombination of ions is expected to be negligible, as this process would result in the

Figure 1.25. Reaction Energy Diagram[a]

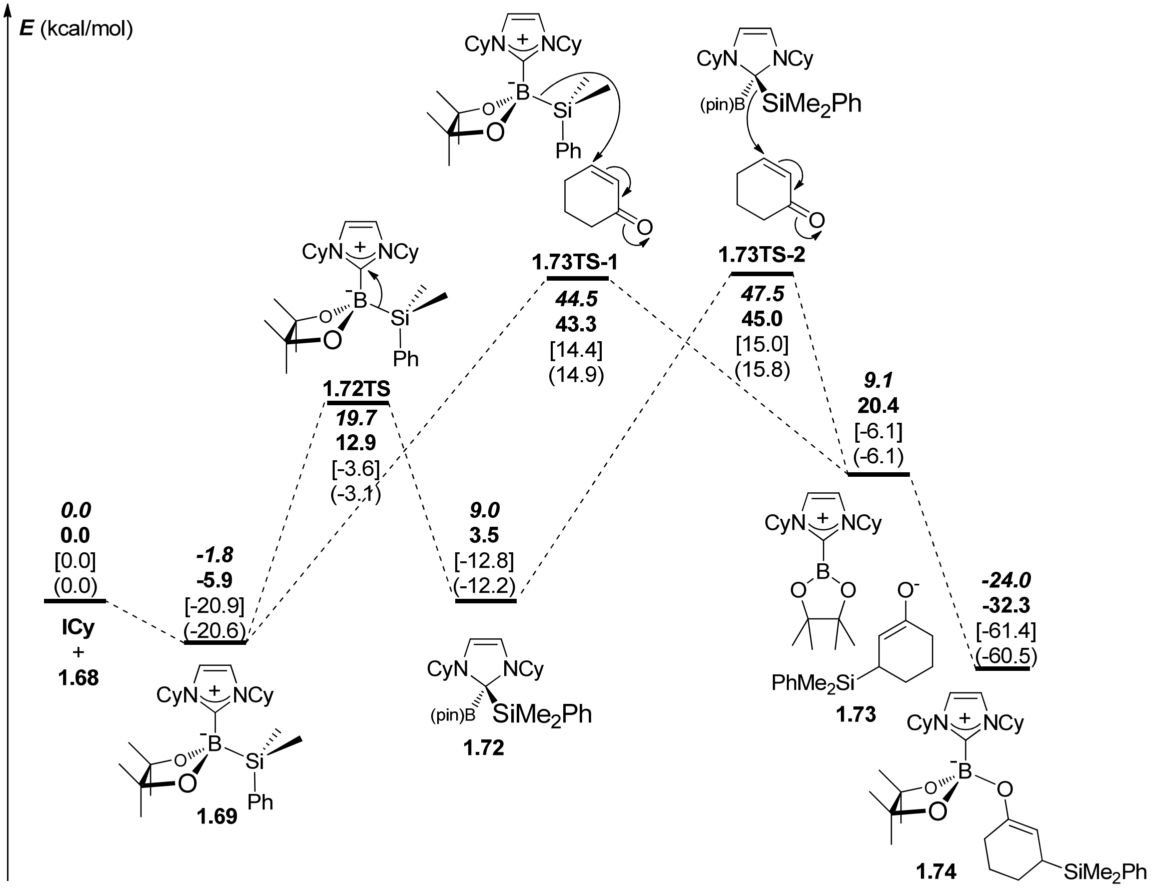

[a] All energies are in kcal/mol. The values in ***italicized bold*** are relative Gibbs free energies, including solvation energies. The values in **bold** are relative gas-phase Gibbs free energies, the values in brackets are gas-phase enthalpies, the values in parantheses are gas-phase ZPE-corrected electronic energies.

formation of a bond and disappearance of the charge separation. The energy of the intermediate **1.73** is significantly lowered when solvation energies are included (8.8 kcal/mol in the latter case *vs* 20.4 kcal/mol in the former case). Recombination of the ionic fragments of the tight ion pair **1.73** affords **1.74** and significantly lowers the energy of the system.

The transition state energies **1.73TS-1** and **1.73TS-2** indicate that the process should be practically unobservable at ambient temperature. Indeed, the reaction conditions necessitate the presence of superstoichiometric quantities of water and methanol.[135] Because formation of the C-Si bond in transition states **1.73TS-1** and **1.73TS-2** results in the formation of a "naked" enolate within the tight ion pair **1.73**, it is possible that protic additives effectively stabilize the developing negative charge at the oxygen atom of the carbonyl of the enone.

As shown in Figure 1.26, the relative Gibbs energies for transition states **1.75TS-1** and **1.75TS-2** have either decreased slightly or even increased due to incorporation of water. Inclusion of polarized continuum solvation models results in further increase in Gibbs free energies. However, the ZPE-corrected electronic energies and enthalpies have decreased nearly two-fold as a result of inclusion of water. The relative increase in Gibbs free energies is likely due to significant negative entropic contribution, which is increased because of incorporation of a fourth molecule in the transition state. However, given the relative concentration of water and methanol in the reaction solution, the reaction would be expected to be pseudo zero order in the protic additive and thus its contribution to the entropy of the transition state should be minimal. It is thus reasonable to assume that enthalpies and ZPE-corrected electronic energies are superior descriptors in this particular reaction system. Furthermore, polarized continuum solvation models may not be adequate at describing the solvation of the intermediates and the transition states in this case; however, explicit inclusion of tetrahydrofuran in calculations is prohibitively expensive from the computational standpoint. The limitations of implicit solvation models are discussed elsewhere.[7b]

---

(135) O'Brien, J. *Unpublished Results*.

Upon formation of the tight ion pair **1.75** immediate protonation of the resulting enolate is most likely to ensue, and the resulting NHC-borenium ion is trapped with the hydroxide or methoxide ion, thus liberating the free NHC. Indeed, experimental studies demonstrate that boron enolate is not formed under these reaction conditions as no reaction was observed with benzaldehyde.[135] However, NHC was found to catalyze addition of **1.68** to benzaldehyde, which is in contrast to the experimental observations in conjugate addition of boron to *α,β*-unsaturated carbonyls (see section 1.3.2.3). Transition

Figure 1.26. Reaction Energy Diagram[a]

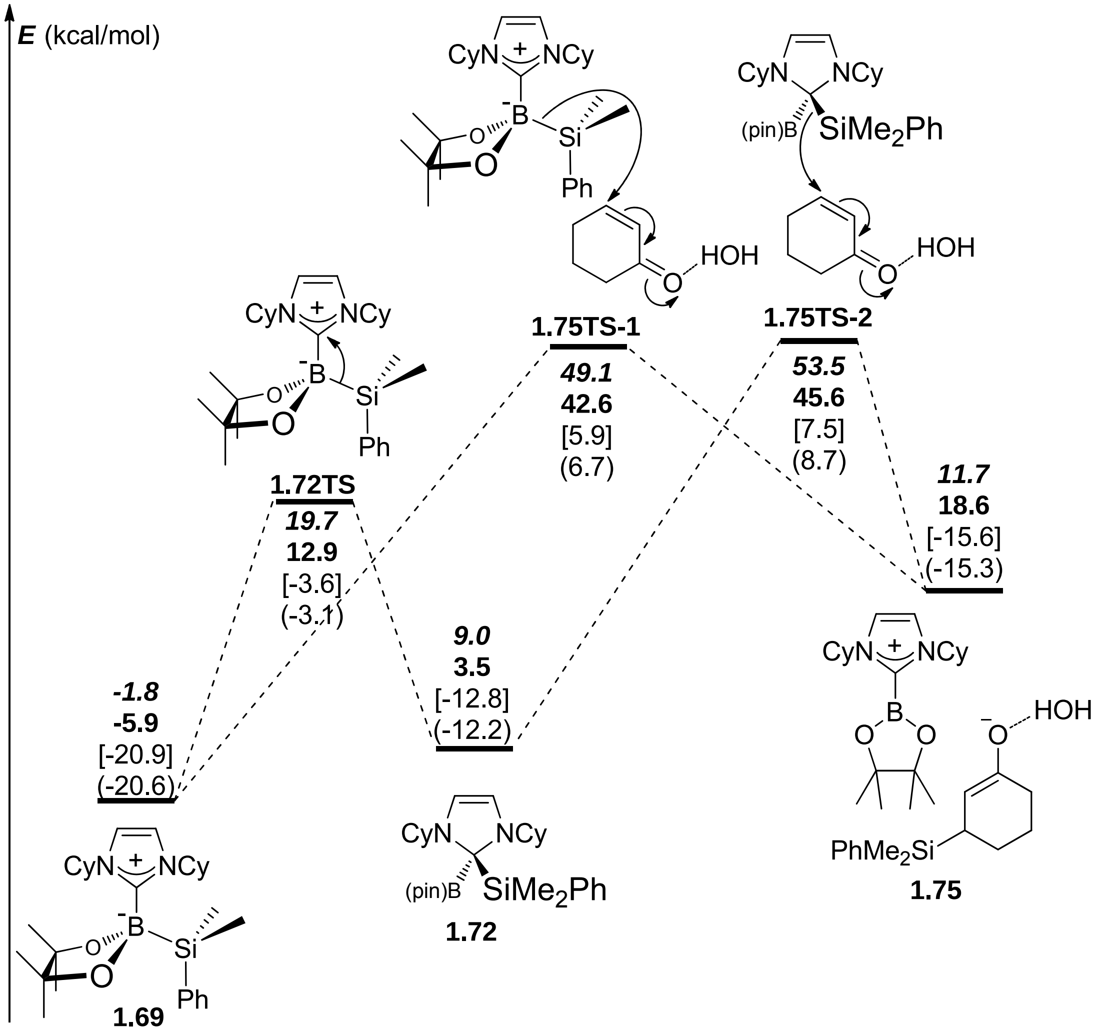

[a] All energies are in kcal/mol. The values in ***italicized bold*** are relative Gibbs free energies, including solvation energies. The values in **bold** are relative gas-phase Gibbs free energies, the values in brackets are gas-phase enthalpies, the values in parantheses are gas-phase ZPE-corrected electronic energies.

states for silicon addition to benzaldehyde were calculated as shown in Figure 1.27. Although the Gibbs free energy of the transition state **1.76TS** is relatively high (40.9 kcal/mol in the gas phase), it is comparable to the transition state energies **1.73TS-1** and **1.73-TS2**. Similarly, the enthalpies and ZPE-corrected electronic energies are relatively close to those of gas phase transition states for conjugate addition of silicon (Figure 1.25).

The geometries of the transition states shown in Figures 1.25, 1.26, and 1.27 are shown in Figure 1.28. The transition state structure **1.72TS**, which effectively constitutes an oxidative insertion of C_{NHC}(II) to B-Si bond, can be viewed as a result of migration of the silyl group due to the overlap of the B-Si bond with the partially occupied p-orbital of the C_{NHC} center. The pinacolatoborolane ring is coplanar with that of the NHC, while the

Figure 1.27. Reaction Energy Diagram[a]

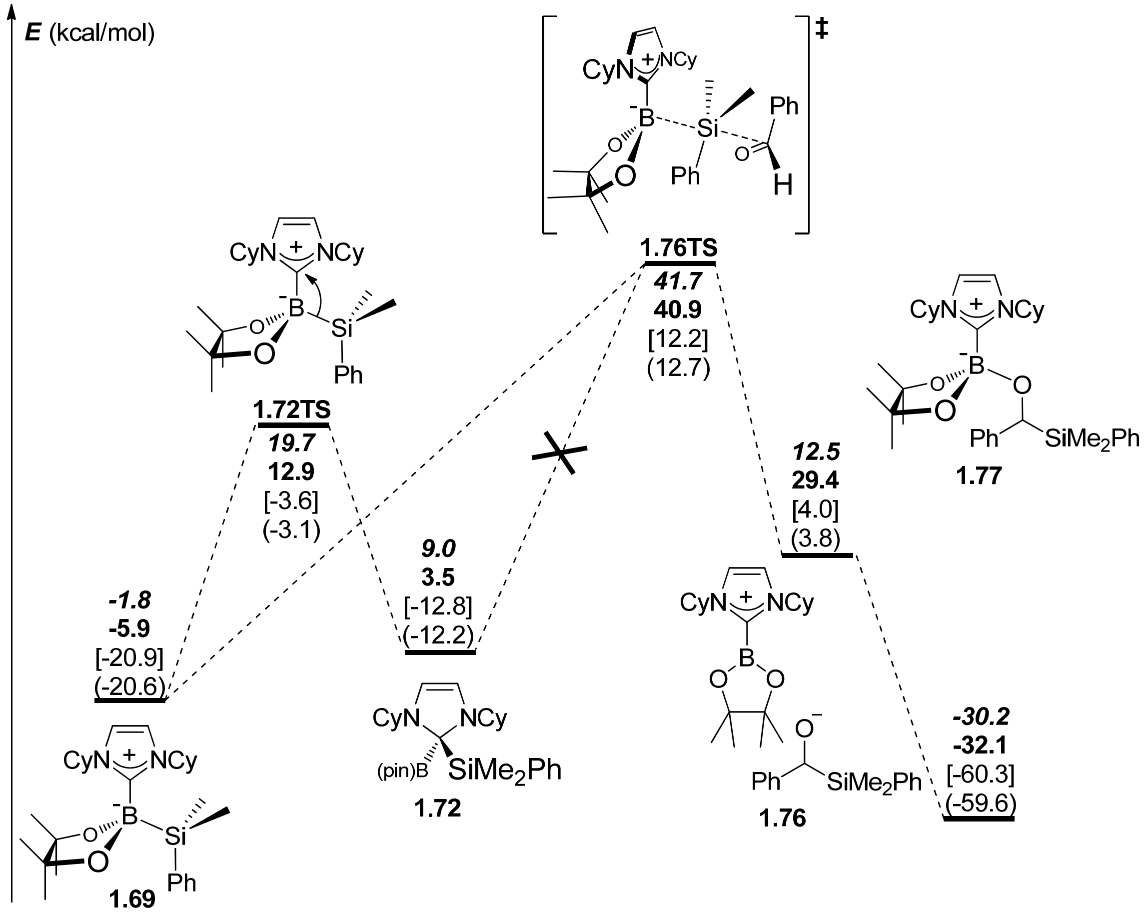

[a] All energies are in kcal/mol. The values in ***italicized bold*** are relative Gibbs free energies, including solvation energies. The values in **bold** are relative gas-phase Gibbs free energies, the values in brackets are gas-phase enthalpies, the values in parantheses are gas-phase ZPE-corrected electronic energies.

Figure 1.28. Key Transition State Structures [a,b]

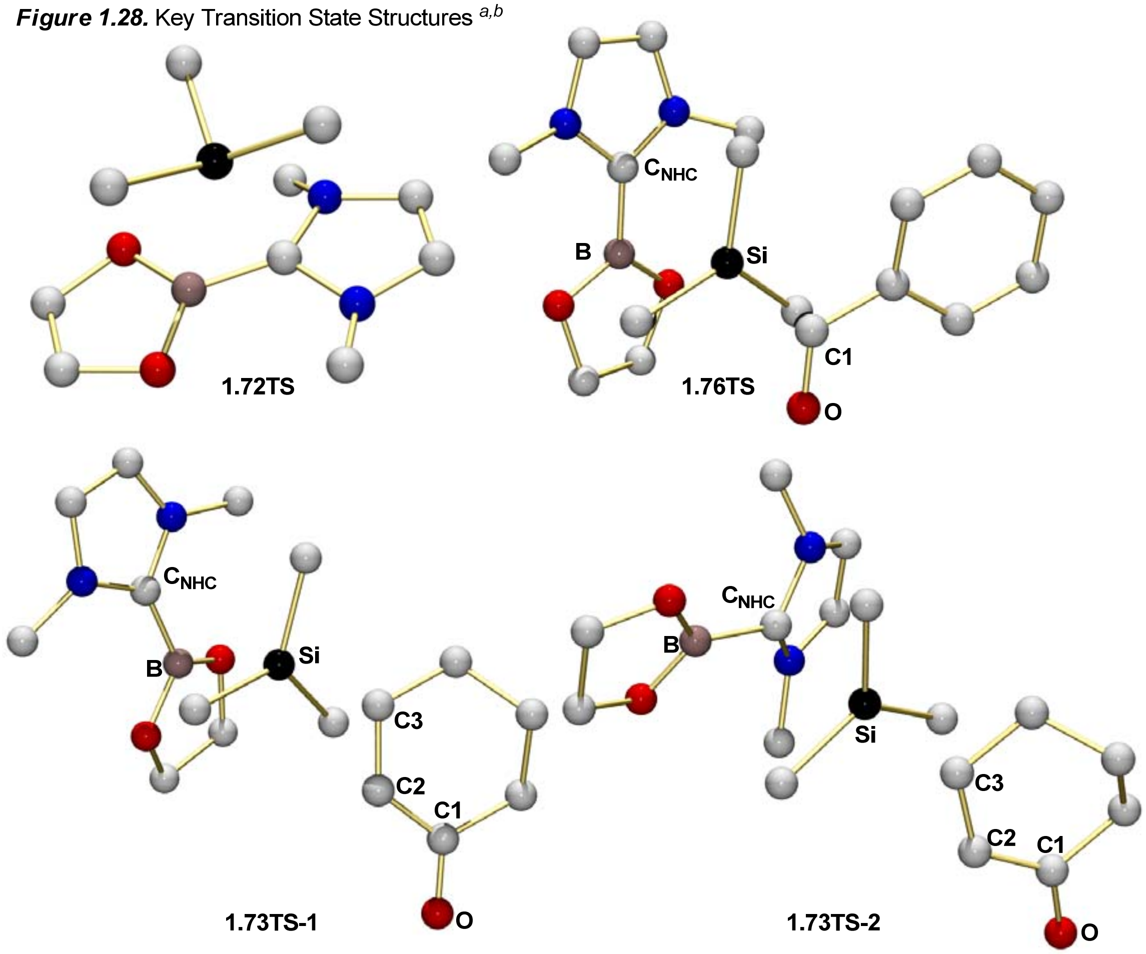

[a] Hydrogen atoms were eliminated for clarity. [b] Key bond lengths: (a) **1.76TS**: C1-O: 1.260Å; C1-Si: 2.476Å; Si-B: 3.124Å; Si-C_{NHC}: 3.170Å; (b) **1.73TS-1**: C1-O: 1.242Å; C1-C2: 1.440Å; C2-C3: 1.393Å; C3-Si: 2.412Å; Si-B: 2.810Å; Si-C_{NHC}: 3.057Å; (c) **1.73TS-2**: C1-O: 1.243Å ; C1-C2: 1.439Å; C2-C3: 1.401Å; C3-Si: 2.368Å; Si-B: 3.089Å; Si-C_{NHC}: 2.567Å.

silicon atom remains in the plane, containing B-C_{NHC} bond and bisecting the two aforementioned rings. These structural elements can be seen to some extent in C- Si bond-forming transition state geometries. For example, in transition state structures **1.73TS-1** and **1.73TS-2** the bond lengths B-Si and C_{NHC}-Si become closer in magnitude than in the corresponding starting materials **1.69** and **1.72** as is the case for the transition state **1.72TS**. Thus, the structure of the NHC ligand may result in a merger of the transition states **1.73TS-1** and **1.73TS-2** so as to afford a bifurcation on a potential energy surface, where transition state **1.72TS** lies along the perpendicular coordinate.[136] Indeed,

---

(136) Ess, D. H.; Wheeler, S. E.; Iafe, R. G.; Xu, L.; Çelebi-Ölcüm, N.; Houk, K. N. *Angew. Chem. Int. Ed.*

geometry optimization of transition states for reactions **1.69→1.76** and **1.72→1.76** gave similar structures, which upon subjection to internal reaction coordinate calculations gave the same starting material **1.69**, *i.e.* **1.72** was found to be not connected to the transition state **1.76TS**. The bond B-Si and C_{NHC}-Si bond lengths are very similar in their magnitudes: 3.124Å and 3.170Å, respectively. Examination of the imaginary vibration mode for the transition state **1.76TS** indicated that both C_{NHC} and B atoms are undergoing a vibration in the direction of the Si center. Thus it is possible that the potential energy surface (PES) for 1,2-addition of silicon to benzaldehyde involves a bifurcation, where the coordinate for migration of the Si group is orthogonal to the reaction coordinate for silicon addition to the carbonyl group. In order to confirm that the PES is bifurcated additional theoretical studies such as 2D PES scans are necessary. Canonical transition state theory is not formulated to handle the bifurcated potential energy surfaces; contributions of each pathway **1.69→1.76** and **1.72→1.76** cannot be assessed directly, and thus molecular dynamics calculations are necessary.[136]

The geometries of the transition states **1.73TS-1**, **1.73TS-2**, and **1.76TS** are best described as S_E2 transition states, where Si adopts a trigonal bipyramidal geometry. Although trigonal bipyramidal pentacoordinate hypervalent organosilicon compounds are well known as isolable stable compounds,[137] their formation imposes electronic requirements on the ligands at the Si center: some of the ligands must be electronegative, and these electronegative ligands occupy axial positions. These structural requirements are due to the fact that the axial ligands and the Si center comprise a *3-center-4-electron bonding system*.[138] In the present case the methyl groups are relatively electropositive, the formally negatively-charged boryl fragment is strongly electropositive, and the carbonyl carbon is net *electronegative and electron-withdrawing*. Thus, the C_3-axis within the structures of the transition states **1.73TS-1** and **1.73TS-2** can be viewed as *a 3-center-2-*

2008, *47*, 7592-7601.

(137) (a) Corriu, R. J. P. *Pure. Appl. Chem.* **1988**, *60*, 99-106; (b) Chuit, C.; Corriu, R. J. P.; Reye, C.; Young, J. C. *Chem. Rev.* **1993**, *93*, 1371-1448; (c) Holmes, R. *Chem. Rev.* **1996**, *96*, 927-950; (c) Kost, D.; Kalikhman, I. in *The Chemistry of Organic Silicon Compounds*, Volume 2 (Eds: Rappoport, Z.; Apeloig, Y.), John Wiley & Sons, Ltd.: Chichester, UK, 2003.

(138) (a) Musher, J. I. *Angew. Chem. Int. Ed. in Engl.* **1969**, *8*, 54-68; (b) Denmark, S. E. *Chimia* **2008**, *62*, 37-40.

electron bonding system. Consequently, the structures **1.73TS-1** and **1.73TS-2** are transition states and not intermediates.

Within the transition state **1.73TS-1** the enolate formation is advanced to a similar degree as in the transition state **1.73TS-2**; however, both of these transition states are slightly more advanced than **1.60TS-2** but less advanced than **1.60TS-1**. However, unlike the transition states involving diboron reagents the substrate molecule is farther removed from the steric bulk of the NHC ligand, and thus the enantioselective variant of the silicon addition would be reliant upon the relay of stereogenicity through the equatorial substituents at the Si center (in the appropriate transition states), whereas the enantioselective boron addition reaction is expected to be more sensitive to the modifications of the ligand structure.

1.3.2.5. Conclusion

The conjugate addition of boron and silicon reagents to α,β-unsaturated carbonyls are similar in terms of the overall nature of the pathways, through which the desired reaction takes place. However, geometric and electronic differences are notable in the transition states. In particular, while the addition of boron proceeds such that partially-populated *p*-orbital of the terminal boron atom prevents addition to strongly electrophilic carbon centers such as the carbon of a carbonyl group, the importance of $\sigma^*_{\text{B-Si}}$ in addition of silicon appears to play a less pronounced role, as evidenced by the fact that the addition of silicon to aldehydes is as facile as that to enones and enoates.

The relative weakness of B-Si bond (88.6 kcal/mol *vs* 104.6 kcal/mol for $B_2(pin)_2$) facilitates the NHC insertion (12.9 kcal/mol for **1.72TS** *vs* 18.2 kcal/mol for **1.65TS**). Given the difference between the energy for the NHC insertion into the B-X bond (X = B or Si) and the energy for the downstream processes, the addition of silicon is under Curtin-Hammett control, *i.e.* the downstream steps will define the contributions of each pathway. Another factor that affects the insertion step is the electronic structure of a carbene. The S-T gap of saturated carbenes is lower than that of corresponding unsaturated variants, and thus the insertion step is likely to be more facile with the saturated NHCs. Another factor affecting the preference for a specific pathway is steric hindrance of NHC catalyst and of the nucleophilic reagent employed. However, generalization of the steric bulk present at the catalyst is not possible in this case, as steric pressure points differ for each pathway, though reactions of diboron reagents are more prone to differentiation between the pathways through steric interactions between the NHC catalyst and the electrophile (enone, enoate, *etc*.) The complicating factor in the silicon addition to α,β-unsaturated carbonyls is the possibility of merging transition states **1.73TS-1** and **1.73TS-2** with sufficiently sterically hindered unsaturated NHCs, thereby leading to bifurcations in PES.

1.4. Experimental

1.4.1. Theoretical Investigation of Transition Metal Complexes of N-Heterocyclic Carbenes and Phosphines

All geometries were optimized with tight or very tight convergence criteria at PBEh level of theory in Gaussian 03. Revision E01.[139,140] In all calculations ultrafine grids and tight SCF convergence criteria were employed. The basis sets employed for geometry optimizations were all electron split valence Pople-style basis sets 6-311G(d,p) on H, C, N, O, F and 6-311G(2df,p) on P, Cl, and 1st row transition metals;[141] the basis sets for C, N, O, F, P, Cl, and the 1st row transition metals were augmented with a set of diffuse basis functions. For the 2nd row transition metals the basis sets were Dunning-style correlation consistent basis sets aug-cc-pVTZ-PP with small core Dirac-Hartree-Fock quasirelativistic pseudopotentials.[142] The minimum nature of the stationary points was ascertained by absence of imaginary vibrational modes in output of frequency calculations. All geometries (Cartesian coordinates) are listed in Table 1.13.

---

(139) Hybrid Perdew-Burke-Ernzerhof density functional: Ernzerhof, M.; Perdew, J. P. *J. Chem. Phys.* **1998**, *109*, 3313-3320.

(140) Gaussian 03. Revision E01: Frisch, M. J.; Trucks, G. B.; Schlegel, H. B.; Scuseria, G. E.; Rob, M. A.; Cheeseman, J. R.; Montgomery, J. A., Jr; Vreven, T.; Kudin, K. N.; Burant, J. C.; Millam, J. M.; Iyengar, S. S.; Tomasi, J.; Barone, V.; Mennuci, B.; Cossi, M.; Scalmani, G.; Rega, N.; Petersson, G. A.; Nakatsuji, H.; Hada, M.; Ehara, M.; Toyota, K.; Fukuda, R.; Hasegawa, J.; Ishida, M.; Nakajima, T.; Honda, Y.; Kitao, O.; Nakai, H.; Klene, M.; Li, X.; Knox, J. E.; Hratchian, H. P.; Cross, J. B.; Bakken, V.; Adamo, C.; Jaramillo, J.; Gomperts, R.; Stratmann, R. E.; Yazyev, O.; Austin, A. J.; Cammi, R.; Pomelli, C.; Ochterski, J. W.; Ayala, P. Y.; Morokuma, K.; Voth, G. A.; Salvador, P.; Dannenberg, J. J.; Zakrzewski, V. G.; Dapprich, S.; Daniels, A. D.; Strain, M. C.; Farkas, O.; Malick, D. K.; Rabuck, A. D.; Raghavachari, K.; Foresmjan, J. B.; Ortiz, J. V.; Cui, Q.; Baboul, A. G.; Clifford, S.; Cioslowski, J.; Stefanov, B. B.; Liu, G.; Liashenko, A.; Piskorz, P.; Komaromi, I.; Martin, R. L.; Fox, D. J.; Keith, T.; Al-Laham, M. A.; Peng, C. Y.; Nanayakkara, A.; Challacombe, M.; Gill, P. M. W.; Johnson, B.; Chen, W.; Wong, M. W.; Gonzalez, C.; Pople, J. A. *Gaussian 03* (Gaussian, Inc., Wallingford, CT, 2003).

(141) All electron split valence basis sets for 1st and 2nd row main group elements: (a) Krishnan, R.; Binkley, J. S.; Seeger, R.; Pople, J. A. *J. Chem. Phys.* **1980**, *72*, 650-654; (b) McLean, A. D.; Chandler, G. S. *J. Chem. Phys.* **1980**, *72*, 5639-5648. Wachters-Hay all electron split valence basis sets for 1st row transition metals: (c) Wachters, A. J. H. *J. Chem. Phys.* **1970**, *52*, 1033-1036; (d) Hay, P. J. *J. Chem. Phys.* **1977**, *66*, 4377-4384. Scaling factors applied to the Wachters-Hay basis sets: (e) Raghavachari, K.; Trucks, G. W. *J. Chem. Phys.* **1989**, *91*, 1062-1065.

(142) Stuttgart-Dresden quasirelativistic Dirac-Hartree-Fock pseudopotentials for Cu and Pd: (a) Figgen, D.; Rauhut, G.; Dolg, M.; Stoll, H. *Chem. Phys.* **2005**, *311*, 227-244. The energy-consistent basis sets for Cu and Pd: (b) Peterson, K. A.; Puzzarini, C. *Theor. Chem. Acc.* **2005**, *114*, 283-296. The energy-consistent basis sets and pseudopotentials: (c) Peterson, K. A.; Figgen, D.; Dolg, M.; Stoll, H. *J. Chem. Phys.* **2007**, *126*, 124101.

Density functional theory cannot be used for meaningful QTAIM calculations, as kinetic and potential energies are not explicitly defined, as parts of the former and the latter are included in exchange-correlation energy.[7b] In order to obtain meaningful results correlation energies must be included in the calculations and thus 2nd order Møller-Plesset method was employed.[143] Stability calculations on the optimized geometries at HF level of theory generated the minimum HF or UHF wavefunctions. The resulting wavefunctions were used as initial guesses in MP2(full) or UMP2(full) single-point energy calculations. The basis sets employed were Dunning's all electron correlation consistent basis sets cc-pVTZ for H, aug-cc-pVTZ for the remaining atoms, except I, for which Sadlej's pVTZ all-electron basis set was used.[144] The formatted checkpoint files from MP2 and UMP2 single-point energy calculations were converted into extended wavefunction files, which were used as inputs for QTAIM calculations with AIMAll (Version 09.04.23).[145] All calculations in AIMAll were carried out with methods implemented therein with *Very High* and *Sky High* basin quadrature grids. The quality of data for each compound was assessed by the following criteria: the magnitude of the sum of all atomic charges in a molecule is less than $1 \cdot 10^{-3}$, the magnitude of the sum of Lagrangian of each atom Ω $|\Sigma L(\Omega)|$ is less than $1 \cdot 10^{-3}$ a.u. (0.6 kcal/mol), molecular virial ratio is approximately equal to 2 (within 1 ppt). Note that due to difficulties associated with locating interatomic surfaces for the backbone carbon atoms of the NHC in **1.5i**, the quality of the data was only assessed by its virial ratio and individual Lagrangians of all atoms with the exception of the aforementioned two carbon atoms.

---

(143) (a) Møller, C.; Plesset, M. S. *Phys. Rev.* **1934**, *46*, 618-622; (b) Bartlett, R. J. *Ann. Rev. Phys. Chem.* **1981**, *32*, 359-401.

(144) All electron correlation consistent basis sets for H and 1st row main group elements: (a) Dunning, T. H., Jr. *J. Chem. Phys.* **1989**, *90*, 1007-1023; (b) Kendall, R. A.; Dunning, T. H., Jr. *J. Chem. Phys.* **1992**, *96*, 6796-6806. All electron correlation consistent basis sets for 2nd row main group elements: (c) Woon, D. E.; Dunning, T. H., Jr. *J. Chem. Phys.* **1993**, *98*, 1358-1371. All electron correlation consistent basis sets for 1st row transition metals: (d) Balabanov, N. B.; Peterson, K. A. *J. Chem. Phys.* **2005**, *123*, 064107. All electron correlation consistent basis sets for 2nd row transition metals: see Ref. 133c. The all electron basis set for iodine: (e) Sadlej, A. J. *Theor. Chim. Acta* **1992**, *81*, 339-354.

(145) AIMAll (Version 09.04.23): Keith, T. A. 2010 (aim.tkgristmill.com).

The contour maps of ρ and $\nabla^2\rho$ in Figures 1.2, 1.12, and 1.13 were generated with MORPHY98 from the MP2 wavefunctions, obtained as described above.[146]

Table 1.13. Geometries of Ligands IMe, SIMe, and PMe$_3$, and transition metal complexes **1.1i-1.19i**, **1.1s-1.19s**, **1.1p-1.19p**.

IMe

Atom	X	Y	Z
C1	0.00E+00	0.00E+00	1.84E+00
C2	0.00E+00	1.28E+00	-2.28E+00
C3	-1.57E-16	-1.28E+00	-2.28E+00
N4	0.00E+00	-2.00E+00	2.27E-01
H5	0.00E+00	2.60E+00	-3.83E+00
H6	-3.19E-16	-2.60E+00	-3.83E+00
N7	2.45E-16	2.00E+00	2.27E-01
C8	0.00E+00	4.59E+00	1.08E+00
H9	0.00E+00	4.57E+00	3.13E+00
H10	1.68E+00	5.59E+00	4.08E-01
H11	-1.68E+00	5.59E+00	4.08E-01
C12	-5.63E-16	-4.59E+00	1.08E+00
H13	1.68E+00	-5.59E+00	4.08E-01
H14	-5.60E-16	-4.57E+00	3.13E+00
H15	-1.68E+00	-5.59E+00	4.08E-01

SIMe

Atom	X	Y	Z
C1	0.00E+00	0.00E+00	1.91E+00
C2	2.36E-01	-1.42E+00	-2.31E+00
C3	-2.36E-01	1.42E+00	-2.31E+00
N4	0.00E+00	2.02E+00	3.81E-01
H5	2.14E+00	-1.91E+00	-2.99E+00
H6	1.14E+00	2.48E+00	-3.45E+00
N7	-1.07E-16	-2.02E+00	3.81E-01
C8	3.03E-01	-4.58E+00	1.24E+00
H9	1.15E-01	-4.59E+00	3.29E+00
H10	-1.14E+00	-5.82E+00	4.22E-01
H11	2.17E+00	-5.34E+00	7.36E-01
C12	-3.03E-01	4.58E+00	1.24E+00
H13	-2.17E+00	5.34E+00	7.36E-01
H14	-1.15E-01	4.59E+00	3.29E+00
H15	1.14E+00	5.82E+00	4.22E-01
H16	-2.14E+00	1.91E+00	-2.99E+00
H17	-1.14E+00	-2.48E+00	-3.45E+00

PMe3

Atom	X	Y	Z
P1	-3.14E-05	-6.08E-05	-1.13E+00
C2	5.28E-01	3.02E+00	5.22E-01
H3	-9.25E-01	4.38E+00	-4.18E-02
H4	4.87E-01	2.81E+00	2.58E+00
H5	2.36E+00	3.80E+00	-3.47E-02
C6	-2.88E+00	-1.05E+00	5.22E-01
H7	-3.33E+00	-2.99E+00	-4.05E-02
H8	-2.68E+00	-9.83E-01	2.58E+00
H9	-4.47E+00	1.43E-01	-3.57E-02
C10	2.35E+00	-1.97E+00	5.22E-01
H11	2.19E+00	-1.83E+00	2.58E+00
H12	2.11E+00	-3.94E+00	-3.41E-02
H13	4.25E+00	-1.39E+00	-4.22E-02

---

(146) MORPHY98, a program written by Popelier, P. L. A. with a contribution from Bone, R. G. A. (UMIST, Manchester, England, EU, 1998).

Table 1.13 (continued).

1.1i

Atom	X	Y	Z
C1	2.07E+00	3.44E-16	-1.42E-01
C2	6.15E+00	1.27E+00	-2.17E-01
C3	6.15E+00	-1.27E+00	-2.17E-01
N4	3.66E+00	-2.02E+00	-1.47E-01
H5	7.69E+00	2.61E+00	-2.39E-01
H6	7.69E+00	-2.61E+00	-2.39E-01
N7	3.66E+00	2.02E+00	-1.47E-01
C8	2.93E+00	4.66E+00	1.94E-02
H9	1.24E+00	4.82E+00	1.19E+00
H10	4.47E+00	5.71E+00	8.94E-01
H11	2.54E+00	5.45E+00	-1.85E+00
C12	2.93E+00	-4.66E+00	1.94E-02
H13	4.47E+00	-5.71E+00	8.94E-01
H14	1.24E+00	-4.82E+00	1.19E+00
H15	2.54E+00	-5.45E+00	-1.85E+00
Fe16	-1.70E+00	-2.82E-16	6.90E-02
C17	-2.01E+00	2.73E+00	-1.87E+00
O18	-2.32E+00	4.43E+00	-3.19E+00
C19	-2.01E+00	-2.73E+00	-1.87E+00
O20	-2.32E+00	-4.43E+00	-3.19E+00
C21	-1.12E+00	-1.86E-16	3.38E+00
O22	-6.83E-01	-1.14E-16	5.51E+00
C23	-5.00E+00	-8.32E-16	6.62E-01
O24	-7.12E+00	-1.19E-15	1.08E+00

1.1p

Atom	X	Y	Z
Fe1	1.31E+00	1.29E-04	2.65E-05
C2	1.19E+00	-9.98E-01	3.20E+00
O3	1.08E+00	-1.64E+00	5.27E+00
C4	1.19E+00	-2.27E+00	-2.46E+00
O5	1.08E+00	-3.74E+00	-4.06E+00
C6	1.19E+00	3.27E+00	-7.34E-01
O7	1.08E+00	5.38E+00	-1.21E+00
C8	4.66E+00	3.80E-04	-3.78E-04
O9	6.82E+00	4.89E-04	-7.05E-04
P10	-2.90E+00	7.42E-05	-9.31E-06
C11	-4.37E+00	-3.04E+00	6.82E-01
H12	-6.43E+00	-2.89E+00	6.47E-01
H13	-3.75E+00	-4.42E+00	-7.20E-01
H14	-3.76E+00	-3.69E+00	2.54E+00
C15	-4.37E+00	9.29E-01	-2.97E+00
H16	-6.43E+00	8.82E-01	-2.83E+00
H17	-3.76E+00	2.84E+00	-3.47E+00
H18	-3.75E+00	-3.55E-01	-4.47E+00
C19	-4.37E+00	2.11E+00	2.29E+00
H20	-6.43E+00	2.01E+00	2.18E+00
H21	-3.76E+00	1.59E+00	4.19E+00
H22	-3.76E+00	4.05E+00	1.93E+00

1.1s

Atom	X	Y	Z
C1	-1.97E+00	1.42E-02	-7.15E-02
C2	-6.16E+00	-1.41E+00	-1.57E-01
C3	-6.14E+00	1.45E+00	-4.53E-01
N4	-3.49E+00	2.05E+00	1.30E-02
H5	-7.19E+00	-2.37E+00	-1.67E+00
H6	-6.68E+00	2.05E+00	-2.36E+00
N7	-3.48E+00	-2.04E+00	-2.33E-01
C8	-2.78E+00	-4.64E+00	1.70E-01
H9	-8.44E-01	-4.74E+00	8.66E-01
H10	-4.03E+00	-5.46E+00	1.60E+00
H11	-2.94E+00	-5.75E+00	-1.57E+00
C12	-2.77E+00	4.67E+00	2.78E-01
H13	-4.18E+00	5.62E+00	1.46E+00
H14	-9.41E-01	4.79E+00	1.21E+00
H15	-2.68E+00	5.64E+00	-1.55E+00
Fe16	1.79E+00	-3.53E-03	7.00E-02
C17	1.98E+00	-2.60E+00	-2.06E+00
O18	2.19E+00	-4.21E+00	-3.51E+00
C19	2.10E+00	2.82E+00	-1.73E+00
O20	2.43E+00	4.57E+00	-2.98E+00
C21	1.29E+00	-1.45E-01	3.38E+00
O22	9.15E-01	-2.38E-01	5.52E+00
C23	5.10E+00	-1.08E-01	5.67E-01
O24	7.23E+00	-1.81E-01	9.20E-01
H25	-7.36E+00	2.42E+00	9.01E-01
H26	-6.97E+00	-2.01E+00	1.66E+00

1.2i

Atom	X	Y	Z
C1	-2.22E+00	0.00E+00	-1.46E-01
C2	-6.31E+00	-1.27E+00	-1.92E-01
C3	-6.31E+00	1.27E+00	-1.92E-01
N4	-3.81E+00	2.02E+00	-1.40E-01
H5	-7.85E+00	-2.61E+00	-2.05E-01
H6	-7.85E+00	2.61E+00	-2.05E-01
N7	-3.81E+00	-2.02E+00	-1.40E-01
C8	-3.08E+00	-4.66E+00	1.70E-02
H9	-1.41E+00	-4.83E+00	1.21E+00
H10	-4.64E+00	-5.72E+00	8.63E-01
H11	-2.66E+00	-5.43E+00	-1.85E+00
C12	-3.08E+00	4.66E+00	1.70E-02
H13	-4.64E+00	5.72E+00	8.63E-01
H14	-1.41E+00	4.83E+00	1.21E+00
H15	-2.66E+00	5.43E+00	-1.85E+00
Fe16	1.50E+00	0.00E+00	2.82E-02
C17	1.85E+00	-2.74E+00	-1.86E+00
O18	2.21E+00	-4.46E+00	-3.15E+00
C19	1.85E+00	2.74E+00	-1.86E+00
O20	2.21E+00	4.46E+00	-3.15E+00

Table 1.13 (continued).

C21	1.04E+00	-5.38E-06	3.34E+00
O22	7.11E-01	-8.68E-06	5.50E+00
P23	5.57E+00	-3.87E-06	6.83E-01
H24	6.49E+00	-1.29E-05	3.19E+00
H25	7.09E+00	-2.00E+00	-2.34E-01
H26	7.09E+00	2.00E+00	-2.34E-01

1.2s

Atom	X	Y	Z
C1	-2.12E+00	1.91E-02	-7.80E-02
C2	-6.31E+00	-1.40E+00	-1.26E-01
C3	-6.28E+00	1.45E+00	-4.45E-01
N4	-3.64E+00	2.06E+00	4.08E-02
H5	-7.38E+00	-2.37E+00	-1.61E+00
H6	-6.81E+00	2.04E+00	-2.37E+00
N7	-3.63E+00	-2.03E+00	-2.53E-01
C8	-2.94E+00	-4.63E+00	1.46E-01
H9	-9.93E-01	-4.74E+00	8.11E-01
H10	-4.17E+00	-5.45E+00	1.59E+00
H11	-3.12E+00	-5.75E+00	-1.59E+00
C12	-2.93E+00	4.67E+00	2.83E-01
H13	-4.34E+00	5.64E+00	1.44E+00
H14	-1.10E+00	4.80E+00	1.23E+00
H15	-2.80E+00	5.62E+00	-1.55E+00
Fe16	1.58E+00	1.49E-03	3.55E-02
C17	1.82E+00	-2.58E+00	-2.07E+00
O18	2.07E+00	-4.20E+00	-3.52E+00
C19	1.95E+00	2.84E+00	-1.69E+00
O20	2.33E+00	4.62E+00	-2.90E+00
C21	1.20E+00	-1.87E-01	3.34E+00
O22	9.17E-01	-3.14E-01	5.51E+00
P23	5.67E+00	-1.26E-01	5.87E-01
H24	6.66E+00	-3.24E-01	3.06E+00
H25	7.13E+00	-2.09E+00	-5.05E-01
H26	7.22E+00	1.90E+00	-2.21E-01
H27	-7.52E+00	2.43E+00	8.87E-01
H28	-7.08E+00	-1.98E+00	1.71E+00

1.2p

Atom	X	Y	Z
Fe1	-1.11E+00	-5.88E-05	-1.68E-04
C2	-1.05E+00	3.31E+00	-3.79E-01
O3	-1.01E+00	5.48E+00	-6.26E-01
C4	-1.05E+00	-1.98E+00	-2.68E+00
O5	-1.01E+00	-3.28E+00	-4.43E+00
C6	-1.05E+00	-1.33E+00	3.06E+00
O7	-1.01E+00	-2.20E+00	5.06E+00
P8	-5.23E+00	4.92E-04	1.73E-04
H9	-6.56E+00	-1.38E+00	-1.86E+00
H10	-6.56E+00	-9.22E-01	2.12E+00
H11	-6.56E+00	2.30E+00	-2.62E-01
P12	3.03E+00	-7.87E-06	-6.39E-05
C13	4.52E+00	1.24E+00	-2.85E+00
H14	6.58E+00	1.18E+00	-2.71E+00
H15	3.91E+00	1.19E-01	-4.48E+00
H16	3.91E+00	3.19E+00	-3.15E+00
C17	4.52E+00	1.85E+00	2.50E+00
H18	6.58E+00	1.76E+00	2.37E+00
H19	3.91E+00	3.82E+00	2.34E+00
H20	3.91E+00	1.13E+00	4.33E+00
C21	4.52E+00	-3.09E+00	3.55E-01
H22	6.58E+00	-2.93E+00	3.38E-01
H23	3.91E+00	-3.94E+00	2.14E+00
H24	3.91E+00	-4.32E+00	-1.19E+00

1.3i

Atom	X	Y	Z
C1	-2.36E+00	-1.14E-01	7.61E-02
C2	-6.23E+00	-1.88E+00	7.67E-02
C3	-6.57E+00	6.50E-01	1.07E-01
N4	-4.19E+00	1.70E+00	1.14E-01
H5	-7.58E+00	-3.40E+00	8.12E-02
H6	-8.26E+00	1.78E+00	1.40E-01
N7	-3.67E+00	-2.31E+00	6.12E-02
C8	-2.69E+00	-4.88E+00	-6.69E-02
H9	-7.39E-01	-4.91E+00	5.63E-01
H10	-3.83E+00	-6.07E+00	1.18E+00
H11	-2.80E+00	-5.57E+00	-2.01E+00
C12	-3.84E+00	4.42E+00	-1.13E-02
H13	-5.38E+00	5.33E+00	1.01E+00
H14	-2.07E+00	4.97E+00	8.81E-01
H15	-3.84E+00	5.07E+00	-1.97E+00
Fe16	1.41E+00	3.49E-01	-3.50E-03
Cl17	1.74E+00	-2.45E+00	-3.36E+00
Cl18	2.03E+00	-2.54E+00	3.27E+00
C19	4.88E+00	2.34E-01	-1.45E-01
O20	7.01E+00	8.31E-02	-2.40E-01
C21	1.14E+00	2.56E+00	-2.52E+00
O22	9.87E-01	3.95E+00	-4.15E+00
C23	1.34E+00	2.44E+00	2.64E+00
O24	1.32E+00	3.74E+00	4.34E+00

1.3s

Atom	X	Y	Z
C1	2.29E+00	-9.63E-02	-2.51E-02
C2	6.26E+00	-1.97E+00	9.38E-02
C3	6.59E+00	8.72E-01	-1.22E-01
N4	4.01E+00	1.78E+00	2.36E-01
H5	6.80E+00	-2.69E+00	1.96E+00
H6	7.86E+00	1.66E+00	1.31E+00
N7	3.54E+00	-2.27E+00	-2.43E-01
C8	2.59E+00	-4.83E+00	-3.12E-01

Table 1.13 (continued).

H9	5.82E-01	-4.85E+00	-7.18E-01
H10	3.59E+00	-5.86E+00	-1.80E+00
H11	2.93E+00	-5.76E+00	1.51E+00
C12	3.63E+00	4.47E+00	7.68E-02
H13	4.00E+00	5.17E+00	-1.84E+00
H14	1.71E+00	4.98E+00	6.01E-01
H15	4.91E+00	5.41E+00	1.39E+00
Fe16	-1.49E+00	3.35E-01	2.99E-02
Cl17	-1.90E+00	-2.78E+00	3.11E+00
Cl18	-2.01E+00	-2.19E+00	-3.53E+00
C19	-4.97E+00	2.03E-01	6.78E-02
O20	-7.10E+00	3.91E-02	8.51E-02
C21	-1.29E+00	2.24E+00	2.80E+00
O22	-1.20E+00	3.43E+00	4.59E+00
C23	-1.37E+00	2.71E+00	-2.36E+00
O24	-1.32E+00	4.19E+00	-3.91E+00
H25	7.28E+00	1.45E+00	-1.99E+00
H26	7.29E+00	-3.03E+00	-1.34E+00

1.3p

Atom	X	Y	Z
Fe1	-1.10E+00	0.00E+00	3.06E-01
Cl2	-1.06E+00	-3.25E+00	-2.61E+00
Cl3	-1.06E+00	3.25E+00	-2.61E+00
C4	-4.54E+00	5.11E-06	-1.79E-01
O5	-6.64E+00	6.76E-06	-5.75E-01
C6	-1.08E+00	-2.50E+00	2.56E+00
O7	-1.06E+00	-4.10E+00	3.98E+00
C8	-1.08E+00	2.50E+00	2.56E+00
O9	-1.06E+00	4.10E+00	3.98E+00
P10	3.20E+00	0.00E+00	-8.81E-02
C11	4.78E+00	-2.72E+00	1.31E+00
H12	6.81E+00	-2.65E+00	9.25E-01
H13	4.48E+00	-2.75E+00	3.36E+00
H14	3.99E+00	-4.44E+00	4.90E-01
C15	4.78E+00	2.72E+00	1.31E+00
H16	4.48E+00	2.75E+00	3.36E+00
H17	6.81E+00	2.65E+00	9.25E-01
H18	3.99E+00	4.44E+00	4.90E-01
C19	4.30E+00	-1.32E-05	-3.33E+00
H20	3.58E+00	1.67E+00	-4.29E+00
H21	6.37E+00	-1.33E-05	-3.34E+00
H22	3.58E+00	-1.67E+00	-4.29E+00

1.4i

Atom	X	Y	Z
C1	2.46E+00	-2.74E-16	-1.26E-01
C2	6.54E+00	1.27E+00	-2.00E-01
C3	6.54E+00	-1.27E+00	-2.00E-01
N4	4.05E+00	-2.02E+00	-1.34E-01
H5	8.08E+00	2.61E+00	-2.19E-01
H6	8.08E+00	-2.61E+00	-2.19E-01
N7	4.05E+00	2.02E+00	-1.34E-01
C8	3.31E+00	4.66E+00	-1.17E-02
H9	1.62E+00	4.84E+00	1.15E+00
H10	4.85E+00	5.73E+00	8.43E-01
H11	2.92E+00	5.41E+00	-1.89E+00
C12	3.31E+00	-4.66E+00	-1.17E-02
H13	4.85E+00	-5.73E+00	8.43E-01
H14	1.62E+00	-4.84E+00	1.15E+00
H15	2.92E+00	-5.41E+00	-1.89E+00
C16	-1.83E+00	2.98E+00	-2.00E+00
O17	-2.14E+00	4.70E+00	-3.28E+00
C18	-1.83E+00	-2.98E+00	-2.00E+00
O19	-2.14E+00	-4.70E+00	-3.28E+00
C20	-1.02E+00	-6.73E-06	3.66E+00
O21	-6.78E-01	-1.02E-05	5.81E+00
C22	-5.12E+00	-3.21E-06	5.66E-01
O23	-7.25E+00	-6.80E-06	8.96E-01
Ru24	-1.55E+00	1.72E-16	6.69E-02

1.4s

Atom	X	Y	Z
C1	-2.38E+00	2.56E-02	-5.85E-02
C2	-6.57E+00	-1.39E+00	-1.48E-01
C3	-6.53E+00	1.47E+00	-4.32E-01
N4	-3.89E+00	2.07E+00	3.76E-02
H5	-7.60E+00	-2.34E+00	-1.66E+00
H6	-7.07E+00	2.09E+00	-2.34E+00
N7	-3.89E+00	-2.02E+00	-2.38E-01
C8	-3.19E+00	-4.63E+00	9.66E-02
H9	-1.23E+00	-4.75E+00	7.12E-01
H10	-4.40E+00	-5.47E+00	1.56E+00
H11	-3.43E+00	-5.71E+00	-1.66E+00
C12	-3.15E+00	4.68E+00	2.48E-01
H13	-4.55E+00	5.67E+00	1.41E+00
H14	-1.31E+00	4.81E+00	1.16E+00
H15	-3.06E+00	5.62E+00	-1.60E+00
C16	1.79E+00	-2.80E+00	-2.26E+00
O17	1.96E+00	-4.40E+00	-3.71E+00
C18	1.96E+00	3.11E+00	-1.78E+00
O19	2.30E+00	4.90E+00	-2.95E+00
C20	1.18E+00	-2.48E-01	3.67E+00
O21	8.74E-01	-3.92E-01	5.81E+00
C22	5.23E+00	-1.31E-01	4.77E-01
O23	7.36E+00	-2.11E-01	7.45E-01
Ru24	1.64E+00	-1.02E-02	7.34E-02
H25	-7.76E+00	2.44E+00	9.23E-01
H26	-7.37E+00	-1.99E+00	1.67E+00

Table 1.13 (continued).

1.4p

Atom	X	Y	Z
C1	-1.07E+00	-2.57E-04	3.63E+00
O2	-9.64E-01	-4.09E-04	5.80E+00
C3	-1.07E+00	3.14E+00	-1.81E+00
O4	-9.63E-01	5.02E+00	-2.90E+00
C5	-1.07E+00	-3.14E+00	-1.81E+00
O6	-9.63E-01	-5.02E+00	-2.90E+00
C7	-4.82E+00	2.19E-06	-1.28E-03
O8	-6.97E+00	2.32E-06	-1.88E-03
Ru9	-1.19E+00	0.00E+00	-3.38E-04
P10	3.28E+00	2.53E-16	-2.59E-04
C11	4.74E+00	2.70E+00	1.56E+00
H12	6.80E+00	2.57E+00	1.49E+00
H13	4.12E+00	4.44E+00	6.32E-01
H14	4.12E+00	2.77E+00	3.53E+00
C15	4.74E+00	2.32E-04	-3.12E+00
H16	6.80E+00	2.21E-04	-2.97E+00
H17	4.12E+00	-1.67E+00	-4.16E+00
H18	4.12E+00	1.67E+00	-4.16E+00
C19	4.74E+00	-2.70E+00	1.56E+00
H20	4.12E+00	-4.44E+00	6.32E-01
H21	6.80E+00	-2.57E+00	1.49E+00
H22	4.12E+00	-2.77E+00	3.53E+00

1.5i

Atom	X	Y	Z
C1	-2.05E-16	3.08E-16	-2.46E+00
C2	-6.28E-01	1.11E+00	-6.54E+00
C3	6.28E-01	-1.11E+00	-6.54E+00
N4	9.86E-01	-1.77E+00	-4.05E+00
H5	-1.29E+00	2.27E+00	-8.08E+00
H6	1.29E+00	-2.27E+00	-8.08E+00
N7	-9.86E-01	1.77E+00	-4.05E+00
C8	-2.29E+00	4.04E+00	-3.27E+00
H9	-1.60E+00	4.57E+00	-1.40E+00
H10	-1.88E+00	5.55E+00	-4.61E+00
H11	-4.33E+00	3.73E+00	-3.18E+00
C12	2.29E+00	-4.04E+00	-3.27E+00
H13	4.33E+00	-3.73E+00	-3.18E+00
H14	1.60E+00	-4.57E+00	-1.40E+00
H15	1.88E+00	-5.55E+00	-4.61E+00
C16	3.63E+00	2.96E-02	1.43E+00
O17	5.79E+00	4.22E-02	1.27E+00
C18	-1.52E-16	-3.08E+00	3.45E+00
O19	1.38E-02	-4.86E+00	4.70E+00
C20	1.54E-15	3.08E+00	3.45E+00
O21	-1.38E-02	4.86E+00	4.70E+00
C22	-3.63E+00	-2.96E-02	1.43E+00
O23	-5.79E+00	-4.22E-02	1.27E+00
Ru24	1.32E-16	-1.98E-16	1.58E+00

1.5s

Atom	X	Y	Z
C1	2.38E+00	0.00E+00	0.00E+00
C2	6.56E+00	1.44E+00	7.69E-02
C3	6.56E+00	-1.44E+00	-7.69E-02
N4	3.89E+00	-1.98E+00	-5.18E-01
H5	7.18E+00	2.32E+00	-1.69E+00
H6	7.72E+00	-2.17E+00	-1.61E+00
N7	3.89E+00	1.98E+00	5.18E-01
C8	3.11E+00	4.55E+00	9.52E-01
H9	1.14E+00	4.56E+00	1.54E+00
H10	4.28E+00	5.38E+00	2.45E+00
H11	3.32E+00	5.71E+00	-7.58E-01
C12	3.11E+00	-4.55E+00	-9.52E-01
H13	3.32E+00	-5.71E+00	7.58E-01
H14	1.14E+00	-4.56E+00	-1.54E+00
H15	4.28E+00	-5.38E+00	-2.45E+00
C16	-1.52E+00	-2.44E+00	2.69E+00
O17	-1.37E+00	-3.88E+00	4.30E+00
C18	-3.52E+00	-2.27E+00	-2.10E+00
O19	-4.76E+00	-3.60E+00	-3.29E+00
C20	-3.52E+00	2.27E+00	2.10E+00
O21	-4.76E+00	3.60E+00	3.29E+00
C22	-1.52E+00	2.44E+00	-2.69E+00
O23	-1.37E+00	3.88E+00	-4.30E+00
Ru24	-1.67E+00	0.00E+00	0.00E+00
H25	7.18E+00	-2.32E+00	1.69E+00
H26	7.72E+00	2.17E+00	1.61E+00

1.5p

Atom	X	Y	Z
C1	1.40E+00	3.60E+00	2.21E-16
O2	1.49E+00	5.76E+00	4.13E-16
C3	2.80E+00	-1.07E-01	-3.25E+00
O4	3.83E+00	-1.52E-01	-5.16E+00
C5	2.80E+00	-1.07E-01	3.25E+00
O6	3.83E+00	-1.52E-01	5.16E+00
C7	1.01E+00	-3.66E+00	-4.18E-16
O8	8.51E-01	-5.81E+00	-6.05E-16
Ru9	1.20E+00	-3.06E-02	0.00E+00
P10	-3.27E+00	1.20E-01	2.72E-16
C11	-4.83E+00	-1.40E+00	2.68E+00
H12	-6.88E+00	-1.28E+00	2.52E+00
H13	-4.26E+00	-3.38E+00	2.77E+00
H14	-4.21E+00	-4.84E-01	4.43E+00
C15	-4.83E+00	-1.40E+00	-2.68E+00
H16	-6.88E+00	-1.28E+00	-2.52E+00
H17	-4.21E+00	-4.84E-01	-4.43E+00
H18	-4.26E+00	-3.38E+00	-2.77E+00
C19	-4.74E+00	3.24E+00	-7.48E-06
H20	-4.14E+00	4.29E+00	-1.67E+00

Table 1.13 (continued).

H21	-6.80E+00	3.08E+00	-6.97E-06
H22	-4.14E+00	4.29E+00	1.67E+00

1.6i

Atom	X	Y	Z
C1	2.60E+00	5.77E-16	-1.23E-01
C2	6.68E+00	1.27E+00	-1.71E-01
C3	6.68E+00	-1.27E+00	-1.71E-01
N4	4.19E+00	-2.02E+00	-1.22E-01
H5	8.22E+00	2.61E+00	-1.82E-01
H6	8.22E+00	-2.61E+00	-1.82E-01
N7	4.19E+00	2.02E+00	-1.22E-01
C8	3.45E+00	4.66E+00	-9.03E-03
H9	1.78E+00	4.84E+00	1.18E+00
H10	5.00E+00	5.74E+00	8.04E-01
H11	3.01E+00	5.39E+00	-1.89E+00
C12	3.45E+00	-4.66E+00	-9.03E-03
H13	5.00E+00	-5.74E+00	8.04E-01
H14	1.78E+00	-4.84E+00	1.18E+00
H15	3.01E+00	-5.39E+00	-1.89E+00
C16	-1.70E+00	2.99E+00	-1.97E+00
O17	-2.08E+00	4.74E+00	-3.21E+00
C18	-1.70E+00	-2.99E+00	-1.97E+00
O19	-2.08E+00	-4.74E+00	-3.21E+00
C20	-9.87E-01	-5.91E-06	3.62E+00
O21	-7.98E-01	-1.15E-05	5.79E+00
Ru22	-1.35E+00	-3.01E-16	2.77E-02
P23	-5.69E+00	-1.95E-06	5.53E-01
H24	-6.70E+00	-5.99E-06	3.02E+00
H25	-7.16E+00	2.00E+00	-4.23E-01
H26	-7.16E+00	-2.00E+00	-4.23E-01

1.6s

Atom	X	Y	Z
C1	-2.51E+00	3.79E-02	-5.96E-02
C2	-6.70E+00	-1.37E+00	-1.09E-01
C3	-6.67E+00	1.49E+00	-4.15E-01
N4	-4.02E+00	2.08E+00	7.90E-02
H5	-7.78E+00	-2.33E+00	-1.59E+00
H6	-7.18E+00	2.08E+00	-2.34E+00
N7	-4.03E+00	-2.00E+00	-2.57E-01
C8	-3.33E+00	-4.62E+00	6.50E-02
H9	-1.35E+00	-4.74E+00	6.12E-01
H10	-4.49E+00	-5.45E+00	1.57E+00
H11	-3.63E+00	-5.70E+00	-1.68E+00
C12	-3.29E+00	4.69E+00	2.64E-01
H13	-4.71E+00	5.70E+00	1.38E+00
H14	-1.47E+00	4.82E+00	1.22E+00
H15	-3.14E+00	5.60E+00	-1.60E+00
C16	1.64E+00	-2.73E+00	-2.32E+00
O17	1.87E+00	-4.33E+00	-3.79E+00
C18	1.85E+00	3.17E+00	-1.65E+00
O19	2.31E+00	5.01E+00	-2.72E+00
C20	1.13E+00	-3.66E-01	3.61E+00
O21	9.56E-01	-5.92E-01	5.78E+00
Ru22	1.44E+00	-3.42E-03	3.83E-02
P23	5.79E+00	-1.78E-01	4.68E-01
H24	7.19E+00	-2.11E+00	-7.48E-01
H25	7.31E+00	1.88E+00	-3.17E-01
H26	6.85E+00	-4.74E-01	2.90E+00
H27	-7.91E+00	2.46E+00	9.18E-01
H28	-7.46E+00	-1.96E+00	1.73E+00

1.6p

Atom	X	Y	Z
C1	-9.60E-01	3.57E+00	-5.20E-01
O2	-9.38E-01	5.73E+00	-8.33E-01
C3	-9.62E-01	-2.24E+00	-2.83E+00
O4	-9.43E-01	-3.59E+00	-4.54E+00
C5	-9.61E-01	-1.34E+00	3.35E+00
O6	-9.41E-01	-2.14E+00	5.38E+00
Ru7	-1.00E+00	2.61E-04	1.06E-04
P8	-5.38E+00	1.92E-03	-4.51E-04
H9	-6.71E+00	2.30E+00	-3.32E-01
H10	-6.71E+00	-1.43E+00	-1.82E+00
H11	-6.71E+00	-8.57E-01	2.15E+00
P12	3.39E+00	-6.85E-05	-2.83E-04
C13	4.87E+00	1.15E+00	-2.89E+00
H14	6.93E+00	1.09E+00	-2.75E+00
H15	4.25E+00	-1.36E-02	-4.48E+00
H16	4.25E+00	3.09E+00	-3.24E+00
C17	4.87E+00	1.93E+00	2.44E+00
H18	4.25E+00	1.26E+00	4.30E+00
H19	6.93E+00	1.83E+00	2.33E+00
H20	4.25E+00	3.89E+00	2.23E+00
C21	4.87E+00	-3.08E+00	4.47E-01
H22	6.93E+00	-2.93E+00	4.23E-01
H23	4.25E+00	-3.87E+00	2.25E+00
H24	4.25E+00	-4.35E+00	-1.06E+00

1.7i

Atom	X	Y	Z
C1	-2.67E+00	-7.10E-02	7.91E-02
C2	-6.61E+00	-1.66E+00	6.87E-02
C3	-6.83E+00	8.80E-01	8.31E-02
N4	-4.41E+00	1.83E+00	9.66E-02
H5	-8.03E+00	-3.12E+00	7.26E-02
H6	-8.47E+00	2.08E+00	1.01E-01
N7	-4.07E+00	-2.21E+00	7.03E-02
C8	-3.20E+00	-4.82E+00	-2.21E-02
H9	-1.25E+00	-4.92E+00	6.15E-01
H10	-4.39E+00	-5.94E+00	1.24E+00

Table 1.13 (continued).

H11	-3.33E+00	-5.53E+00	-1.95E+00
C12	-3.91E+00	4.52E+00	-3.06E-03
H13	-5.61E+00	5.52E+00	6.18E-01
H14	-2.37E+00	5.03E+00	1.26E+00
H15	-3.46E+00	5.12E+00	-1.92E+00
Cl16	1.46E+00	-2.80E+00	-3.38E+00
Cl17	1.74E+00	-2.83E+00	3.34E+00
C18	5.01E+00	7.69E-02	-1.43E-01
O19	7.14E+00	-1.16E-01	-2.30E-01
C20	1.16E+00	2.65E+00	-2.63E+00
O21	1.10E+00	4.08E+00	-4.24E+00
C22	1.36E+00	2.58E+00	2.69E+00
O23	1.42E+00	3.95E+00	4.35E+00
Ru24	1.33E+00	2.72E-01	-6.19E-03

1.7s

Atom	X	Y	Z
C1	-2.60E+00	-7.79E-02	-1.50E-02
C2	-6.62E+00	-1.83E+00	1.30E-01
C3	-6.87E+00	1.01E+00	-1.28E-01
N4	-4.26E+00	1.85E+00	2.19E-01
H5	-7.68E+00	-2.88E+00	-1.29E+00
H6	-7.54E+00	1.58E+00	-2.01E+00
N7	-3.91E+00	-2.22E+00	-1.99E-01
C8	-3.03E+00	-4.81E+00	-2.39E-01
H9	-1.03E+00	-4.88E+00	-6.49E-01
H10	-3.39E+00	-5.71E+00	1.59E+00
H11	-4.06E+00	-5.82E+00	-1.72E+00
C12	-3.79E+00	4.52E+00	1.82E-02
H13	-5.07E+00	5.53E+00	1.29E+00
H14	-1.87E+00	4.98E+00	5.60E-01
H15	-4.12E+00	5.20E+00	-1.91E+00
Cl16	1.77E+00	-2.53E+00	-3.57E+00
Cl17	1.68E+00	-3.04E+00	3.16E+00
C18	5.10E+00	1.10E-01	4.93E-02
O19	7.23E+00	-6.63E-02	6.14E-02
C20	1.33E+00	2.80E+00	-2.47E+00
O21	1.33E+00	4.32E+00	-4.00E+00
C22	1.26E+00	2.39E+00	2.87E+00
O23	1.21E+00	3.65E+00	4.61E+00
Ru24	1.41E+00	2.74E-01	2.12E-02
H25	-8.11E+00	1.86E+00	1.29E+00
H26	-7.19E+00	-2.51E+00	2.00E+00

1.7p

Atom	X	Y	Z
Cl1	-8.09E-01	-3.30E+00	-2.89E+00
Cl2	-8.09E-01	3.30E+00	-2.89E+00
C3	-4.70E+00	-7.50E-16	-2.84E-01
O4	-6.80E+00	-1.09E-15	-6.68E-01
C5	-1.10E+00	-2.61E+00	2.65E+00
O6	-1.13E+00	-4.18E+00	4.12E+00
C7	-1.10E+00	2.61E+00	2.65E+00
O8	-1.13E+00	4.18E+00	4.12E+00
Ru9	-1.03E+00	-1.53E-16	2.38E-01
P10	3.49E+00	5.49E-16	1.76E-03
C11	4.99E+00	-2.73E+00	1.46E+00
H12	7.03E+00	-2.67E+00	1.17E+00
H13	4.59E+00	-2.77E+00	3.49E+00
H14	4.22E+00	-4.44E+00	5.91E-01
C15	4.99E+00	2.73E+00	1.46E+00
H16	4.59E+00	2.77E+00	3.49E+00
H17	7.03E+00	2.67E+00	1.17E+00
H18	4.22E+00	4.44E+00	5.91E-01
C19	4.69E+00	6.18E-16	-3.20E+00
H20	6.75E+00	9.45E-16	-3.16E+00
H21	3.98E+00	-1.67E+00	-4.18E+00
H22	3.98E+00	1.67E+00	-4.18E+00

1.8i

Atom	X	Y	Z
C1	-1.73E+00	1.15E-01	-2.00E-05
C2	-5.95E+00	7.12E-01	-8.44E-05
C3	-5.54E+00	-1.80E+00	1.68E-04
N4	-2.96E+00	-2.14E+00	2.05E-04
H5	-7.68E+00	1.78E+00	-1.93E-04
H6	-6.84E+00	-3.37E+00	3.23E-04
N7	-3.61E+00	1.87E+00	-1.97E-04
C8	-3.29E+00	4.58E+00	-4.69E-04
H9	-2.27E+00	5.18E+00	-1.69E+00
H10	-5.16E+00	5.45E+00	-5.58E-04
H11	-2.27E+00	5.18E+00	1.69E+00
C12	-1.73E+00	-4.60E+00	4.52E-04
H13	-3.18E+00	-6.06E+00	5.97E-04
H14	-5.58E-01	-4.79E+00	-1.69E+00
H15	-5.58E-01	-4.79E+00	1.69E+00
Ru16	1.93E+00	3.11E-01	-3.56E-05
Cl17	2.27E+00	-1.04E+00	-4.09E+00
Cl18	2.27E+00	-1.04E+00	4.09E+00
C19	2.64E+00	3.60E+00	-3.65E-04
H20	1.45E+00	5.28E+00	-5.34E-04
H21	4.69E+00	3.97E+00	-3.99E-04

1.8s

Atom	X	Y	Z
C1	-1.64E+00	2.98E-01	-1.06E-01
C2	-6.00E+00	-1.98E-01	-4.85E-01
C3	-5.42E+00	2.53E+00	2.09E-01
N4	-2.75E+00	2.39E+00	8.37E-01
H5	-7.24E+00	-3.76E-01	-2.13E+00
H6	-5.71E+00	3.82E+00	-1.39E+00
N7	-3.50E+00	-1.22E+00	-1.01E+00

Table 1.13 (continued).

C8	-3.37E+00	-3.92E+00	-1.46E+00
H9	-1.44E+00	-4.58E+00	-1.30E+00
H10	-4.51E+00	-4.91E+00	-4.63E-02
H11	-4.11E+00	-4.37E+00	-3.34E+00
C12	-1.54E+00	4.63E+00	1.83E+00
H13	-2.72E+00	5.38E+00	3.36E+00
H14	3.14E-01	4.17E+00	2.58E+00
H15	-1.30E+00	6.08E+00	3.77E-01
Ru16	1.94E+00	-4.24E-01	-1.48E-01
Cl17	1.54E+00	-3.46E+00	2.90E+00
Cl18	3.84E+00	3.39E+00	-8.66E-01
C19	1.85E+00	-1.83E+00	-3.22E+00
H20	2.54E-01	-1.84E+00	-4.53E+00
H21	3.60E+00	-2.71E+00	-3.92E+00
H22	-6.53E+00	3.21E+00	1.81E+00
H23	-6.86E+00	-1.24E+00	1.09E+00

1.8p

Atom	X	Y	Z
Ru1	-1.54E+00	1.71E-16	2.87E-01
Cl2	-1.99E+00	-4.05E+00	-1.12E+00
Cl3	-1.99E+00	4.05E+00	-1.12E+00
C4	-1.55E+00	1.72E-16	3.67E+00
H5	4.68E-02	0.00E+00	4.99E+00
H6	-3.43E+00	3.31E-06	4.56E+00
P7	2.58E+00	-2.32E-06	-3.38E-02
C8	3.59E+00	-3.23E-06	-3.31E+00
H9	5.66E+00	-5.18E-06	-3.44E+00
H10	2.84E+00	-1.68E+00	-4.25E+00
H11	2.84E+00	1.68E+00	-4.25E+00
C12	4.14E+00	2.72E+00	1.36E+00
H13	6.19E+00	2.61E+00	1.07E+00
H14	3.39E+00	4.43E+00	4.94E-01
H15	3.75E+00	2.78E+00	3.38E+00
C16	4.14E+00	-2.72E+00	1.36E+00
H17	3.39E+00	-4.43E+00	4.94E-01
H18	6.19E+00	-2.61E+00	1.07E+00
H19	3.75E+00	-2.78E+00	3.38E+00

1.9i

Atom	X	Y	Z
C1	-2.21E+00	9.89E-02	-2.29E-01
C2	-6.27E+00	1.19E+00	4.68E-01
C3	-6.27E+00	-1.17E+00	-5.23E-01
N4	-3.78E+00	-1.79E+00	-9.47E-01
H5	-7.81E+00	2.38E+00	1.06E+00
H6	-7.81E+00	-2.43E+00	-9.62E-01
N7	-3.78E+00	1.93E+00	6.22E-01
C8	-2.93E+00	4.26E+00	1.78E+00
H9	-9.02E-01	4.44E+00	1.44E+00
H10	-3.92E+00	5.87E+00	9.46E-01
H11	-3.26E+00	4.21E+00	3.81E+00
C12	-2.92E+00	-4.25E+00	-1.80E+00
H13	-3.93E+00	-4.80E+00	-3.51E+00
H14	-9.00E-01	-4.12E+00	-2.19E+00
H15	-3.21E+00	-5.66E+00	-3.23E-01
Rh16	1.60E+00	7.20E-02	-1.65E-01
Cl17	1.15E+00	-1.67E+00	3.88E+00
C18	1.72E+00	2.76E+00	-3.10E+00
H19	5.66E-03	3.90E+00	-3.14E+00
H20	3.45E+00	3.86E+00	-3.07E+00
C21	1.70E+00	3.22E-01	-4.14E+00
H22	3.42E+00	-4.75E-01	-4.92E+00
H23	-2.14E-02	-4.18E-01	-4.98E+00
C24	5.53E+00	1.07E+00	8.04E-01
H25	6.13E+00	2.70E+00	-2.87E-01
H26	5.44E+00	1.32E+00	2.84E+00
C27	5.53E+00	-1.30E+00	-2.33E-01
H28	5.45E+00	-2.96E+00	9.72E-01
H29	6.14E+00	-1.61E+00	-2.17E+00

1.9s

Atom	X	Y	Z
C1	2.12E+00	2.13E-01	2.26E-01
C2	6.29E+00	1.19E+00	-7.66E-01
C3	6.23E+00	-1.21E+00	8.40E-01
N4	3.59E+00	-1.29E+00	1.65E+00
H5	7.31E+00	9.43E-01	-2.55E+00
H6	6.67E+00	-2.90E+00	-2.73E-01
N7	3.61E+00	1.64E+00	-1.22E+00
C8	2.78E+00	3.54E+00	-2.97E+00
H9	7.18E-01	3.54E+00	-3.01E+00
H10	3.45E+00	5.42E+00	-2.41E+00
H11	3.48E+00	3.12E+00	-4.88E+00
C12	2.67E+00	-3.48E+00	3.00E+00
H13	3.73E+00	-3.72E+00	4.76E+00
H14	6.71E-01	-3.19E+00	3.42E+00
H15	2.85E+00	-5.19E+00	1.85E+00
Rh16	-1.67E+00	1.30E-01	1.25E-01
Cl17	-1.10E+00	-2.90E+00	-3.07E+00
C18	-1.89E+00	3.65E+00	1.98E+00
H19	-2.11E-01	4.78E+00	1.64E+00
H20	-3.65E+00	4.63E+00	1.58E+00
C21	-1.85E+00	1.70E+00	3.78E+00
H22	-3.57E+00	1.16E+00	4.77E+00
H23	-1.22E-01	1.31E+00	4.83E+00
C24	-5.59E+00	6.79E-01	-1.22E+00
H25	-6.22E+00	2.58E+00	-7.85E-01
H26	-5.44E+00	2.01E-01	-3.21E+00
C27	-5.61E+00	-1.19E+00	5.77E-01
H28	-5.49E+00	-3.16E+00	2.99E-02
H29	-6.26E+00	-8.08E-01	2.48E+00

Table 1.13 (continued).

H30	7.51E+00	-1.13E+00	2.46E+00
H31	7.13E+00	2.80E+00	2.45E-01

1.9p

Atom	X	Y	Z
Rh1	-1.21E+00	2.16E-01	0.00E+00
Cl2	-9.06E-01	-4.20E+00	5.69E-06
C3	-1.33E+00	3.97E+00	-1.33E+00
H4	3.68E-01	4.46E+00	-2.38E+00
H5	-3.06E+00	4.36E+00	-2.35E+00
C6	-1.33E+00	3.97E+00	1.33E+00
H7	-3.06E+00	4.36E+00	2.35E+00
H8	3.68E-01	4.46E+00	2.38E+00
C9	-5.17E+00	-2.29E-01	-1.30E+00
H10	-5.74E+00	1.43E+00	-2.35E+00
H11	-5.09E+00	-1.99E+00	-2.34E+00
C12	-5.17E+00	-2.29E-01	1.30E+00
H13	-5.09E+00	-1.99E+00	2.34E+00
H14	-5.74E+00	1.43E+00	2.35E+00
P15	3.15E+00	1.02E-01	-1.96E-06
C16	4.46E+00	-1.57E+00	-2.71E+00
H17	6.51E+00	-1.72E+00	-2.56E+00
H18	3.61E+00	-3.45E+00	-2.78E+00
H19	3.97E+00	-5.65E-01	-4.44E+00
C20	4.99E+00	3.03E+00	-9.54E-06
H21	4.56E+00	4.16E+00	1.67E+00
H22	7.01E+00	2.59E+00	-9.67E-06
H23	4.56E+00	4.16E+00	-1.67E+00
C24	4.46E+00	-1.57E+00	2.71E+00
H25	3.61E+00	-3.45E+00	2.78E+00
H26	6.51E+00	-1.72E+00	2.56E+00
H27	3.97E+00	-5.65E-01	4.44E+00

1.10i

Atom	X	Y	Z
C1	-2.24E+00	3.67E-01	-4.93E-02
C2	-6.40E+00	-4.81E-01	-4.74E-02
C3	-6.14E+00	2.06E+00	-1.69E-01
N4	-3.59E+00	2.55E+00	-1.74E-01
H5	-8.06E+00	-1.65E+00	-1.46E-02
H6	-7.54E+00	3.54E+00	-2.47E-01
N7	-4.00E+00	-1.49E+00	3.03E-02
C8	-3.52E+00	-4.19E+00	1.06E-01
H9	-1.61E+00	-4.53E+00	7.70E-01
H10	-4.86E+00	-5.06E+00	1.42E+00
H11	-3.75E+00	-5.00E+00	-1.78E+00
C12	-2.52E+00	5.07E+00	-1.82E-01
H13	-2.61E+00	5.91E+00	1.70E+00
H14	-5.43E-01	4.97E+00	-7.73E-01
H15	-3.55E+00	6.25E+00	-1.52E+00
Rh16	1.52E+00	3.17E-01	-1.82E-02

Cl17	5.64E+00	1.56E+00	-1.84E-01
Cl18	1.42E+00	-2.39E+00	-3.20E+00
Cl19	1.32E+00	-1.70E+00	3.64E+00

1.10s

Atom	X	Y	Z
C1	-1.82E+00	-1.87E-02	-2.03E-01
C2	-6.07E+00	9.42E-01	-7.06E-02
C3	-5.67E+00	-1.44E+00	-1.64E+00
N4	-3.01E+00	-2.02E+00	-1.14E+00
H5	-6.92E+00	5.34E-01	1.78E+00
H6	-6.87E+00	-3.01E+00	-1.05E+00
N7	-3.49E+00	1.84E+00	2.66E-01
C8	-3.01E+00	4.05E+00	1.80E+00
H9	-1.06E+00	4.67E+00	1.55E+00
H10	-4.23E+00	5.59E+00	1.15E+00
H11	-3.40E+00	3.67E+00	3.80E+00
C12	-1.98E+00	-4.44E+00	-1.89E+00
H13	-1.54E+00	-4.48E+00	-3.91E+00
H14	-2.71E-01	-4.82E+00	-8.13E-01
H15	-3.38E+00	-5.89E+00	-1.46E+00
Rh16	1.66E+00	4.03E-01	5.81E-01
Cl17	3.55E+00	-2.01E+00	-2.25E+00
Cl18	1.28E+00	-2.40E+00	3.83E+00
Cl19	2.39E+00	3.89E+00	-1.84E+00
H20	-5.94E+00	-1.11E+00	-3.66E+00
H21	-7.22E+00	2.36E+00	-1.03E+00

1.10p

Atom	X	Y	Z
Rh1	1.34E+00	2.49E-06	-6.28E-01
Cl2	1.56E+00	-4.26E+00	-1.24E+00
Cl3	2.15E+00	3.75E-06	3.49E+00
Cl4	1.56E+00	4.26E+00	-1.24E+00
P5	-2.69E+00	-5.15E-06	1.51E-01
C6	-3.78E+00	-2.72E+00	1.90E+00
H7	-2.77E+00	-2.80E+00	3.70E+00
H8	-5.81E+00	-2.55E+00	2.22E+00
H9	-3.35E+00	-4.44E+00	8.34E-01
C10	-4.36E+00	-8.53E-06	-2.84E+00
H11	-6.40E+00	-1.24E-05	-2.50E+00
H12	-3.84E+00	1.69E+00	-3.91E+00
H13	-3.84E+00	-1.69E+00	-3.91E+00
C14	-3.78E+00	2.72E+00	1.90E+00
H15	-5.81E+00	2.55E+00	2.22E+00
H16	-2.77E+00	2.80E+00	3.70E+00
H17	-3.35E+00	4.44E+00	8.34E-01

Table 1.13 (continued).

1.11i

Atom	X	Y	Z
C1	1.52E+00	0.00E+00	0.00E+00
C2	5.61E+00	-1.28E+00	0.00E+00
C3	5.61E+00	1.28E+00	0.00E+00
N4	3.11E+00	2.02E+00	0.00E+00
H5	7.16E+00	-2.61E+00	2.04E-06
H6	7.16E+00	2.61E+00	0.00E+00
N7	3.11E+00	-2.02E+00	0.00E+00
C8	2.26E+00	-4.61E+00	2.77E-06
H9	1.98E-01	-4.59E+00	2.51E-06
H10	2.93E+00	-5.60E+00	-1.69E+00
H11	2.93E+00	-5.60E+00	1.69E+00
C12	2.26E+00	4.61E+00	-3.30E-06
H13	2.93E+00	5.60E+00	-1.69E+00
H14	1.98E-01	4.59E+00	-3.53E-06
H15	2.93E+00	5.60E+00	1.69E+00
C16	-2.37E+00	-3.35E-06	-3.73E+00
H17	-1.60E+00	1.73E+00	-4.54E+00
H18	-1.60E+00	-1.73E+00	-4.54E+00
C19	-4.77E+00	-3.12E-06	-2.59E+00
H20	-5.88E+00	-1.73E+00	-2.51E+00
H21	-5.88E+00	1.73E+00	-2.51E+00
C22	-2.37E+00	3.25E-06	3.73E+00
H23	-1.60E+00	-1.73E+00	4.54E+00
H24	-1.60E+00	1.73E+00	4.54E+00
C25	-4.77E+00	2.95E-06	2.59E+00
H26	-5.88E+00	1.73E+00	2.51E+00
H27	-5.88E+00	-1.73E+00	2.51E+00
Ni28	-2.07E+00	1.15E-16	0.00E+00

1.11s

Atom	X	Y	Z
C1	1.17E-16	0.00E+00	-1.41E+00
C2	-1.42E+00	-2.36E-01	-5.59E+00
C3	1.42E+00	2.36E-01	-5.59E+00
N4	2.04E+00	-1.42E-01	-2.93E+00
H5	-1.89E+00	-2.18E+00	-6.17E+00
H6	2.46E+00	-1.07E+00	-6.80E+00
N7	-2.04E+00	1.42E-01	-2.93E+00
C8	-4.60E+00	-1.46E-01	-2.06E+00
H9	-4.63E+00	2.01E-01	-2.62E-02
H10	-5.84E+00	1.21E+00	-3.00E+00
H11	-5.32E+00	-2.06E+00	-2.42E+00
C12	4.60E+00	1.46E-01	-2.06E+00
H13	5.32E+00	2.06E+00	-2.42E+00
H14	4.63E+00	-2.01E-01	-2.62E-02
H15	5.84E+00	-1.21E+00	-3.00E+00
C16	7.04E-03	3.72E+00	2.44E+00
H17	1.74E+00	4.53E+00	1.68E+00
H18	-1.72E+00	4.53E+00	1.67E+00
C19	3.77E-16	2.60E+00	4.84E+00
H20	-1.73E+00	2.52E+00	5.95E+00
H21	1.72E+00	2.52E+00	5.96E+00
C22	-7.04E-03	-3.72E+00	2.44E+00
H23	-1.74E+00	-4.53E+00	1.68E+00
H24	1.72E+00	-4.53E+00	1.67E+00
C25	-1.79E-15	-2.60E+00	4.84E+00
H26	1.73E+00	-2.52E+00	5.95E+00
H27	-1.72E+00	-2.52E+00	5.96E+00
Ni28	-1.79E-16	0.00E+00	2.15E+00
H29	1.89E+00	2.18E+00	-6.17E+00
H30	-2.46E+00	1.07E+00	-6.80E+00

1.11p

Atom	X	Y	Z
C1	-1.94E+00	3.73E+00	-4.52E-02
H2	-1.14E+00	4.55E+00	1.66E+00
H3	-1.24E+00	4.55E+00	-1.80E+00
C4	-4.33E+00	2.61E+00	2.41E-02
H5	-5.49E+00	2.51E+00	-1.67E+00
H6	-5.39E+00	2.50E+00	1.78E+00
C7	-1.94E+00	-3.73E+00	-4.52E-02
H8	-1.24E+00	-4.55E+00	-1.80E+00
H9	-1.14E+00	-4.55E+00	1.66E+00
C10	-4.33E+00	-2.61E+00	2.41E-02
H11	-5.39E+00	-2.50E+00	1.78E+00
H12	-5.49E+00	-2.51E+00	-1.67E+00
Ni13	-1.64E+00	2.09E-06	-7.31E-02
P14	2.44E+00	5.86E-06	-3.34E-02
C15	4.15E+00	2.66E+00	-1.45E+00
H16	6.20E+00	2.46E+00	-1.21E+00
H17	3.72E+00	2.77E+00	-3.46E+00
H18	3.53E+00	4.42E+00	-5.69E-01
C19	3.72E+00	-1.10E-04	3.18E+00
H20	3.04E+00	-1.67E+00	4.19E+00
H21	5.79E+00	-1.07E-04	3.18E+00
H22	3.04E+00	1.67E+00	4.19E+00
C23	4.15E+00	-2.66E+00	-1.45E+00
H24	3.72E+00	-2.76E+00	-3.46E+00
H25	6.20E+00	-2.46E+00	-1.21E+00
H26	3.53E+00	-4.42E+00	-5.69E-01

1.12i

Atom	X	Y	Z
C1	2.04E+00	1.13E-16	8.81E-06
C2	6.13E+00	1.28E+00	-5.85E-02
C3	6.13E+00	-1.28E+00	5.85E-02
N4	3.63E+00	-2.01E+00	9.22E-02
H5	7.68E+00	2.60E+00	-1.20E-01
H6	7.68E+00	-2.60E+00	1.19E-01
N7	3.63E+00	2.01E+00	-9.21E-02

Table 1.13 (continued).

C8	2.78E+00	4.61E+00	-2.11E-01
H9	7.17E-01	4.58E+00	-2.04E-01
H10	3.46E+00	5.67E+00	1.43E+00
H11	3.45E+00	5.51E+00	-1.94E+00
C12	2.78E+00	-4.61E+00	2.11E-01
H13	3.45E+00	-5.51E+00	1.94E+00
H14	7.17E-01	-4.58E+00	2.04E-01
H15	3.46E+00	-5.67E+00	-1.43E+00
C16	-2.33E+00	2.36E-01	4.01E+00
H17	-1.57E+00	-1.44E+00	4.91E+00
H18	-1.57E+00	2.01E+00	4.71E+00
C19	-4.71E+00	1.68E-01	2.86E+00
H20	-5.81E+00	1.89E+00	2.65E+00
H21	-5.81E+00	-1.57E+00	2.85E+00
C22	-2.33E+00	-2.36E-01	-4.01E+00
H23	-1.57E+00	1.44E+00	-4.91E+00
H24	-1.57E+00	-2.01E+00	-4.71E+00
C25	-4.71E+00	-1.68E-01	-2.86E+00
H26	-5.81E+00	-1.89E+00	-2.65E+00
H27	-5.81E+00	1.57E+00	-2.85E+00
Pd28	-1.88E+00	-2.53E-06	-5.76E-05

1.12s

Atom	X	Y	Z
C1	-1.94E+00	-4.32E-16	0.00E+00
C2	-6.12E+00	-1.44E+00	1.21E-02
C3	-6.12E+00	1.44E+00	-1.21E-02
N4	-3.46E+00	1.99E+00	-4.47E-01
H5	-6.73E+00	-2.24E+00	-1.81E+00
H6	-7.31E+00	2.24E+00	-1.50E+00
N7	-3.46E+00	-1.99E+00	4.47E-01
C8	-2.59E+00	-4.56E+00	6.14E-01
H9	-5.48E-01	-4.53E+00	8.91E-01
H10	-3.49E+00	-5.53E+00	2.21E+00
H11	-3.02E+00	-5.62E+00	-1.12E+00
C12	-2.59E+00	4.56E+00	-6.14E-01
H13	-3.02E+00	5.62E+00	1.12E+00
H14	-5.48E-01	4.53E+00	-8.91E-01
H15	-3.49E+00	5.53E+00	-2.21E+00
C16	2.41E+00	6.76E-01	3.96E+00
H17	1.66E+00	2.52E+00	4.46E+00
H18	1.65E+00	-8.92E-01	5.04E+00
C19	4.80E+00	4.80E-01	2.82E+00
H20	5.90E+00	-1.25E+00	3.01E+00
H21	5.90E+00	2.17E+00	2.43E+00
C22	2.41E+00	-6.76E-01	-3.96E+00
H23	1.66E+00	-2.52E+00	-4.46E+00
H24	1.65E+00	8.92E-01	-5.04E+00
C25	4.80E+00	-4.80E-01	-2.82E+00
H26	5.90E+00	1.25E+00	-3.01E+00
H27	5.90E+00	-2.17E+00	-2.43E+00
Pd28	1.96E+00	4.35E-16	0.00E+00
H29	-6.73E+00	2.24E+00	1.81E+00
H30	-7.31E+00	-2.24E+00	1.50E+00

1.12p

Atom	X	Y	Z
C1	-1.77E+00	-4.04E+00	-1.14E-02
H2	-9.98E-01	-4.81E+00	-1.75E+00
H3	-9.65E-01	-4.82E+00	1.71E+00
C4	-4.19E+00	-2.99E+00	1.33E-02
H5	-5.27E+00	-2.90E+00	1.76E+00
H6	-5.30E+00	-2.89E+00	-1.71E+00
C7	-2.05E+00	4.02E+00	-4.84E-03
H8	-1.30E+00	4.84E+00	1.73E+00
H9	-1.31E+00	4.84E+00	-1.74E+00
C10	-4.39E+00	2.81E+00	4.86E-03
H11	-5.49E+00	2.64E+00	-1.72E+00
H12	-5.47E+00	2.64E+00	1.74E+00
Pd13	-1.45E+00	1.04E-02	-1.17E-02
P14	2.91E+00	5.12E-02	-6.60E-03
C15	4.56E+00	3.07E+00	-4.16E-01
H16	3.98E+00	4.37E+00	1.07E+00
H17	6.62E+00	2.84E+00	-3.48E-01
H18	4.03E+00	3.89E+00	-2.23E+00
C19	4.39E+00	-1.13E+00	2.89E+00
H20	3.76E+00	-3.07E+00	3.24E+00
H21	6.46E+00	-1.10E+00	2.77E+00
H22	3.79E+00	2.97E-02	4.49E+00
C23	4.48E+00	-1.88E+00	-2.41E+00
H24	6.54E+00	-1.79E+00	-2.25E+00
H25	3.87E+00	-3.85E+00	-2.21E+00
H26	3.92E+00	-1.23E+00	-4.29E+00

1.13i

Atom	X	Y	Z
C1	-2.25E-01	0.00E+00	0.00E+00
C2	-4.30E+00	-1.28E+00	0.00E+00
C3	-4.30E+00	1.28E+00	0.00E+00
N4	-1.81E+00	2.02E+00	0.00E+00
H5	-5.85E+00	-2.61E+00	0.00E+00
H6	-5.85E+00	2.61E+00	0.00E+00
N7	-1.81E+00	-2.02E+00	0.00E+00
C8	-9.58E-01	-4.62E+00	0.00E+00
H9	1.10E+00	-4.62E+00	0.00E+00
H10	-1.64E+00	-5.60E+00	1.69E+00
H11	-1.64E+00	-5.60E+00	-1.69E+00
C12	-9.58E-01	4.62E+00	0.00E+00
H13	-1.64E+00	5.60E+00	1.69E+00
H14	1.10E+00	4.62E+00	0.00E+00
H15	-1.64E+00	5.60E+00	-1.69E+00
Cu16	3.43E+00	0.00E+00	0.00E+00
H17	6.31E+00	0.00E+00	0.00E+00

Table 1.13 (continued).

1.13s

Atom	X	Y	Z
C1	1.38E-01	0.00E+00	0.00E+00
C2	4.31E+00	1.44E+00	-1.47E-01
C3	4.31E+00	-1.44E+00	1.47E-01
N4	1.63E+00	-2.04E+00	-1.40E-01
H5	5.45E+00	2.40E+00	1.28E+00
H6	5.45E+00	-2.40E+00	-1.28E+00
N7	1.63E+00	2.04E+00	1.40E-01
C8	7.67E-01	4.61E+00	1.35E-02
H9	-1.28E+00	4.63E+00	2.20E-01
H10	1.61E+00	5.74E+00	1.53E+00
H11	1.26E+00	5.48E+00	-1.80E+00
C12	7.67E-01	-4.61E+00	-1.35E-02
H13	1.26E+00	-5.48E+00	1.80E+00
H14	-1.28E+00	-4.63E+00	-2.20E-01
H15	1.61E+00	-5.74E+00	-1.53E+00
Cu16	-3.53E+00	-1.96E-16	0.00E+00
H17	-6.41E+00	-3.56E-16	0.00E+00
H18	4.98E+00	-2.04E+00	2.02E+00
H19	4.98E+00	2.04E+00	-2.02E+00

1.13p

Atom	X	Y	Z
Cu1	-3.01E+00	-3.71E-05	1.51E-05
H2	-5.90E+00	-6.11E-05	-4.34E-05
P3	1.19E+00	7.50E-06	7.59E-06
C4	2.69E+00	-1.64E+00	-2.64E+00
H5	4.75E+00	-1.56E+00	-2.51E+00
H6	2.09E+00	-3.62E+00	-2.65E+00
H7	2.09E+00	-7.84E-01	-4.42E+00
C8	2.69E+00	3.11E+00	-1.04E-01
H9	2.09E+00	4.22E+00	1.53E+00
H10	4.75E+00	2.96E+00	-9.87E-02
H11	2.09E+00	4.11E+00	-1.81E+00
C12	2.69E+00	-1.46E+00	2.74E+00
H13	2.09E+00	-3.43E+00	2.89E+00
H14	4.75E+00	-1.39E+00	2.61E+00
H15	2.09E+00	-4.88E-01	4.46E+00

1.14i

Atom	X	Y	Z
C1	-8.80E-01	5.45E-05	3.70E-04
C2	-4.96E+00	-1.28E+00	-5.62E-04
C3	-4.96E+00	1.28E+00	-5.61E-04
N4	-2.46E+00	2.02E+00	8.45E-05
H5	-6.50E+00	-2.61E+00	-8.33E-04
H6	-6.50E+00	2.61E+00	-8.29E-04
N7	-2.46E+00	-2.02E+00	8.45E-05
C8	-1.62E+00	-4.62E+00	2.37E-04
H9	4.43E-01	-4.62E+00	2.39E-03
H10	-2.30E+00	-5.60E+00	1.69E+00
H11	-2.29E+00	-5.60E+00	-1.69E+00
C12	-1.62E+00	4.62E+00	2.37E-04
H13	-2.30E+00	5.60E+00	1.69E+00
H14	4.43E-01	4.62E+00	2.34E-03
H15	-2.29E+00	5.60E+00	-1.69E+00
C16	6.40E+00	1.58E-04	-5.93E-04
H17	7.18E+00	-4.98E-01	1.86E+00
H18	7.18E+00	-1.36E+00	-1.36E+00
H19	7.18E+00	1.86E+00	-4.98E-01
Cu20	2.76E+00	-5.27E-05	2.66E-04

1.14s

Atom	X	Y	Z
C1	-7.86E-01	5.28E-05	5.37E-04
C2	-4.96E+00	-1.44E+00	1.50E-01
C3	-4.96E+00	1.43E+00	-1.51E-01
N4	-2.29E+00	2.04E+00	1.45E-01
H5	-5.62E+00	-2.03E+00	2.03E+00
H6	-6.11E+00	2.40E+00	1.27E+00
N7	-2.28E+00	-2.04E+00	-1.44E-01
C8	-1.42E+00	-4.61E+00	-1.28E-02
H9	6.31E-01	-4.63E+00	-2.26E-01
H10	-1.91E+00	-5.48E+00	1.81E+00
H11	-2.27E+00	-5.74E+00	-1.53E+00
C12	-1.42E+00	4.61E+00	1.42E-02
H13	-2.27E+00	5.74E+00	1.53E+00
H14	6.29E-01	4.63E+00	2.30E-01
H15	-1.91E+00	5.47E+00	-1.81E+00
C16	6.50E+00	1.07E-04	-9.40E-04
H17	7.28E+00	-5.68E-01	1.84E+00
H18	7.28E+00	-1.31E+00	-1.41E+00
H19	7.29E+00	1.87E+00	-4.29E-01
Cu20	2.86E+00	4.00E-04	5.54E-05
H21	-5.62E+00	2.03E+00	-2.03E+00
H22	-6.11E+00	-2.40E+00	-1.27E+00

1.14p

Atom	X	Y	Z
C1	-5.94E+00	-7.71E-04	7.43E-04
H2	-6.71E+00	-3.65E-01	1.89E+00
H3	-6.71E+00	1.82E+00	-6.30E-01
H4	-6.71E+00	-1.46E+00	-1.26E+00
Cu5	-2.29E+00	1.11E-03	-1.10E-03
P6	1.88E+00	3.28E-04	-3.85E-04
C7	3.39E+00	2.93E+00	-1.05E+00
H8	2.79E+00	4.48E+00	1.69E-01
H9	5.45E+00	2.78E+00	-9.95E-01
H10	2.79E+00	3.36E+00	-2.97E+00
C11	3.38E+00	-5.57E-01	3.06E+00
H12	2.78E+00	-2.39E+00	3.80E+00

Table 1.13 (continued).

H13	5.45E+00	-5.31E-01	2.91E+00
H14	2.78E+00	8.98E-01	4.40E+00
C15	3.39E+00	-2.37E+00	-2.01E+00
H16	2.79E+00	-2.10E+00	-3.97E+00
H17	5.45E+00	-2.26E+00	-1.91E+00
H18	2.78E+00	-4.26E+00	-1.42E+00

1.15i

Atom	X	Y	Z
C1	0.00E+00	0.00E+00	-1.27E+00
C2	0.00E+00	1.28E+00	-5.34E+00
C3	-1.57E-16	-1.28E+00	-5.34E+00
N4	0.00E+00	-2.02E+00	-2.84E+00
H5	0.00E+00	2.61E+00	-6.88E+00
H6	-3.19E-16	-2.61E+00	-6.88E+00
N7	2.47E-16	2.02E+00	-2.84E+00
C8	0.00E+00	4.63E+00	-2.01E+00
H9	0.00E+00	4.65E+00	5.21E-02
H10	1.69E+00	5.60E+00	-2.69E+00
H11	-1.69E+00	5.60E+00	-2.69E+00
C12	-5.67E-16	-4.63E+00	-2.01E+00
H13	1.69E+00	-5.60E+00	-2.69E+00
H14	-5.69E-16	-4.65E+00	5.21E-02
H15	-1.69E+00	-5.60E+00	-2.69E+00
C16	0.00E+00	-3.27E-16	5.88E+00
N17	0.00E+00	-4.49E-16	8.08E+00
Cu18	0.00E+00	-1.30E-16	2.35E+00

1.15s

Atom	X	Y	Z
C1	1.18E+00	0.00E+00	0.00E+00
C2	5.34E+00	1.44E+00	-1.41E-01
C3	5.34E+00	-1.44E+00	1.41E-01
N4	2.66E+00	-2.04E+00	-1.30E-01
H5	6.47E+00	2.40E+00	1.30E+00
H6	6.47E+00	-2.40E+00	-1.30E+00
N7	2.66E+00	2.04E+00	1.30E-01
C8	1.80E+00	4.62E+00	1.36E-02
H9	-2.47E-01	4.66E+00	2.26E-01
H10	2.65E+00	5.73E+00	1.54E+00
H11	2.30E+00	5.49E+00	-1.80E+00
C12	1.80E+00	-4.62E+00	-1.36E-02
H13	2.30E+00	-5.49E+00	1.80E+00
H14	-2.47E-01	-4.66E+00	-2.26E-01
H15	2.65E+00	-5.73E+00	-1.54E+00
C16	-5.99E+00	0.00E+00	0.00E+00
N17	-8.19E+00	0.00E+00	0.00E+00
Cu18	-2.46E+00	0.00E+00	0.00E+00
H19	6.02E+00	-2.05E+00	2.00E+00
H20	6.02E+00	2.05E+00	-2.00E+00

1.15p

Atom	X	Y	Z
C1	-5.40E+00	-2.88E-05	8.06E-06
N2	-7.59E+00	-3.35E-04	1.72E-05
Cu3	-1.85E+00	2.79E-04	-1.44E-05
P4	2.32E+00	2.63E-05	-1.68E-05
C5	3.77E+00	3.08E+00	-5.32E-01
H6	3.16E+00	4.39E+00	9.36E-01
H7	5.84E+00	2.94E+00	-5.07E-01
H8	3.16E+00	3.82E+00	-2.36E+00
C9	3.77E+00	-2.00E+00	-2.40E+00
H10	5.84E+00	-1.91E+00	-2.29E+00
H11	3.16E+00	-3.95E+00	-2.13E+00
H12	3.16E+00	-1.39E+00	-4.27E+00
C13	3.77E+00	-1.08E+00	2.93E+00
H14	3.16E+00	-3.01E+00	3.34E+00
H15	5.84E+00	-1.03E+00	2.80E+00
H16	3.16E+00	1.29E-01	4.49E+00

1.16i

Atom	X	Y	Z
C1	0.00E+00	0.00E+00	-7.80E-01
C2	0.00E+00	-1.28E+00	-4.85E+00
C3	1.57E-16	1.28E+00	-4.85E+00
N4	0.00E+00	2.02E+00	-2.36E+00
H5	0.00E+00	-2.61E+00	-6.40E+00
H6	3.19E-16	2.61E+00	-6.40E+00
N7	-2.47E-16	-2.02E+00	-2.36E+00
C8	0.00E+00	-4.63E+00	-1.52E+00
H9	0.00E+00	-4.64E+00	5.37E-01
H10	-1.69E+00	-5.60E+00	-2.21E+00
H11	1.69E+00	-5.60E+00	-2.21E+00
C12	5.67E-16	4.63E+00	-1.52E+00
H13	-1.69E+00	5.60E+00	-2.21E+00
H14	5.68E-16	4.64E+00	5.37E-01
H15	1.69E+00	5.60E+00	-2.21E+00
F16	0.00E+00	0.00E+00	6.10E+00
Cu17	0.00E+00	0.00E+00	2.75E+00

1.16s

Atom	X	Y	Z
C1	6.88E-01	-1.91E-16	0.00E+00
C2	4.86E+00	-1.43E+00	1.58E-01
C3	4.86E+00	1.43E+00	-1.58E-01
N4	2.18E+00	2.04E+00	1.51E-01
H5	6.01E+00	-2.41E+00	-1.25E+00
H6	6.01E+00	2.41E+00	1.25E+00
N7	2.18E+00	-2.04E+00	-1.51E-01
C8	1.33E+00	-4.62E+00	-1.38E-02
H9	-7.20E-01	-4.65E+00	-2.60E-01
H10	2.20E+00	-5.75E+00	-1.51E+00

Table 1.13 (continued).

H11	1.79E+00	-5.47E+00	1.82E+00
C12	1.33E+00	4.62E+00	1.38E-02
H13	1.79E+00	5.47E+00	-1.82E+00
H14	-7.20E-01	4.65E+00	2.60E-01
H15	2.20E+00	5.75E+00	1.51E+00
F16	-6.20E+00	1.72E-15	1.29E-16
Cu17	-2.85E+00	7.91E-16	0.00E+00
H18	5.50E+00	2.02E+00	-2.04E+00
H19	5.50E+00	-2.02E+00	2.04E+00

1.16p

Atom	X	Y	Z
F1	-5.63E+00	-5.76E-05	2.70E-05
Cu2	-2.28E+00	6.96E-05	-7.46E-06
P3	1.77E+00	3.81E-05	-2.23E-06
C4	3.25E+00	2.84E+00	-1.28E+00
H5	5.31E+00	2.70E+00	-1.22E+00
H6	2.64E+00	3.11E+00	-3.23E+00
H7	2.64E+00	4.48E+00	-1.87E-01
C8	3.25E+00	-2.53E+00	-1.82E+00
H9	5.31E+00	-2.41E+00	-1.73E+00
H10	2.64E+00	-4.36E+00	-1.08E+00
H11	2.64E+00	-2.40E+00	-3.79E+00
C12	3.25E+00	-3.13E-01	3.10E+00
H13	5.31E+00	-2.98E-01	2.95E+00
H14	2.64E+00	1.24E+00	4.31E+00
H15	2.64E+00	-2.08E+00	3.98E+00

1.17i

Atom	X	Y	Z
C1	0.00E+00	0.00E+00	-1.41E+00
C2	0.00E+00	1.28E+00	-5.48E+00
C3	-1.57E-16	-1.28E+00	-5.48E+00
N4	0.00E+00	-2.02E+00	-2.99E+00
H5	0.00E+00	2.61E+00	-7.02E+00
H6	-3.19E-16	-2.61E+00	-7.02E+00
N7	2.47E-16	2.02E+00	-2.99E+00
C8	0.00E+00	4.63E+00	-2.15E+00
H9	0.00E+00	4.64E+00	-8.65E-02
H10	1.69E+00	5.60E+00	-2.83E+00
H11	-1.69E+00	5.60E+00	-2.83E+00
C12	-5.67E-16	-4.63E+00	-2.15E+00
H13	1.69E+00	-5.60E+00	-2.83E+00
H14	-5.68E-16	-4.64E+00	-8.65E-02
H15	-1.69E+00	-5.60E+00	-2.83E+00
Cl16	0.00E+00	-1.70E-16	6.13E+00
Cu17	0.00E+00	0.00E+00	2.17E+00

1.17s

Atom	X	Y	Z
C1	-1.31E+00	-4.38E-16	0.00E+00
C2	-5.48E+00	-1.44E+00	-1.51E-01
C3	-5.48E+00	1.44E+00	1.51E-01
N4	-2.80E+00	2.04E+00	-1.41E-01
H5	-6.14E+00	-2.03E+00	-2.03E+00
H6	-6.62E+00	2.40E+00	-1.27E+00
N7	-2.80E+00	-2.04E+00	1.41E-01
C8	-1.94E+00	-4.62E+00	1.39E-02
H9	1.04E-01	-4.65E+00	2.45E-01
H10	-2.81E+00	-5.74E+00	1.52E+00
H11	-2.42E+00	-5.48E+00	-1.81E+00
C12	-1.94E+00	4.62E+00	-1.39E-02
H13	-2.42E+00	5.48E+00	1.81E+00
H14	1.04E-01	4.65E+00	-2.45E-01
H15	-2.81E+00	5.74E+00	-1.52E+00
Cl16	6.24E+00	2.08E-15	0.00E+00
Cu17	2.28E+00	7.58E-16	0.00E+00
H18	-6.14E+00	2.03E+00	2.03E+00
H19	-6.62E+00	-2.40E+00	1.27E+00

1.17p

Atom	X	Y	Z
Cl1	-5.64E+00	-1.48E-04	-1.34E-05
Cu2	-1.67E+00	1.70E-04	4.33E-05
P3	2.43E+00	8.29E-05	-1.93E-06
C4	3.90E+00	-1.43E+00	2.77E+00
H5	5.96E+00	-1.37E+00	2.64E+00
H6	3.29E+00	-4.34E-01	4.47E+00
H7	3.29E+00	-3.40E+00	2.93E+00
C8	3.90E+00	-1.68E+00	-2.63E+00
H9	3.29E+00	-8.38E-01	-4.41E+00
H10	5.96E+00	-1.60E+00	-2.50E+00
H11	3.29E+00	-3.65E+00	-2.61E+00
C12	3.90E+00	3.12E+00	-1.42E-01
H13	5.96E+00	2.97E+00	-1.35E-01
H14	3.29E+00	4.09E+00	-1.86E+00
H15	3.29E+00	4.24E+00	1.48E+00

1.18i

Atom	X	Y	Z
C1	0.00E+00	0.00E+00	-2.44E+00
C2	0.00E+00	-1.28E+00	-6.51E+00
C3	1.57E-16	1.28E+00	-6.51E+00
N4	0.00E+00	2.02E+00	-4.02E+00
H5	0.00E+00	-2.61E+00	-8.06E+00
H6	3.19E-16	2.61E+00	-8.06E+00
N7	-2.47E-16	-2.02E+00	-4.02E+00
C8	0.00E+00	-4.63E+00	-3.18E+00
H9	0.00E+00	-4.64E+00	-1.12E+00

Table 1.13 (continued).

H10	-1.69E+00	-5.60E+00	-3.86E+00
H11	1.69E+00	-5.60E+00	-3.86E+00
C12	5.67E-16	4.63E+00	-3.18E+00
H13	-1.69E+00	5.60E+00	-3.86E+00
H14	5.68E-16	4.64E+00	-1.12E+00
H15	1.69E+00	5.60E+00	-3.86E+00
Br16	0.00E+00	-1.49E-16	5.36E+00
Cu17	0.00E+00	0.00E+00	1.15E+00

1.18s

Atom	X	Y	Z
C1	0.00E+00	0.00E+00	-2.35E+00
C2	-2.47E-01	1.42E+00	-6.51E+00
C3	2.47E-01	-1.42E+00	-6.51E+00
N4	1.10E-16	-2.05E+00	-3.84E+00
H5	-2.16E+00	1.89E+00	-7.17E+00
H6	-1.11E+00	-2.48E+00	-7.65E+00
N7	1.40E-16	2.05E+00	-3.84E+00
C8	-3.01E-01	4.61E+00	-2.97E+00
H9	-7.77E-02	4.66E+00	-9.27E-01
H10	1.13E+00	5.83E+00	-3.83E+00
H11	-2.18E+00	5.34E+00	-3.46E+00
C12	3.01E-01	-4.61E+00	-2.97E+00
H13	2.18E+00	-5.34E+00	-3.46E+00
H14	7.77E-02	-4.66E+00	-9.27E-01
H15	-1.13E+00	-5.83E+00	-3.83E+00
Br16	0.00E+00	-1.52E-16	5.47E+00
Cu17	0.00E+00	0.00E+00	1.26E+00
H18	2.16E+00	-1.89E+00	-7.17E+00
H19	1.11E+00	2.48E+00	-7.65E+00

1.18p

Atom	X	Y	Z
Br1	-4.85E+00	-2.33E-04	2.39E-04
Cu2	-6.41E-01	8.88E-04	-9.12E-04
P3	3.48E+00	1.55E-04	-1.93E-04
C4	4.95E+00	2.95E+00	-9.97E-01
H5	4.34E+00	4.48E+00	2.49E-01
H6	7.01E+00	2.81E+00	-9.50E-01
H7	4.34E+00	3.41E+00	-2.92E+00
C8	4.95E+00	-6.13E-01	3.06E+00
H9	4.34E+00	-2.46E+00	3.76E+00
H10	7.01E+00	-5.85E-01	2.92E+00
H11	4.34E+00	8.19E-01	4.41E+00
C12	4.95E+00	-2.34E+00	-2.06E+00
H13	7.01E+00	-2.23E+00	-1.96E+00
H14	4.34E+00	-4.23E+00	-1.50E+00
H15	4.34E+00	-2.03E+00	-4.01E+00

1.19i

Atom	X	Y	Z
C1	0.00E+00	0.00E+00	-3.31E+00
C2	0.00E+00	1.28E+00	-7.38E+00
C3	-1.57E-16	-1.28E+00	-7.38E+00
N4	0.00E+00	-2.02E+00	-4.88E+00
H5	0.00E+00	2.61E+00	-8.92E+00
H6	-3.19E-16	-2.61E+00	-8.92E+00
N7	2.47E-16	2.02E+00	-4.88E+00
C8	0.00E+00	4.63E+00	-4.04E+00
H9	0.00E+00	4.64E+00	-1.98E+00
H10	1.69E+00	5.60E+00	-4.73E+00
H11	-1.69E+00	5.60E+00	-4.73E+00
C12	-5.67E-16	-4.63E+00	-4.04E+00
H13	1.69E+00	-5.60E+00	-4.73E+00
H14	-5.68E-16	-4.64E+00	-1.98E+00
H15	-1.69E+00	-5.60E+00	-4.73E+00
I16	0.00E+00	-1.35E-16	4.85E+00
Cu17	0.00E+00	0.00E+00	3.05E-01

1.19s

Atom	X	Y	Z
C1	0.00E+00	0.00E+00	-3.21E+00
C2	1.51E-01	-1.44E+00	-7.38E+00
C3	-1.51E-01	1.44E+00	-7.38E+00
N4	1.31E-01	2.04E+00	-4.70E+00
H5	2.02E+00	-2.03E+00	-8.05E+00
H6	1.28E+00	2.40E+00	-8.52E+00
N7	-1.31E-01	-2.04E+00	-4.70E+00
C8	-1.23E-16	-4.62E+00	-3.84E+00
H9	-2.23E-01	-4.65E+00	-1.79E+00
H10	-1.51E+00	-5.74E+00	-4.70E+00
H11	1.82E+00	-5.48E+00	-4.33E+00
C12	7.10E-16	4.62E+00	-3.84E+00
H13	-1.82E+00	5.48E+00	-4.33E+00
H14	2.23E-01	4.65E+00	-1.79E+00
H15	1.51E+00	5.74E+00	-4.70E+00
I16	0.00E+00	1.38E-16	4.96E+00
Cu17	0.00E+00	0.00E+00	4.09E-01
H18	-2.02E+00	2.03E+00	-8.05E+00
H19	-1.28E+00	-2.40E+00	-8.52E+00

Table 1.13 (continued).

1.19p

Atom	X	Y	Z
I1	4.35E+00	0.00E+00	0.00E+00
Cu2	-1.98E-01	-3.00E-05	2.84E-05
P3	-4.35E+00	0.00E+00	-9.67E-06
C4	-5.81E+00	-2.21E+00	-2.20E+00
H5	-7.87E+00	-2.11E+00	-2.10E+00
H6	-5.20E+00	-1.78E+00	-4.12E+00
H7	-5.20E+00	-4.13E+00	-1.76E+00
C8	-5.81E+00	3.01E+00	-8.14E-01
H9	-7.87E+00	2.87E+00	-7.77E-01
H10	-5.20E+00	4.46E+00	5.24E-01
H11	-5.20E+00	3.59E+00	-2.70E+00
C12	-5.81E+00	-8.00E-01	3.01E+00
H13	-7.88E+00	-7.63E-01	2.88E+00
H14	-5.20E+00	-2.68E+00	3.60E+00
H15	-5.20E+00	5.45E-01	4.46E+00

1.4.2. Mechanistic Investigation of NHC-catalyzed Conjugate Addition of Boron and Silicon

1.4.2.1. Experimental

General: Infrared (IR) spectra were recorded on a Bruker alpha spectrophotometer (ATR mode), $\tilde{\nu}_{\text{max}}$ in cm^{-1}. Bands are characterized as broad (br), strong (s), medium (m), or weak (w). ^{1}H NMR spectra were recorded on a Varian Unity INOVA 400 (400 MHz) spectrometer. Chemical shifts are reported in ppm from tetramethylsilane with the solvent resonance resulting from incomplete deuteration as the internal standard ($CDCl_3$: *d* 7.26 ppm). Data are reported as follows: chemical shift, integration, multiplicity (s = singlet, d = doublet, t = triplet, q = quartet, br = broad, m = multiplet), and coupling constants (Hz). For clarity ^{1}H NMR peaks are treated as first-order coupled spin systems; strongly coupled ^{1}H NMR spectra are reported following Pople notation[147] where possible. ^{13}C NMR spectra were recorded on a Varian Unity INOVA 400 (100 MHz) spectrometer with complete proton decoupling. Chemical shifts are reported in ppm from tetramethylsilane with the solvent resonance as the internal standard ($CDCl_3$: *d* 77.16 ppm). High-resolution mass spectrometry analysis was performed on a Micromass LCT ESI-MS (positive mode) at the Mass Spectrometry Facility, Boston College.

---

(147) Bernstein, H. J.; Pople, J. A.; Schneider, W. G. *Can. J. Chem.* **1957**, *35*, 65-81.

Unless otherwise noted, all reactions were carried out with distilled and degassed solvents under an atmosphere of dry N_2 in oven (135 °C) or flame-dried glassware with standard dry box or vacuum-line techniques. Solvents were purified under a positive pressure of dry argon by a modified Innovative Technologies purification system: toluene, benzene and pentane were purified through a copper oxide and alumina column; CH_2Cl_2 and Et_2O were purged with Ar and purified by passage through two alumina columns. Tetrahydrofuran (Aldrich) was purified by distillation from sodium benzophenone ketyl, followed by a vacuum transfer from benzophenone ketyl immediately prior to use unless otherwise specified. Dimethylformamide (extra dry over 4Å mol. sieves) was purchased from Acros and used as received. All work-up and purification procedures were carried out with reagent grade solvents (purchased from Doe & Ingalls) under air.

The data presented in Tables 1.11 and 1.12, and Scheme 1.6 was disclosed elsewhere along with experimental procedures and characterization data.[148]

Reagents:

1,3-Dicyclohexylimidazolium tetrafluoroborate (**ICy·HBF$_4$**) was purchased from Aldrich or TCI America and purified by silica gel chromatography followed by trituration from CH_2Cl_2/hexanes. It was also prepared as described elsewhere.[149]

Bis(pinacolato)diboron ($B_2(pin)_2$) was a gift from Frontier Scientific. It was purified by recrystallization from hot anhydrous pentane, followed by sublimation at 55 °C under high vacuum. The sublimed $B_2(pin)_2$ was subsequently dried under high vacuum at 50 °C for 3 days.

Dimethylphenylsilylpinacolatoborane (DMPS-Bpin) was purchased from Aldrich and distilled *in vacuo* prior to use.

3-cyclopropyl-2-cyclohexen-1-one (**1.51**) was prepared following a procedure disclosed elsewhere.[150]

Preparation of Reagents with Embedded Radical Traps:

---

[148] Lee, K.; Zhugralin, A. R.; Hoveyda, A. H. *J. Am. Chem. Soc.* **2009**, *131*, 7253-7255.

[149] Böhm, V. P. W.; Weskamp, T.; Gstöttmayer, C. W. K.; Herrmann, W. A. *Angew. Chem. Int. Ed.* **2000**, *39*, 1602-1604.

[150] Piers, E.; Banville, J.; Lau, C. K.; Nagakura, I. *Can. J. Chem.* **1982**, *60*, 2965-2975.

2-cyclopropyl-2-cyclohexen-1-one (**1.53**) was prepared following a modified procedure.[151] Under dry N_2 atmosphere in a flame-dried round-bottom flask were mixed anhydrous zinc chloride (1.1969 g, 8.7814 mmol, 1.13 equiv.) and 16 mL of [0.58M] cyclopropyl magnesium bromide solution in THF (9.3 mmol, 1.2 equiv.) The resulting milky-white mixture was allowed to stir at 22 ^oC for 30 min, at which time was added dropwise a solution of 2-iodo-2-cyclohexen-1one[152] (1.7249 g, 7.7687 mmol, 1.00 equiv.) and $[Pd(PPh_3)_2Cl_2]$ (241.5 mg, 0.3441 mmol, 0.0443 equiv.) in DMF (20 mL). The reaction mixture was allowed to stir at 22 ^oC for 12h, at which time aqueous 10% (wt.) citric acid was added dropwise to quench the excess organometallics. The mixture was diluted with Et_2O, layers were separated, and the aqueous layer was washed 2x with Et_2O. Combined organic layers were dried over anhydrous $MgSO_4$, filtered and concentrated *in vacuo* to give brown oil. Purification by silica gel chromatography (5:1 hexanes:Et_2O), followed by bulb-to-bulb distillation (200 ^oC, high vacuum) gave the title product as a colorless oil (660.7 mg, 4.851 mmol, 62% yield). ^1H NMR ($CDCl_3$, 400 MHz): δ 6.42 (1H, dd, J = 4.3, 4.3 Hz), 2.45–2.42 (2H, m), 2.33–2.29 (2H, m), 1.98–1.91 (2H, m), 1.78–1.71 (1H, m), 0.75–0.70 (2H, m), 0.38–0.34 (2H, m). The spectra of the compound were identical to the previously reported spectroscopic data.[153]

3-(2,2-diphenylcyclopropyl)-2-cyclohexen-1-one (**1.55**) was prepared following a modified procedure.[154] Under dry N_2 atmosphere at -20 ^oC was added dropwise a solution of 2,2-diphenylcyclopropyl magnesium bromide (in THF, [0.19M], 25 mL, 4.8 mmol, 0.98 equiv.) to the solution of CuCN (535.9 mg, 5.984 mmol, 1.22 equiv.) and LiBr (1.0247 g, 11.799 mmol, 2.41 equiv.) in THF (5 mL). The resulting creamy yellow mixture was allowed to stir at 0 ^oC for 5 min, at which time was added dropwise at -78 ^oC with vigorous stirring a solution of 3-iodo-2-cyclohexen-1-one (1.0869 g, 4.8953 mmol, 1.00 equiv.) in THF (5 mL). The mixture was allowed to stir at -50 ^oC for 12 h, at which time excess organometallics were quenched by addition of water. The mixture was diluted with water (50 mL) and saturated aqueous NH_4Cl until pH = 7, followed by Et_2O.

---

(151) Negishi, E.; Tan, Z.; Liou, S. –Y.; Liao, B. *Tetrahedron* **2000**, *56*, 10197-10207.
(152) Li, K.; Alexakis, A. *Angew. Chem. Int. Ed.* **2006**, *45*, 7600-7603.
(153) Pattenden, G.; Whybrow, D. *J. Chem. Soc. Perkin Trans. 1* **1981**, 3147-3149.
(154) Majid, T. N.; Yeh, M. C. P.; Knochel, P. *Tetrahedron Lett.* **1989**, *30*, 5069-5072.

Layers were separated, and aqueous layer was washed 2x with Et_2O. Combined organic layers were dried over anhydrous $MgSO_4$, filtered, and concentrated *in vacuo* to give light yellow oil. Purification by silica gel chromatography (2:1 hexanes:Et_2O) gave the title product as a viscous colorless oil (1.0441 g, 3.6206 mmol, 74% yield). IR (neat, ATR mode): 3056 (w), 3023 (w), 2945 (w), 2867 (w), 1660 (s), 1621 (m), 1600 (m), 1494 (m), 1446 (m), 1426 (w), 1396 (w), 1378 (w), 1346 (m), 1324 (m), 1295 (w), 1191 (w), 1179 (w), 1127 (w), 1078 (w), 1038 (w), 1021 (w), 1001 (w), 968 (w), 930 (w), 882 (m), 850 (w), 812 (w), 749 (s), 696 (s), 632 (w), 616 (w), 575 (w), 550 (m), 512 (w), 452 (w), 435 (w) cm^{-1}; ^1H NMR ($CDCl_3$, 400 MHz): δ 7.30–7.15 (10H, m), 5.78 (1H, s), 2.46 (1H, dd, J = 8.0, 6.3 Hz), 2.18 (2H, dddd, J = 39.6, 16.4, 6.4, 6.4 Hz), 2.07 (1H, ddd, J = 17.6, 5.6, 5.6 Hz), 1.99 (1H, dd, J = 6.4, 6.4 Hz), 1.81 (1H, ddd, J = 18.0, 5.6, 5.6 Hz), 1.70–1.66 (2H, m), 1.63 (1H, dd, J = 8.4 , 5.6 Hz); ^{13}C NMR ($CDCl_3$, 100 MHz): δ 199.2, 163.4, 145.9, 140.0, 130.0, 128.6, 128.5, 127.8, 127.1, 126.9, 126.6, 40.3, 37.4, 33.8, 29.8, 22.5, 19.4.

2-(2,2-diphenylcyclopropyl)-2-cyclohexen-1-one (**1.57**) was prepared according to the procedure described for **1.55**. Thus, 2-iodo-2-cyclohexen-1-one[152] (1.5293 g, 6.8878 mmol, 1.00 equiv.), [0.26M] solution of 2,2-diphenylcyclopropyl magnesium bromide in THF (31 mL, 8.1 mmol, 1.2 equiv.), anhydrous $ZnCl_2$ (1.3931 g, 10.221 mmol, 1.48 equiv.), [$Pd(PPh_3)_2Cl_2$] (266.7 mg, 0.3800 mmol, 0.0552 equiv.), and DMF (30 mL) gave the title product as a colorless crystalline solid (870.6 mg, 3.019 mmol, 44% yield) after purification by silica gel chromatography (10:1→5:1 hexanes:Et_2O) and subsequent recrystallization at -15 ^oC from minimum CH_2Cl_2, Et_2O, pentane (excess). IR (neat, ATR mode): IR spectrum needed cm^{-1}; ^1H NMR ($CDCl_3$, 400 MHz): δ 7.60–7.58 (2H, m), 7.28 (2H, dd, J = 7.6, 7.6 Hz), 7.18–7.05 (6H, m), 6.17 (1H, dd, J = 4.0, 4.0 Hz), 2.76 (1H, app t. J = 7.6 Hz), 2.37 (1H, BB' of AA'BB' as app ddd, J = 16.4, 9.6, 4.4 Hz), 2.23 (1H, AA' of AA'BB' as app ddd, J = 16.4, 8.0, 4.4 Hz), 2.21–2.14 (1H, m), 1.96–1.87 (1H, m), 1.86–1.78 (1H, m), 1.71 (1H, dd, J = 6.4, 5.6 Hz), 1.58–1.47 (1H, m), 1.35 (1H, dd, J = 8.4, 5.2 Hz); ^{13}C NMR ($CDCl_3$, 100 MHz): δ 200.2, 146.6, 144.2, 141.2, 136.7, 130.1, 129.2, 128.4, 127.9, 126.3, 126.2, 38.7, 38.3, 25.9, 25.0, 22.8, 15.8.

Test Reactions for Radical Intermediates in Conjugate Addition of Boron to *α,β*-unsaturated carbonyls:

3-cyclopropyl-3-(4,4,5,5-tetramethyl-1,3,2-dioxaborolan-2-yl)cyclohexenone (**1.52**). Under dry N_2 atmosphere in a flame-dried vial were mixed 1,3-dicyclohexylimidazolium tetrafluoroborate (10.6 mg, 0.0331 mmol, 0.0957 equiv.), NaO*t*-Bu (3.8 mg, 0.040 mmol, 0.12 equiv.), vacuum transferred THF (2.0 mL). The resulting mixture was allowed to stir at 22 ^{o}C for 2 h, at which time were added $B_2(pin)_2$ (93.4 mg, 0.368 mmol, 1.08 equiv.), and cyclohexenone **1.51** (46.6 mg, 0.342 mmol, 1.00 equiv.) The reaction mixture was allowed to stir at 22 ^{o}C for 6 h, at which time water (2 mL) was added with vigorous stirring. And the mixture was allowed to stir at 22 ^{o}C for 15 min, at which time it was diluted with EtOAc (~4 mL), layers were separated, and the aqueous layer was washed 3x with EtOAc. Combined organic layers were dried over anhydrous $MgSO_4$, filtered, and concentrated *in vacuo* to give white solid. Purification by silica gel chromatography gave the title product as a colorless oil (77.1 mg, 0.292 mmol, 85% yield). IR (neat, ATR mode): 3080 (w), 2978 (m), 2934 (w), 2872 (w), 1710 (s), 1447 (w), 1390 (m), 1372 (s), 1310 (s), 1281 (m), 1262 (m), 1229 (w), 1212 (m), 1167 (m), 1141 (s), 1125 (s), 1111 (m), 1088 (w), 1071 (w), 1035 (w), 1018 (w), 968 (w), 916 (m), 853 (s), 824 (w), 775 (w), 730 (s), 693 (w), 669 (m), 647 (m), 579 (w), 539 (w), 520 (w), 478 (w), 461 (w), 426 (w), 412 (w) cm^{-1}; ^{1}H NMR ($CDCl_3$, 400 MHz): δ 2.43 (1H, B of AB, J_{AB} = 14.0 Hz), 2.22–2.16 (2H, m), 2.05–1.90 (2H, m), 1.98 (1H, A of AB, J_{AB} = 14.0 Hz), 1.73–1.62 (1H, m), 1.46 (1H, app ddd, J = 12.8, 12.8, 2.4 Hz), 1.16 (12H, s), 0.72–0.65 (1H, m), 0.36–0.21 (4H, m); ^{13}C NMR ($CDCl_3$, 100 MHz): δ 212.0, 83.6, 48.4, 41.4, 32.6, 24.9, 24.7, 24.4, 18.9, 1.5, 1.0; HRMS (ESI+): Calcd for $C_{15}H_{26}BO_3$ $[M+H]^+$: 265.19750. Found 265.19750. No products due to ring-opening of the cyclopropane ring were observed.

2-cyclopropyl-3-(4,4,5,5-tetramethyl-1,3,2-dioxaborolan-2-yl)cyclohexenone (**1.54** and *O*-**1.54**). Cyclohexenone **1.53** was subjected to the same reaction conditions as above (see **1.52**). Thus, cyclohexenone **1.53** (30.1 mg, 0.221 mmol, 1.00 equiv.), 1,3-dicyclohexylimidazolium tetrafluoroborate (14.2 mg, 0.0444 mmol, 0.201 equiv.), NaO*t*-

Bu (4.6 mg, 0.048 mmol, 0.22 equiv.), $B_2(pin)_2$ (63.2 mg, 0.249 mmol, 1.13 equiv.), and THF (1.5 mL) furnished the major product **1.54** as a colorless oil (39.1 mg, 0.148 mmol, 67% yield) and the minor product *O*-**1.54** as a colorless oil (4.4 mg, 0.017 mmol, 8% yield) after purification by silica gel chromatography (10:1 hexanes:Et_2O). ***Major product*****:** IR (neat, ATR mode): 3079 (w), 2978 (m), 2931 (m), 2853 (w), 1707 (s), 1449 (w), 1406 (w), 1372 (s), 1323 (s), 1257 (m), 1213 (m), 1167 (m), 1142 (s), 1047 (w), 1019 (m), 983 (m), 971 (m), 925 (w), 905 (w), 871 (w), 852 (s), 813 (w), 735 (m), 716 (w), 688 (m), 668 (m), 578 (w), 527 (w), 441 (w) cm^{-1}; ^1H NMR ($CDCl_3$, 400 MHz): δ 2.55–2.47 (1H, m), 2.24–2.18 (1H, m), 2.03–1.88 (2H, m), 1.80-1.66 (3H, m), 1.62–1.58 (1H, m), 1.23 (6H, s), 1.22 (6H, s), 1.13–1.04 (1H, m), 0.54–0.42 (2H, m), 0.22–0.18 (1H, m), 0.14–0.09 (1H, m); ^{13}C NMR ($CDCl_3$, 100 MHz): δ 213.3, 83.6, 83.4, 57.1, 40.4, 27.9, 25.1, 24.9, 24.5, 10.8, 5.4, 4.1; HRMS (ESI+): Calcd for $C_{15}H_{26}BO_3$ $[M+H]^+$: 265.19750. Found 265.19700. ***Minor product*****:** IR (neat, ATR mode): 2979 (m), 2933 (m), 2866 (w), 1707 (m), 1450 (w), 1432 (w), 1380 (s), 1371 (s), 1322 (s), 1274 (w), 1247 (m), 1213 (m), 1166 (w), 1141 (s), 1106 (w), 1081 (m), 1040 (w), 1024 (w), 987 (w), 973 (w), 957 (w), 910 (m), 887 (m), 868 (w), 850 (m), 840 (w), 820 (w), 729 (s), 696 (w), 676 (w), 662 (w), 647 (w), 575 (w); ^1H NMR ($CDCl_3$, 400 MHz): δ 3.72 (1H, s), 2.75 (1H, ddd, J = 14.0, 14.0, 6.4 Hz), 2.48 (1H, dddd, J = 13.6, 2.0, 2.0, 2.0 Hz), 2.19–2.13 (1H, m), 1.66 (1H, dddd, J = 27.6, 13.2, 4.4, 4.4 Hz), 1.47 (1H, dd, J = 13.6, 3.6 Hz), 1.33–1.27 (1H, m), 1.28 (12H, s), 0.84–0.78 (1H, m), 0.41-0.34 (1H, m), 0.31-0.24 (1H, m), 0.15-0.09 (1H, m); ^{13}C NMR ($CDCl_3$, 100 MHz): δ 213.6, 83.5, 77.4, 76.4, 37.8, 29.4, 25.2, 25.1, 25.0, 24.9, 14.5, 2.6, -0.3. No products due to ring-opening of the cyclopropane ring were observed.

2-(2,2-diphenylcyclopropyl)-3-(4,4,5,5-tetramethyl-1,3,2-dioxaborolan-2-yl)cyclohexenone 1.58. Following the procedure described above compound **1.58** was prepared in 45% yield. IR (ATR) mode: 3023 (w), 2975 (w), 2929 (w), 2860 (w), 1703 (s), 1599 (w), 1494 (m), 1446 (m), 1409 (m), 1371 (m), 1261 (s), 1228 (s), 1215 (m) cm^{-1}; ^1H NMR ($CDCl_3$, 400 MHz): δ 7.26 (m, 8H), 7.18–7.11 (m, 2H), 2.54–2.44 (m, 1H), 2.29 (d, J = 13.9 Hz, 1H), 2.19–2.04 (m, 2H), 2.02–1.87 (m, 2H), 1.79 (d, J = 2.4 Hz, 1H), 1.74 (d, *J* = 10.6 Hz, 1H), 1.70–1.56 (m, 1H), 1.50 (t, *J* = 5.6 Hz, 1H), 1.18 (dd, *J* = 8.8, 5.2 Hz, 1H), 1.08 (s, 6H), 1.05 (s, 6H); ^{13}C NMR ($CDCl_3$, 100 MHz): δ 213.39, 146.85, 140.48, 130.25, 128.83, 128.46, 128.31, 126.44, 126.24, 83.47, 50.32, 40.03, 37.16, 28.11, 26.17, 24.84, 24.50, 22.44, 17.85.

3-(dimethyl(phenyl)silyl)-2-(2,2-diphenylcyclopropyl)cyclohexenone 1.71. Under N_2 atmosphere in a flamed-dried vial were mixed enone **1.57** (20.4 mg, 0.0707 mmol, 1.00 equiv), ICy·HBF_4 (2.2 mg, 0.069 mmol, 0.094 equiv), $PhMe_2SiB(pin)$ (22.8 mg, 0.0873 mmol, 1.23 equiv), DBU (3.0 mg, 0.020 mmol, 0.28 equiv), MeOH (0.056 mL), THF (0.011 mL). To the resulting mixture was added H_2O (0.11 mL) with stirring. Resulting mixture was allowed to stir at 22 °C for 24 h, at which time the mixture was diluted with Et_2O. Layers were separated, and aqueous layer was washed 3 x with Et_2O. Combined organic layers were dried over anhydrous $MgSO_4$, filtered, and concentrated *in vacuo* to give colorless solid. Purification by silica gel chromatography (50:1 Hexanes:Et_2O) afforded **1.71** as a colorless oil, which solidified upon standing (7.2 mg, 0.017 mmol, 24% yield). No products due to cyclopropane ring opening were observed. IR (ATR mode): 3056 (w), 3023 (w), 2927 (m), 2857 (w), 2836 (w), 1663 (m), 1600 (w), 1494 (m), 1446 (w), 1428 (w), 1369 (w), 1352 (w), 1253 (m), 1193 (m), 1171 (m), 1137 (m), 1118 (m), 1077 (w), 1023 (m) cm^{-1}; ^{1}H NMR ($CDCl_3$, 400 MHz): δ 7.60 – 7.55 (m, 2H), 7.42–7.27 (m, 5H), 7.25–7.06 (m, 8H), 2.66–2.58 (m, 1H), 2.02 (t, *J* = 5.8 Hz, 1H), 1.65 (dd, *J* = 6.9, 5.1 Hz, 1H), 1.52–1.44 (m, 1H), 1.41–1.36 (m, 1H), 1.36–1.26 (m, 1H), 1.26–1.15 (m, 1H), 1.07–0.95 (m, 1H), 0.77 (dd, *J* = 16.0, 5.4 Hz, 1H), 0.47 (s, 3H); ^{13}C NMR ($CDCl_3$, 101 MHz): δ 147.73, 147.44, 142.12, 138.39, 133.52, 130.63, 129.70, 128.17, 127.97, 127.88, 127.86, 126.08, 125.50, 112.57, 35.08, 30.90, 30.47, 28.35, 26.36, 23.25, 22.62, 18.70, 0.16, 0.01.

1.4.2.2. *X-Ray Crystal Structure of **1.59***

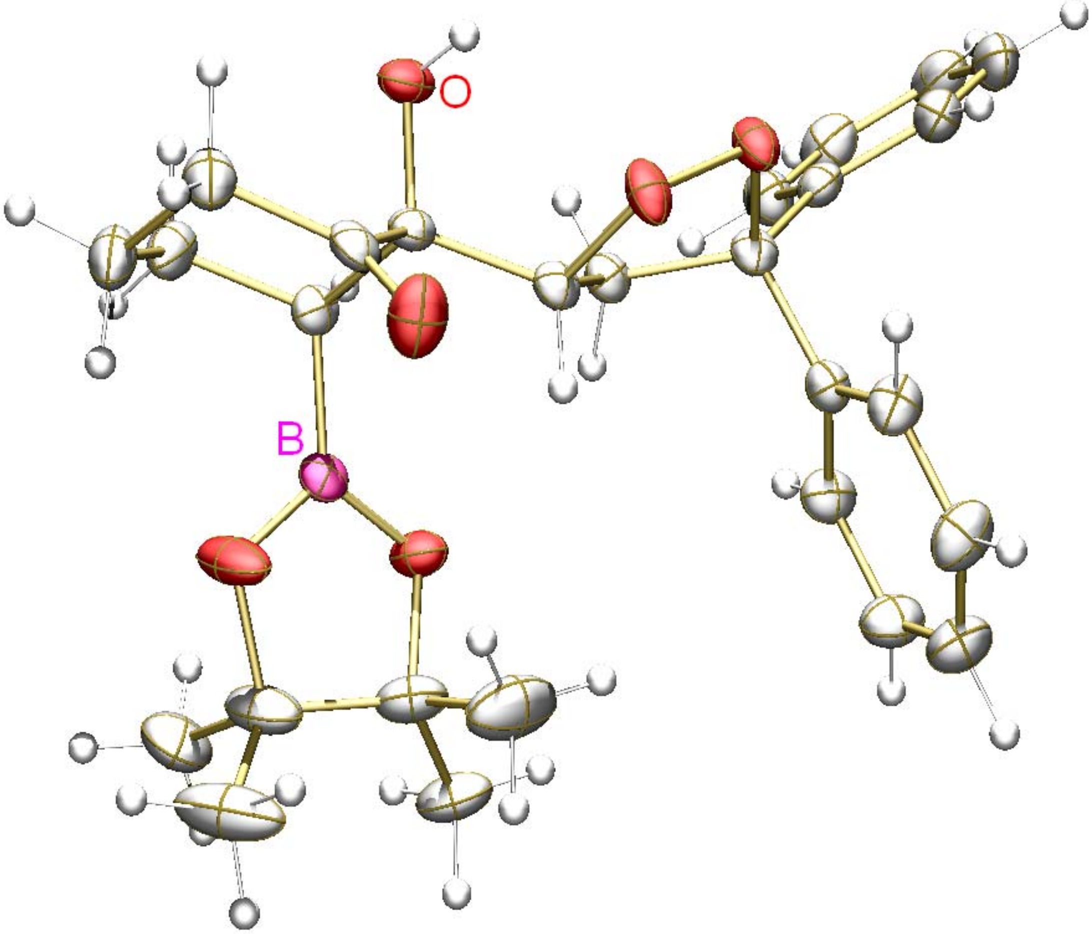

Identification code	C27H33BO6	
Empirical formula	C27 H33 B O6	
Formula weight	464.34	
Temperature	143(2) K	
Wavelength	0.71073 Å	
Crystal system	Orthorhombic	
Space group	P b c a	
Unit cell dimensions	a = 18.8781(9) Å	a= 90°.
	b = 12.1056(5) Å	b= 90°.
	c = 21.2885(9) Å	g = 90°.

Volume	4865.1(4) Å^3
Z	8
Density (calculated)	1.268 Mg/m^3
Absorption coefficient	0.088 mm^{-1}
F(000)	1984
Crystal size	0.17 x 0.02 x 0.02 mm^3
Theta range for data collection	1.91 to 26.00°.
Index ranges	-23<=h<=23, -14<=k<=14, -26<=l<=26
Reflections collected	64871
Independent reflections	4780 [R(int) = 0.0899]
Completeness to theta = 26.00°	100.0 %
Absorption correction	Semi-empirical from equivalents
Max. and min. transmission	0.9983 and 0.9853
Refinement method	Full-matrix least-squares on F^2
Data / restraints / parameters	4780 / 0 / 310
Goodness-of-fit on F^2	1.009
Final R indices [I>2sigma(I)]	R1 = 0.0450, wR2 = 0.0943
R indices (all data)	R1 = 0.0840, wR2 = 0.1110
Extinction coefficient	na
Largest diff. peak and hole	0.408 and -0.214 e.Å^{-3}

Table 1.14. Atomic coordinates (x 10^4) and equivalent isotropic displacement parameters (Å^{2}x 10^3) for sad. U(eq) is defined as one third of the trace of the orthogonalized U^{ij} tensor.

	x	y	z	U(eq)
B(1)	1503(1)	522(2)	2566(1)	23(1)
O(1)	1491(1)	-2315(1)	2112(1)	39(1)
O(2)	920(1)	296(1)	2912(1)	45(1)

O(3)	1377(1)	1282(1)	2103(1)	31(1)
O(4)	3147(1)	-1286(1)	2353(1)	29(1)
O(5)	3074(1)	-1134(1)	708(1)	27(1)
O(6)	2561(1)	-1597(1)	1175(1)	28(1)
C(1)	1953(1)	-1955(2)	2449(1)	25(1)
C(2)	2078(1)	-2348(2)	3109(1)	32(1)
C(3)	1940(1)	-1379(2)	3560(1)	36(1)
C(4)	2374(1)	-368(2)	3379(1)	33(1)
C(5)	2256(1)	-8(2)	2690(1)	24(1)
C(6)	2424(1)	-988(1)	2247(1)	21(1)
C(7)	365(1)	1074(2)	2719(1)	43(1)
C(8)	599(1)	1370(2)	2052(1)	36(1)
C(9)	-346(1)	505(2)	2775(2)	65(1)
C(10)	409(1)	2068(2)	3166(1)	53(1)
C(11)	372(1)	502(2)	1562(1)	61(1)
C(12)	410(1)	2515(2)	1826(1)	42(1)
C(13)	2316(1)	-680(1)	1559(1)	22(1)
C(14)	2745(1)	312(1)	1343(1)	24(1)
C(15)	2888(1)	21(2)	659(1)	23(1)
C(16)	2231(1)	197(2)	251(1)	24(1)
C(17)	1970(1)	1269(2)	182(1)	30(1)
C(18)	1373(1)	1473(2)	-176(1)	37(1)
C(19)	1026(1)	609(2)	-470(1)	39(1)
C(20)	1281(1)	-451(2)	-405(1)	38(1)
C(21)	1882(1)	-657(2)	-48(1)	30(1)
C(22)	3531(1)	577(2)	369(1)	25(1)
C(23)	3791(1)	1568(2)	608(1)	32(1)
C(24)	4360(1)	2090(2)	320(1)	38(1)
C(25)	4675(1)	1627(2)	-200(1)	39(1)
C(26)	4420(1)	643(2)	-440(1)	39(1)
C(27)	3850(1)	125(2)	-162(1)	31(1)

Bond lengths [Å] and angles [°] for sad.

B(1)-O(2)	1.352(3)
B(1)-O(3)	1.369(3)
B(1)-C(5)	1.582(3)
O(1)-C(1)	1.211(2)
O(2)-C(7)	1.468(2)
O(3)-C(8)	1.475(2)
O(4)-C(6)	1.429(2)
O(4)-H(4O)	0.85(2)
O(5)-C(15)	1.445(2)
O(5)-O(6)	1.4959(17)
O(6)-C(13)	1.454(2)
C(1)-C(2)	1.502(3)
C(1)-C(6)	1.532(3)
C(2)-C(3)	1.539(3)
C(2)-H(2A)	0.9900
C(2)-H(2B)	0.9900
C(3)-C(4)	1.523(3)
C(3)-H(3A)	0.9900
C(3)-H(3B)	0.9900
C(4)-C(5)	1.546(3)
C(4)-H(4A)	0.9900
C(4)-H(4B)	0.9900
C(5)-C(6)	1.548(2)
C(5)-H(5)	1.0000
C(6)-C(13)	1.527(3)
C(7)-C(9)	1.513(3)
C(7)-C(8)	1.530(3)
C(7)-C(10)	1.536(3)
C(8)-C(12)	1.510(3)
C(8)-C(11)	1.540(3)
C(9)-H(9A)	0.9800
C(9)-H(9B)	0.9800
C(9)-H(9C)	0.9800

C(10)-H(10A)	0.9800
C(10)-H(10B)	0.9800
C(10)-H(10C)	0.9800
C(11)-H(11A)	0.9800
C(11)-H(11B)	0.9800
C(11)-H(11C)	0.9800
C(12)-H(12A)	0.9800
C(12)-H(12B)	0.9800
C(12)-H(12C)	0.9800
C(13)-C(14)	1.519(2)
C(13)-H(13)	1.0000
C(14)-C(15)	1.522(3)
C(14)-H(14A)	0.9900
C(14)-H(14B)	0.9900
C(15)-C(22)	1.520(3)
C(15)-C(16)	1.530(3)
C(16)-C(21)	1.380(3)
C(16)-C(17)	1.396(3)
C(17)-C(18)	1.383(3)
C(17)-H(17)	0.9500
C(18)-C(19)	1.383(3)
C(18)-H(18)	0.9500
C(19)-C(20)	1.377(3)
C(19)-H(19)	0.9500
C(20)-C(21)	1.388(3)
C(20)-H(20)	0.9500
C(21)-H(21)	0.9500
C(22)-C(23)	1.391(3)
C(22)-C(27)	1.392(3)
C(23)-C(24)	1.388(3)
C(23)-H(23)	0.9500
C(24)-C(25)	1.375(3)
C(24)-H(24)	0.9500
C(25)-C(26)	1.383(3)

C(25)-H(25)	0.9500
C(26)-C(27)	1.380(3)
C(26)-H(26)	0.9500
C(27)-H(27)	0.9500
O(2)-B(1)-O(3)	112.73(17)
O(2)-B(1)-C(5)	123.92(18)
O(3)-B(1)-C(5)	123.33(17)
B(1)-O(2)-C(7)	107.35(16)
B(1)-O(3)-C(8)	105.99(15)
C(6)-O(4)-H(4O)	106.5(15)
C(15)-O(5)-O(6)	104.73(12)
C(13)-O(6)-O(5)	107.00(11)
O(1)-C(1)-C(2)	123.62(18)
O(1)-C(1)-C(6)	121.84(17)
C(2)-C(1)-C(6)	114.39(16)
C(1)-C(2)-C(3)	108.37(16)
C(1)-C(2)-H(2A)	110.0
C(3)-C(2)-H(2A)	110.0
C(1)-C(2)-H(2B)	110.0
C(3)-C(2)-H(2B)	110.0
H(2A)-C(2)-H(2B)	108.4
C(4)-C(3)-C(2)	111.34(17)
C(4)-C(3)-H(3A)	109.4
C(2)-C(3)-H(3A)	109.4
C(4)-C(3)-H(3B)	109.4
C(2)-C(3)-H(3B)	109.4
H(3A)-C(3)-H(3B)	108.0
C(3)-C(4)-C(5)	112.84(17)
C(3)-C(4)-H(4A)	109.0
C(5)-C(4)-H(4A)	109.0
C(3)-C(4)-H(4B)	109.0
C(5)-C(4)-H(4B)	109.0
H(4A)-C(4)-H(4B)	107.8
C(4)-C(5)-C(6)	109.46(15)

C(4)-C(5)-B(1)	113.70(16)
C(6)-C(5)-B(1)	113.19(15)
C(4)-C(5)-H(5)	106.7
C(6)-C(5)-H(5)	106.7
B(1)-C(5)-H(5)	106.7
O(4)-C(6)-C(13)	109.90(15)
O(4)-C(6)-C(1)	108.52(14)
C(13)-C(6)-C(1)	112.19(15)
O(4)-C(6)-C(5)	107.07(14)
C(13)-C(6)-C(5)	111.78(14)
C(1)-C(6)-C(5)	107.17(14)
O(2)-C(7)-C(9)	108.58(17)
O(2)-C(7)-C(8)	101.78(16)
C(9)-C(7)-C(8)	115.8(2)
O(2)-C(7)-C(10)	106.8(2)
C(9)-C(7)-C(10)	110.9(2)
C(8)-C(7)-C(10)	112.13(19)
O(3)-C(8)-C(12)	108.95(16)
O(3)-C(8)-C(7)	101.63(16)
C(12)-C(8)-C(7)	116.19(19)
O(3)-C(8)-C(11)	106.17(17)
C(12)-C(8)-C(11)	110.2(2)
C(7)-C(8)-C(11)	112.9(2)
C(7)-C(9)-H(9A)	109.5
C(7)-C(9)-H(9B)	109.5
H(9A)-C(9)-H(9B)	109.5
C(7)-C(9)-H(9C)	109.5
H(9A)-C(9)-H(9C)	109.5
H(9B)-C(9)-H(9C)	109.5
C(7)-C(10)-H(10A)	109.5
C(7)-C(10)-H(10B)	109.5
H(10A)-C(10)-H(10B)	109.5
C(7)-C(10)-H(10C)	109.5
H(10A)-C(10)-H(10C)	109.5

H(10B)-C(10)-H(10C)	109.5
C(8)-C(11)-H(11A)	109.5
C(8)-C(11)-H(11B)	109.5
H(11A)-C(11)-H(11B)	109.5
C(8)-C(11)-H(11C)	109.5
H(11A)-C(11)-H(11C)	109.5
H(11B)-C(11)-H(11C)	109.5
C(8)-C(12)-H(12A)	109.5
C(8)-C(12)-H(12B)	109.5
H(12A)-C(12)-H(12B)	109.5
C(8)-C(12)-H(12C)	109.5
H(12A)-C(12)-H(12C)	109.5
H(12B)-C(12)-H(12C)	109.5
O(6)-C(13)-C(14)	105.29(14)
O(6)-C(13)-C(6)	108.09(14)
C(14)-C(13)-C(6)	114.33(15)
O(6)-C(13)-H(13)	109.7
C(14)-C(13)-H(13)	109.7
C(6)-C(13)-H(13)	109.7
C(13)-C(14)-C(15)	101.61(14)
C(13)-C(14)-H(14A)	111.4
C(15)-C(14)-H(14A)	111.4
C(13)-C(14)-H(14B)	111.4
C(15)-C(14)-H(14B)	111.4
H(14A)-C(14)-H(14B)	109.3
O(5)-C(15)-C(22)	105.32(14)
O(5)-C(15)-C(14)	101.35(14)
C(22)-C(15)-C(14)	115.28(16)
O(5)-C(15)-C(16)	111.91(15)
C(22)-C(15)-C(16)	110.88(15)
C(14)-C(15)-C(16)	111.57(15)
C(21)-C(16)-C(17)	118.66(18)
C(21)-C(16)-C(15)	122.96(17)
C(17)-C(16)-C(15)	118.37(16)

C(18)-C(17)-C(16)	120.72(18)
C(18)-C(17)-H(17)	119.6
C(16)-C(17)-H(17)	119.6
C(19)-C(18)-C(17)	120.04(19)
C(19)-C(18)-H(18)	120.0
C(17)-C(18)-H(18)	120.0
C(20)-C(19)-C(18)	119.6(2)
C(20)-C(19)-H(19)	120.2
C(18)-C(19)-H(19)	120.2
C(19)-C(20)-C(21)	120.53(19)
C(19)-C(20)-H(20)	119.7
C(21)-C(20)-H(20)	119.7
C(16)-C(21)-C(20)	120.48(18)
C(16)-C(21)-H(21)	119.8
C(20)-C(21)-H(21)	119.8
C(23)-C(22)-C(27)	118.86(18)
C(23)-C(22)-C(15)	121.05(17)
C(27)-C(22)-C(15)	120.01(17)
C(24)-C(23)-C(22)	120.3(2)
C(24)-C(23)-H(23)	119.9
C(22)-C(23)-H(23)	119.9
C(25)-C(24)-C(23)	120.2(2)
C(25)-C(24)-H(24)	119.9
C(23)-C(24)-H(24)	119.9
C(24)-C(25)-C(26)	119.9(2)
C(24)-C(25)-H(25)	120.0
C(26)-C(25)-H(25)	120.0
C(27)-C(26)-C(25)	120.2(2)
C(27)-C(26)-H(26)	119.9
C(25)-C(26)-H(26)	119.9
C(26)-C(27)-C(22)	120.5(2)
C(26)-C(27)-H(27)	119.8
C(22)-C(27)-H(27)	119.8

Symmetry transformations used to generate equivalent atoms:

Table 1.15. Anisotropic displacement parameters (Å^{2}x 10^3) for sad. The anisotropic displacement factor exponent takes the form: $-2\square^{2}[\, h^{2} a^{*2} U^{11} + ... + 2\, h\, k\, a^{*}\, b^{*}\, U^{12} \,]$

	U^{11}	U^{22}	U^{33}	U^{23}	U^{13}	U^{12}
B(1)	26(1)	17(1)	26(1)	-4(1)	1(1)	2(1)
O(1)	44(1)	41(1)	32(1)	0(1)	-2(1)	-18(1)
O(2)	32(1)	39(1)	64(1)	22(1)	15(1)	15(1)
O(3)	23(1)	32(1)	37(1)	6(1)	-3(1)	3(1)
O(4)	22(1)	30(1)	34(1)	-7(1)	-2(1)	7(1)
O(5)	33(1)	22(1)	26(1)	1(1)	7(1)	4(1)
O(6)	40(1)	20(1)	25(1)	-4(1)	9(1)	-2(1)
C(1)	28(1)	22(1)	26(1)	-6(1)	5(1)	7(1)
C(2)	42(1)	26(1)	28(1)	1(1)	3(1)	6(1)
C(3)	53(1)	33(1)	22(1)	1(1)	2(1)	13(1)
C(4)	44(1)	30(1)	25(1)	-7(1)	-6(1)	8(1)
C(5)	26(1)	21(1)	24(1)	-5(1)	-2(1)	1(1)
C(6)	19(1)	20(1)	24(1)	-3(1)	0(1)	3(1)
C(7)	29(1)	33(1)	66(2)	12(1)	8(1)	10(1)
C(8)	24(1)	31(1)	54(2)	2(1)	-8(1)	2(1)
C(9)	29(1)	36(1)	129(3)	24(2)	16(2)	5(1)
C(10)	48(2)	53(2)	56(2)	-8(1)	11(1)	22(1)
C(11)	50(2)	55(2)	77(2)	-24(2)	-30(1)	10(1)
C(12)	32(1)	35(1)	60(2)	9(1)	-14(1)	5(1)
C(13)	25(1)	18(1)	24(1)	-5(1)	1(1)	2(1)
C(14)	26(1)	21(1)	24(1)	-4(1)	1(1)	0(1)
C(15)	28(1)	17(1)	25(1)	-2(1)	1(1)	3(1)
C(16)	25(1)	24(1)	23(1)	-1(1)	3(1)	-2(1)
C(17)	31(1)	25(1)	35(1)	-4(1)	-2(1)	-1(1)
C(18)	35(1)	30(1)	46(1)	-1(1)	-6(1)	6(1)
C(19)	33(1)	41(1)	42(1)	2(1)	-10(1)	1(1)
C(20)	43(1)	32(1)	38(1)	-2(1)	-12(1)	-8(1)

C(21)	39(1)	22(1)	30(1)	0(1)	-3(1)	-1(1)
C(22)	24(1)	27(1)	23(1)	5(1)	-3(1)	3(1)
C(23)	33(1)	32(1)	32(1)	1(1)	4(1)	-1(1)
C(24)	36(1)	38(1)	39(1)	8(1)	-4(1)	-8(1)
C(25)	25(1)	58(2)	36(1)	19(1)	-1(1)	-6(1)
C(26)	32(1)	60(2)	25(1)	7(1)	4(1)	6(1)
C(27)	32(1)	37(1)	26(1)	2(1)	-1(1)	4(1)

Table 1.16. Hydrogen coordinates (x 10^4) and isotropic displacement parameters (Å^{2}x 10^3) for sad.

	x	y	z	U(eq)
H(4O)	3243(12)	-1800(20)	2093(11)	43
H(2A)	2572	-2610	3155	38
H(2B)	1755	-2969	3208	38
H(3A)	1430	-1188	3552	43
H(3B)	2062	-1604	3994	43
H(4A)	2883	-533	3443	40
H(4B)	2247	253	3661	40
H(5)	2614	578	2599	28
H(9A)	-363	-123	2485	98
H(9B)	-724	1028	2670	98
H(9C)	-410	240	3206	98
H(10A)	255	1843	3587	79
H(10B)	102	2661	3012	79
H(10C)	899	2333	3185	79
H(11A)	495	-237	1714	91
H(11B)	617	644	1165	91
H(11C)	-141	549	1496	91
H(12A)	553	3058	2143	63
H(12B)	-102	2562	1759	63

H(12C)	658	2667	1431	63
H(13)	1802	-545	1477	27
H(14A)	3191	383	1584	29
H(14B)	2470	1005	1380	29
H(17)	2204	1865	384	36
H(18)	1202	2206	-221	44
H(19)	614	746	-714	46
H(20)	1044	-1045	-606	45
H(21)	2055	-1391	-9	36
H(23)	3578	1888	969	39
H(24)	4532	2769	483	45
H(25)	5067	1982	-393	47
H(26)	4638	323	-799	47
H(27)	3673	-545	-333	38

Table 1.17. Torsion angles [°] for sad.

O(3)-B(1)-O(2)-C(7)	-7.6(2)
C(5)-B(1)-O(2)-C(7)	171.04(19)
O(2)-B(1)-O(3)-C(8)	-13.9(2)
C(5)-B(1)-O(3)-C(8)	167.44(17)
C(15)-O(5)-O(6)-C(13)	-23.31(16)
O(1)-C(1)-C(2)-C(3)	-116.1(2)
C(6)-C(1)-C(2)-C(3)	59.4(2)
C(1)-C(2)-C(3)-C(4)	-53.9(2)
C(2)-C(3)-C(4)-C(5)	54.8(2)
C(3)-C(4)-C(5)-C(6)	-56.5(2)
C(3)-C(4)-C(5)-B(1)	71.2(2)
O(2)-B(1)-C(5)-C(4)	-26.4(3)
O(3)-B(1)-C(5)-C(4)	152.16(18)
O(2)-B(1)-C(5)-C(6)	99.4(2)
O(3)-B(1)-C(5)-C(6)	-82.1(2)
O(1)-C(1)-C(6)-O(4)	-130.42(18)

C(2)-C(1)-C(6)-O(4)	53.93(19)
O(1)-C(1)-C(6)-C(13)	-8.8(2)
C(2)-C(1)-C(6)-C(13)	175.56(15)
O(1)-C(1)-C(6)-C(5)	114.27(19)
C(2)-C(1)-C(6)-C(5)	-61.38(19)
C(4)-C(5)-C(6)-O(4)	-59.63(19)
B(1)-C(5)-C(6)-O(4)	172.41(15)
C(4)-C(5)-C(6)-C(13)	179.96(15)
B(1)-C(5)-C(6)-C(13)	52.0(2)
C(4)-C(5)-C(6)-C(1)	56.65(19)
B(1)-C(5)-C(6)-C(1)	-71.32(19)
B(1)-O(2)-C(7)-C(9)	147.3(2)
B(1)-O(2)-C(7)-C(8)	24.7(2)
B(1)-O(2)-C(7)-C(10)	-93.1(2)
B(1)-O(3)-C(8)-C(12)	151.26(19)
B(1)-O(3)-C(8)-C(7)	28.09(19)
B(1)-O(3)-C(8)-C(11)	-90.1(2)
O(2)-C(7)-C(8)-O(3)	-31.4(2)
C(9)-C(7)-C(8)-O(3)	-148.96(17)
C(10)-C(7)-C(8)-O(3)	82.4(2)
O(2)-C(7)-C(8)-C(12)	-149.49(18)
C(9)-C(7)-C(8)-C(12)	93.0(2)
C(10)-C(7)-C(8)-C(12)	-35.7(3)
O(2)-C(7)-C(8)-C(11)	81.9(2)
C(9)-C(7)-C(8)-C(11)	-35.7(3)
C(10)-C(7)-C(8)-C(11)	-164.29(19)
O(5)-O(6)-C(13)-C(14)	-4.81(17)
O(5)-O(6)-C(13)-C(6)	-127.39(14)
O(4)-C(6)-C(13)-O(6)	54.87(18)
C(1)-C(6)-C(13)-O(6)	-65.96(18)
C(5)-C(6)-C(13)-O(6)	173.62(14)
O(4)-C(6)-C(13)-C(14)	-62.01(19)
C(1)-C(6)-C(13)-C(14)	177.16(15)
C(5)-C(6)-C(13)-C(14)	56.7(2)

O(6)-C(13)-C(14)-C(15)	29.40(18)
C(6)-C(13)-C(14)-C(15)	147.88(15)
O(6)-O(5)-C(15)-C(22)	161.67(13)
O(6)-O(5)-C(15)-C(14)	41.23(16)
O(6)-O(5)-C(15)-C(16)	-77.77(16)
C(13)-C(14)-C(15)-O(5)	-43.53(17)
C(13)-C(14)-C(15)-C(22)	-156.66(15)
C(13)-C(14)-C(15)-C(16)	75.72(18)
O(5)-C(15)-C(16)-C(21)	-2.2(3)
C(22)-C(15)-C(16)-C(21)	115.1(2)
C(14)-C(15)-C(16)-C(21)	-115.0(2)
O(5)-C(15)-C(16)-C(17)	177.28(16)
C(22)-C(15)-C(16)-C(17)	-65.4(2)
C(14)-C(15)-C(16)-C(17)	64.5(2)
C(21)-C(16)-C(17)-C(18)	0.1(3)
C(15)-C(16)-C(17)-C(18)	-179.38(18)
C(16)-C(17)-C(18)-C(19)	0.3(3)
C(17)-C(18)-C(19)-C(20)	-0.4(3)
C(18)-C(19)-C(20)-C(21)	0.1(4)
C(17)-C(16)-C(21)-C(20)	-0.5(3)
C(15)-C(16)-C(21)-C(20)	179.01(19)
C(19)-C(20)-C(21)-C(16)	0.4(3)
O(5)-C(15)-C(22)-C(23)	-135.11(18)
C(14)-C(15)-C(22)-C(23)	-24.3(3)
C(16)-C(15)-C(22)-C(23)	103.7(2)
O(5)-C(15)-C(22)-C(27)	48.1(2)
C(14)-C(15)-C(22)-C(27)	158.87(17)
C(16)-C(15)-C(22)-C(27)	-73.2(2)
C(27)-C(22)-C(23)-C(24)	-0.2(3)
C(15)-C(22)-C(23)-C(24)	-177.10(18)
C(22)-C(23)-C(24)-C(25)	-0.6(3)
C(23)-C(24)-C(25)-C(26)	0.7(3)
C(24)-C(25)-C(26)-C(27)	0.1(3)
C(25)-C(26)-C(27)-C(22)	-0.9(3)

C(23)-C(22)-C(27)-C(26)	0.9(3)
C(15)-C(22)-C(27)-C(26)	177.84(18)

Symmetry transformations used to generate equivalent atoms:

Table 1.18. Hydrogen bonds for sad [Å and °].

D-H...A	d(D-H)	d(H...A)	d(D...A)	<(DHA)
O(4)-H(4O)...O(3)#1	0.85(2)	2.43(2)	3.1246(19)	139(2)

Symmetry transformations used to generate equivalent atoms:
#1 -x+1/2,y-1/2,z

1.4.2.3. Computational Methods and Results

The calculations were carried out on model structures, in which ICy was replaced for IMe, $B_2(pin)_2$ was replaced for bisglycolato-diboron ($B_2(glycol)_2$), and the model version of **1.68** was trimethylsilyl-glycolatoboron (TMSB(glycol)). All calculations were carried out in Gaussian 09, Rev A.1.[155] The geometries were optimized with tight convergence criteria with the exception of the model version of **1.68**, for which loose convergence criteria were used due to the presence of a soft vibrational mode corresponding to the dihedral angles along B-Si bond. Also, the tight ion pairs **1.73**, **1.75**, and **1.76** were optimized with normal convergence criteria due to presence of soft vibrational modes, corresponding to vibrations associated with the motion of one ion of

---

(155) Gaussian 09, Revision A.1, Frisch, M. J.; Trucks, G. W.; Schlegel, H. B.; Scuseria, G. E.; Robb, M. A.; Cheeseman, J. R.; Scalmani, G.; Barone, V.; Mennucci, B.; Petersson, G. A.; Nakatsuji, H.; Caricato, M.; Li, X.; Hratchian, H. P.; Izmaylov, A. F.; Bloino, J.; Zheng, G.; Sonnenberg, J. L.; Hada, M.; Ehara, M.; Toyota, K.; Fukuda, R.; Hasegawa, J.; Ishida, M.; Nakajima, T.; Honda, Y.; Kitao, O.; Nakai, H.; Vreven, T.; Montgomery, J. A. Jr.; Peralta, J. E.; Ogliaro, F.; Bearpark, M.; Heyd, J. J.; Brothers, E.; Kudin, K. N.; Staroverov, V. N.; Kobayashi, R.; Normand, J.; Raghavachari, K.; Rendell, A.; Burant, J. C.; Iyengar, S. S.; Tomasi, J.; Cossi, M.; Rega, N.; Millam, N. J.; Klene, M.; Knox, J. E.; Cross, J. B.; Bakken, V.; Adamo, C.; Jaramillo, J.; Gomperts, R.; Stratmann, R. E.; Yazyev, O.; Austin, A. J.; Cammi, R.; Pomelli, C.; Ochterski, J. W.; Martin, R. L.; Morokuma, K.; Zakrzewski, V. G.; Voth, G. A.; Salvador, P.; Dannenberg, J. J.; Dapprich, S.; Daniels, A. D.; Farkas, Ö.; Foresman, J. B.; Ortiz, J. V.; Cioslowski, J.; Fox, D. J. *Gaussian 09* (Gaussian, Inc., Wallingford CT, 2009).

the tight ion pair with respect to the other. In all cases M06L density functional was employed with 6-31+G(d,p) basis sets on H, C, N, O, B, and 6-31+G(2df) basis set on Si.[121,156] Geometries of transition states were optimized with Berny algorithm; as input guess structures were located with relaxed potential energy surface scans at the same level of theory. Solvation energies were calculated on the gas-phase optimized structures at the same level of theory as above with integral equation formalism variant of polarizable continuum model (IEFPCM) with default scaling (α=1.1) of atomic radii.[129] The molecule envelope consisted of DFT-optimized atoms of united atom topological model (UAKS).[129] All ^{11}B NMR spectra were calculated at M06L/6-311++G(3d2f,2df,2p)//M06L/6-31+G(2df,d,p) level of theory including IEFPCM solvation model as described above.[157]

Energies of compounds depicted in Schemes 1.22, 1.24-1.27 (ZPE-corrected electronic energies, standard enthalpies, and standard Gibbs free energies) are listed in Table 1.19.

---

(156) Basis sets for H, C, N, O, B: (a) Hehre, W. J.; Fitchfield, R.; Pople, J. A. *J. Chem. Phys.* **1971**, *56*, 2257-2261; (b) Hariharan, P. C.; Pople, J. A. *Theor. Chim. Acta* **1973**, *28*, 213-222. Basis sets for Si: (c) Francl, M. M.; Pietro, W. J.; Hehre, W. J.; Binkley, J. S.; Gordon, M. S.; DeFrees, D. J.; Pople, J. A. *J. Chem. Phys.* **1982**, *77*, 3654-3665.

(157) The basis set 6-311++G(3d2f) for 2nd row main group elements: (a) see Ref. 136b; (b) Tratz, C. M.; Fast, P. L.; Truhlar, D. G. *Phys. Chem. Comm.* **1999**, *2*, 70-79.

Table 1.19. Absolute Energies for NHC-Catalyzed Addition of B_2(glycol)$_2$ or TMS-B(glycol) to Cyclohexenone and Benzaldehyde[a]

Compound	E+ZPE	H	G
B_2(glycol)$_2$	-507.813089	-507.802634	-507.850829
TMS-B(glycol)	-663.033405	-663.019734	-663.074373
ime	-304.639576	-304.631616	-304.670492
PhCHO	-345.436896	-345.429595	-345.467497
1.25	-812.482810	-812.464735	-812.529911
1.26	-308.515134	-308.508065	-308.545082
1.65TS	-812.447717	-812.429946	-812.492352
1.65	-812.474728	-812.456759	-812.521382
1.60TS-1	-1120.977978	-1120.954386	-1121.028553
1.60TS-2	-1120.978722	-1120.954155	-1121.031896
C-1.61	-1121.061608	-1121.037661	-1121.113851
O-1.61	-1121.073176	-1121.049070	-1121.126576
1.66	-1121.062765	-1121.038762	-1121.115057
1.66TS-1	-1120.954979	-1120.930939	-1121.005833
1.67	-1157.994573	-1157.970390	-1158.048558
1.67TS	-1157.895385	-1157.870958	-1157.948368
1.69	-967.705752	-967.684703	-967.754263
1.72	-967.692416	-967.671702	-967.739367
1.72TS	-967.677894	-967.657133	-967.724374
1.73	-1276.197868	-1276.169120	-1276.257388
1.73TS-1	-1276.164374	-1276.136534	-1276.220974
1.73TS-2	-1276.162882	-1276.135474	-1276.218307
1.74	-1276.284595	-1276.257310	-1276.341382
1.75	-1352.610953	-1352.578936	-1352.676447
1.75TS-1	-1352.575999	-1352.544751	-1352.638274
1.75TS-2	-1352.572782	-1352.542111	-1352.633430
1.76	-1313.103780	-1313.074553	-1313.165515
1.76TS	-1313.089595	-1313.061518	-1313.147193
1.77	-1313.204788	-1313.176957	-1313.263458

[a] All values are in units of hartree.

1.4.3. NMR Spectra

Unless otherwise noted all spectra are ^{1}H NMR spectra. Spectra for compounds B_2(pin)$_2$, **1.25**, **1.68**, and **1.69** are ^{11}B NMR spectra (chemical shifts are relative to the external standard $BF_3 \cdot OEt_2$ in d_8-THF).

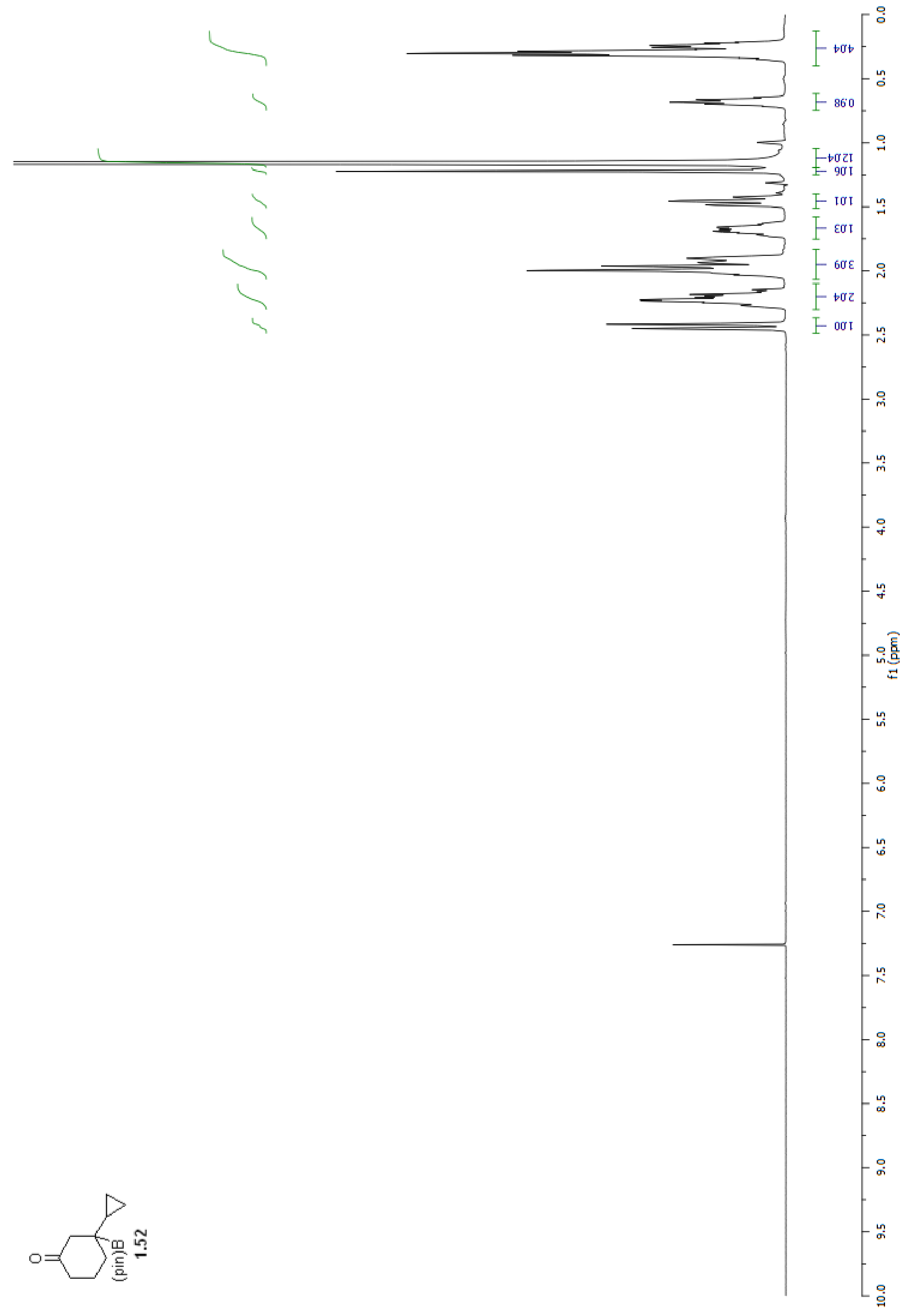
O
(pin)B
4.04
0.98
12.04
1.06
1.01
1.03
3.09
2.04
1.00
0.0
0.5
1.0
1.5
2.0
2.5
3.0
3.5
4.0
4.5
5.0
5.5
6.0
6.5
7.0
7.5
8.0
8.5
9.0
9.5
10.0
f1 (ppm)

1.52

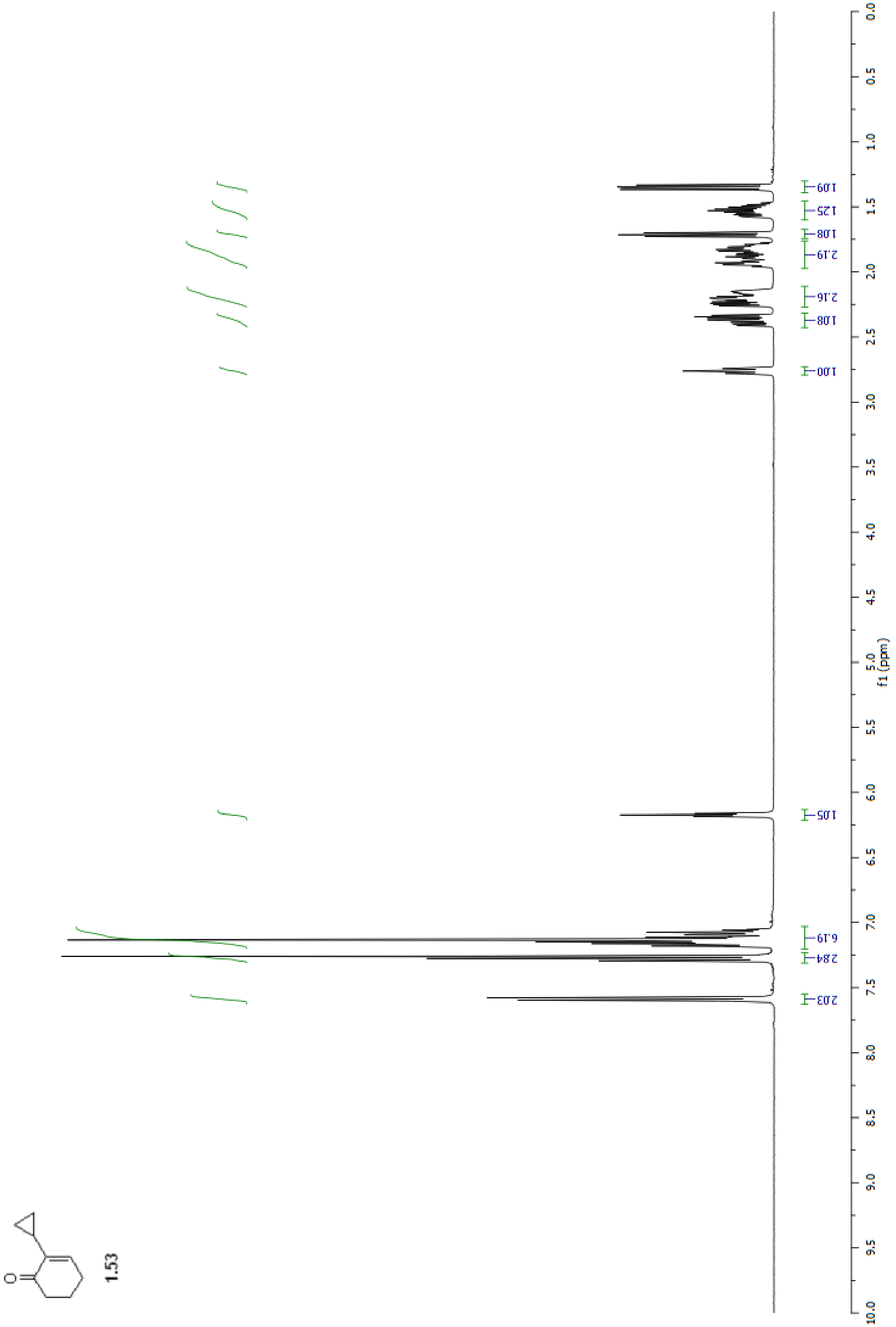
1.09
1.25
1.08
2.19
2.16
1.08
1.00
1.05
6.19
2.84
2.03
0.0
0.5
1.0
1.5
2.0
2.5
3.0
3.5
4.0
4.5
5.0
f1 (ppm)
5.5
6.0
6.5
7.0
7.5
8.0
8.5
9.0
9.5
10.0

1.53

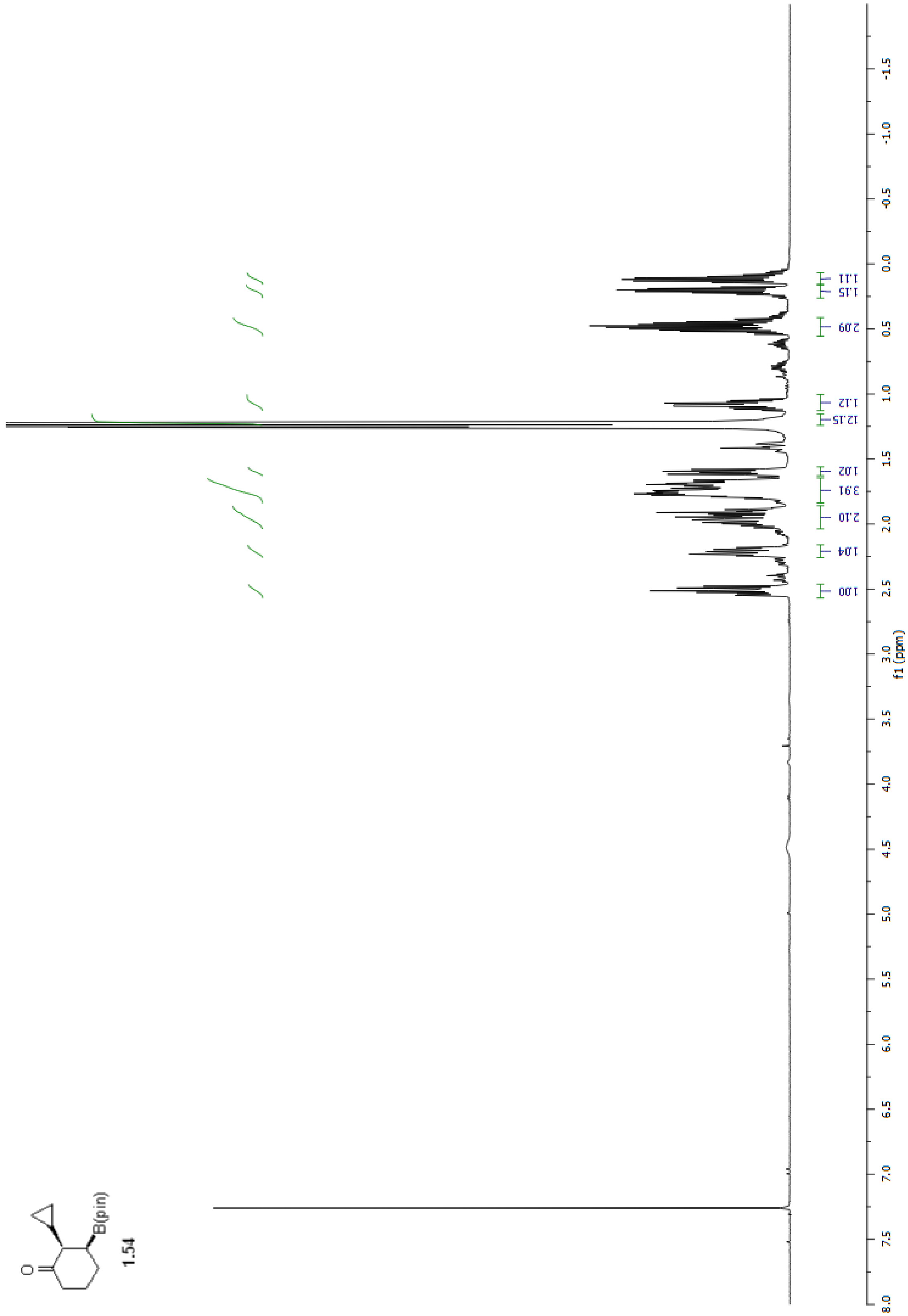
O
B(pin)
1.11
1.15
2.09
1.12
12.15
1.02
3.91
2.10
1.04
1.00
-1.5
-1.0
-0.5
0.0
0.5
1.0
1.5
2.0
2.5
3.0
3.5
4.0
4.5
5.0
5.5
6.0
6.5
7.0
7.5
8.0
f1 (ppm)

1.54

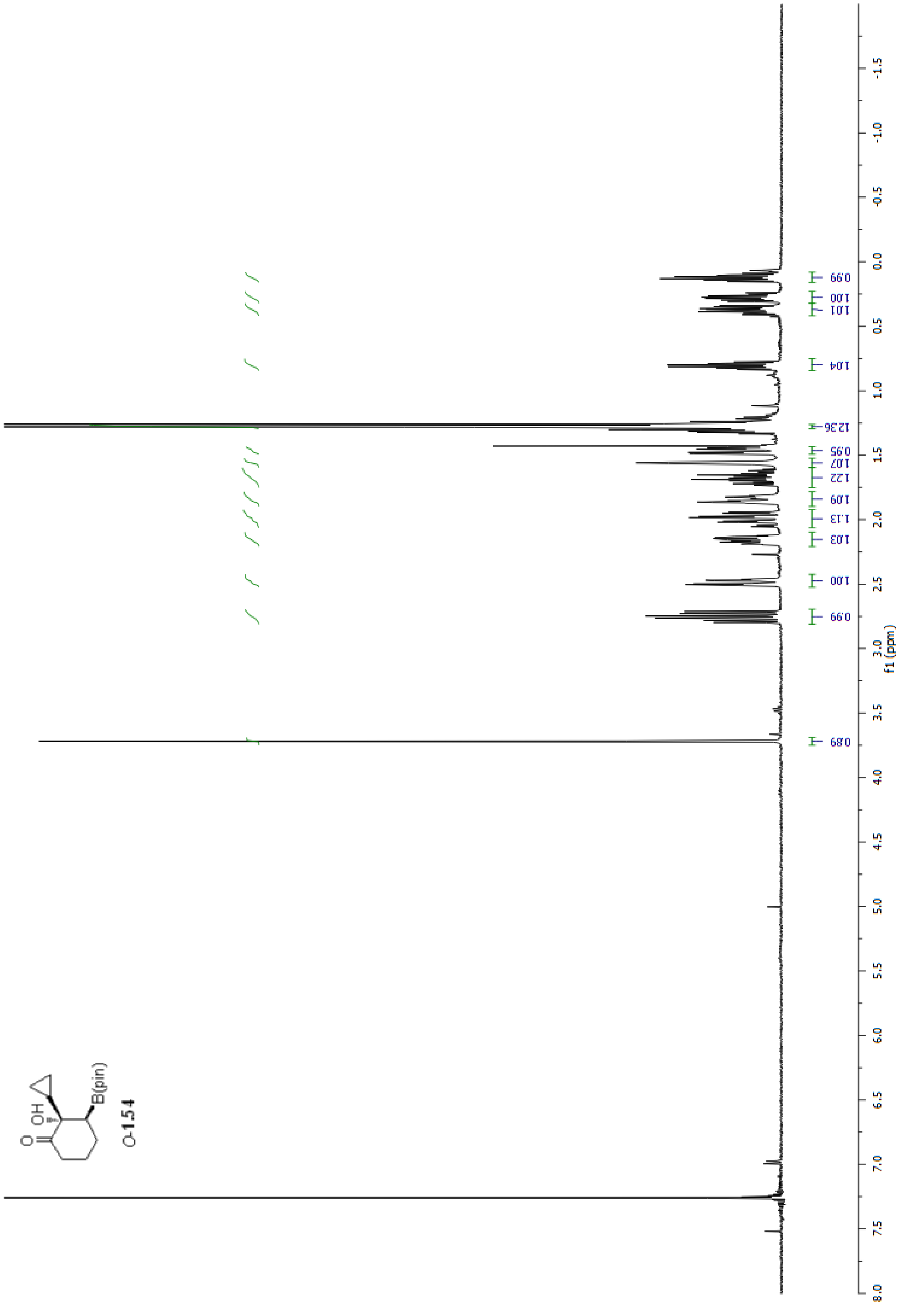
O
OH
B(pin)
0.99
1.00
1.01
1.04
12.36
0.95
1.07
1.22
1.09
1.13
1.03
1.00
0.99
0.89
f1 (ppm)
8.0
7.5
7.0
6.5
6.0
5.5
5.0
4.5
4.0
3.5
3.0
2.5
2.0
1.5
1.0
0.5
0.0
-0.5
-1.0
-1.5

O-1.54

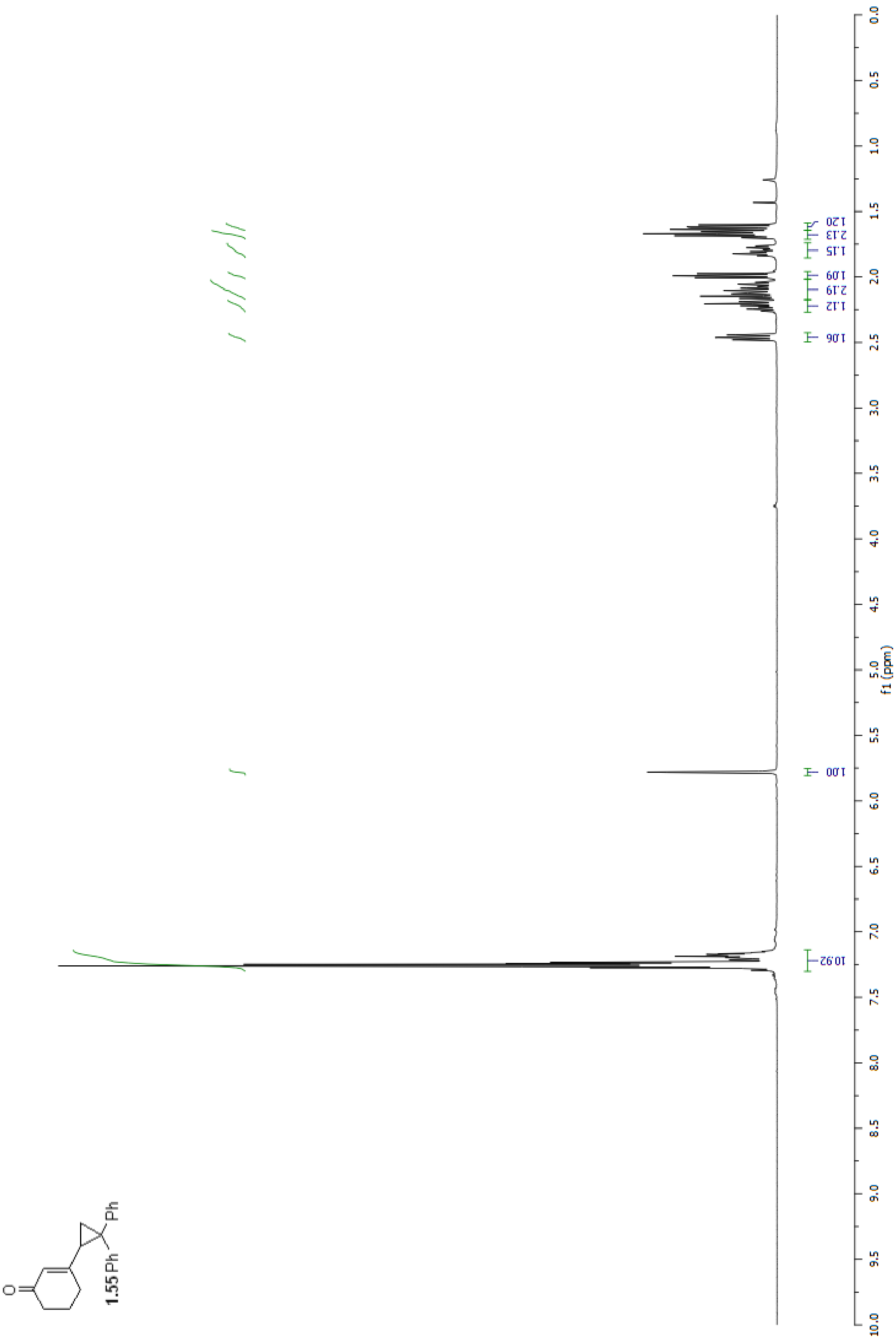
1.55
O
Ph
Ph
1.20
2.13
1.15
1.09
2.19
1.12
1.06
1.00
10.92
0.0
0.5
1.0
1.5
2.0
2.5
3.0
3.5
4.0
4.5
5.0
5.5
6.0
6.5
7.0
7.5
8.0
8.5
9.0
9.5
10.0
f1 (ppm)

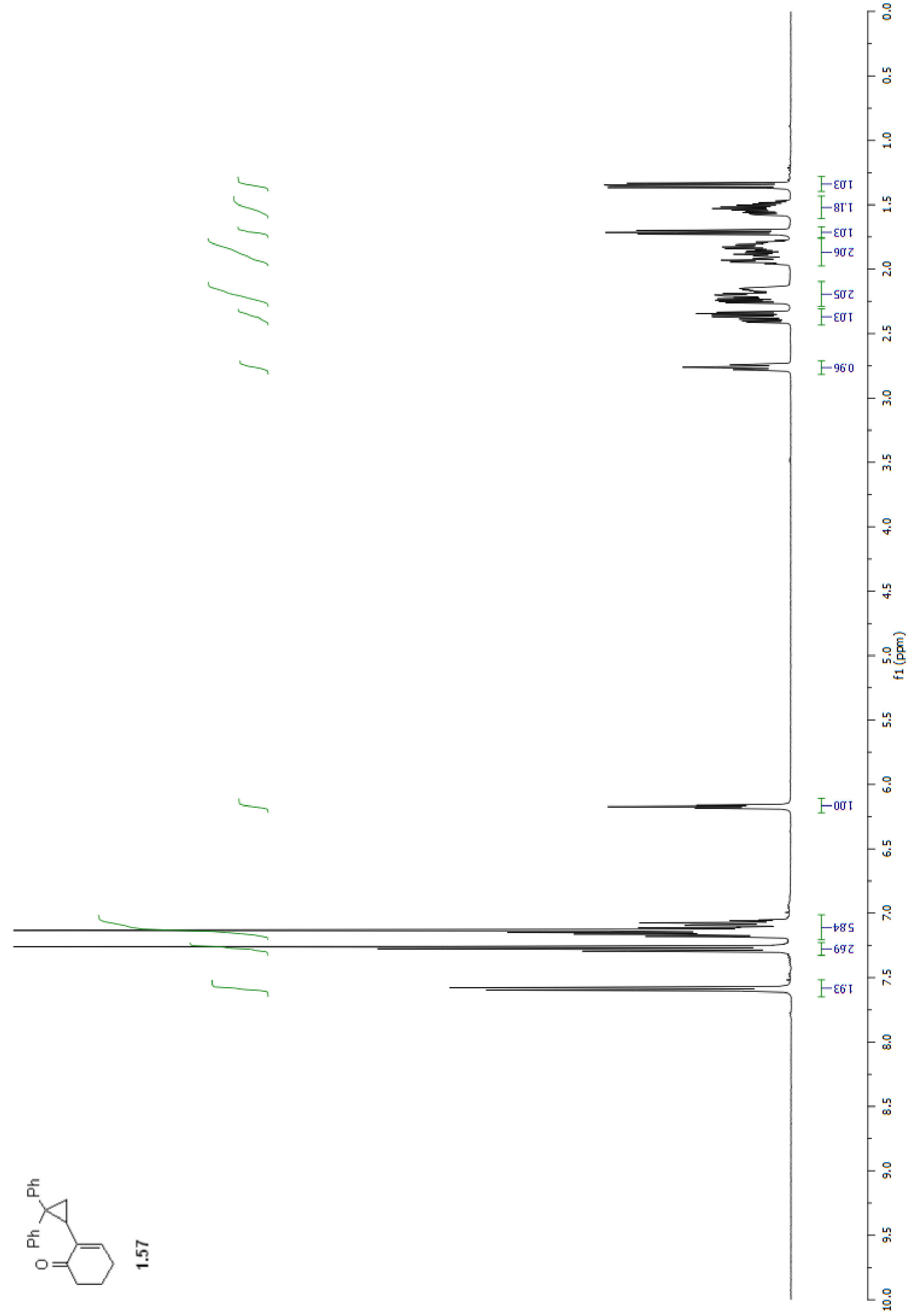
O
Ph
Ph
1.03
1.18
1.03
2.06
2.05
1.03
0.96
1.00
5.84
2.69
1.93
0.0
0.5
1.0
1.5
2.0
2.5
3.0
3.5
4.0
4.5
5.0
f1 (ppm)
5.5
6.0
6.5
7.0
7.5
8.0
8.5
9.0
9.5
10.0

1.57

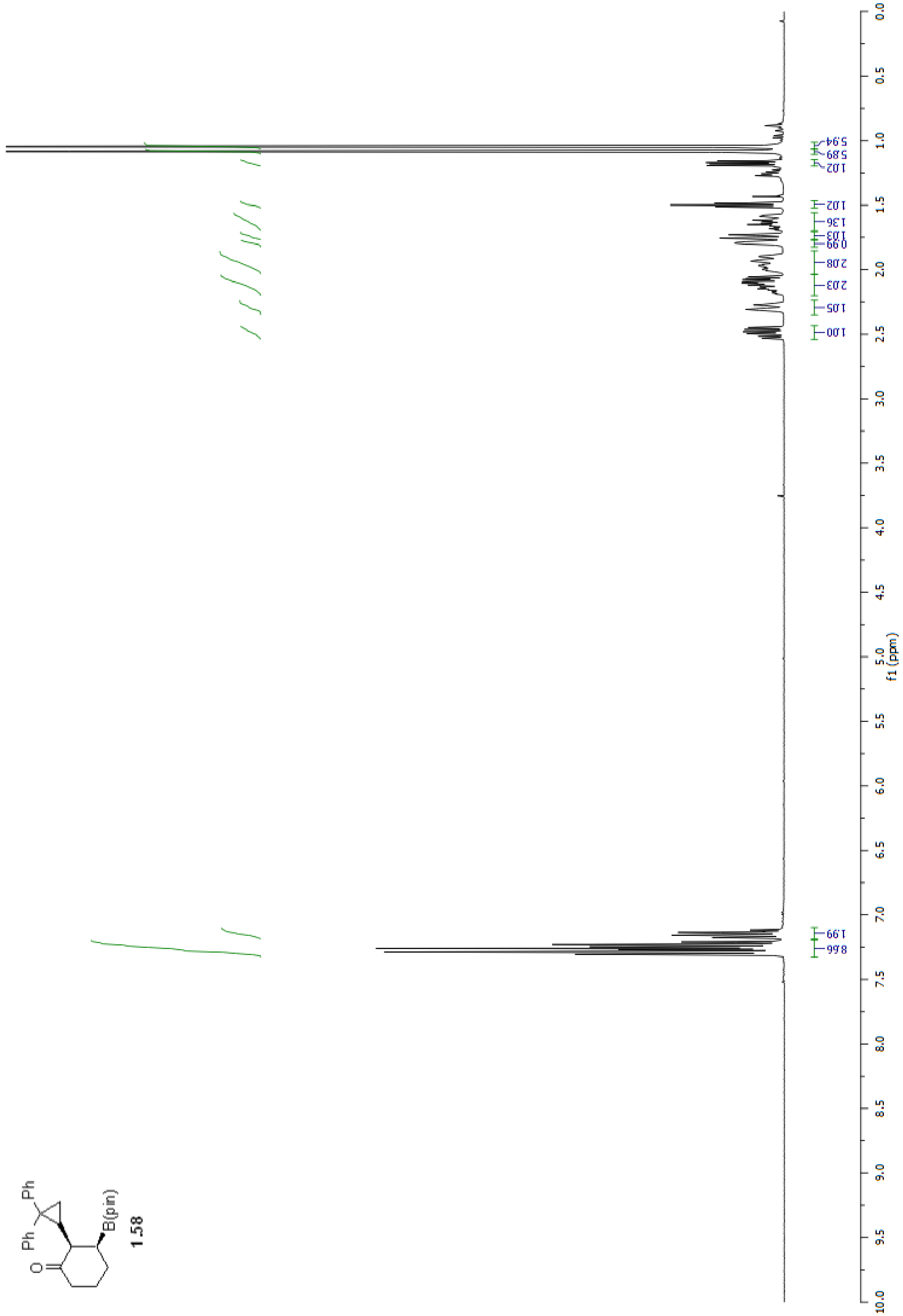
O
Ph
Ph
B(pin)
5.94
5.89
1.02
1.02
1.36
1.03
0.99
2.08
2.03
1.05
1.00
1.99
8.66
0.0
0.5
1.0
1.5
2.0
2.5
3.0
3.5
4.0
4.5
5.0
5.5
6.0
6.5
7.0
7.5
8.0
8.5
9.0
9.5
10.0
f1 (ppm)

1.58

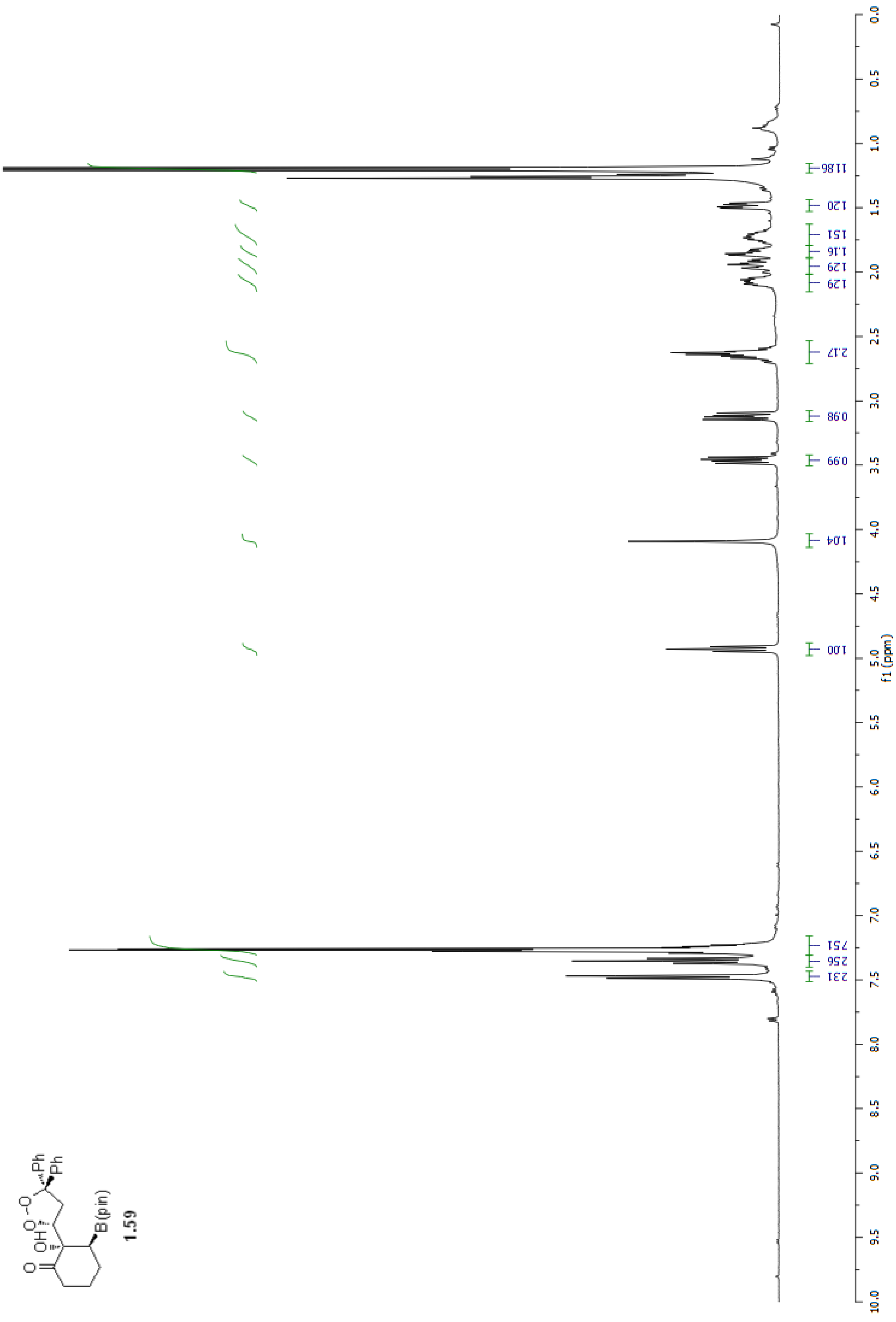
O
OH
O
O
Ph
Ph
B(pin)
11.86
1.20
1.51
1.16
1.29
1.29
2.17
0.98
0.99
1.04
1.00
7.51
2.56
2.31
0.0
0.5
1.0
1.5
2.0
2.5
3.0
3.5
4.0
4.5
5.0
5.5
6.0
6.5
7.0
7.5
8.0
8.5
9.0
9.5
10.0
f1 (ppm)

1.59

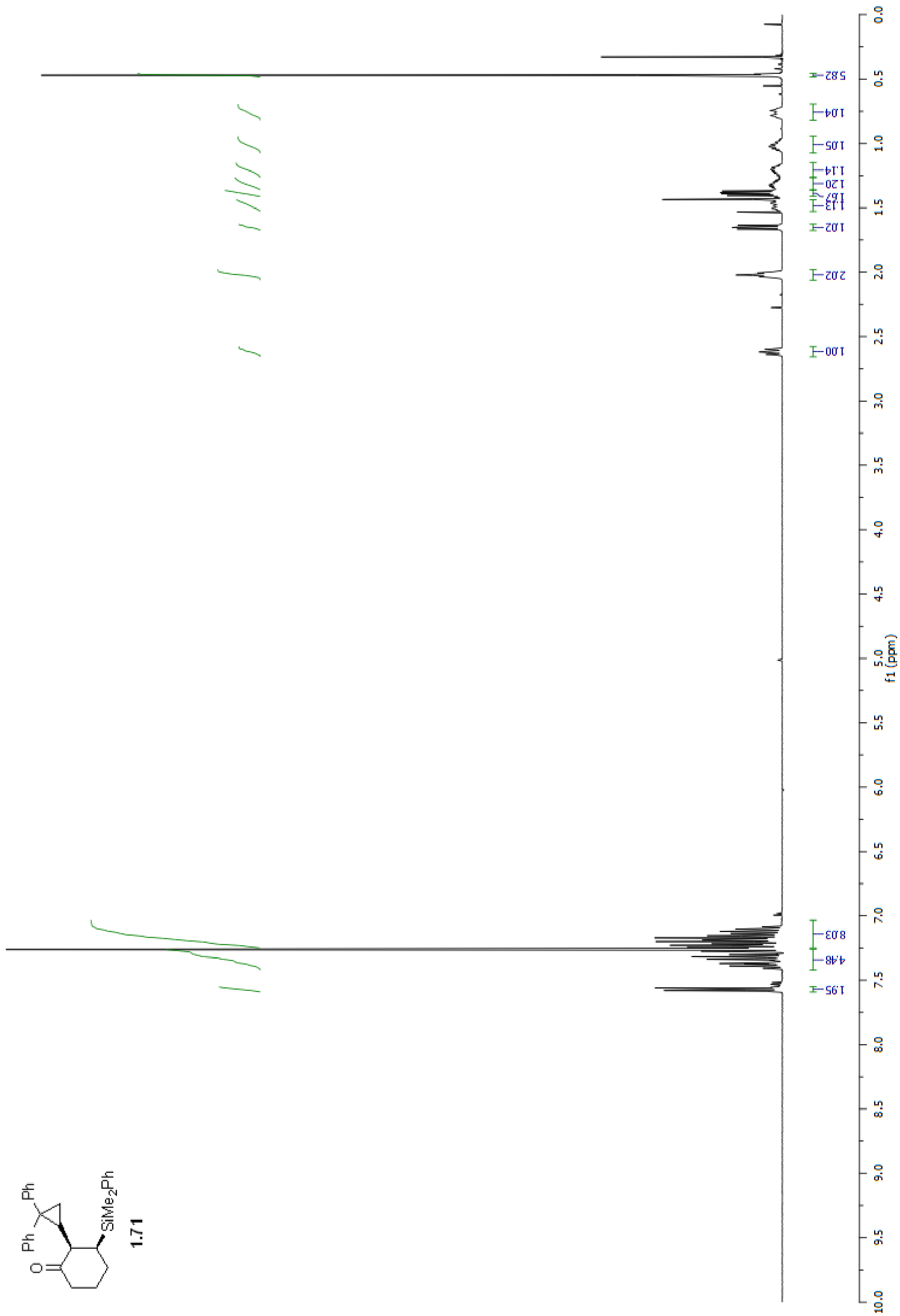
O
Ph
Ph
SiMe$_2$Ph
1.71
5.82
1.04
1.05
1.14
1.20
1.27
1.13
1.02
2.02
1.00
8.03
4.48
1.95
0.0
0.5
1.0
1.5
2.0
2.5
3.0
3.5
4.0
4.5
5.0
5.5
6.0
6.5
7.0
7.5
8.0
8.5
9.0
9.5
10.0
f1 (ppm)

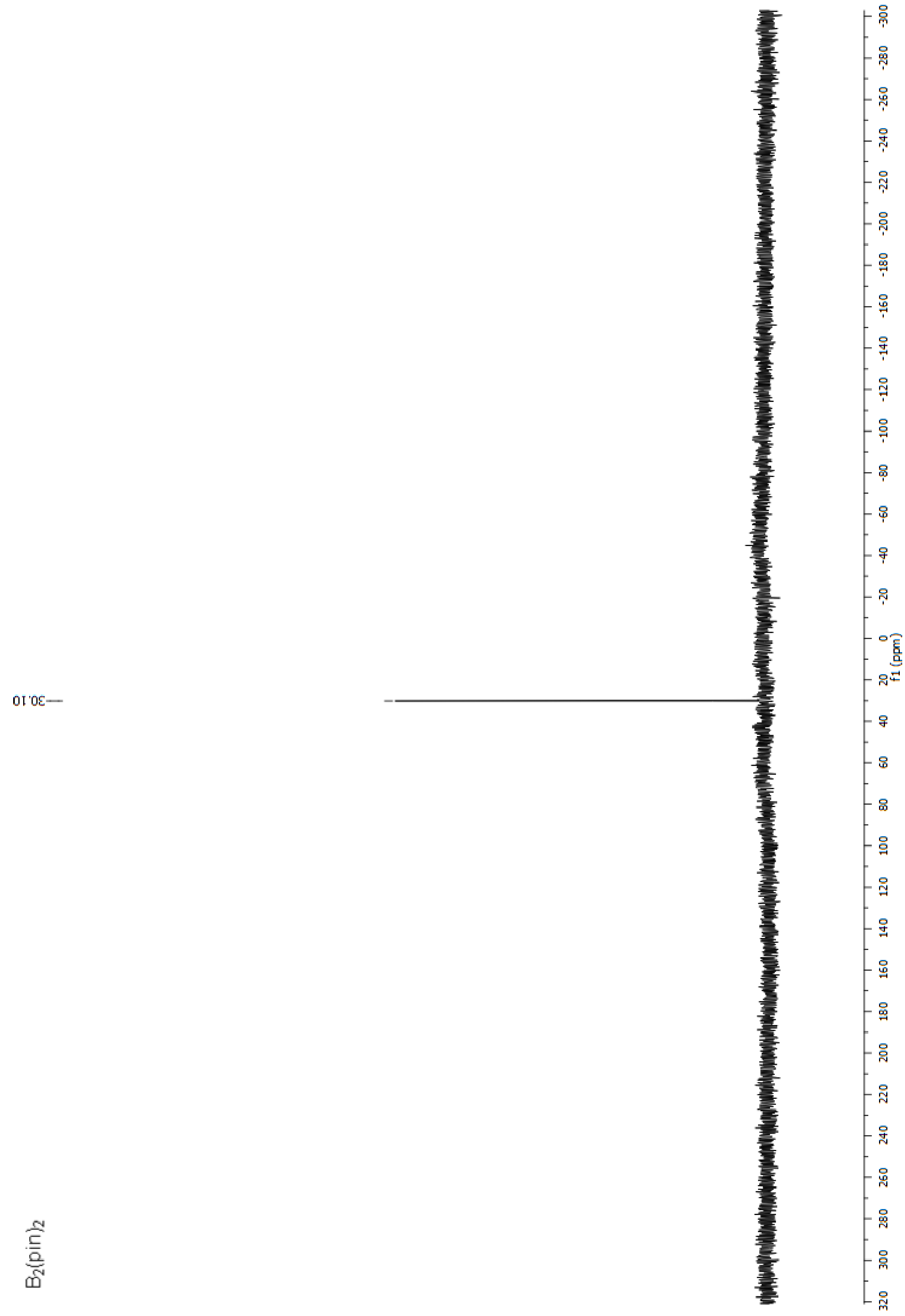
B$_2$(pin)$_2$
30.10
f1 (ppm)
320
300
280
260
240
220
200
180
160
140
120
100
80
60
40
20
0
-20
-40
-60
-80
-100
-120
-140
-160
-180
-200
-220
-240
-260
-280
-300

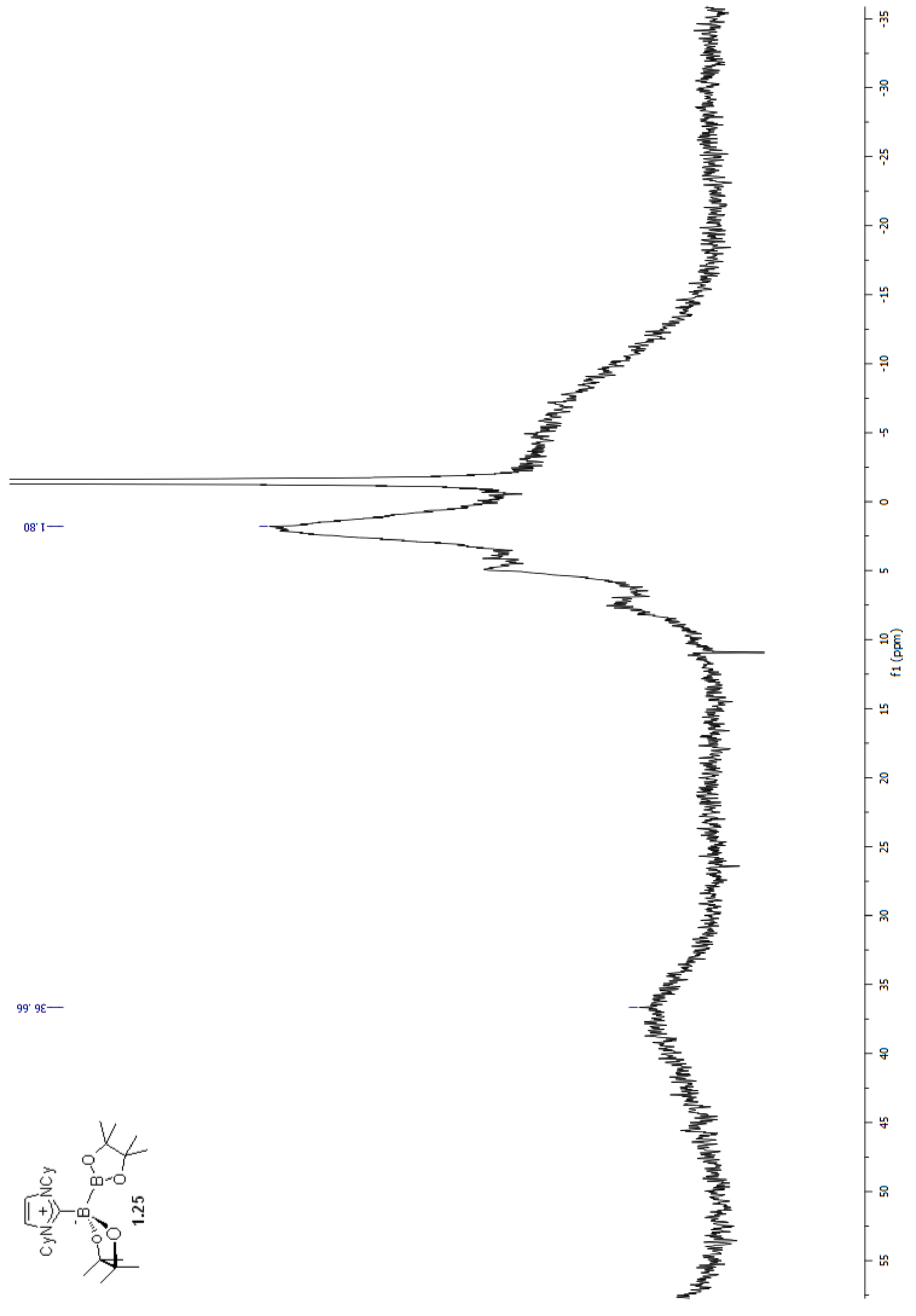

CyN
NCy
+
B
B
O
O
O
O
36.66
1.80
55
50
45
40
35
30
25
20
15
10
5
0
-5
-10
-15
-20
-25
-30
-35
f1 (ppm)

1.25

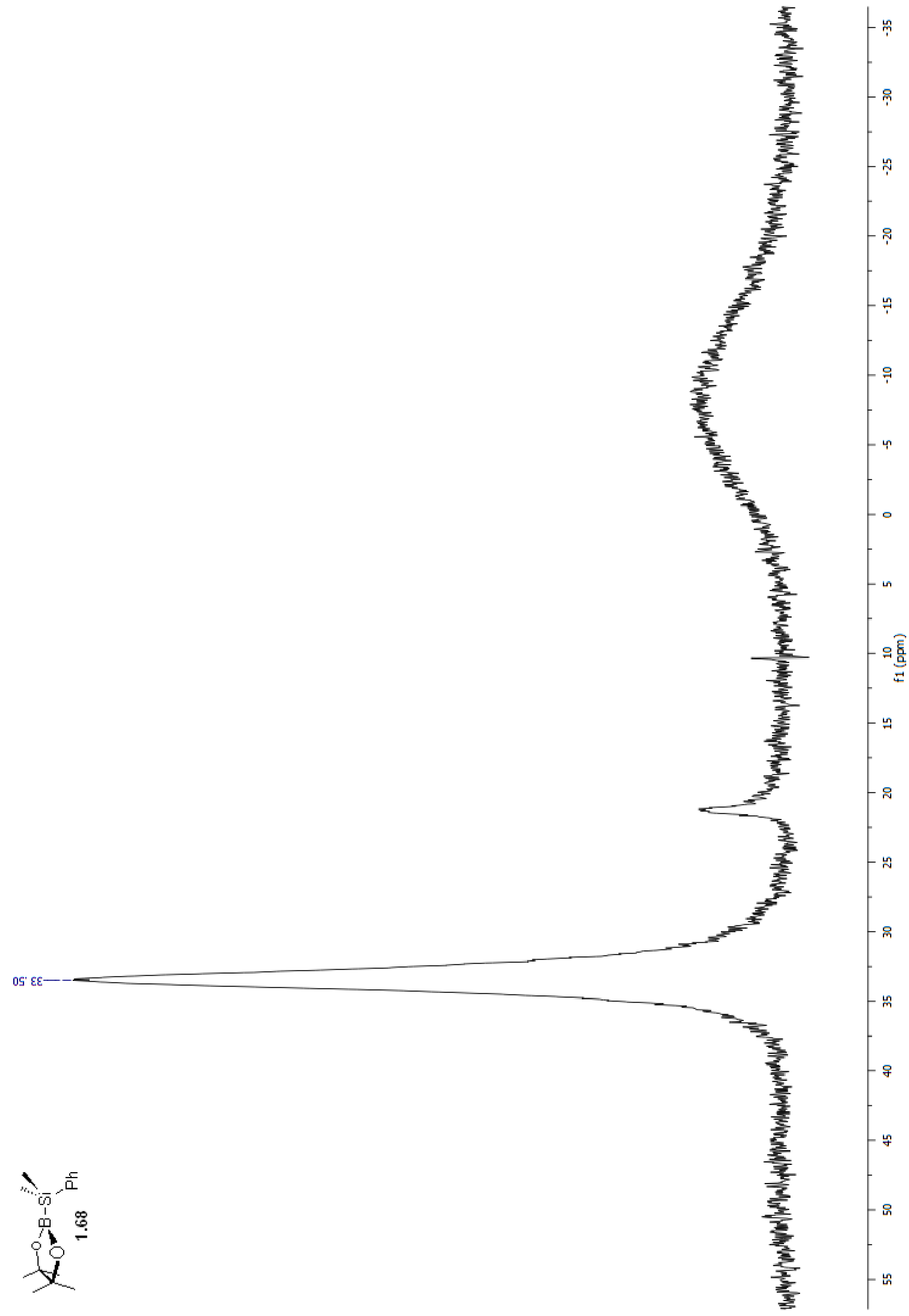
1.68

O
B
Si
Ph
33.50
f1 (ppm)
55
50
45
40
35
30
25
20
15
10
5
0
-5
-10
-15
-20
-25
-30
-35

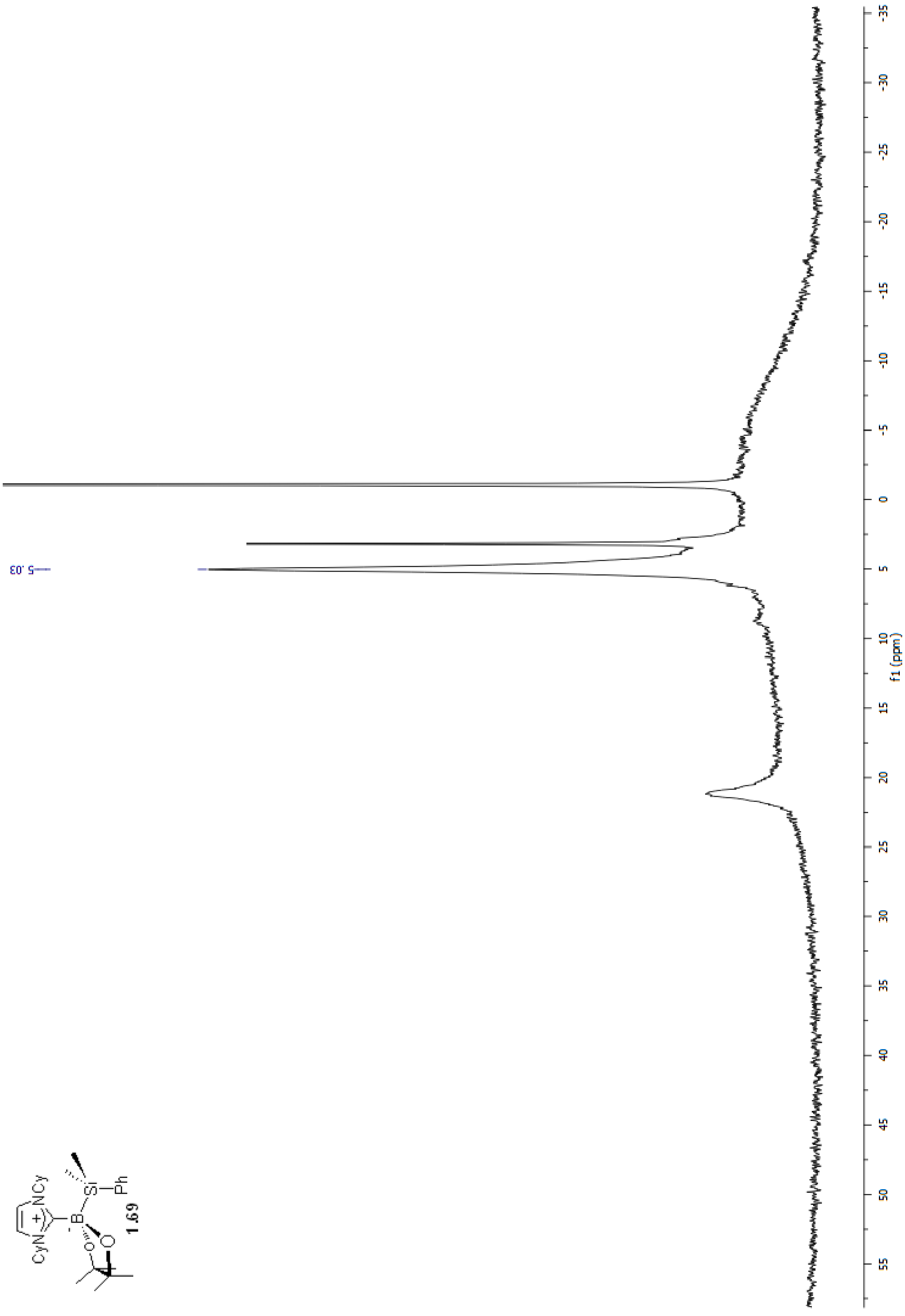
5.03
-35
-30
-25
-20
-15
-10
-5
0
5
10
15
20
25
30
35
40
45
50
55
f1 (ppm)
CyN
NCy
+
B
-
Si
Ph
O

1.69

Chapter 2

Development of New Catalysts and Methods for Stereoselective Ru-catalyzed Olefin Metathesis. Mechanistic Investigation of Action of the Stereogenic-at-Ru Olefin Metathesis Catalysts through Isolation of Key Reactive Intermediates

2.1. Introduction

Olefin metathesis[1] ("metathesis" from the Greek *μετάθεσις*: "transposition") constitutes a rearrangement process, wherein C-C double bonds of olefinic substrates are broken and different C-C double bonds are formed. This transformation can be performed catalytically or non-catalytically as shown in Scheme 2.1. The stepwise photothermal olefin metathesis sequence constitutes a [2+2] photocycloaddition, followed by the pyrolytic cleavage of the cyclobutane generated in the previous step.[2] Stepwise

---

(1) For reviews on olefin metathesis see: (a) *Handbook of Metathesis*; Grubbs, R. H., Eds.; WILEY-VCH Verlag GmbH & Co. KGaA: Weinheim, 2003; (b) Hoveyda, A. H.; Zhugralin, A. R. *Nature* **2007**, *450*, 243-251. For a review on well-defined early transition metal-based olefin metathesis catalysts see: (c) Schrock, R. R.; Hoveyda, A. H. *Angew. Chem. Int. Ed.* **2003**, *42*, 4592-4633. For a report on well-defined Re-based olefin metathesis catalyst see: (d) Toreki, R.; Schrock, R. R. *J. Am. Chem. Soc.* **1990**, *112*, 2448-2449. For reviews on well-defined Ru-based olefin metathesis catalysts see: (e) Trnka, T. M.; Grubbs, R. H. *Acc. Chem. Res.* **2001**, *34*, 18-29; (f) Samojłowicz, C.; Michał, B.; Grela, K. *Chem. Rev.* **2009**, *109*, 3708-3742; (g) Vougioukalakis, G. C.; Grubbs, R. H. *Chem. Rev.* **2010**, *110*, 1746-1787. For a report on well-defined Os-bases olefin metathesis catalyst see: (h) Castarlenas, R.; Esteruelas. M. A.; Oñate, E. *Organometallics* **2005**, *24*, 4343-4346.

(2) (a) Bryce-Smith, D.; Gilbert, A. *Tetrahedron Lett.* **1964**, *47*, 3471-3473; (b) Story, P. R.; Busch, P. *Adv. Org. Chem.* **1972**, *8*, 67-95; (c) Lange, G. L.; Huggins, M. –A.; Neidert, E. *Tetrahedron Lett.* **1976**, *49*, 4409-4412; (d) Wender, P. A.; Lechleiter, J. C. *J. Am. Chem. Soc.* **1977**, *99*, 267-268; (e) Salomon, R. G.; Coughlin, D. J.; Easler, E. M. *J. Am. Chem. Soc.* **1979**, *101*, 3961-3962; (f) Wilson, S. R.; Phillips, L. R.; Pelister, Y.; Huffman, J. C. *J. Am. Chem. Soc.* **1979**, *101*, 7373-7379; (g) Williams, J. R.; Callahan, J. F. *J. Chem. Soc. Chem. Commun.* **1979**, 404-405; (h) Wender, P. A.; Hubbs, J. C. *J. Org. Chem.* **1980**, *45*, 365-

Scheme 2.1. Approaches to Olefin Metathesis

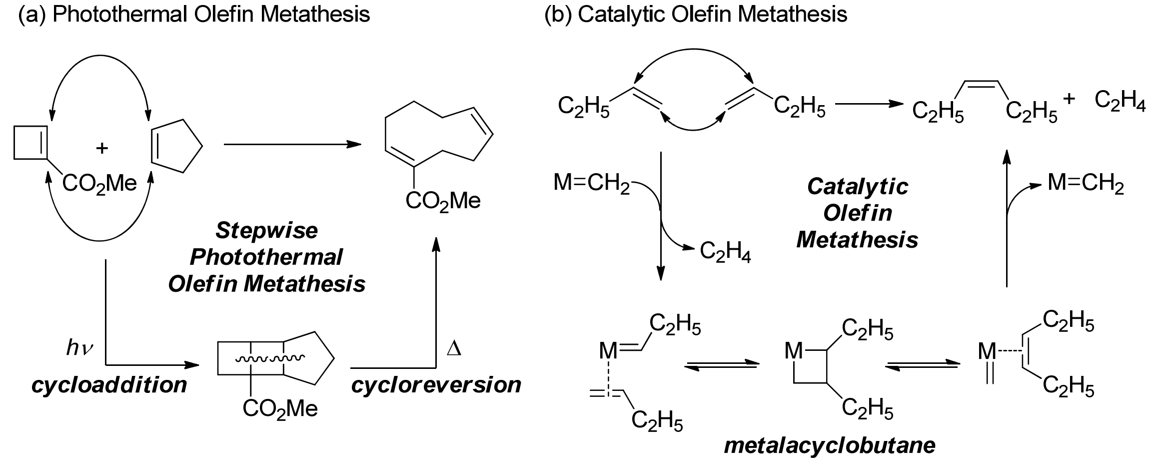

photothermal olefin metathesis is directly related to the catalytic olefin metathesis; if M was made to equal a carbon atom, the process (b) turns into the process (a). Thus, in the case when M = C the [2+2] cycloaddition is a thermally-forbidden process.[3] When M = transition metal, this process is allowed; however, if M = $d^{>6}$ transition metal the cycloreversion of metalacyclobutane is competing with reductive elimination.[4] The briefly outlined in Scheme 2.1 mechanism for catalytic olefin metathesis involving metal carbene/alkylidene[5] and metalacyclobutane intermediates was put forward by Chauvin and co-workers and subsequently was corroborated experimentally.[6] The following mechanistic discussions assume that all catalytic olefin metathesis reactions described herein follow the Chauvin mechanism.

It is the purpose of the present section to describe the electronic requirements imposed on the key steps of the catalytic olefin metathesis in the context of the

---

367; (i) Wender, P. A.; Letendre, L. J. *J. Org. Chem.* **1980**, *45*, 367-368; (j) Wender, P. A.; Lechleiter, J. C. *J. Am. Chem. Soc.* **1980**, *102*, 6340-6341.

(3) Woodward, R. B.; Hoffmann, R. *Angew. Chem. Int. Ed. in Engl.* **1969**, *9*, 781-932.

(4) Eisenstein, O.; Hoffmann, R. *J. Am. Chem. Soc.* **1981**, *103*, 5582-5584.

(5) For the discussion regarding the distinction between carbenes and alkylidenes see section 1.1.2.4.

(6) For the original report on the mechanism of metal-catalyzed olefin metathesis see: (a) Hérisson, J. –L.; Chauvin, Y. *Makromol. Chem.* **1971**, *141*, 161-176; (b) Soufflet, J. –P.; Commereuc, D.; Chauvin, Y. *C. R. Hebd. Seances Acad. Sci C: Sci. Chim.* **1973**, *276*, 169-171. For the related Nobel lecture see: (c) Chauvin, Y. *Angew. Chem. Int. Ed.* **2006**, *45*, 3740-3765. For mechanistic studies of the mechanism of metal-catalyzed olefin metathesis see: (d) Casey, C. P.; Burkhardt, T. J. *J. Am. Chem. Soc.* **1974**, *96*, 7808-7809; (e) Katz, T. J.; McGinnis, J. *J. Am. Chem. Soc.* **1975**, *97*, 1592-1594; (f) Katz, T. J.; Rothchild, R. *J. Am. Chem. Soc.* **1976**, *98*, 2519-2526; (g) Grubbs, R. H.; Carr, D. D.; Hoppin, C.; Burk, P. L. *J. Am. Chem. Soc.* **1976**, *98*, 3478-3483.

mechanism. Further discussion will relate to control of olefin metathesis stereoselectivities by means of modifications of either ancillary or reactive and dynamically exchangeable ligands, *i.e.* olefins. Throughout this section particular attention will be given to Ru-catalyzed olefin metathesis. Although the introductory discussion is based on data disclosed previously by our and other groups, the provided rationalizations may differ from the ones given in the relevant publications, as the ultimate goal of the present section is to provide a coherent and sound mechanistic model for Ru-catalyzed olefin metathesis.

2.1.1. Development of Well-defined Olefin Metathesis Catalysts: Mechanistic Aspects

Following a number of experimental observations,[7] catalytic olefin metathesis was recognized as a "transalkylidenation" reaction by Calderon and co-workers.7[g-h] The first catalytically active well-defined metal carbene complex was disclosed by Casey and Burkhardt.[8] Despite this milestone the main applications of olefin metathesis were those utilizing ill-defined catalytic systems in large-scale commodity chemicals synthesis such as Shell Higher Olefin Process (SHOP) or in polymer synthesis.[9] The lack of applications of ill-defined olefin metathesis catalytic systems in the fine chemical synthesis can be attributed to the necessity for strongly Lewis-acidic additives such as alkyl aluminum halides. Also, control of reactivity and selectivity of ill-defined catalysts is difficult due to necessity to design ancillary ligands in the absence of information regarding the structures of catalytically active species. With the advent of well-defined olefin metathesis catalysts (Scheme 2.2), particularly the Schrock-type Mo- and W-alkylidenes and Grubbs-type Ru-carbenes, the catalytic olefin metathesis has become an invaluable

---

(7) (a) Ziegler, K.; Holzkamp, E.; Breil, H.; Martin, H. *Angew. Chem.* **1955**, *67*, 541-547; (b) Truett, W. L.; Johnson, D. R.; Robinson, I. M.; Montague, B. A. *J. Am. Chem. Soc.* **1960**, *82*, 2337-2340; (c) Banks, R. L.; Bailey, G. C. *Ind. Eng. Chem. Prod. Res. Dev.* **1964**, *3*, 170-173; (d) Natta, G.; Dall'asta, G.; Mazzanti, G. *Angew. Chem. Int. Ed. in Engl.* **1964**, *3*, 723-729; (e) Michelotti, F. W.; Keaveney, W. P. *J. Polym. Sci. Part A: Polym. Chem.* **1965**, *3*, 895-905; (f) Bradshaw, C. P. C.; Howman, E. J.; Turner, L. *J. Catalysis* **1967**, *7*, 269-276; (g) Calderon, N.; Chen, H. Y.; Scott, K. W. *Tetrahedron Lett.* **1967**, *34*, 3327-3329; (h) Calderon, N.; Ofstead, E. A.; Ward, J. P.; Judy, W. A.; Scott, K. W. *J. Am. Chem. Soc.* **1968**, *90*, 4133-4140.

(8) (a) Casey, C. P.; Burkhardt, T. J. *J. Am. Chem. Soc.* **1973**, *95*, 5833-5834; (b) Casey, C. P.; Burkhardt, T. J. *J. Am. Chem. Soc.* **1974**, *96*, 7808-7809.

(9) (a) Weissermel, K.; Arpe, H. –J. *Industrial Organic Chemistry*, 4rd Ed.; WILEY-VCH Verlag GmbH & Co. KGaA: Weinheim, 2003; (b) Mol, J. C. *J. Mol. Catal. A: Chem.* **2004**, *213*, 39-45.

Scheme 2.2. Representative Well-defined Olefin Metathesis Catalysts

High Oxidation State Early Transition Metal-based Catalysts

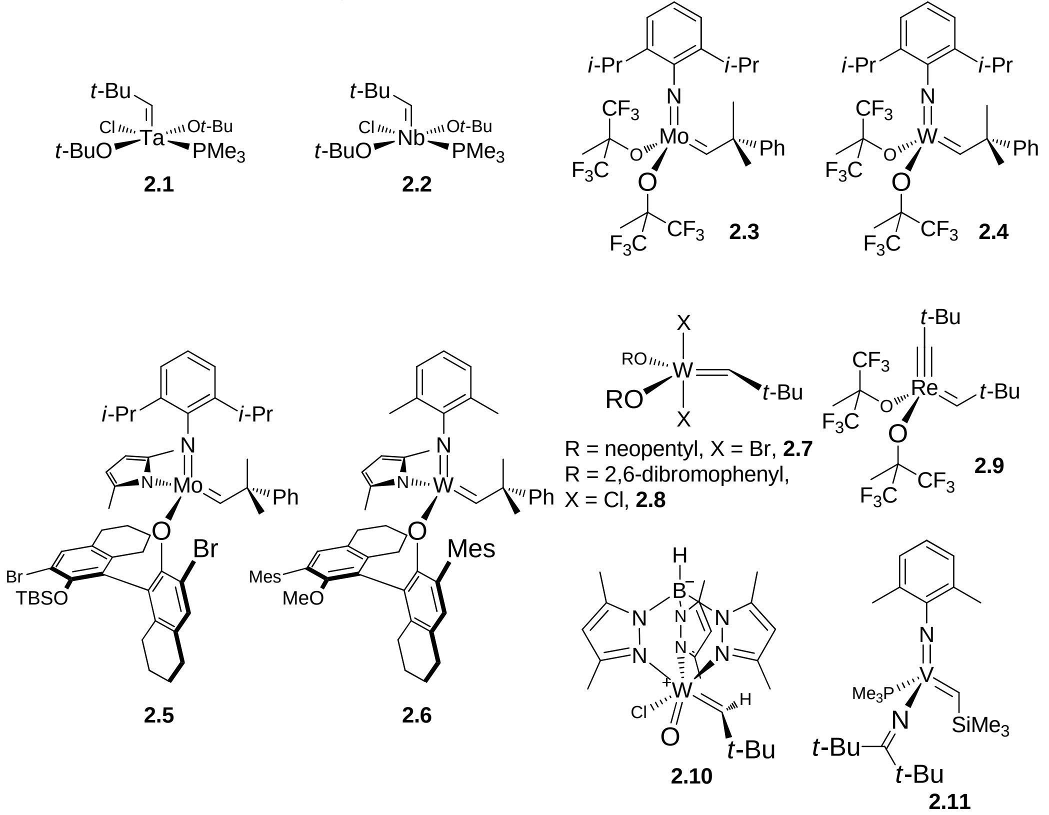

Low Oxidation State Late Transition Metal-based Catalysts

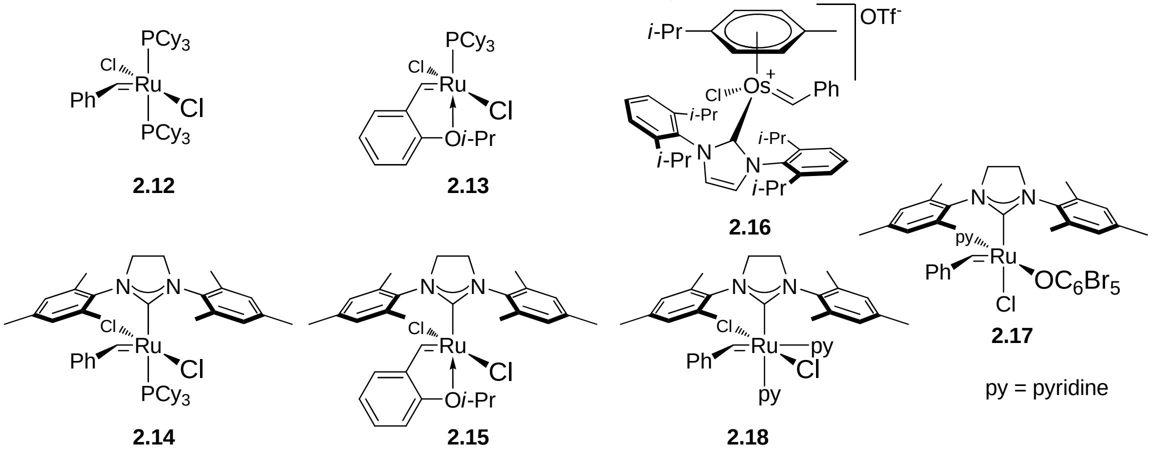

method among C-C bond-forming processes.[1,10] The main advantages of olefin

---

[10] For reviews on applications of olefin metathesis in synthesis of natural products and other molecules of interest see: (a) Nicolaou, K. C.; Bulger, P. G.; Sarlah, D. *Angew. Chem. Int. Ed.* **2005**, *44*, 4490-4527; (b) Gradillas, A.; Pérez-Castells, J. *Angew. Chem. Int. Ed.* **2006**, *45*, 6086-6101; (c) Dietrich-Buchecker, C.; Rapenne, G.; Sauvage, J. –P. *Coord. Chem. Rev.* **1999**, *185-186*, 167-176; (d) Hoveyda, A. H.; Malcolmson, S. J.; Meek, S. J.; Zhugralin, A. R. *Angew. Chem. Int. Ed.* **2010**, *49*, 34-44; (e) *Metathesis in*

metathesis are that it does not involve charge separation, thereby rendering it orthogonal to most polar transformations. Furthermore, olefin metathesis is an atom-economical green process furnishing environmentally benign (for example, ethylene in case of most ring-closing metathesis reactions) or no byproducts. [11,12]

Following the disclosure of $(CO)_5W{=}CPh_2$ as a well-defined olefin metathesis catalyst,[8] the initial breakthroughs occurred in catalyst development involving early transition metal alkylidenes.[13] Among the major milestones in the development of olefin metathesis catalysts were the complexes **2.1** and **2.2**, which proved to be competent olefin metathesis catalysts under mild reaction conditions (25 °C) and were reisolable, following the reaction, thereby providing addition evidence for the transalkylidenation mechanism involving metal carbenes/alkylidenes.[14] However, Ta- and Nb-based olefin metathesis catalysts were relatively short lived, and thus it was not until the complexes **2.3** and **2.4** were disclosed that the potential of olefin metathesis in fine chemical synthesis began to be realized.[15] Other metal alkylidene complexes were disclosed (for example, complexes **2.7-2.11**);[16] however, their olefin metathesis activities were often low at mild reaction conditions or limited to ring-opening metathesis polymerization reactions. Throughout

---

Natural Product Synthesis; Cossy, J.; Arseniyadis, S.; Meyer, C. Eds.; WILEY-VCH Verlag GmbH & Co. KGaA, Weinheim, 2010.

(11) Trost, B. M. *Science* **1991**, *254*, 1471-1478.

(12) (a) Clavier, H.; Grela, K.; Kirschning, A.; Mauduit, M.; Nolan, S. P. *Angew. Chem. Int. Ed.* **2007**, *46*, 6786-6801; (b) *Green Metathesis Chemistry: Great Challenges in Synthesis, Catalysis and Nanotechnology*; Dragutan, V.; Demonceau, A.; Dragutan, I.; Finkelshtein, E. Sh., Eds. In NATO Science for Peace and Security Series – A: Chemistry and Biology: Springer, Dodrecht, the Netherlands, 2010.

(13) (a) Schrock, R. R. *Acc. Chem. Res.* **1979**, *12*, 98-104; (b) Schrock, R. R. *Chem. Rev.* **2002**, *102*, 145-179. For the original disclosure of Ta alkylidene see: (c) Schrock, R. R. *J. Am. Chem. Soc.* **1974**, *96*, 6796-6797.

(14) (a) Schrock, R. R.; Rocklage, S.; Wengrovius, J.; Rupprecht, G.; Fellmann, J. *J. Mol. Catal.* **1980**, *8*, 73-83; (b) Rocklage, S. M.; Fellmann, J. D.; Rupprecht, G. A.; Messerle, L. W.; Schrock, R. R. *J. Am. Chem. Soc.* **1981**, *103*, 1440-1447.

(15) Complex **2.3**: (a) Murdzek, J. S.; Schrock, R. R. *Organometallics* **1987**, *6*, 1373-1374. Complex **2.4**: (b) Schrock, R. R.; DePue, R. T.; Feldman, J.; Schaverien, C. J.; Dewan, J. C.; Liu, A. H. *J. Am. Chem. Soc.* **1988**, *110*, 1423-1435.

(16) Complex **2.7**: (a) Kress, J.; Aguero, A.; Osborn, J. A. *J. Mol. Catal.* **1986**, *36*, 1-12. Complex **2.8**: (b) Quignard, F.; Leconte, M.; Basset, J. –M. *J. Chem. Soc. Chem. Commun.* **1985**, 1816-1817. Complex **2.9**: (c) Toreki, R.; Schrock, R. R. *J. Am. Chem. Soc.* **1990**, *112*, 2448-2449; (d) Toreki, R.; Schrock, R. R.; Davis, W. M. *J. Am. Chem. Soc.* **1992**, *114*, 3367-3380; (e) Toreki, R.; Vaughan, G. A.; Schrock, R. R.; Davis, W. M. *J. Am. Chem. Soc.* **1993**, *115*, 127-137. Complex **2.10**: (f) Blosch, L. L.; Abboud, K.; Boncella, J. M. *J. Am. Chem. Soc.* **1991**, *113*, 7066-7068. Complex **2.11**: (g) Yamada, J.; Fujiki, M.; Nomura, K. *Organometallics* **2005**, *24*, 2248-2250.

the studies of early transition metal alkylidene complexes it was found that Mo-based catalysts exhibit highest activities, primarily due to the fact that the decomposition pathways are not as easily energetically accessible for such complexes as those for Ta-, Nb- and Re-based complexes.[1c,17] Furthermore, potential energy surface for Mo-catalyzed olefin metathesis is generally more flat (*i.e.* no deep valleys and high energy transition states), whereas complexes based on other early transition metals exhibit either an energetically low lying metalacyclobutane (Ti and W) or higher energy transition states (Re).[1c,18] Recent breakthrough in early transition metal-based catalyst design involved the introduction of the stereogenic-at-metal complexes **2.5** and **2.6** and derivatives thereof, which were shown to possess a set of unique reactivity and selectivity profiles.[19]

Although ill-defined catalytic systems based on low oxidation Ru salts were among the early disclosures of catalytic olefin metathesis,[7f,9b,20] well-defined Ru carbenes that are competent olefin metathesis catalysts were not prepared until Grubbs and co-workers demonstrated that structures of the type **2.12** are capable of catalyzing olefin metathesis.[1e,21,22] The modification of the originally disclosed Ru allylidene gave a more

---

(17) (a) Leduc, A. –M.; Salameh, A.; Soulivong, D.; Chabanas, M.; Basset, J. –M.; Copéret, C.; Solans-Monfort, X.; Clot, E.; Eisenstein, O.; Böhm, V. P. W.; Röper, M. *J. Am. Chem. Soc.* **2008**, *120*, 6288-6297; (b) Solans-Monfort, X.; Copéret, C.; Eisenstein, O. *J. Am. Chem. Soc.* **2010**, *132*, 7750-7757.

(18) (a) Solans-Monfort, X.; Clot, E.; Copéret, C.; Eisenstein, O. *J. Am. Chem. Soc.* **2005**, *127*, 14015-14025; (b) Poater, A.; Solans-Monfort, X.; Clot, E.; Copéret, C.; Eisenstein, O. *J. Am. Chem. Soc.* **2007**, *129*, 8207-8216

(19) For the original disclosure of the complex **2.5** see: (a) Malcolmson, S. J.; Meek, S. J.; Sattely, E. S.; Schrock, R. R.; Hoveyda, A. H. *Nature* **2008**, *456*, 933-937. For the disclosure of the complex **2.6** see: (b) Jiang, A. J.; Zhao, Y.; Schrock, R. R.; Hoveyda, A. H. *J. Am. Chem. Soc.* **2009**, *131*, 16630-16631. For applications of the stereogenic-at-metal complexes **2.5**, **2.6**, and the derivatives thereof see: (c) Sattely, E. S.; Meek, S. J.; Malcolmson, S. J.; Schrock, R. R.; Hoveyda, A. H. *J. Am. Chem. Soc.* **2009**, *131*, 943-953; (d) Ibrahem, I.; Yu, M.; Schrock, R. R.; Hoveyda, A. H. *J. Am. Chem. Soc.* **2009**, *131*, 3844-3845; (e) Flook, M. M.; Jiang, A. J.; Schrock, R. R.; Müller, P.; Hoveyda, A. H. *J. Am. Chem. Soc.* **2009**, *131*, 7962-7963; (f) Lee, Y. –J.; Schrock, R. R.; Hoveyda, A. H. *J. Am. Chem. Soc.* **2009**, *131*, 10652-10661; (g) Marinescu, S. C.; Schrock, R. R.; Müller, P.; Hoveyda, A. H. *J. Am. Chem. Soc.* **2009**, *131*, 10840-10841.

(20) (a) Mutch, A.; Leconte, M.; Lefebvre, F.; Basset, J. –M. *J. Mol. Catal. A: Chem.* **1998**, *133*, 191-199; (b) Hamilton, J. G.; Ivin, K. J.; McCann, G. M.; Rooney, J. J. *J. Chem. Soc., Chem. Commun.* **1984**, 1379-1381.

(21) Nguyen, S. T.; Johnson, L. K.; Grubbs, R. H.; Ziller, J. W. *J. Am. Chem. Soc.* **1992**, *114*, 3974-3975.

(22) Other Ru-carbenes such as Roper carbenes were found to be inert under olefin metathesis reaction conditions: (a) Nguyen, S. B. *PhD Thesis*, California Institute of Technology, 1995. For examples of Roper carbenes see: (b) Gallop, M. A.; Roper, W. R. *Adv. Organomet. Chem.* **1986**, *25*, 121-198; (c) Roper, W. R. *J. Organomet. Chem.* **1986**, *300*, 167-190; (d) Brothers, P. J.; Roper, W. R. *Chem. Rev.* **1988**, *88*, 1293-1326.

active initiator **2.12**.[23a] Substitution of the phosphine ligand by a weaker π-acidic ligand (NHC) resulted in enhanced catalyst activity (complex **2.14**).[23b-f] The complexes **2.13** and **2.15** were introduced by our group to decrease the concentration of free phosphine in the reaction mixture, as free phosphine can be detrimental to the reactivity of the catalytic species.[24,25] Rapid olefin metathesis initiators based on Ru were disclosed; complex **2.18** was found to exhibit superior rates of initiation to those of complexes **2.14** or **2.15**.[23g] Another rapid initiator that exhibited high rates of initiation and propagation was **2.17**.[26] It should be noted that despite structural differences of the starting Ru complexes, in all cases the propagating species are fundamentally similar; this aspect of Ru-catalyzed olefin metathesis is going to be discussed below. Os-Based olefin metathesis catalysts were not developed to the same extent as were Ru-based catalyst.[27] To the best of my knowledge there is only a single instance of a published olefin metathesis active Os-based catalyst (complex **2.16**); the activities, however, are significantly lower than those of the corresponding Ru-based catalysts.[28] It should be noted that the propagating species in olefin metathesis catalyzed by **2.16** most likely involve a triflate version of the

---

(23) (a) Schwab, P.; France, M. B.; Ziller, J. W.; Grubbs, R. H. *Angew. Chem. Int. Ed.* **1995**, *34*, 2039-2041; (a) Schwab, P.; Grubbs, R. H.; Ziller, J. W. *J. Am. Chem. Soc.* **1996**, *118*, 100-110; (b) Scholl, M.; Trnka, T. M.; Morgan, J. P.; Grubbs, R. H. *Tetrahedron Lett.* **1999**, *40*, 2247-2250; (c) Scholl, M.; Ding, S.; Lee, C. W.; Grubbs, R. H. *Org. Lett.* **1999**, *1*, 953-956; (d) Weskamp, T.; Schattenmann, W. C.; Spiegler, M.; Herrmann, W. A. *Angew. Chem. Int. Ed.* **1998**, *37*, 2490-2493; (e) Huang, J.; Stevens, E. D.; Nolan, S. P.; Petersen, J. L. *J. Am. Chem. Soc.* **1999**, *121*, 2674-2678; (f) Trnka, T. M.; Morgan, J. P.; Sanford, M. S.; Wilhelm, T. E.; Scholl, M.; Choi, T. –L.; Ding, S.; Day, M. W.; Grubbs, R. H. *J. Am. Chem. Soc.* **2003**, *125*, 2546-2558; (g) Love, J. A.; Sanford, M. S.; Day, M. W.; Grubbs, R. H. *J. Am. Chem. Soc.* **2003**, *125*, 10103-10109.

(24) Complex **2.13**: (a) Kingsbury, J. S.; Harrity, J. P. A.; Bonitatebus, P. J., Jr.; Hoveyda, A. H. *J. Am. Chem. Soc.* **1999**, *121*, 791-799. Complex **2.15**: (b) Garber, S. B.; Kingsbury, J. S.; Gray, B. L.; Hoveyda, A. H. *J. Am. Chem. Soc.* **2000**, *122*, 8168-8179. Shortly after the report in (b) a related work was disclosed: (c) Gessler, S.; Randl, S.; Blechert, S. *Tetrahedron Lett.* **2000**, *41*, 9973-9976.

(25) (a) Hong, S. H.; Day, M. W.; Grubbs, R. H. *J. Am. Chem. Soc.* **2004**, *126*, 7414-7415; (b) Hong, S. H.; Wenzel, A. G.; Salguero, T. T.; Day, M. W.; Grubbs, R. H. *J. Am. Chem. Soc.* **2007**, *129*, 7961-7968.

(26) Conrad, J. C.; Parnas, H. H.; Snelgrove, J. L.; Fogg, D. E. *J. Am. Chem. Soc.* **2005**, *127*, 11882-1183.

(27) It is generally noted that 5d-transition metals provide less active catalysts than their 4d-counterparts due to formation of stronger M-element bonds in the complexes of the former metals. For the discussion comparing the transition metal triad Fe/Ru/Os see: Esteruelas, M. A.; Oro, L. A. *Chem. Rev.* **1998**, *98*, 577-588.

(28) Castarlenas, R.; Esteruelas, M. A.; Oñate, E. *Organometallics* **2005**, *24*, 4343-4346.

propagating species in olefin metathesis catalyzed by Grubbs-type NHC-Ru catalysts (**2.14**, **2.15**, **2.17**, and **2.18**).[29]

From the examples of well-defined olefin metathesis catalysts illustrated in Scheme 2.2 it is clear that the structural diversity of the high oxidation state early transition metal alkylidenes is greater than that of the low oxidation state late transition metal carbenes. The main reason for this disparity can be attributed to the following factors: (1) an olefin metathesis active M-C double bond has a dominant alkylidene character and a minor carbene character;[5] (2) electronic and structural demands associated with the synthesis of metal carbenes, in which metal has a partially occupied *d*-shell (see section 2.1.2).

The nature of the M-C double bond can be clearly seen through consideration of the molecular orbital diagrams.[30] In a molecule of ethylene the two :CH_2 fragments can be considered as being in a ground triplet state; metal alkylidenes are analogous to ethylene. The main distinction in bonding between ethylene and metal alkylidene can be seen in [2+2] reaction between either two molecules of ethylene or a molecule of metal alkylidene and ethylene. In case of the formation transformation the process is a symmetry forbidden [π2a+π2s] reaction; however, the latter is symmetry allowed, because of the d_π orbital at the metal center (Figure 2.1). Metal alkylidene π-bonds are usually polarized towards the C atom, as evidenced by their nucleophilic character.

Figure 2.1. Cycloaddition Reactions

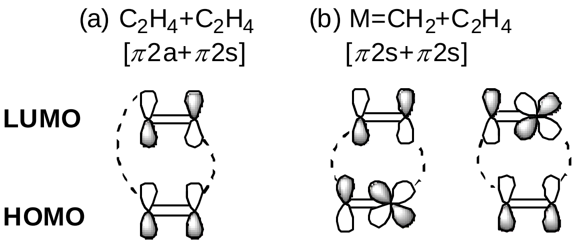

---

(29) The design of complex **2.16** is based on related Ru complexes. The phosphine-bearing Ru(cymene) complex: (a) Fürstner, A.; Picquet, M.; Bruneau, C.; Dixneuf, P. H. *Chem. Commun.* **1998**, 1315-1316. The NHC-bearing Ru(cymene) complex: (b) Jafarpour, L.; Huang, J.; Stevens, E. D.; Nolan, S. P. *Organometallics* **1999**, *18*, 3760-3763. For the discussion regarding the mechanism of action of the Ru(cymene) carbene complexes in olefin metathesis see: (c) Castarlenas, R.; Vovard, C.; Fischmeister, C.; Dixneuf, P. H. *J. Am. Chem. Soc.* **2006**, *128*, 4079-4089; (d) Ahr, M.; Thieuleux, C.; Copéret, C.; Fenet, B.; Basset, J. –M. *Adv. Synth. Catal.* **2007**, *349*, 1587-1591. The mono-triflate analogue of **2.15** was found to be a competent olefin metathesis catalyst: (d) Krause, J. O.; Nuyken, O.; Wurst, K.; Buchmeiser, M. R. *Chem. Eur. J.* **2004**, *10*, 777-784.

(30) (a) See Figure 1.8 in section 1.1.2.4. For the discussion of molecular orbital diagrams of metal carbenes, metal alkylidenes, and ethylene see: (b) Taylor, T. E.; Hall, M. B. *J. Am. Chem. Soc.* **1984**, *106*, 1576-1584.

Therefore, HOMO of metal alkylidene can be viewed as having a greater coefficient at the carbon center, and consequently the cycloaddition between an olefin and metal alkylidene is comparable to a carbometalation reaction (Scheme 2.3).[31]

Scheme 2.3. Metalacyclobutane Formation as a Carbometalation Reaction

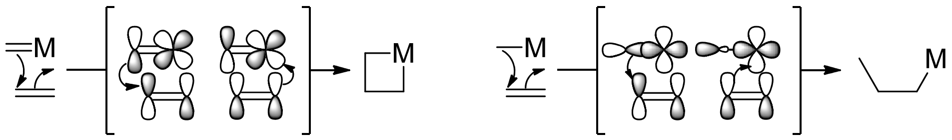
(a) Metalacyclobutane formation (b) Carbometalation reaction

Metal carbene bond, on the other hand, is comprised of metal and carbon fragments in singlet ground states. The bond is generally polarized towards the metal center, as evidenced by the electrophilic character of metal carbenes; the $\pi_{\text{M-C}}$ bond is a Lewis base (metal) Lewis acid (carbon) pair; the HOMO coefficient is greater at the d_π-orbital of the metal than p-orbital of the carbene carbon. On the other hand the LUMO coefficient is greater at the p-orbital of the carbene carbon atom and smaller at the d_π-orbital of the metal. As illustrated in Figure 2.1, there are two contributing interactions that result in the formation of a metalacyclobutane.[32] It is useful to consider the limits or extremes within a reaction (*i.e.* cases where one of the interactions is negligible). The first such case involves the dominant contribution of donation from the metal carbene bonding orbital $\pi_{\text{M-C}}$ into the $\pi^*_{\text{C-C}}$; in order for a reaction to occur the coefficient at the p-orbital at the carbene carbon atom must be sufficiently large in order to contribute significantly enough to bonding, as otherwise the olefin would stay bound to a metal center as a metalacyclopropane and no metalacyclobutane would form. Sufficient increases in coefficient at the p-orbital of the carbene carbon atom effectively endow the M-C bond with an alkylidene character, and thus it is possible that at the limit of the $\pi_{\text{M-C}}\rightarrow\pi^*_{\text{C-C}}$ interaction the p-orbital coefficient is required to be at the alkylidene level. The

---

(31) For example, addition of alkyl zirconocene and titanocene complexes to C-C multiple bonds is considered to involve the donation σ(M-C)→π^*(C-C) as a dominant interaction: Negishi, E. *Dalton Trans.* **2005**, 827-848.

(32) These interactions effectively constitute a Dewar-Chatt-Duncanson model for an olefin bonding to a metal carbene rather than a metal center. For the discussion of donation/backdonation model of Dewar, Chatt, and Duncanson see: (a) Dewar, M. J. S. *Bull. Chim. Soc. Fr.* **1951**, *18*, C71-C79; (b) Chatt, J.; Duncanson, L. A. *J. Chem. Soc.* **1953**, 2939-2947.

other extreme involves the donation from the $\pi_{C\text{-}C}$ into $\pi^*_{M\text{-}C}$; the coefficient at the *p*-orbital of the carbene carbon atom needs to be sufficiently high (*i.e.* carbene needs to be sufficiently electrophilic) in order to compete with interaction between the $\pi_{C\text{-}C}$ of olefin and the d_σ-orbital of the metal center. However, enhanced electrophilicity of the carbene carbon atom may result in competitive outer sphere cyclopropanation processes, as observed for Rh carbenes.[33] Overall, electrophilic carbenes that would be expected to undergo olefin metathesis fall into the narrow window, which is limited by alkylidene character on one hand and the competing cyclopropanation processes on the other. However, experimental evidence suggests that catalytically active in olefin metathesis Ru-carbenes are electrophilic.[34]

2.1.2. Synthesis of Metal Carbenes/Alkylidenes

Before the discussion of the mechanism of olefin metathesis it is useful to consider the methods for synthesis of metal-carbon double bonds. Common methods for the synthesis of metal non-heteroatom substituted carbene and alkylidene complexes involve transmetalation of an alkylidene moiety (from the corresponding ylide),[35] cyclopropene ring-opening,[36] dehydration of propargyl alcohol,[29] formal double oxidative addition,[37] synthesis of oligo-alkyl metal complexes and subsequent α-hydrogen abstraction,[38] or protonation of metal carbyne/alkylidyne complexes.[39] The most common methods are summarized in Scheme 2.4.

---

(33) For the discussion of the mechanism of Rh-catalyzed cyclopropanation see: (a) Nowlan, D. T.; Gregg, T. M.; Davies, H. M. L.; Singleton, D. A. *J. Am. Chem. Soc.* **2003**, *125*, 15902-15911; (b) Howell, J. A. S. *Dalton Trans.* **2007**, 1104-1114; (c) Bonge, H. T.; Hansen, T. *J. Org. Chem.* **2010**, *75*, 2309-2320.

(34) Decomposition of Ru carbenes is consistent with the electrophilic nature of these complexes.

(35) For transmetalation of carbenes from the corresponding diazocompounds see: (a) Mango, F. D.; Dvoretzky, I. *J. Am. Chem. Soc.* **1965**, *88*, 1654-1657; (b) see Ref 22c; (c) Hill, A. W.; Roper, W. R.; Waters, J. M.; Wright, A. H. *J. Am. Chem. Soc.* **1983**, *105*, 5939-5940 (d) Schwab, P.; Grubbs, R. H.; Ziller, J. W. *J. Am. Chem. Soc.* **1996**, *118*, 100-110. For transmetalation of carbenes from the sulfur ylides see: (e) Gandelman, M.; Rybtchinski, B.; Ashkenazi, N.; Gauvin, R. M.; Milstein, D. *J. Am. Chem. Soc.* **2001**, *123*, 5372-5373. For transmetalation of carbenes/alkylidenes from phosphorus ylides see: (f) Buijink, J. F.; Tueben, J. H.; Kooijman, H.; Spek, A. L. *Organometallics* **1994**, *13*, 2922-2924.

(36) (a) Ref. 21; (b) de la Mata, F. J.; Grubbs, R. H. *Organometallics* **1996**, *15*, 577-584.

(37) Belderrain, T. R.; Grubbs, R. H. *Organometallics* **1997**, *16*, 4001-4003.

(38) See Refs. 1c, 13, 15.

(39) Caskey, S. R.; Stewart, M. H.; Ahn, Y. J.; Johnson, M. J. A.; Rowsell, J. L. C.; Kampf, J. W. *Organometallics* **2007**, *26*, 1912-1923.

Scheme 2.4. Representative Methods for Preparation of Complexes with Metal-Carbon Double Bonds

(a) Transmetalation

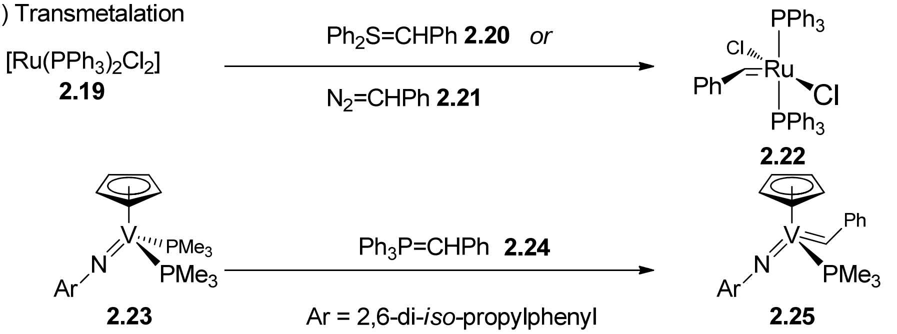

(1)

(2)

(b) Cyclopropene Ring-Opening

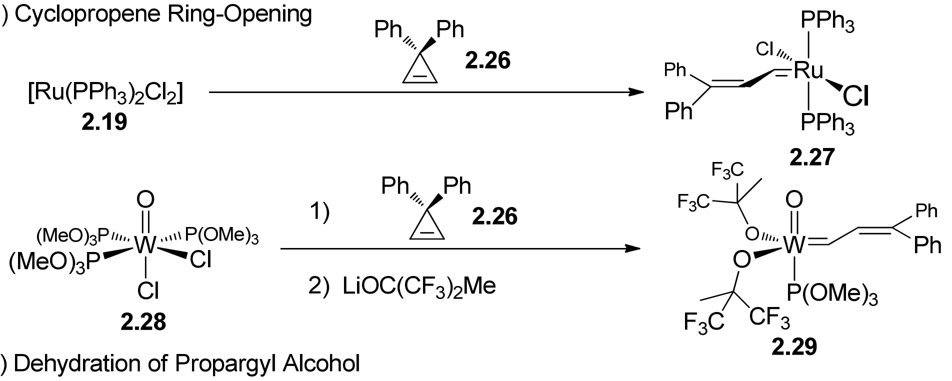

(3)

(4)

(c) Dehydration of Propargyl Alcohol

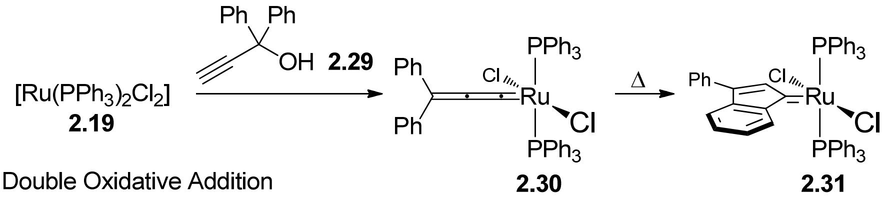

(5)

(d) Double Oxidative Addition

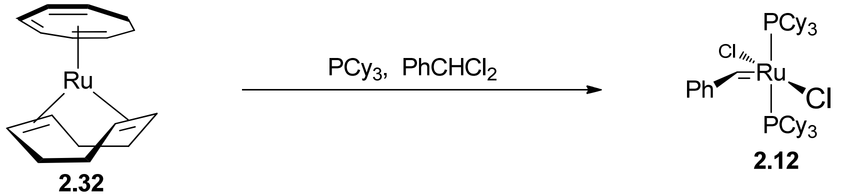

(6)

(e) Alkylation of Transition Metal Center with Subsequent α-Hydrogen Abstraction

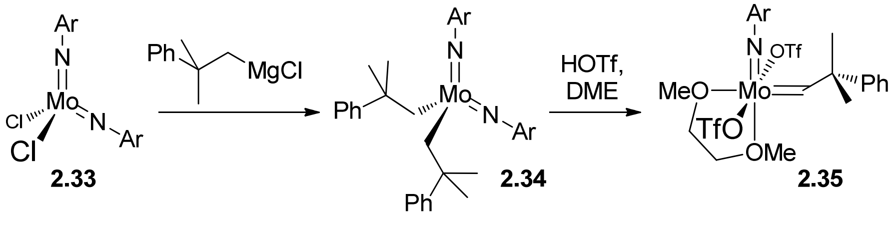

(7)

(f) Protonation of Carbyne

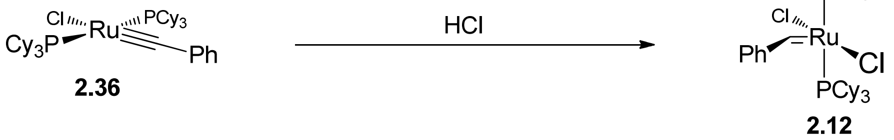

(8)

The methods for synthesis of metal-carbon double bonds impose electronic constraints on the metal center in question. Methods such as transmetalation, cyclopropene ring-opening, and dehydration of propargylic alcohol necessitate a Lewis amphoteric metal center; in other words, the metal atom in question has to exhibit both Lewis acidic and Lewis basic properties. Double oxidative addition requires employment of electron rich metal centers in low oxidation states such as Ru (0) (eq 6 in Scheme 2.4). Alkylation of transition metal center followed by the α-hydrogen abstraction applies to high oxidation states electron poor metal centers; however, this method is largely limited to the early transition metals, as middle to late transition metals tend to exhibit outer sphere reactivity in high oxidation states. Protonation of metal carbynes/alkylidynes requires the carbyne carbon atom to exhibit nucleophilic properties. This method has limited applicability, because prior synthesis of metal-carbon triple bonds is necessary.

Preparation of Ru-based olefin metathesis catalysts is usually carried out by means of either carbene transmetalation from the corresponding diazocompounds or dehydration of propargyl alcohol. Subsequent carbene exchange allows for preparation of other Ru complexes.[1f-g] As stated above, nearly all of the olefin metathesis active Ru carbene complexes generate Grubbs-type propagating Ru complexes in the catalytic cycle. Stability of the requisite low valent low oxidation state metal carbene complexes with partially filled *d* shell is partly responsible for the paucity of this class of catalysts. There are three notable major limitations in the synthesis of Ru carbenes: (1) low valent late transition metal carbene complexes can undergo unimolecular rearrangements, affording a metal carbyne hydride species or metal olefin complexes;[40,41] (2) highly

---

(40) Strictly, the equilibrium between metal carbene and metal carbyne hydride complexes should not inhibit olefin metathesis reaction; as long as metal carbene species are present in the reaction mixture cycloaddition/cycloreversion with an olefin can occur. However, alternative pathways are open; for example, metal carbyne hydride can undergo hydrometalation with olefins to give alkyl metals. In one case, it was found that cationic Ru hydride carbyne species are short-lived olefin metathesis catalysts: (a) González-Herrero, P.; Weberndörfer, B.; Ilg, K.; Wolf, J.; Werner, H. *Angew. Chem. Int. Ed.* **2000**, *39*, 3266-3269. For a review on equilibria between metal alkyl, carbene, and carbyne complexes see: (b) Caulton, K. G. *J. Organomet. Chem.* **2001**, *617-618*, 56-64. For examples of 1,2-hydrogen atom migrations see: (c) Espuelas, J.; Esteruelas, M. A.; Lahoz, F. J.; Oro, L. A.; Ruiz, N. *J. Am. Chem. Soc.* **1993**, *115*, 4683-4689; (d) Spivak, G. J.; Coalter, J. N.; Oliván, M.; Eisenstein, O.; Caulton, K. G. *Organometallics* **1998**, *17*, 999-1001; (e) González-Herrero, P.; Weberndöfer, B.; Ilg, K.; Wolf, J.; Werner, H. *Organometallics* **2001**, *20*, 3672-3685; (f) Esteruelas, M. A.; González, A. I.; López, A. M.; Oñate, E.

electrophilic late transition metal carbenes undergo a competitive outer sphere cyclopropanation reactions;[42] (3) electrophilic late transition metal carbenes effect intramolecular C-H activations, thereby deactivating or losing the carbene moiety.[43] These limitations are illustrated in Scheme 2.5.

Scheme 2.5. Late Transition Metal Carbenes Deactivation Pathways

(a) Unimolecular Rearrangements

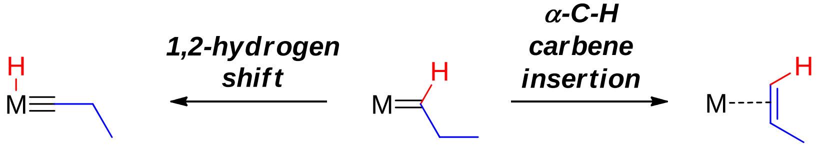

(b) Outer Sphere Cyclopropanation and C-H Insertion

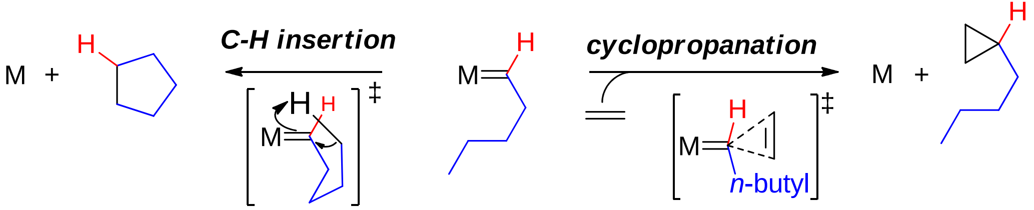

Organometallics **2003**, *22*, 414-425; (g) Bolaño, T.; Castarlenas, R.; Esteruelas, M. A.; Oñate, E. *Organometallics* **2007**, *26*, 2037-2041; (h) Brown, C. C.; Ancelet, T. A.; Stephan, D. W. *Organometallics* **2010**, *29*, 4369-4374.

(41) Strongly electrophilic metal carbenes can be viewed as carbocations that are weakly stabilized through backdonation from a metal center, thus, isomerization of an alkyl carbene to an olefin constitutes an organometallic variant of 1,2-hydride shift in Bamford-Stevens reactions carried out in aprotic solvents: (a) Bamford, W. R.; Stevens, T. S. *J. Chem. Soc.* **1952**, 4735-4740. For examples of metal carbene rearrangements affording metal olefin complexes see: (b) Casey, C. P.; Miles, W. H.; Tukada, H. *J. Am. Chem. Soc.* **1985**, *107*, 2924-2931; (c) Roger, C.; Bodner, G. S.; Hatton, W. G.; Gladysz, J. A. *Organometallics* **1991**, *10*, 3266-3274; (d) Ozerov, O. V.; Watson, L. A.; Pink, M.; Caulton, K. G. *J. Am. Chem. Soc.* **2003**, *125*, 9604-9605 (e) Paneque, M.; Poveda, M. L.; Santos, L. L.; Carmona, E.; Lledós, A.; Ujaque, G.; Mereiter, K. *Angew. Chem. Int. Ed.* **2004**, *43*, 3708-3711. The isomerizations of late transition metal carbenes to give olefins have been noted in Au- and Pt-catalyzed cycloisomerizations: (e) Echavarren, A. M.; Méndez, M.; Muñoz, M. P.; Nevado, C.; Martín-Matute, B.; Nieto-Oberhuber, C.; Cárdenas, D. J. *Pure Appl. Chem.* **2004**, *76*, 453-463; (f) Zhang, L.; Sun, J.; Kozmin, S. A. *Adv. Synth. Catal.* **2006**, *348*, 2271-2296. Alternatively, this isomerization can be a result of a sequence of β-hydride elimination and reductive elimination. It should be noted that late transition metal are more prone to β-eliminations than early transition metals: (g) Marks, T. J.; Gagne, M. R.; Nolan, S. P.; Schock, L. E.; Seyam, A. M.; Stern, D. *Pure Appl. Chem.* **1989**, *61*, 1665-1672.

(42) For examples of Ru-catalyzed cyclopropanation reactions see: (a) Nishiyama, H. Ruthenium-Catalyzed Cyclopropanation. In *Ruthenium in Organic Synthesis*; Murahashi, S. –I., Ed.; Wiley-VCH Verlag GmbH & Co. KGaA, Weinheim, 2005; (b) Nishiyama, H.; Itoh, Y.; Matsumoto, H.; Park, S. –B.; Itoh, K. *J. Am. Chem. Soc.* **1994**, *116*, 2223-2224. For the mechanism of Rh-catalyzed cyclopropanation reactions see Ref. 33. For mechanistic studies of Cu-catalyzed cyclopropanations see: (c) Straub, B.; Gruber, I.; Rominger, F.; Hofmann, P. *J. Organomet. Chem.* **2003**, *684*, 124-143.

(43) For examples of transition metal carbene insertions into C-H bonds see: (a) Díaz-Requejo, M. M.; Belderrain, T. R.; Nicasio, M. C.; Pérez, P. J. *Dalton Trans.* **2006**, 5559-5566; (b) Davies, H. M. L.; Dick, A. R. *Top. Curr. Chem.* **2010**, *292*, 303-345.

Thus, a competent olefin metathesis catalysts based on electrophilic carbenes have to fulfill the following criteria: (1) electrophilicity of the carbene carbon atom is limited by the occurrence of side reactions (b) in Scheme 2.5; (2) metal center has to be sufficiently electron poor to ascertain that the equilibrium between metal hydride carbyne and metal carbene tautomers strongly favors the latter; (3) the metal center must be reluctant to undergo β-hydride eliminations.[41g] These criteria favor early transition metal alkylidenes over late transition metal carbenes; it is surprising that low oxidation state Ru carbenes are capable of catalyzing olefin metathesis. The next section will address the mechanism of Ru-catalyzed olefin metathesis, while accounting for the aforementioned criteria.

2.1.3. Mechanism of Ru-Catalyzed Olefin Metathesis and Factors Governing the Catalyst Activity

2.1.3.1. Electronic Structure of Ru Carbene Complexes

Before the discussion of the mechanism of olefin metathesis it is imperative to consider the electronic structure of the Ru carbene complexes. The useful information in this respect can be gleaned from spectral and structural data.

As illustrated in Scheme 2.6 the ^{1}H NMR chemical shifts of the carbene protons in Grubbs-type complexes **2.12**, **2.14**, and **2.38**[44] are consistently downfield from those in styrene-etherate Ru complexes **2.37**,[24a,45] **2.15**, and **2.39**[46]. The effect of changing halide ligands from more electronegative chlorides to less electronegative iodides does not have a pronounced effect on ^{1}H NMR carbene proton chemical shift in Grubbs-type complexes **2.14** and **2.38**; however, the same chemical shift in styrene etherate complexes is sensitive to the nature of the X ligands (compare **2.15** and **2.39**). The main reason for the difference in chemical shifts between carbene protons in **2.15** and **2.39** can be attributed

---

(44) Complex **2.38**: Sanford, M. S.; Love, J. A.; Grubbs, R. H. *J. Am. Chem. Soc.* **2001**, *123*, 6543-6554.

(45) Note that Ru complex **2.37** is shown in place of the complex **2.13**, because *X*-ray crystal structure of the latter is not available. However, ^{1}H NMR chemical shift of the carbene proton of **2.13** is 17.46 ppm, and thus **2.38** can be considered a reasonable model for this complex.

(46) Complex **2.39**: Wappel, J.; Urbina-Blanco, C. A.; Abbas, M.; Albering, J. H.; Saf, R.; Nolan, S. P.; Slugovc, C. *Beilstein J. Org. Chem.* **2010**, *6*, 1091-1098.

Scheme 2.6. ^{1}H NMR and Structural Data for Ru Complexes **2.12**-**2.15** and Key Interactions

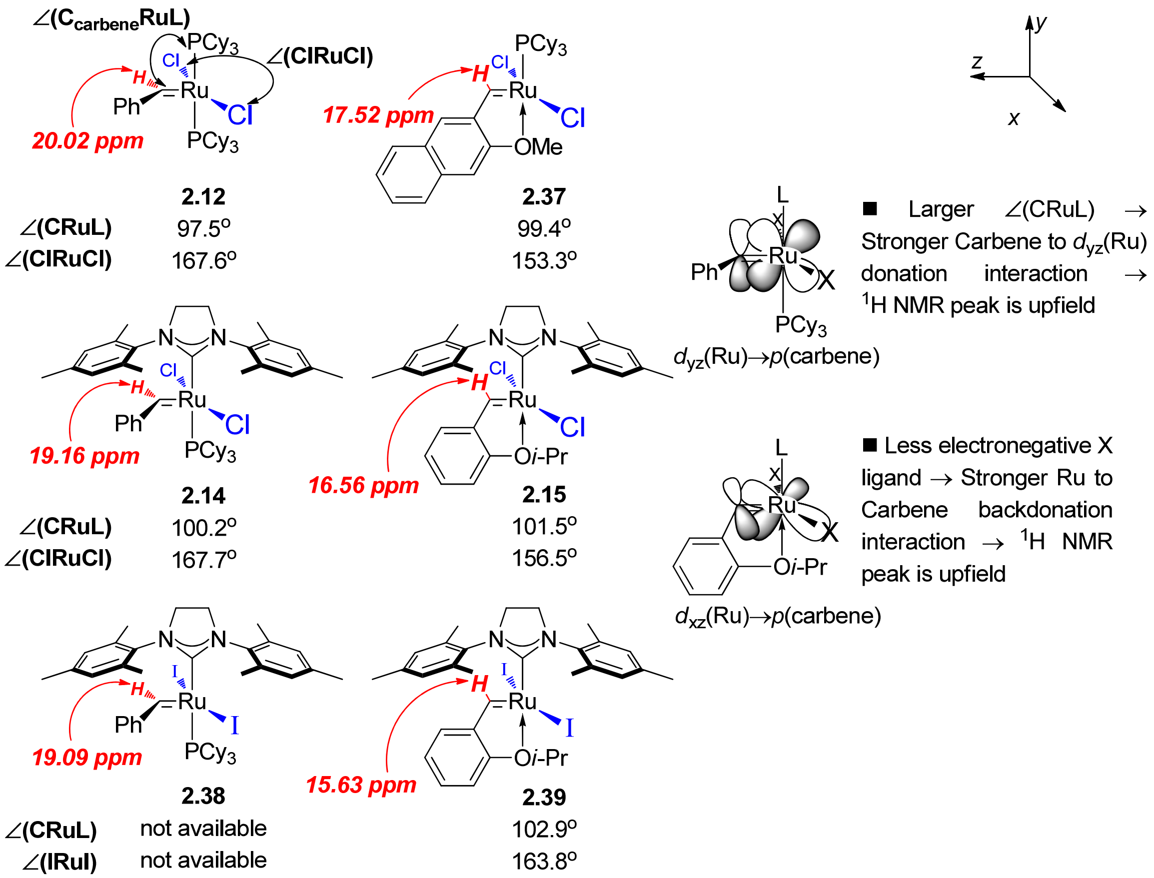

to the fact that the halide ligands are not perpendicular to the carbene carbon atom and instead are distorted such that the X ligands overlap with d_{xz}(Ru) orbital. It can be concluded that the ^{1}H NMR carbene proton chemical shift can be utilized to gauge the degree of backdonation from the d_π orbitals of Ru into the empty p orbital of the carbene carbon: stronger backdonation from Ru to carbene carbon atom results in a more downfield ^{1}H NMR carbene proton chemical shift.

In each orientation of the carbene there is a filled d_π orbital on Ru to backdonate into carbene carbon atom's p(carbene) orbital. The orientation of the empty p(carbene) orbital in complexes **2.12**, **2.14**, and **2.38** is such that it overlaps with d_{yz}(Ru) orbital, which rests in plane of the L (NHC or phosphine) and PCy$_3$ ligands. On the other hand, the p(carbene) orbital in complexes **2.15**, **2.37**, and **2.39** rests in plane of the halide ligands. Thus, the observed dependence of ^{1}H NMR chemical shifts of the carbene protons on the carbene orientation can be understood in light of the nature of ligands coplanar with *p*(carbene). Both NHC and phosphine ligands are π-acidic, whereas the halide ligands can be considered as predominantly σ-donors with a weak π interaction component. Therefore, d_{yz}(Ru) orbital is expected to be less populated due to π-backdonation into the NHC and phosphine ligands.[47] On the other hand d_{xz}(Ru) orbital is more electron rich than d_{yz}(Ru) due to its overlap with the halide ligands, and thus the degree of π-backdonation into *p*(carbene) orbital is greater in complexes **2.15**, **2.37**, and **2.39**, as evidenced by the relatively upfield ^{1}H NMR chemical shift of their carbene protons. As described previously NHC ligands are weaker π-acceptors than phosphines; thus, substitution of PCy_3 for SIMes leads to an upfield chemical shift of the carbene proton (compare complexes **2.14** and **2.12**). Another orbital interaction that should be considered is that between the donating lone pair of the phosphine or NHC and d_{yz}; if the ligand is perpendicular with respect to the carbene carbon atom the donor ligand's lone pair is in the node of the d_{yz}(Ru) orbital, but deformation away from orthogonality (*i.e.* increase in $\angle$CRuL angle) leads to partial overlap between the lone pair and d_{yz}(Ru). As illustrated in Scheme 2.7, deformation away from orthogonality is greater in the case of **2.14** than in **2.13**, thus the relatively upfield ^{1}H NMR chemical shift of the carbene proton in **2.14** is partially due to geometric reasons. On the other hand, the π-accepting orbitals of PCy_3 and SIMes ligands do not overlap with d_{xz}(Ru) and thus the difference between the carbene proton chemical shifts in complexes **2.37** and **2.15** cannot be accounted for by analogy with the complexes **2.13** and **2.14**.[48] Consider NHC-Ru-carbene complexes **2.40** and **2.41** (Scheme 2.7).[49] The ^{1}H NMR chemical shifts of carbene protons in these complexes are close to that in **2.37** and **2.13**; in fact, the relevant chemical shift (18.37 ppm) in **2.41** is downfield of the all other chemical shifts in the series. The difference between complexes **2.40-2.41** and **2.15** is the presence of the aryl ring above the carbene

---

(47) For the discussion addressing the nature of the NHC-metal and phosphine-metal bonding see Chapter 1, section 1.2 of the present dissertation and references therein.

(48) Although it is tempting to assume that NHC ligands are stronger electron donors than phosphines and thus complexes with the former ligand would have a more electron rich Ru center, the present assumption about electron donating ability of the NHC ligands is contrary to the findings described in the preceding chapter (section 1.2).

(49) Complex **2.40**: (a) Vougioukalakis, G. C.; Grubbs, R. H. *J. Am. Chem. Soc.* **2008**, *130*, 2234-2245. Complex **2.41**: (b) Fournier, P. –A.; Savoie, J.; Stenne, B.; Bédard, M.; Grandbois, A.; Collins, S. K. *Chem. Eur. J.* **2008**, *14*, 8690-8695.

proton. Thus, the relative upfield shift of the carbene proton in **2.15** can be attributed to anistropic effect due to the benzene ring of the *N*-substituent of the NHC ligand.

Scheme 2.7. ^{1}H NMR Chemical Shifts of Carbene Protons for Ru Complexes **2.40**-**2.41**

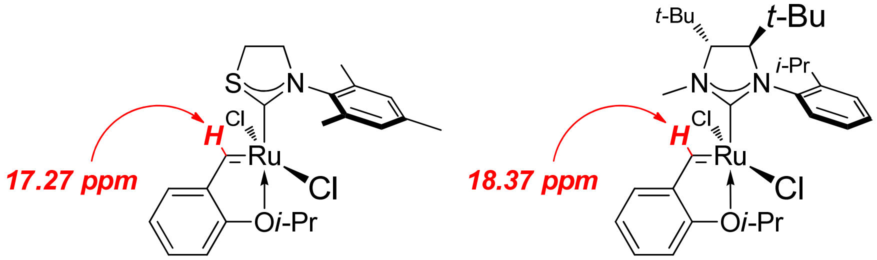

2.40 **2.41**

The key interactions described above will be utilized to analyze the catalytic cycle of Ru-catalyzed olefin metathesis below.

2.1.3.2. Catalytic Cycle of Ru-catalyzed Olefin Metathesis

Since the disclosure of well-defined Ru-based olefin metathesis catalysts **2.12**-**2.15** considerable effort was dedicated to experimental[50] and theoretical[51] studies into the details of the catalytic cycle of Ru-catalyzed olefin metathesis. The catalytic cycle inferred from these studies is shown in Scheme 2.8. The illustrated catalytic cycle is for a degenerate process with a terminal olefin.

The precatalyst **I** initiates through decoordination of the ligand L to afford 14-electron Ru(II) carbene complex **II**, which upon reaction with the terminal olefin

---

(50) Key publications outlining experimental studies addressing the catalytic cycle of Ru-catalyzed olefin metathesis: (a) Dias, E. L.; Nguyen, S. T.; Grubbs, R. H. *J. Am. Chem. Soc.* **1997**, *119*, 3887-3897; (b) Ulman, M.; Grubbs, R. H. *Organometallics* **1998**, *17*, 2484-2489; (c) Adlhart, C.; Hinderling, C.; Baumann, H.; Chen, P. *J. Am. Chem. Soc.* **2000**, *122*, 8204-8214; (d) Adlhart, C.; Volland, M. A. O.; Hofmann, P.; Chen, P. *Helv. Chim. Acta* **2000**, *83*, 3306-3311; (e) Sanford, M. S.; Love, J. A.; Grubbs, R. H. *J. Am. Chem. Soc.* **2001**, *123*, 6543-6554; (f) Volland, M. A. O.; Adlhart, C.; Kiener, C. A.; Chen, P.; Hofmann, P. *Chem. Eur. J.* **2001**, *7*, 4621-4632; (g) Adlhart, C.; Chen, P. *Helv. Chim. Acta* **2003**, *86*, 941-951; (h) Romero, P. E.; Piers, W. E. *J. Am. Chem. Soc.* **2005**, *127*, 5032-5033; (i) Wenzel, A. G.; Grubbs, R. H. *J. Am. Chem. Soc.* **2006**, *128*, 16048-16049; (j) Romero, P. E.; Piers, W. E. *J. Am. Chem. Soc.* **2007**, *129*, 1698-1704; (k) van der Eide, E. F.; Romero, P. E.; Piers, W. E. *J. Am. Chem. Soc.* **2008**, *130*, 4485-4491; (l) van der Eide, E. F.; Piers, W. E. *Nature Chem.* **2010**, *2*, 571-576.

(51) Key publications outlining theoretical studies addressing the catalytic cycle of Ru-catalyzed olefin metathesis: (a) Adlhart, C.; Chen, P. *Angew. Chem. Int. Ed.* **2002**, *41*, 4484-4487; (b) Cavallo, L. *J. Am. Chem. Soc.* **2002**, *124*, 8965-8973; (c) Adlhart, C.; Chen, P. *J. Am. Chem. Soc.* **2004**, *126*, 3496-3510; (d) Occhipinti, G.; Bjørsvik, H. –R.; Jensen, V. R. *J. Am. Chem. Soc.* **2006**, *128*, 6952-6964; (e) Correa, A.; Cavallo, L. *J. Am. Chem. Soc.* **2006**, *128*, 13352-13353; (f) Benitez, D.; Tkatchouk, E.; Goddard, W. A., III *Chem. Commun.* **2008**, 6194-6196; (g) Rowley, C. N.; van der Eide, E. F.; Piers, W. E.; Woo, T. K. *Organometallics* **2008**, *27*, 6043-6045. Ref. 43c is a combined theoretical/experimental study.

$RCH{=}CH_2$ furnishes 16-electron olefin complex **III**. Rotation of the olefin such that its π-system is brought into alignment with the Ru-carbene π-system results in a cycloaddition reaction delivering metalacyclobutane **IV**. For the degenerate process shown (after the first cycle) cycloreversion of complex **IV** constitutes a microscopic reverse of the **III**→**IV** reaction and yields complex **V** which is identical to **III**. Decoordination of the terminal olefin from **V** regenerates 14 electron complex **II**. All reactions in Scheme 2.8 are reversible, and thus thermoneutral olefin metathesis reactions such as cross metathesis over time tend toward thermodynamic equilibrium.

Scheme 2.8. Generic Catalytic Cycle for Ru-Catalyzed Olefin Metathesis

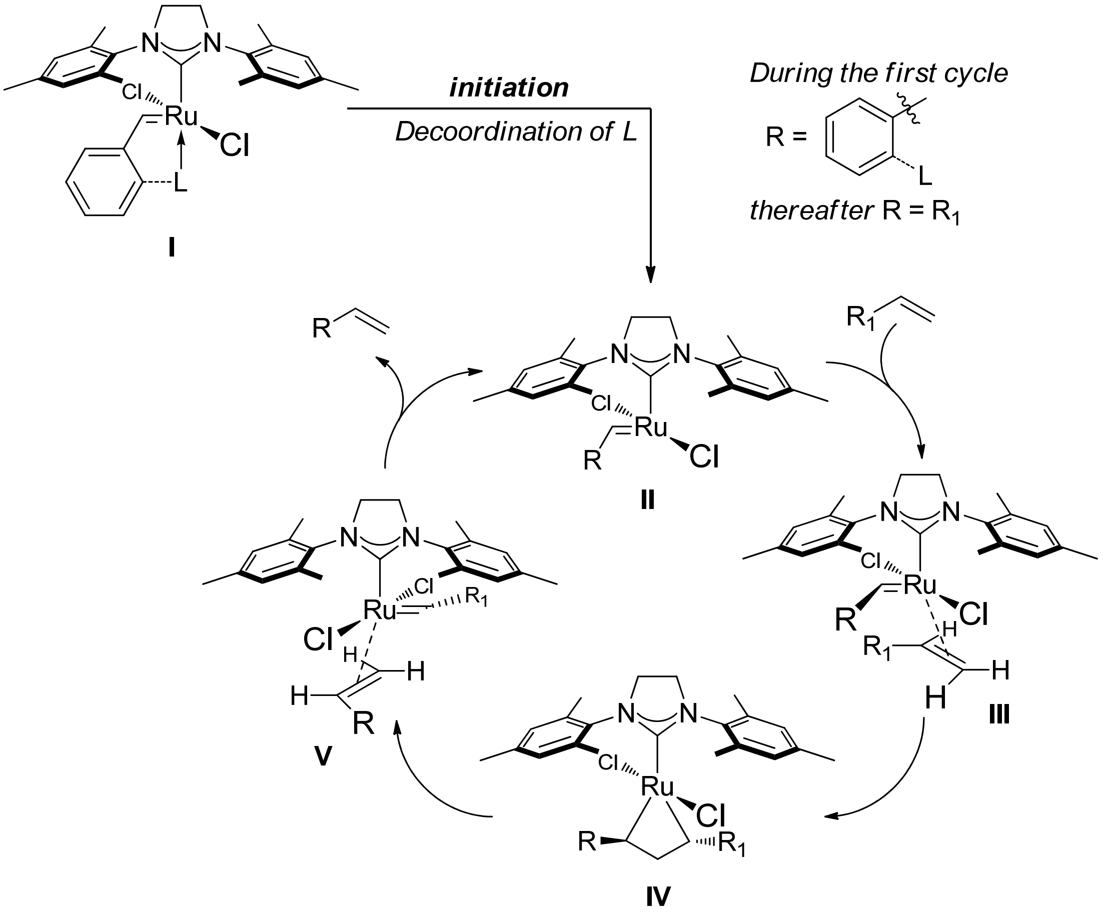

The step **III**→**IV** deserves particular attention. As illustrated above complex **III** is ligated to an olefin, which is not aligned to undergo a [2+2] cycloaddition with Ru carbene. There are four possible conformations for olefin and carbene in complex **III**, among these only one (**IIId**) exhibits correct alignment between Ru-carbene and olefin π-

systems for the cycloaddition to occur (Scheme 2.9). The conformation **IIIa** (inactive olefin orientation) is lowest in energy when R is not proton; however, if R = H, conformation **IIIb** (inactive carbene orientation) is lowest in energy.[52] Inactive carbene orientation is stabilized through the backdonation interaction d_{xz}(Ru)→p(carbene), which as described above is weaker in Ru-chloride complexes than in Ru-iodide complexes, and thus the rate of formation of the active conformer **IIId** is greater with the former complexes than with the latter. Formation of complex **IV** is also more favorable for Ru-chloride complexes, because chloride ligands are weaker *trans*-effect ligands than iodides. Thus, trigonal bipyramidal complex **IV** with two chloride ligands in axial positions is expected to be lower in energy than the corresponding diiodide complex.

Scheme 2.9. Conformation of Complex **III**

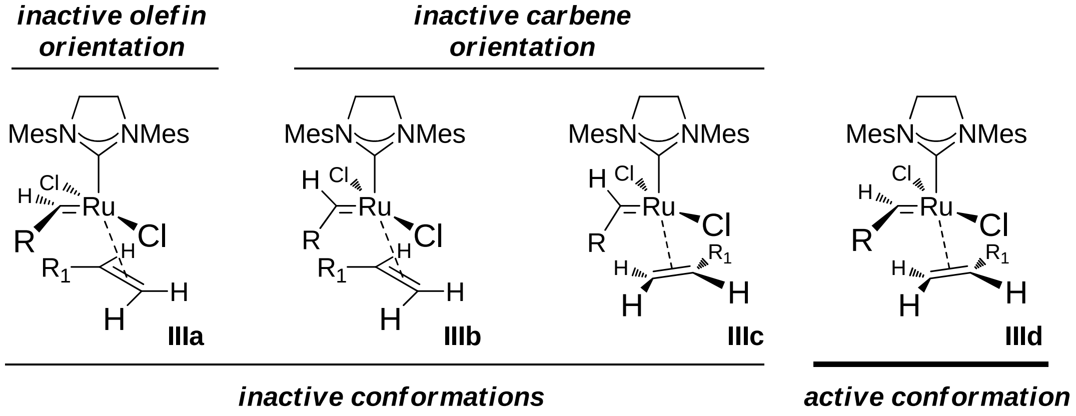

Development of Ru-based catalysts for olefin metathesis has been predominantly focused on facilitating the catalyst initiation,[53] while few attempts have been made at altering the structure of the reactive intermediates.[54] The main causes for the focus of

---

(52) (a) Straub, B. F. *Angew. Chem. Int. Ed.* **2005**, *44*, 5974-5978; (b) Straub, B. F. *Adv. Synth. Catal.* **2007**, *349*, 204-214.

(53) For a recent review on attempts at facilitating the inititation step by means of structural modifications to the benzylidene ligand see: Diesendruck, C. E.; Tzur, E.; Lemcoff, N. G. *Eur. J. Inorg. Chem.* **2009**, 4185-4203.

(54) Main areas of catalyst structure modification were concerned with changes to the NHC structure: (a) Ritter, T.; Day, M. W.; Grubbs, R. H. *J. Am. Chem. Soc.* **2006**, *128*, 11768-11769; (b) Berlin, J. M.; Campbell, K.; Ritter, T.; Funk, T. W.; Chlenov, A.; Grubbs, R. H. *Org. Lett.* **2007**, *9*, 1339-1342; (c) Stewart, I. C.; Douglas, C. J.; Grubbs, R. H. *Org. Lett.* **2008**, *10*, 441-444; (d) Ref. 48a. Other catalyst structure modifications involved changes to the X ligands: (e) Krause, J. O.; Wurst, K.; Buchmeiser, M. R. *Chem. Eur. J.* **2004**, *10*, 777-784; (f) Halbach, T. S.; Mix, D.; Fischer, D.; Maechling, S.; Krause, J. O.;

catalyst development research on the initiation step are as follows: (1) among the ligands on Ru center in Ru-based olefin metathesis catalysts the carbene ligand is most easily modifiable, (2) the stereoelectronic effects of structural changes to the carbene ligand are well-understood and are generally predictable, (3) the rate of Ru-catalyst initiation was found to be slower than the rate of propagation steps in cases where the rate comparison studies were carried out.[55]

2.1.3.3. Initiation of Ru-based Olefin Metathesis Catalysts

Studies of catalyst initiation shed light on the mechanism of Ru-catalyzed olefin metathesis. Although, it is generally observed that NHC bearing complexes **2.14** and **2.15** are more active catalysts than their phosphine congeners **2.12** and **2.13**, the rate of initiation of the NHC-Ru complexes was found to be slower than that of the phosphine-Ru complexes, indicating that the propagation steps in the catalytic cycle involving NHC-Ru complexes are faster than those involving phosphine-Ru complexes. This observation was unexpected, as the original intent of designing complex **2.14** was to employ a stronger *trans*-effect ligand to facilitate decoordination of the PCy_3 ligand and thus the rate of catalyst initiation.[56] Investigation of near-edge region of Ru K-edge *X*-Ray absorption spectra (XAS) of complexes **2.12** and **2.14** indicated that Ru center is more electron rich in the former than in the latter complex.[57] Thus, in concert with experimental observation phosphine decoordination would be expected to be more facile in the case of complex **2.12**. Indeed, this observation is consistent with NHC ligands being less electron donating than phosphines. Furthermore, π-backdonation constitutes a larger share of metal-phosphine bonding energy than of metal-NHC bonding energy,[58] and thus ligand bonding energy is lower for a phosphine within a complex, in which said

---

Sievers, C.; Blechert, S.; Nuyken, O.; Buchmeiser, M. R. *J. Org. Chem.* **2005**, *70*, 4687-4694; (g) Ref. 43; (h) Ref. 26.

(55) (a) Sanford, M. S.; Ulman, M.; Grubbs, R. H. *J. Am. Chem. Soc.* **2001**, *123*, 749-750; (b) Ref. 50a; (c) Ref. 50e.

(56) Grubbs and co-workers, relying on the Tolman electronic parameters for NHC and phosphine ligands, assumed that NHC ligands are stronger donors and thus stronger *trans*-effect ligands. For the discussion regarding the electron donating abilities of NHC and phosphine ligands see Chapter 1 (section 1.2).

(57) Getty, K.; Delgado-Jaime, M. U.; Kennepohl, P. *J. Am. Chem. Soc.* **2007**, *129*, 15774-15776.

(58) Tonner, R.; Heydenrych, G.; Frenking, G. *Chem. Asian J.* **2007**, *2*, 1555-1567.

phosphine is coordinated to a metal bearing more π-acidic ligands. In other words, phosphine decoordination is more facile for complexes in which stronger π-acidic ligands are present. Grubbs and co-workers rationalized the enhanced relative to **2.12** catalytic activitiy of **2.14** by considering the steps downstream to phosphine decoordination, indicating that olefin affinity of the NHC-Ru complexes is higher than that of the phosphine-Ru complexes; there is a 4 orders of magnitude increase in favoring reaction **II→III** over coordination of a phosphine for complex **2.14** relative to complex **2.12**.[50e] In concert with the results of Grubbs and co-workers, Chen and co-workers explained the enhanced catalytic activities of NHC-Ru complexes over those of phosphine-Ru complexes by invoking the concept of commitment (Figure 2.2).[50g] Despite higher activation barrier for catalyst initiation complex **2.14** exhibits higher commitment to the product forming steps than complex **2.12**.

Figure 2.2. High *vs* Low Commitment Reaction Coordinates

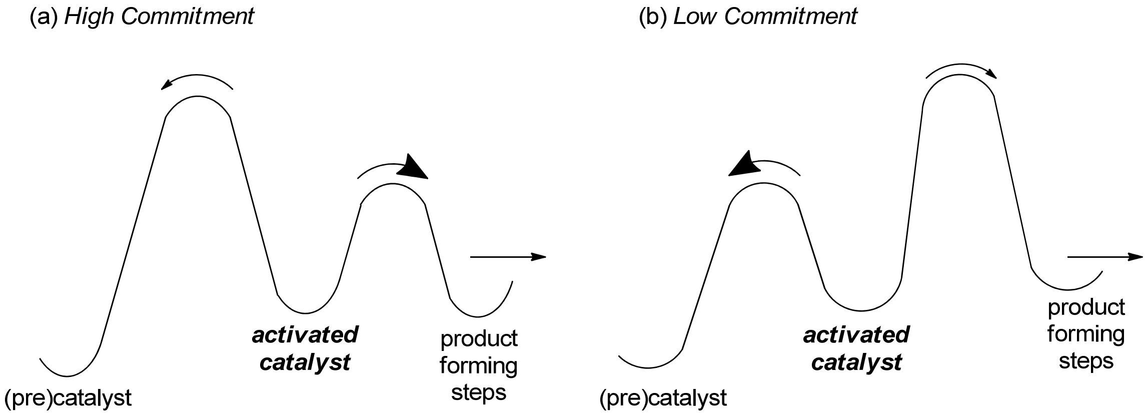

2.1.3.4. Kinetic Details of the Catalytic Cycle of Ru-catalyzed Olefin Metathesis

As described above the catalytic cycle for Ru-catalyzed olefin metathesis consists of 4 steps (Scheme 2.8): (1) olefin coordination (**II→III**); (2) cycloaddition (**III→IV**); (3) cycloreversion (**IV→V**); (4) olefin decoordination (**V→II**). Computational investigation of these steps is challenging due to the fact that olefin coordination and decoordination steps are not handled correctly by a majority of currently available density functional, because significant changes in dispersive forces are not properly accounted for. For example, the popular B3LYP[59] density functional predicts that olefin coordination is endothermic, which is inconsistent with experiments.[51f] However, Zhao and Truhlar developed M06 suite of density functionals, which are corrected for medium-range correlations, thereby leading to improved treatment of dispersive forces.[60] Predictive ability of these density functionals in Ru-catalyzed olefin metathesis was confirmed experimentally by Chen and co-workers and computationally by Zhao and Truhlar.[61] Thus, the discussion below will only refer to computational investigations that were carried out with M06 density functional.[62]

Here, it is important to make a distinction between thermoneutral and exothermic olefin metathesis reactions. The enthalpy difference between starting materials and products in thermoneutral olefin metathesis is close to zero, *i.e.* there is no *enthalpic* driving force; for example, olefin cross metathesis and olefin ring-closing metathesis reactions are generally thermoneutral. Ring-opening olefin metathesis reactions of strained cyclic molecules are generally exothermic, *i.e.* ring strain is the source of thermal driving force for the reaction.

Most of the computational studies (with M06 density functional) were carried out on the thermoneutral olefin metathesis reactions, particularly, on basic cross metathesis reactions. The key study of cross-metathesis reaction in Scheme 2.10 by Goddard and co-workers indicated that the rate-determining step is product decoordination (**V→II**). All other steps within the catalytic cycle were found to be 5.2-5.8 kcal/mol lower in energy (ΔH with self-consistent Poisson-Boltzmann continuum solvation model,[63] CH_2Cl_2 was

---

(59) Becke, A. D. *J. Chem. Phys.* **1993**, *98*, 5648-5652.

(60) (a) Zhao, Y.; Truhlar, D. G. *J. Chem. Phys.* **2006**, *125*, 194101; (b) Zhao, Y.; Truhlar, D. G. *Theor. Chem. Acc.* **2008**, *120*, 215-241; (c) Zhao, Y.; Truhlar, D. G. *Acc. Chem. Res.* **2008**, *41*, 157-167.

(61) Chen and co-workers found that phosphine decoordination energy (bond dissociation energy) in complex **2.14** was 40.2 kcal/mol. The calculated phosphine-Ru bond dissociation energy was found to be 40.3 kcal/mol. (a) Torker, S.; Merki, D.; Chen, P. *J. Am. Chem. Soc.* **2008**, *130*, 4808-4814; (b) Zhao, Y.; Truhlar, D. G. *J. Chem. Theory Comput.* **2009**, *5*, 324-333.

(62) Due to the size of the fully elaborated Ru complexes no computational studies have been done with correlated wavefunction methods (*e.g.* Møller-Plesset, QCISD, CCSD, etc.) with the exception of model studies in Ref. 61b. It should be noted that the computational studies on Ru-catalyzed olefin metathesis with M06 density functional appeared after the studies outlined in section 2.2 were carried out. The importance of these theoretical studies and experimental work in Ref. 50l will become apparent in section 2.2.

(63) Tomasi, J.; Mennucci, B.; Cammi, R. *Chem. Rev.* **2005**, *105*, 2999-3093.

employed as a solvent).[51f] Furthermore, it was found that an alternative pathway, in which metalacyclobutane is formed *syn* with respect to the NHC ligand is higher in energy by 5.5-6.5 kcal/mol than the pathway shown in Scheme 2.8.

Scheme 2.10. Theoretically Investigated Cross Metathesis Reactions

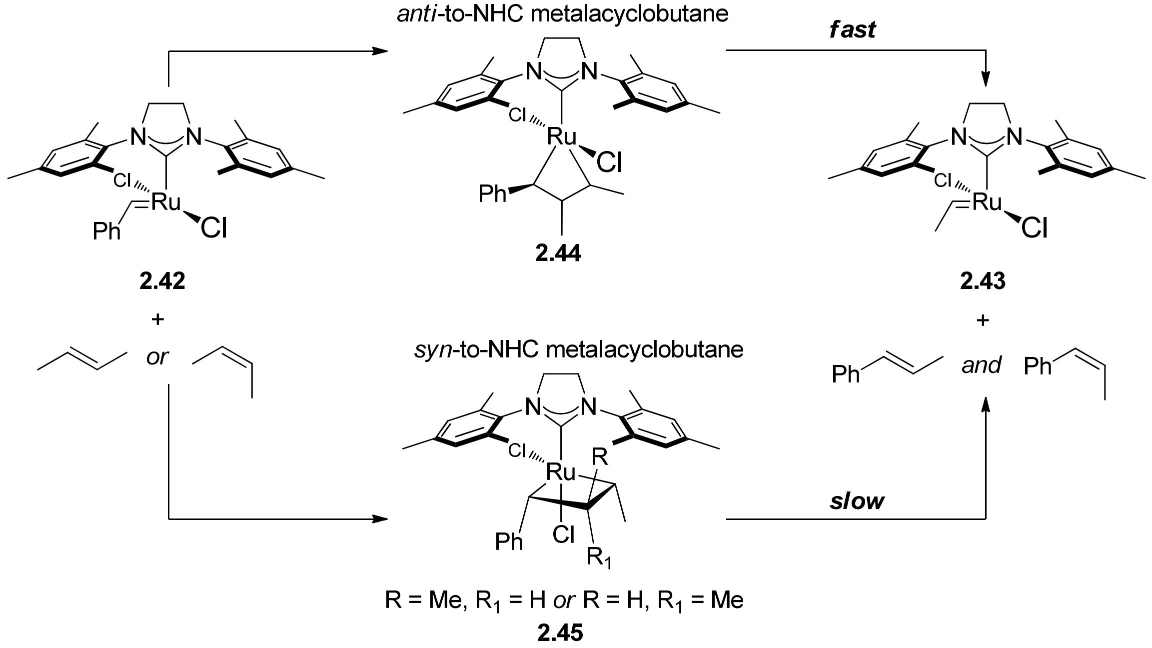

In concert with the computational studies described above, Piers and co-workers experimentally established that in thermoneutral olefin metathesis reactions (ring-closing olefin metathesis) the rate determining step is product decoordination (**V**→**II**).[50l]

2.1.4. Stereoselective Olefin Metathesis

Stereoselective catalytic olefin metathesis has been the subject of numerous investigations over the past three decades. The most obvious stereochemical property that can be determined through olefin metathesis is *E*:*Z* selectivity of the resulting olefin (Scheme 2.11).[64] However, aside from planar stereogenicity it is not immediately obvious how central stereogenicity can be controlled through stereoselective (enantioselective) olefin metathesis, as no tetrahedral carbon centers are formed or destroyed in the course

---

(64) *E*/*Z* Selectivities in catalytic olefin metathesis have been the subject of investigation for the past three decades. For discussions concerning *E*/*Z* selectivities in catalytic olefin metathesis see: (a) Katz, T. J.; Hersh, W. H. *Tetrahedron Lett.* **1977**, *6*, 585-588; (b) Ref. 16a; (c) Tallarico, J. A.; Randall, M. L.; Snapper, M. L. *Tetrahedron* **1997**, *53*, 16511-16520; (d) Ritter, T.; Hejl, A.; Wenzel, A. G.; Funk, T. W.; Grubbs, R. H. *Organometallics* **2006**, *25*, 5740-5745; (e) Ref. 19b; (f) Ref. 19d.

of the reaction. As illustrated in Scheme 2.11 stereogenicity of can be controlled through either a desymmetrization process or a kinetic resolution.

Scheme 2.11. Catalytic Stereoselective Olefin Metathesis

(a) *Control of E/Z Selectivity of the Product Olefin*

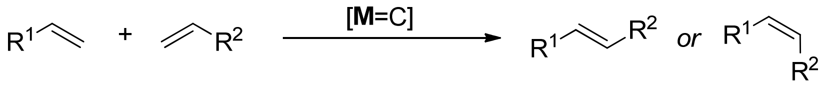

(b) *Control of Planar Stereogenicity in Catalytic Olefin Metathesis*

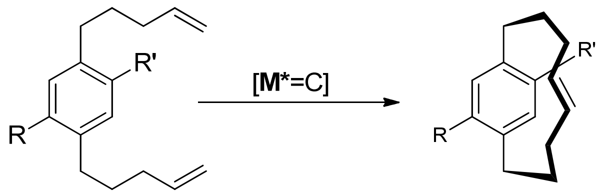

(c) *Kinetic Resolution of Racemic Chiral Substrates*

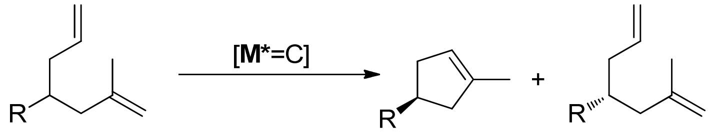

(d) *Desymmetrization of Substrates Bearing Enantiotopic sp²-Carbon Atoms*

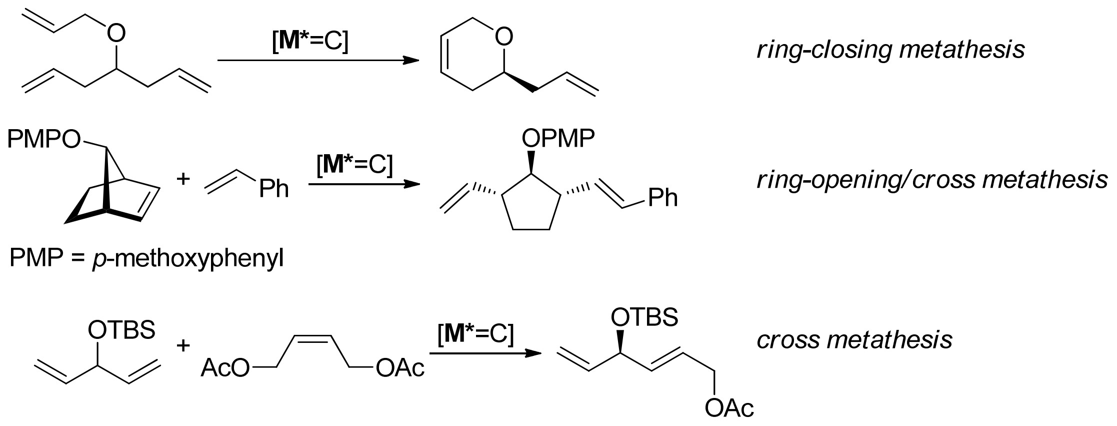

2.1.4.1. *Enantioselective Olefin Metathesis*

The first report on chiral well-defined olefin metathesis catalyst **2.46** (Scheme 2.12), in which enantioselective olefin metathesis of small molecules was proposed as feasible, was that of Schrock and co-workers.[65] However, it was not until Grubbs and co-

---

(65) McConville, D. H.; Wolf, J. R.; Schrock, R. R. *J. Am. Chem. Soc.* **1993**, *115*, 4413-4414.

workers reported the first example of kinetic resolution through Mo-catalyzed enantioselective ring-closing metathesis; however, k_{rel} values[66] were poor ($k_{rel} \leq 2.06$).[67] Shortly thereafter our group reported an efficient version of the above kinetic resolution protocol.[68] Fundamental limitation of kinetic resolution, however, is the fact that the

Scheme 2.12. Chiral Well-Defined Olefin Metathesis Catalysts

Chiral Mo-Based Olefin Metathesis Catalysts

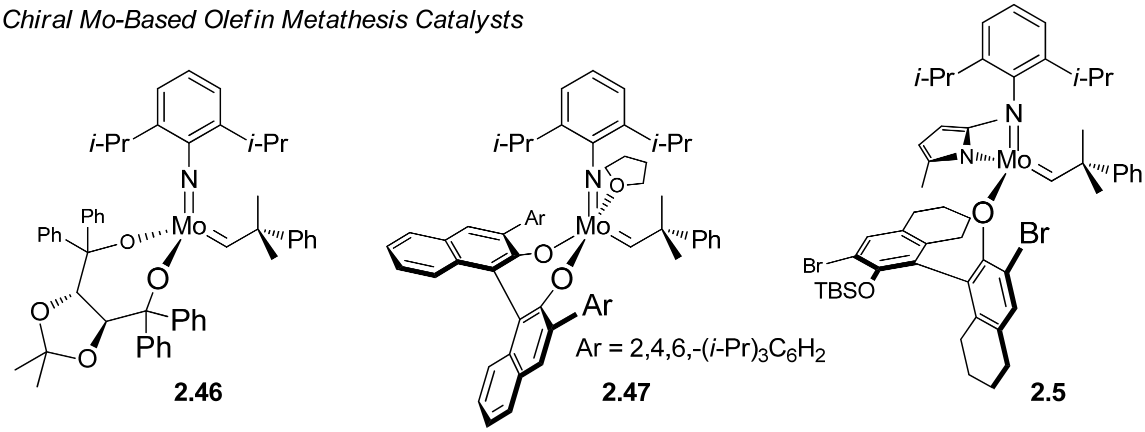

Chiral Ru-Based Olefin Metathesis Catalysts

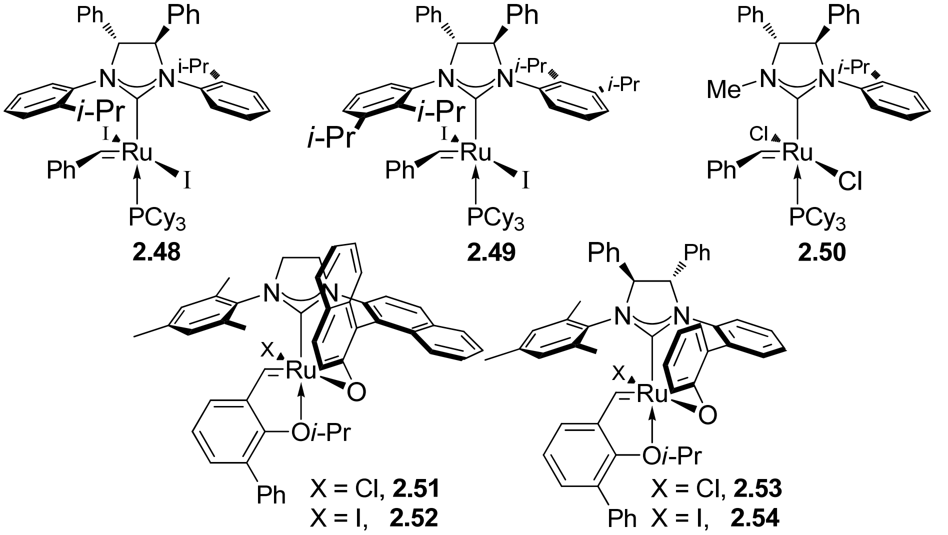

---

(66) The ratio of favored to unfavored rate constants for enantiodetermining step can be calculated from the formula $k_{rel} = \frac{\ln(1-C)(1-ee)}{\ln(1-C)(1+ee)}$, where C = conversion of starting material and *ee* = enantiomeric excess of the remaining starting material. See: Balavoine, G.; Moradpour, A.; Kagan, H. B. *J. Am. Chem. Soc.* **1974**, *96*, 5152-5158.

(67) (a) Fujimura, O.; Grubbs, R. H. *J. Am. Chem. Soc.* **1996**, *118*, 2499-2500; (b) Fujimura, O.; Grubbs, R. H. *J. Org. Chem.* **1998**, *63*, 824-832.

(68) Alexander, J. B.; La, D. S.; Cefalo, D. R.; Hoveyda, A. H.; Schrock, R. R. *J. Am. Chem. Soc.* **1998**, *120*, 4041-4042.

maximum possible yield of a desired compound is 50%, and thus following the aforementioned promising results our group and others pursued desymmetrization reactions as described below. Many chiral Mo-based and Ru-based olefin metathesis catalysts (for representative examples see Scheme 2.12)[69] were designed and prepared to meet the needs of enantioselective olefin metathesis method development.

Perhaps the most developed class of enantioselective olefin metathesis reactions falls into the category of exothermic olefin metathesis reactions (Scheme 2.13). Within enantioselective ring-opening cross metathesis the enantiodetermining step occurs in the exothermic region of the mechanism, and the following thermoneutral cross-metathesis

Scheme 2.13. Enantioselective Ring-Opening Olefin Metathesis

(a) Enantioselective Ring-Opening/Ring-Closing Olefin Metathesis

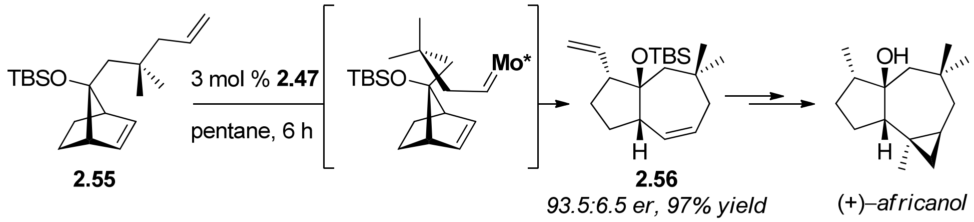

(b) Enantioselective Ring-Opening/Cross Olefin Metathesis

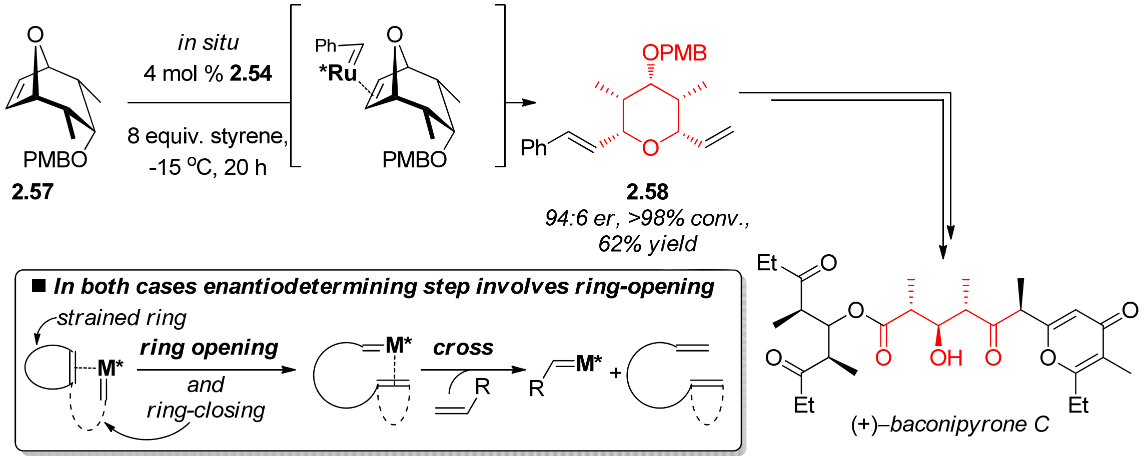

---

(69) For a review summarizing Mo-diolate olefin metathesis catalysts prepared before 2003 see Ref. 1c. For monoalkoxide monopyrrolide Mo alkylidene complexes related to **2.5** see Ref. 19. Complex **2.48**: (a) Seiders, T. J.; Ward, D. W.; Grubbs, R. H. *Org. Lett.* **2001**, *3*, 3225-3228. Complex **2.49**: (b) Funk, T. W.; Berlin, J. M.; Grubbs, R. H. *J. Am. Chem. Soc.* **2006**, *128*, 1840-1846. Complex **2.50**: (c) Fournier, P. –A.; Collins, S. K. *Organometallics* **2007**, *26*, 2945-2949. Complex **2.51**: (d) Van Veldhuizen, J. J.; Gillingham, D. G.; Garber, S. B.; Kataoka, O.; Hoveyda, A. H. *J. Am. Chem. Soc.* **2003**, *125*, 12502-12508. Complex **2.52**: (e) Gillingham, D. G.; Kataoka, O.; Garber, S. B.; Hoveyda, A. H. *J. Am. Chem. Soc.* **2004**, *126*, 12288-12290. Complexes **2.53** and **2.54**: (f) Van Veldhuizen, J. J.; Campbell, J. E.; Giudici, R. E.; Hoveyda, A. H. *J. Am. Chem. Soc.* **2005**, *127*, 6877-6882.

reaction is not enantiodetermining.[70] The utility of Mo- and Ru-catalyzed enantioselective ring-opening/cross metathesis was demonstrated by the total syntheses of (+)–africanol and (+)–baconipyrone.[71] In both syntheses the core of each natural product is constructed efficiently through enantioselective olefin metathesis, which in a single step sets absolute stereochemical identity of three stereogenic centers found within the final products.

In spite of the evident power of ring-opening olefin metathesis that was demonstrated above, the most widely used versions of catalytic olefin metathesis are thermoneutral: ring-closing metathesis and cross metathesis.[10] Enantioselective variants of thermoneutral catalytic olefin metathesis are not as well developed;[72] although, many

---

(70) For examples of Mo-catalyzed enantioselective ring-opening metathesis desymmetrizations see: (a) La, D. S.; Ford, J. G.; Sattely, E. S.; Bonitatebus, P. J.; Schrock, R. R.; Hoveyda, A. H. *J. Am. Chem. Soc.* **1999**, *121*, 11603-11604; (b) Weatherhead, G. S.; Ford, J. G.; Alexanian, E. J.; Schrock, R. R.; Hoveyda, A. H. *J. Am. Chem. Soc.* **2000**, *122*, 1828-1829; (c) La, D. S.; Sattely, E. S.; Ford, J. G.; Schrock, R. R.; Hoveyda, A. H. *J. Am. Chem. Soc.* **2001**, *123*, 7767-7778; (d) Cefalo, D. R.; Kiely, A. F.; Wuchrer, M.; Jamieson, J. Y.; Schrock, R. R.; Hoveyda, A. H. *J. Am. Chem. Soc.* **2001**, *123*, 3139-3140; (e) Ref. 71a; (f) Ref. 19d; (g) Cortez, G. A.; Schrock, R. R.; Hoveyda, A. H. *Angew. Chem. Int. Ed.* **2007**, *46*, 4534-4538. For examples of Ru-catalyzed enantioselective ring-opening metathesis desymmetrizations see: (h) Van Veldhuizen, J. J.; Garber, S. B.; Kingsbury, J. S.; Hoveyda, A. H. *J. Am. Chem. Soc.* **2002**, *124*, 4954-4955; (i) Refs. 69d-f; (j) Berlin, J. M.; Goldberg, S. D.; Grubbs, R. H. *Angew. Chem. Int. Ed.* **2006**, *45*, 7591-7595; (k) Maison, W.; Büchert, M.; Deppermann, N. *Beilstein J. Org. Chem.* **2007**, *3*, doi: 10.1186/1860-5397-3-48. For a comparative study of Mo- and Ru-catalyzed enantioselective ring-opening/cross metathesis see: (l) Cortez, G. A.; Baxter, C. A.; Schrock, R. R.; Hoveyda, A. H. *Org. Lett.* **2007**, *9*, 2871-2874.

(71) Total synthesis of (+)–africanol: (a) Weatherhead, G. S.; Cortez, G. A.; Schrock, R. R.; Hoveyda, A. H. *Proc. Nat. Acad. Sci.* **2004**, *101*, 5805-5809. Total synthesis of (+)–baconipyrone: (b) Gillingham, D. G.; Hoveyda, A. H. *Angew. Chem. Int. Ed.* **2007**, *46*, 3860-3864.

(72) For examples of Mo-catalyzed enantioselective ring-closing metathesis desymmetrizations see: (a) La, D. S.; Alexander, J. B.; Cefalo, D. R.; Graf, D. D.; Hoveyda, A. H.; Schrock, R. R. *J. Am. Chem. Soc.* **1998**, *120*, 9720-9721; (b) Zhu, S. S.; Cefalo, D. R.; La, D. S.; Jamieson, J. Y.; Davis, W. M.; Hoveyda, A. H.; Schrock, R. R. *J. Am. Chem. Soc.* **1999**, *121*, 8251-8259; (c) Burke, S. D.; Müller, N.; Beaudry, C. M. *Org. Lett.* **1999**, *1*, 1827-1829; (d) Dolman, S. J.; Sattely, E. S.; Hoveyda, A. H.; Schrock, R. R. *J. Am. Chem. Soc.* **2002**, *124*, 6991-6997; (e) Kiely, A. F.; Jernelius, J. A.; Schrock, R. R.; Hoveyda, A. H. *J. Am. Chem. Soc.* **2002**, *124*, 2868-2869; (f) Dolman, S. J.; Schrock, R. R.; Hoveyda, A. H. *Org. Lett.* **2003**, *5*, 4899-4902; (g) Sattely, E. S.; Cortez, G. A.; Moebius, D. C.; Schrock, R. R.; Hoveyda, A. H. *J. Am. Chem. Soc.* **2005**, *127*, 8526-8533; (h) Lee, A. –L.; Malcolmson, S. J.; Puglisi, A.; Schrock, R. R.; Hoveyda, A. H. *J. Am. Chem. Soc.* **2006**, *128*, 5153-5157; (i) Ref. 19a; (j) 19c; (k) Harvey, J. S.; Malcolmson, S. J.; Dunne, K. S.; Meek, S. J.; Thompson, A. L.; Schrock, R. R.; Hoveyda, A. H.; Gouverneur, V. *Angew. Chem. Int. Ed.* **2009**, *48*, 762-766. For examples of Ru-catalyzed enantioselective ring-closing metathesis see: (l) Ref. 69a-d; (m) Ref. 49b; (n) Savoie, J.; Stenne, B.; Collins, S. K. *Adv. Synth. Catal.* **2009**, *351*, 1826-2832; (o) Stenne, B.; Timperio, J.; Savoie, J.; Dudding, T.; Collins, S. K. *Org. Lett.* **2010**, *12*, 2032-2035. For examples of ring-closing metathesis reactions, in which planar and axial stereogenicity is controlled see: (p) Ogasawara, M.; Watanabe, S.; Fan, L.; Nakajima, K.; Takahashi, T. *Organometallics* **2006**, *25*, 5201-5203; (q) Grandbois, A.; Collins, S. K. *Chem. Eur. J.* **2008**, *14*, 9323-9329.

Mo-catalyzed enantioselective ring-closing metathesis protocols (Scheme 2.14) were developed no methods involving enantioselective cross metathesis were reported to date.[72a-k,p]

Scheme 2.14. Mo-Catalyzed Enantioselective Ring-Closing Olefin Metathesis

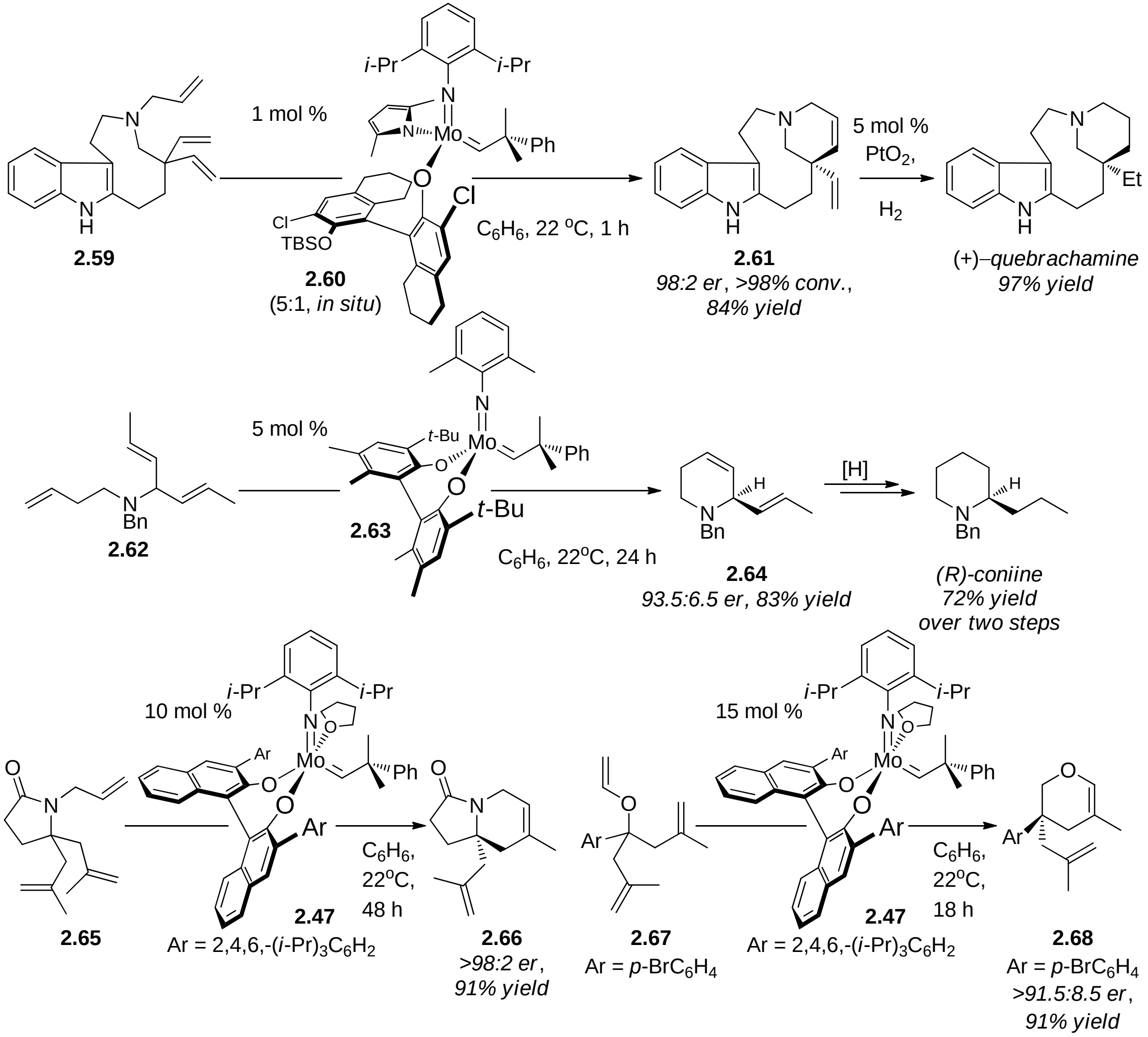

As shown in Scheme 2.14, Mo-catalyzed enantioselective ring-closing metathesis protocols involving desymmetrizations of terminal olefins,[19a,72a,72g] 1,2-disubstituted and 1,1-disubstituted olefins were developed.[72] Efficiency of Mo-catalyzed enantioselective ring-closing metathesis is generally very high; however, there are limitations in cases where proximal Lewis-basic moieties are present (**2.65→2.66**) and in the presence of enol ethers (**2.67→2.68**). Furthermore, sensitivity of the alkylidene group to acidic protons and molecular oxygen limits the applicability of the catalytic processes. Thus, development of Ru-catalyzed olefin metathesis protocols is important for biological applications in aqueous media.[73] However, Ru-catalyzed enantioselective ring-closing

Scheme 2.15. Thermoneutral Ru-Catalyzed Enantioselective Olefin Metathesis

(a) *Ru-Catalyzed Enantioselective Ring-Closing Metathesis*

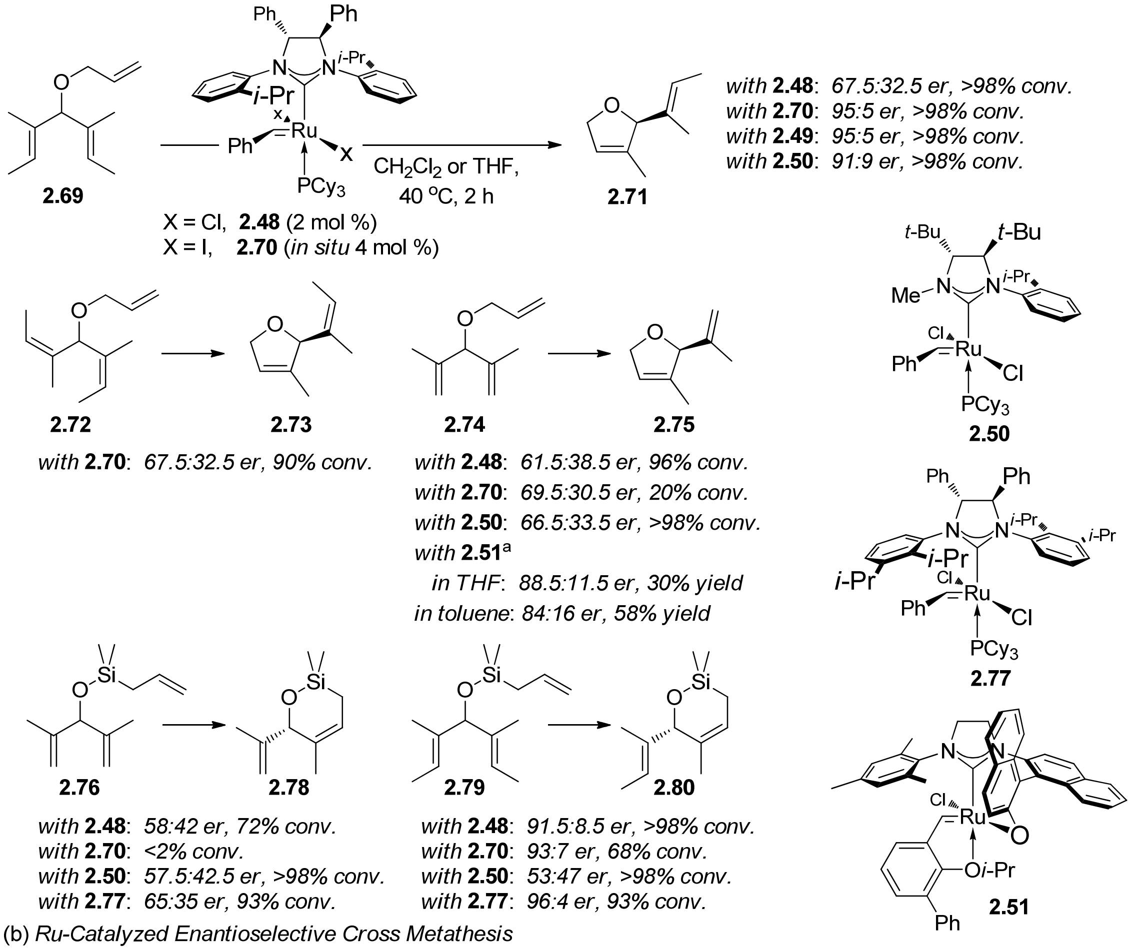

(b) *Ru-Catalyzed Enantioselective Cross Metathesis*

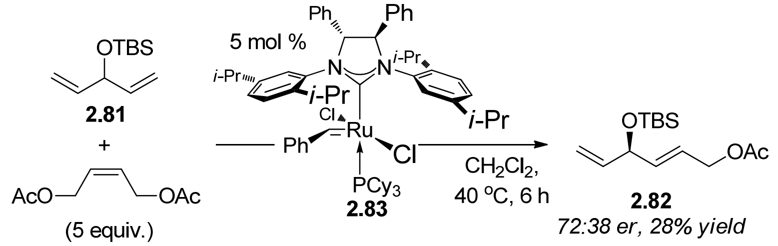

[a] Conditions for enantioselective RCM reactions with **2.51**: 5 mol % catalyst, solvent, 60 °C, 24 h.

---

(73) For a review on catalytic olefin metathesis in aqueous media see: (a) Burtscher, D.; Grela, K. *Angew. Chem. Int. Ed.* **2009**, *48*, 442-454. For examples of biological applications of olefin metathesis see: (b) Lin, Y. A.; Chalker, J. M.; Floyd, N.; Bernardes, G. J. L.; Davis, B. G. *J. Am. Chem. Soc.* **2008**, *130*, 9642-9643; (b) Lin, Y. A.; Chalker, J. M.; Davis, B. G. *J. Am. Chem. Soc.* **2010**, *132*, 16805-16811.

metathesis remains in its infancy despite a decade of intense research in this area (Scheme 2.15),[72l-o,q] and only a single instance of a very inefficient Ru-catalyzed cross metathesis was reported.[70j]

As shown in Scheme 2.15, Ru-catalyzed enantioselective ring-closing metathesis necessitates desymmetrization of trisubstituted olefins (compare **2.69→2.71** to **2.74→2.75**).[69a-d] Furthermore, the substitution pattern of the desymmetrized trisubstituted olefins is important for enantioselectivity (compare **2.69→2.71** to **2.72→2.73**).[69a] However, desymmetrization of 1,1-disubstituted olefins proved to be most enantioselective if catalyzed by the stereogenic-at-Ru complex **2.51** (**2.74→2.75**); the yields for the reaction are relatively low due to volatility of the desired product and in the case of THF formation of a substrate dimer **2.84**, which was isolated in 30% yield. It is worth noting that Mo-catalyzed transformations involving trisubstituted olefins surpass Ru-catalyzed protocols in the reaction efficiency, for example, the reaction **2.69** undergoes RCM in the presence of 1 mol % **2.63** to give **2.71** after 5 min in 93% yield and >98:2 er.[72a]

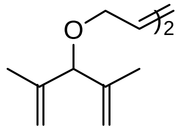

2.84

A pronounced effect due to the catalyst structure was observed for halide ligands; in most cases iodide ligands proved to render Ru-catalyzed processes more enantioselective than those with catalysts bearing chloride ligands (Scheme 2.15).[74] However, such an increase in enantioselectivities comes at the expense of reactivities; in certain cases no reaction is observed with Ru-iodide catalysts (for example, **2.76→2.78**).

Variation of other parameters of the reaction conditions such as temperature and reactive media proved to be inconsequential to enantioselectivities; however, reactivity of Ru catalysts proved to be sensitive to the temperature of the reaction medium.[69b]

The modified version of the selectivity model originally proposed by Grubbs and co-workers is depicted in Scheme 2.16.[69b] Upon initiation of the complex **2.70** the 14-electron species **2.85** and **2.88** are formed. These complexes can coordinate a diastereotopic olefin either *trans* or *cis* to the NHC ligand. In both *cis* complexes **2.89**

---

[74] The halide ligand effect in Ru-catalyzed enantioselective ring-closing metathesis was studied computationally in: Costabille, C.; Cavallo, L. *J. Am. Chem. Soc.* **2004**, *126*, 9592-9600.

Scheme 2.16. Enantioselectivity Model of Ru-catalyzed Enantioselective Ring Closing Metathesis with **2.70**

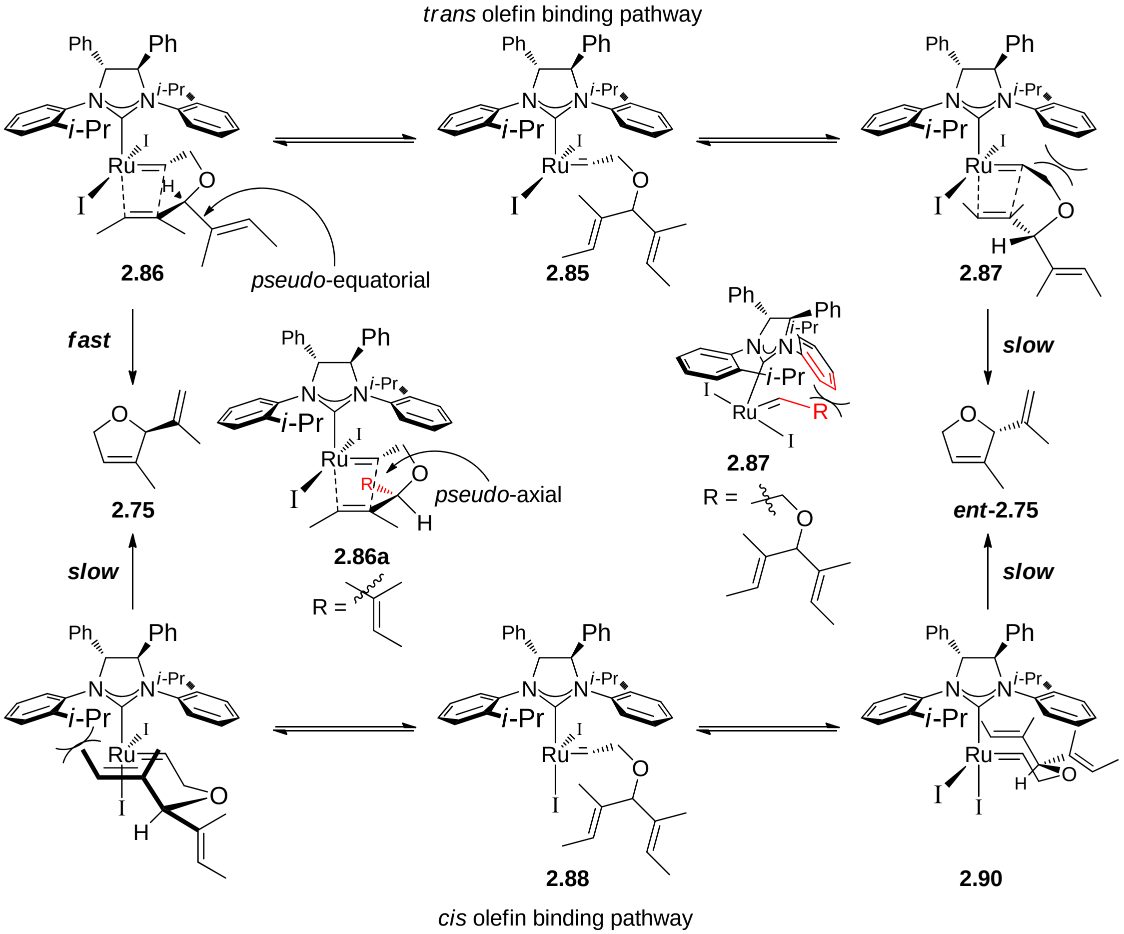

and **2.90** the terminal methyl group of the 2-butenyl moiety will interact with the *N*-aryl groups of the NHC ligands as shown, thereby preventing productive cycloreversion of *cis*-metalacyclobutanes generated from **2.89** and **2.90**. Thus, it is reasonable to assume that the reaction will proceed solely through the *trans* olefin binding pathway shown in Scheme 2.16. Within the *trans* olefin binding pathway there are two possible carbene rotormers **2.86** and **2.87**. The latter is disfavored through the steric interaction between the methylene group of the carbene substituent and the edge of the *N*-aryl substituent of the NHC ligand. Thus, the preferred mode of coordination is signified by the structure **2.86**. Differentiation between the diastereotopic butenyl groups can be seen through comparison of the structures **2.86** and **2.86a**. In the latter the diastereotopic butenyl group occupies *pseudo*-axial position within the forming five-member ring, whereas in the former the butenyl group is *pseudo*-equatorial. Therefore, the pathway through **2.86** is preferred as others have been ruled out.

In the absence of the terminal methyl group the *cis* olefin binding pathway may be operative (through intermediates related to **2.89** and **2.90**). Indeed, Ru-catalyzed enantioselective RCM reactions of both **2.72** and **2.74** proceed with low levels of enantioselectivity; in both cases the diastereotopic olefin that binds Ru center orients a proton towards the NHC ligand (**2.89a-b** and **2.90a-b**) instead of the methyl group in the case of **2.69** (intermediates **2.89** and **2.90**).

Scheme 2.17. Enantiodetermining Intermediates in RCM of **2.69**, **2.72**, and **2.74**

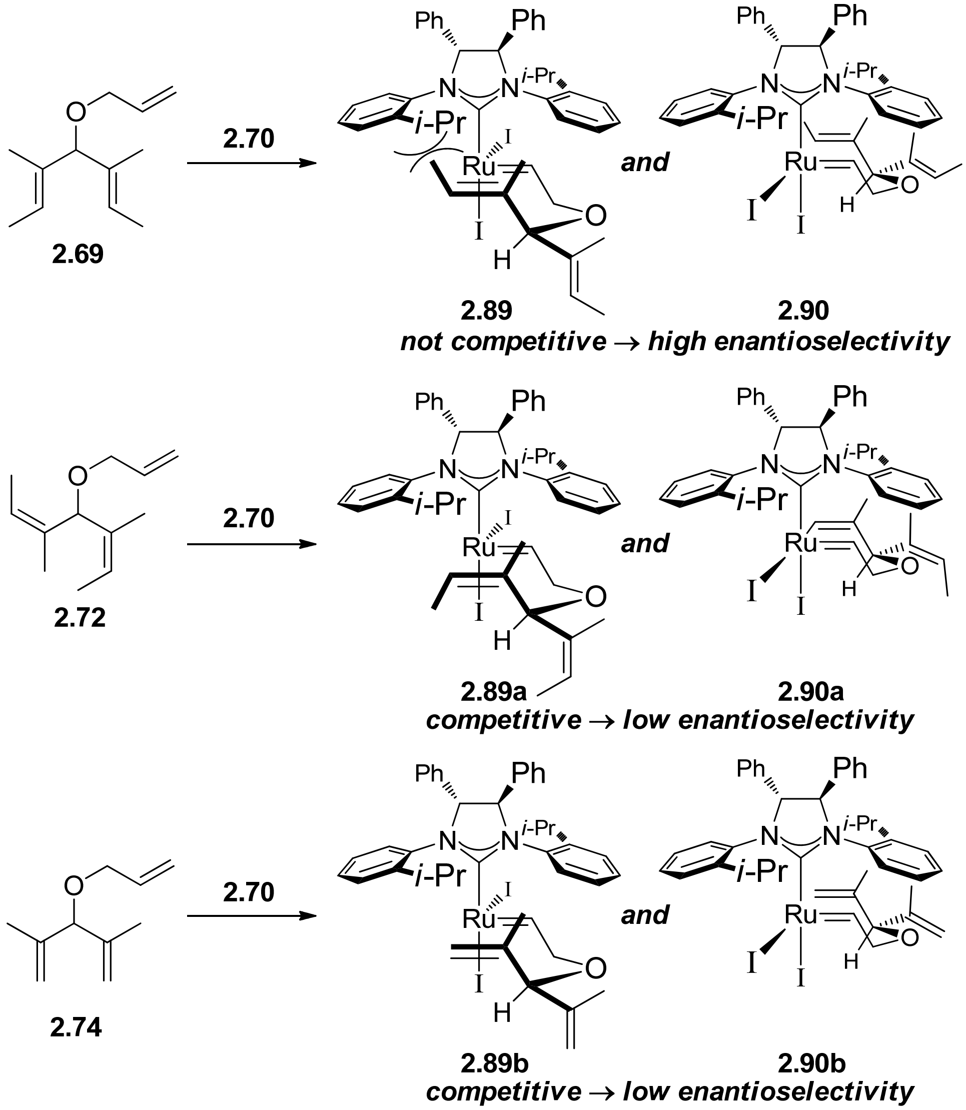

As stated above, catalyst **2.51** provides highest enantioselectivities in enantioselective RCM desymmetrization of 1,1-disubstituted olefins (**2.74**→**2.75**). However, the reason for this preference is not clear at present, because *cis*-to-NHC pathway is expected to afford opposite enantiomer to the one observed, and thus if this mechanism is operative low levels of enantioselectivity would be expected as well.

As demonstrated in this section design of Ru-based catalysts for enantioselective RCM presents challenges of distinguishing between *cis*-to-NHC and *trans*-to-NHC pathways. Further attempts at catalyst design are outlined in the section 2.2.

2.1.4.2. Diastereoselective Olefin Metathesis

The section above addressed Ru-catalyzed stereoselective olefin metathesis, in which stereoselectivities of reactions are controlled through steric interactions between the chiral NHC ligand and the substrate that does not bear stereogenic centers. The alternative approach to stereoselective olefin metathesis involves utilization of chiral substrates bearing diastereotopic olefins with achiral catalysts.

The first reported diastereoselective olefin metathesis method was reported by Lautens and co-workers (Scheme 2.18, **2.91**→**2.92a**+**2.92b** and **2.93**→**2.94a**+**2.94b**).[75] Shortly thereafter a related method was reported on diastereoselective ring-closing metathesis; this method was applied towards a formal total synthesis of (-)–aspidospermine.[76]

Blechert and co-workers reported a diastereoselective ring rearrangement metathesis method, which constitutes a ring-opening/ring-closing metathesis reaction (Scheme 2.18, **2.93**→**2.94a**+**2.94b** and **2.95**→**2.96a**+**2.96b**).[77] A few other diastereoselective olefin metathesis methods have also appeared in literature;[78] however,

---

(75) Lautens, M.; Hughes, G. *Angew. Chem. Int. Ed.* **1999**, *38*, 129-131.

(76) (a) Fukuda, Y.; Sasaki, H.; Shindo, M.; Shishido, K. *Tetrahedron Lett.* **2002**, *43*, 2047-2049; (b) Fukuda, Y.; Shindo, M.; Shishido, K. *Org. Lett.* **2003**, *5*, 749-751.

(77) Böhrsch, V.; Neidhöfer, J.; Blechert, S. *Angew. Chem. Int. Ed.* **2006**, *45*, 1302-1305.

(78) (a) Schmidt, B.; Wildemann, H. *J. Org. Chem.* **2000**, *65*, 5817–5822; (b) Layton, M. E.; Morales, C. A.; Shair, M. D. *J. Am. Chem. Soc.* **2002**, *124*, 773–775; (c) Evans, P. A.; Cui, J.; Buffone, G. P. *Angew. Chem. Int. Ed.* **2003**, *42*, 1734–1737; (d) Wallace, D. J. *J. Mol. Catal. A: Chem.* **2006**, *254*, 78–84; (e) Hooper, A. M.; Dufour, S.; Willaert, S.; Pouvreau, S.; Pickett, J. A. *Tetrahedron Lett.* **2007**, *48*, 5991–5994.

Scheme 2.18. Representative Diastereoselective Olefin Metathesis Reactions

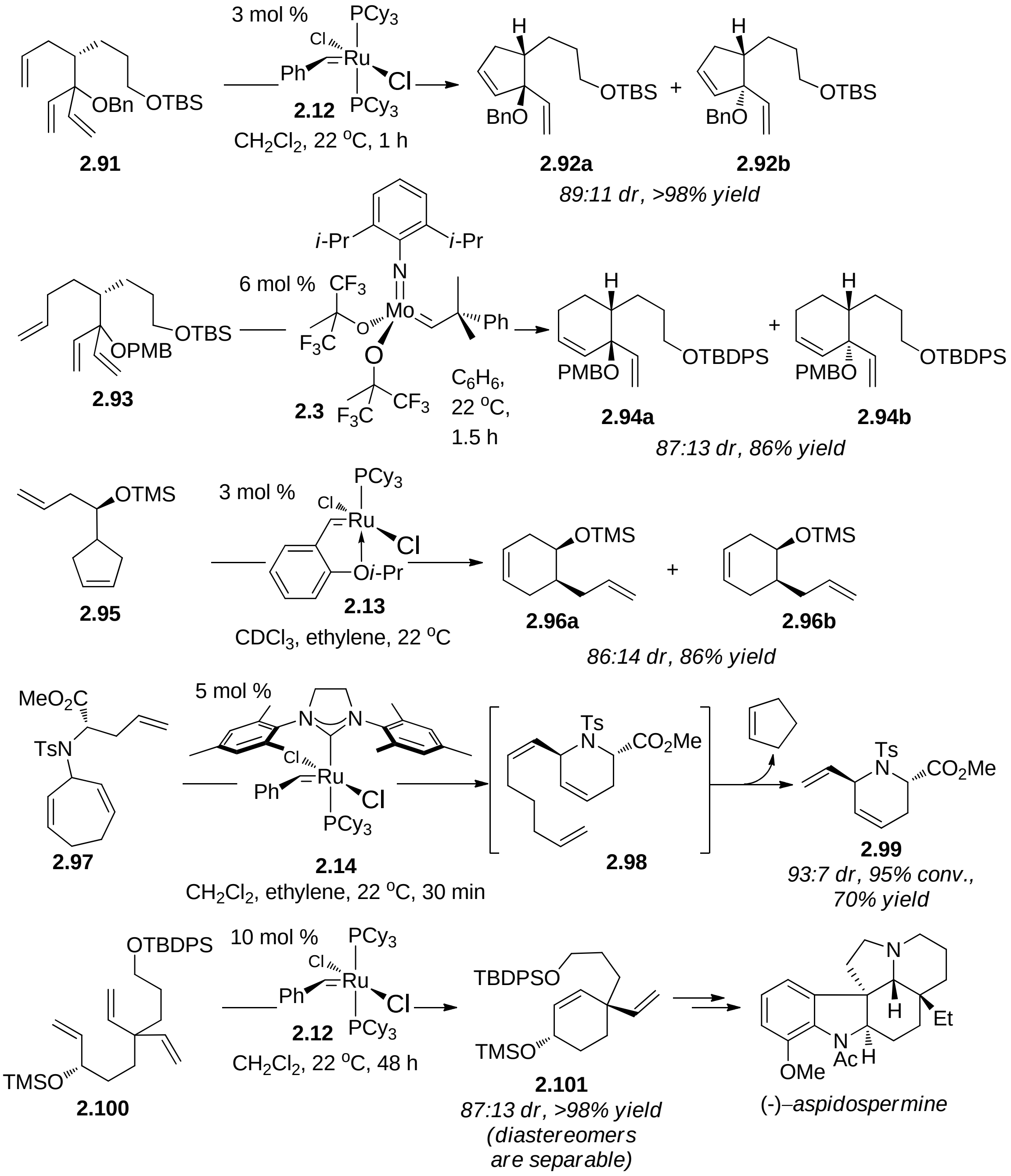

the common feature of all these methods is that these transformations involve a stereodetermining ring-closing metathesis step (diastereoselective ring-closing metathesis: DRCM). Thus, within the stereodetermining olefin coordination/ cycloaddition sequence a bicyclic intermediate forms, within which the present

Scheme 2.19. Model of Control of Diastereoselectivity in DRCM of **2.100**

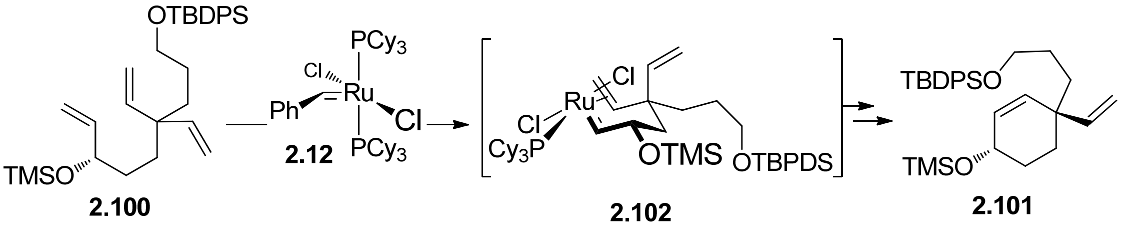

substituents at the stereogenic center and the prostereogenic center can adapt axial-axial, axial-equatorial, and equatorial-equatorial positions (equatorial-equatorial conformer is depicted in Scheme 2.19). For example, compound **2.100** upon reaction with the complex **2.12** forms the carbene **2.102**, in which one of the diastereotopic vinyl groups coordinates to Ru center, whereas the other diastereotopic vinyl group occupies the *pseudo*-axial position and the more sterically hindered TBDPS-protected alkoxy group occupies the *pseudo*-equatorial position. The relatively small energetic difference between complex **2.102** and its equatorial-vinyl-axial-alkoxy diastereomer translates into less than perfect diastereoselectivities (luckily, in the case shown in Scheme 2.19, the diastereomers are separable by silica gel chromatography). On the other hand, utilization of substrates with *tertiary* prostereogenic centers would render this reaction non-selective, because Ru catalyst would be capable of initiating on all of the olefins within such substrate.

The major limitation of diastereoselective olefin metathesis lies in the fact that the stereodetermining step should be cyclic and the diastereotopic olefins sufficiently sterically hindered to prevent competitive initiation of a metal catalyst on the diastereotopic olefins. Utilization of secondary interactions such as hydrogen bonding in stereodetermining step of diastereoselective olefin metathesis may thus assist in overcoming the aforementioned limitations. Development of such a method is the topic of the section 2.4.

2.1.5. Fluxional Behavior of Ru-based Olefin Metathesis Catalysts

Conformational fluxionality of pentavalent compounds has been well-documented over the past half a century. Pentavalent trigonal bipyramidal PF_5 is a case in point; its structure is well-defined in solid state,[79] but PF_5 exhibits fluxional behavior in solution[80] with a barrier for axchange of axial and equatorial fluorine of only 3.1 kcal/mol.[81] Berry proposed a mechanism to account for the dynamic behavior of PF_5 in solution phase, this mechanism became known as Berry pseudorotation (BPR).[82] Subsequently, Muetterties proposed additional five modes, which could account for dynamic behavior of pentavalent complexes (all mechanisms are depicted in Scheme 2.20).[83] Additional mechanism was proposed by Ugi and co-workers, which was called turnstile rotation (TR).[84] Ugi and co-workers argues that mechanisms **M2**-**M6** are not valid on the grounds that they violate the law of conservation of angular momentum.[85] Furthermore, it was concluded that **M1** (BPR) and **M7** (TR) cannot be differentiated experimentally. However, in a recent theoretical study Lammertsma and co-workers found that BPR and TR are, in fact, the same mechanism.[86] Mechanisms **M2** and **M4** are effectively sequences of BPR, in which the intermediates are destabilized such that they become non-stationary points on the potential energy surface.[86] Mechanisms **M5** and **M6** were suggested as implausible, as they proceed through high energy pentagonal planar transition states (Scheme 2.20).[83]

Pentavalent Ru complexes are known to be fluxional.[87] Indeed, olefin metathesis

---

(79) Mootz, D.; Wiebcke, M. *Z. Anorg. Allg. Chem.* **1987**, *545*, 35-42.

(80) Gutowsky, H. S.; Liehr, A. D. *J. Chem. Phys.* **1953**, *20*, 1652-1653; (b) Gutowsky, H. S.; McCall, D. W.; Slichter, C. P. *J. Chem. Phys.* **1953**, *21*, 279-292; (c) Maier, L.; Schmutzler, R. *Chem. Commun.* **1969**, 961-962.

(81) (a) Bernstein, L. S.; Kim, J. J.; Pitzer, K. S.; Abramowitz, S.; Levin, I. W. *J. Chem. Phys.* **1975**, *62*, 3671-3675; (b) Bernstein, L. S.; Abramowitz, S.; Levin, I. W. *J. Chem. Phys.* **1976**, *64*, 3228-3236.

(82) (a) Berry, R. S. *J. Chem. Phys.* **1960**, *32*, 933-938; (b) Berry, R. S. *Rev. Mod. Phys.* **1960**, *32*, 447-454.

(83) (a) Muetterties, E. L. *J. Am. Chem. Soc.* **1969**, *91*, 1636-1643; (b) Muetterties, E. L. *J. Am. Chem. Soc.* **1969**, *91*, 4115-4122.

(84) Gillespie, P.; Hoffman, P.; Klusacek, H.; Marquarding, D.; Pfohl, S.; Ramirez, F.; Tsolis, E. A.; Ugi, I. *Angew. Chem. Int. Ed. in Engl.* **1971**, *10*, 687-715.

(85) Mechanisms **M2**-**M4** do not violate the law of angular momentum conservation, because in the internal coordinates each one of these modes can be represented as two opposing half turns, for example, within **M2** exchange of *e* and *a* ligands has to undergo only a half turn if the ligands *e'*, *e"*, and *a'* undergo an opposing half turn. Thus, the latter half turn would cancel out the angular momentum vector due to the former half turn; however, in the laboratory frame of reference this transformation would appear as net **M2**.

(86) Couzijn, E. P. A.; Slootweg, J. C.; Ehlers, A. W.; Lammertsma, K. *J. Am. Chem. Soc.* **2010**, *132*, 18127-18140.

(87) (a) Hoffman, P. R.; Caulton, K. G. *J. Am. Chem. Soc.* **1975**, *97*, 4221-4228; (b) Barnard, C. F. J.; Daniels, J. A.; Jeffery, J.; Mawby, R. J. *J. Chem. Soc. Dalton Trans.* **1976**, 953-961; (c) Krassowski, D. W.; Nelson, J. H.; Brower, K. R.; Hauenstein, D.; Jacobson, R. A. *Inorg. Chem.* **1988**, *27*, 4294-4307.

Scheme 2.20. Permutational Isomerization Mechanisms

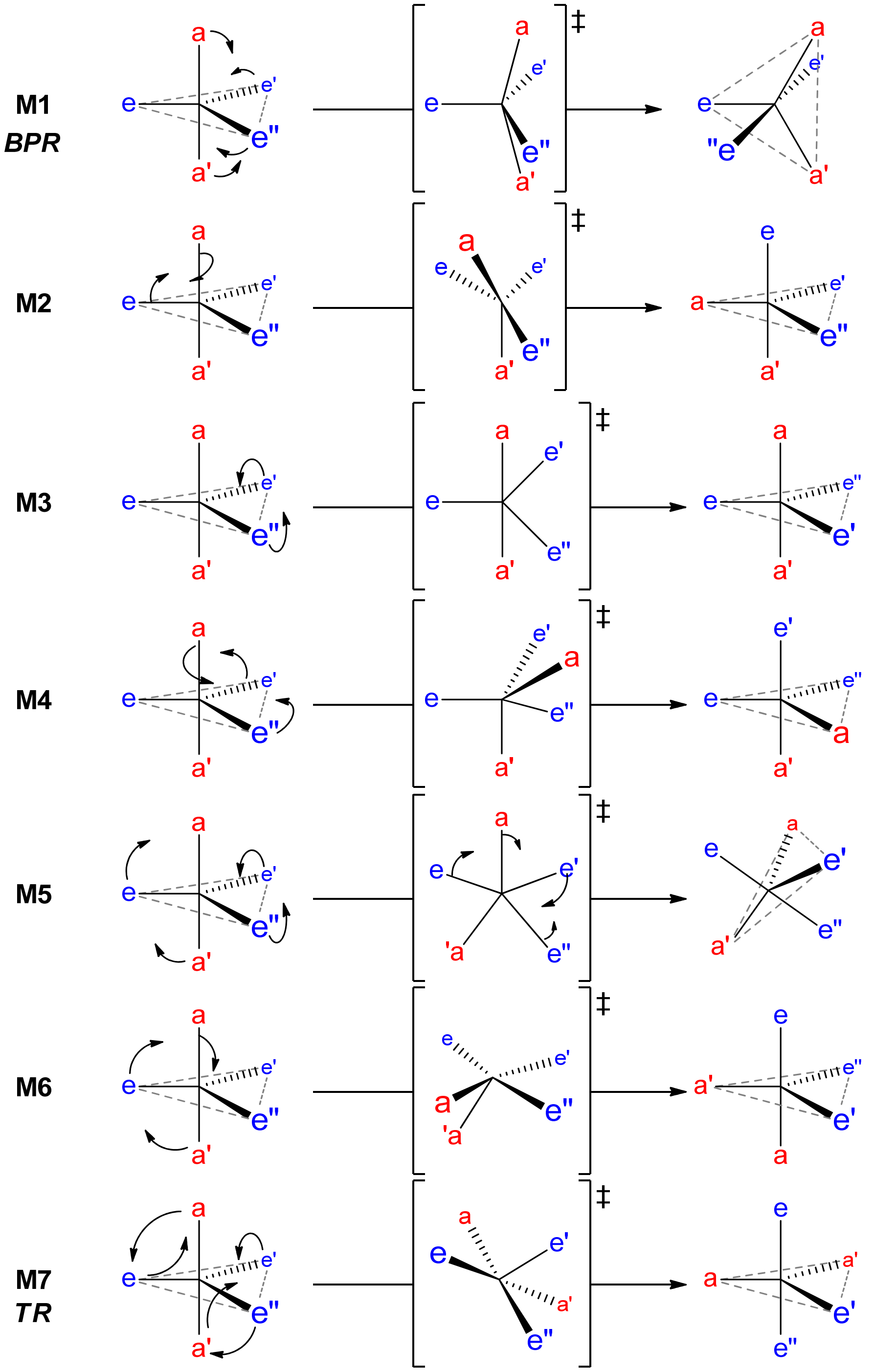

mechanism can be viewed as manifestation of the fluxional behavior of the Ru-based complexes; the cycloaddition/cycloreversion sequence is effectively a sequence of two Berry pseudorotations (Scheme 2.21).

Scheme 2.21. Olefin Metathesis as a Sequence of Berry Pseudorotations

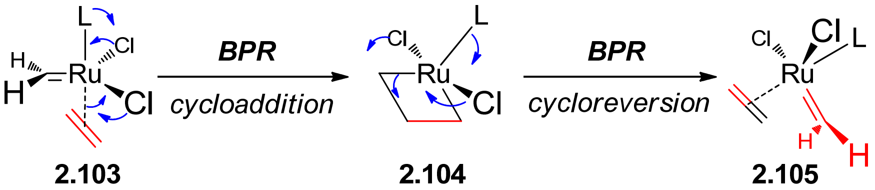

The generic olefin metathesis reaction between Ru-methylene complex and ethylene is shown in Scheme 2.21. The cycloaddition step is effected upon rotation of the ethylene molecule such that there is an overlap between its and Ru-carbene's π-systems within **2.103**. Concomitant distortion of the Ru complex leads to the trigonal bipyramidal metalacyclobutane **2.104**. Further distortion of **2.104** with concomitant breakage of the metalacyclobutane ring to give **2.105** in an overall cycloreversion process that is also a Berry pseudorotation.

Because olefin metathesis reaction constitutes a manifestation of the fluxional behavior of Ru-based olefin metathesis catalysts, it is reasonable to expect these Ru complexes to undergo non-metathesis permutational isomerizations (polytopal rearrangements). In the case of Mo-based catalysts non-metathesis polytopal rearrangements have been observed.[88] However, no unambiguous evidence for non-metathesis isomerizations of Ru-based olefin metathesis catalysts was reported to date. The rearrangement processes that has been studied in this respect is the *cis*-*trans* isomerization of the Ru-carbene chelates (Scheme 2.22). Grubbs, Schrodi and co-workers reported that complex **2.106** is isolated in equilibrium with **2.109**;[89] the ratios of the complexes were found to be solvent-dependent, with polar solvents favoring formation of

Scheme 2.22. *Cis-Trans* Isomerization of Ru-based Olefin Metathesis Catalysts

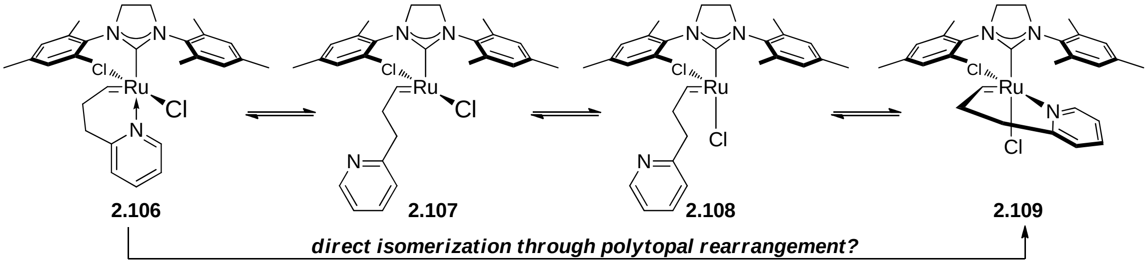

---

[88] Marinescu, S. C.; Schrock, R. R.; Li, B.; Hoveyda, A. H. *J. Am. Chem. Soc.* **2009**, *131*, 58-59.
[89] Ung, T.; Hejl, A.; Grubbs, R. H.; Schrodi, Y. *Organometallics* **2004**, *23*, 5399-5401.

complex **2.109**, as it is significantly more polar due to the *cis* arrangement of electronegative chloride ligands.[90] Subsequently, Goddard and co-workers investigated theoretically the equilibrium between **2.106** and **2.109**; however, only decoordination/recoordination pathway was considered (Scheme 2.22).[90] Only recently the polytopal rearrangement mechanism was investigated computationally.[91] The decoordination/recoordination pathway was found to be close in energy to the polytopal rearrangement pathway; however, no unambiguous experimental evidence was provided. In the section 2.4 of this chapter, unambiguous experimental evidence will be provided for non-metathesis polytopal rearrangements of Ru-based olefin metathesis catalysts.

2.2. Development of New Chiral N-Heterocyclic Carbenes for Ru-catalyzed Enantioselective Ring-Closing Metathesis

The importance of development of thermoneutral enantioselective olefin metathesis (*e.g.* RCM) protocols was described above. However, methods involving Ru-catalyzed enantioselective RCM are limited in their scope to desymmetrizations of trisubstituted olefins. Thus, to address this deficiency I set out to design and prepare chiral NHC-Ru complexes. Taking into account the relatively poor activity of stereogenic-at-Ru complexes in thermoneutral olefin metathesis,[69d] it was decided to test monodentate NHC-Ru dihalide complexes.

For a rapid and practical systematic study a chiral NHC scaffold must fulfill the following requirements: (1) scaffold must be modular, (2) the source of chirality must be easily accessible, (3) synthesis of a scaffold must be expeditious. Thus, as a starting point the general structure of the stereogenic-at-Ru complex **2.53** was chosen (Scheme 2.23). The C_1-symmetric ligand scaffold depicted in Scheme 2.23 fulfills the aforementioned requirements. The ligand structure is modular with three diversity elements, represented by the two *N*-aryl substituents and the ligand backbone. The source of chirality for this ligand is commercially available diphenylethylenediamine; both enantiomers are readily

---

(90) Benitez, D.; Goddard, W. A., III *J. Am. Chem. Soc.* **2005**, *127*, 12218-12219.

(91) Poater, A.; Ragone, F.; Correa, A.; Szadkowska, A.; Barbasiewicz, M.; Grela, K.; Cavallo, L. *Chem. Eur. J.* **2010**, *EarlyView*.

Scheme 2.23. Design of a Modular Chiral NHC-Ru Scaffold

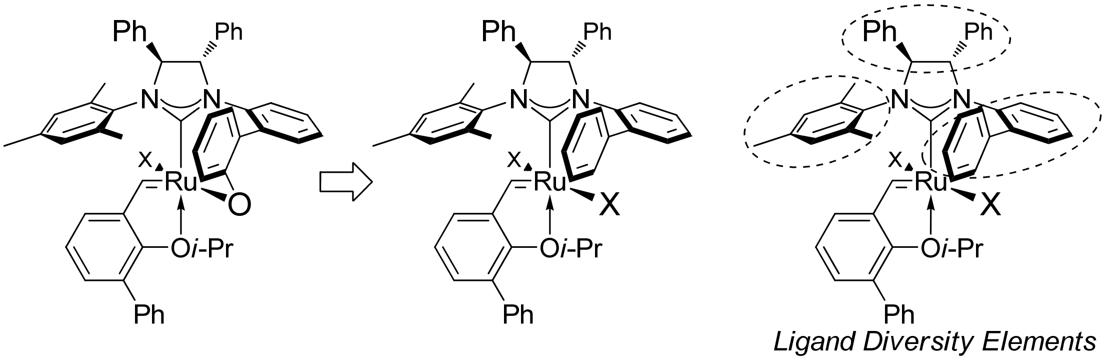

available at the same price. Synthesis of ligands can be achieved in 3 steps: two C-N cross coupling reactions,[92] followed by the cyclization of the diamine to give the imidazolium ring.[93]

2.2.1. Chiral Ru Complexes Bearing C_1-symmetric NHC Ligands

2.2.1.1. Structures of the Chiral Ru Complexes

Chiral Ru-carbenes that were developed in the course of the present study are depicted in Scheme 2.24. As the Ru iodides were found to catalyze enantioselective RCM reactions with higher enantioselectivities than the corresponding Ru chlorides, the present study will focus primarily on the former.

The Ru complexes in Scheme 2.24 were designed with the purpose of probing the diversity elements that were outlined in Scheme 2.23. Thus, complexes **2.110-2.114** assess the effect of the *syn*-to-reactive carbene *N*-aryl group of the NHC ligand on enantioselectivity of RCM reactions. Complexes **2.115-2.120** and **2.124** test the impact of the *anti*-to-reactive carbene *N*-biaryl group of the NHC ligand on the levels of enantioselectivity in RCM reactions. Complexes **2.121-2.123** and **2.125** address the possibility for cooperativity between the backbone substituents and the *syn*-to-reactive carbene *N*-aryl group of the NHC ligand, whereas complexes **2.126** and **2.127** examine

---

(92) (a) Wolfe, J. P.; Wagaw, S.; Buchwald, S. L. *J. Am. Chem. Soc.* **1996**, *118*, 7215-7216. (b) Driver, M. S.; Hartwig, J. F. *J. Am. Chem. Soc.* **1996**, *18*, 7217-7218. For reviews see: (c) Wolfe, J. P.; Wagaw, S.; Marcoux, J. –F.; Buchwald, S. L. *Acc. Chem. Res.* **1998**, *31*, 805-818. (d) Hartwig, J. F. *Angew. Chem. Int. Ed.* **1998**, *37*, 2046-2047. (e) Yang, B. H.; Buchwald, S. L. *J. Organomet. Chem.* **1999**, *576*, 125-146.

(93) Saba, S.; Brescia, A.; Kaloustian, M. K. *Tetrahedron Lett.* **1991**, *32*, 5031-5034.

Scheme 2.24. Representative New Chiral C_1-symmetric Monodentate NHC-Ru Complexes

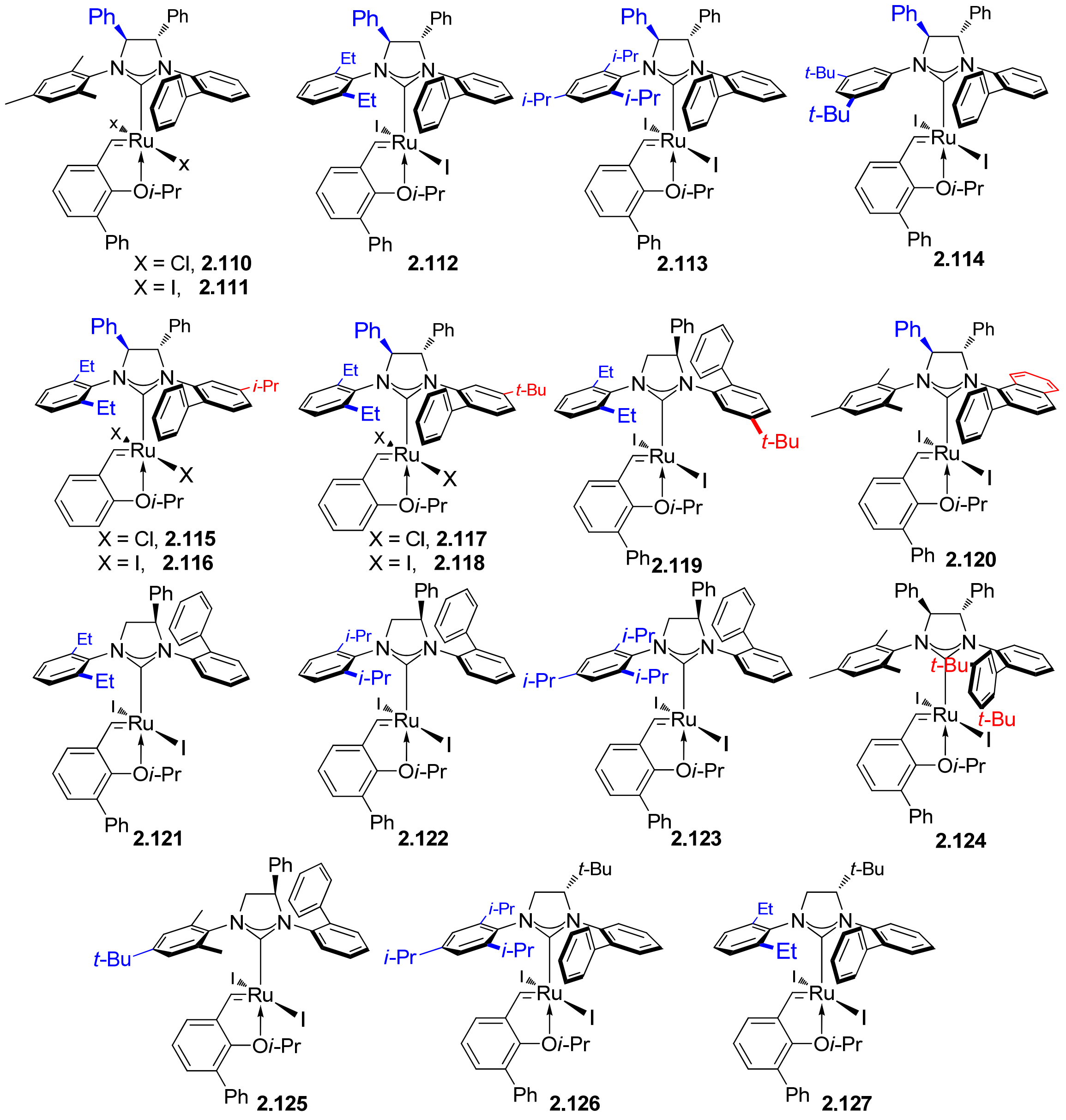

cooperativity between the backbone and the *anti*-to-reactive carbene *N*-biaryl group of the NHC ligand.

2.2.1.2. Synthesis of Chiral Ru Complexes

Catalysts based on (*S*,*S*)-diphenylethylenediamine ((*S*,*S*)-DPEDA) (**2.110-2.118**, **2.120**, **2.124**) were prepared as shown in Scheme 2.25a. The synthesis of **2.111** began with Buchwald-Hartwig cross-coupling between (*S*,*S*)-DPEDA and biphenyl iodide

Scheme 2.25. Synthesis of Chiral Ru Complexes

(a) *Preparation of Chiral NHC-Ru Complexes from (S,S)-DPEDA*

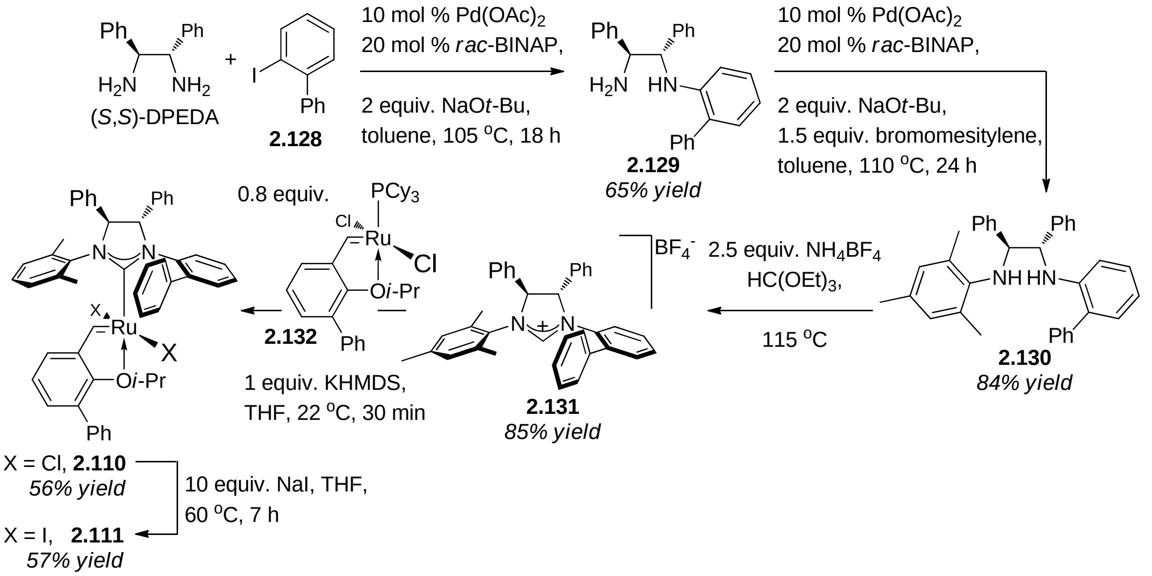

(b) *Preparation of Chiral NHC-Ru Complexes from Aminoalcohols*

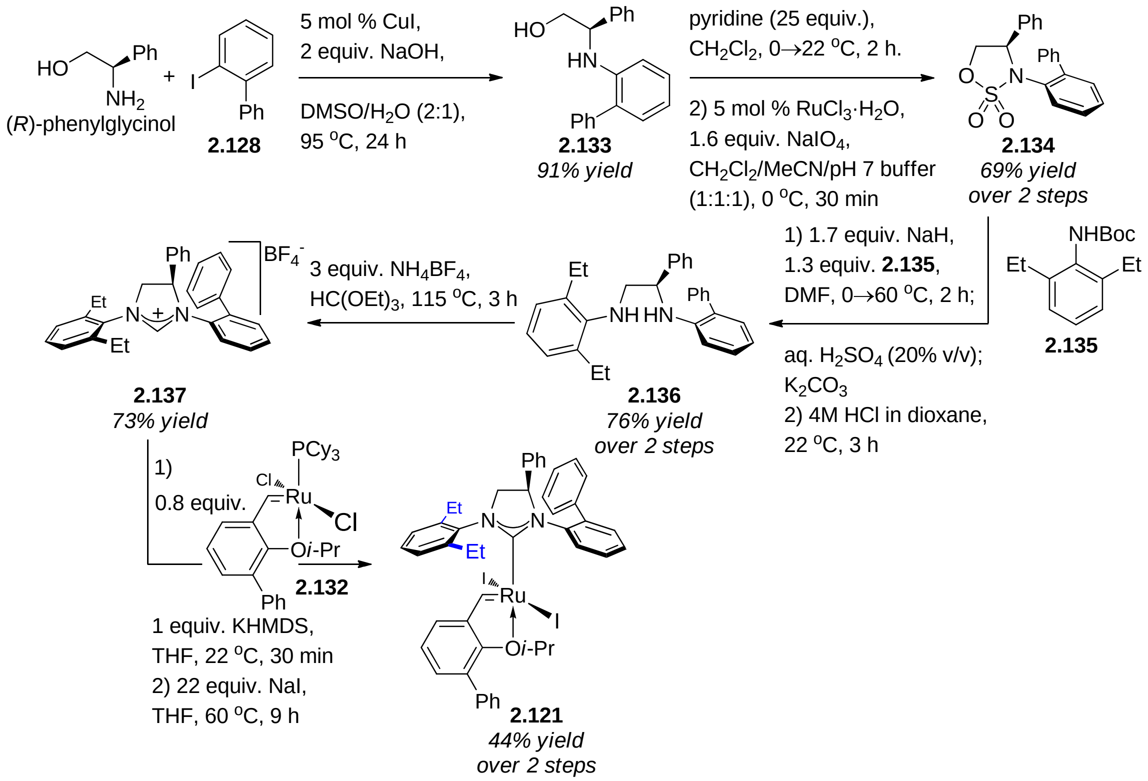

2.128, followed by another Buchwald-Hartwig coupling with bromomesitylene to give diamine **2.130** in 55% overall yield.[92] Cyclization of diamine **2.130** in neat triethyl orthoformate in the presence of NH_4BF_4 gave chiral imidazolinium salt **2.131** in 85% yield.[93] Deprotonation of **2.131** with KHMDS in the presence of phosphine-Ru complex **2.132** gave NHC-Ru dichloride complex **2.110** in 56% yield, which upon treatment with excess NaI at elevated temperatures afforded **2.111** in 57% isolated yield.

Catalysts based on aminoalcohols (**2.119**, **2.121-2.123**, and **2.125-2.127**) were prepared as shown in Scheme 2.25b. Cross-coupling between (*R*)-phenylglycinol and biphenyl iodide **2.128** furnished aminoalcohol **2.133** in 91% yield, which was converted to cyclic sulfamidate **2.134** by a two step process. Nucleophilic substitution of the sulfamidate with deprotonated aniline **2.135**,[94] followed by removal of a Boc group under acidic conditions afforded diamine **2.136**, which was cyclized in neat triethyl orthoformate to give imidazolinium salt **2.137** in 38% yield over 5 steps. Substitution of phosphine ligand in **2.132** with deprotonated **2.137**, followed by substitution of chloride ligands for iodides afforded complex **2.121** in 44% yield over two steps.

2.2.2. Structure-Selectivity Studies of Ru-catalyzed Enantioselective RCM

Enantioselective ring-closing metathesis reactions that were employed in the present structure-selectivity relationship study are shown in Table 2.1. Substrate choice was guided by the necessity for sufficient structural diversity. Thus, substrates **2.65** and **2.67** bear quaternary prostereogenic centers, whereas substrates **2.138** and **2.140** bear tertiary prostereogenic centers. Also, substrates **2.65** and **2.140** bear substituents at the α-position relatively to the prostereogenic centers, while substrates **2.67** and **2.138** have no substituents between the prostereogenic centers and the terminal olefins. It is worth noting that all substrates depicted in Table 1 form 6-memberred rings upon RCM; all attempts at RCM of 5-memberred rings unexpectedly failed, suggesting that the structural parameters governing formation of 5-memberred rings are vastly different from those governing formation of 6-memberred rings.[95]

As illustrated in Table 2.1, chiral NHC-Ru iodide complexes proved to be more enantioselective than chlorides and thus the study was primarily focused on the former

---

(94) Baldwin, J. E.; Spivey, A. C.; Schofield, C. J. *Tetrahedron Asym.* **1990**, *1*, 881-884.

(95) The difference between RCM of 5- and 6-memberred rings was noted previously in Ref. 69d.

Table 2.1. Catalyst Screening Studies in Ru-catalyzed Enantioselective RCM

Entry	Catalyst	Time (h)	Conv. (%)^a	*er* (%)^{b,c}	Entry	Catalyst	Time (h)	Conv. (%)^a	*er* (%)^{b,c}	Entry	Catalyst	Time (h)	Conv. (%)^a	*er* (%)^{b,c}
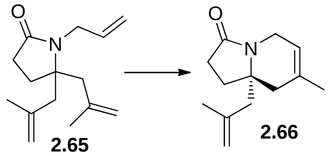 **2.65** → **2.66**					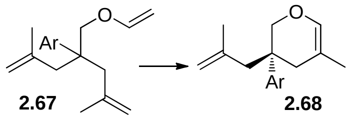 **2.67** → **2.68** Ar = (4-bromo)phenyl					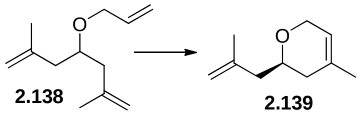 **2.138** → **2.139**				
1	**2.110**	12	>98	42:58	17	**2.110**	12	>98	56:44	35	**2.113**	24	57^g	62:24
2	**2.111**	36	24	60.5:39.5	18	**2.111**	36	88	77.5:22.5	36	**2.121**	24	>98	54:46
3	**2.112**	36	35	53:47	19	**2.112**	36	>98	77.5:22.5	37	**2.122**	24	37^h	54:46
4	**2.113**	36	2	91.5:8.5	20	**2.113**	36	>98	67:33	38	**2.125**	24	>98	<53:47
5	**2.114**	36	>98	54:46	21	**2.114**	36	<2	nd	39	**2.127**	24	>98	<53:47
6	**2.115**	12	>98	38.5:61.5	22	**2.116**	36	>98	41.5:58.5	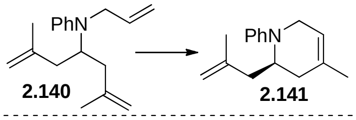 **2.140** → **2.141**				
7	**2.117**	12	>98	37:63	23	**2.117**	12	>98	42.5:57.5					
8	**2.120**	36	>98	54:46	24	**2.118**	36	47	37.5:62.5					
9	**2.121**	24	73	46:54	25	**2.119**	36	47	41:59	40	**2.111**	36	83	59:41
10	**2.122**	36	>98^{e,f}	57:43	26	**2.120**	36	>98	65.5:34.5	41	**2.113**	24	24	58:42
11	**2.123**	24	53^e	54:46	27	**2.121**	24	28	79.5:20.5	42	**2.122**	36	13	55.5:44.5
12	**2.124**	36	11	57:43	28	**2.122**	24	25	79.5:20.5	43	**2.125**	24	79	55.5:44.5
13	**2.125**	24	>98	52.5:47.5	29	**2.123**	24	>98	75:25					
14	**2.126**	24	10^e	53.5:46.5	30	**2.124**	36	89	72.5:27.5					
15	**2.127**	24	26^e	57.5:42.5	31	**2.125**	24	21	79.5:20.5					
16	**2.51**	24	>98^e	71:29	32	**2.126**	24	66	72.5:27.5					
					33	**2.127**	24	19	76:24					
					34	**2.51**	24	>98	41:59					

All reactions were run at 22 ^{o}C in dry C_6H_6 (0.1M) under dry N_2 atmosphere with 5 mol % catalyst loadin. [a] Conversion to product was determined by ^{1}H-NMR; [b] Enantioselectivities were determined by HPLC and GC; [c] For clarity absolute sense of enantioselectivity is adjusted with respect to absolute stereoconfiguration of the catalys.; [e] Reaction was performed at 60 ^{o}. [f] The reaction furnished a mixture of the desired product and unidentified byproducts; [g] 96:4 mixture of RCM:dimer products; [h] 3:1 mixture of RCM:dimer products

class of complexes. Among the substrates compounds **2.65** and **2.67**, bearing quaternary prostereogenic centers proved to be most amenable to improvements in enantioselectivities; thus, the study mainly focused on trienes **2.65** and **2.67**.

The possible catalytic pathways are outlined in Scheme 2.26. All reactions shown in the scheme are reversible; however, for clarity only ligand rotations are depicted as equilibria. After the initiation step ruthenacyclobutane **VI** is formed (R" = H for propagating intermediate), to which two open pathways are available: path A ($k_{\mathbf{VI\text{-}VIII}}$>>$k_1$) or path B ($k_1$>>$k_{\mathbf{VI\text{-}VIII}}$). Note that all intermediates on path A are even-numbered, and all intermediates on path B are odd-numbered. Path A should be

Scheme 2.26. Mechanistic model for Ru-catalyzed Enantioselective RCM

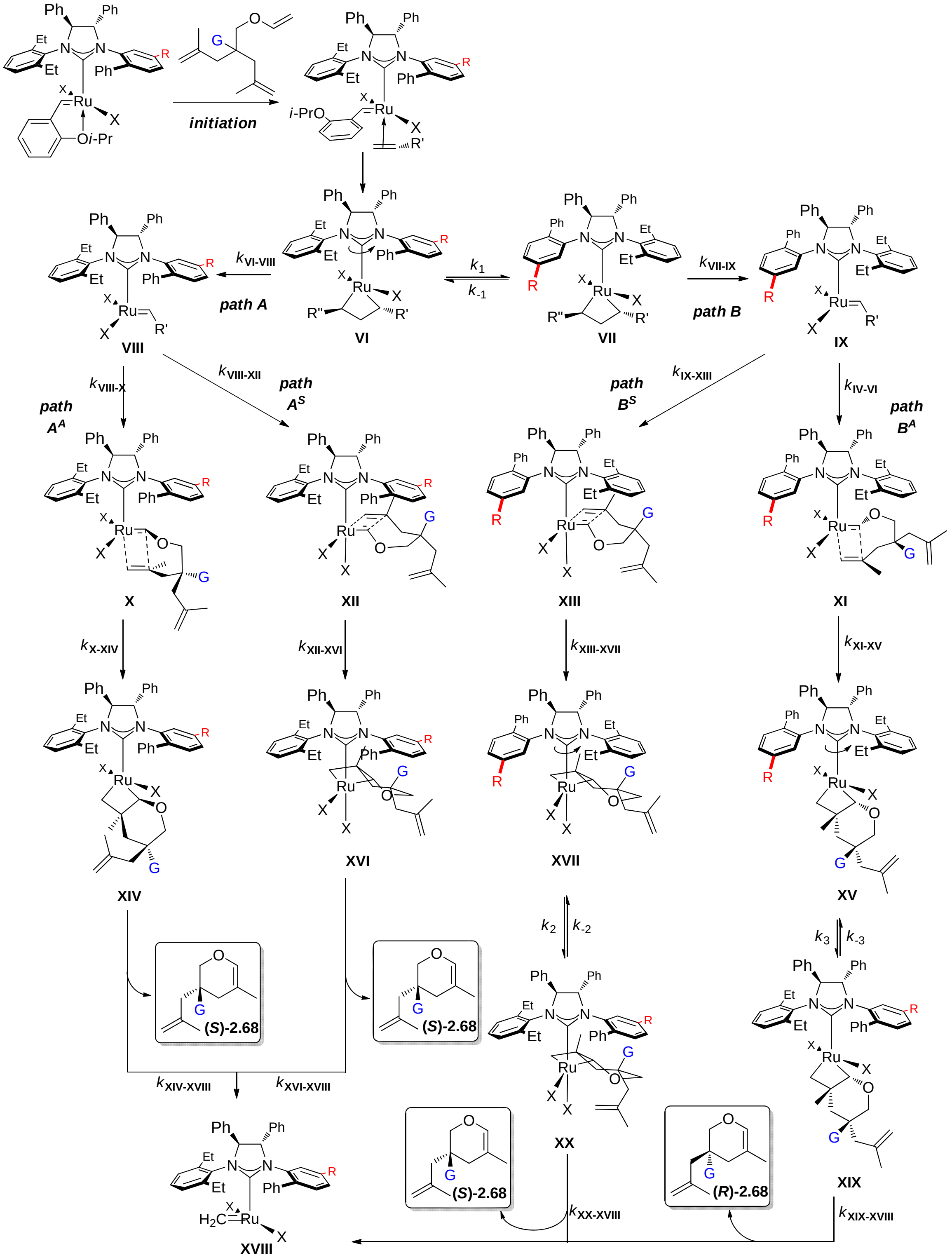

predominant if the steric bulk of the ligand prevents ligand from rotation, making path A accessible, even though barrier to **VIII** is presumably higher than that leading to **IX** (Hammond's postulate). Path B is likely to predominate if the ligand rotation is facile for the aforementioned reason.

Intermediate Ru-carbenes **VIII** and **IX** can undergo metathesis through coordinating enantiotopic olefin of a substrate either *trans*-to-NHC (path A^A: **X**, and path B^A: **XI**) or *cis*-to-NHC (path A^S: **XII**, and path B^S: **XIII**). The diastereomers of Ru-carbenes **X** and **XII** are consistent with the mechanistic model proposed by Grubbs and co-workers.**Error! Bookmark not defined.**[b] However, given the aforementioned necessity for desymmetrization of trisubstituted olefins to achieve high enantioselectivity, it is likely that path A^A is non-selective due to lack of halide ligand differentiation described above, and reactions of trisubstituted olefins favor path A^S (lower $k_{\mathbf{VIII\text{-}X}}$ or $k_{\mathbf{X\text{-}XIV}}$). The diastereomer **XI** is consistent with the model described above, but from the structure of **XIII** alone the mode of olefin coordination depicted appears to be only slightly favored for disubstituted olefins.

Figure 2.3. Double-tier gearing effect in NHC-$RuCl_2$ and NHC-RuI_2 complexes

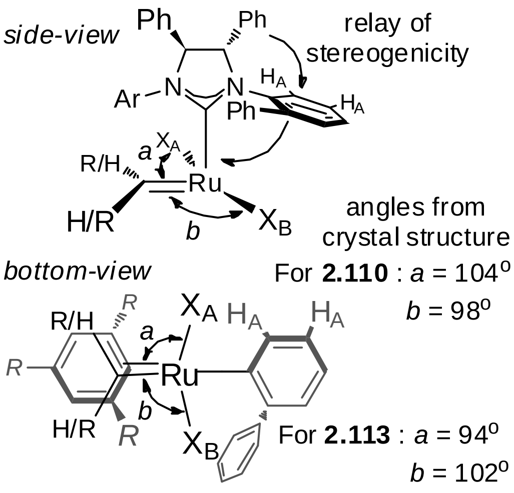

The enantioinduction observed in enantioselective RCM reactions above is likely due to distortion, imparted by the NHC on halide ligands on Ru (Figure 2.3). Assuming only *trans*-to-NHC coordination of olefins during the reaction, in order to favor only one diastereomeric transition state, resulting in a single enantiomer, ideally only one diastereomer of Ru=CH*R* carbene needs to be present in the reaction system. As depicted in Figure 2.3, the crystal structure of **2.113** (X = I) reveals that a steric interaction between H_A of the NHC ligand and I_A iodide ligand results in compression of the angle *a*, whereas I_B is capable of adopting wider angles *b*, while maintaining overlap with *d*-orbitals of Ru. Thus, *R* substituent of Ru=CH*R* would have a less pronounced steric interaction with iodide ligand in *R*-*cis*-to-I_B diastereomer than in

R-cis-to-I_A, where the movement of X_A is restricted by H_A atoms of the NHC ligand. In **2.110** (X = Cl) inequality of angles *a* > *b* is likely due to hydrogen bonding between H_A and Cl_A (downfield shift of H_A in ^{1}H-NMR);[96] however, in the course of the reaction the angle *b* may require a larger value than the one observed for *a*. The latter statement is supported by the experimental data (*vide supra*), where NHC-$RuCl_2$ complexes provide the same absolute sense of enantioselectivity as NHC-RuI_2 complexes.

Figure 2.4. *Syn*-pentane interactions in RCM intermediates *path B*

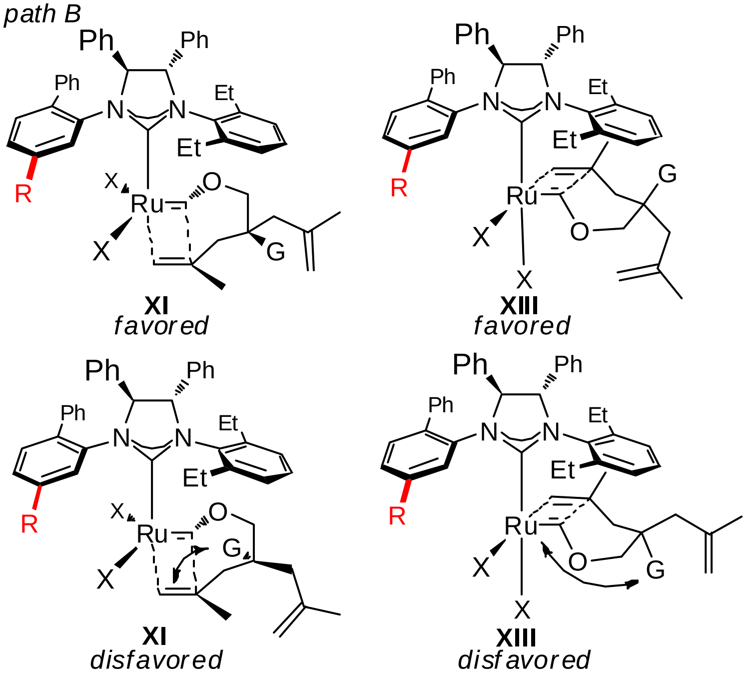

XI *favored*

XIII *favored*

XI *disfavored*

XIII *disfavored*

Assuming a single diastereomer of each carbene, the enantiomeric excess in all pathways shown in Scheme 2.26 is due to *syn*-pentane interaction between methyl and either methallyl or H groups (if G = H, **2.138** and **2.140**). For bulky quaternary prostereogenic center-bearing substrates (G = Ph; **2.67**), aryl ring is likely to occupy the same position as H atom in substrate **2.138**, because the ring being formed in **X** and **XII** adjusts its conformation to accommodate the steric bulk of aryl and methallyl groups such that in the favored conformer the bulkier aryl ring avoids *syn*-pentane interaction with the formed metalacyclobutane (Figure 2.4).

Ruthenacyclobutanes **XIV** and **XVI** (path A) exhibit similar interactions (Figure 2.4) to Ru-olefin complexes **XI**and **XII**, which in turn furnish the single enantiomer **(*S*)-2.58**. Given the above-stated assumption for path B ($k_1 >> k_{\mathbf{I\text{-}III}}$), the same assumption should hold for ruthenacyclobutanes **XV** and **XVII**. Thus, upon rapid ligand rotation

---

[96] Lane, D. R.; Beavers, C. M.; Olmstead, M. M.; Schore, N. E. *Organometallics* **2009**, *28*, 6789-6797.

atropisomeric **XIX** and **XX** are formed. They in turn are cleaved productively to afford opposite enantiomers [**XIX→(*R*)-2.68**, **XX→(*S*)-2.68**].

Based on the analysis of the mechanistic model presented in Scheme 2.26 *a priori* there appears to be no single major pathway for Ru-catalyzed olefin metathesis. However, the catalyst screening studies demonstrate that different pathways can be disfavored. In our attempt to design a highly selective Ru-based olefin metathesis catalyst we attempted to disfavor paths A^A, A^S, and B^S, because these pathways can be disfavored by designing chiral NHC ligand bearing necessary strategically placed aliphatic/aromatic groups. Paths A^A and A^S can be disfavored, as stated above, by facilitating equilibrium **VI⇆VII** ($k_1 >> k_{\mathbf{VI\text{-}VIII}}$). Path B^S can be disfavored by employing ligands that sterically disfavor *syn*-to-NHC olefin coordination. Only path B^A appears to be clearly amenable to preferring a single Ru=CHR diastereomer by sterically distorting halide ligands on Ru center. Furthermore, mechanism involving *trans*-to-NHC olefin coordination has been shown theoretically[51] and inferred[50] experimentally to be a major – if not exclusive – pathway for Ru-catalyzed olefin metathesis.

The experimental data in Table 2.1 can be used to infer the following trends. Triene **2.67** appears to undergo olefin metathesis predominantly through *trans*-to-NHC mode of olefin coordination (paths A^A and B^A), because of disfavored interaction between the aryl rings of the substrate and the NHC in intermediates **XII** and **XIII**. On the other hand substrate **2.138**, bearing tertiary prostereogenic center, can undergo olefin metathesis through all paths A^A, A^S, B^A, and B^S. This hypothesis is largely supported by absence of switch in absolute sense of enantioselectivity for **2.67→2.68** between NHC-$RuCl_2$ and NHC-RuI_2 complexes, and by observed relatively high enantioselectivity for RuI_2 complexes (as compared to substrates bearing less bulky prochiral centers). Observed reversal in absolute sense of enantioselectivity for **2.65→2.66** (entries 1 and 2 in Table 2.1) suggests either change in the mode of reactivity (switch between predominating paths B^A and B^S) or alteration of the chiral pocket of the intermediate Ru-carbene complex. Although the latter possibility cannot be ruled out (crystal structures analysis), the fact that no reversal is observed in the absolute stereoconfiguration of the

RCM product **2.68** supports the former (entries 16 and 17). Complexes **2.114** and **2.120** likely function through both paths A and B, because the atropisomers (such as **VIII** and **IX**) of both complexes are close in energy and the barrier to rotation is likely to be small. Thus, enantioselectivities in enantioselective RCM reactions catalyzed by **2.114** and **2.120** are low (entries 5, 8, 20, 25). Complex **2.114** (like **2.120**) was prepared to maximize the interaction between the NHC backbone phenyl ring and the sterically more imposing naphthyl (R, R' = $(CH)_4$) or *m-tert*-butyl groups (R' = *t*-Bu), thus, resulting in minimal dihedral angle θ (structure **2.142**) and maximum steric interaction between R and halide ligand on Ru. However, steric interaction between naphthalene moiety and iodide ligand resulted in larger angle θ. In complex **2.114**, on the other hand, lack of *o*-substituents on the aryl ring resulted in rapid rotation of the ring with respect to the imidazolinylidene ring (two *m-tert*-butyl groups appear as a single peak in ^{1}H-NMR spectrum). Since the rapid rotation of the aryl ring results in essentially cylindrical achiral environment, ARCM reactions with complex **2.114** proceed with very low enantioselectivities (entries 5 and 20).

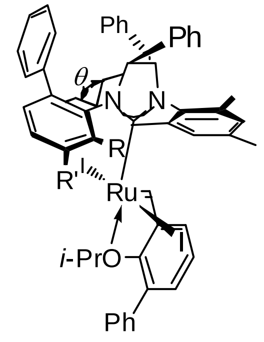

2.142

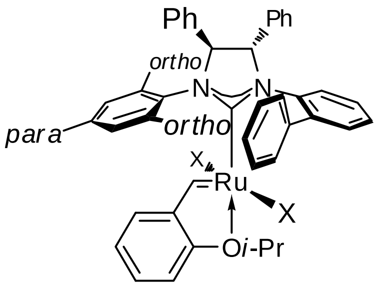

2.143

Complexes **2.111**, **2.112**, and **2.113** were tested to probe the effect of increased steric bulk close to reacting Ru-carbene, which may be responsible for eliminating pathways involving *syn*-to-NHC olefin coordination (paths A^S and B^S). Interestingly, in **2.65→2.66** (entries 2, 3, and 4) the presence of *para*-substituent (structure **2.143**) appears to enhance the observed enantioselectivities (entries 2 and 3); however, the current model (Scheme 2.26) fails to account for such an effect. Presence of bulky *o-iso*-propyl groups in **2.113** seems to disfavor *syn*-to-NHC reactivity (path B^S), and path A is likely disfavored due to facile equilibrium **VI⇆VII**. Thus, the predominant operating path is B^A. However, in **2.67→2.68** (entries 2, 3, 4) the increased steric bulk in **2.113** (as compared to **2.111** and **2.112**) results in lower selectivity possibly due to the mismatched interaction inherent in *pseudo*-C_2-symmetry of complexes such as **2.113**, which is an artifact of the C_2-symmetric backbone. The two possible diastereomers of **VI** (path B^A) are shown in Figure 2.5. The diastereomer $\mathbf{IX_a}$ is disfavored for reasons described previously, whereas the diastereomer $\mathbf{IX_b}$ is disfavored due to the tilt of 2,4,6-tri-*iso*-propylphenyl ring, resulting from steric interaction between the phenyl ring and of the backbone and bulky *o*-*iso*-propyl group. Complex **2.122** was prepared in order to alleviate the mismatched interaction present in **2.113**. Although in reaction **2.67→2.68** enantioselectivities were restored (entry 29), in reactions **2.65→2.66** and **2.138→2.139** (entries 10 and 42) enantioselectivities diminished significantly. However, complex **2.122** lacks the bulky *para*-substituent, which as observed before enhances the enantioselectivity in **2.65→2.66**. Thus, complexes **2.123** and **2.125** were prepared to test the effect of a bulky *para*-substituent on enantioselectivity. In all of the reactions tested (entries 13, 31, 38, and 43) no effect of *p*-*t*-butyl group was observed. However, reaction **2.67→2.68** merits mention due to the low observed reactivity; unlike **2.122**, complex **2.125** appeared to have fully initiated (no ^{1}H-NMR peak of *iso*-propoxybenzylidene Ru-carbene was present), but a new carbene peak was observed in ^{1}H NMR ($CDCl_3$) spectrum (δ 13.6 ppm), it was tentatively assigned as a Fischer Ru-carbene complex.

Figure 2.5. Mismatched interactions in pseudo-C_2-symmetric NHC-Ru complexes.

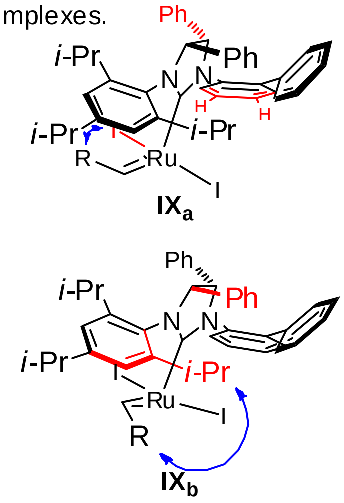

Because the substrate **2.67** exhibited modest enantioselectivity in enantioselective RCM, likely due to predominantly operating path B^A, we expected the enantioselectivity to be increased by minimizing angle θ shown in **2.142**. Thus, complexes **2.115-2.118** were prepared. However, in **2.67→2.68** they demonstrate lower selectivity with opposite absolute sense of enantioinduction. The likely cause for this observation is the preference for path A due to steric bulk present on the biphenyl moiety (*m*-*iso*-propyl and *m*-*tert*-butyl groups in **2.116** and **2.118** respectively). Ligand rotation, hindered by bulky *m*-

substituents (R' = *i*-Pr or *t*-Bu in structure **2.142**), significantly slows down due to steric interaction between the NHC and halide ligands on Ru in the transition state (**VI→VII**). Thus, path A is competitive with path B ($k_{\mathbf{VI\text{-}VIII}} \geq k_1$). The main mode of reactivity on path A is likely to involve *anti*-to-NHC coordination of olefins (path A^A) for aforementioned arguments regarding the bulky quaternary prostereogenic center-bearing substrates.

Dichloride complexes **2.115** and **2.117** on the other hand do not catalyze enantioselective RCM **2.65→2.66** with an opposite sense of enantioselectivity (entries 1, 6, and 7), implying that NHC-RuCl$_2$ ring closing **2.65→2.66** is competitive with the ligand rotation ($k_{\mathbf{VI\text{-}VIII}} \geq k_1$); reactivity of Ru chloride catalyst is high enough to compete with the ligand rotation **VI→VII**.

Among enantioselective reactions depicted in Table 2.1 the only case that can be deemed as approaching synthetically useful levels of enantioselectivity is shown in entry 4 (91.5:8:5 *er*). However, reaction conversion at 22 ^{o}C is <5%, at higher temperatures competitive decomposition to unidentified byproducts occurs, and thus development of methods employing the catalyst **2.113** would be of limited potential.

The complexity of the catalytic cycle of enantioselective RCM with C_1-symmetric monodentate NHC-Ru carbenes and presence of multiple competitive pathways that are difficult to control prompted me to consider other possible chiral NHC-Ru scaffolds.

2.2.3. Attempts at Synthesis of Chiral Tridentate NHC-Ru Complex

To achieve enhanced control over stereoselectivity in Ru-catalyzed thermoneutral olefin metathesis catalyst scaffold needs to preclude the possibility of multiple competitive pathways. Because pathways A^A, A^S, B^A, and B^S (Scheme 2.26) are competitive, and the structure of monodentate NHC ligands cannot be readily modified to prefer only one of the pathways without hampering the overall reaction efficiency, the most plausible strategy is to limit the number of accessible pathways to only one. For example, C_2-symmetric NHC structures would render pathways A and B identical. However, as was demonstrated by Grubbs and co-workers this approach does not result in improvement of enantioselectivities in enantioselective RCM involving desymmetrizations of 1,1-disubstituted olefins. As described in section 2.1.4.1, possible competition due to *cis*-to-NHC pathways (A^S and B^S) could be responsible for low enantioselectivities in desymmetrizations of 1,1-disubstituted olefins. Possible strategy that would disallow pathways A^S and B^S involves tethering X ligands to the NHC; in other words halide ligands can be replaced for pseudohalides (sulfonates, carboxylates) that can be tethered to the NHC. Indeed, among chiral Ru-based olefin metathesis catalysts complex **2.51**, bearing chiral bidentate NHC ligand, provides highest levels of enantioselectivity in desymmetrization **2.74**→**2.75** (Scheme 2.15). Thus, it was hypothesized that a chiral C_2-symmetric tridentate NHC ligand meets the described structural constraints. Another important criterion for tridentate ligand design is the length of tethers.[97] For example, in complexes **2.51**-**2.54** the bidentate ligand and Ru center form 8-memberred rings. It was hypothesized that smaller rings could be incorporated as well if tethers were of sufficient flexibility. Ligand flexibility is also important, because $C_{carbene}$-Ru-X angles change between reactive complexes within the catalytic cycle. Taking the aforementioned criteria into account chiral imidazolium **2.147** was designed and prepared as shown in Scheme 2.27.

The imidazolium salt **2.147** was prepared from commercially available sulfonate **2.144** through the following sequence. Chlorination of **2.144** with $SOCl_2$ with catalytic amounts of DMF, followed by trapping the resulting sulfonyl chloride with *i*-BuOH under basic conditions and the aldehyde reduction with $LiAlH_4$ furnished **2.145** in 10% yield over 3 steps. The overall yield of **2.145** was low due to competitive dichlorination of the carbonyl group during the first step. Substitution reaction of in situ prepared from **2.145** triflate with dihydroimidazole **2.146**[98] afforded **2.147** in 52% yield.

Scheme 2.27. Preparation of Chiral bis-Sulfonate Imidazolinium Salt **2.147**

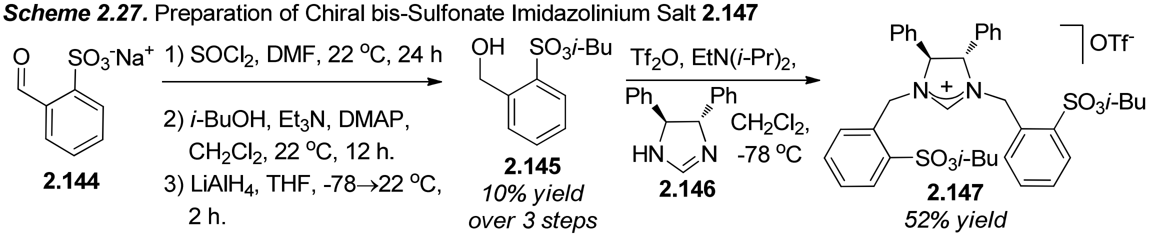

---

[97] In a related study of chiral Ru complexes, bearing bidentate NHC ligands, it was noticed that complexes, in which the tether length was such that a 7-memberred ruthenacycle would have formed upon chelation, could not be formed under all conditions screened. Baxter, C. A. *Unpublished Results.*

[98] Diaz, D. D.; Finn, M. G. *Org. Lett.* **2004**, *6*, 43-46.

Installation of the imidazolinium salt on Ru was expected to be achieved through deprotonation of the imidazolinium salt, substitution of phosphine on Ru and deprotection of the sulfonate groups, followed by the abstraction of halide ligands (Scheme 2.28) to give **2.150**. Although, complex **2.149** was readily accessible through a standard protocol, subsequent attempts at deprotection of the sulfonates followed by abstraction of a halide ligand with concomitant trapping of the cationic Ru with sulfonates proved unfruitful.

Scheme 2.28. Attempts at Synthesis of Chiral Tridentate NHC-Ru Complex

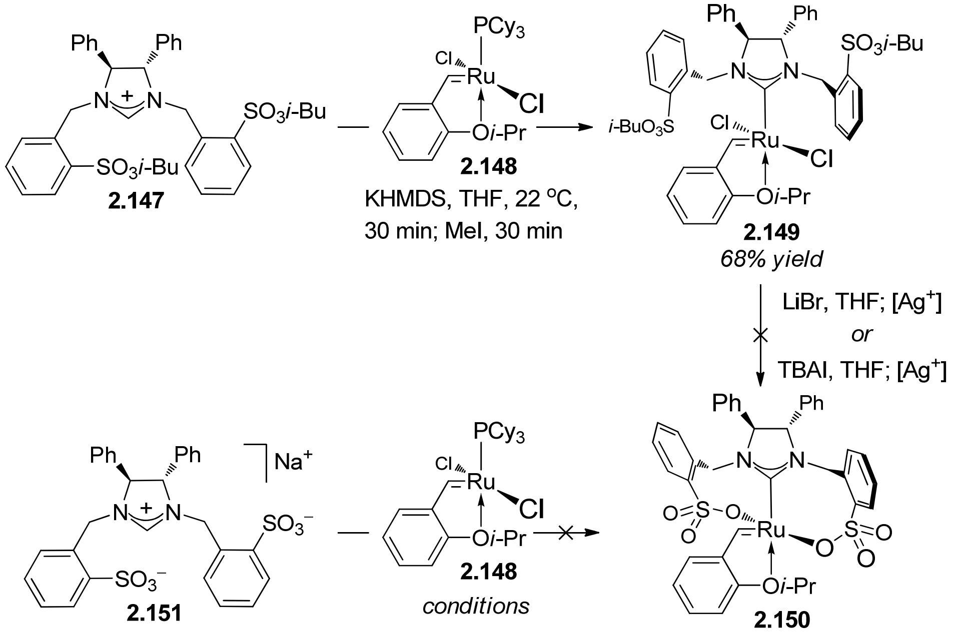

entry	*conditions*	*result*
1	KHMDS, THF, 22 °C, 30 min	*a*
2	*t*-BuMgCl, Et$_2$O, THF, -78 °C, 10 min	*a*
3	Et$_2$Zn, C$_6$D$_6$, 22 °C, 30 min	*b*
4	Ag$_2$CO$_3$, THF/C$_6$H$_6$, 70 °C, 2 h	*b*
5	Ag$_2$O, Me$_4$NCl, THF, 22 °C, 14 h	*a*

a No conversion

b Decomposition of Ru carbene as inferred from absence of peaks in >12 ppm region of ^{1}H NMR spectra

To overcome difficulties with deprotection of sulfonate groups in the presence of Ru-carbene imidazolinium salt **2.151** was prepared (see Supporting Information for details). Deprotonation of **2.151** with KHMDS in the presence of complex **2.148** did not lead to formation of new Ru-carbenes as evidenced by ^{1}H NMR spectrum of the reaction mixture. Alternative approach to synthesis of **2.150** involved the use of transmetalating agents with imidazolinium salt **2.151** such as NHC-Mg, NHC-Zn, and NHC-Ag.[99] However, treatment of **2.151** with *t*-BuMgCl or Et_2Zn, followed by **2.148** resulted in either no conversion (*t*-BuMgCl) or decomposition of Ru-carbenes (Et_2Zn). The presence of EtZn-sulfonate is most likely responsible for the observed decomposition of Ru carbenes, as ethyl group may undergo transmetalation with Ru center, generating alkyl Ru-carbenes. Attempts at carbene transfer *via* NHC-Ag were not fruitful and led to either decomposition of Ru-carbenes under forcing conditions (entry 4, Scheme 2.28) or no conversion (entry 5, Scheme 2.28).[100]

The complications described above in the synthesis of **2.150** led us to abandon this structure. The major limitations in the synthesis of Ru complexes described herein were associated with protection/deprotection of sulfonate groups. Unfortunately, removal of protecting groups for sulfonates often involves the use of Lewis basic solvents such as piperidine or harsh conditions,[101] and thus incorporation of sulfonates into structures with Ru-carbenes proves to be a significant obstacle in design and synthesis of chiral Ru olefin metathesis catalysts for enantioselective thermoneutral olefin metathesis.

2.2.4. Conclusion

Development of chiral Ru olefin metathesis catalysts remains a significant challenge. Despite the fact that well-defined Ru-based olefin metathesis catalysts were disclosed only a few years after Mo-complexes, by comparison to the developments in

---

(99) For examples of NHC-Mg and NHC-Zn complexes see: (a) Arduengo, A. J. III; Rasika Dias, H. V.; Davidson, F.; Harlow, R. W. *J. Organomet. Chem.* **1993**, *462*, 13-18. (b) Herrmann, W. A.; Runte, O.; Artus, G. *J. Organomet. Chem.* **1995**, *501*, C1-C4. (c) Arduengo, A. J. III; Davidson, F.; Krafczyk, R.; Marshall, W. J.; Tamm, M. *Organometallics* **1998**, *17*, 3375-3382. (d) Schumann, H.; Gottfriedsen, J.; Glanz, M.; Dechert, S.; Demtschuk, J. *J. Organomet. Chem.* **2001**, *617*, 588-600. (e) Lee, Y.; Li, B.; Hoveyda, A. H. *J. Am. Chem. Soc.* **2009**, *131*, 11625-11633. For reviews on NHC-Ag complexes see: (f) Garrison, J. C.; Youngs, W. J. *Chem. Rev.* **2005**, *105*, 3978-4008. (g) Lin, I. J. B.; Vasam, C. S. *Coord. Chem. Rev.* **2007**, *251*, 642-670. For a report on the use of NHC-Ag complexes as transmetalating agents for Ru carbenes see: (g) Ref. 69f.

(100) Complications in NHC-Ag complex synthesis are discussed in detail in: Lin, J. C. Y.; Huang, R. T. W.; Lee, C. S.; Bhattacharyya, A.; Hwang, W. S.; Lin, I. J. B. *Chem. Rev.* **2009**, *109*, 3561-3598.

(101) For a discussion regarding protecting groups for sulfonates see: Simpson, L. S.; Widlanski, T. S. *J. Am. Chem. Soc.* **2006**, *128*, 1605-1610.

the area of stereoselective Mo-catalyzed olefin metathesis the area of stereoselective Ru-catalyzed olefin metathesis remains undeveloped. The reasons for such a dichotomy are manifold. For example, comparison of molybdacyclobutanes and ruthenacyclobutanes divulges the first among the problems of Ru-catalyzed stereoselective olefin metathesis (Figure 2.6). Molybdacyclobutanes carry two sterically different groups (imido and X^2 = alkoxide) *cis*-to-metalacyclobutane and ruthenacyclobutanes carry two sterically similar groups (X = Cl, I) *cis*-to-metalacyclobutane, and thus stereocontrol through steric interactions is difficult to achieve through modification of chiral NHC ligand structure in Ru complexes, whereas imido groups and alkoxides of Mo complexes offer diversity of choices for control of the metalacyclobutane substitution pattern through steric interactions. Although substitution of X ligands on Ru for alkoxides would be expected to lead to catalysts capable of highly stereoselective olefin metathesis, reactivity of Ru bisalkoxides is extremely low due to diminished Lewis acidity of the Ru center.[102] Thus, substitution of X ligands for chiral (and possibly tethered to NHC sulfonates) would be highly beneficial for future development of Ru-based chiral olefin metathesis complexes.

Figure 2.6. Comparison of Mo-catalyzed and Ru-catalyzed Olefin Metatheses

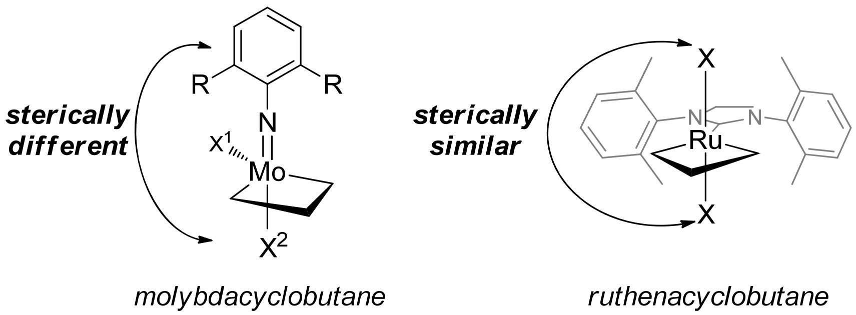

Perhaps, the more fundamental limitation of Ru-based complexes in stereoselective olefin metathesis lies in the fact that low valent 14-electron species **II** (Scheme 2.8) are high in energy; therefore, rate determining step is likely product decoordination (by >5 kcal/mol) – a step, stereoselectivity within which is difficult to control with a ligand *trans* to the leaving olefin.[51f] Some strides in addressing this problem have been made through changing the electronegativity of X ligands; for

---

[102] Sanford, M. S. *PhD Thesis*, California Institute of Technology, 2001.

example, substitution of chlorides for iodides leads to enhanced enantioselectivities, an observation that at least partly can be attributed to enhanced facility of product decoordination. Somewhat circumstantial evidence for the problem of product decoordination is found in the fact that Ru-catalyzed exothermic olefin metathesis (*e.g.* enantioselective ring-opening/cross metathesis) was developed to a much greater extent than the thermoneutral variant. This problem can be addressed through incorporation of a small weakly Lewis basic side-arm within the structure of a chiral NHC such that the decoordination process is rendered associative rather than dissociative, thereby leading to lowering of the transition state energies for product decoordination and possibly rendering other steps (cycloaddition or cycloreversion) rate-determining.

The third obstacle in the way of designing chiral Ru-based olefin metathesis catalysts is the fact that pathways *cis*-to-NHC and *trans*-to-NHC appear to be competitive; the equivalents of these processes in Mo-catalyzed olefin metathesis are *cis*-to-imido ligand and *trans*-to-imido ligand, the former process was found computationally[103] and inferred experimentally[1c,88] to be operative. Thus, understanding the mechanism, through which *cis*-to-NHC pathway may operate, and factors that affect its facility will provide further information for future catalyst design. To date, computational studies only demonstrated that *cis*-to-NHC olefin-Ru coordination transition state is significantly higher in energy; however, other steps are energetically comparable to *trans*-to-NHC pathway.[51c] On the other hand, *trans*-to-NHC olefin coordination can lead to *cis*-to-NHC ruthenacyclobutane (through polytopal rearrangements) and thus *cis*-to-NHC pathway should be considered as competitive.

Although it may be argued that Mo-catalyzed olefin metathesis can be viewed as complimentary to Ru-catalyzed olefin metathesis by virtue of the ability of the former to effect highly stereoselective processes, there are areas of application where Mo-based catalysts will not be able meet the demand: aqueous and biological applications of olefin metathesis. Thus, development of chiral Ru-based olefin metathesis catalysts will remain an important objective in the area of catalyst design.

---

(103) (a) Wu, Y. –D.; Peng, Z. –H. *J. Am. Chem. Soc.* **1997**, *119*, 8043-8049. (b) Goumans, T. P. M.; Ehlers, A. W.; Lammertsma, K. *Organometallics* **2005**, *24*, 3200-3206.

2.3. Isolation of Reactive Intermediates in Olefin Metathesis Catalyzed by Stereogenic-at-Ru Complexes and Observation of Non-Metathesis Fluxional Behavior of the Ru-based Olefin Metathesis Catalyst

The section above addressed design and synthesis of chiral Ru complexes for thermoneutral olefin metathesis. It is exothermic olefin metathesis that chiral Ru complexes are capable of effecting with high levels of enantioselectivity.[70h-l] However, chiral monodentate NHC-Ru complexes are not as efficient catalysts in these transformations as bidentate NHC-Ru complexes; for example, as shown in Scheme 2.29 chiral bidentate NHC-Ru complex **2.54** afforded the desired **2.153** in 62% yield and no inseparable bis-cross product **2.155** was detected. Reaction **2.152**→**2.153** catalyzed by complexes **2.13** and **2.15**, on the other hand, resulted in a competitive formation of bis-cross product **2.155**, which proved inseparable. Furthermore, in reactions catalyzed by monodentate NHC-Ru complexes competitive stilbene formation was observed (as much as 2 equiv. of styrene were converted to stilbene in the course of **2.152**→**2.153** catalyzed by complexes **2.15**), whereas minimal or no stilbene formation was observed in all ring-opening cross metathesis reactions catalyzed by **2.54**.

Scheme 2.29. Enantioselective Ring-Opening/Cross Metathesis: Monodentate vs Bidentate Chiral NHC-Ru Complexes

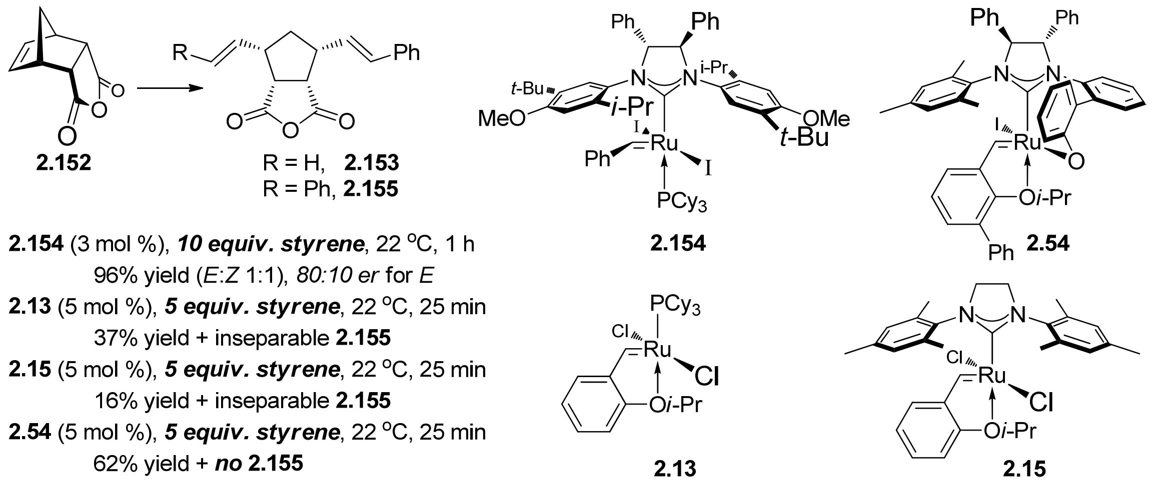

2.154 (3 mol %), ***10 equiv. styrene***, 22 °C, 1 h
96% yield (*E*:*Z* 1:1), *80:10 er* for *E*
2.13 (5 mol %), ***5 equiv. styrene***, 22 °C, 25 min
37% yield + inseparable **2.155**
2.15 (5 mol %), ***5 equiv. styrene***, 22 °C, 25 min
16% yield + inseparable **2.155**
2.54 (5 mol %), ***5 equiv. styrene***, 22 °C, 25 min
62% yield + ***no*** **2.155**

These experimental observations can be rationalized by considering the catalytic cycle of Ru-catalyzed enantioselective ring-opening/cross metathesis (ROCM) depicted in Scheme 2.30. Although the mechanisms shown are standard there is a feature that defines the difference between monodentate and bidentate NHC Ru complexes: Ru center

Scheme 2.30. Catalytic Cycles for Ring-Opening/Cross Metathesis with Bidentate and Monodentate NHC Ru Complexes

(a) *Monodentate NHC Ru Complex in ROCM*

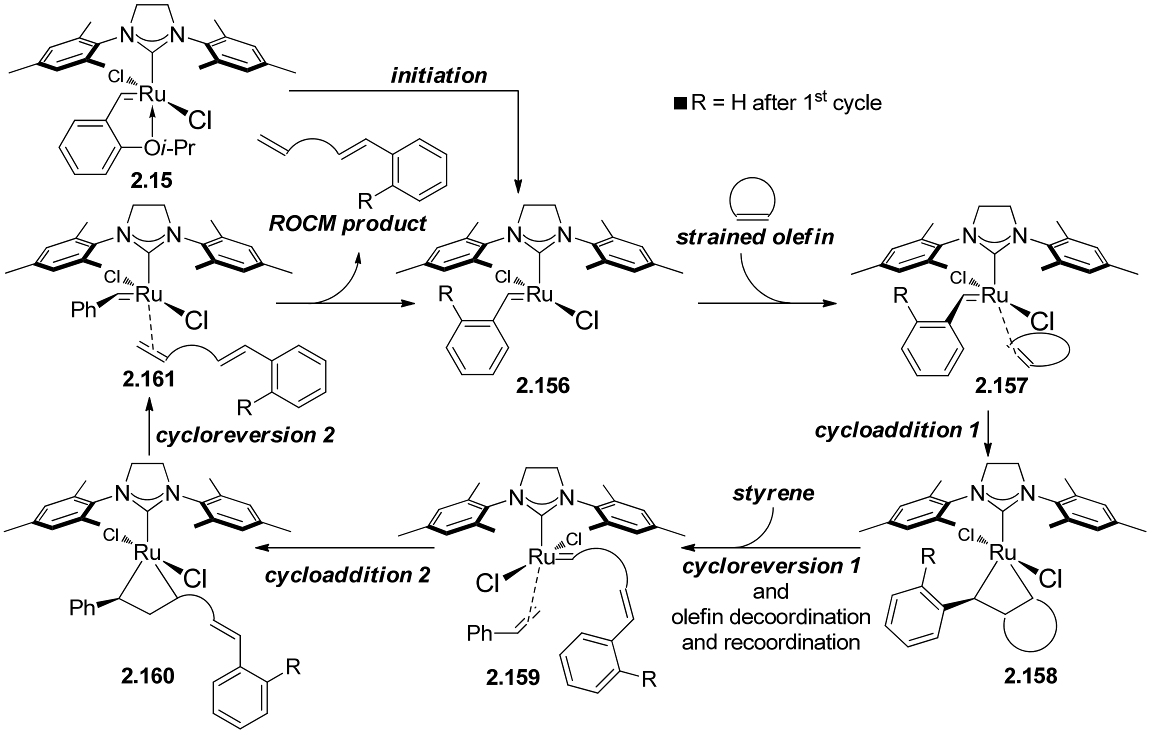

(b) *Bidentate NHC Ru Complex in ROCM*

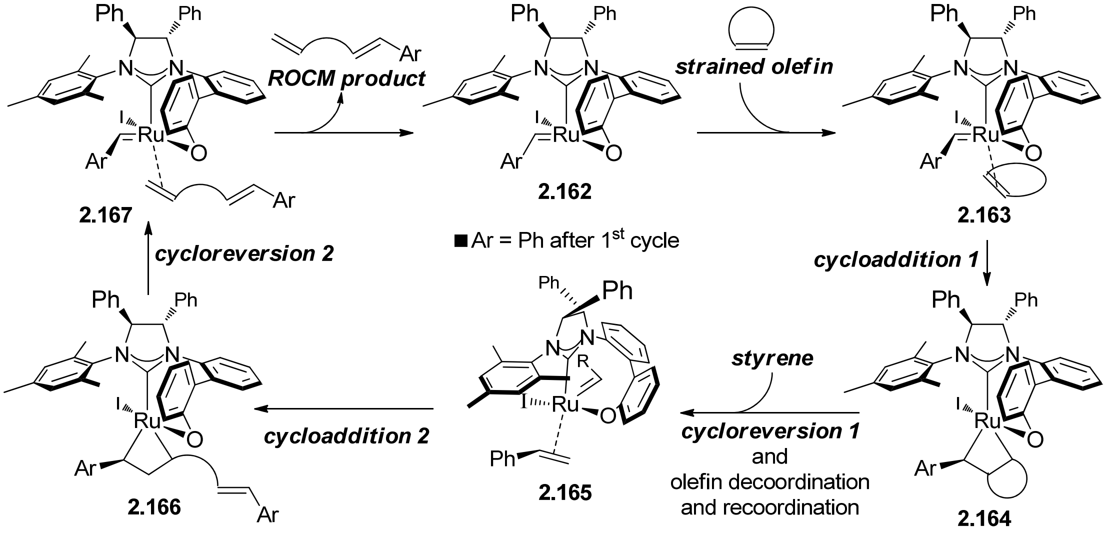

in bidentate NHC Ru complex is stereogenic, and with each olefin metathesis (cycloaddition/ productive cycloreversion) Ru center undergoes stereomutation. As shown in Scheme 2.30 each productive ring-opening cross metathesis reaction consists of two olefin metatheses: ring opening metathesis and cross metathesis; ring opening step is exothermic and cross metathesis step is thermoneutral. Thus, each productive ring-opening cross metathesis results in a *net retention of stereochemical identity of the Ru center*. Consideration of diastereomeric carbenes is mute for monodentate NHC Ru complexes, because in cases of dissymmetric carbenes a rotation along C_{NHC}-Ru bond equilibrates out carbene orientations (similar to **VI⇆VII**, Scheme 2.26) and in cases of symmetric carbenes the two carbene orientations are identical.

As a consequence of the fact that Ru is a stereogenic center, the two accessible carbene orientations (compare **2.163** and **2.165**) are diastereomeric, the carbene orientation in **2.163** (*syn*-to-mesityl group of the NHC) is referred to as *exo* carbene, whereas carbene orientation in **2.165** (in the *endo* orientation with respect to 8-memberred aza-oxo-ruthenacycle) is called *endo* carbene. The energetic difference (ΔG^{o}) between **2.162** (Ar = Ph) and its diastereomer at Ru was calculated to be 6.3 kcal/mol in favor of **2.162** (see the supporting information for details). Thus, access to the diastereomeric would be expected to be more efficient with strained olefins, whereas the reverse reaction is likely to be more facile with small sterically non-demanding olefins such as styrene due to α-branching in the *endo* carbene that resulted from the ring opening of a strained bicyclic molecule. By rendering Ru center stereogenic dual site reactivity was effectively incorporated into the catalysts **2.51**-**2.54**, thereby accounting for the observed high efficiencies in ROCM reactions as exemplified by Scheme 2.29. Similar approach was utilized by Chen and co-workers in the design of stereogenic-at-Ru complexes for applications in selective copolymerization of cyclooctene and norbornene.[104]

---

(104) (a) Bornand, M.; Chen, P. *Angew. Chem. Int. Ed.* **2005**, *44*, 7909-7911. (b) Bornand, M.; Torker, S.; Chen, P. *Organometallics* **2007**, *26*, 3585-3596. (c) Torker, S.; Müller, A.; Chen, P. *Angew. Chem. Int. Ed.* **2010**, *49*, 3762-3766. (d) Torker, S.; Müller, A.; Sigrist, R.; Chen, P. *Organometallics* **2010**, *29*, 2735-2751.

Despite the inferred experimental evidence for the intermediacy of diastereomeric carbenes in olefin metathesis, in only one report observation of diastereomeric Ru carbenes under olefin metathesis reaction conditions (cross metathesis) was reported.[104b] It was necessary to confirm the intermediacy of diastereomeric carbenes in olefin metathesis reactions catalyzed by **2.51-2.54** in order to confirm that the hypothesis described above was indeed operative.

We reasoned that a reaction of **2.54** with a terminal olefin would afford only a thermodynamic mixture of diastereomeric carbenes (*i.e.* a significantly less thermodynamically-stable *endo* diastereomer is unlikely to be observable); however, treatment of **2.54** with a strained olefin, bearing a chelating moiety, would allow for trapping of *endo* carbene complex. Indeed, upon treatment of **2.54** with cyclobutene **2.168** in C_6D_6 a major new Ru carbene complex **2.169** (17.07 ppm) was observed by ^1H NMR (Figure 2.7), which was isolated by silica gel chromatography in 42% yield. The absolute stereochemical identity of (*C*)-Ru center was confirmed through observation of heteronuclear *n*O*e* between the ^1H of the carbene and the F atom of **2.171** (prepared from **2.170** as shown in Figure 1), and the relative stereochemistry of the cyclobutene ring-opening was established through NOESY of **2.169** (see the Supporting Information for details). Calculated ^1H NMR chemical shift of the carbene **2.169** was consistent with the experimentally observed spectrum (calculated: δ 17.01 ppm in $CDCl_3$; experimental: δ 16.82 ppm in $CDCl_3$).

In order to confirm that the isolated *endo* carbene is a competent intermediate in Ru-catalyzed olefin metathesis, complex **2.169** was treated with 11 equiv. of styrene, furnishing ring-opening/cross metathesis product **2.172** in 51% yield and two new carbenes (17.68 and 16.41 ppm), as observed by ^1H NMR (Figure 2.8). The peak at 17.68 ppm was attributed to **2.173**, which could not be isolated due to decomposition. Upon isolation the major Ru carbene (**2.174**) was identified as the (*A*)-Ru diastereomeric carbene complex, with the chelating *iso*-propoxide ligand *trans* with respect to the NHC ligand. Formation of complex **2.174** cannot be rationalized by invoking the olefin metathesis mediated stereomutation of Ru center; however, non-metathesis unimolecular

Figure 2.7. Synthesis of *Endo*-carbene Through a Single Ring-Opening Metathesis Reaction. (a) Unpurified reaction mixture; (b) Pure **2.54**; (c) Purified **2.169**; (d) key observed ^{19}F-^{1}H *nOe*.

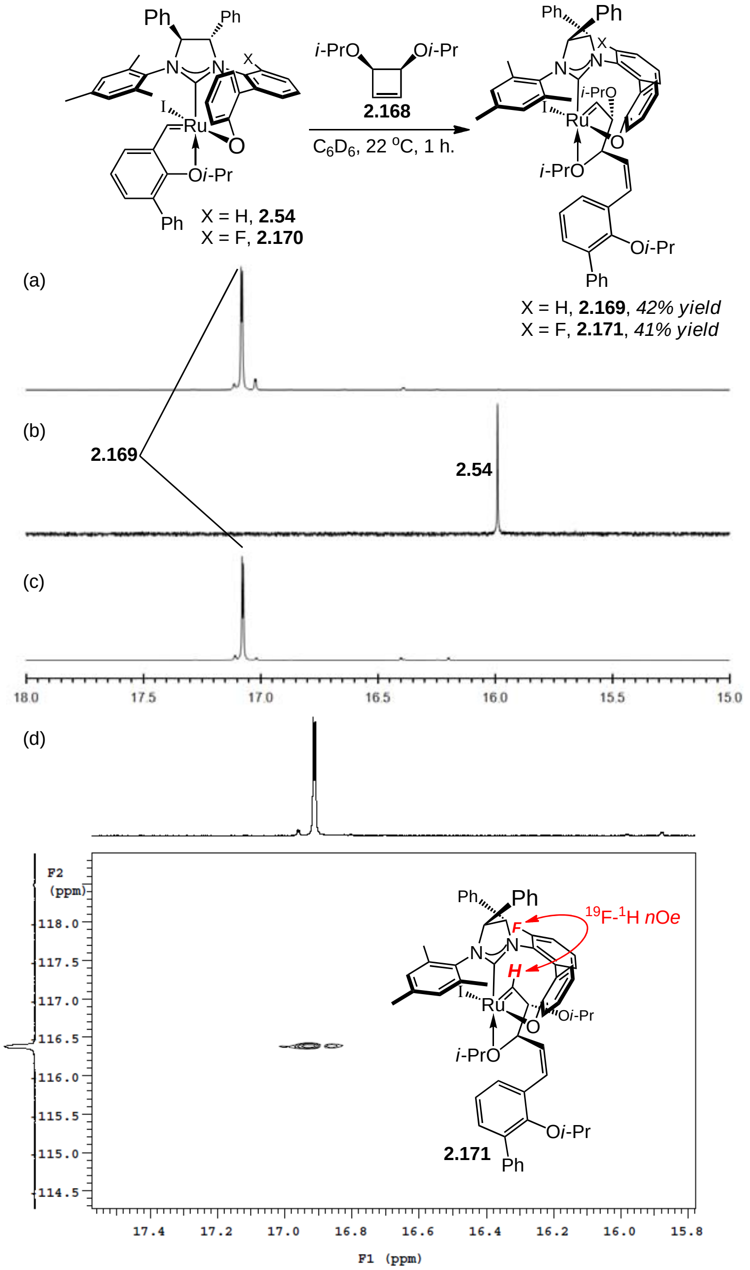

isomerizations such as polytopal rearrangements could account for the present observation.[82-86] Indeed, the presence of styrene proved inconsequential for the isomerization of **2.169** to **2.174**, as this reaction was found to proceed in the absence of styrene (Figure 2.9).

Figure 2.8. Isomerization of **2.169** in the Presence of Styrene.
(a) unpurified reaction mixture; (b) **2.54** treated with styrene

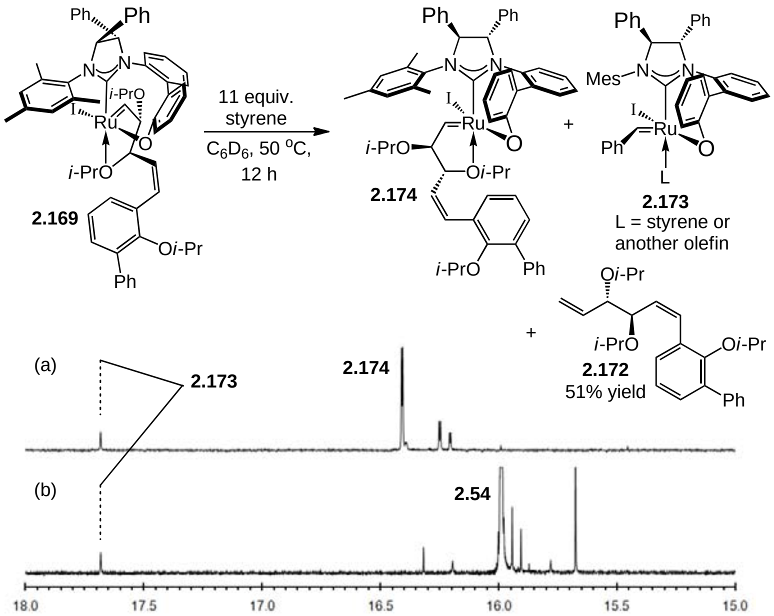

Figure 2.9. Isomerization of **2.169** Under Thermal Conditions. ^{1}H NMR spectra: (a) pure **2.169**; (b) reaction mixture after 6 h; (c) isolated **2.175**; (d) isolated **2.174**.

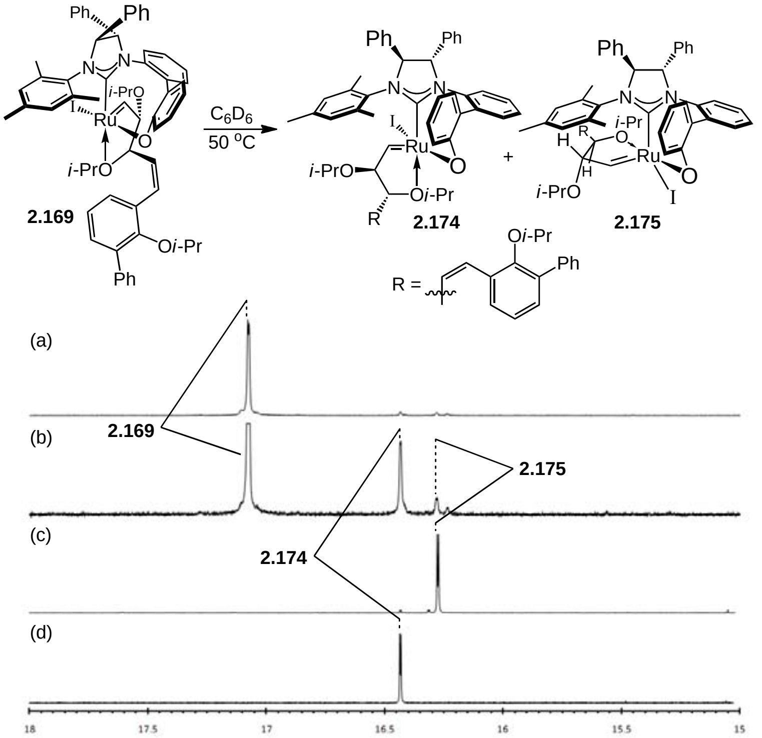

As shown in Figure 2.9, in addition to carbene **2.174**, Ru complex **2.175**, bearing *exo* carbene moiety with the pendant *iso*- propoxy group chelated *syn* to the NHC ligand, was observed in the reaction mixture. Appearance of **2.175** (^{1}H NMR peak at 16.24 ppm) is transient; following the initial increase in its relative area, the ^{1}H NMR peak at 16.24 ppm diminishes over time to give that corresponding to complex **2.174**.

Despite the transient nature of **2.175**, it was separated from other carbenes by silica gel chromatography, as **2.54**, **2.169**, and **2.174** are significantly less polar. The structure of **2.175** was confirmed by solution-phase spectroscopic studies (see the Supporting Information). The calculated structure of **2.175** was found to have a relatively larger dipole moment than the other three carbene complexes (9.49D for **14** compared to 2.76D, 3.88D, and 2.62D for **2.54**, **2.169**, and **2.174**, respectively), thus accounting for the ease of separation of **2.174** by silica gel chromatography.[90]

Figure 2.10. Plot of Forward Rates against Initial Concentrations of **2.169**. **X** = **2.169**.

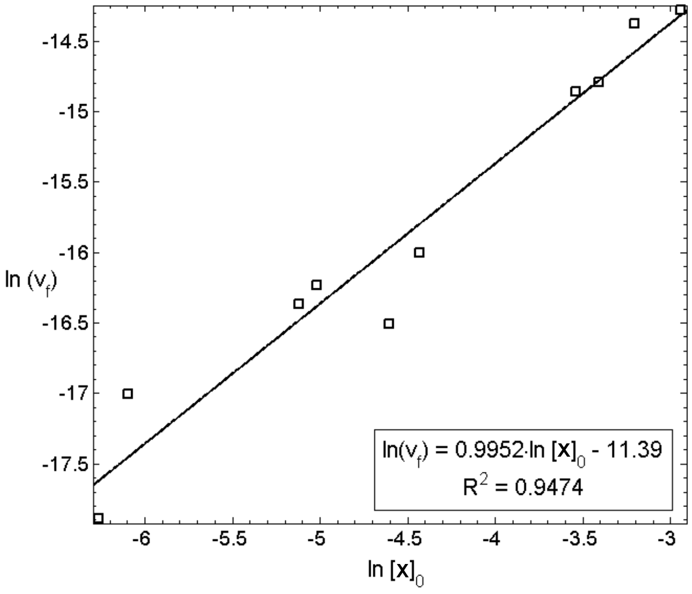

The mechanism of non-metathesis isomerization of **2.169** to **2.174** was investigated further. Thus, kinetics experiments indicated that isomerization of **2.169** is 1st order with respect to the concentration of **2.169** as illustrated in Figure 2.10. This observation is consistent with a polytopal rearrangement.

The non-metathesis unimolecular isomerization reaction of **2.169** constitutes a polytopal rearrangement of a pentacoordinate fluxional complex. The fluxional behavior of Ru complexes manifests itself in the mechanism of olefin metathesis. The cycloaddition/cycloreversion sequence within the catalytic cycle of the Ru-catalyzed olefin metathesis can be classified as a series of two Berry pseudorotations,[82] in the course of which C-C and C-Ru bonds of a metalacyclobutane are formed and broken (section 2.1.5). In competition with olefin metathesis (*i.e.* metathesis through Berry pseudorotations), non-metathesis polytopal rearrangements occur that do not involve formation or breakage of a metalacyclobutane,[87] as evidenced by the observed formation of **2.174**. The mechanism of the polytopal rearrangement of **2.169** involves a distortion to a trigonal bipyramidal geometry, in which the oxygen atom of the phenoxy ligand and the iodide ligand occupy axial positions.[87]**Error! Bookmark not defined.**[a] The facility of this distortion is augmented weaker electron donating ligands (these ligands must occupy axial position in the Berry pseudorotation intermediates).[105] Thus, the isomerization of **2.169** to **2.174** could be accelerated through coordination of Lewis acid to the oxygen atom of the phenoxy ligand; simplest Lewis acid that could be used here is a proton. Consistent with our proposal, in the presence of catalytic amounts of AcOH complex **2.169** underwent isomerization to **2.175** in 68% conversion after 1 h at ambient temperature (Scheme 2.31). To rule out the possibility that isomerization of **2.169** to **2.175** is accelerated by coordination of AcOH to the Ru center, test reactions with acetone, DMSO, and methanol were performed. In all of these reactions acceleration was not observed.

Scheme 2.31. Polytopal Rearrangements of Stereogenic-at-Ru Complexes

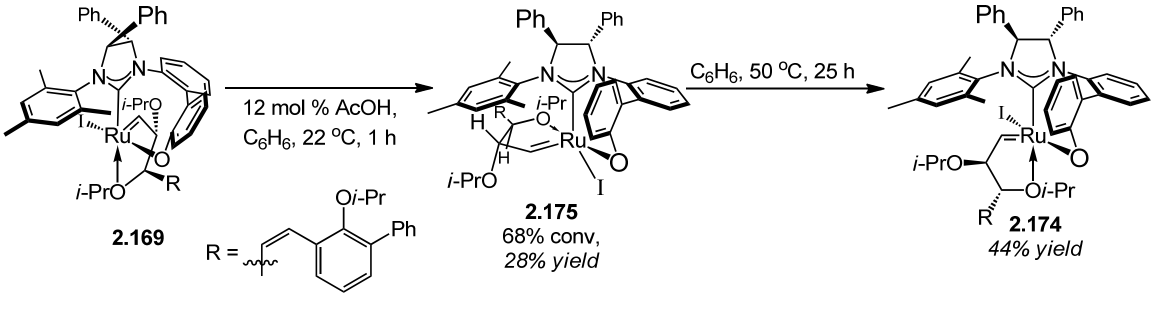

---

(105) Goldfield, S. A.; Raymond, K. N. *Inorg. Chem.* **1974**, *13*, 770-775.

The presence of protic additives did not affect the rate of isomerization of **2.175** to **2.174**, perhaps due to fact that the phenoxy ligand occupies the axial position in complex **2.175**. This isomerization reaction, however, can be effected thermally as shown in Scheme 2.31. The rearrangement **2.175→2.174** can also proceed through dissociation/association of the *iso*-propoxy ligand; however, theoretical studies of quinoline-chelated non-stereogenic-at-Ru olefin metathesis catalysts revealed that the polytopal rearrangement and dissociation/association pathways are close in energy.[91]

The rearrangement reaction **2.169→2.175** can be viewed as a net Mutterties' type 4 or type 2 rearrangement. Rearrangement **2.175→2.174** is a net Mutterties' type 2 rearrangement.[83-84] However, as was demonstrated recently, these rearrangements constitute a series of Berry pseudorotations.[86] The aforementioned acceleration of isomerization of **2.169** to **2.175** in the presence of AcOH is in agreement with the mechanism that involves Berry pseudorotations.[87a]

The observation of non-metathesis isomerization of *endo* carbenes to *exo* carbenes presented herein may account for lower enantioselectivities and yields observed for some of the less reactive cross partners[96] in enantioselective ROCM. For example, the enantioselective ROCM of strained oxabicycles (**2.176**) with styrene in the presence of the catalyst **2.52** proceeds with high enantiomeric ratio (up to 97:3 er) and good yield; however, upon substituting the cross partner for vinylcyclohexane both enantioselectivities and yields erode (Scheme 2.32).[69e] Presumably, the more slowly reacting vinylcyclohexane allows for a higher degree of isomerization of the corresponding *endo* carbene to the *exo* carbene, which undergoes a reaction with either another oxabicycle (affording oligomers, thereby decreasing the yield of the desired product) or another molecule of vinylcyclohexane, furnishing the desired product and the *endo* cyclohexylmethylidene. The latter, upon reacting with another molecule of oxabicycle, may lead to erosion of enantioselectivity, as the stereodetermining step is changed from *exo→endo* to *endo→exo*.

Scheme 2.32. Erosion of enantioselectivities and yields due to non-metathesis isomerization of carbenes.

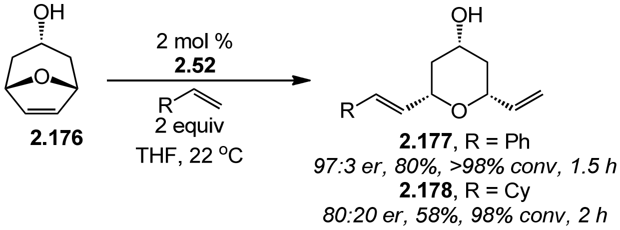

The non-metathesis isomerization of higher energy carbenes to the lower energy diastereomers may account in part for the errors in co-polymerization of norbornene and cyclooctene as observed by Chen and co-workers.[104]

An important ramification of the fact that polytopal rearrangements are operative in olefin metathesis catalysts is that *olefin coordination to Ru does not necessarily lead to a trans-to-NHC pathway and may, in fact, result in a cis-to-NHC ruthenacyclobutane.* As *cis*-to-NHC olefin coordination transition states were found to be much higher in energy, while downstream steps were determined to be energetically competitive with *trans*-to-NHC pathway, the likely cause for the erosion of enantioselectivity in enantioselective RCM desymmetrizations of 1,1-disubstituted olefins can be found in polytopal rearrangements of reactive intermediates, thereby leading to scrambling between *cis*-to-NHC and *trans*-to-NHC pathways (for the full discussion see 2.1.4.1. and 2.2).

In conclusion we have demonstrated that stereogenic-at-Ru complexes can undergo polytopal rearrangements, which account for a number of previously unexplained experimental observations. The present observations of non-metathesis polytopal rearrangements suggest new strategies for Ru-based catalyst design, in which polytopal rearrangements could be rendered faster than olefin metathesis reaction such that the catalytic system is under Curtin-Hammett control. In cases where reactivities of both diastereomeric carbenes need to be harnessed (*e.g.* enantioselective ROCM or alternating co-polymerization), rendering polytopal rearrangements significantly slower than the olefin metathesis reaction would be beneficial.

2.4. Hydrogen Bonding as a Stereocontrolling Interaction in Ru-catalyzed Diastereoselective Ring-Opening/Cross Metathesis

2.4.1. Introduction

The above study demonstrated that the presence of protic additives facilitates polytopal rearrangements between diastereomeric Ru carbenes. Olefin metathesis reaction (cycloaddition/cycloreversion) is also a series of polytopal rearrangements (Berry pseudorotations). Thus, protic additives would be expected to accelerate olefin metathesis as well. Indeed, in 1999 Hoye and co-workers observed a rate enhancement in Ru-catalyzed RCM of allylic alcohols.[106] In their report a number of hypotheses were posited to explain the 60-fold increase in the rate of RCM. Although the authors did not specify the favored hypothesis, it is in our opinion that hydrogen bonding (H-bonding) between halide ligand of Ru-complex[107] and the alcohol of the substrate presents a most viable possibility. The rest of the hypotheses are not kinetically viable, as 18-e^- Ru-complex is unlikely to form rapidly a ruthenacyclobutane,[51c] and the halide substitution with an alcohol is unfavorable[108]. Thus, if H-bonding is a true reason of reactivity enhancement, existence of an intermediate with an intramolecular H-bond can be conjectured (Scheme 2.33, **2.179**); resulting temporary ring-structure could enhance diastereoselection of subsequent reactions. On the other hand if no hydrogen bonding occurs the carbene orientation is expected to be controlled through minimization of $A_{1,3}$-strain as depicted in Scheme 2.33 (**2.180**).[109] The carbene orientation due to minimization

---

(106) Hoye, T. R.; Zhao, H. *Org. Lett.* **1999**, *1*, 1123-1125.

(107) For an example of intramolecular hydrogen bond between Ru-Cl and a pendant alcohol see: (a) Kayaki, Y.; Shimokawatoko, Y.; Ikariya, T. *Inorg. Chem.* **2007**, *46*, 5791-5797. For other examples of intramolecules hydrogen bonding with metal halides see: (b) Aullón, G.; Bellamy, D.; Brammer, L.; Bruton, E. A.; Orpen, A. G. *Chem. Commun.* **1998**, 653–654. (c) Peris, E.; Lee, J. C., Jr.; Rambo, J. R.; Eisenstein, O.; Crabtree, R. H. *J. Am. Chem. Soc.* **1995**, *117*, 3485–3491. (d) Flower, K. R.; Pritchard, R. G.; Warren, J. E. *Eur. J. Inorg. Chem.* **2003**, 1929–1938. (e) Park, Y. J.; Kim, J. –S.; Youm, K. –T.; Lee, N. –K.; Ko, J.; Park, H–s.; Jun, M–J. *Angew. Chem., Int. Ed.* **2006**, *45*, 4290–4294. (f) Ainscough, E. W.; Brodie, A. M.; Derwahl, A.; Freeman, G. H.; Otter, C. A. *Polyhedron* **2007**, *26*, 5398–5405. (g) Köcher, S.; Lutz, M.; Spek, A. L.; Walfort, B.; Rüffer, T.; van Klink, G. P. M.; van Koten, G.; Lang, H. *J. Organomet. Chem.* **2008**, *693*, 2244–2250.

(108) Fagnou, K.; Lautens, M. *Angew. Chem. Int. Ed.* **2002**, *41*, 26-47.

(109) For a review on $A_{1,3}$-strain as a controlling factor in stereoselective transformations see: Hoffmann, R. W. *Chem. Rev.* **1989**, *89*, 1841-1860.

Scheme 2.33. Carbene Orientations Controlled by Hydrogen Bonding or $A_{1,3}$-Strain

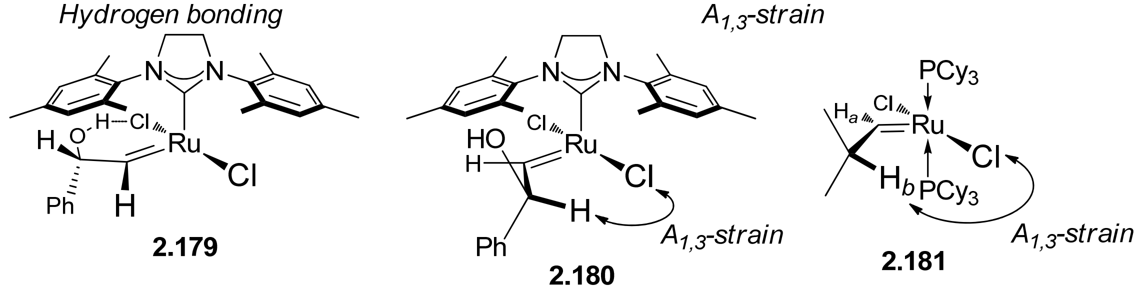

of $A_{1,3}$-strain is consistent with the observation that ^{1}H NMR coupling constant between the methine H_b and carbene proton H_a in **2.181** is 10.2 Hz, whereas the same coupling in the corresponding terminal alkene (3-methylbut-1-ene) is 6.6 Hz.[96] This observation is consistent with the *anti* relationship between H_a and H_b in **2.181**. Relative stereochemical identity of a product from the downstream transformation thus can serve as a marker for presence or absence of hydrogen bonding in the relevant intermediates and transition states. Ring-opening metathesis as a downstream transformation would provide the maximum amount of information regarding the intermediacy of carbenes such as **2.179**, because formation of either *E* or *Z* olefins is possible, and stereochemical identity of each olefin stereoisomer can be helpful in determining the mode of the reaction. The overall transformation would constitute a substrate-directed diastereoselective ring-opening cross metathesis (DROCM) – an unprecedented transformation for a number of reasons.[110]

Unlike the previously disclosed diastereoselective olefin metathesis reactions,[111] in which steric interactions were utilized to effect stereoselective ring-closing metathesis transformations, the use of hydrogen bonding as a catalyst-directing interaction in the present study is unprecedented in olefin metathesis. Furthermore, the present study constitutes the first example of diastereoselective ring-opening/cross metathesis (DROCM).

---

(110) For reviews on substrate-directed reactions see: (a) Sawamura, M.; Ito, Y. *Chem. Rev.* **1992**, *92*, 851-871. (b) Hoveyda, A. H.; Evans, D. A.; Fu, G. C. *Chem. Rev.* **1993**, *93*, 1307-1370.

(111) For a full discussion of diastereoselective olefin metathesis see Section 2.1.4.2 and Refs. 75-78.

2.4.2. Substrate-Directed Diastereoselective Ring-Opening/Cross Metathesis

To test the above hypothesis the effect of *α*-hydroxyl group within a cross partner in DROCM was assessed (Scheme 2.34). Ring-opening/cross metathesis reaction of cyclopropene **2.182** with 1-octene gave **2.183** in 83% conv after 4 h; however, substitution of the alkyl chain for a hydroxymethylene group (allyl alcohol) improved reaction efficiency such that reaction was complete[112] after *5 min* in the presence of only *0.5 mol %* of **2.15**. Incorporation of the *α*-stereogenic center into the cross partner (*R*-**2.185**) as a marker for presence of hydrogen bonding in the relevant stereodetermining transition state did not diminish reaction efficiency; DROCM of **2.182** with *R*-**2.185 in** the presence of the catalyst **2.15** afforded *S*,*R*-**2.186** in 87% yield and 96:4 dr after 5 min. On the other hand, employment of substrates lacking in *α*-hydroxyl group significantly diminished the reaction efficiency and most importantly, in concert with the above

Scheme 2.34. Effect of Hydrogen Bonding on ROCM Reaction Efficiency

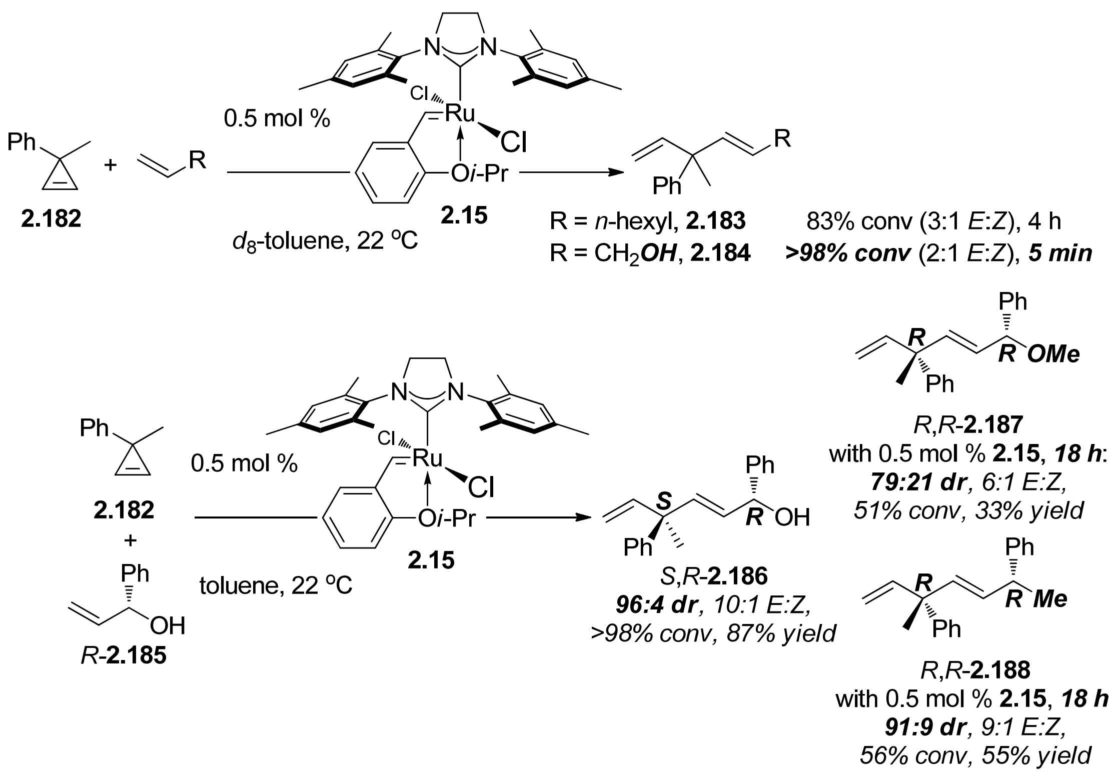

---

(112) As judged by the ratio of starting material and internal standard peak areas in ^{1}H NMR spectrum of an unpurified reaction mixture.

Table 2.2. Ru-Catalyzed DROCM of Cyclopropenes and Enantiomerically Enriched Chiral Allylic Alcohols[a]

entry	reaction	mol % **2.15**; time	yield (%)[b]	*E*:*Z*[c]	*dr*[d]
1	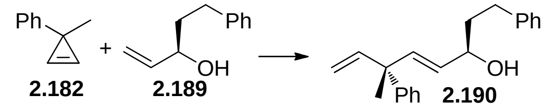 **2.182** + **2.189** → **2.190**	0.5; 15 min	80	4:1	91:9
2	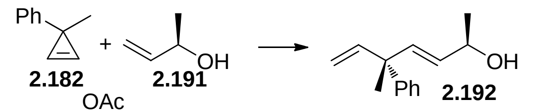 **2.182** + **2.191** → **2.192**	0.5; 15 min	64	6:1	95:5
3	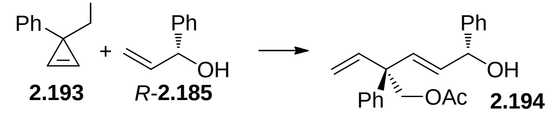 **2.193** + *R*-**2.185** → **2.194**	5.0; 4 h[e]	80	8:1	95:5
4	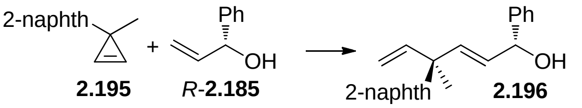 **2.195** + *R*-**2.185** → **2.196**	0.5; 5 min	76	10:1	96:4
5	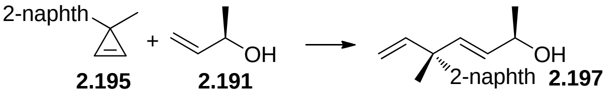 **2.195** + **2.191** → **2.197**	0.5; 15 min	84	6:1	97:3
6	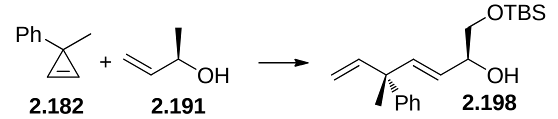 **2.182** + **2.191** → **2.198**	0.5; 15 min	71	11:1	89:11

[a] All reactions were run under dry N_2 atmosphere at 22 °C in dry and degassed toluene. For experimental details, including enantiomeric purity of chiral allylic alcohols see the supporting information. [b] Yields of purified products (*E*/*Z* mixtures). [c] Based on analysis of 400 MHz ^{1}H NMR spectra of unpurified reaction mixtures. [d] Based on HPLC analysis of the *E* olefin products. [e] Chiral allylic alcohol was added slowly *via* syringe pump.

hypothesis, resulted in formation of products with the opposite relative sense of stereochemical identity (*R*,*R*-**2.187** and *R*,*R*-**2.188**). Similarly high reaction efficiencies and high diastereoselectivities were observed with other cyclopropenes and chiral allylic alcohols (Table 2.2).

In support of H-bonding hypothesis theoretical studies (DFT) on reactive intermediates were carried out. The effect of H-bonding is most pronounced on H of alcohol, as the O-H bond is polarized by interaction with Cl. Unexpectedly, H-bonding interaction results in higher charge on carbene C, rendering it more electrophilic, while olefinic C_{sp^2} atoms of cyclopropene became more nucleophilic, as evidenced by diminished corresponding positive charge. Thus, formation of ruthenacyclobutane is likely to be facilitated if in the transition state leading to ruthenacyclobutane the

Figure 2.11. Stereochemical Model and Charges (APT) in Ru-catalyzed DROCM

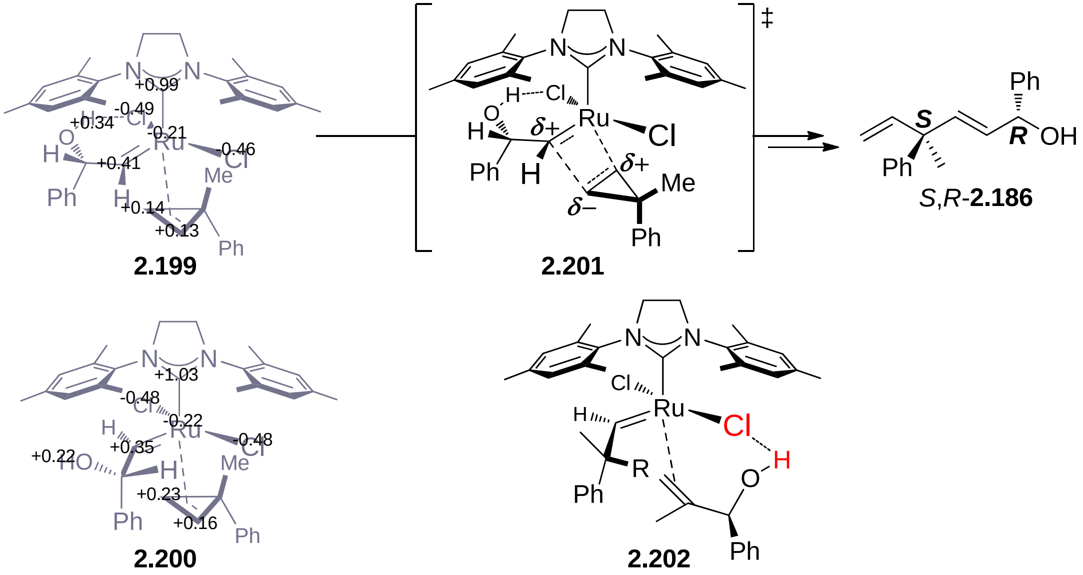

cyclopropene π-cloud attacks partially populated through backbonding p-orbital of carbene, and the resulting δ+ on C_{sp^2} of cyclopropene (C_α of ruthenacyclobutane) is trapped by filled d-orbital of Ru of appropriate symmetry (Figure 2.11). Resulting ruthenacyclobutane bears relative δ+ and δ- charges on C_α and C_β respectively – consistent with the observed ^{1}H-NMR chemical shifts for ruthenacyclobutane.[50j] Ruthenacyclobutane intermediate structures were not analyzed as corresponding stationary points were not located, probably due to nearly barrierless reorganization of ruthenacyclobutane structures to either the starting Ru-carbene olefin complex or the resulting ring-opened Ru complex. It should be noted that the overall reaction rate acceleration is most likely not due to lowering of the transition state **2.201**, but instead due to facilitation of coordination (possibly through associative mechanism) of the chiral allylic alcohol **2.185** to Ru complex through hydrogen bonding, thereby leading to **2.202**.

To test the H-bonding hypothesis reactions were performed with protic additives. As illustrated in Table 2.3, presence of 10 equiv of protic additives did not result in a significantly diminished diastereoselectivities; however, reaction efficiencies suffered, particularly, with the sterically hindered t-butanol. It is likely that the protic additives do not disrupt the hydrogen bond between the allylic alcohol and instead sterically hindered additives slow down the reaction, as they compete more efficiently with chiral allylic alcohols for *intermolecular* hydrogen bonding with halides of the Ru complex.

Table 2.3. Effect of Protic Additives on Ru-catalyzed DROCM of **2.182**[a]

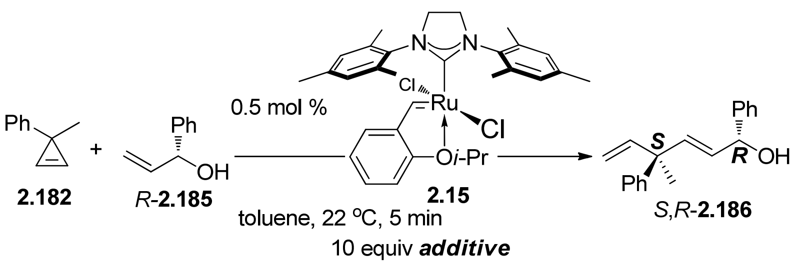

entry	additive	conv (%)[b]	*E*:*Z*[b]	dr[c]
1	none	>98	10:1	96:4
2	*t*-BuOH	38	9:1	94.5:5.5
3	H_2O	88	8:1	93.5:6:5

[a] See the supporting information for experimental details; the additive was first mixed mixed with a solution of Ru complex prior to addition of the substrates. [b] Based on analysis of 400 MHz ^1H NMR spectra of unpurified reaction mixtures. [c] Based on HPLC analysis.

The present method is not limited to cyclopropenes; other strained olefins undergo DROCM with similar efficiencies (Table 2.4). As shown in Table 2.4, DROCM of TBS-protected cyclobutenediol **2.203** with *R*-**2.185** in the presence of the catalyst **2.204** affords the desired product in high yield with good diastereoselectivity; however, the *E* and *Z* diastereomers result from the carbene addition to the different C_{sp^2}-centers of cyclobutene (Figure 2.12), thereby leading to formation of *S*,*R*,*R*-**2.205** and *R*,*S*,*R*-**2.206** – ROCM products with opposite formed in the course of the reaction stereogenic centers. Reactions in the presence of **2.15** proved to be as efficient as those with **2.204**, but difficult to monitor as the likely competitive cross-metathesis of the cross partner with the desired product generates the *meso*-byproduct thus diminishing the yield. Therefore, **2.204** was chosen as an optimal catalyst for this transformation. As illustrated in Table 2.4, reactions with Bn-protected cyclobutene and pyrazolidine **2.211** are also highly diastereoselective and efficient (entries 1 and 3). Interestingly, preference for the formation of the *Z*-DROCM product was observed for **2.209** and **2.210**. However, relative stereochemical identity of the products does not permit extension of the mode

Table 2.4. Ru-Catalyzed DROCM of Strained Olefins and Enantiomerically Enriched Chiral Allylic Alcohols[a]

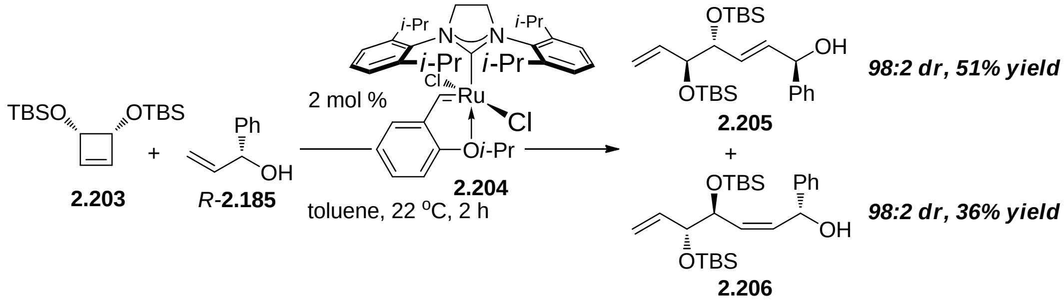

entry	time	*E* product	yield (%)[b]	*dr*[c]	*Z* product	yield (%)[b]	*dr*[c]
1	2 h	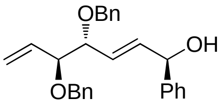 **2.207**	45	98:2	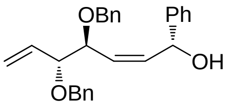 **2.208**	36	97:3
2	2 h	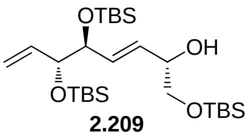 **2.209**	27	90:10	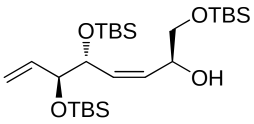 **2.210**	48	83:17
3	2.5 h	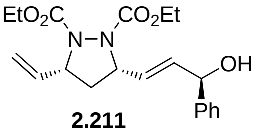 **2.211**	46	>98:2	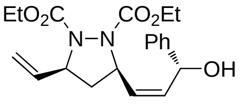 **2.212**	27	>98:2

[a] All reactions were run under dry N_2 atmosphere at 22 °C in dry and degassed toluene. [b] Yields of purified products. [c] Based on HPLC analysis.

Scheme 2.35. Ru-Catalyzed DROCM of Cyclobutene in the Absence of α-Hydroxyl Group

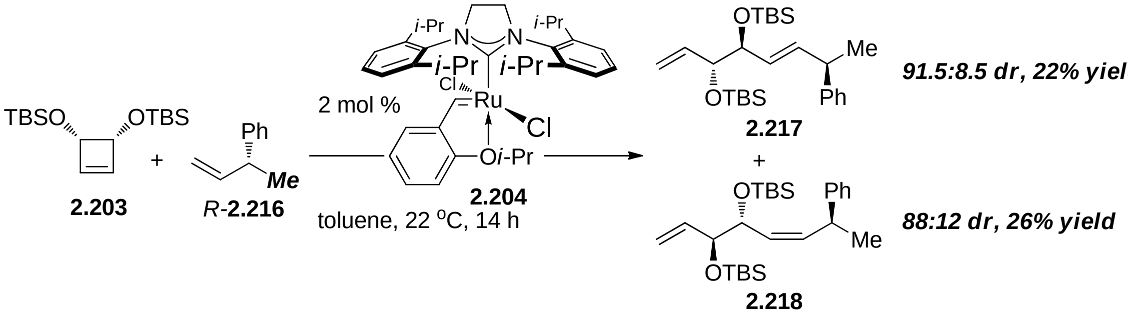

proposed by Snapper and co-workers for *Z*-selective ring-opening/cross metathesis of cyclobutenes.[64c]

To test whether hydrogen bonding interaction is responsible for the observed diastereoselectivities the reaction with (*R*)-phenylbutene (**2.216**) was tested (Scheme 2.35). This reaction proved to be less efficient than the corresponding reaction with allylic alcohol *R*-**2.185**, requiring 14 h for the former against 2 h for the latter. Most importantly, the relative stereochemistry of the products was consistent with the model based on minimization of $A_{1,3}$-strain (Scheme 2.33).

The mechanistic model for DROCM of cyclobutenes is similar to that of cyclopropenes (Figure 2.12). The Ru-alkene complex in its ground state bears the alkene in inactive conformation, wherein the *π*-cloud of cyclobutene is not in alignment with Ru-carbene for cycloaddition to take place. Upon rotation of the cyclobutene either *syn* or *anti* ruthenacyclobutanes are generated, which upon cycloreversion afford either *Z*- or *E*-alkene.

Figure 2.12. Formation of *E* and *Z* Diastereomers in DROCM of Cyclobutenes

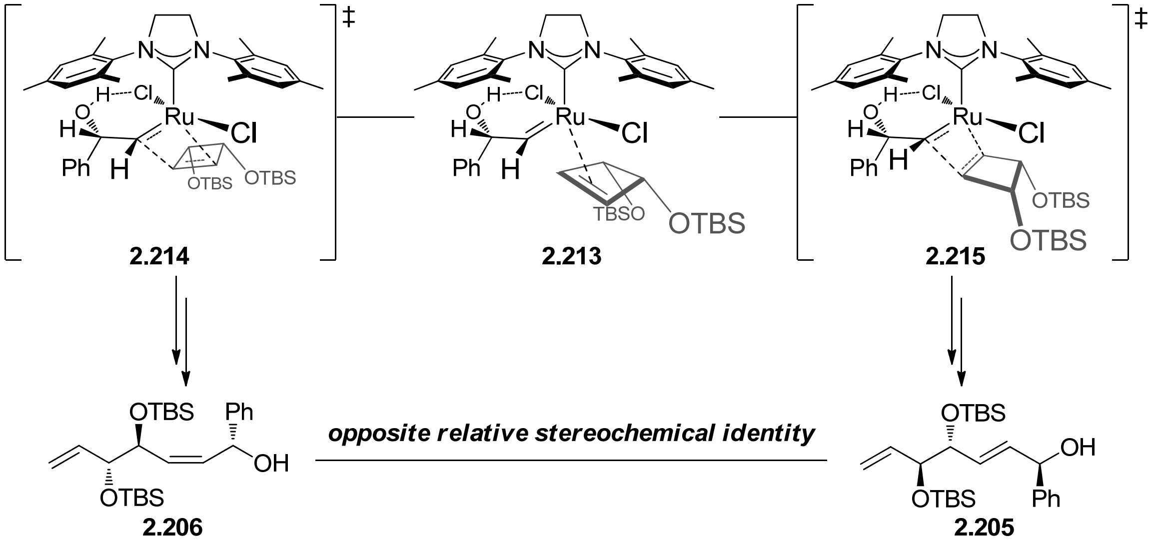

2.4.3. *Conclusion*

In conclusions the study presented herein demonstrated that hydrogen bonding can be utilized as a secondary directing interaction in diastereoselecting ring-opening/cross metathesis. Relative stereochemical identity of desymmetrization products was utilized as a marker for presence of hydrogen bonding interactions in relevant transition states and intermediates. Furthermore, by confirming that hydrogen bonding occurs in the course of Ru-catalyzed olefin metathesis (*i.e.* Berry pseudorotations) the hypothesis that acceleration of non-metathesis isomerization (Section 2.3) due to hydrogen bonding with AcOH is supported.

2.5. Experimental

2.5.1. General Information

Infrared (IR) spectra were recorded on a Bruker alpha spectrophotometer (ATR mode), $\tilde{\nu}_{\max}$ in cm^{-1}. Bands are characterized as broad (br), strong (s), medium (m), or weak (w). ^{1}H NMR spectra were recorded on a Varian Unity INOVA 400 (400 MHz) spectrometer. Chemical shifts are reported in ppm from tetramethylsilane with the solvent resonance resulting from incomplete deuteration as the internal standard ($CDCl_3$: δ 7.26 ppm). Data are reported as follows: chemical shift, integration, multiplicity (s = singlet, d = doublet, t = triplet, q = quartet, br = broad, m = multiplet), and coupling constants (Hz). For clarity ^{1}H NMR peaks are treated as first-order coupled spin systems; strongly coupled ^{1}H NMR spectra are reported following Pople notation[113] where possible. ^{13}C NMR spectra were recorded on a Varian Unity INOVA 400 (100 MHz) spectrometer with complete proton decoupling. Chemical shifts are reported in ppm from tetramethylsilane with the solvent resonance as the internal standard ($CDCl_3$: δ 77.16 ppm). High-resolution mass spectrometry analysis was performed on a Micromass LCT ESI-MS (positive mode) at the Mass Spectrometry Facility, Boston College. Enantiomeric ratios of starting materials and diastereomeric ratios of products were determined by GLC analysis (Alltech Associated Chiraldex GTA column (30 m x 0.25 mm) or Betadex 120 column (30 m x 0.25 mm)) or HPLC analysis (Daicel Chiracel/Chiralpak OD, AS, OJ-H, and AD columns) in comparison with authentic racemic materials. For GLC analysis, the inlet and detector temperatures were set to 250 °C and runs were isothermal of the temperature given using ultra high purity helium as the carrier gas. Specific rotations were measured on a Rudolph Research Analytical Autopol IV Polarimeter.

---

(113) Bernstein, H. J.; Pople, J. A.; Schneider, W. G. *Can. J. Chem.* **1957**, *35*, 65–81.

Unless otherwise noted, all reactions were carried out with distilled and degassed solvents under an atmosphere of dry N_2 in oven (135 °C) or flame-dried glassware with standard dry box or vacuum-line techniques. Solvents were purified under a positive pressure of dry Ar by a modified Innovative Technologies purification system: toluene, benzene and pentane were purified through a copper oxide and alumina column; CH_2Cl_2 and Et_2O were purged with Ar and purified by passage through two alumina columns. Tetrahydrofuran (Aldrich) was purified by distillation from sodium benzophenone ketyl immediately prior to use unless otherwise specified. All work-up and purification procedures were carried out with reagent grade solvents (purchased from Doe & Ingalls) under air.

2.5.2. Chiral Imidazolinium Salts

Preparation of Chiral Imidazolinium Salts from (S,S)-DPEDA

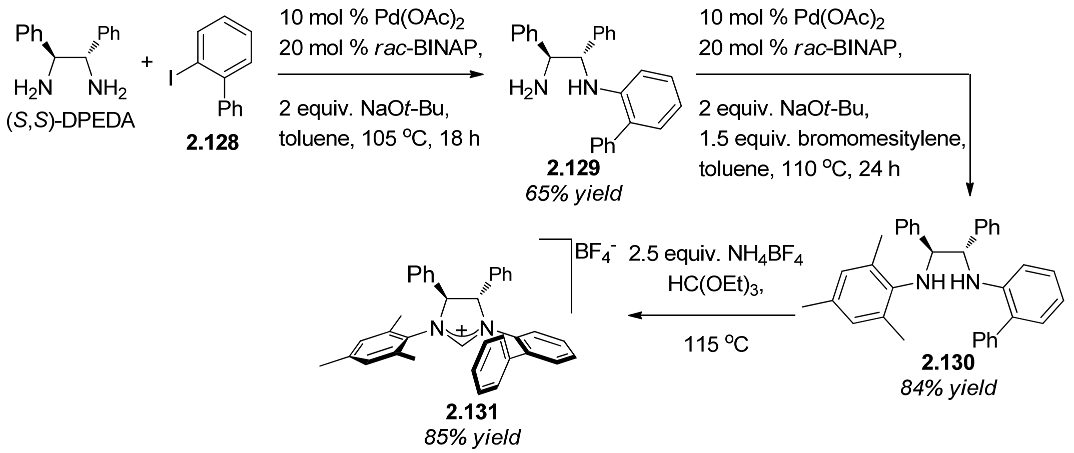

Imidazolinium Tetrafluoroborate 2.131 was prepared by the following sequence: Under dry N_2 atmosphere in a flame-dried round bottom flask, equipped with a flame-dried reflux condenser were mixed (*S*,*S*)-DPEDA (1.4996 g, 7.0735 mmol, 1.00 equiv.), $Pd(OAc)_2$ (165.9 mg, 0.7390 mmol, 0.10 equiv.), *rac*-BINAP (898.1 mg, 1.442 mmol, 0.20 equiv.), iodobiphenyl **2.128** (2.0857 g, 7.4224 mmol, 1.05 equiv.), NaO*t*-Bu (1.5015 g, 15.623 mmol, 2.21 equiv.), and 47 mL of toluene. The resulting mixture was allowed to stir at 105 °C for 18 h, at which time the mixture was allowed to cool to 22 °C, diluted with H_2O (~20 mL). Layers were separated, and aqueous layer was washed 3x with Et_2O. Combined organic layers were dried over anhydrous $MgSO_4$, filtered, and concentrated *in* *vacuo* to give brown oil. Purification by silica gel chromatography (4:1 Petroleum Ether:EtOAc) afforded diamine **2.129** as an off-white solid (2.2236 g, 6.129 mmol, 87% yield). ^{1}H NMR ($CDCl_3$, 400 MHz): δ 7.55-7.50 (2H, m), 7.46-7.39 (3H, m), 7.35-7.31 (4H, m), 7.29-7.21 (4H, m), 7.19-7.16 (2H, m), 7.03 (1H, dd, J = 7.4, 1.7 Hz), 6.96 (1H, ddd, J = 7.2, 7.4, 1.7 Hz), 6.62 (1H, ddd, J = 7.4, 7.4, 1.1 Hz), 6.21 (1H, dd, J = 8.2, 0.9 Hz), 5.34 (1H, d, J = 5.6 Hz), 4.48 (1H, dd, J = 5.5, 3.8 Hz), 4.30 (1H, d, J = 3.6 Hz), 1.17 (2H, s). Diamine **2.129** was converted to diamine **2.130** following a modified procedure described for **2.129**. Purification of **2.130** was carried out by silica gel chromatography (20:1 Petroleum Ether:EtOAc). ^{1}H NMR ($CDCl_3$, 400 MHz) δ 7.53–7.47 (2H, m), 7.45–7.38 (2H, m), 7.36–7.30 (2H, m), 7.20–7.02 (10H, m), 6.86–6.80 (2H, m), 6.74 (1H, ddd, J = 7.4, 7.4, 1.1 Hz), 6.59 (2H, s), 6.47 (1H, d, J = 7.6 Hz), 5.61 (1H, d, J = 3.3 Hz), 4.75 (1H, dd, J = 7.8, 3.4 Hz), 4.28 (1H, d, J = 7.8 Hz), 3.38 (1H, s), 2.10 (3H, s), 1.90–1.83 (6H, s). Diamine **2.130** (1.2467 g, 2.5811 mmol, 1.00 equiv) and NH_4BF_4 (682.3 mg, 6.508 mmol, 2.52 equiv.) were suspended in freshly distilled $HC(OEt)_3$ (7 mL) in a flame-dried flask under dry N_2 atmosphere. A needle was inserted into the septum on the flask, and the mixture inside was allowed to stir at 115 ^{o}C for 4 h, at which time excess $HC(OEt)_3$ was removed *in vacuo* to give brown oil. Purification by silica gel chromatography (1:1 Petroleum Ether:EtOAc → 100% EtOAc), followed by trituration from CH_2Cl_2/petroleum ether gave imidazolinium tetrafluoroborate **2.131** as a white powder, which was dried in Abderhalden apparatus under high vacuum over refluxing 2-propanol for 24 h (1.2783 g, 2.2001 mmol, 85% yield). IR (neat): 3049 (w), 2936 (w), 2854 (w), 1633 (s), 1482 (m), 1457 (m), 1274 (m), 1211 (m), 1060 (m), 909 (w), 859 (w), 758 (m), 733 (s), 708 (s) cm^{-1}; ^{1}H NMR ($CDCl_3$, 400 MHz): δ 8.79 (1H, s), 7.85–7.79 (1H, m), 7.70–7.62 (3H, m), 7.49 (2H, ddd, J = 7.6, 4.2, 2.9 Hz), 7.45–7.32 (5H, m), 7.31 – 7.22 (4H, m), 7.14 (2H, dd, J = 10.6, 4.9 Hz), 6.92 (1H, s), 6.67 (1H, s), 6.62–6.54 (2H, m), 5.42 (1H, B of AB, J_{AB} = 9.7 Hz), 5.26 (1H, A of AB, J_{AB} = 9.6 Hz), 2.54 (3H, s), 2.20 (3H, s), 1.82 (3H, s); ^{13}C NMR (CDCl3, 100 MHz): δ 158.4, 140.2, 139.0, 138.0, 135.5, 135.1, 135.0, 132.3, 131.8, 131.2, 130.7, 130.4, 130.2, 130.1, 130.1, 130.0, 129.9, 129.8, 129.8, 129.5, 129.1, 128.9, 128.8, 128.7, 128.0, 75.1, 72.7, 21.1, 19.3, 18.4; HRMS Calcd for $C_{36}H_{33}N_2$ [M-BF_4] (ES+): 493.2644, Found: 493.2645.

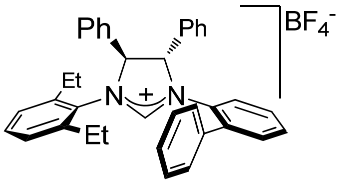

2.219

Imidazolinium Tetrafluoroborate 2.219 was prepared following the same procedure as described for **2.131**. Characterization data is available elsewhere.[114]

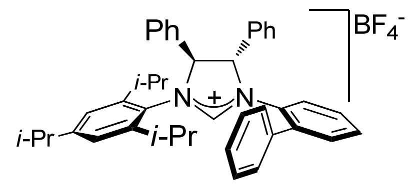

2.220

Imidazolinium Tetrafluoroborate 2.220 was prepared following the same procedure as described for **2.131**. IR (neat): 3061 (m), 2964 (s), 2930 (m), 2871 (m), 1617 (s), 1457 (s) cm^{-1}; ^1H NMR ($CDCl_3$, 400 MHz): δ 8.93 (1H, s), 7.77–7.65 (6H, m), 7.54–7.46 (3H, m), 7.43–7.32 (8H, m), 7.30–7.20 (6H, m), 7.12 (3H, dd, J = 7.8, 7.8 Hz), 7.08 (1H, d, J = 2.0 Hz), 6.78 (1H, d, J = 2Hz), 6.36 (2H, d, J = 7.2 Hz), 5.29 (1H, B of AB, J_{AB} = 9.6 Hz), 5.22 (1H, A of AB, J_{AB} = 9.6 Hz), 3.22 (1H, septet, J = 6.8 Hz), 2.83 (1H, septet, J = 6.8 Hz), 2.42 (1H, septet, J = 6.8 Hz), 1.52 (3H, d, J = 6.4 Hz), 1.39 (3H, d, 6.8 Hz), 1.21–1.17 (9H, m), 0.38 (3H, d, J = 6.8 Hz); ^{13}C NMR ($CDCl_3$, 100 MHz): δ 157.7, 151.9, 146.5, 145.8, 139.1, 138.3, 134.7, 131.4, 131.2, 130.4, 130.4, 130.3, 129.9, 129.8, 129.7, 129.3, 128.9, 128.8, 127.6, 125.3, 123.2, 122.6, 72.5, 34.2, 29.5, 28.9, 26.0, 25.1, 24.6, 23.8, 23.8, 22.4; HRMS Calcd for $C_{42}H_{45}N_2$ [M-BF_4] (ES^+): 577.3583, Found: 577.3603. Optical rotation: $[\alpha]_D^{20}$ -242.2 (*c* 1.00, $CHCl_3$).

---

(114) Lee, K.; Hoveyda, A. H. *J. Org. Chem.* **2009**, *74*, 4455-4462.

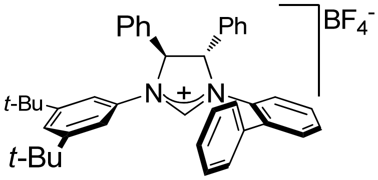

2.221

Imidazolinium Tetrafluoroborate 2.221 was prepared following the same procedure as described for **2.131**. IR (neat): 3066 (m), 2963 (s), 2871 (m), 1619 (s), 1586 (s), 1458 (s) cm^{-1}; ^{1}H NMR ($CDCl_3$, 400 MHz): δ 9.23 (1H, s), 7.62–7.57 (1H, m), 7.53–7.47 (2H, m), 7.47–7.40 (3H, m), 7.39–7.33 (6H, m), 7.33–7.31 (2H, m), 7.31–7.27 (2H, m), 7.27–7.25 (1H, m), 7.20–7.14 (2H, m), 7.03–7.00 (2H, m), 6.97–6.92 (2H, m), 5.59 (1H, d, J = 9.0 Hz), 4.76 (1H, d, J = 9.0 Hz), 1.20 (18H, s); ^{13}C NMR ($CDCl_3$, 100 MHz): δ 155.33, 153.17, 138.14, 137.86, 135.18, 133.94, 133.88, 131.84, 131.31, 130.37, 130.15, 129.91, 129.78, 129.69, 129.56, 129.38, 129.26, 128.61, 128.16, 127.29, 122.73, 115.91, 75.96, 74.74, 35.24, 31.19; HRMS Calcd for $C_{41}H_{43}N_2$ [M-BF_4] (ES$^+$): 563.3426, Found: 563.3411. Optical rotation: $[\alpha]_D^{20}$ –221.0 (c 1.00, $CHCl_3$).

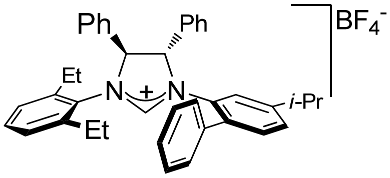

2.222

Imidazolinium Tetrafluoroborate 2.222 was prepared following the same procedure as described for **2.131**. Characterization data is available elsewhere.[114]

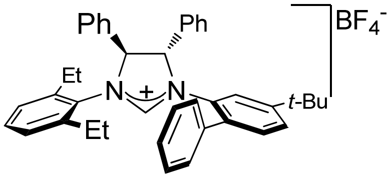

2.223

Imidazolinium Tetrafluoroborate 2.223 was prepared following the same procedure as described for **2.131**. Characterization data is available elsewhere.[114]

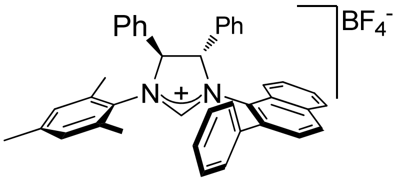

2.224

Imidazolinium Tetrafluoroborate 2.224 was prepared following the same procedure as described for **2.131** from 1-iodo-2-phenylnaphthalene[115] and was isolated a mixture of rotomers (50:1). The data below is only for the major rotomer. IR (ATR mode): 3055 (w), 2920 (w), 1616 (s), 1603 (m), 1495 (w), 1455 (w), 1370 (w), 1269 (m), 1179 (m), 1163 (s), 1066 (s), 1021 (s), 999 (m), 971 (m), 888 (m), 862 (m), 830 (m), 767 (s), 753 (s), 740 (w), 730 (m), 710 (m), 699 (s), 654 (w), 647 (w), 636 (m), 619 (w), 603 (w) cm^{-1}; ^{1}H NMR (CDCl$_3$, 400 MHz): δ 9.13 (1H, s), 7.88 (2H, dd, J = 8.2, 5.5 Hz), 7.81–7.73 (7H, m), 7.65–7.58 (1H, m), 7.51–7.44 (1H, m), 7.41 (1H, d, J = 8.4 Hz), 7.32–7.26 (1H, m), 7.20–7.14 (3H, m), 7.14–7.08 (5H, m), 6.97 (1H, s), 6.72 (1H, s), 6.48 (2H, d, J = 7.3 Hz), 5.63 (1H, d, J = 11.7 Hz), 5.33 (1H, d, J = 11.8 Hz), 2.75 (3H, s), 2.21 (3H, s), 1.85 (3H, s); ^{13}C NMR (CDCl$_3$, 100 MHz); δ 159.00, 140.58, 139.16, 137.52, 136.73, 133.95, 133.54, 132.46, 131.16, 131.06, 131.00, 130.65, 130.45, 130.21, 130.17, 129.74, 129.59, 129.35, 129.09, 128.89, 128.71, 128.64, 128.58, 128.40, 127.83, 127.25, 126.84, 121.35, 74.02, 72.59, 21.12, 19.24, 18.16.

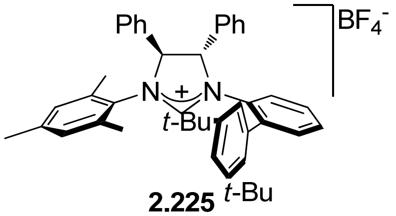

2.225

Imidazolinium Tetrafluoroborate 2.225 was prepared following the same procedure as described for **2.131**. Characterization data is available elsewhere.[114]

---

(115) Yue, D.; Cà, N. D.; Larock, R. C. *Org. Lett.* **2004**, *6*, 1581-1584.

Preparation of Chiral Imidazolinium Salts from Aminoalcohols

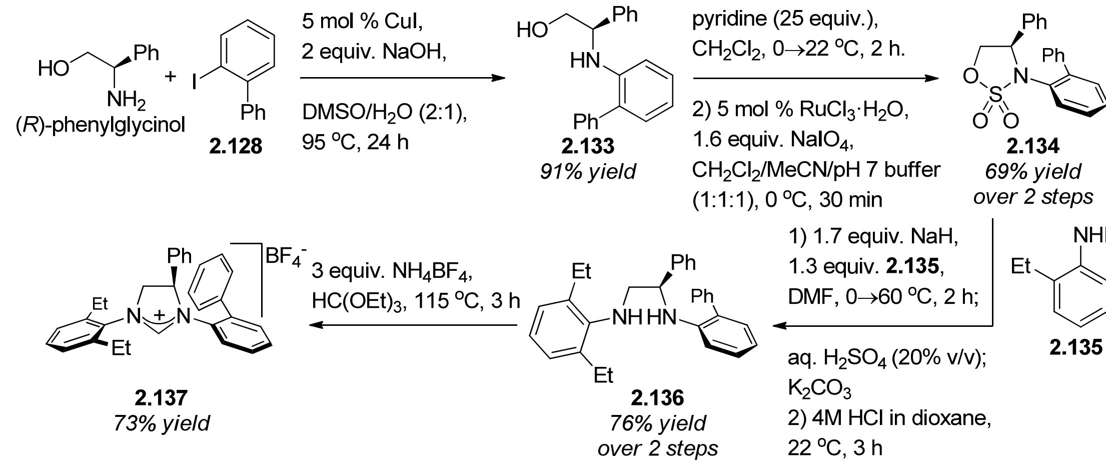

Imidazolinium Tetrafluoroborate 2.137 was prepared through the following sequence: In a vial were mixed (*R*)-phenylglycinol (558.1 mg, 4.068 mmol 1.00 equiv), iodobiphenyl **2.128** (1.3989 g, 4.9943 mmol, 1.23 equiv), CuI (54.0 mg, 0.283 mmol, 0.0696 equiv), NaOH (332.4 mg, 8.310 mmol, 2.07 equiv). The vial was purged with N$_2$, and DMSO and water were added *via* syringe. The vial was capped with a cap and the mixture was allowed to stir at 95 °C for 24 h, at which time the mixture was allowed to cool to 22 °C, diluted with H$_2$O (4 mL) and washed 3x with CH$_2$Cl$_2$. Combined organic layers were washed 3x with aqueous 0.1M NaOH, brine, dried over anhydrous MgSO$_4$, filtered, and concentrated *in vacuo* to give colorless oil. Purification by silica gel chromatography (4:1 Petroleum Ether:EtOAc) afforded **2.133** as a colorless oil (978.5 mg, 3.381 mmol, 83% yield). ^{1}H NMR (CDCl$_3$, 400 MHz): δ 7.49 (4H, d, J = 4.5 Hz), 7.42–7.38 (m, 1H), 7.37–7.24 (5H, m), 7.13–7.05 (2H, m), 6.76 (1H, ddd, J = 7.4, 7.4, 1.1 Hz), 6.52 (1H, d, J = 8.0 Hz), 4.73 (s, 1H), 4.53 (s, 1H), 3.85–3.81 (1H, m), 3.66–3.63 (1H, m), 1.59 (1H, br s). Thionyl chloride (1.6 mL, 21.9 mmol, 1.65 equiv) and anhydrous pyridine (27 mL, $3.3 \cdot 10^2$ mmol, 25 equiv) were added to CH$_2$Cl$_2$ (20 mL) at 0 °C. A solution of **2.133** (3.8389 g, 13.28 mmol, 1.00 equiv) in CH$_2$Cl$_2$ (100 mL) was added dropwise through an addition funnel with vigorous stirring at 0 °C. The funnel was rinsed with 13 mL of CH$_2$Cl$_2$, and the resulting mixture was allowed to warm slowly to 22 °C with stirring. After 2 h water was added to the mixture. Layers were separated, and aqueous layer was washed 3x with CH$_2$Cl$_2$. Combined organic layers were washed with brine, dried over anhydrous $MgSO_4$, filtered, and concentrated *in vacuo* to give a mixture of diastereomeric cyclic sulfimidates as a light yellow oil, which was used without further purification assuming quantitative yield. In a round bottom flask the mixture of diastereomeric cyclic sulfimidates was dissolved in CH_2Cl_2 (30 mL) and acetonitrile (30 mL). To this mixture are 0 ^{o}C was added with vigorous $RuCl_3{\cdot}H_2O$ (138.4 mg, 0.6672 mmol, 0.050 equiv.). The mixture was allowed to stir for 10 min before $NaIO_4$ (4.5468 g, 21.258 mmol, 1.60 equiv.) and pH 7 buffer solution (30 mL) were added. After 20 mins the reaction mixture was allowed to warm to 22 ^{o}C, and filtered through a pad of Celite. Residual solids on the Celite were rinsed with dichloromethane. Combined filtrates were washed with brine, dried over anhydrous $MgSO_4$, filtered, and concentrated *in vacuo* to give brown oil, which was filtered through a pad of silica gel with CH_2Cl_2 to remove Ru impurities, affording a cyclic sulfamidate **2.134** as a light yellow oil that solidifies upon standing (3.2137 g, 9.156 mmol, 69% yield over two steps). ^{1}H NMR ($CDCl_3$, 400 MHz) δ 7.71–7.69 (1H, m), 7.51–7.41 (5H, m), 7.35–7.26 (2H, m), 7.20 (4H, dddd, J = 10.2, 8.7, 3.4, 2.0 Hz), 7.01–6.95 (2H, m), 4.58 (1H, dd, J = 8.5, 6.9 Hz), 4.49 (1H, dd, t, J = 7.0, 7.0 Hz), 4.34 (1H, dd, J = 8.5, 7.3 Hz). Under dry N_2 atmosphere in a flame-dried round bottom flask were mixed at 0 ^{o}C NaH (71.6 mg, 2.98 mmol, 1.72 equiv) and 2 mL of dry DMF with stirring. Then, Boc-protected aniline **2.135** (572.9 mg, 2.30 mmol, 1.33 equiv) was added dropwise with stirring as a solution in 5 mL of dry DMF. Resulting mixture was allowed to stir at 0 ^{o}C for 30 min, at which time sulfamidate **2.134** (607.5 mg, 1.73 mmol, 1.00 equiv) was added as a solution in 10 mL of dry DMF. Resulting mixture was allowed to stir at 60 ^{o}C for 2 h, at which time it was allowed to cool to 0 ^{o}C, and excess NaH was quenched by dropwise addition of H_2O, followed by dropwise addition of 15 mL of aqueous H_2SO_4 (20% v/v). The mixture was allowed to stir at 80 ^{o}C for 2 h, at which time it was allowed to cool to 0 ^{o}C and pH of the mixture was adjusted to 10 by slow addition of sat. aq. K_2CO_3. Resulting mixture was filtered, diluted with H_2O and CH_2Cl_2. Layers were separated and aqueous later was washed 2x with CH_2Cl_2. Combined organic layers were dried over anhydrous $MgSO_4$, filtered, and concentrated *in vacuo* to give yellow oil, to which was added at 0 ^{o}C 16 mL of 4M HCl in dioxane (16 mmol, 9.2 equiv). Resulting solution was allowed to stir at 22 °C for 3 h, at which time at 0 °C pH of the mixture was adjusted to 10 with sat. aq. $NaHCO_3$ and sat. aq. K_2CO_3. The mixture was washed 3x with Et_2O. Combined organic layers were dried over anhydrous $MgSO_4$, filtered, and concentrated *in vacuo* to give brown-yellow oil. Purification by silica gel chromatography gave diamine **2.136** as a foaming light yellow solid (555.6 mg, 1.323 mmol, 76% yield). ^1H NMR ($CDCl_3$, 400 MHz): δ 7.56 (2H, dd, J = 8.1, 1.1 Hz), 7.52–7.47 (2H, m), 7.41–7.34 (5H, m), 7.31–7.27 (1m, 0H), 7.13 (1H, dd, J = 7.4, 1.6 Hz), 7.11–7.06 (1H, m), 6.98–6.90 (3H, m), 6.75 (1H, ddd, J = 7.4, 7.4, 1.1 Hz), 6.47 (1H, d, J = 8.1 Hz), 5.22 (1H, d, J = 6.0 Hz), 4.65 (1H, dd, J = 10.1, 5.9 Hz), 3.23 (1H, dd, J = 11.6, 4.2 Hz), 3.03 (1H, dd, J = 11.7, 6.2 Hz), 2.89 (1H, s), 2.37–2.21 (4H, m), 1.01 (1H, t, J = 7.6 Hz). Diamine **2.136** (555.6 mg, 1.323 mmol, 1.00 equiv) and NH_4BF_4 (418.1 mg, 3.988 mmol, 3.01 equiv.) were suspended in freshly distilled $HC(OEt)_3$ (4 mL) in a flame-dried flask under dry N_2 atmosphere. A needle was inserted into the septum on the flask, and the mixture inside was allowed to stir at 115 °C for 3 h, at which time excess $HC(OEt)_3$ was removed *in vacuo* to give brown oil. Purification by silica gel chromatography (1:1 Petroleum Ether:EtOAc → 1:3 Petroleum Ether:EtOAc), followed by trituration from minimum CH_2Cl_2, a few drops of EtOAc, and a large excess of petroleum ether gave imidazolinium tetrafluoroborate **2.137** as a white powder, which was dried in Abderhalden apparatus under high vacuum over refluxing 2-propanol for 24 h (1.2783 g, 2.2001 mmol, 85% yield). ^1H NMR ($CDCl_3$, 400 MHz): δ 8.30 (1H, s), 7.68–7.63 (1H, m), 7.57–7.48 (3H, m), 7.43–7.32 (6H, m), 7.29 (4H, dd, J = 7.2, 1.7 Hz), 7.25–7.15 (3H, m), 5.58 (1H, dd, J = 12.3, 8.8 Hz), 4.54 (1H, dd, J = 12.3, 12.3 Hz), 4.07 (1H, dd, J = 12.2, 8.9 Hz), 2.68–2.53 (3H, m), 2.51–2.42 (1H, m), 1.34–1.28 (3H, m), 1.26 (3H, t, J = 7.5 Hz); ^{13}C NMR ($CDCl_3$, 100 MHz): δ 158.1, 141.6, 141.0, 137.9, 137.6, 135.8, 134.7, 131.5, 131.4, 131.2, 131.2, 130.3, 129.9, 129.8, 129.7, 129.4, 129.0, 128.9, 128.1, 127.4, 127.2, 66.8, 59.9, 23.9, 23.8, 15.1, 14.7.

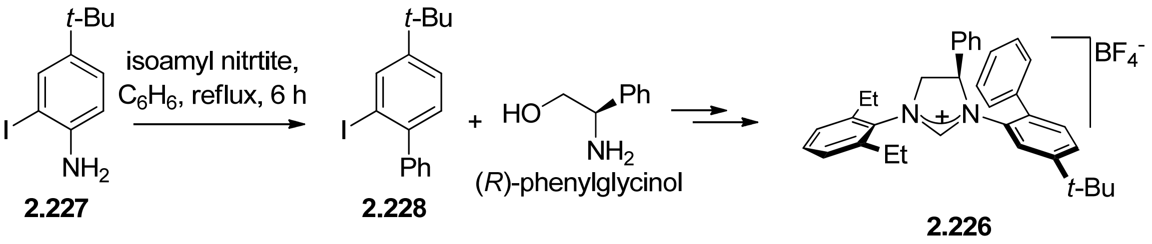

Imidazolinium Tetrafluoroborate 2.226 was prepared following the procedure described for **2.137** from (*R*)-phenylglycinol and biaryl iodide **2.228**, which was prepared following a modified procedure from **2.227**.[116] Note that two rotomers are produced in the cyclization reaction; however, major rotomer is separable from minor by silica gel chromatography (1:1 → 1:4 Petroleum Ether:EtOAc). IR (ATR mode): 3080 (w), 3031 (w), 2974 (w), 2903 (w), 1629(s), 1607 (m), 1549 (w), 1484 (m), 1459 (m), 1446 (w), 1397 (w), 1381 (w), 1365 (w), 1336 (w), 1272 (w), 1246 (w), 1233 (w), 1214 (m), 1057 (m), 1013 (w), 963 (s), 910 (s), 899 (m), 867 (w), 852 (w), 822 (m), 761 (m), 739 (m), 703 (s), 663 (w), 627 (w), 610 (w) cm^{-1}; ^1H NMR ($CDCl_3$, 400 MHz): δ 8.06 (1H, s), 7.57 (1H, s), 7.52 (3H, ddt, J = 7.0, 4.5, 1.8 Hz), 7.47 (1H, m), 7.44–7.38 (6H, m), 7.38–7.35 (2H, m), 7.32–7.28 (2H, m), 7.19 (3H, m), 5.88 (1H, dd, J = 12.4, 9.1 Hz), 4.67 (1H, dd, J = 12.3, 12.3 Hz), 4.11 (1H, dd, J = 12.1, 8.1 Hz), 2.69–2.50 (3H, m), 2.45 (1H, dq, J = 15.1, 7.5 Hz), 1.30 (3H, t, J = 7.6 Hz), 1.27 (9H, s), 1.26 (3H, t, J = 7.6 Hz); ^{13}C NMR ($CDCl_3$, 100 MHz): δ 157.59, 153.54, 141.89, 140.89, 137.94, 135.08, 134.46, 131.36, 131.16, 131.13, 131.08, 130.30, 129.70, 129.46, 129.19, 128.63, 128.45, 127.41, 127.01, 126.70, 124.46, 67.17, 59.67, 35.05, 31.01, 23.86, 23.75, 15.07, 14.74.

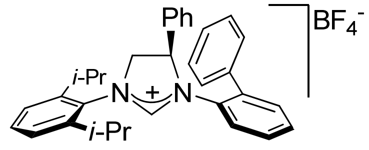

2.229

Imidazolinium Tetrafluoroborate 2.226 was prepared following the procedure described for **2.137**. IR (ATR mode): 3061 (w), 2963 (w), 2929 (w), 2871 (w), 1626 (s), 1582 (w), 1493 (w), 1476 (w), 1459 (w), 1440 (w), 1366 (w), 1331 (w), 1283 (w), 1251 (m), 1183 (w), 1056 (s), 1006 (s), 936 (w), 917 (w), 886 (w), 862 (w), 808 (w), 772 (m),

---

(116) Edler, R.; Voβ, J. *Chem. Ber.* **1989**, *122*, 187-191.

756 (s), 738(s), 698 (s), 658 (w), 636 (w), 611 (w) cm^{-1}; ^{1}H NMR (CDCl$_3$, 400 MHz): δ 8.48 (1H, s), 7.77 (1H, d, J = 8.0 Hz), 7.58–7.51 (4H, m), 7.49–7.36 (6H, m), 7.34–7.23 (6H, m), 5.50 (1H, dd, J = 12.3, 8.3 Hz), 4.47 (1H, dd, J = 12.3, 12.3 Hz), 4.11 (1H, dd, J = 12.3, 8.4 Hz), 2.97 (2H, m), 1.35 (6H, d, J = 6.8 Hz), 1.33 (6H, d, J = 7.2 Hz), 1.22 (3H, d, J = 6.9 Hz); ^{13}C NMR (CDCl$_3$, 100 MHz): δ 158.2, 146.6, 146.2, 138.2, 137.3, 134.8, 131.7, 131.5, 131.3, 130.4, 130.2, 130.1, 129.9, 129.5, 129.4, 129.0, 128.0, 128.0, 125.4, 125.2, 66.7, 61.3, 29.2, 28.9, 25.2, 25.1, 24.6, 24.4; HRMS Calcd for $C_{33}H_{35}N_2$ [M-BF$_4$] (ES$^+$): 459.2800, Found: 459.2801.

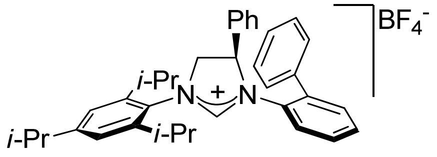

2.230

Imidazolinium Tetrafluoroborate 2.230 was prepared following the procedure described for **2.137**. IR (ATR mode): 3060 (w), 2962 (w), 2930 (w), 2871 (w), 1620 (s), 1459 (w), 1387 (w), 1366 (w), 1278 (w), 1240 (m), 1209 (w), 1183 (w), 1052 (s), 1032 (s), 942 (w), 880 (w), 762 (m), 701 (s), 654 (w), ,639 (w), 609 (w) cm^{-1}; ^{1}H NMR (CDCl$_3$, 400 MHz): δ 8.35 (1H, s, 1H), 7.75 (1H, dd, J = 7.9, 1.1 Hz), 7.57–7.48 (3H, m), 7.46–7.34 (6H, m), 7.31–7.22 (4H, m), 7.09 (2H, dd, J = 11.0, 2.0 Hz), 5.54 (1H, dd, J = 12.4, 8.4 Hz), 4.47 (1H, dd, J = 12.4, 12.4 Hz), 4.08 (1H, dd, J = 12.3, 8.5 Hz), 3.01–2.84 (3H, m), 1.34 (3H, d, J = 6.7 Hz), 1.33 (3H, d, J = 6.8 Hz), 1.31 (3H, d, J = 6.8 Hz), 1.25 (6H, d, J = 6.9 Hz), 1.22 (3H, d, J = 6.9 Hz); ^{13}C NMR (CDCl$_3$, 100 MHz): δ 158.09, 152.46, 146.35, 145.82, 138.11, 137.39, 134.91, 131.52, 131.33, 130.39, 130.16, 130.00, 129.88, 129.42, 129.01, 128.03, 127.95, 127.24, 123.37, 123.16, 66.71, 61.29, 34.55, 29.20, 28.92, 25.29, 25.10, 24.62, 24.49, 23.99.

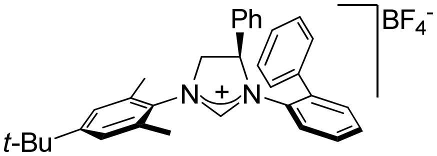

2.231

Imidazolinium Tetrafluoroborate 2.231 was prepared following the procedure described for **2.137**. IR (ATR mode): 3061 (w), 2956 (w), 2871 (w), 1625 (s), 1602 (w), 1483 (m), 1460 (m), 1398 (w), 1313 (w), 1251 (w), 1230 (m), 1203 (m), 1203 (w), 1057 (s), 1011 (s), 975 (m), 922 (w), 886 (w), 851 (w), 769 (m), 739 (m), 702 (s), 648 (w), 631 (w), 613 (w) cm^{-1}; ^{1}H NMR (CDCl$_3$, 500 MHz): δ 8.19 (1H, s, 1H), 7.71 (1H, d, J = 7.8 Hz), 7.55–7.50 (3H, m), 7.42–7.37 (4H, m), 7.35–7.32 (3H, m), 7.30–7.27 (2H, m), 7.24 (1H, dd, J = 7.5, 1.6 Hz), 7.13 (2H, s), 5.64 (1H, dd, J = 12.4, 8.8 Hz), 4.56 (1H, dd, J = 12.4, 12.4 Hz), 4.05 (1H, dd, J = 12.4, 8.8 Hz), 2.28 (6H, broad d, J = 39.2 Hz), 1.29 (9H, s); ^{13}C NMR (CDCl$_3$, 125 MHz): δ 158.0, 154.0, 138.0, 137.4, 134.8, 131.5, 131.4, 130.3, 130.0, 129.9, 129.8, 129.5, 129.1, 128.9, 128.2, 127.4, 126.7, 66.7, 58.6, 34.8, 31.2, 18.1.

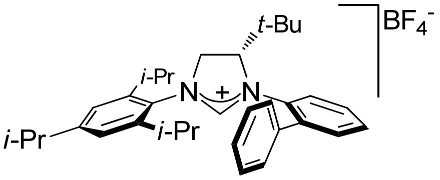

2.232

Imidazolinium Tetrafluoroborate 2.232 was prepared following the procedure described for **2.137**. IR (ATR mode): 3062 (w), 2962 (w), 2872 (w), 1627 (s), 1597 (w), 1508 (w), 1471 (m), 1404 (w), 1388 (w), 1370 (w), 1339 (w), 1321 (w), 1260 (m), 1241 (w), 1210 (w), 1184 (w), 1053 (s), 942 (w), 879 (w), 765 (m), 748 (m), 705 (m), 655 (w) cm^{-1}; ^{1}H NMR (CDCl$_3$, 400 MHz): δ 8.98 (1H, s), 7.87 (1H, broad s), 7.62 (2H, dd, J = 7.7, 7.7 Hz), 7.53 (6H, broad s), 7.47–7.31 (4H, broad m), 7.12 (1H, broad s), 7.09 (1H, d, J = 1.6 Hz), 3.90–3.81 (1H, broad m), 3.72–3.58 (2H, broad m), 3.07–2.80 (3H, m), 1.41 (6H, broad s), 1.36 (3H, d, J = 6.8 Hz), 1.27 (9H, d, J = 7.3 Hz), 0.77 (broad s, 9H); ^{13}C NMR (CDCl$_3$, 126 MHz): δ 160.5, 152.3, 146.1 (broad), 145.2 (broad), 138.5 (broad), 137.4 (broad), 133.5 (broad), 131.6 (broad), 130.7 (broad), 130.3, 129.3, 129.0, 128.8, 127.2, 123.4 (broad), 123.0, 70.1 (broad), 55.9, 35.4, 34.5, 29.0 (broad), 25.6, 25.3, 25.1, 24.2, 23.9.

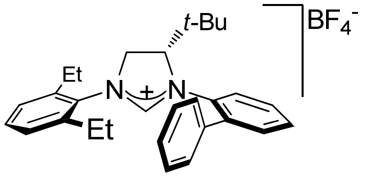

2.233

Imidazolinium Tetrafluoroborate 2.233 was prepared following the procedure described for **2.137**. IR (ATR mode): 3062 (w), 2967 (w), 2877 (w), 1627 (s), 1587 (w), 1467 (w), 1444 (w), 1404 (w), 1373 (w), 1257 (m), 1216 (w), 1197 (w), 1049 (s), 1030 (s), 869 (w), 813 (w), 768 (m), 749 (m), 705 (m), 659 (w) cm^{-1}; ^{1}H NMR (CDCl$_3$, 400 MHz): δ 8.75 (1H, broad s), 7.77 (1H, broad s), 7.60–7.45 (5H, m), 7.44–7.28 (4H, m), 7.22 (1H, s), 7.21 (1H, s), 3.92–3.77 (2H, broad m), 3.61 (1H, broad s), 2.81 (1H, broad s), 2.76–2.66 (1H, m), 2.64–2.59 (2H, broad m), 1.43 – 1.18 (6H, broad m), 0.76 (9H, s); ^{13}C NMR (CDCl$_3$, 100 MHz): δ 160.5, 141.6, 140.7, 138.2, 137.7, 133.8, 131.7, 131.4, 131.2, 130.8, 130.2, 130.1, 129.5, 129.1, 128.9, 128.5, 128.4, 127.6, 127.4, 70.4, 54.7, 35.5, 25.7, 24.1, 15.3, 15.0.

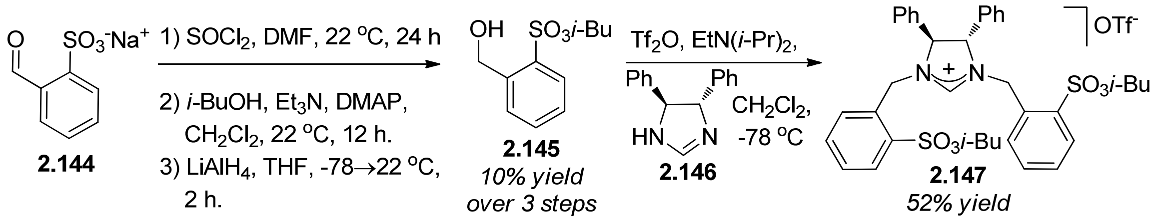

Imidazolinium Triflate 2.147 was prepared according to the following sequence. Under N$_2$ atmosphere in a flame-dried round bottom flask at 0 °C sodium sulfonate **2.144** (2.5081 g, 12.048 mmol, 1.00 equiv) was dissolved in SOCl$_2$ (7 mL), DMF (0.30 mL, 3.9 mmol, 0.32 equiv) was added with vigorous stirring. The resulting mixture was allowed to stir at 22 °C for 6 h, at which time the mixture was poured into crushed ice/water, to which 50 mL of CH$_2$Cl$_2$ was subsequently added. Layers were separated, and aqueous layer was washed 3 x 20 mL with CH$_2$Cl$_2$. Combined organic layers were dried over anhydrous MgSO$_4$, filtered, and concentrated *in vacuo* to give yellow oil, which was used without further purification assuming quantitative yield. Under N$_2$ atmosphere in a flame-dried rount bottom flask yellow oil obtained from previous step was dissolved in CH$_2$Cl$_2$ (10 mL). At 0 °C Et$_3$N (2.0 mL, 14 mmol) was added dropwise with vigorous stirring, followed by *i*-BuOH (1.4 mL, 15 mmol). Resulting mixture was allowed to stir at 22 °C for 24 h, at which time 40 mL of CH$_2$Cl$_2$ was added. The mixture was washed 2 x 20 mL with 1M aqueous KHSO$_4$, dried over anhydrous MgSO$_4$, filtered, and concentrated *in* *vacuo* to give yellow-brown oil. Purification by silica gel chromatography (5:1 Hexanes:EtOAc) afforded the desired *i*-Bu-sulfonatobenzaldehyde as a light yellow oil (445.2 mg, 1.837 mmol, 15% yield). ^{1}H NMR ($CDCl_3$, 500 MHz): δ 10.75 (1H, d, J = 0.7 Hz), 8.29 (1H, dd, J = 7.0, 1.0 Hz), 8.08 (1H, dd, J = 7.5, 1.5 Hz), 7.81–7.74 (2H, m), 3.89 (2H, d, J = 6.5 Hz), 1.97 (1H, dp, J = 13.3, 6.5 Hz), 0.90 (6H, d, J = 7.0 Hz). Under N_2 atmosphere in a flame-dried round bottom flask were mixed $LiAlH_4$ (69.3 mg, 1.824 mmol, 0.99 equiv) and THF (5 mL). At -78 ^{o}C to this mixture was added dropwise a solution of *i*-Bu-sulfonatobenzaldehyde (445.2 mg, 1.837 mmol, 1.00 equiv) in 5 mL of THF. Resulting mixture was allowed to stir at -78 ^{o}C for 30 min and at 0 ^{o}C for 2 h, at which time 5 mL of Et_2O were added, followed by dropwise addition of saturated aqueous Rochelle's salt with vigorous stirring until the solids turn into white powder and the solution becomes clear. The mixture was filtered, solids were washed with 50 mL of Et_2O. Combined organic layers were concentrated *in vacuo* to give **2.145** (308.5 mg, 1.263 mmol, 69% yield) as a light yellow oil, which was sufficiently pure to be used without further purification. ^{1}H NMR ($CDCl_3$, 400 MHz): δ 7.98 (1H, dd, J = 7.7, 0.8 Hz), 7.71–7.64 (2H, m), 7.50–7.45 (1H, m), 4.95 (2H, d, J = 6.8 Hz), 3.82 (2H, d, J = 6.8 Hz), 1.96 (1H, dp, J = 13.2, 6.8 Hz), 0.90 (6H, d, J = 6.8 Hz). Under N_2 atmosphere in a flame-dried vial were mixed1.0 mL of CH_2Cl_2 and Tf_2O (0.10 mL, 0.59 mmol, 2.6 equiv). At -78 ^{o}C was added dropwise Hünig's base (0.32 mL, 3.3 mmol, 15 equiv) with vigorous stirring, followed by a solution of **2.145** (123.2 mg, 0.5043 mmol, 2.24 equiv) in 0.5 mL of CH_2Cl_2. The resulting mixture was allowed to stir at -78 ^{o}C for 30 min, at which time a solution of diphenyl-dihydroimidazole **2.146**[98] (50.0 mg, 0.225 mmol, 1.00 equiv) in 1.5 mL of CH_2Cl_2 were added dropwise with vigorous stirring. Resulting mixture was allowed to stir and warm to 22 ^{o}C over 3 h, at which time 5 mL of CH_2Cl_2 were added. The resulting mixture was washed with 1M aqueous $KHSO_4$ (2 x 5 mL), dried over anhydrous $MgSO_4$, filtered and concentrated *in vacuo* to give yellow oil. Purification by silica gel chromatography (1:1 Hexanes:EtOAc → 100% EtOAc) afforded imidazolinium triflate **2.147** as a colorless solid. IR (ATR mode): 3068 (w), 2965 (w), 2877 (w), 1637 (m), 1497 (w), 1470 (w), 1457 (w), 1396 (m), 1255 (s), 1223 (m), 1179 (s), 1152 (s), 1066 (w), 1029 (s), 960 (m), 938 (s), 908 (m), 841 (m), 818 (m), 757 (m), 698 (s), 637 (s), 617 (s), 599 (s) cm^{-1}; ^{1}H NMR ($CDCl_3$, 400 MHz): δ 8.67 (1H, s), 7.94 (2H, dd, J = 7.8, 1.2 Hz), 7.59 (2H, td, J = 7.6, 1.2 Hz), 7.48 (4H, dt, J = 14.0, 4.4 Hz), 7.34 (6H, dd, J = 5.0, 1.6 Hz), 7.21 (4H, dd, J = 6.4, 3.0 Hz), 5.09 (2H, B of AB, J_{AB} = 15.3 Hz), 4.92 (2H, s), 4.91 (2H, A of AB, J_{AB} = 15.2 Hz), 3.75 (4H, d, J = 6.6 Hz), 1.91 (2H, dp, J = 13.4, 6.6 Hz), 0.85 (12G, dd, J = 6.6, 2.2 Hz); ^{13}C NMR ($CDCl_3$, 100 MHz): δ 159.9, 135.1, 134.6, 134.3, 133.4, 131.0, 130.4, 130.1, 129.9, 129.8, 127.9, 77.6, 74.5, 48.4, 28.1, 18.7.

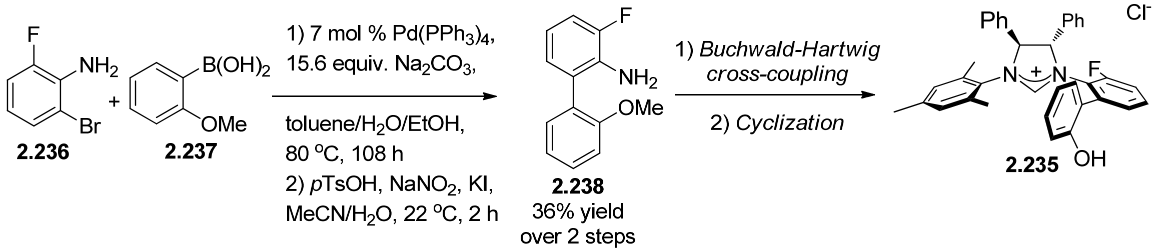

Imidazolinium Chloride 2.235 was prepared following a modified procedure. In a round-bottom flask, equipped with a reflux condenser, under N_2-atmosphere were mixed $Pd(PPh_3)_4$ (5.0 g, 4.3 mmol, 0.071 equiv), aniline **2.236** (11.5907 g, 60.997 mmol, 1.00 equiv), boronic acid **2.237** (13.4037 g, 88.205 mmol, 1.45 equiv), Na_2CO_3 (100.7 g, 950.5 mmol, 15.6 equiv), toluene (300 mL), ethanol (90 mL), H_2O (230 mL). The resulting mixture was allowed to stir at 80 °C for 108 h, at which time it was allowed to cool to 22 °C, and the layers were separated. Aqueous layer was washed with EtOAc (2 x 50 mL). Combined organic layers were dried over anhydrous $MgSO_4$, filtered, and concentrated *in vacuo* to give black-brown oil. Purification by silica gel chromatography (10:1 hexanes:EtOAc) gave the desired biaryl as a colorless oil (13.0415 g, 60.03 mmol, 98% yield). ^{1}H NMR ($CDCl_3$, 400 MHz): δ 7.40-7.36 (m, 1H), 7.26 (dd, J = 7.2, 1.6 Hz, 1H), 7.08-6.98 (m, 3H), 6.91 (dt, J = 7.6, 1.2 Hz, 1H), 6.77-6.71 (m, 1H), 3.82 (s, 3H), 3.77 (br s, 2H). The product from the previous step was subjected to Sandmeyer reaction conditions as follows. In a round bottom flask under ambient atmosphere were mixed the biaryl (5.1696 g, 15.755 mmol, 1.00 equiv.), *p*-toluenesulfonic acid hydrate (9.0120 g, 47.377 mmol, 3.01 equiv.), acetonitrile (205 mL). To the resulting solution at 0 °C was added dropwise with vigorous stirring the solution of $NaNO_2$ (2.1515 g, 31.19 mmol, 1.97 equiv.), and KI (6.4454 g, 38.825 mmol, 2.46 equiv.), in H_2O (20 mL). The resulting mixture was allowed to stir at 22 °C for 2 h, at which time it was poured into the saturated aqueous $Na_2S_2O_3$ solution. The layers were separated, and the aqueous layer was washed with EtOAc (3 x 75 mL). Combined organic layers were dried over anhydrous $MgSO_4$, filtered, and concentrated *in vacuo* to give brown oil. Purification by silica gel chromatography (20:6:1 hexanes:CH_2Cl_2:Et_3N) gave the desired aryl iodide **2.238** as a yellow oil (1.9297 g, 5.8802 mmol, 37% yield). ^1H NMR ($CDCl_3$, 400 MHz): δ 7.44-7.39 (m, 1H), 7.36-7.31 (m, 1H), 7.11-7.09 (m, 1H), 7.07-7.00 (m, 3H), 6.98 (dd, J = 8.0, 0.4 Hz, 1H)), 3.78 (s, 3H). The aryl iodide **2.238** obtained above was subjected to Buchwald Hartwig cross-coupling conditions as follows. In a round bottom flask attached to a reflux condenser under N_2-atmosphere were mixed $Pd_2(dba)_3$ (233.7 mg, 0.2552 mmol, 0.050 equiv.) (*S*, *S*)-diphenyl-ethylenediamine (1.6629 g, 7.84 mmol, 1.54 equiv.), aryl iodide (1.6679 g, 5.083 mmol, 1.00 equiv.), *rac*-BINAP (641.1 mg, 1.029 mmol, 0.203 equiv.), and sodium *t*-butoxide (1.2551g, 13.05 mmol, 2.57 equiv.). Anhydrous toluene (52 mL) was added and the mixture was allowed to stir for 24 h at 100 °C. The mixture was allowed to cool to 22 °C and then passed through a short plug of silica gel with copious amounts of EtOAc. The solvents were removed *in vacuo* to give brown oil. Purification by silica gel chromatography (4:1 hexanes:EtOAc) afforded the desired diamine as a yellow foaming solid (1.5696 g, 3.805 mmol, 75% yield). ^1H NMR ($CDCl_3$, 400 MHz): δ 7.53-7.44 (m, 1H), 7.33-7.27 (m, 2H), 7.24-7.22 (m, 4H), 7.20-7.10 (m, 4H), 7.08-7.02 (m, 2H)), 6.97-6.85 (m, 3H), 6.72-6.61 (m, 1H), 5.17-4.85 (m, 1H), 4.72-4.67 (m, 1H), 4.21-4.12 (m, 1H), 3.73-3.72 (m, 3H), 1.33 (br s, 2H). In a round bottom flask attached to a reflux condenser under N_2-atmosphere were mixed $Pd_2(dba)_3$ (168.9 mg, 0.1844 mmol, 0.053 equiv.) diamine (1.4216 g, 3.446 mmol, 1.00 equiv.), bromomesitylene (2.1213 g, 10.655 mmol, 3.09 equiv.), *rac*-BINAP (450.6 mg, 0.7236 mmol, 0.209 equiv.), and sodium *t*-butoxide (852.6 g, 8.871 mmol, 2.57 equiv.). Anhydrous toluene (40 mL) was added and the mixture was allowed to stir for 40 h at 110 °C. The mixture was allowed to cool to 22 °C and then passed through a short plug of silica gel with copious amounts of EtOAc. The solvents were removed *in vacuo* to give brown oil. Purification by silica gel chromatography (19:1 hexanes:EtOAc) afforded the desired diamine as a yellow foaming solid (1.2995 g, 2.448 mmol, 71% yield). ^{1}H NMR (CDCl$_3$, 400 MHz): δ 7.39-7.36 (m, 1H), 7.20-7.13 (m, 2H), 7.08-6.97 (m, 7H), 6.92-6.81 (m, 4H), 6.75-6.62 (5H), 5.05-4.91 (m, 1H), 4.58-4.56 (m, 1H), 4.31-4.29 (m, 1H), 3.71-3.66 (m, 3H), 3.59 (br s, 1H), 2.13 (s, 3H), 1.94-1.92 (m, 6H) To a round bottom flask cooled to 0 ^{o}C under N$_2$-atmosphere were added prepared above diamine (1.5460 g, 2.9132 mmol, 1.00 equiv.) and CH$_2$Cl$_2$ (50 mL). Neat boron tribromide (2.00 mL, 21.2 mmol, 7.27 equiv.) was added dropwise followed by allowing the reaction mixture to stir for 6h at 22 ^{o}C. The saturated aqueous sodium bicarbonate solution was added to basify the reaction mixture. CH$_2$Cl$_2$ layer was separated and the aqueous layer was washed with EtOAc (2x50 mL). Combined organic layers were dried over anhydrous MgSO$_4$, filtered, and concentrated *in vacuo* to give brown oil. Purification by silica gel chromatography (199:1 hexanes:EtOAc) gave diamine-phenol (1.4127 g, 2.734 mmol, 94% yield). ^{1}H NMR (CDCl$_3$, 400 MHz): δ 8.81 (br s, 1H), 7.35-7.31 (m, 1H), 7.10-6.91 (m, 12H), 6.77-6.74 (m, 2H), 6.69-6.68 (m, 2H), 6.64 (s, 2H), 5.11 (br s, 1H), 4.58-4.56 (m, 1H), 4.47-4.43 (m, 1H), 3.50 (br s, 1H), 2.12 (s, 3H), 2.04 (s, 6H). To a round bottom flask under N$_2$-atmosphere were added diamine phenol (1.1863 g, 2.296 mmol, 1.00 equiv.) and anhydrous methanol (23 mL), and the flask was allowed to cool to -78 ^{o}C. 4M HCl:dioxane (5.00 mL, 20.00 mmol, 8.71 euiv.) was added dropwise and the reaction mixture was allowed to stir for 30 mins at -78 ^{o}C. White precipitates were observed, and the mixture was allowed to warm to 22 ^{o}C and stirred for 1h. The volatiles were removed *in vacuo* to give white powder, which was further washed with pentane (20 mL) and Et$_2$O (20 mL). The solid was dried under high vacuum, and transferred to a round bottom flask containing triethylorthoformate (4.00 mL, 24.05 mmol, 10.5 equiv.) with an attached short path distillation apparatus under N$_2$-atmosphere. The reaction mixture was allowed to stir for 4 h at 110 ^{o}C. The mixture was cooled to 22 ^{o}C and excess triethylorthoformate was removed *in vacuo*. The cannula filtration with Et$_2$O (2x10 mL) afforded white powder (545.6 mg, 0.9689 mmol, 42% yield). Imidazolinium chloride **2.235** was isolated as a mixture of rotomer (8.3:1.0). IR (ATR mode): 3034 (w), 2919 (w), 2851 (w), 2705 (w), 2567 (w), 1618 (s), 1600 (s), 1494 (s), 1469 (s), 1446 (s), 1377 (s), 1263 (s), 1218 (s), 1182 (s), 1157 (s), 1119 (s), 1080 (s), 1032 (s), 1003 (s), 923 (s), 899 (s), 854 (s), 795 (s), 758 (s), 727 (s), 698 (s), 639 (s), 631 (s), 553 (s), 516 (s), 453 (s), 407 (s) cm^{-1}; ^{1}H NMR (CDCl$_3$, 400 MHz): δ 10.87 (s, 1H), 8.87 (s, 1H), 7.77-7.75 (m, 1H), 7.56-7.52 (m, 1H), 7.34-7.32 (m, 5H), 7.15-7.09 (m, 7H), 6.93 (s, 2H), 6.82-6.79 (m, 2H), 6.76 (s, 1H), 5.42 (d, J = 10.4 Hz, 1H), 5.31 (d, J = 10.8 Hz, 1H), 2.55 (s, 3H), 2.23 (s, 3H), 2.02 (s, 3H); ^{13}C NMR (CDCl$_3$, 100 MHz): δ 159.0, 158.9, 156.4, 155.2, 140.7, 138.8, 138.2, 134.1, 133.6, 131.6, 131.5, 131.2, 131.0, 130.8, 130.6, 130.2, 129.8, 129.59, 129.56, 129.3, 129.1, 128.4, 128.1, 127.94, 127.91, 127.5, 127.4, 123.97, 123.95, 121.1, 120.9, 120.1, 118.8, 115.2, 114.9, 75.7, 71.6, 20.9, 18.7, 18.5; ^{19}F NMR (CDCl$_3$, 376 MHZ): δ -127.4; HRMS (ESI$^+$): Calcd for $C_{36}H_{32}O N_2F$ [M-Cl]: 527.2499. Found: 527.2498. $[\alpha]_D^{23.8}$ -203.0 (*c* 0.66, CDCl$_3$).

2.5.3. Chiral NHC-Ru Complexes

Complexes 2.110 and 2.111. Under dry N$_2$ atmosphere in a flame-dried vial were mixed imidazolinium tetrafluoroborate **2.131** (83.0 mg, 0.143 mmol, 1.27 equiv), Ru complex **2.132** (74.2 mg, 0.113 mmol, 1.00 equiv), KHMDS (28.1 mg, 0.147 mmol, 1.30 equiv). These solids were dissolved in THF (1.4 mL) with vigorous stirring, the resulting mixture was allowed to stir for 30 min at 22 °C, when iodomethane (0.6 mL) was added, and the mixture was allowed to stir for another 15 min, at which time the solution was loaded directly onto TSI silica gel column (10x0.5 cm), which was eluted with 100% CH$_2$Cl$_2$. Collected eluent was concentrated *in vacuo* to give green-brown foaming solid. Purification by TSI silica gel chromatography (3:1→2:1→3:2 pentane:CH$_2$Cl$_2$ and in cases when unreacted **2.132** remains the eluent gradient is 100% toluene→2:1→3:2 pentane:CH$_2$Cl$_2$), followed by trituration from CH$_2$Cl$_2$/pentane afforded complex **2.110** as a green to light green solid (55.8mg, 0.0628 mmol, 0.56% yield). ^{1}H NMR (CDCl$_3$, 400 MHz): δ 17.01 (1H, s), 9.48–9.40 (1H, m), 8.08 (2H, s), 7.50–7.45 (1H, m), 7.44–7.38 (3H, m), 7.37–7.30 (5H, m), 7.27 (2H, ddd, J = 7.2, 7.2, 1.6 Hz), 7.23–7.13 (2H, m), 7.03 (2H, dd, J = 7.7, 7.7 Hz), 6.98 (1H, d, J = 1.2 Hz), 6.96 (1H, s), 6.85 (1H, ddd, J = 7.5, 1.8, 1.8 Hz), 6.80 (1H, s), 6.58 (2H, d, J = 7.8 Hz), 5.29 (2H, s), 4.51–4.44 (1H, m), 2.58 (3H, s), 2.36 (3H, s), 1.93 (3H, s), 1.13 (3H, d, J = 6.3 Hz), 1.04 (3H, d, J = 6.3 Hz). Under dry N_2 atmosphere in a flame-dried vial were mixed complex **2.110** (55.8 mg, 0.0628 mmol, 1.00 equiv), anhydrous NaI (97.3 mg, 0.649 mmol, 10.3 equiv), and THF (0.6 mL). Resulting mixture was allowed to stir at 60 °C for 7 h, at which time volatiles were removed *in vacuo* to give brown solid. Purification by TSI silica gel chromatography (3:1→2:1→3:2 pentane:CH_2Cl_2), followed by trituration from CH_2Cl_2/pentane furnished complex **2.111** as an olive green solid (39.3 mg, 0.0367 mmol, 32% yield over 2 steps). IR (ATR mode): 3054 (w), 3027 (w), 2970 (w), 2918 (w), 2864 (w), 1685 (w), 1601 (w), 1562 (w), 1494 (m), 1478 (m), 1456 (m), 1423 (m), 1397 (m), 1374 (m), 1343 (m), 1307 (w), 1279 (m), 1225 (s), 1191 (m), 1160 (w), 1103 (w), 1088 (w), 1028 (w), 1010 (w), 933 (w), 903 (w), 872 (w), 855 (w), 818 (w), 774 (s), 757 (m), 699 (s), 646 (w), 633(w), 609 (w) cm^{-1}; ^1H NMR ($CDCl_3$, 400 MHz): δ 16.12 (1H, s), 9.58 (1H, dd, J = 7.6, 0.9 Hz), 8.07 (2H, s), 7.71–7.50 (6H, m), 7.48–7.30 (9H, m), 7.28–7.23 (3H, m), 7.22–7.13 (2H, m), 7.06 (2H, dd, J = 7.6, 7.6 Hz), 6.97–6.85 (3H, m), 6.80 (1H, s), 6.78 (2H, s), 5.32 (1H, B of AB, J_{AB} = 8.8 Hz), 5.27 (1H, A of AB, J_{AB} = 8.7 Hz), 4.64 (1H, app. septet, J = 6.4 Hz), 2.72 (3H, s), 2.32 (3H, s), 2.09 (3H, s), 1.39 (2H, d, J = 6.3 Hz), 1.21 (3H, d, J = 6.2 Hz); ^{13}C NMR ($CDCl_3$, 100 MHz): δ 305.3, 211.8, 191.2, 150.4, 147.8, 142.2, 141.1, 140.1, 140.0, 139.6, 138.3, 136.9, 136.4, 135.4, 135.3, 135.0, 133.6, 132.0, 130.9, 130.5, 130.0, 129.3, 129.1, 128.9, 128.8, 128.7, 128.6, 128.3, 128.0, 127.9, 127.8, 127.2, 123.3, 122.3, 122.3, 77.6, 77.3, 70.9, 22.6, 22.2, 21.9, 21.18, 21.16.

Complex 2.112 was prepared from imidazolinium tetrafluoroborate **2.219** following the procedure described for complex **2.111** via corresponding NHC-$RuCl_2$ complex **2.219c**: ^1H NMR ($CDCl_3$, 400 MHz): δ 16.81 (1H, s), 9.43 (1H, d, J = 7.2 Hz), 8.11 (1H, s), 7.64–7.60 (3H, m), 7.59–7.54 (2H, m), 7.50–7.44 (2H, m), 7.43–7.38 (4H, m), 7.37–7.32 (5H, m), 7.31–7.26 (3H, m), 7.23–7.18 (1H, m), 7.13 (1H, t, J = 7.4 Hz), 7.08 (1H, d, J = 7.4 Hz), 7.00 (2H, t, J = 7.6 Hz), 6.95 (1H, dd, J = 7.6, 7.6 Hz), 6.82 (1H, dd, J = 7.6, 1.6 Hz), 6.47 (2H, d, J = 7.3 Hz), 5.35 (1H, B of AB, J = 8.8 Hz), 5.24 (1H, A of AB, J = 9.2 Hz), 4.48 (1H, hept., J = 6.4 Hz), 3.20 (1H, dq, J = 15.2, 7.6 Hz), 2.84 (1H, dq, J = 15.0, 7.4 Hz), 2.56 (1H, dq, *J* = 15.0, 7.6 Hz), 2.19 (1H, dq, *J* = 15.2, 7.6 Hz), 1.24 (3H, t, *J* = 7.6 Hz), 1.11 (3H, d, *J* = 6.4 Hz), 1.05 (3H, d, *J* = 6.4 Hz), 0.78 (3H, t, *J* = 7.6 Hz). Complex **2.112**: ^{1}H NMR (CDCl$_3$, 400 MHz): δ 15.92 (1H, s), 9.61–9.57 (1H, m), 8.10 (2H, s), 7.66–7.53 (5H, m), 7.46–7.30 (9H, m), 7.29–7.23 (4H, m), 7.23–7.17 (1H, m), 7.14 (1H, dd, *J* = 7.4, 7.4 Hz), 7.06 (1H, d, *J* = 7.6 Hz), 7.03 (2H, dd, *J* = 7.7, 7.7 Hz), 6.90 (1H, dd, *J* = 7.4, 7.4 Hz), 6.85 (1H, dd, *J* = 7.5, 1.9 Hz), 6.70 (2H, d, *J* = 7.9 Hz), 5.34 (1H, d, *J* = 8.6 Hz), 5.27 (1H, d, *J* = 8.6 Hz), 4.70–4.58 (1H, m), 3.61 (1H, dq, *J* = 15.1, 7.5 Hz), 2.88–2.69 (2H, m), 2.25 (1H, dq, *J* = 15.2, 7.5 Hz), 1.40 (3H, d, *J* = 6.3 Hz), 1.26 (3H, t, *J* = 7.4 Hz), 1.20 (3H, d, *J* = 6.2 Hz), 0.80 (3H, t, *J* = 7.5 Hz).

Complex 2.113 was prepared from imidazolinium tetrafluoroborate **2.220** following the procedure described for complex **2.111** via corresponding NHC-RuCl$_2$ complex **2.220c**: ^{1}H NMR (CDCl$_3$, 400 MHz): δ 16.86 (1H, s), 9.41–9.36 (1H, m), 8.16 (2H, s), 7.68–7.52 (6H, m), 7.44 (3H, d, *J* = 7.2 Hz), 7.42–7.38 (3H, m), 7.37–7.32 (6H, m), 7.29 (2H, dd, *J* = 7.4, 7.4 Hz), 7.22–7.18 (2H, m), 7.13 (1H, dd, *J* = 7.4, 7.4 Hz), 7.02–6.96 (3H, m), 6.93 (1H, td, *J* = 7.5, 0.7 Hz), 6.79 (1H, dd, *J* = 7.3, 1.2 Hz), 6.30 (2H, d, *J* = 7.7 Hz), 5.44 (1H, B of AB, J_{AB} = 8.9 Hz), 5.19 (1H, A of AB, J_{AB} = 9.0 Hz), 4.54 (1H, hept., *J* = 6.4 Hz), 3.62 (1H, hept., *J* = 6.8 Hz), 3.03 (1H, hept., *J* = 6.8 Hz), 2.88 (1H, hept., *J* = 6.8 Hz), 1.40 (3H, d, *J* = 5.3 Hz), 1.38 (3H, d, *J* = 5.2 Hz), 1.31 (3H, d, *J* = 6.9 Hz), 1.15 (6H, d, *J* = 6.3 Hz), 1.00 (3H, d, *J* = 6.4 Hz), 0.97 (3H, d, *J* = 6.7 Hz), 0.17 (3H, d, *J* = 6.7 Hz). Complex **2.113**: IR (ATR mode): 3054 (w), 2960 (w), 2926 (w), 2865 (w), 1601 (m), 1561 (m), 1498 (m), 1479 (m), 1457 (m), 1421 (w), 1383 (w), 1340 (s), 1277 (m), 1260 (m), 1225 (m), 1191 (w), 1177 (w), 1088 (w), 1069 (w), 1028 (w), 1009 (w), 935 (w), 902 (w), 880 (w), 856 (w), 820 (w), 752 (s), 737 (m), 698 (s), 646 (m), 609 (m) cm^{-1}; ^{1}H NMR (CDCl$_3$, 400 MHz): δ 16.16 (1H, s), 9.70 (1H, d, *J* = 7.6 Hz), 8.17 (2H, broad s), 7.63–7.60 (3H, m), 7.54 (4H, d, *J* = 7.2 Hz), 7.43–7.32 (6H, m), 7.32–7.30 (1H, m), 7.29 (1H, s), 7.28–7.26 (1H, m), 7.23–7.17 (2H, m), 7.11 (1H, dd, *J* = 7.4, 7.4 Hz), 6.98–6.94 (3H, m), 6.85 (1H, dd, *J* = 7.2, 7.2 Hz), 6.80 (1H, dd, *J* = 7.5, 1.9 Hz), 6.38 (2H, d, *J* = 7.6 Hz), 5.57 (1H, d, *J* = 8.2 Hz), 5.28 (1H, d, *J* = 8.2 Hz), 4.72 (1H, app. septet, *J* = 6.4 Hz), 3.94 (1H, app. septet, *J* = 6.4 Hz), 3.04–2.96 (1H, m), 2.95–2.87 (1H, m), 1.45 (3H, d, *J* = 6.3 Hz), 1.35 (3H, d, *J* = 6.6 Hz), 1.34 (3H, d, *J* = 6.6 Hz), 1.30 (3H, d, *J* = 6.8 Hz), 1.29 (3H, d, *J* = 6.0 Hz), 1.27 (3H, d, *J* = 6.4 Hz), 0.88 (3H, d, *J* = 6.4 Hz), 0.07 (3H, d, *J* = 6.6 Hz); ^{13}C NMR ($CDCl_3$, 100 MHz): δ 298.4, 212.4, 150.6, 150.3, 149.8, 147.4, 146.4, 146.3, 141.6, 141.5, 140.9, 139.9, 137.4, 135.0, 134.7, 133.8, 133.5, 131.7, 130.2, 130.1, 129.5, 129.4, 129.1, 129.0, 128.5, 128.3, 128.3, 128.2, 128.1, 127.8, 127.6, 124.7, 123.5, 122.8, 122.5, 78.1, 77.4, 69.3, 34.4, 28.6, 28.5, 27.72, 27.66, 25.7, 24.6, 24.5, 22.9, 22.2, 14.2.

Complexes 2.115 and 2.116 were prepared from imidazolinium tetrafluoroborate **2.222** following the procedure described for complex **2.111**. Complex **2.115** was isolated as a 25:1 mixture of rotomers, only data for major rotomer is reported: ^{1}H NMR ($CDCl_3$, 400 MHz): δ 16.68 (1H, s), 8.88 (1H, s), 8.23 (2H, s), 7.66–7.58 (3H, m), 7.54–7.47 (1H, m), 7.44 (1H, dd, *J* = 7.7, 7.7 Hz), 7.31 (5H, dd, *J* = 7.9, 7.9 Hz), 7.27–7.24 (3H, m), 7.22–7.05 (4H, m), 7.00 (2H, dd, *J* = 7.6, 7.6 Hz), 6.89 (3H, dd, *J* = 13.6, 7.4 Hz), 6.47 (2H, d, *J* = 8.0 Hz), 5.31 (1H, B of AB, J_{AB} = 9.2 Hz), 5.25 (1H, A of AB, J_{AB} = 9.3 Hz), 5.09–4.99 (1H, m), 3.24–3.13 (1H, m), 3.13–3.06 (1H, m), 2.85 (1H, dq, *J* = 14.8, 7.3 Hz), 2.75–2.63 (1H, m), 2.19 (1H, dq, *J* = 15.4, 7.6 Hz), 1.66 (3H, d, *J* = 6.1 Hz), 1.49 (3H, d, *J* = 6.1 Hz), 1.31 (3H, d, *J* = 6.8 Hz), 1.23 (3H, dd, *J* = 7.9, 7.0 Hz), 1.13 (3H, d, *J* = 6.8 Hz), 0.85 (3H, dd, *J* = 8.0, 7.0 Hz). Complex **2.116**: IR (ATR mode): 3049 (w), 3027 (w), 2960 (w), 2930 (w), 2873 (w), 1589 (w), 1577 (w), 1475 (w), 1455 (m), 1386 (m), 1343 (w), 1299 (w), 1174 (s), 1157 (m), 1114 (m), 1097 (m), 1057 (m), 1037 (m), 1008 (w), 934 (w), 897 (w), 880 (w), 842 (W), 814 (w), 772 (w), 744 (s), 719 (w), 699 (s), 639 (m), 609 (m) cm^{-1}; ^{1}H NMR ($CDCl_3$, 400 MHz): δ 15.61 (1H, s), 9.15 (1H, d, *J* = 1.5 Hz), 8.27 (2H, d, *J* = 6.7 Hz), 7.65–7.51 (4H, m), 7.38 (1H, dd, *J* = 7.0, 7.0 Hz), 7.35 (2H, d, *J* = 7.1 Hz), 7.26–7.21 (4H, m), 7.20–7.14 (1H, m), 7.11 (1H, dddd, *J* = 7.2, 7.2, 1.2, 1.2 Hz), 7.06 (1H, d, *J* = 7.2 Hz), 7.00 (2H, dd, *J* = 7.7, 7.7 Hz), 6.94 (1H, d, *J* = 8.5 Hz), 6.89 (1H, dd, *J* = 7.6, 1.8 Hz), 6.82 (1H, ddd, *J* = 7.2, 7.2, 0.8 Hz), 6.61 (2H, d, *J* = 7.2 Hz), 5.32 (1H, B of AB, *J* = 9.0 Hz), 5.28 (1H, A of AB, *J* = 9.0 Hz), 5.15 (1H, hept., *J* = 6.4 Hz), 3.56–3.47 (1H, m), 3.12 (1H, hept., *J* = 6.8 Hz), 2.95–2.77 (2H, m), 2.38–2.28 (1H, m), 1.76 (3H, d, *J* = 6.2 Hz), 1.68 (3H, d, *J* = 6.2 Hz), 1.30 (3H, d, *J* = 6.9 Hz), 1.23

(3H, t, *J* = 7.5 Hz), 1.10 (3H, d, *J* = 6.9 Hz), 0.85 (3H, t, *J* = 7.5 Hz); ^{13}C NMR ($CDCl_3$, 100 MHz): *δ* 298.4, 211.4, 153.0, 150.2, 145.2, 144.3, 142.7, 141.1, 140.1, 140.0, 137.6, 135.0, 134.8, 132.9, 130.8, 130.5, 129.3, 128.9, 128.8, 128.73, 128.68, 128.3, 128.2, 128.0, 127.6, 126.7, 126.3, 124.9, 124.6, 123.5, 122.1, 113.8, 76.0, 71.0, 32.9, 26.6, 25.5, 24.6, 22.9, 21.1, 14.4, 13.3.

Complexes 2.117 and 2.118 were prepared from imidazolinium tetrafluoroborate **2.223** following the procedure described for complex **2.111**. Complex **2.117** was isolated as a 7.3:1 mixture of rotomers, only data for major rotomer is reported: IR (ATR mode): 3061 (w), 3030 (w), 2962 (w), 2933 (w), 2873 (w), 1589 (w), 1577 (w), 1475 (m), 1455 (m), 1410 (m), 1385 (m), 1344 (m), 1290 (m), 1232 (s), 1219 (s), 1177 (m), 1157 (m), 1141 (m), 1114 (m), 1099 (w), 1036 (w), 1008 (w), 938 (w), 908 (w), 842 (w), 807 (w), 774 (w), 744 (s), 699 (s), 643 (w), 609 (w) cm^{-1}; ^{1}H NMR ($CDCl_3$, 400 MHz): *δ* 16.58 (1H, s), 8.62 (1H, d, *J* = 1.9 Hz), 8.30 (2H, dd, *J* = 6.4, 2.8 Hz), 7.60 (3H, dd, *J* = 6.9, 2.9 Hz), 7.51–7.47 (1H, m), 7.42 (1H, d, *J* = 7.7 Hz), 7.37 (1H, dd, *J* = 8.1, 2.0 Hz), 7.33–7.29 (4H, m), 7.25 (2H, dd, *J* = 7.2, 7.2 Hz), 7.22–7.15 (2H, m), 7.12 (1H, dd, *J* = 7.4, 7.4 Hz), 7.08 (1H, d, *J* = 7.1 Hz), 6.97 (2H, dd, *J* = 7.7, 7.7 Hz), 6.89 (1H, d, *J* = 8.3 Hz), 6.86 (2H, d, *J* = 4.5 Hz), 6.39 (2H, d, *J* = 7.3 Hz), 5.26 (1H, B of AB, J_{AB} = 9.3 Hz), 5.23 (1H, A of AB, J_{AB} = 9.2 Hz), 5.05–4.96 (1H, hept., *J* = 6.4 Hz), 3.14 (1H, dq, *J* = 15.2, 7.7 Hz), 2.87 (1H, dq, *J* = 15.1, 7.4 Hz), 2.69 (1H, dq, *J* = 15.0, 7.4 Hz), 2.16 (1H, dq, *J* = 15.3, 7.5 Hz), 1.58 (3H, d, *J* = 6.2 Hz), 1.46 (3H, d, *J* = 6.2 Hz), 1.28 (9H, s), 1.22 (3H, t, *J* = 7.5 Hz), 0.83 (3H, t, *J* = 7.6 Hz); ^{13}C NMR ($CDCl_3$, 100 MHz): δ 295.6, 207.9, 152.5, 151.6, 145.2, 144.4, 143.1, 140.9, 139.8, 137.7, 137.2, 137.0, 134.4, 131.5, 130.8, 130.3, 129.9, 129.8, 129.6, 129.4, 129.0, 128.9, 128.8, 128.6, 128.4, 128.3, 128.3, 128.2, 127.9, 127.6, 127.4, 126.6, 126.4, 126.2, 125.3, 122.8, 122.4, 113.2, 75.2, 71.3, 35.2, 31.5, 31.2, 24.0, 23.7, 22.50, 22.46, 14.4, 13.2. Complex **2.118** was isolated as a 19:1 mixture of rotomers, only data for major rotomer is reported: IR (ATR mode): 3057 (w), 3027 (w), 2959 (w), 2929 (w), 2872 (w), 1588 (w), 1577 (w), 1544 (w), 1475 (w), 1454 (m), 1385 (m), 1343 (w), 1298 (w), 1287 (w), 1223 (s), 1174 (m), 1156 (m), 1140 (m), 1113 (w), 1097 (w), 1036 (w), 1007 (w), 934 (w), 901 (w), 882 (w), 842 (w), 807 (w), 773 (w), 743 (s), 719 (w), 698 (s), 638 (m), 621 (w), 610 (w) cm^{-1}; ^{1}H NMR (CDCl$_3$, 400 MHz): δ 15.39 (1H, s), 8.72 (1H, d, *J* = 1.9 Hz), 8.41–8.38 (2H, m), 7.65–7.59 (3H, m), 7.52 (1H, ddd, *J* = 8.8, 7.2, 2.0 Hz), 7.41–7.37 (3H, m), 7.34 (1H, dd, *J* = 8.1, 2.0 Hz), 7.28 (1H, s), 7.23 (2H, dd, *J* = 7.2, 7.2 Hz), 7.19–7.13 (1H, m), 7.10 (1H, dd, *J* = 7.6, 7.6 Hz), 7.06 (1H, d, *J* = 8.4 Hz), 6.99–6.91 (3H, m), 6.87 (1H, dd, *J* = 7.6, 1.8 Hz), 6.81 (1H, dd, *J* = 7.1, 7.1 Hz), 6.52 (2H, d, *J* = 7.2 Hz), 5.37 (1H, B of AB, J_{AB} = 9.4 Hz), 5.30 (1H, A of AB, *J* = 9.4 Hz), 5.15 (1H, hept., *J* = 6.4 Hz), 3.54 (1H, dq, *J* = 15.2, 7.6 Hz), 2.97 (1H, dq, *J* = 15.0, 7.4 Hz), 2.86 (1H, dq, *J* = 14.8, 7.3 Hz), 2.44 (1H, dq, *J* = 15.2, 7.6 Hz), 1.71 (3H, d, *J* = 6.3 Hz), 1.68 (3H, d, *J* = 6.3 Hz), 1.29 (9H, s), 1.24 (3H, t, *J* = 7.4 Hz), 0.89 (3H, t, *J* = 7.5 Hz); ^{13}C NMR (CDCl$_3$, 100 MHz): δ 294.4, 210.9, 152.6, 151.9, 145.1, 144.3, 142.7, 141.0, 140.1, 138.8, 137.8, 135.7, 134.6, 131.9, 130.9, 130.5, 130.0, 129.3, 128.9, 129.3, 128.9, 128.7, 128.6, 128.5, 128.4, 128.3, 127.9, 127.5, 127.3, 126.3, 124.9, 123.4, 122.1, 114.1, 76.9, 71.3, 35.7, 31.8, 31.4, 25.5, 24.5, 23.2, 22.9, 22.5, 14.5, 14.2, 13.3.

Complex 2.119 was prepared from imidazolinium tetrafluoroborate **2.226** following the procedure described for complex **2.111** via NHC-RuCl$_2$ complex **2.226c**. Complex **2.234c** was isolated as a mixture of rotomers (84:16). Data only for major rotomer is shown: ^{1}H NMR (CDCl$_3$, 400 MHz): δ 16.73 (1H, s), 8.65 (1H, s), 8.22 (2H, d, *J* = 7.2 Hz), 7.64 (2H, d, *J* = 7.2 Hz), 7.60–7.57 (2H, m), 7.51 (2H, t, *J* = 7.4 Hz), 7.48–7.36 (8 H, m), 7.35–7.33 (2H, m), 7.32–7.26 (6H, m), 7.25–7.15 (2H, m), 6.98 (1H, dd, *J* = 7.6 Hz), 6.78 (1H, dd, *J* = 7.5, 1.6 Hz), 4.64 (1H, dd, *J* = 11.4, 5.2 Hz), 4.40 (1H, dq, *J* = 12.6, 6.4 Hz), 4.05 (1H, dd, *J* = 11.0, 11.0 Hz), 3.79 (1H,dd, *J* = 10.4, 5.2 Hz), 3.14 (1H, dq, *J* = 15.2, 7.6 Hz), 2.90 (2H, apparent dqd, *J* = 15.4, 7.6, 3.8 Hz), 2.73 (1H, dq, *J* = 15.2, 7.4 Hz), 1.43 (3H, t, *J* = 7.6 Hz), 1.27 (9H, s), 1.04 (3H, d, *J* = 7.6 Hz), 1.03 (3H, t, *J* = 8.8 Hz), 0.99 (3H, d, *J* = 6.4 Hz), 0.88 (3H, d, *J* = 6.2 Hz). Complex **2.214** was isolated as a mixture of rotomers (94:6). Data only for major rotomer is shown: IR (ATR mode): 3056 (w), 3028 (w), 2963 (w), 2930 (w), 2870 (w), 1685 (w), 1584 (w), 1457 (m), 1422 (m), 1408 (m), 1374 (m), 1333 (m), 1279 (m), 1222 (s), 1177 (m), 1140 (m), 1101 (m), 1077 (w), 1027 (w), 929 (w), 904 (w), 815 w), 757 (s), 739 (m), 698 (s), 663 (m), 642 (w), 607 (w) cm^{-1}; ^1H NMR ($CDCl_3$, 400 MHz): δ 15.66 (1H, s), 8.52 (1H, s), 8.33 (2H, d, *J* = 7.2 Hz), 7.62–7.56 (5H, m), 7.53 (2H, d, *J* = 7.8 Hz), 7.49–7.26 (18H, m), 7.24–7.17 (2H, m), 6.91 (1H, dd, *J* = 7.6 Hz), 6.83 (1H, dd, *J* = 7.6, 1.6 Hz), 4.66 (2H, dd overlapping with a multiplet, *J* = 11.4, 4.8 Hz), 4.05 (1H, dd, *J* = 11.0, 11.0 Hz), 3.87 (1H, dd, *J* = 10.5, 4.8 Hz), 3.44–3.32 (1H, m), 3.21 (1H, dq, *J* = 15.2, 7.6 Hz), 3.05–2.89 (2H, m), 1.43 (3H, t, *J* = 7.6 Hz), 1.23 (9H, s), 1.17 (3H, d, *J* = 6.4 Hz), 1.14 (3H, d, *J* = 6.4 Hz), 1.10 (3H, t, *J* = 7.6 Hz); ^{13}C NMR ($CDCl_3$, 100 MHz): δ 211.8, 152.4, 149.9, 147.7, 143.8, 143.7, 140.5, 140.2, 139.6, 139.3, 139.0, 138.2, 137.5, 136.7, 134.7, 134.4, 131.3, 130.2, 129.50, 129.45, 129.2, 129.1, 128.7, 128.6, 128.3, 128.23, 128.17, 127.8, 127.7, 127.3, 127.2, 127.1, 127.0, 126.9, 126.7, 125.8, 125.4, 125.2, 124.9, 124.2, 124.1, 123.3, 123.2, 121.8, 65.4, 62.2, 35.7, 31.9, 25.4, 24.5, 22.22, 22.21, 21.9, 14.9, 14.1.

Complex 2.120 was prepared from imidazolinium tetrafluoroborate **2.224** following the procedure described for complex **2.111** via corresponding NHC-$RuCl_2$ complex **2.224c**, which was isolated as an inseparable 70:22:8 mixture of rotomers. Only data for major rotomer is presented. Complex **2.224c**: ^1H NMR ($CDCl_3$, 400 MHz): δ 16.86 (1H, s, 1H), 8.51 (1H, d, *J* = 9.1 Hz), 8.15 (2H, s), 7.99 (1H, d, *J* = 8.4 Hz), 7.81–7.52 (9H, m), 7.43 (2H, ddd, *J* = 14.4, 7.4, 4.1 Hz), 7.37–7.23 (13H, m), 7.21–7.13 (4H, m), 7.12–7.02 (5H, m), 7.01–6.87 (5H, m), 6.77 (1H, d, *J* = 6.9 Hz), 6.69 (1H, dd, *J* = 9.2, 5.8 Hz), 6.52 (2H, d, *J* = 7.5 Hz), 6.44 (1H, d, *J* = 7.8 Hz), 6.33 (1H, d, *J* = 6.5 Hz), 5.57 (1H, d, *J* = 11.9 Hz), 5.36 (1H, d, *J* = 11.9 Hz), 4.43 (1H, dq, *J* = 12.4, 6.2 Hz), 3.05 (3H, s), 2.24 (s, 3H), 1.79 (3H, s), 0.89 (3H, d, *J* = 6.7 Hz), 0.85 (3H, d, *J* = 6.2 Hz). Complex **2.120** is an inseparable 79:3:18 mixture of rotomers. Only data for major diastereomer is presented: ^1H NMR ($CDCl_3$, 400 MHz): δ 16.45 (1H, s), 9.60 (1H, d, *J* = 8.3 Hz), 7.88–7.83 (1H, m), 7.76 (1H, dd, *J* = 8.2, 3.9 Hz), 7.66–7.63 (4H, m), 7.60–7.55 (1H, m), 7.49–7.39 (4H, m), 7.37–7.27 (9H, m), 7.22–7.16 (1H, m), 7.15–7.10 (3H, m), 7.09–7.02 (2H, m), 7.01–6.94 (4H, m), 6.89 (1H, s), 6.86 (1H, d, *J* = 7.5 Hz), 6.84 (1H, s), 6.59 (2H, d, *J* = 7.3 Hz), 5.74 (1H, d, *J* = 11.0 Hz), 5.59 (1H, d, *J* = 11.0 Hz), 4.37–4.26 (1H, m), 2.95 (3H, s), 2.38 (3H, s), 2.29 (3H, s), 0.63 (3H, d, *J* = 6.2 Hz), 0.54 (3H, d, *J* = 6.3 Hz).

Complex 2.121 was prepared from imidazolinium tetrafluoroborate **2.137** following the procedure described for complex **2.111** via corresponding NHC-$RuCl_2$ complex **2.137c**: IR (ATR mode): 3054 (w), 2963 (w), 2929 (w), 2874 (w), 1686 (w), 1599 (w), 1579 (w), 1561 (w), 1494 (m), 1475 (m), 1459 (m), 1422 (m), 1376 (w), 1305 (w), 1279 (m), 1226 (s), 1203 (m), 1175 (m), 1156 (w), 1101 (w), 1089 (m), 1067 (m), 1027 (m), 1010 (w), 927 (w), 901 (m), 853 (w), 816 (m), 774 (m), 752 (s), 700 (s), 653 (m), 609 (w) cm^{-1}; ^1H NMR ($CDCl_3$, 400 MHz): δ 16.80 (1H, s), 9.35 (1H, d, *J* = 7.7 Hz), 8.03 (2H, d, *J* = 7.4 Hz), 7.61–7.53 (4H, m), 7.51 (2H, d, *J* = 8.1 Hz), 7.48–7.28 (16H, m), 7.25–7.19 (1H, m), 6.98 (1H, dd, *J* = 7.5, 7.5 Hz), 6.84 (1H, dd, *J* = 7.5, 1.5 Hz), 4.66 (1H, dd, *J* = 11.2, 4.6 Hz), 4.49 (1H, hept., *J* = 6.4 Hz), 4.06 (1H, dd, *J* = 10.8, 10.8 Hz), 3.74 (1H, dd, *J* = 10.4, 4.4 Hz), 2.97 (2H, apparent ddq, *J* = 31.1, 15.5, 7.7 Hz), 2.80 (2H, apparent ddq, *J* = 31.1, 15.5, 7.7 Hz), 1.38 (3H, t, *J* = 7.6 Hz), 1.08 (6H, d, *J* = 6.3 Hz), 1.04 (3H, t, *J* = 7.2 Hz). Complex **2.121**: IR (ATR mode): 3056 (w), 3031 (w), 2963 (w), 2929 (w), 2873 (w), 1561 (w), 1458 (m), 1436 (m), 1421 (m), 1409 (m), 1373 (m), 1332 (w), 1305 (m), 1277 (m), 1220 (s), 1177 (m), 1103 (m), 1086 (m), 1068 (m), 1027 (w), 1010 (w), 933 (w), 902 (m), 856 (w), 815 (m), 773 (m), 756 (s), 734 (m), 699 (s), 648 (m), 610 (w) cm^{-1}; ^1H NMR ($CDCl_3$, 400 MHz): δ 15.85 (1H, s), 9.35–9.29 (1H, m), 8.08 (2H, d, *J* = 7.5 Hz), 7.58 (3H, dd, *J* = 8.3, 1.4 Hz), 7.54 (2H, d, *J* = 8.0 Hz), 7.50–7.44 (3H, m), 7.43–7.32 (10H, m), 7.30 (2H, d, *J* = 7.8 Hz), 7.25–7.19 (1H, m), 6.93 (1H, dd, *J* = 7.4, 7.4 Hz), 6.88 (1H, dd, *J* = 7.5, 1.9 Hz), 4.69 (1H, dd, *J* = 11.2, 4.3 Hz), 4.64 (1H, dd, *J* = 6.2, 6.2 Hz), 4.06 (1H, dd, *J* = 10.9, 10.9 Hz), 3.79 (1H, dd, *J* = 10.5, 4.3 Hz), 3.28– 3.11 (2H, m), 2.90 (2H, dqd, *J* = 15.2, 7.5, 2.7 Hz), 1.35 (3H, t, *J* = 7.2, 7.2 Hz), 1.35 (3H, d, *J* = 6.4 Hz), 1.24 (3H, d, *J* = 6.2 Hz), 1.08 (3H, t, *J* = 7.6 Hz); ^{13}C NMR ($CDCl_3$, 100 MHz): δ 303.5, 214.2, 150.4, 147.4, 144.0, 143.8, 141.9, 140.6, 140.4, 139.6, 138.9, 136.2, 135.0, 132.9, 131.8, 130.7, 129.3, 129.3, 129.1, 129.0, 128.7, 128.4, 128.2, 128.0, 127.9, 127.4, 127.3, 126.0, 123.2, 122.6, 122.1, 77.3, 64.1, 63.1, 25.4, 24.9, 22.5, 22.0, 14.8, 14.5.

Complex 2.122 was prepared from imidazolinium tetrafluoroborate **2.229** following the procedure described for complex **2.111** via corresponding NHC-$RuCl_2$ complex **2.229c**:

^{1}H NMR (CDCl$_3$, 400 MHz): δ 16.83 (1H, s), 9.43 (1H, dd, J = 7.7, 0.9 Hz), 8.04 (2H, d, J = 7.3 Hz), 7.63 (1H, dd, J = 9.9, 5.6 Hz), 7.58 (2H, d, J = 7.0 Hz), 7.54 (3H, dd, J = 11.4, 4.6 Hz), 7.49–7.43 (5H, m), 7.42–7.37 (8H, m), 7.36–7.28 (7H, m), 7.24–7.19 (1H, m), 6.97 (1H, dd, J = 7.2 Hz), 6.81 (1H, dd, J = 7.5, 1.7 Hz), 4.69 (1H, dd, J = 11.1, 4.8 Hz), 4.52 (1H, hept., J = 6.4 Hz), 4.05 (1H, dd, J = 10.8, 10.8 Hz), 3.77 (1H, dd, J = 10.8, 4.8 Hz), 3.65 (1H, hept., J = 6.8 Hz), 3.35 (1H, hept., J = 6.8 Hz), 1.37 (3H, d, J = 6.9 Hz), 1.21 (3H, d, J = 6.7 Hz), 1.13 (3H, d, J = 6.3 Hz), 1.10 (3H, d, J = 6.3 Hz), 0.99 (3H, d, J = 6.6 Hz), 0.92 (3H, d, J = 7.3 Hz). Complex **2.122**: IR (ATR mode): 3056 (w), 3029 (w), 2960 (w), 2922 (w), 2862 (w), 1599 (w), 1578 (w), 1561 (w), 1493 (w), 1469 (w), 1455 (m), 1435 (m), 1421 (m), 1402 (m), 1383 (m), 1372 (m), 1326 (m), 1305 (m), 1283 (m), 1269 (m), 1245 (m), 1219 (s), 1205 (m), 1176 (m), 1103 (m), 1071 (w), 1053 (w), 1028 (w), 1009 (m), 949 (m), 933 (w), 898 (w), 856 (w), 824 (w), 809 (w), 778 (m), 759 (s), 737 (m), 699 (s), 646 (m), 611 (m) cm^{-1}; ^{1}H NMR (CDCl$_3$, 400 MHz): δ 16.07 (1H, s), 9.49 (1H, d, J = 7.3 Hz), 8.07 (2H, d, J = 7.1 Hz), 7.65–7.55 (4H, m), 7.53 (2H, d, J = 8.0 Hz), 7.50 (2H, d, J = 7.8 Hz), 7.47–7.33 (10H, m), 7.30 (2H, dd, J = 7.4, 7.4 Hz), 7.22 (2H, dd, J = 7.2, 7.2 Hz), 6.93–6.82 (2H, m), 4.80–4.65 (2H, m), 4.12 (1H, dd, J = 10.7, 10.7 Hz), 3.93–3.83 (2H, m), 3.51 (1H, hept., J = 6.8 Hz), 1.43 (3H, d, J = 6.2 Hz), 1.36 (3H, d, J = 6.8 Hz), 1.27 (3H, d, J = 6.2 Hz), 1.22 (3H, d, J = 6.6 Hz), 1.15 (3H, d, J = 6.5 Hz), 0.90 (3H, d, J = 6.8 Hz); ^{13}C NMR (CDCl$_3$, 100 MHz): δ 300.5, 214.6, 150.6, 148.8, 148.6, 146.9, 142.1, 140.6, 140.5, 139.7, 137.6, 136.2, 134.9, 133.0, 131.8, 130.6, 129.8, 129.2, 128.9, 128.7, 128.6, 128.3, 128.2, 127.9, 127.4, 125.4, 124.9, 123.0, 122.5, 122.3, 77.3, 64.9, 63.9, 28.2, 28.0, 27.3, 26.1, 25.4, 25.3, 22.7, 22.0.

Complex 2.123 was prepared from imidazolinium tetrafluoroborate **2.230** following the procedure described for complex **2.111** via corresponding NHC-RuCl$_2$ complex **2.230c**: ^{1}H NMR (CDCl$_3$, 400 MHz): δ 16.85 (1H, s), 9.41 (1H, d, J = 7.7 Hz), 8.03 (2H, d, J = 7.4 Hz), 7.58 (2H, d, J = 7.1 Hz), 7.53 (2H, dd, J = 8.0, 8.0 Hz), 7.49–7.41 (3H, m), 7.41–7.26 (12H, m), 7.22 (1H, d, J = 7.0 Hz), 7.20 (1H, d, J = 2.0 Hz), 6.95 (1H, dd, J = 7.5, 7.5 Hz), 6.79 (1H, dd, J = 7.5, 1.5 Hz), 4.66 (1H, dd, J = 10.8, 4.8 Hz), 4.51 (1H, hept., J = 6.4 Hz), 4.03 (1H, dd, J = 10.8, 10.8 Hz), 3.75 (1H, dd, J = 10.8, 4.8 Hz), 3.60

(1H, hept., *J* = 6.8 Hz), 3.31 (1H, hept., *J* = 6.8 Hz), 3.10 (1H, hept., *J* = 6.8 Hz), 1.44 (6H, d, *J* = 6.8 Hz), 1.36 (3H, d, *J* = 6.8 Hz), 1.19 (3H, d, *J* = 6.8 Hz), 1.11 (3H, d, *J* = 6.4 Hz), 1.09 (3H, d, *J* = 6.4 Hz), 0.97 (3H, *J* = 6.8 Hz), 0.92 (3H, d, *J* = 6.8 Hz). Complex **2.123**: IR (ATR mode): 3055 (w), 2960 (m), 2926 (w), 2865 (w), 1601 (w), 1562 (w), 1469 (m), 1457 (m), 1438 (m), 1421 (m), 1409 (m), 1383 (m), 1373 (m), 1335 (m), 1318 (m), 1304 (m), 1281 (m), 1255 (m), 1224 (s), 1198 (m), 1176 (m), 1103 (m), 1088 (m), 1069 (m), 1028 (w), 1010 (w), 935 (w), 903 (m), 879 (w), 856 (w), 818 (w), 756 (s), 735 (m), 699 (s), 650 (m), 611 (w) cm^{-1}; ^1H NMR ($CDCl_3$, 400 MHz): δ 16.10 (1H, s), 9.50 (1H, d, *J* = 7.4 Hz), 8.08 (2H, d, *J* = 7.3 Hz), 7.58 (2H, d, *J* = 8.4 Hz), 7.57–7.44 (6H, m), 7.43–7.32 (8H, m), 7.30 (3H, dd, *J* = 4.9, 2.8 Hz), 7.23 (d, *J* = 7.6 Hz), 7.21 (1H, d, *J* = 2.0 Hz), 6.89 (1H, dd, *J* = 7.2, 7.2 Hz), 6.84 (1H, dd, *J* = 7.5, 1.9 Hz), 4.76–4.66 (2H, m), 4.12 (1H, dd, *J* = 10.8, 10.8 Hz), 3.93–3.81 (2H, m, 2H), 3.48 (1H, hept, *J* = 6.8 Hz), 3.07 (1H, hept., *J* = 6.8 Hz), 1.44 (3H, d, *J* = 6.8 Hz), 1.42 (6H, d, *J* = 6.8 Hz), 1.36 (3H, d, *J* = 6.8 Hz), 1.28 (3H, d, *J* = 6.4 Hz), 1.23 (3H, d, *J* = 6.8 Hz), 1.16 (3H, d, *J* = 6.8 Hz), 0.91 (3H, d, *J* = 6.8 Hz); ^{13}C NMR (101 MHz, $CDCl_3$) δ 300.8, 214.5, 150.52, 150.48, 148.3, 148.1, 146.93, 146.90, 142.1, 140.62, 140.57, 139.7, 136.2, 135.3, 134.8, 132.9, 131.9, 130.6, 129.2, 128.9, 128.7, 128.6, 128.3, 128.1, 127.9, 127.4, 123.1, 123.0, 122.7, 122.4, 122.3, 64.8, 63.9, 34.6, 28.2, 28.0, 27.3, 26.2, 25.4, 25.3, 24.50, 24.48, 22.8, 22.7, 22.0.

Complex 2.124 was prepared from imidazolinium tetrafluoroborate **2.225** following the procedure described for complex **2.111** via corresponding NHC-$RuCl_2$ complex **2.225c**: ^1H NMR (400 MHz, $CDCl_3$): δ 17.08 (1H, s), 9.52 (1H, dd, *J* = 7.6, 1.2 Hz), 8.36 (1H, dd, *J* = 1.5, 1.5 Hz), 7.68 (1H, dd, *J* = 1.8, 1.8 Hz), 7.58–7.54 (2H, m), 7.49 (2H, d, *J* = 7.2 Hz), 7.47 (1H, ddd, *J* = 7.6, 7.6, 1.6 Hz) 7.43–7.37 (3H, m), 7.36–7.31 (3H, m), 7.30 (1H, dd, *J* = 7.4, 1.2 Hz), 7.25–7.19 (3H, m), 7.15 (1H, dd, *J* = 7.5, 7.5 Hz), 6.98–6.95 (4H, m), 6.83 (1H, dd, *J* = 7.5, 1.7 Hz), 6.73 (1H, s), 6.19 (2H, d, *J* = 7.2 Hz), 5.74 (1H, B of AB, J_{AB} = 6.8 Hz), 5.08 (1H, A of AB, J_{AB} = 6.8 Hz), 4.51–4.42 (1H, m), 2.53 (3H, s), 2.34 (3H, s), 1.61 (3H, s), 1.40 (9H, s), 1.37 (9H, s), 1.14 (3H, d, *J* = 6.3 Hz), 1.06 (3H, d, *J* = 6.3 Hz). Complex **2.124**: IR (ATR mode): 3060 (w), 3031 (w), 2961 (w), 2866 (w), 1590 (w), 1562 (w), 1477 (m), 1456 (m), 1422 (m), 1395 (m), 1374 (m), 1341 (w), 1306 (w), 1279 (m), 1243 (m), 1225 (s), 1190 (m), 1161 (w), 1103 (w), 1088 (w), 1076 (w), 1028 (w), 1003 (w), 934 (w), 902 (m), 881 (w), 855 (w), 818 (w), 756 (s), 736 (m), 719 (w), 699 (s), 645 (w), 620 (w), 608 (w) cm^{-1}; ^{1}H NMR (CDCl$_3$, 400 MHz): δ 16.09 (1H, s, 1H), 9.58 (1H, dd, J = 7.7, 1.1 Hz), 8.63 (1H, dd, J = 1.6 Hz), 7.64 (1H, dd, J = 1.8, 1.8 Hz), 7.62 (2H, broad overlapping s), 7.58–7.54 (2H, m), 7.45 (1H, ddd, J = 7.5, 7.5, 1.7 Hz), 7.39 (3H, dd, J = 7.3, 2.0 Hz), 7.36–7.27 (5H, m), 7.25–7.22 (1H, m), 7.19 (1H, dd, J = 7.5, 1.6 Hz), 7.13 (1H, dd, J = 7.5, 7.5 Hz), 7.10 (1H, dd, J = 1.6, 1.6 Hz), 6.98–6.94 (3H, m), 6.91 (1H, dd, J = 7.6, 7.6 Hz), 6.86 (1H, dd, J = 7.5, 1.9 Hz), 6.70 (1H, d, J = 1.4 Hz), 6.32 (2H, d, J = 7.2 Hz), 5.81 (1H, B of AB, J_{AB} = 7.4 Hz), 5.18 (1H, A of AB, J_{AB} = 7.5 Hz), 4.68–4.55 (1H, m), 2.72 (3H, s), 2.33 (3H, s), 1.72 (3H, s), 1.42 (9H, s), 1.42 (3H, d, J = 6.0 Hz) 1.36 (9H, s), 1.17 (3H, d, J = 6.2 Hz); ^{13}C NMR (CDCl$_3$, 100 MHz): δ 306.0, 211.2, 151.2, 150.9, 150.4, 147.9, 142.1, 141.2, 140.7, 140.5, 139.6, 138.4, 138.4, 136.9, 135.4, 135.2, 134.9, 134.4, 132.0, 130.7, 130.5, 129.2, 129.1, 129.0, 128.9, 128.8, 128.7, 128.6, 128.3, 128.1, 127.9, 127.8, 127.6, 127.4, 125.8, 123.3, 123.1, 122.2, 122.2, 122.0, 77.4, 77.0, 70.3, 35.9, 35.2, 32.1, 31.8, 31.1, 29.9, 22.7, 21.9, 21.8, 21.2; HRMS Calcd for $C_{60}H_{64}N_2ORuI_2$ [M$^+$] (ES$^+$): 1184.2151, Found: 1184.2162.

Complex 2.125 was prepared from imidazolinium tetrafluoroborate **2.231** following the procedure described for complex **2.111** via corresponding NHC-RuCl$_2$ complex **2.231c**: ^{1}H NMR (CDCl$_3$, 400 MHz): δ 16.94 (1H, s), 9.30 (1H, dd, J = 7.6, 1.0 Hz), 8.02 (2H, d, J = 7.2 Hz), 7.58 (2H, d, J = 8.4 Hz), 7.51 (2H, dd, J = 8.0, 8.0 Hz), 7.48 – 7.39 (6H, m), 7.38–7.33 (6H, m), 7.31 (3H, dd, J = 8.0, 8.0 Hz), 7.24–7.20 (2H, m), 6.99 (1H, dd, J = 7.6, 7.6 Hz), 6.87 (1H, dd, J = 7.5, 1.7 Hz), 4.63 (1H, dd, J = 11.2, 4.3 Hz), 4.49 (1H, hept., J = 6.4 Hz), 4.07 (1H, dd, J = 10.8, 10.8 Hz), 3.72 (1H, dd, J = 10.5, 4.3 Hz), 2.55 (3H, s), 2.39 (3H, s), 1.46 (9H, s), 1.08 (6H, d, J = 6.4 Hz). Complex **2.125**: IR (ATR mode): 3053 (w), 2961 (w), 1561 (m), 1492 (m), 1478 (m), 1457 (m), 1435 (m), 1421 (m), 1410 (m), 1373 (w), 1305 (m), 1275 (m), 1223 (s), 1203 (m), 1177 (m), 1103 (m), 1087 (m), 1068 (m), 1028 (w), 1010 (w), 934 (w), 903 (m), 871 (w), 855 (w), 818 (w), 773 (m), 756 (m), 748 (m), 735 (m), 699 (s), 649 (m), 621 (w), 611 (m) cm^{-1}; ^{1}H NMR

($CDCl_3$, 400 MHz): δ 16.06 (1H, s), 9.29 (2H, dd, *J* = 7.2, 1.6 Hz), 8.09 (2H, d, *J* = 7.0 Hz), 7.60 (2H, d, *J* = 8.2 Hz), 7.58–7.51 (2H, m), 7.51–7.45 (3H, m), 7.44–7.27 (10H, m), 7.25–7.18 (2H, m), 6.95–6.89 (2H, m), 4.73–4.61 (2H, m), 4.05 (1H, dd, *J* = 10.8, 10.8 Hz), 3.78 (1H, dd, *J* = 10.8, 4.2 Hz), 2.66 (3H, s), 2.59 (3H, s), 1.46 (9H, s), 1.35 (3H, d, *J* = 6.2 Hz), 1.29 (3H, d, *J* = 6.2 Hz); ^{13}C NMR ($CDCl_3$, 100 MHz): δ 213.3, 152.2, 150.4, 147.4, 141.9, 140.7, 140.4, 139.7, 138.0, 137.5, 137.2, 136.3, 135.0, 132.7, 131.9, 130.7, 129.3, 129.0, 128.7, 128.4, 128.2, 128.0, 127.9, 127.5, 126.8, 126.0, 123.1, 122.7, 122.2, 77.3, 64.1, 61.7, 34.8, 31.7, 22.4, 22.1, 20.8, 20.5.

Complex 2.126 was prepared from imidazolinium tetrafluoroborate **2.232** following the procedure described for complex **2.111**: ^{1}H NMR ($CDCl_3$, 400 MHz): δ 16.09 (1H, s), 9.71 (1H, dd, *J* = 7.2, 0.8 Hz), 8.01 (2H, broad s), 7.58–7.53 (3H, m), 7.49–7.44 (4H, m), 7.43–7.30 (6H, m), 7.28 (1H, d, *J* = 2.1 Hz), 7.25 (1H, d, *J* = 2.1 Hz), 6.84 (1H, dd, *J* = 7.2, 7.2 Hz), 6.75 (1H, dd, *J* = 7.2, 1.8 Hz), 4.66 (1H, hept., *J* = 6.4), 3.82 (1H, hept., *J* = 6.8 Hz), 3.77–3.66 (2H, m), 3.57 (1H, dd, *J* = 10.4, 5.4 Hz), 3.41 (1H, hept., *J* = 6.8 Hz), 3.07 (1H, hept., 6.8 Hz), 1.42 (6H, d, *J* = 6.8 Hz), 1.38 (3H, d, *J* = 6.8 Hz), 1.36 (3H, d, *J* = 6.8 Hz), 1.26 (3H, d, *J* = 6.4 Hz), 1.22 (3H, d, *J* = 6.8 Hz), 1.16 (3H, d, *J* = 6.4 Hz), 1.14 (3H, d, *J* = 6.8 Hz), 0.80 (9H, s).

Complex 2.127 was prepared from imidazolinium tetrafluoroborate **2.233** following the procedure described for complex **2.111** via corresponding NHC-$RuCl_2$ complex **2.233c**: ^{1}H NMR ($CDCl_3$, 400 MHz): δ 16.73 (1H, s), 9.60 (1H, d, *J* = 7.6 Hz), 7.98 (2H, broad s), 7.64 (1H, ddd, *J* = 7.7, 5.8, 3.4 Hz), 7.59–7.55 (3H, m, 3H), 7.49–7.37 (10H, m), 7.35–7.30 (2H, m), 6.95 (1H, dd, *J* = 7.6, 7.6 Hz), 6.77 (1H, dd, *J* = 7.6, 1.6 Hz), 4.44 (1H, hept., *J* = 6.4 Hz), 3.72–3.63 (2H, m), 3.54 (1H, dd, *J* = 10.4, 6.4 Hz), 3.02 (1H, dq, *J* = 15.2, 7.6 Hz), 2.88–2.69 (3H, m), 1.36 (3H, t, *J* = 7.6 Hz), 1.14 (3H, t, *J* = 7.6 Hz), 1.05 (3H, d, *J* = 6.4 Hz), 1.01 (3H, d, *J* = 6.4 Hz), 0.76 (9H, s). Complex **2.127**: IR (ATR mode): 3056 (w), 2960 (w), 2872 (w), 1562 (w), 1478 (m), 1458 (m), 1421 (m), 1399 (m), 1372 (m), 1340 (w), 1307 (w), 1277 (m), 1241 (m), 1225 (s), 1204 (m), 1177 (m), 1103 (m), 1088 (m), 1068 (m), 1029 (w), 1011 (w), 934 (w), 903 (m), 874 (w), 856 (m), 815 (w), 758 (m), 749 (m), 733 (m), 701 (s), 670 (w), 641 (m), 610 (m) cm^{-1}; ^{1}H NMR

($CDCl_3$, 400 MHz): δ 15.77 (1H, s), 9.55 (1H, d, J = 7.8 Hz), 8.04 (1H, broad s), 7.60–7.54 (4H, m), 7.49–7.44 (4H, m), 7.42–7.30 (8H, m), 6.90 (1H, dd, J = 7.6, 7.6 Hz), 6.80 (1H, dd, J = 7.6, 1.8 Hz), 4.61 (1H, hept., J = 6.4 Hz), 3.74–3.64 (1H, m), 3.55 (1H, dd, J = 9.0, 7.0 Hz), 3.20 (1H, dq, J = 15.4, 7.6 Hz), 3.13–2.98 (2H, m), 2.86 (1H, dq, J = 15.2, 7.6 Hz), 1.34 (3H, t, J = 7.6 Hz), 1.31 (3H, d, J = 6.8 Hz), 1.23 (3H, d, J = 6.0 Hz), 1.21 (3H, t, J = 7.6 Hz), 0.80 (9H, s); ^{13}C NMR ($CDCl_3$, 100 MHz): δ 303.5, 214.2, 150.3, 147.5, 145.2, 143.9, 143.7, 140.5, 139.7, 139.3, 136.5, 134.9, 133.4, 131.8, 131.5, 129.4, 129.3, 129.1, 128.7, 128.5, 128.2, 127.8, 127.5, 126.1, 123.1, 122.6, 120.9, 77.0, 68.1, 56.9, 36.4, 26.5, 25.8, 24.8, 22.5, 22.1, 15.5, 14.3.

Complex 2.149 was prepared from was prepared from imidazolinium triflate **2.147** following the procedure described for complex **2.111** with the exception that solution of KHMDS in THF was added *via* syringe pump (over 15 min). IR (ATR mode): 3066 (w), 2961 (w), 2927 (w), 2873 (w), 1590 (w), 1576 (w), 1472 (m), 1453 (m), 1410 (m), 1358 (s), 1300 (m), 1242 (w), 1208 (m), 1179 (s), 1139 (w), 1096 (m), 1065 (m), 1037 (w), 969 (m), 928 (s), 881 (w), 843 (m), 816 (m), 759 (s), 700 (s), 645 (w), 615 (w) cm^{-1}; ^{1}H NMR ($CDCl_3$, 400 MHz): δ 16.11 (1H, s), 8.20 (1H, d, J = 7.6 Hz), 8.15 (1H, d, J = 7.6 Hz), 8.06 (1H, d, J = 7.0 Hz), 7.91 (1H, dd, J = 7.8, 1.2 Hz), 7.64 (2H, dt, J = 8.8, 3.8 Hz), 7.59 (2H, d, J = 7.2 Hz), 7.54 (2H, d, J = 7.2 Hz), 7.46 (4H, dd, J = 13.4, 6.2 Hz), 7.41–7.29 (6H, m), 7.23 (1H, d, J = 7.4 Hz), 7.04 (1H, d, J = 8.6 Hz), 6.89 (1H, t, J = 7.4 Hz), 6.00 (1H, broad d, J = 18.0 Hz), 5.85 (1H, B of AB, J = 17.0 Hz), 5.49 (1H, A of AB, J = 17.0 Hz), 5.36 (1H, dt, J = 12.2, 6.2 Hz), 5.19 (1H, broad s), 4.85 (2H, s), 3.68 (1H, dd, J = 9.2, 7.0 Hz), 3.64 (1H, dd, J = 9.4, 7.0 Hz), 3.53 (1H, dd, J = 9.2, 6.6 Hz), 3.37 (1H, dd, J = 9.4, 6.6 Hz), 1.86 (3H, d, J = 6.0 Hz), 1.85 (3H, d, J = 6.0 Hz), 0.77 (3H, d, J = 6.8 Hz), 0.72 (3H, d, J = 6.8 Hz), 0.64 (3H, d, J = 6.0 Hz), 0.62 (3H, d, J = 6.8 Hz); ^{13}C NMR ($CDCl_3$, 100 MHz): δ 215.8, 153.7, 144.3, 139.1, 138.8, 136.6, 134.7, 134.5, 134.0, 133.7, 133.2, 131.3, 130.9, 130.4, 129.9, 129.7, 129.5, 129.1, 128.8, 127.9, 127.9, 127.1, 127.0, 123.5, 122.6, 113.6, 76.7, 76.3, 76.2, 72.0, 50.2, 31.7, 28.1, 28.0, 22.8, 22.7, 22.6, 18.8, 18.72, 18.71, 18.69, 14.3.

Complex 2.169. To a 1-dram vial under N_2-atmosphere were added Ru-complex **2.54** (102.6 mg, 0.1069 mmol, 1.36 equiv.) and cyclobutene **2.168** (13.4 mg, 0.0787 mmol, 1.00 equiv.). C_6H_6 (3.0 mL) was added and the reaction mixture was allowed to stir for 2 h at 22 °C, at which time the solvent was removed *in vacuo* to give a dark brown solid. Purification by silica gel chromatography (30% to 60% CH_2Cl_2 in pentane) afforded the desired Ru-complex 2.**169** (27.2 mg, 0.0241 mmol, 31% yield). IR (ATR mode): 3060 (w), 3030 (w), 2962 (w), 2921 (w), 2869 (w), 1735 (w), 1601 (w), 1586 (w), 1557 (w), 1494 (w), 1469 (w), 1432(w), 1399 (w), 1380 (w), 1343 (w), 1273 (w), 1258 (w), 1215 (w), 1176 (w), 1139 (w), 1108 (w), 1060 (w), 1026 (w), 1006 (w), 933 (w), 905 (w), 857 (s), 795 (s), 757 (s), 739 (s), 698 (s), 674 (s), 607 (s), 575 (w), 556 (w), 524 (w); ^{1}H NMR ($CDCl_3$, 400 MHz): δ 16.82 (d, J = 1.6 Hz, 1H), 7.68 (d, J = 7.6 Hz, 1H), 7.54-7.52 (m, 1H) 7.49-7.47 (m, 2H), 7.40-7.39 (m, 4H), 7.37-7.31 (m, 4H), 7.29-7.27 (m, 2H), 7.20-7.14 (m, 2H), 7.12-7.08 (m, 1H), 7.05-7.03 (m, 2H), 7.00 (m, 1H), 6.97-6.90 (m, 6H), 6.78 (s, 1H), 6.62 (s, 1H) 6.17 (d, J = 7.6 Hz, 2H), 5.70 (dd, J = 12.0, 10.4 Hz, 1H), 5.01-4.96 (m, 2H), 4.83-4.81 (m, 1H), 4.16-4.10 (m, 1H), 3.77-3.71 (m, 1H), 3.58-3.52 (m, 1H), 2.95 (dd, J = 6.4, 1.6 Hz, 1H), 2.50 (s, 3H), 2.17 (s, 3H), 2.11 (s, 3H), 1.56 (d, J = 6.0 Hz, 3H), 1.08 (d, J = 6.0 Hz, 3H), 1.00 (d, J = 6.0 Hz, 3 H), 0.97-0.95 (m, 6H), 0.74 (d, J = 6.4 Hz, 3 H); ^{13}C NMR ($CDCl_3$, 100 MHZ): δ 212.4, 166.97, 153.1, 140.8, 140.5, 140.4, 139.5, 137.8, 137.3, 137.2, 136.9, 136.7, 135.5, 132.3, 131.7, 130.8, 130.7, 130.5, 130.1, 129.9, 129.7, 129.4, 129.3, 128.9, 128.8, 128.8, 128.7, 128.6, 128.3, 128.2, 128.1, 128.0, 127.9, 126.9, 126.8, 126.7, 123.4, 123.2, 117.4, 94.8, 77.2, 76.4, 76.3, 75.4, 75.3, 73.5, 71.1, 24.3, 23.5, 22.3, 21.8, 21.6, 21.3, 21.2, 20.1, 19.9; HRMS (ESI+): Calcd for $C_{62}H_{65}IN_2O_4Ru$ [M+H]: 1131.3129. Found: 1131.3143. 2D NMR spectra are shown in in the NMR section.

Complex 2.170. Prepared according to standard procedure.[69f] IR (ATR mode): 3032 (w), 2970 (w), 2919 (w), 2736 (w), 1686 (w), 1604 (w), 1588 (w), 1559 (w), 1484 (w), 1459 (w), 1435 (w), 1422 (w), 1400 (w), 1381 (w), 1371 (w), 1344 (w), 1284 (w), 1264 (w), 1237 (w), 1200 (w), 1176 (w), 1158 (w), 1116 (w), 1102 (w), 1091 (s), 1075 (s), 1029 (s), 1004 (s), 931 (s), 902 (s), 847 (s), 808 (s), 795 (s), 781 (s), 760 (s), 736 (s), 699 (s), 671 (s), 632 (s), 610 (s), 602 (s), 574 (s), 558 (s), 541 (s), 519 (s), 489 (s), 464(s); ^{1}H NMR (CDCl$_3$, 400 MHz): δ 15.45 (s, 1H), 7.49-7.47 (m, 2H), 7.39-7.30 (m, 7 H), 7.18-7.14 (m, 3H), 7.08-7.00 (m, 4H), 6.96 (m, 1H), 6.93-6.89 (m, 1H), 6.83-6.81 (m, 1H), 6.79 (m, 1H), 6.53 (d, *J* = 8.0 Hz, 1H), 6.40 (d, *J* = 7.6 Hz, 1H), 5.09 (s, 2H), 4.45-4.38 (m, 1H), 2.65 (s, 3H), 2.32 (s, 3H), 1.52 (s, 3H), 0.88 (d, *J* = 6.0 Hz, 3H), 0.73 (d, *J* = 6.4 Hz, 3H); ^{13}C NMR (CDCl$_3$, 100 MHZ): δ 281.1, 219.4, 170.4, 160.9, 158.3, 149.7, 147.8, 145.4, 139.8, 139.3, 138.5, 137.8, 136.5, 136.3, 135.1, 132.4, 132.3, 131.9, 131.8, 130.7, 130.6, 130.1, 129.8, 129.6, 126.59, 129.4, 129.39, 129.2, 129.1, 128.9, 128.8, 128.7, 128.6, 128.57, 128.4, 128.2, 127.9, 127.7, 127.4, 127.38, 127.3, 126.6, 126.5, 125.5, 123.9, 123.6, 121.1, 117.2, 116.7, 116.4, 78.1, 74.9, 21.3, 20.9, 20.8, 20.4, 19.2; ^{19}F NMR (CDCl$_3$, 376 MHZ): δ -105.4; HRMS (ESI+): Calcd for $C_{52}H_{46}IFN_2O_2Ru$ [M+H]: 978.1632. Found: 978.1641.

Complex 2.171. Prepared according to the procedure for **2.169**. IR (neat): 3031 (w), 2970 (w), 2924 (w), 1954 (w), 1719 (w), 1687 (w), 1589 (w), 1459 (w), 1433 (s), 1401 (s), 1380 (s), 1344 (s), 1256 (s), 1217 (s), 1177 (s), 1141 (s), 1106 (s), 1079 (s), 1035 (s), 1004 (s), 933 (s), 901 (s), 847 (s), 794 (s), 759 (s), 698 (s), 671 (s), 633 (s), 607 (s), 573 (s); ^{1}H NMR (CDCl$_3$, 400 MHz): δ 16.96 (d, *J* = 2.4 Hz, 1H), 7.63 (d, *J* = 6.0 Hz, 1H), 7.52-7.49 (m, 3H), 7.39-7.28 (m, 12H), 7.25-7.21 (m, 2H), 7.14-7.09 (m, 2H), 7.07-7.00 (m, 10H), 6.88-6.85 (m, 1H), 6.82 (s, 1H), 6.79-6.78 (m, 1H), 6.63 (s, 1H), 6.22 (d, *J* = 7.2 Hz, 2H), 5.64 (dd, *J* = 12.0, 10.0 Hz, 1H), 5.19 (d, *J* = 10.4 Hz, 1H), 5.00 (dd, *J* = 10.4, 5.6 Hz, 1H), 4.85 (d, *J* = 10.4 Hz, 1H), 4.18-4.12 (m, 1H), 3.78-3.72 (m, 1H), 3.71-3.65 (m, 1H), 3.17 (dd, *J* = 5.6, 2.4 Hz, 1H), 2.59 (s, 3H), 2.19 (s, 3H), 2.18 (s, 3H), 1.59 (d, *J* = 6.0 Hz, 3H), 1.15 (d, *J* = 6.4 Hz, 3H), 1.04-1.02 (m, 6H), 0.98 (d, *J* = 6.0 Hz, 3H), 0.77 (d, *J* = 6.0 Hz, 3H); ^{13}C NMR (CDCl$_3$, 100 MHZ): δ 214.3, 167.5, 160.2, 158.2, 153.3, 143.4, 139.7, 137.7, 137.6, 137.4, 137.3, 137.1, 136.8, 135.9, 131.2, 130.9, 130.8, 130.7, 130.5, 130.1, 129.8, 129.6, 129.4, 129.3, 129.1, 129.06, 128.7, 128.5, 128.2, 127.9, 127.6, 127.0, 123.8, 123.7, 118.1, 115.0, 114.9, 94.1, 76.5, 76.3, 76.1, 75.6, 73.7, 71.2, 24.5, 23.9, 22.5, 22.2, 21.9, 21.4, 21.3, 20.9, 20.2; ^{19}F NMR (CDCl$_3$, 376 MHZ): δ -

116.4; HRMS (ESI+): Calcd for $C_{62}H_{65}IFN_2O_2Ru$ [M+H]: 1149.3017. Found: 1149.3005. 2D NMR spectra are shown in in the NMR section.

Complex 2.175. To a 1-dram vial under N_2-atmosphere were added Ru-complex **2.169** (10.9 mg, 0.00964 mmol, 1.00 equiv.) and C_6D_6 (0.50 mL), and the reaction mixture was allowed to stir for 25 h at 50 °C, at which time the solvent was removed *in vacuo* to give a dark brown solid. Purification by silica gel chromatography (30% to 80% CH_2Cl_2 in pentane) afforded the desired Ru-complex **2.175** (4.8 mg, 0.0042 mmol, 44% yield). IR (in CH_2Cl_2): 3032 (w), 2970 (w), 2923 (w), 1961 (w), 1758 (w), 1728 (w), 1667 (w), 1637 (w), 1601 (w), 1587 (w), 1495 (w), 1470 (w), 1439 (w), 1380 (w), 1345 (w), 1263 (w), 1236 (w), 1216 (w), 1176 (w), 1155 (w), 1140 (w), 1106 (w), 1061 (w), 1027 (w), 1005 (w), 933 (w), 905 (s), 856 (w), 797 (w), 758 (w), 734 (s), 698 (s), 672 (w), 634 (w), 607 (w), 573 (w), 527 (w), 471 (w); ^1H NMR ($CDCl_3$, 400 MHz): δ 15.99 (d, J = 2.4 Hz, 1H), 8.21 (dd, J = 8.0, 1.2 Hz, 1H), 7.66 (dd, J = 7.6, 1.6 Hz, 1H), 7.52-7.48 (m, 3H), 7.38-7.35 (m, 3H), 7.31-7.28 (m, 2H), 7.24-7.21 (m, 6H), 7.17-7.13 (m, 6H), 7.12-7.08 (m, 2H), 7.02 (d, J = 12.4 Hz, 1H), 6.96-6.94 (m, 3H), 6.91 (m, 1H), 6.79 (dt, J = 7.2, 1.2 Hz, 1H), 6.69-6.68 (m, 2H), 6.53 (dd, J = 8.0, 0.8 Hz, 1H), 5.88 (d, J = 12.4 Hz, 2H), 4.90 (dd, J = 10.4, 6.0 Hz, 1H), 4.84 (d, J = 12.0 Hz, 1H), 4.04-3.98 (m, 1H), 3.78-3.72 (m, 1H), 3.50 (dd, J = 6.0, 2.4 Hz, 1H), 3.47-3.41 (m, 1H), 2.25 (s, 3H), 1.88 (s, 3H), 1.79 (s, 3H), 1.03 (d, J = 6.0 Hz, 3H), 0.99 (d, J = 6.4 Hz, 3H), 0.96 (d, J = 6.0 Hz, 3H), 0.81-0.78 (m, 6H), 0.74 (d, J = 6.4 Hz, 3H); ^{13}C NMR ($CDCl_3$, 100 MHZ): δ 220.6, 169.5, 153.3, 142.5, 139.8, 139.7, 138.2, 137.5, 137.4, 136.5, 135.8, 135.6, 134.8, 131.8, 131.3, 131.0, 130.9, 130.7, 130.6, 130.57, 130.52, 130.3, 130.1, 129.8, 129.7, 129.6, 129.5, 129.2, 129.16, 128.96, 128.8, 128.5, 128.4, 128.3, 128.2, 128.15, 127.8, 127.0, 123.8, 123.6, 121.6, 116.9, 96.1, 83.9, 75.6, 75.58, 75.3, 74.7, 73.2, 73.0, 70.8, 23.7, 23.4, 23.1, 22.9, 22.5, 22.2, 22.1, 21.9, 21.86, 21.7, 21.2, 20.9, 20.4, 19.0; HRMS (ESI+): Calcd for $C_{62}H_{65}IN_2O_4Ru$ [M+H]: 1131.3129. Found: 1131.3160. 2D NMR spectra are shown in in the NMR section.

Complex 2.174. To a 1-dram vial under N_2-atmosphere were added Ru-complex **2.175** (20.2 mg, 0.0179 mmol, 1.00 equiv.) and acetic acid (0.13 mg, 0.0021 mmol, 0.12 equiv.). C_6H_6 (0.12 mL) was added and the reaction mixture was allowed to stir for 1 h at 22 °C, at which time the solvent was removed *in vacuo* to give a dark brown solid. Purification by silica gel chromatography (30% to 70% CH_2Cl_2 in pentane) afforded the desired Ru-complex **2.174** (5.6 mg, 0.0049 mmol, 28% yield). IR (in CH_2Cl_2): 3030 (w), 2972 (w), 2918 (w), 1734 (w), 1655 (w), 1602 (w), 1587 (w), 1496 (w), 1465 (w), 1450 (w), 1425 (w), 1402 (w), 1380 (w), 1370 (w), 1343 (w), 1264 (w), 1215 (s), 1176 (w), 1139 (w), 1107 (s), 1074 (w), 1013 (w), 933 (w), 910 (w), 854 (s), 794 (s), 760 (w), 734 (s), 698 (s), 649 (w), 607 (w), 573 (w), 552 (w), 524 (w), 461 (w), 411 (w); ^{1}H NMR ($CDCl_3$, 400 MHz): δ 16.07 (d, J = 2.0 Hz, 1H), 7.90 (dd, J = 6.0, 1.2 Hz, 1H), 7.59-7.49 (m, 9H), 7.42-7.27 (m, 21H), 7.14-7.10 (m, 3H), 7.08-7.03 (m, 5H), 6.88 (s, 1H), 6.84 (d, , J = 9.6 Hz, 2H), 6.73 (s, 1H), 6.55 (d, J = 6.0 Hz, 1H), 6.37 (d, J = 6.0 Hz, 2H), 5.80 (dd, J = 8.8, 7.2 Hz, 1H), 5.73 (dd, J = 10.0, 8.8 Hz, 1H), 5.09 (d, J = 7.2 Hz, 1H), 4.96 (dd, J = 8.0, 6.0 Hz, 1H), 4.85 (d, J = 7.2 Hz, 1H), 4.63 (d, J = 7.2 Hz, 1H), 4.32-4.29 (m, 1H), 4.27 (d, J = 1.2 Hz, 1H), 4.04 (d, J = 1.6 Hz, 1H), 3.93-3.90 (m, 1H), 3.86-3.81 (m, 1H), 3.78-3.73 (m, 1H), 3.71-3.66 (m, 1H), 3.50-3.43 (m, 1H), 3.19 (dd, J = 6.4, 1.6 Hz, 1H), 2.59 (s, 3H), 2.24 (s, 3H), 1.52 (s, 3H); ^{13}C NMR ($CDCl_3$, 100 MHz): δ 216.7, 170.4, 160.8, 153.6, 153.4, 143.5, 139.8, 139.7, 139.5, 139.4, 138.1, 137.22, 137.17, 136.6, 136.1, 135.9, 135.8, 135.2, 132.1, 132.0, 131.9, 131.2, 131.1, 130.9, 130.8, 130.5, 130.4, 130.2, 129.9, 129.7, 129.3, 129.2, 129.1, 129.0, 128.9, 128.8, 128.5, 128.3, 128.2, 128.16, 127.5, 127.0, 123.5, 123.48, 123.2, 117.1, 99.6, 83.3, 78.0, 76.1, 75.7, 75.6, 74.7, 73.1, 72.7, 71.9, 69.1, 69.08, 45.4, 29.9, 23.5, 23.2, 22.9, 22.8, 22.5, 22.4, 22.3, 22.2, 21.9; HRMS (ESI+): Calcd for $C_{62}H_{65}IN_2O_4Ru$ [M+H]: 1131.3129. Found: 1131.3141. 2D NMR spectra are shown in in the NMR section.

2.5.4. Ring-Opening/Cross Olefin Metathesis Products

2.5.4.1. Preparation of the Starting Materials

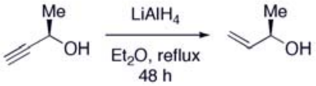

(*R*)-3-Buten-2-ol 2.191. A flame-dried round-bottom flask, equipped with a stirbar and reflux condenser, was charged with 451 mg (11.8 mmol, 0.8 equiv) lithium aluminum hydride under a N_2 atmosphere. Anhydrous Et_2O (15 mL) was added, and the resulting suspension was allowed to stir vigorously and cooled to 0 °C. (*R*)-3-Butyn-2-ol (1.000 g, 14.3 mmol, 1.0 equiv) was dissolved in 5.0 mL anhydrous Et_2O and the resulting mixture was added to the LAH suspension dropwise (five min) through a syringe. The solution was brought to a gentle reflux, and stirring was allowed to proceed for 48 hours. At this time, the mixture was cooled to 0 °C, and saturated aqueous Rochelle's salt was added, dropwise, until gas evolution ceased (CAUTION: extremely exothermic), at which point the mixture had formed a suspension of fine gray-white solids. Addition of 20 mL Et_2O was followed by removal of the solids through a pad of celite, which was subsequently washed with an additional 20 mL Et_2O; the resulting filtrate was concentrated (care must be taken, since product is volatile). The resulting clear, colorless oil was distilled under vacuum at 22 °C, affording 318 mg desired product as clear colorless oil (4.41 mmol, 31% yield). The identity of the product was ascertained through ^1H NMR analysis, which proved consistent with previous reports.[117] The spectrum also revealed the presence of 13% *R*-2-butanol (not separable from the desired product). Enantiomeric ratio (91:9 er) was measured by GLC chromatography (*b*-dextran, 15 psi, 40°C).

(*S*)-1-(*t*-Butyldimethylsilyloxy)but-3-en-2-ol. This material was prepared from commercially available enantiomerically enriched materials through a modified literature

---

[117] Helfer, D. F.; Phaho, D. S.; Atwood, J. D. *Organometallics*, **2006**, *25*, 410–415.

procedure.[118] Enantiomeric ratio (>98:<2 er) was measured by GLC chromatography (*b*-dextran, 15 psi, 60-120°C, +0.5°C/min).

(*S*)-3-Phenyl-1-butene 2.216. Prepared based on a previously reported procedure.[69f] Enantiomeric ratio (93.5:6.5 er) was established by enantioselective GLC in comparison to authentic racemic sample (Chiraldex β-dex, 15 psi, 60 °C).

(*R*)-5-Phenylpent-1-en-3-ol 2.189. This material was prepared in enantiomerically enriched form through an unpublished procedure (spectral data consistent reported literature values).[119] Enantiomeric ratio (93:7 er) was established by HPLC analysis in comparison with authentic racemic material (Daicel Chiralpak OJ-H column, 95:5 hexanes:2-propanol, 1.0 mL/min, 210 nm). The absolute configuration of **2.189** was assigned as *R*, based on a previous report.[120]

Cyclopropene 2.182. This material was prepared according to a previously reported procedure.[121]

Cyclopropene 2.195. This material was synthesized according to a previously reported procedure from 2-isopropenylnaphthalene,[121] and was isolated as a clear, colorless liquid in 63% yield (129 mg, 0.717 mmol). IR(neat): 3054 (w), 2966 (w), 2944 (w), 2862 (w), 1638 (m), 1627 (m), 1597 (m), 1504 (m), 1452 (m), 1374 (w), 1273 (m), 1188 (m), 1129 (m), 1063 (m), 992 (m), 959 (m), 947 (m), 889 (m), 855 (s), 818 (s), 773 (s), 762 (s), 740 (s), 619 (s), 594 (s), 473 (s) cm^{-1};^{1}H NMR (CDCl$_3$, 400 MHz): 7.81 (2H, br d, *J* = 8.0 Hz), 7.76 (1H, d, *J* = 8.4 Hz), 7.71 (1H, s), 7.48-7.40 (2H, m), 7.36 (2H, s), 7.34 (1H, ddd, *J* = 8.4, 1.6, 1.6 Hz), 1.76 (3H, t, *J* = 0.8 Hz); ^{13}C NMR (CDCl$_3$, 100 MHz): 147.5, 133.5, 131.6, 127.7, 127.6, 127.3, 126.0, 125.1, 124.8, 124.7, 115.9, 25.7, 22.3; HRMS (ESI+): Calcd for $C_{14}H_{13}$ (M$^+$): 181.10173. Found: 181.10177.

---

(118) Chaudray, S. K.; Hernandez, O. *Tetrahedron Lett.* **1979**, *20*, 99–102

(119) Molander, G. A.; Jean-Gerard, L. *J. Org. Chem.* **2009**, *74*, 1297–1303.

(120) Binder, J . T.; Kirsch, S. F. *Chem. Commun.* **2007**, 4164–4166.

(121) Rubin, M.; Gevorgyan, V. *Synthesis* **2004**, 796–800

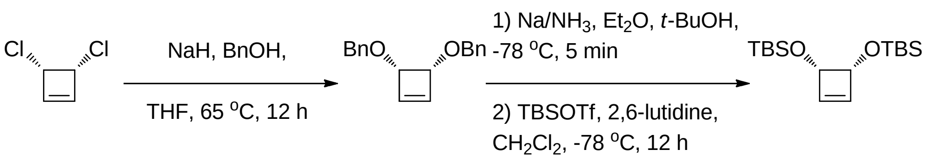

3,4-Bis(benzyloxy)-*cis*-cyclobutene. This material was prepared by a modification of a previously reported procedure.[122] In a flame-dried round-bottom flask equipped with a reflux condenser, were mixed NaH (1.380 g, 57.6 mmol, 2.24 equiv) and THF (25 mL). To this slurry was added benzyl alcohol (14.0 mL, 135 mmol, 5.25 equiv) in a drop-wise manner at 0 °C with vigorous stirring. The mixture was allowed to stir at 0 °C until all solids dissolved (~15 min). 3,4-Dichloro-*cis*-cyclobutene (3.180 g, 25.9 mmol, 1.00 equiv) was added and the mixture was allowed to stir at 65 °C for 12 h. After the flask was allowed to cool to 22 °C, H_2O was added (drop-wise; 25 mL) while stirring continued. The resulting solution was diluted with diethyl ether (100 mL). Layers were separated and aqueous layer was washed with Et_2O (2 x 50 mL). The combined organic layers were washed with brine, dried over anhydrous $MgSO_4$, filtered, and concentrated *in vacuo* to afford brown oil. Purification by silica gel chromatography (10:1 hexanes:Et_2O) afforded the desired product as a colorless oil (1.78 g, 6.67 mmol, 78% yield). IR (neat): 3087 (w), 3061 (w), 3030 (w), 2861 (m), 2771 (w), 1952 (w), 1873 (w), 1810 (w), 1606 (w), 1586 (w), 1496 (m), 1453 (m), 1396 (w), 1378 (w), 1332 (m), 1299 (w), 1255 (w), 1207 (m), 1161 (s), 1102 (s), 1062 (s), 1026 (s), 943 (w), 906 (w), 840 (w), 802 (m), 730 (s), 695 (s), 656 w), 610 (w), 592 (w), 556 (w), 516 (w), 459 (w) cm^{-1}; ^1H NMR ($CDCl_3$, 400 MHz): δ 7.40-7.27 (10H, m), 6.38-6.37 (2H, m), 4.76 (2H, B of AB, J_{AB} = 11.6 Hz), 4.76-4.75 (2H, m), 4.65 (2H, A of AB, J_{AB} = 11.6 Hz); ^{13}C NMR ($CDCl_3$, 100 MHz): δ 142.2, 138.8, 128.5, 128.0, 127.7, 81.4, 71.0; HRMS (ESI+): Calcd for $C_{18}H_{18}O_2$ (M^+): 266.1307. Found: 266.1311.

3,4-Bis(*tert*-butyldimethylsilyloxy)-*cis*-cyclobutene (2.203). In a two-neck flask equipped with a Dewar condenser, anhydrous NH_3 (~40 mL) was condensed at -78 °C with stirring (to avoid freezing ammonia), and sodium metal (952 mg, 41.4 mmol, 8.34

---

(122) Kirmse, W.; Scheidt, F.; Vater, H-J. *J. Am. Chem. Soc.* **1978**, *100*, 3945–3946.

equiv.) was dissolved, causing the solution to turn blue. Bis-benzylcyclobutene, described above, (1.32 g, 4.96 mmol, 1.00 equiv.) was added to this mixture as a solution in dry Et_2O (10 mL) and *t*-BuOH (3.6 mL). The resulting mixture was allowed to stir for 5 min, and NH_4Cl (s) was added carefully until blue color dissipated. The resulting mixture was diluted with with 1:1 mixture of CH_2Cl_2:Et_2O (50 mL) (added slowly to avoid rapid refluxing ammonia), and was allowed to warm slowly to 22 °C while stirring was allowed to continue. The solution was diluted with an equal mixture of CH_2Cl_2:Et_2O (50 mL), filtered, and concentrated *in vacuo* to afford *meso*-cyclobut-1-en-3,4-diol (435 mg, 5.06 mmol, >98% yield) as an off-white solid. IR (neat): 3316 (br s), 3251 (br s), 3053 (w), 2961 (m), 2912 (m), 2853 (m), 1451 (m), 1410 (m), 1316 (m), 1277 (m), 1208 (w), 1179 (m), 1157 (s), 1096 (s), 1034 (s), 978 (s), 947 (w), 916 (m), 810 (s), 767 (s), 697 (w), 615 (s), 567 (s), 490 (m), 478 (m), 440 m) cm^{-1}; ^1H NMR ($CDCl_3$, 400 MHz): δ 6.41-6.40 (2H, m), 4.81-4.80 (2H, m), 2.41 (2H, br s); ^{13}C NMR ($CDCl_3$, 100 MHz): δ 144.5, 73.9.

In a round-bottom flask were mixed *meso*-cyclobut-1-en-3,4-diol (435 mg, 5.06 mmol, 1.00 equiv), CH_2Cl_2 (50 mL), 2,6-lutidine (1.80 mL, 15.5 mmol, 3.07 equiv). The mixture was allowed to cool to –78 °C, and *tert*-butyldimethylsilyl triflate (2.90 mL, 12.6 mmol, 2.49 equiv) was added in a drop-wise fashion. The mixture was allowed to warm to 22 °C with stirring. After 12 hours, the solution was allowed to cool to –78 °C and methanol (~2 mL) was added, drop-wise. The resulting mixture was allowed to warm to 22 °C and volatiles were removed *in vacuo* to leave behind biphasic (colorless/brown) oil. Purification by silica gel chromatography (50:1 hexanes:Et_2O) delivered **2.203** (1.18 g, 3.74 mmol, 74% yield over 2 steps) as a colorless oil. IR (neat): 3047 (w), 2954 (m), 2929 (m), 2884 (m), 2857 (m), 1472 (m), 1463 (m), 1407 (w), 1389 (w), 1360 (m), 1295 (w), 1220 (s), 1192 (s), 1174 (s), 1120 (s), 1059 (w), 1006 (w), 987 (w), 921 (m), 895 (m), 861 (s), 832 (s), 772 (s), 695 (m), 671 (m), 652 (m), 580 (w), 518 (w), 478 (w) cm^{-1}; ^1H-NMR ($CDCl_3$, 400 MHz): δ 6.27-6.26 (2H, m), 4.84-4.83 (2H, m), 0.91 (18H, s), 0.10 (6H, s), 0.09 (6H, s); ^{13}C-NMR ($CDCl_3$, 100 MHz): δ 143.0, 76.3, 26.2, 18.6, –4.0, –4.4. HRMS (ESI+): Calcd for $C_{16}H_{35}O_2Si_2$ $(M+H)^+$: 315.2176. Found: 315.2179.

2.5.4.2. Ru-Catalyzed DROCM Reactions

(See section below regarding proof of stereochemical identities of all products)

■ Reactions of Cyclopropenes

General Procedure for Ru-catalyzed DROCM of cyclopropenes. **(1*R*,4*S*,*E*)-4-methyl-1,4-diphenylhexa-2,5-dien-1-ol (2.186).** Cyclopropene **2.182** (24.6 mg, 0.189 mmol, 1.5 equiv) and (*R*)-1-phenyl-2-propen-1-ol **(2.185)** (95.5:4.5 er; 16.9 mg, 0.126 mmol, 1.0 equiv) were weighed into a one-dram vial charged with a stir bar. The vial was purged with nitrogen for ~5 seconds, and toluene (0.660 mL) was added. A solution of Ru complex **2.15** (0.590 mg in 0.290 mL of toluene, 0.005 equiv) was added as a single portion (total volume of toluene is 0.950 mL, or 0.2 M with respect to **2.185**). The vial was capped and the solution was allowed to stir for 5 min. After 5 min, the reaction was quenched by loading the mixture onto a short column of SiO_2 and eluted with 1:1 hexanes/Et_2O. The volatiles were evaporated and the resulting pale yellow residue was purified by silica gel chromatography (10:1 to 6:1 hexanes:Et_2O) to afford 28.9 mg of **2.186** as a clear, colorless oil (10:1 *E:Z*, 0.109 mmol, 87% yield). IR (neat): 3541 (br m), 3349 (m), 3083 (m), 3059 (m), 3028 (m), 3003 (m), 2972 (m), 2928 (m), 2872 (m), 1491 (m), 1445 (m), 1027 (m), 1001 (m), 976 (m), 915 (m), 763 (m), 670 (m) cm^{-1}; *E*-isomer (major): ^1H NMR ($CDCl_3$, 400 MHz): δ 7.41–7.35 (4H, m), 7.33-7.27 (5H, m), 7.26-7. 21 (1H, m), 6.07 (1H, dd, J = 17.2, 10.4 Hz), 6.05 (1H, dd, J = 14.4, 0.8 Hz), 5.69 (1H, dd, J = 15.6, 6.4 Hz), 5.28 (1H, dd, J = 6.4, 2.8 Hz), 5.13 (1H, dd, J = 10.4, 1.2 Hz), 5.00 (1H, dd, J = 17.6, 1.2 Hz), 1.94 (1H, d, J = 3.6 Hz), 1.52 (3H, s); ^{13}C NMR ($CDCl_3$, 100 MHz): δ 146.2, 145.1, 143.3, 139.1, 138.8, 133.1, 130.8, 128.7, 128.6, 128.4, 128.3, 127.8, 127.6, 127.3, 127.2, 126.4, 113.1, 75.3, 65.3, 47.4, 25.6; HRMS (ESI+): Calcd for $C_{19}H_{19}$ $[M\text{-}OH]^+$: 247.14917. Found: 247.14868; Diastereomeric ratio was established by HPLC analysis of the derived enone (see below).

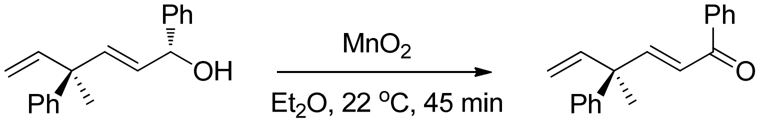

(*S*,*E*)-4-Methyl-1,4-diphenylhexa-2,5-dien-1-one. An oven-dried two-dram vial equipped with a stir bar was charged with **2.186** (17.9 mg, 0.068 mmol, 1 equiv). Diethyl ether (2.0 mL) was added through a syringe followed by manganese dioxide (179 mg, 10 mg/mg of substrate, ~30 equiv). The resulting suspension was allowed to stir vigorously until the reaction was determined to be complete according to TLC analysis (45 min). The mixture was filtered through a short pad of celite, which was then washed with diethyl ether (3 x 5.0 mL). The volatiles were removed *in vacuo*, affording a colorless oil, which was purified by silica gel chromatography (15:1 hexanes:Et$_2$O). Enone **2.186a** (10:1 *E:Z*) was isolated as a clear, colorless oil (14.5 mg, 0.055 mmol, 81% yield). The following data is for the *E*-**2.186a** (major). IR (neat): 3084 (w), 3058 (w), 3026 (w), 2973 (w), 2928 (w), 1725 (w), 1670 (s), 1615 (s), 1598 (m), 1579 (m), 1492 (m), 1447 (m), 1329 (m), 1293 (m), 1226 (m), 1015 (m), 920 (m), 764 (m), 698 (m) cm^{-1}; ^{1}H NMR (CDCl$_3$, 400 MHz): □□7.92-7.90 (2H, m), 7.58-7.54 (1H, m), 7.49-7.44 (2H, m), 7.37-7.30 (4H, m), 7.27-7.23 (2H, m), 6.83 (1H, d, *J* = 15.6 Hz), 6.14 (1H, dd, *J* = 17.4, 10.4 Hz), 5.26 (1H, dd, *J* = 10.8, 1.2 Hz), 5.11 (1H, dd, *J* = 17.2, 0.8 Hz), 1.64 (3H, s). Diastereomeric ratio was established by HPLC analysis in comparison with authentic racemic material (91.5:8.5 er shown; after correction for 95.5:4.5 er of starting material, results in a diastereoselectivity of 96:4 dr; Daicel Chiralpak OD column (99.5:0.5 hexanes:2-propanol, 0.7 mL/min, 220 nm) was used.

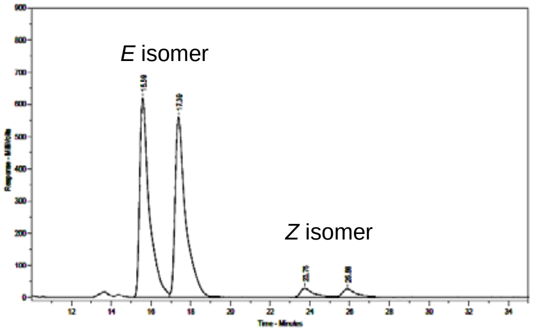

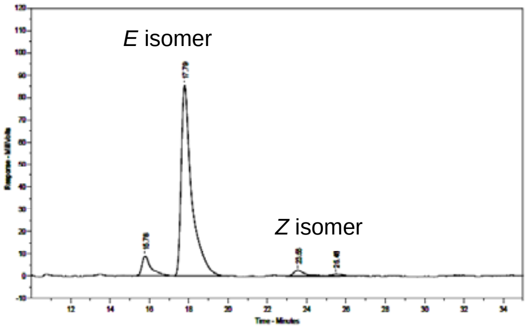

Peak #	Retention time	Area	Area %	Peak #	Retention time	Area	Area %

	(min)				(min)		
1	15.59	20612370	47.015	1	15.78	286595	7.967
2	17.39	20588760	46.961	2	17.79	3158918	87.814
3	23.75	1335308	3.046	3	23.56	110317	3.067
4	25.88	1305651	2.978	4	25.48	41447	1.152

(1*R*,4*R*,*E*)-1-Methoxy-4-methyl-1,4-diphenyl-hexa-2,5-diene (2.187). The previously described procedure was used except that the reaction was allowed to proceed for 18 hours. IR (neat): 3084 (w), 3059 (w), 3027 (w), 2974 (w), 2931 (w), 2820 (w), 1634 (w), 1600 (w), 1492 (m), 1446 (m), 1409 (w), 1369 (w), 1308 (w), 1187 (w), 1156 (w), 1086 (m), 1028 (w), 1000 (w), 975 (m), 912 (m), 850 (w), 762 (m), 731 (m), 697 (s), 635 (w), 620 (w), 572 (w), 538 (w), 431 (w) cm^{-1}; ^{1}H NMR (CDCl$_3$, 400 MHz): δ 7.36–7.27 (*E*/*Z*, 6H, m), 7.24 (*E*/*Z*, 3H, s), 7.20-7.15 (*E*/*Z*, 1H, m), 6.04 (*E*, 1H, dd, *J* = 17.4, 10.6 Hz; *Z*, 1H, overlapping dd, *J* = 17.2, 10.4 Hz), 5.95 (*E*, 1H, dd, *J* = 15.6, 0.8 Hz; *Z*, 1H, overlapping dd, *J* = 15.6, 0.8 Hz), 5.55 (*E*/*Z*, 1H, dd, *J* = 15.6, 6.8 Hz), 5.10 (*E*, 1H, dd, *J* = 10.8, 1.2 Hz; *Z*, 1H, overlapping dd, *J* = 10.8, 0.8 Hz), 4.97 (*E*, 1H, dd, *J* = 17.6, 0.8 Hz; *Z*, 1H, overlapping dd, *J* = 17.2, 0.8 Hz), 4.67 (*E*/*Z*, 1H, d, *J* = 6.8 Hz), 3.32 (*E*/*Z*, 3H, s), 1.49 (*Z*, 3H, s), 1.47 (*E*, 3H, s); ^{13}C NMR (CDCl$_3$, 100 MHz): δ 146.3, 146.0, 145.0, 141.6, 139.8, 139.0, 129.3, 128.6, 128.3, 127.6, 127.2, 126.9, 126.3, 113.1, 84.5, 56.5, 47.6, 29.8, 28.8, 25.6; HRMS (ESI+): Calcd for $C_{19}H_{19}$ [M-OMe]$^+$ 247.1487. Found: 247.1492. Diastereomeric ratio was determined by analysis of a derivative (see below).

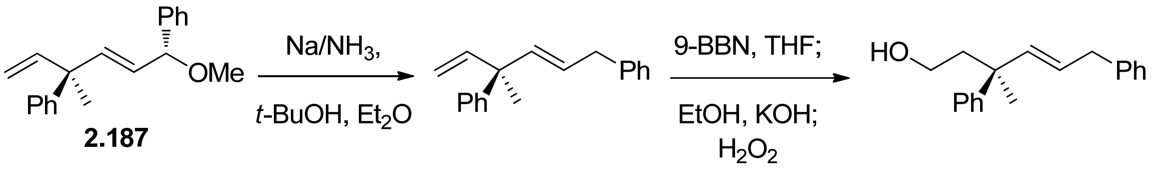

Following the conditions described for **2.203**, methyl ether **2.187** (10.5 mg, 0.038 mmol, 1 equiv) and Na(0) metal (10.4 mg, 0.045 mmol, 12 equiv), after purification by silica gel chromatography (100% hexanes) afforded the derived reduced intermediate (see above Scheme) as a clear, colorless oil (8.4 mg, 0.034 mmol, 89% yield, >98:2 *E*:*Z*). ^{1}H NMR

($CDCl_3$, 400 MHz): δ 7.33–7.27 (6H, m), 7.24-7.22 (4H, m), 6.12 (1H, dd, J = 17.4, 10.6 Hz), 5.79 (1H, d, J = 15.9 Hz), 5.63 (1H, dt, J = 15.5, 6.7 Hz), 5.15 (1H, dd, J = 10.8, 1.6Hz), 5.05 (1H, dd, J = 17.2, 1.2 Hz), 3.43 (2H, d, J = 6.6 Hz), 1.49 (3H, s); HRMS (ESI+): Calcd for $C_{19}H_{20}$ [M^+]: 249.1643. Found: 249.1632.

An oven-dried vial equipped with a stir bar was charged with 8.4 mg of diene product obtained from the above reduction (0.034 mmol, 1 equiv), and after purging for one minute, 9-BBN in THF was added (0.500 mL) under N_2. The resulting mixture was allowed to stir for 18 h at 22 °C, after which time it was allowed to cool to 0 °C. Ethanol (1.0 mL) was added, followed by aqueous KOH (1mL); drop-wise addition of H_2O_2 (0.5 mL, 35% wt/v; strongly exothermic) was subsequently performed. The mixture was allowed to stir for 5 h at 22 °C, after which the reaction was quenched by addition of an aqueous solution of HCl (10 mL). Layers were separated,, and the aqueous layer was washed with CH_2Cl_2 (3 x 10mL). The organic layers were combined, dried with $MgSO_4$, and concentrated *in vacuo*. The resulting yellow oil was purified by silica gel chromatography (10% EtOAc/hexanes), affording the desired alcohol (same as alcohol *R*-**f** in the section below regarding proof of stereochemistry) as yellow oil (5.8 mg, 0.022 mmol, 64% yield). ^{1}H NMR ($CDCl_3$, 400 MHz): δ 7.43-7.29 (5H, m), 7.22-7.07 (5H, m), 5.77 (1H, d, J = 16.0 Hz), 5.65 (1H, dt, J = 15.8, 6.7 Hz), 3.67-3.56 (2H, m), 3.42 (2H, d, J = 6.8 Hz), 2.17-2.03 (3H, m), 1.42 (3H, s); HRMS (ESI+): Calcd for $C_{19}H_{22}O$ [$M+NH_4^+$]: 284.2014. Found: 284.2003. Diastereomeric ratio was established by HPLC analysis in comparison with authentic racemic material (75:25 er). Correction for 95:5 er of starting material results in a diastereoselectivity of 79:21 dr; Daicel Chiralpak AS column (97:3 hexanes:2-propanol, 0.5 mL/min, 220 nm) was used.

Please note: The *E* and *Z* product isomers bear the quaternary stereogenic center of *opposite* stereoconfiguration. Due to isomerization of the *Z* isomer to the *E* isomer under dissolving metal reduction conditions, the observed diastereomeric ratio of **2.187b** presents a lower limit for the diastereoselectivity of the catalytic DROCM reaction (**2.182**→**2.187**). Separation of *E* and *Z* isomers of **5** could not be achieved by silica gel or

AgNO$_3$-impregnated silica gel chromatography.

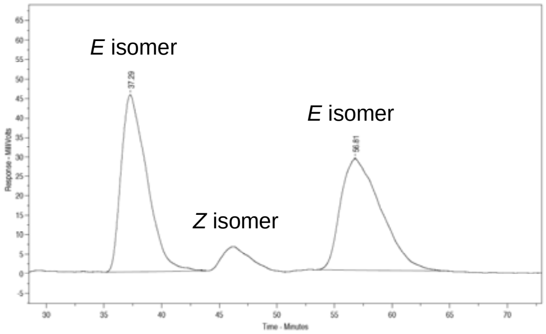

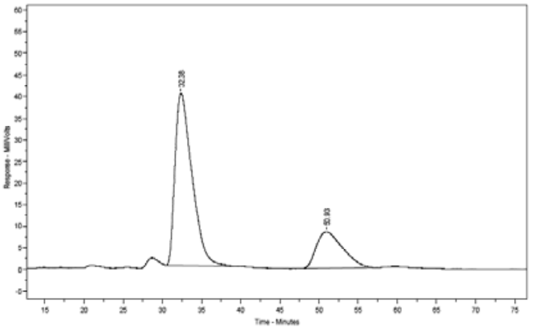

Peak #	Retention time (min)	Area	Area %	Peak #	Retention time (min)	Area	Area %
1	37.29	7085191	50.395	1	32.38	6015720	75.473
2	56.81	6974189	49.605	2	50.93	1954920	24.527

(2*S*,5*S*,*E*)-5-Methyl-2,5-diphenylhepta-3,6-diene (2.188). The previously described procedure was used except that 18 hours of reaction time. Silica gel chromatography (100% hexanes) afforded the desired product, which was isolated as the *E* isomer (>98% *E*). It should be noted that the unpurified product was obtained as a 9:1 *E*:*Z* mixture. IR (neat): 3082 (w), 3059 (w), 3025 (w), 2966 (m), 2928 (w), 2871 (w), 1633 (w), 1600 (w), 1491 (m), 1446 (m), 1409 (w), 1370 (w), 1285 (w), 1184 (w), 1156 (w), 1073 (w), 1028 (w), 1008 (m), 999 (m), 976 (m), 913 (m), 841 (w), 760 (s), 696 (s), 535 (m) cm^{-1}; ^{1}H NMR (CDCl$_3$, 400 MHz): δ 7.34-7.28 (6H, m), 7.25-7.18 (4H, m), 6.09 (1H, dd, J = 17.4, 10.6 Hz), 5.75 (1H, dd, J = 15.8, 1.0 Hz), 5.63 (1H, dd, J = 16, 6.4 Hz), 5.12 (1H, dd, J = 10.4, 1.2 Hz), 5.00 (1H, dd, J = 17.4, 1.4 Hz), 3.53 (1H, apparent quintet, J = 7.0 Hz), 1.49 (3H, s), 1.40 (3H, d, J = 6.8 Hz); ^{13}C NMR (CDCl$_3$, 100 MHz): δ 147.1, 146.5, 145.8, 136.1, 133.6, 128.6, 128.3, 127.4, 127.4, 126.2, 126.2, 112.7, 47.6, 42.5, 26.0, 21.8; HRMS (ESI+): Calcd for $C_{20}H_{23}$ [M+H]$^+$: 263.1800 Found: 263.1793. Diastereomeric ratio was established by HPLC analysis of a derived lactone (below).

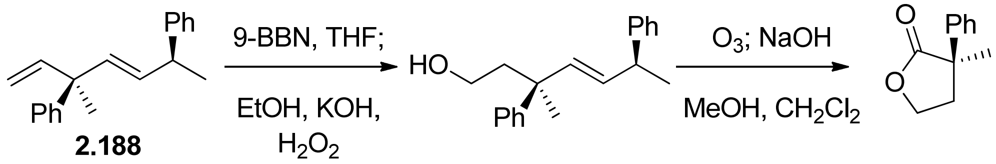

Please note: For purpose of clarity, *R,R*-**2.188** product is discussed shown in Scheme 2.34 of the text

Following well-established procedures,[123,124] the above sequence was carried out on diene **5** (73% and 51% yield, respectively). Diastereomeric ratio (dr) was established by HPLC analysis in comparison with authentic racemic material (85:15 er). After correction for 94:6 er of starting material, diastereoselectivity is calculated as 91:9 dr; Daicel Chiralpak OJ-H column (9:1 hexanes:2-propanol, 0.7 mL/min, 210 nm) was used.

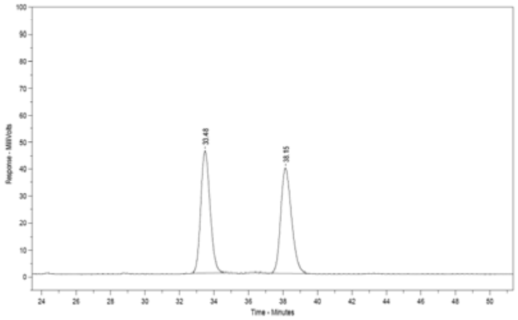

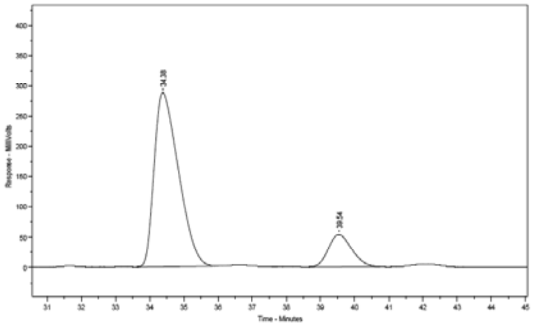

Peak #	Retention time (min)	Area	Area %	Peak #	Retention time (min)	Area	Area %
1	33.48	1695685	50.009	1	34.38	14177810	84.862
2	38.15	1695055	49.991	2	39.54	2529071	15.138

(3*R*,6*R*,*E*)-6-Methyl-1,6-diphenylocta-4,7-dien-3-ol (2.190). The previously described procedure was used except that 3 equiv of cyclopropene **2.182** was used, and the reaction was allowed to proceed for 15 minutes. Silica gel chromatography (5% EtOAc in hexanes) afforded the desired product was isolated as a 4:1 *E:Z* mixture. IR (neat): 3347 (br w), 3083 (w), 3059 (w), 3025 (w), 2971 (w), 2928 (w), 2860 (w), 1634 (w), 1600 (w), 1493 (m), 1454 (m), 1445 (m), 1409 (w), 1369 (w), 1303 (w) 1156 (w), 1099 (w) 1050

([123]) Marshall, J. A.; Garofalo, A. W. *J. Org. Chem.* **1993**, *58*, 3675–3680.

([124]) Spielvogel, D. J.; Buchwald, S. L. *J. Am. Chem. Soc.* **2002**, *124*, 3500–3501.

(w), 1029 (m), 1000 (w), 979 (m), 915 (m), 820 (w), 764 (m), 747 (m), 699 (s), 536 (w), 495 (w) cm $^{-1}$; ^{1}H NMR ($CDCl_3$, 400 MHz: δ 7.35-7.28 (*E*/*Z*, 3H, m), 7.24-7.18 (*E*/*Z*, 3H, m), 6.21 (*Z*, 1H, dd, *J* = 17.4, 10.6 Hz), 6.08 (*E*, 1H, dd, *J* = 17.4, 10.6 Hz), 5.93 (*E*, 1H, dd, *J* = 16.0, 1.2 Hz), 5.82 (*Z*, 1H, dd, *J* = 12.4, 0.8 Hz), 5.52 (*E*, 1H, dd, *J* = 16.0, 6.8 Hz), 5.45 (*Z*, 1H, dd, *J* = 11.6, 10.0 Hz), 5.16 (*E*, 1H/*Z*, 0.5H, dd, *J* = 10.6, 1.4 Hz), 5.11 (*Z*, 0.5H, dd, *J* = 10.4 Hz, 1.2 Hz), 5.07 (*Z*, 0.5H, dd, *J* = 17.6, 1.4 Hz), 5.03 (*E*, 1H, dd, *J* = 17.2, 1.2 Hz; *Z*, 0.5H, overlapping dd, *J* = 17.6, 1.2 Hz), 4.19 (*E*, 1H, dd, *J* = 13.0, 6.2 Hz), 3.99 (*Z*, 1H, ddd, *J* = 13.4, 8.8, 4.5 Hz), 2.80-2.66 (*E*, 2H, m), 2.58-2.51 (*Z*, 1H, m), 2.50-2.31 (*Z*, 1H, m), 1.98-1.82 (*E*, 2H, m), 1.64-1.47 (*Z*, 2H, overlapping m), 1.58 (*E*/*Z*, 1H, s), 1.52 (*E*, 3H, s), 1.45 (*Z*, 3H, s); ^{13}C NMR ($CDCl_3$, 100 MHz): δ 146.3, 145.3, 142.1, 139.0 138.7, 134.0, 131.5, 128.6, 128.6, 128.5, 128.4, 127.3, 126.4, 126.0, 125.9, 113.1, 112.7, 72.6, 67.0, 47.4, 39.2, 38.3, 32.0, 31.9, 30.5, 29.0, 25.7; HRMS (ESI+): Calcd for $C_{21}H_{24}O$ $[M+NH_4]^+$: 310.2171. Found: 310.2184. Diastereomeric ratio was established by HPLC analysis of the derived enone (see below).

(3*R*,*E*)-6-Methyl-1,6-diphenylocta-4,7-dien-3-one (enone derived from 2.190). This material was accessed by the oxidation procedure with MnO_2 (73% yield). The desired a,*b*-unsaturated ketone was obtained as the pure *E* isomer (>98:<2 *E*:*Z*); the *Z* isomer did not undergo oxidation, and the *E* enone was readily separated from *Z* alcohol. IR (neat): 3084 (w), 3060 (w), 3026 (w), 2969 (w), 2926 (w), 1697 (w), 1673 (m), 1621 (m), 1601 (w), 1493 (m), 1446 (m), 1408 (w), 1367 (w), 1291 (w), 1167 (w), 1095 (m), 1073 (m), 1029 (m), 986 (m), 919 (w), 862 (w), 765 (m), 748 (m), 697 (s) 536 (m), 512 (w) cm^{-1}; ^{1}H NMR ($CDCl_3$, 400 MHz): δ 7.34-7.28 (4H, m), 7.24-7.18 (6H, m), 7.01 (1H, d, *J* = 16.0 Hz), 6.06 (1H, d, *J* = 16.0 Hz), 6.05 (1H, dd, *J* = 17.6, 10.0 Hz), 5.21 (1H, d, *J* = 10.4 Hz), 5.03 (1H, d, *J* = 17.2 Hz), 2.96-2.88 (4H, m), 1.54 (3H, s). Diastereomeric ratio was established by HPLC analysis in comparison with authentic racemic material (85:15 er); after correction for 93.5:6.5 er of starting material, diastereoselectivity is calculated as 91:9 dr). Daicel Chiralpak OJ-H column (95:5 hexanes:2-propanol, 0.5 mL/min, 220 nm) was used.

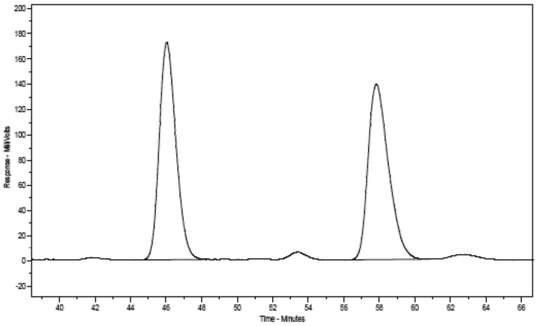

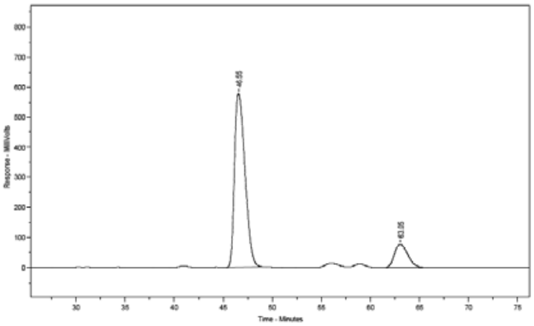

Peak #	Retention time (min)	Area	Area %	Peak #	Retention time (min)	Area	Area %
1	46.27	37524860	50.145	1	46.55	42969890	85.314
2	61.56	37307450	49.855	2	63.05	2529071	14.686

(2*R*,5*R*,*E*)-5-Methyl-5-phenylhepta-3,6-dien-2-ol (2.192). The previously described procedure was followed except that 1.3 equiv of cyclopropene **2.182** was used and the reaction was allowed to proceed for 15 minutes. Silica gel chromatography (10% EtOAc in hexanes) afforded the desired product (colorless oil) was isolated as a 6:1 *E:Z* mixture. IR (neat): 3341 (br m), 3084 (w), 3057 (w), 3023 (w), 2971 (m), 2929 (w), 2872 (w), 1634 (w), 1599 (w), 1492 (m), 1445 (m), 1409 (w), 1368 (m), 1289 (w), 1128 (w), 1057 (m), 1029 (w), 1000 (w), 977 (m), 945 (w) 914 (m), 867 (w), 844 (w), 764 (m), 734 (w), 698 (s), 592 (w) 534 (m), 432 (w) cm^{-1}; ^{1}H NMR (CDCl$_3$, 400 MHz): δ 7.39-7.30 (*E*:*Z*, 4H, m), 7.24-7.20 □□□*Z*, 1H, m), 6.25 (*Z*, 1H, dd, *J* = 17.4, 10.6 Hz), 6.08 (*E*, 1H, dd, *J* = 17.6, 10.4 Hz), 5.90 (*E*, 1H, d, *J* = 15.6 Hz), 5.74 (*Z*, 1H, d, *J* = 11.2 Hz), 5.54 (*E*, 1H, dd, *J* = 16.0, 6.4 Hz), 5.42 (*Z*, 1H, dd, *J* = 11.4, 9.4 Hz), 5.15 (*E/Z*, 1H, dd, *J* = 10.6, 1.0 Hz), 5.02 (*Z*, 1H, dd, *J* = 17.2, 1.2 Hz; *E*, 1H, overlapping dd, *J* = 17.6, 0.8 Hz), 4.40-4.34 (*E*, 1H, m), 4.20-4.16 (*Z*, 1H, m), 1.70 (*Z*, 1H, s), 1.62 (*E*, 1H, s), 1.51 (*E/Z*, 3H, s), 1.31 (*E*, 3H, d, *J* = 6.4 Hz), 1.05 (*Z*, 0.5H, d, *J* = 6.4 Hz), 0.97 (*Z*, 0.5H, d, *J* = 6.4 Hz); ^{13}C NMR (CDCl$_3$, 100 MHz): δ 146.4, 145.3, 137.9, 137.3, 135.3, 132.8, 128.6, 128.5, 128.3, 127.2, 127.2, 126.4, 113.0, 112.7, 69.2, 63.9, 47.3, 29.3, 25.6, 23.8, 22.4; HRMS (ESI+): Calcd for $C_{14}H_{17}$ [M-OH]$^+$: 185.1330. Found: 185.1337. Diastereomeric ratio was established by HPLC analysis of the corresponding enone (below).

(5*R*,*E*)-5-Methyl-5-phenylhepta-3,6-dien-2-one and (5*S*,*Z*)-5-methyl-5-phenylhepta-3,6-dien-2-one (enones derived from 2.192). This material was accessed by the oxidation procedure with MnO_2 (71% yield). The desired a,*b*-unsaturated ketone was obtained as the pure *E* isomer (>98:<2 *E:Z*); the *Z* isomer did not undergo oxidation, and the *E* enone was readily separated from *Z* alcohol.

***E* enone**: IR (neat): 3084 (w), 2924 (s), 2853 (m), 1740 (w), 1698 (w), 1677 (s), 1620 (m), 1600 (w), 1492 (w), 1445 (m), 1359 (m), 1287 (w), 1255 (m), 1175 (w), 1027 (w), 987 (m), 921 (m), 862 (w), 802 (w), 766 (m), 735 (w), 700 (s), 684 (w), 565 (m), 536 (w), 473 (w), 408 (w) cm $^{-1}$; ^{1}H NMR ($CDCl_3$, 400 MHz): δ 7.36-7.27 (3H, m), 7.25-7.21 (2H, m), 7.00 (1H, d, *J* = 16.4 Hz), 6.08 (1H, dd, *J* = 17.6, 10.4 Hz), 6.06 (1H, d, *J* = 16.4 Hz), 5.23 (1H, dd, *J* = 10.6, 1.0 Hz), 5.06 (17.6 Hz, 0.8 Hz), 2.28 (3H, s), 1.57 (3H, s).

The corresponding *Z* enone was synthesized by re-subjection of the *Z*-**2.192**, isolated after oxidation of *E*-**2.192** (see above), to MnO_2-mediated oxidation conditions (93% yield).

***Z* enone:** ^{1}H NMR ($CDCl_3$, 400 MHz): δ 7.32-7.27 (4H, m), 7.21-7.16 (1H, m), 6.30 (1H, dd, *J* = 17.4, 10.6 Hz), 6.05 (2H, overlapping dd, *J* = 24.4, 13.2 Hz), 5.16 (1H, d, *J* = 11.2 Hz), 5.08 (1H, d, *J* = 17.6 Hz), 1.95 (3H, s), 1.58 (3H, s). To ascertain the absolute stereochemistry of each isomer, the *Z*-enone was isomerized to the corresponding *E* isomer by treatment with one equivalent of *N*,*N*-dimethylaminopyridine in THF (reflux for 48 h in a sealed vial). The resulting *E* enone was purified as described above. The dr values and relative stereochemistry for the enone isomers were established by HPLC analysis, in comparison with authentic racemic material. For the *E* isomer, 86:14 er was measured; correction for 91:9 er of the starting allylic alcohol results in a diastereoselectivity of 95:5 dr. For the *Z* isomer, 75:25 er was measured; correction for 91:9 er of the starting allylic alcohol points to diastereoselectivity of 82:18 dr. Daicel Chiralpak OJ-H column (100:0 hexanes:2-propanol, 0.5 mL/min, 220 nm) was used.

The data indicate that the *E* and *Z* product isomers have the opposite absolute configuration at the all-carbon quaternary stereogenic center.

HPLC analysis for enone obtained from oxidation of *E*-**8**:

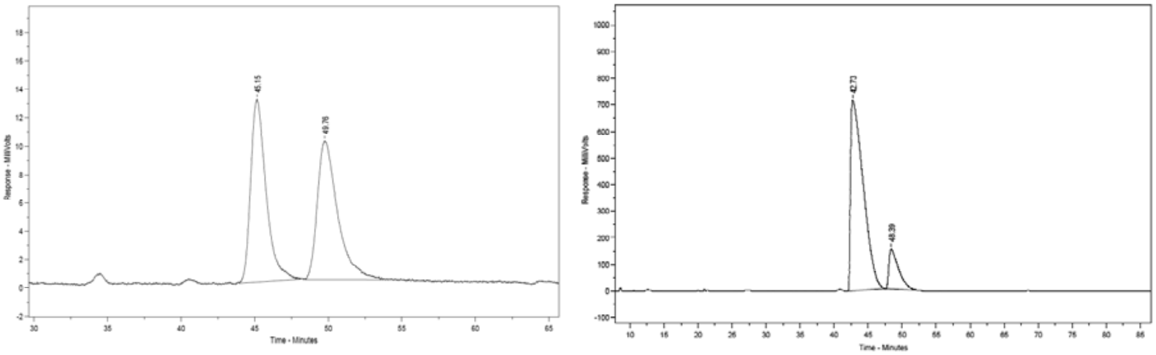

Peak #	Retention time (min)	Area	Area %	Peak #	Retention time (min)	Area	Area %
1	45.15	942274	49.842	1	42.73	92886480	86.101
2	49.76	948244	50.158	2	48.39	14993790	13.899

HPLC analysis for enone obtained from oxidation of *Z*-**8**:

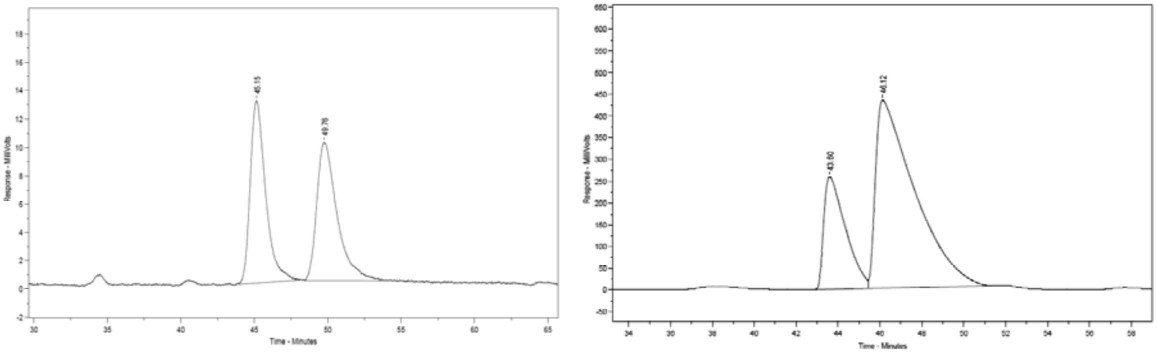

Peak #	Retention time (min)	Area	Area %	Peak #	Retention time (min)	Area	Area %
1	45.15	942274	49.842	1	43.60	18740050	24.976
2	49.76	948244	50.158	2	46.12	5629550	75.024

(2*R*,5*R*,*E*)-5-Hydroxy-2,5-diphenyl-2-vinylpent-3-enyl acetate (2.194). An oven dried vial equipped with stir bar was charged with cyclopropene **2.193** (22.6 mg, 0.120 mmol, 1 equiv) and purged under N_2 for a five seconds. Ru-complex **2.15** (4.6 mg, 0.007 mmol, 0.06 equiv) was then added in 0.05 mL toluene, and mixture was stirred vigorously. (*R*)-Phenyl-2-propen-1-ol (46.6 mg, 0.347 mmol, 2.9 equiv) was added by syringe pump as a solution in 0.80 mL toluene over 4 h. The mixture was then concentrated *in vacuo*, and the product was purified by SiO_2 chromatography (5:1 hexanes:EtOAc) afforded the desired product as amber-colored oil as a 8:1 *E:Z* mixture. IR (neat): 3433 (br w), 3060 (w), 3028 (w), 2920 (w), 2851 (w), 1737 (s), 1671 (w), 1600 (w), 1493 (m), 1448 (m), 1378 (m), 1231 (s), 1033 (m), 980 (w), 922 (m), 851 (w), 803 (w), 762 (m), 698 (s), 634 (w), 604 (w), 542 (w) cm $^{-1}$; ^{1}H NMR ($CDCl_3$, 400 MHz): δ 7.37-7.28 (*E*/*Z*, 10H, m), 6.39 (*Z*, 1H, d, *J* = 17.4, 10.6 Hz), 6.09 (*E*, 1H, d, *J* = 16.4 Hz), 6.07 (*E*, 1H, dd, *J* = 17.6, 10.8 Hz), 5.90 (*Z*, 1H, d, *J* = 8.8 Hz), 5.68 (*E*, 1H, dd, *J* = 15.8, 12.4 Hz), 5.41 (*Z*, 1H, dd, *J* = 10.8, 3.2 Hz), 5.35 (*Z*, 1H, m), 5.28 (*E*, 1H, dd, *J* = 9.6, 1.2 Hz; *E*, 1H, m), 5.10 (*Z*, 1H, d, *J* = 17.6 Hz), 5.00 (*E*, 1H, dd, *J* = 16.4, 0.8 Hz), 4.56 (*Z*, 2H, s), 4.46 (*E*, 2H, s), 2.02 (*Z*, 3H, s), 1.96 (*E*, 3H, s);□^{13}C NMR ($CDCl_3$, 100 MHz): δ 171.2, 143.1, 141.6, 140.7, 134.3, 133.8, 128.8, 128.5, 128.2, 128.0, 127.1, 126.5, 116.7, 68.6, 51.6, 29.9, 21.1; HRMS (ESI+): Calcd for $C_{21}H_{21}O_2$ [M-OH]$^+$: 305.1542. Found: 305.1547. Diastereomeric ratio was established by enantioselective HPLC analysis of the corresponding enone (below).

(*R*,*E*)-5-Oxo-2,5-diphenyl-2-vinylpent-3-enyl acetate (enone derived from 2.194). This material was accessed by the oxidation procedure with MnO_2 (26% yield). The desired a,*b*-unsaturated ketone was obtained as a 9:1 *E*:*Z* mixture. IR (neat): 3058 (w), 3027 (w), 2960 (w), 2919 (w), 2851 (w), 1739 (s), 1670 (m), 1617 (m), 1598 (w), 1579 (w), 1493 (w), 1447 (m), 1378 (m), 1292 (w), 1223 (s), 1179 (w), 1034 (m), 1016 (s), 926 (m), 861 (w), 765 (m), 744 (m), 696 (s), 658 (w), 639 (w), 603 (w), 556 (w) cm^{-1}; ^{1}H NMR ($CDCl_3$, 400 MHz): δ 7.90 (*E*, 1H, dd, *J* = 8.6, 1.4 Hz), 7.81 (*Z*, 1H, d, *J* = 6.8 Hz), 7.59-7.27 (*E*/*Z*, 10H, m), 6.86 (*E*, 1H, d, *J* = 15.6 Hz), 6.73 (*Z*, 1H, d, *J* = 12.8 Hz), 6.28 (*Z*, 1H, d, *J* = 12.8 Hz), 6.11 (*E*, 1H, dd, *J* = 17.6, 10.8 Hz), 5.41 (*E*, 1H, d, *J* = 10.8 Hz), 5.26 (*Z*, 1H, d, *J* = 10.8 Hz), 5.13 (*Z*, 1H, d, *J* = 17.6 Hz), 5.10 (*E*, 1H, d, *J* = 17.6 Hz), 4.56 (*E*, 2H, s), 4.49 (*Z*, 2H, apparent d, *J* = 2.0 Hz), 2.02 (*E*, 3H, s), 1.82 (*Z*, 3H, s). Diastereomeric ratio was established by enantioselective HPLC analysis in comparison with authentic racemic material (91.5:8.5 er). After correction for 95.5:4.5 er of starting allylic alcohol, stereoselectivity is measured as 95:5 dr. Daicel Chiralpak OD column (95:5 hexanes:2-propanol, 0.5 mL/min, 220 nm) was used.

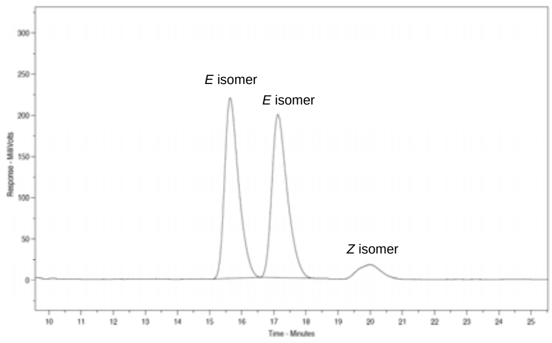

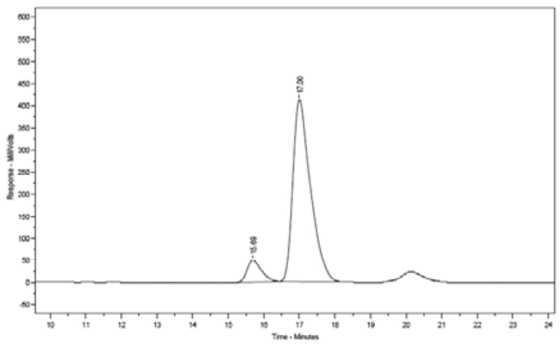

Peak #	Retention time (min)	Area	Area %	Peak #	Retention time (min)	Area	Area %
1	15.64	6679359	50.164	1	15.69	1352589	8.740
2	17.12	6635698	49.836	2	17.00	14123630	91.260

(1*R*,4*S*,*E*)-4-Methyl-4-(naphthalen-2-yl)-1-phenylhexa-2,5-dien-1-ol (2.196). The previously described procedure was followed except that 3 equiv of cyclopropene **2.195** was used. Silica gel chromatography (10% EtOAc in hexanes) afforded the desired product (colorless oil) was isolated as a 10:1 *E:Z* mixture. *E*-isomer (major): IR (neat): 3560 (w), 3359 (m), 3082 (w), 3057 (m), 3027 (m), 2970 (w), 2925 (m), 2871 (w), 2851 (w), 1452 (m), 1001 (m), 977 (m), 917 (m), 857 (m), 818 (m), 747 (s), 699 (s) cm^{-1}; ^{1}H NMR (CDCl$_3$, 400 MHz): δ 7.82-7.75 (3H, m), 7.73 (1H, d, J = 1.6 Hz), 7.48-7.36 (7H, m), 7.32-7.28 (1H, m), 6.15 (1H, dd, J = 17.6, 10.4 Hz), 6.12 (1H, dd, J = 15.6, 1.2 Hz), 5.73 (1H, dd, J = 15.6, 6.4 Hz), 5.31 (1H, br d, J = 5.6 Hz), 5.19 (1H, dd, J = 10.4, 1.2 Hz), 5.04 (1H, d, J = 17.6, 1.2 Hz), 1.95 (1H, d, J = 3.2 Hz), 1.62 (3H, s); ^{13}C NMR (CDCl$_3$, 100 MHz): δ 145.1, 143.7, 143.4, 138.7, 133.5, 132.3, 131.4, 128.8, 128.5, 128.3, 128.2, 127.9, 127.6, 126.6, 126.5, 126.3, 126.2, 126.0, 125.9, 125.5, 125.2, 113.6, 75.4, 69.4, 47.7, 25.8; HRMS (ESI+): Calcd for $C_{23}H_{21}$ [M-OH]$^{+}$: 297.16328. Found: 297.16433. Diastereomeric ratio was established by HPLC analysis of the derived enone (below).

(*S*,*E*)-4-Methyl-4-(naphthalen-2-yl)-1-phenylhexa-2,5-dien-1-one (enone derived from 2.196). This material was accessed by the oxidation procedure with MnO_2 (62% yield). The desired a,*b*-unsaturated ketone was obtained as a 6:1 *E*:*Z* mixture. IR (neat): 3056 (w), 2971 (w), 2922 (w), 2851 (w), 1670 (s), 1651 (m), 1614 (s), 1598 (m), 1448 (w), 1293 (m), 1228 (m), 1015 (m), 747 (m), 696 (m) cm^{-1}; *E*-isomer ^1H NMR ($CDCl_3$, 400 MHz): δ 7.93-7.91 (2H, m), 7.83-7.81 (3H, m), 7.75 (1H, br s), 7.56-7.43 (6H, m), 7.38 (1H, d, J = 16.0 Hz), 6.87 (1H, d, J = 15.2 Hz), 6.21 (1H, dd, J = 17.2, 10.8 Hz), 5.31 (1H, d, J = 10.8 Hz), 5.16 (1H, d, J = 17.2 Hz), 1.73 (3H, s). Diastereomeric ratio was established by HPLC analysis in comparison with authentic racemic material (91.5:8.5 er). After correction for 95.5:4.5 er of the allylic alcohol substrate starting, stereoselectivity is determined as 96:4 dr. Daicel Chiralpak AS column (99.5:0.5 hexanes:2-propanol, 0.5 mL/min, 220 nm) was used.

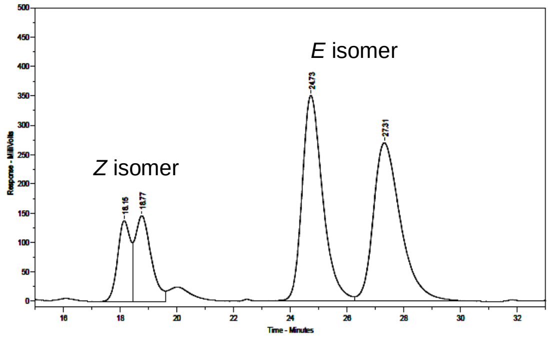

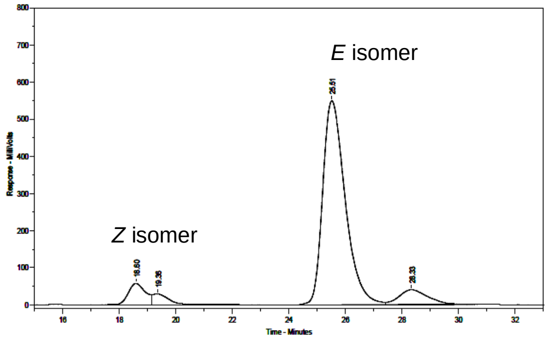

Peak #	Retention time (min)	Area	Area %	Peak #	Retention time (min)	Area	Area %
1	18.15	4348874	9.530	1	18.60	2452672	6.607
2	18.77	5776050	12.658	2	19.36	1348587	3.633
3	24.73	17623390	38.620	3	25.51	30447650	82.022
4	27.31	17884930	39.193	4	28.33	2872363	7.783

(2*R*,5*R*,*E*)-5-Methyl-5-(naphthalen-2-yl)hepta-3,6-dien-2-ol (2.197). The previously described procedure was used except that the reaction was allowed to proceed for 15 minutes. Silica gel chromatography (10% Et_2O in hexanes) afforded the desired product (colorless oil) was isolated as a 6:1 *E:Z* mixture. IR (neat): 3338 (m), 3082 (w), 3056 (m), 2970 (s), 2926 (m), 2871 (m), 1631 (w), 1599 (m), 1504 (m), 1409 (m), 1130 (m), 1061 (m), 1000 (m), 978 (m), 948 (m), 917 (m), 857 (m), 818 (s), 747 (s) cm^{-1}; ^{1}H NMR ($CDCl_3$, 400 MHz): δ 7.82-7.77 (3H *E/Z* and 1H *Z*, 3H, m), 7.73 (*E*, 1H, d, *J* = 1.6 Hz), 7.48-7.42 (*E/Z*, 3H, m), 6.33 (*Z*, 1H, dd, *J* = 17.6, 10.4 Hz), 6.15 (*E,* 1H, dd, *J* = 17.6, 10.8 Hz), 5.97 (*E,* 1H, dd, *J* = 15.6, 0.8 Hz), 5.81 (*Z*, 1H, d, *J* = 10.4 Hz), 5.57 (*E*, 1H, dd, *J* = 15.6, 6.4 Hz), 5.48 (*Z*, 1H, dd, *J* = 11.6, 9.6 Hz), 5.19 (overlapping *E/Z*, 1H, dd, *E*-isomer: *J* = 10.4, 1.2 Hz), 5.05 (overlapping *E/Z*, 1H, dd, *E* isomer: *J* = 17.6, 1.2 Hz), 4.40 (*E*, 1H, dddd, *J* = 6.4, 6.4, 6.3, 6.3 Hz), 4.21-4.16 (*Z*, 1H, m) 1.60 (*E*, 3H, s), 1.59 (*Z*, 1H, s), 1.32 (*E*, 3H, d, *J* = 6.4 Hz), 0.93 (*Z*, 3H, d, *J* = 6.0 Hz); ^{13}C NMR ($CDCl_3$, 100 MHz): δ 145.2, 143.7, 137.2, 135.6, 133.4, 133.2, 132.2, 128.1, 127.8, 127.6, 126.4, 126.3, 126.1, 125.8, 125.3, 124.8, 113.3, 113.0, 69.1, 63.8, 47.4, 25.7, 23.8, 22.5; HRMS (ESI+): Calcd for $C_{18}H_{19}$ $[M-OH]^+$: 235.14868. Found: 235.14889. Diastereomeric ratio was established by HPLC analysis of the derived enone (below).

(*R*,*E*)-5-Methyl-5-(naphthalen-2-yl)hepta-3,6-dien-2-one (enone derived from 2.197). This material was accessed by the oxidation procedure with MnO_2 (97% yield). The desired a,*b*-unsaturated ketone was obtained as a 6:1 *E*:*Z* mixture. IR (neat): 3081 (w), 3056 (w), 3003 (w), 2927 (w), 2873 (w), 1698 (m), 1676 (s), 1620 (m), 1505 (w), 1358 (m), 1256 (m), 987 (m), 922 (m), 819 (m), 749 (m) cm^{-1}; ^{1}H NMR ($CDCl_3$, 400 MHz): δ 7.82-7.80 (3H, m), 7.70 (1H, d, *J* = 1.6 Hz), 7.50-7.45 (2H, m), 7.39 (1H, dd, *J* = 8.4, 1.6 Hz), 7.08 (1H, d, *J* = 16.0 Hz), 6.17 (1H, dd, *J* = 17.6, 10.8 Hz), 6.10 (1H, d, *J* = 16.4 Hz), 5.29 (1H, d, *J* = 10.8 Hz), 5.11 (1H, d, *J* = 17.6 Hz), 2.30 (3H, s), 1.66 (3H, s). Diastereomeric ratio was established by HPLC analysis in comparison with authentic racemic material (88:12 er). After correction for 91:9 er of starting allylic alcohol, diastereoselectivity is measured as 97:3 dr. Daicel Chiralpak OD column (99.8:0.2 hexanes:2-propanol, 1 mL/min, 220 nm) used.

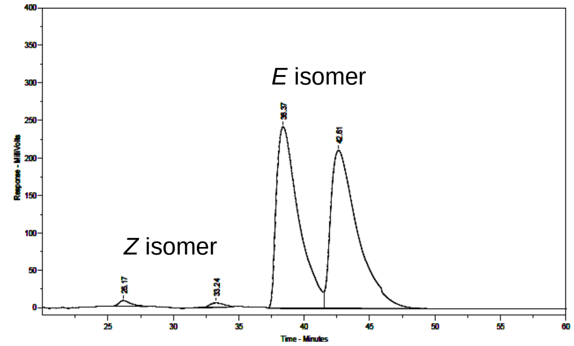

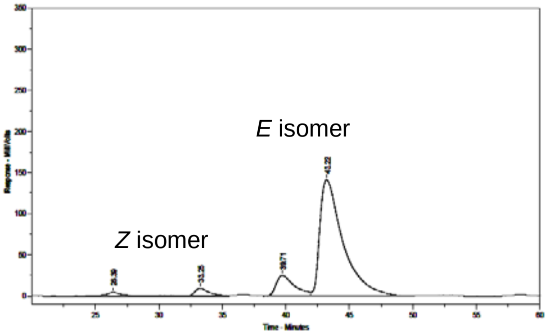

Peak #	Retention time (min)	Area	Area %	Peak #	Retention time (min)	Area	Area %
1	26.17	473406	0.795	1	26.39	407959	1.899
2	33.24	464542	0.780	2	33.25	847978	3.947
3	38.37	28491610	47.817	3	39.71	2423907	11.283
4	42.67	30154670	50.608	4	43.22	17802050	82.870

(2*S*,5*R*,*E*)-1-(*t*-Butyldimethylsilyloxy)-5-methyl-5-phenylhepta-3,6-dien-2-ol (2.198). The previously described procedure was followed except that 2 equiv of cyclopropene **2.182** was used and the reaction was allowed to proceed for 15 minutes. Silica gel chromatography (10% Et_2O in hexanes) afforded the desired product (colorless oil) was isolated as a 11:1 *E:Z* mixture in 71% yield as a colorless oil. *E* isomer (major): IR (neat): 3566 (w), 3433 (w), 3084 (w), 3058 (w), 3023 (w), 2954 (m), 2928 (m), 2857 (m), 1634 (w), 1599 (w), 1492 (m), 1471 (m), 1471 (m), 1463 (m), 1254 (m), 1110 (s), 836 (s), 777 (m), 700 (m) cm^{-1}; ^1H NMR ($CDCl_3$, 400 MHz): δ 7.33-7.28 (4H, m), 7.22-7.19 (1H, m), 6.06 (1H, dd, J = 17.6 Hz, 10.8 Hz), 6.01 (1H, dd, J = 15.6, 1.2 Hz), 5.42 (1H, dd, J=15.6, 6.4 Hz), 5.14 (1H, dd, J = 10.8, 1.2 Hz), 5.01 (1H, dd, J = 17.2, 0.8 Hz), 4.21 (1H, X of ABX, J_{AX} and J_{BX} cannot be determined), 3.66 (1H, B of ABX, J_{AB} = 9.6, J_{BX} = 3.6 Hz), 3.48 (1H, A of ABX, J_{AB} = 10.0, J_{AX} = 7.6 Hz), 2.56 (1H, d, J = 3.6 Hz), 1.50 (3H, s), 0.91 (9H, s), 0.08 (6H, s); ^{13}C NMR ($CDCl_3$, 100 MHz): δ 146.2, 145.1, 139.8, 128.3, 127.3, 127.2, 126.3, 113.0, 73.0, 67.4, 64.5, 47.5, 26.0, 25.6, 18.5, –5.22, –5.17; HRMS (ESI+): Calcd for $C_{20}H_{36}NO_2Si$ $[M+NH_4]^+$: 350.2515. Found: 350.2523.

Diastereomeric ratio was established by enantioselective HPLC analysis of the derived enone (below).

(*R*,*E*)-1-(*t*-Butyldimethylsilyloxy)-5-methyl-5-phenylhepta-3,6-dien-2-one (enone derived from 2.198). This material was accessed by the oxidation procedure with MnO$_2$ (81% yield). The desired a,*b*-unsaturated ketone was obtained as a >98:<2 *E*:*Z* mixture. IR (neat): 2954 (m), 2929 (m), 2886 (w), 2856 (m), 1697 (s), 1617 (s), 1492 (m), 1471 (m), 1463 (m), 1303 (m), 1253 (s), 1105 (s), 1066 (m), 1003 (m), 835 (s), 777 (s), 699 (s) cm^{-1}; ^{1}H NMR (CDCl$_3$, 400 MHz): □□7.32-7.23 (□□□□m), 7.21 (1H, d, *J* = 16.0 Hz), 6.39 (1H, d, *J* = 16.4 Hz), 6.07 (1H, dd, *J* = 17.6, 10.8 Hz), 5.22 (1H, dd, *J* = 10.4, 0.8 Hz), 5.05 (1H, dd, *J* = 17.2, 0.4 Hz), 4.30 (2H, s), 1.54 (3H, s) 0.90 (9H, s), 0.08 (6H, s). Diastereomeric ratio was established by HPLC analysis of the enone in comparison with authentic racemic material (89:11 er). Chiralpak OJ-H (100:0 hexanes:2-propanol, 0.3 mL/min, 220 nm) was used.

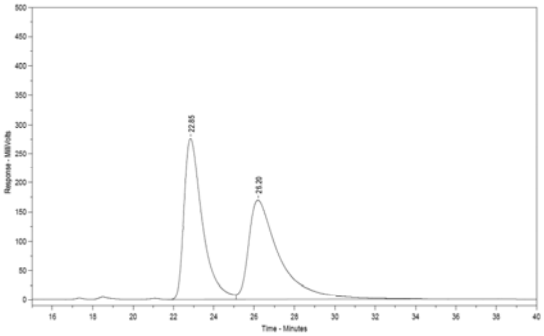

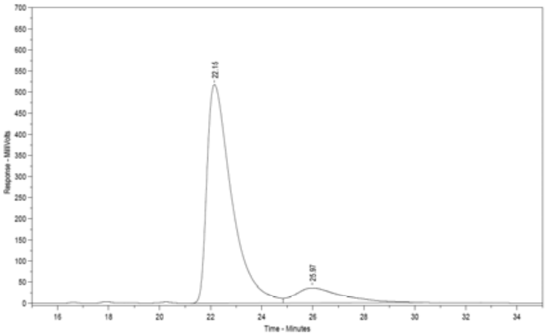

Peak #	Retention time (min)	Area	Area %	Peak #	Retention time (min)	Area	Area %
1	22.85	17374750	49.117	1	22.15	34742070	88.764
2	26.20	17999290	50.883	2	25.97	4397799	11.236

■ Reactions of Cyclobutenes

(1*R*,4*R*,5*S*,*E*)-4,5-Bis(*t*-butyldimethylsilyloxy)-1-phenylhepta-2,6-dien-1-ol (2.205) and (1*R*,4*S*,5*R*,*Z*)-4,5-bis(*t*-butyldimethylsilyloxy)-1-phenylhepta-2,6-dien-1-ol

(2.206): Under N_2 atmosphere, an oven-dried (160 °C) 1-dram vial was charged with cyclobutene **2.203** (49.4 mg, 0.157 mmol, 1.00 equiv), (*R*)-1-phenylprop-2-en-1-ol (*R*-**3**; 95.5:4.5 er; 21.6 mg, 0.161 mmol, 1.03 equiv), and toluene (0.56 mL). Ru complex **2.204** (2.3 mg, 0.0032 mmol, 0.020 equiv) was added as a solution in toluene (0.23 mL). The resulting mixture was allowed to stir for 2 h at 22 °C, after which was transferred directly onto and passed through a silica gel column (5 x 1 cm, 2:1 hexanes:Et_2O), eluted with 2:1 hexanes:Et_2O (30 mL). Volatiles were then removed *in vacuo* to give brown oil, purification of which by silica-gel chromatography (10:1→5:1 hexanes:Et_2O) afforded *E* isomer **2.205** (40.4 mg, 0.090 mmol, 57% yield) as a colorless oil and *Z* isomer **2.206** (25.6 mg 0.057 mmol, 36% yield), also as a colorless oil.

***E* isomer (2.205).** IR (neat): 3390 (br. w), 3029 (w), 2955 (m), 2929 (m), 2885 (m), 2856 (m), 1493 (w), 1472 (m), 1462 (m), 1404 (w), 1389 (w), 1361 (w), 1251 (s), 1188 (w), 1081 (s), 1031 (m), 1004 (m), 971 (m), 939 (m), 922 (m), 831 (s), 774 (s), 698 (s), 670 (m), 614 (w), 550 (w) cm^{-1}; ^1H NMR ($CDCl_3$, 400 MHz): δ 7.38-7.32 (4H, m), 7.29-7.25 (1H, m), 5.89-5.78 (1H, overlapping m), 5.85-5.82 (2H, overlapping m), 5.21 (1H, overlapping apparent d, *J* = 4.0 Hz), 5.18 (1H, ddd, *J* = 17.2, 1.2, 1.2 Hz), 5.11 (1H, ddd, *J* = 10.4, 2.0, 1.2 Hz), 3.99 (1H, ddd, *J* = 5.6, 5.6, 0.8 Hz), 3.96 (1H, ddd, *J* = 5.6, 5.6, 0.8 Hz), 1.81 (1H, d, *J* = 4.0 Hz), 0.87 (9H, s), 0.86 (9H, s), 0.02 (3H, s), 0.01 (3H, s), 0.00 (3H, s), -0.02 (3H, s); ^{13}C NMR ($CDCl_3$, 100 MHz): δ 143.0, 139.0, 133.4, 132.1, 128.6, 127.8, 126.5, 115.9, 78.1, 76.8, 74.8, 26.0, 26.0, 18.4, –4.1, –4.2, –4.4, –4.5; HRMS (ESI+): Calcd for $C_{25}H_{44}O_3Si_2Na$ $[M+Na]^+$: 471.2727. Found: 471.2709.

***Z* isomer (2.206).** IR (neat): 3416 (br. w), 3028 (w), 2954 (m), 2929 (m), 2886 (m), 2856 (m), 1493 (w), 1472 (m), 1462 (m), 1406 (w), 1389 (w), 1361 (w), 1251 (s), 1188 (w), 1071 (s), 1030 (m), 1004 (m), 969 (w), 938 (m), 924 (m), 831 (s), 774 (s), 743 (m), 697 (s), 670 (m), 646 (w), 591 (w), 533 (w) cm^{-1}; ^1H NMR ($CDCl_3$, 400 MHz): δ 7.41 (2H, dd, *J* = 9.2, 1.6 Hz), 7.33 (2H, ddd, *J* = 7.2, 7.2, 1.6 Hz), 7.26 (1H, m), 5.82 (1H, overlapping ddd, *J* = 17.2, 10.4, 6.8 Hz), 5.78 (1H, overlapping ddd, *J* = 11.6, 6.8, 1.2 Hz), 5.46 (1H, d, *J* = 8.4 Hz), 5.44 (1H, obscured m), 5.19 (1H, ddd, *J* = 17.2, 1.6, 1.6

Hz), 5.13 (1H, d, *J* = 10.4 Hz), 4.72 (1H, ddd, *J* = 8.8, 6.4, 1.2 Hz), 3.89 (1H, dd, *J* = 6.4, 6.4 Hz), 3.31 (1H, d, *J* = 2.0 Hz), 0.88 (9H, s), 0.86 (9H, s), 0.05 (3H, s), 0.04 (3H, s), 0.03 (3H, s), -0.00 (3H, s); ^{13}C NMR ($CDCl_3$, 100 MHz): δ 142.9, 138.9, 133.3, 132.0, 128.5, 127.5, 126.4, 116.7, 78.2, 73.0, 71.7, 26.0, 26.0, 18.4, 18.3, –4.26, –4.35, –4.4; HRMS (ESI+): Calcd for $C_{25}H_{44}O_3Si_2Na$ $[M+Na]^+$: 471.2727. Found: 471.2717. Diastereomeric ratios were determined by HPLC analysis of the derived enones (below).

(4*R*,5*S*,*E*)-4,5-Bis(*t*-butyldimethylsilyloxy)-1-phenylhepta-2,6-dien-1-one (enone derived from 2.205). Activated 4 Å molecular sieves (17.0 mg), alcohol **2.205** (14.5 mg, 0.0323 mmol, 1.00 equiv) were dissolved in CH_2Cl_2 (0.20 mL) in a 1-dram vial. To the mixture was added, with stirring, *N*-methylmorpholine oxide (NMO) (6.2 mg, 0.053 mmol, 1.6 equiv), followed by tetrapropylammonium per-ruthenate (TPAP) (0.7 mg, 0.002 mmol, 0.06 equiv). The resulting solution was allowed to stir for one hour at 22 °C, after which, it was directly was loaded and passed through a silica gel column (3 x 0.5 cm) eluted with 20 mL of CH_2Cl_2. The collected fractions were concentrated *in vacuo* to give light yellow-brown oil. Purification by silica gel chromatography (20:1 hexanes:Et_2O) afforded the desired enone (12.3 mg, 0.028 mmol, 85% yield) as a colorless solid, which crystallized upon standing at –15 °C. mp: 57-60 °C; IR (neat): 2954 (m), 2929 (m), 2886 (w), 2857 (m), 1674 (m), 1628 (m), 1599 (w), 1580 (w), 1472 (m), 1463 (m), 1448 (w), 1405 (w), 1389 (w), 1361 (w), 1324 (w), 1286 (m), 1252 (s), 1204 (w), 1178 (w), 1121 (m), 1082 (m), 1004 (m), 991 (m), 974 (m), 925 (m), 831 (s), 813 (s), 775 (s), 691 (s), 588 (w), 561 (w) cm^{-1}; ^{1}H NMR ($CDCl_3$, 400 MHz): δ 7.95-7.93 (2H, m), 7.56 (1H, tt, *J* = 7.2, 1.6 Hz), 7.49-7.45 (2H, m), 7.14-7.05 (2H, m), 5.87 (1H, ddd, *J* = 17.2, 10.4, 6.4 Hz), 5.25 (1H, ddd, *J* = 17.2, 1.6, 1.6 Hz), 5.17 (1H, ddd, *J* = 10.8, 2.0, 0.8 Hz), 4.28 (1H, dd, *J* = 5.6, 3.2 Hz), 4.07 (1H, dd, *J* = 6.0, 5.2 Hz), 0.94 (9H, s), 0.87 (9H, s), 0.09 (3H, s), 0.06 (3H, s), 0.03 (3H, s), 0.02 (3H, s). Diastereomeric ratio for **2.205** was established by HPLC analysis of the derived enone in comparison with authentic racemic material (95.5:4.5 er). Since the enantiomeric purity of the allylic alcohol used was also 95.5:4.5 er, reaction selectivity is measured as >98:2 dr. Daicel Chiralpak OD (99.9:0.1 hexanes:2-propanol, 0.5 mL/min, 254 nm) was used.

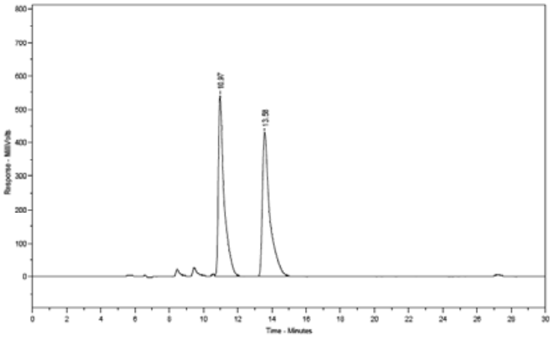

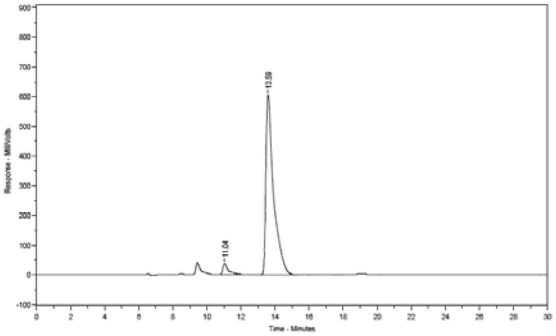

Peak #	Retention time (min)	Area	Area %	Peak #	Retention time (min)	Area	Area %
1	10.97	12586990	49.317	1	11.04	912858	4.560
2	13.58	12935810	50.683	2	13.59	19105100	95.440

(4*S*,5*R*,*Z*)-4,5-Bis(*t*-butyldimethylsilyloxy)-1-phenylhepta-2,6-dien-1-one (enone derived from 2.206). This material was obtained through a similar procedure as used for oxidation of **2.205**. The desired enone was obtained in 89% yield as colorless oil. IR (neat): 3069 (w), 2955 (m), 2929 (m), 2886 (w), 2857 (m), 1708 (w), 1670 (m), 1618 (w), 1598 (w), 1472 (w), 1463 (w), 1449 (w), 1409 (w), 1389 (w), 1361 (w), 1308 (w), 1252 (s), 1230 (m), 1176 (w), 1151 (w), 1109 (m), 1077 (m), 1033 (w), 1004 (m), 996 (m), 938 (w), 922 (w), 870 (w), 835 (s), 811 (m), 777 (s), 745 (m), 722 (w), 688 (m), 671 (w) cm^{-1}; ^{1}H NMR ($CDCl_3$, 400 MHz): δ 7.94-7.92 (2H, m), 7.55 (1H, tt, J = 7.2, 1.2 Hz), 7.48-7.44 (2H, m), 6.85 (1H, dd, J = 12.0, 1.2 Hz), 6.17 (1H, dd, J = 12.0, 8.8 Hz), 5.89 (1H, ddd, J = 16.8, 10.4, 6.4 Hz), 5.26 (1H, ddd, J = 8.4, 3.2, 0.8 Hz), 5.15 (1H, ddd, J = 17.2, 1.6, 1.2 Hz), 5.06 (1H, ddd, J = 10.4, 1.6, 0.8 Hz), 4.23-4.20 (1H, m), 0.89 (9H, s), 0.87 (9H, s), 0.12 (3H, s), 0.05 (6H, s), 0.00 (3H, s). At 22 °C, the *Z* enone undergoes slow isomerization to the *E*-enone, which is the *enantiomer* of the product obtained from oxidation of **2.205**; this process is accelerated in the presence of DMAP (0.2 equiv) in THF (0.5 M). The latter *E* enone isomer was subsequently separated from the *Z*-enone from **2.206** by silica gel chromatography, and was used to determine the diastereomeric purity of **2.206** by HPLC analysis in comparison with authentic racemic material (92.5:7.5 er). Since enantiomeric purity of the starting allylic alcohol is 95.5:4.5 er, the stereoselectivity of the DROCM reactions is measured to 97:3 dr. Daicel Chiralpak OD (99.9:0.1 hexanes:2-propanol, 0.5 mL/min, 254 nm) was used.

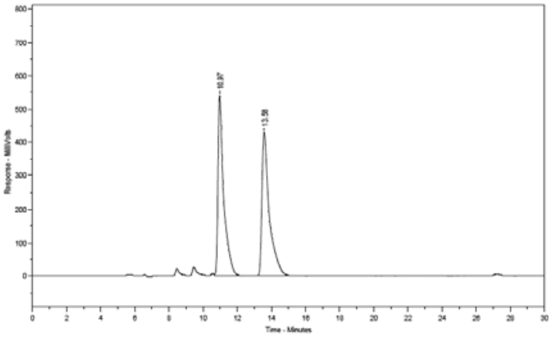

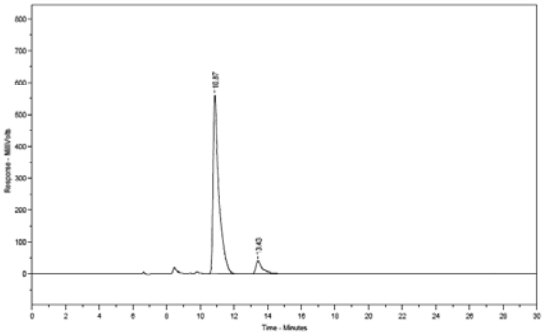

Peak #	Retention time (min)	Area	Area %	Peak #	Retention time (min)	Area	Area %
1	10.97	12586990	49.317	1	10.87	13305590	92.282
2	13.58	12935810	50.683	2	13.43	1112788	7.718

(1*R*,4*R*,5*S*,*E*)-4,5-bis(benzyloxy)-1-phenylhepta-2,6-dien-1-ol (2.207) and (1*R*,4*S*,5*R*,*Z*)-4,5-Bis(benzyloxy)-1-phenylhepta-2,6-dien-1-ol (2.208). This material was obtained through a similar procedure as described above. The *E* isomer was isolated (33.5 mg, 0.084 mmol, 45% yield) as a white solid and the *Z* isomer (26.8 mg, 0.067 mmol, 36% yield) as colorless oil.

***E* isomer (2.207):** mp: 87-90 °C; IR (neat): 3463 (br m), 3061 (w), 3027 (w), 2914 (w), 2869 (m), 1602 (w), 1585 (w), 1496 (m), 1465 (m), 1448 (m), 1384 (m), 1290 (m), 1256 (m), 1218 (w), 1205 (w), 1191 (w), 1177 (w), 1152 (w), 1134 (w), 1101 (s), 1087 (s), 1030 (m), 1004 (m), 981 (s), 968 (s), 952 (s), 923 (m), 912 (w), 897 (w), 862 (w), 814 (w), 757 (m), 746 (s), 732 (s), 714 (s), 695 (s), 650 (m), 627 (m), 603 (m), 582 (m), 503 (m), 490 (m), 462 (m), 436 (m) cm^{-1}; ^{1}H NMR (CDCl$_3$, 400 MHz): δ 7.37-7.23 (15H, m), 5.90 (1H, Y of AXY, J_{XY} = 15.6 Hz), 5.83 (1H, overlapping ddd, J = 17.6, 10.4, 7.6 Hz), 5.79 (1H, overlapping X of AXY, J_{XY} = 15.6 Hz), 5.31 (1H, d, J = 10.4 Hz), 5.28 (1H, dd, J = 17.2, 0.8 Hz), 5.23 (1H, br d, J = 6.0 Hz), 4.63 (1H, B of AB, J_{AB} = 12.4 Hz), 4.62 (1H, B of AB, J_{AB} = 12.0 Hz), 4.48 (1H, A of AB, J_{AB} = 12.0 Hz), 4.41 (1H, A of AB, J_{AB} = 12.0 Hz), 3.90 (1H, dd, J = 7.2, 5.2 Hz), 3.85 (1H, dd, J = 7.2, 5.2 Hz). 1.89 (1H, br s); ^{13}C NMR (CDCl$_3$, 100 MHz): δ 142.8, 138.6, 138.6, 136.7, 135.7, 128.7, 128.7, 128.4, 127.8, 127.5, 126.4, 119.0, 82.6, 81.5, 74.7, 70.9, 70.7; HRMS (ESI+): Calcd for $C_{27}H_{28}O_3Na$ [M+Na]$^+$: 423.1936. Found: 423.1939.

***Z* isomer (2.208):** IR (neat): 3409 (br w), 3063 (w), 3029 (w), 2976 (w), 2866 (m), 1495 (w), 1453 (m), 1422 (w), 1385 (w), 1332 (w), 1206 (w), 1089 (s), 1069 (s), 1027 (s), 994 (m), 929 (m), 911 (m), 846 (w), 732 (s), 696 (s), 646 (w), 611 (w), 535 (w), 460 (w) cm^{-1}; ^{1}H NMR ($CDCl_3$, 400 MHz): δ 7.36-7.21 (15 H, m), 5.91 (1H, ddd, *J* = 11.2, 8.4, 0.8 Hz), 5.83 (1H, ddd, *J* = 18.0, 10.4, 7.6 Hz), 5.52 (1H, ddd. *J* = 11.2, 9.2, 1.2 Hz), 5.32 (1H, obscured), 5.32 (1H, overlapping ddd, *J* = 10.4, 0.8, 0.8 Hz), 5.27 (1H, overlapping ddd, *J* = 17.2, 1.6, 0.8 Hz), 4.65 (1H, B of AB, J_{AB} = 12.4 Hz), 4.62 (1H, B of AB, J_{AB} = 12.0 Hz), 4.50 (1H, A of AB, J_{AB} = 12.4 Hz), 4.46 (1H, ddd, *J* = 9.2, 5.6, 1.2 Hz), 4.37 (1H, A of AB, J_{AB} = 12.0 Hz), 3.79 (1H, dd, *J* = 7.6, 5.6 Hz), 2.37 (1H, br s); ^{13}C NMR ($CDCl_3$, 100 MHz): δ 143.0, 138.5, 138.2, 136.8, 136.5, 129.1, 128.5, 128.5, 128.0, 127.9, 127.8, 127.7, 127.6, 126.3, 119.5, 82.1, 76.7, 70.8, 70.7, 70.4; HRMS (ESI+): Calcd for $C_{27}H_{28}O_3Na$ $[M+Na]^+$: 423.1936. Found: 423.1935. Diastereomeric ratios were determined by HPLC analysis of the derived enones (below).

(4*R*,5*S*,*E*)-4,5-Bis(benzyloxy)-1-phenylhepta-2,6-dien-1-one (2.207). This material was obtained through a similar procedure as used for oxidation of **2.205**. The desired enone was obtained in 65% yield as colorless oil. IR (neat): 3086 (w), 3063 (w), 3030 (w), 2981 (w), 2921 (w), 2864 (w), 1731 (w), 1671 (m), 1625 (m), 1597 (w), 1579 (w), 1496 (w), 1452 (m), 1422 (w), 1390 (w), 1353 (w), 1325 (w), 1280 (m), 1178 (w), 1087 (s), 1069 (s), 1027 (s), 1013 (m), 981 (s), 930 (m), 847 (w), 733 (s), 694 (s), 617 (s), 461 (w), 405 (w) cm^{-1}; ^{1}H NMR ($CDCl_3$, 400 MHz): δ 7.92-7.90 (2H, m), 7.57 (1H, tt, *J* = 7.2, 1.2 Hz), 7.47-7.44 (2H, m), 7.35-7.23 (10H, m), 7.10 (1H, dd, *J* =15.6, 0.8 Hz), 7.00 (1H, dd, *J* = 15.6, 5.6 Hz), 5.88 (1H, ddd, *J* = 17.6, 10.4, 7.6 Hz), 5.38 (1H, d, *J* = 10.0 Hz), 5.35 (1H, d, *J* = 17.6 Hz), 4.69 (1H, B of AB, J_{AB} = 12.0 Hz), 4.65 (1H, B of AB, J_{AB} = 12.0 Hz), 4.57 (1H, A of AB, J_{AB} = 12.0 Hz), 4.42 (1H, A of AB, *J* = 12.0 Hz), 4.19 (1H, ddd, *J* = 5.6, 5.6, 0.8 Hz), 3.95 (1H, dd, *J* = 7.6, 5.6 Hz). Diastereomeric ratio for the *E* product isomer of the reaction in Table S-3 was established by HPLC analysis of the derived enone in comparison with authentic racemic material (93.5:6.5 er). After correction for enantiomeric purity of the starting allylic alcohol (95.5:4.5 er), diastereomeric purity of the product is measured to 98:2 dr. Daicel Chiralpak OD (99.5:0.5 hexanes:2-propanol, 1.0 mL/min, 254 nm) was used.

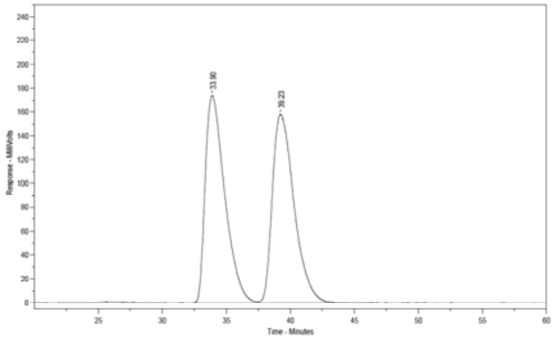

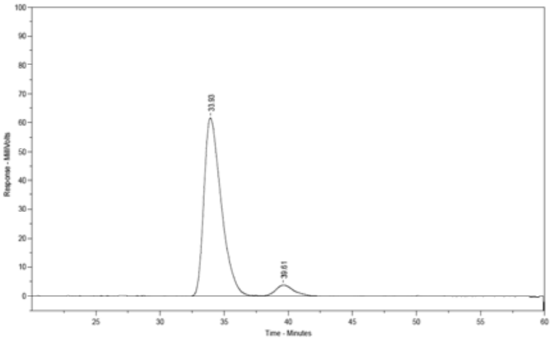

Peak #	Retention time (min)	Area	Area %	Peak #	Retention time (min)	Area	Area %
1	33.90	18405950	49.739	1	33.93	5792403	93.553
2	39.23	18599200	50.261	2	39.61	399144	6.447

(4*S*,5*R*,*Z*)-4,5-Bis(benzyloxy)-1-phenylhepta-2,6-dien-1-one (*Z* isomer oxidation product). This material was obtained through a similar procedure as used for oxidation of **2.205**. The desired enone was obtained in 79% yield as colorless oil. IR (neat): 3086 (w), 3063 (w), 3030 (w), 2981 (w), 2918 (w), 2862 (w), 1725 (w), 1665 (m), 1618 (w), 1596 (w), 1579 (w), 1496 (w), 1449 (m), 1410 (w), 1389 (w), 1298 (w), 1229 (s), 1177 (w), 1158 (w), 1087 (s), 1066 (s), 1027 (m), 1003 (s), 994 (s), 929 (m), 825 (w), 774 (w), 730 (s), 693 (s), 605 (w), 535 (w), 461 (w), 404 (w) cm^{-1}; ^{1}H NMR (CDCl$_3$, 400 MHz): δ 7.94-7.91 (2H, m), 7.57 (1H, tt, J = 8.0, 1.2 Hz), 7.48-7.44 (2H, m), 7.41-7.37 (2H, m), 7.33-7.23 (8H, m), 6.97 (1H, dd, J = 12.0, 1.2 Hz), 6.27 (1H, dd, J = 12.0, 8.4 Hz), 5.97-5.88 (1H, m), 5.29-5.29 (1H, m), 5.25 (1H, ddd, J = 4.0, 0.8, 0.8 Hz), 5.14 (1H, ddd, J = 8.8, 3.6, 1.2 Hz), 4.70 (1H, B of AB, J_{AB} = 12.0 Hz), 4.61 (2H, s), 4.58 (1H, A of AB, J_{AB} = 12.4 Hz), 4.08 (1H, dd, J = 7.6, 3.6 Hz). The resulting *Z* enone undergoes slow isomerization at 22 °C to afford the enantiomer of the enone obtained from oxidation of the corresponding *E* isomer; this process is accelerated in the presence of DMAP (0.2 equiv) in THF (0.5 M). The latter *E* enone isomer was subsequently separated from the enone of the *Z* isomer by silica gel chromatography, and was used to determine the diastereomeric purity of the *Z* isomer by HPLC analysis in comparison with authentic racemic material (92.5:7.5 er). Since enantiomeric purity of the starting allylic alcohol is

95.5:4.5 er, the stereoselectivity of the DROCM reaction is measured to be 98:2 dr. Daicel Chiralpak OD (99.9:0.1 hexanes:2-propanol, 0.5 mL/min, 254 nm) was used.

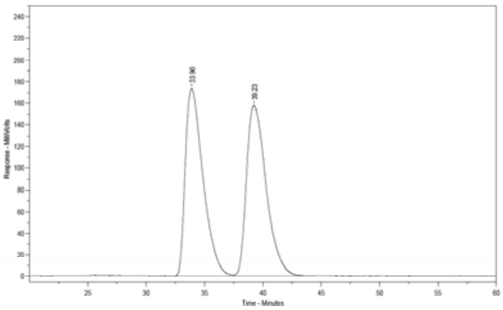

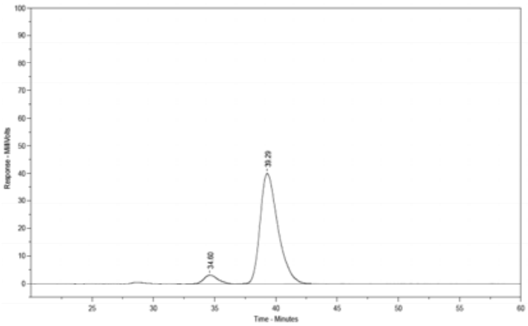

Peak #	Retention time (min)	Area	Area %	Peak #	Retention time (min)	Area	Area %
1	33.90	18405950	49.739	1	34.60	285574	6.565
2	39.23	18599200	50.261	2	39.29	4064144	93.435

(2*S*,5*S*,6*R*,*E*)-5,6-bis(*t*-butyldimethylsilyloxy)-1-(*t*-butyldimethylsilyloxy)octa-3,7-dien-2-ol (2.209) and (2*S*,5*R*,6*S*,*Z*)-5,6-Bis(*t*-butyldimethylsilyloxy)-1-(*t*-butyldimethylsilyloxy)octa-3,7-dien-2-ol (2.210). This material was obtained through a similar procedure as described above. The *E* isomer **2.209** was isolated (23.0 mg, 0.0445 mmol, 27% yield) as colorless oil and the *Z* isomer **2.210** (40.5 mg, 0.0783 mmol, 48% yield), also as colorless oil.

***E* isomer (2.209).** IR (neat): 3581 (br w), 3473 (br w), 2954 (m), 2929 (m), 2886 (m), 2857 (m), 1472 (m), 1463 (m), 1404 (w), 1389 (w), 1361 (w), 1252 (m), 1096 (s), 1005 (m), 970 (m), 938 (m), 922 (m), 831 (s), 774 (s), 669 (m) cm^{-1}; ^{1}H NMR (CDCl$_3$, 400 MHz): δ 5.83 (1H, overlapping ddd, J = 16.8, 10.4, 5.6 Hz), 5.81 (1H, obscured, m), 5.59 (1H, ddd, J = 16.0, 5.6, 0.8 Hz), 5.18 (1H, ddd, J = 17.2, 1.2, 1.2 Hz), 5.11 (1H, ddd, J = 11.2, 1.2, 1.2 Hz), 4.20-4.14 (1H, m), 3.96 (1H, overlapping dd, J = 5.6, 5.6 Hz), 3.93 (1H, overlapping dd, J = 5.6, 5.6 Hz), 3.63 (1H, B of ABX, J_{AB} = 10.0 Hz), 3.40 (1H, A of ABX, J_{AB} = 10.0 Hz), 2.49 (1H, d, J = 2.8 Hz), 0.91 (9H, s), 0.88 (9H, s), 0.88 (9H, s), 0.08 (3H, s), 0.08 (3H, s), 0.04 (3H, s), 0.03 (3H, s), 0.01 (6H, s); ^{13}C NMR (CDCl$_3$, 100 MHz): δ 139.0, 133.2, 115.8, 78.1, 77.0, 72.5, 67.4, 26.1, 26.0, 18.5, 18.4, –4.1, –4.2, –

4.4, –4.5, –5.20, –5.24. HRMS (ES+): Calcd for $C_{26}H_{56}O_4Si_3Na$ $(M+Na)^+$: 539.3384, Found: 539.3368.

***Z* isomer (2.210).** IR (neat): 3572 (br w), 3470 (br w), 3078 (w), 2954 (m), 2929 (m), 2887 (m), 2857 (m), 1472 (m), 1462 (m), 1406 (w), 1389 (w), 1361 (w), 1311 (w), 1252 (m), 1073 (s), 1005 (m), 938 (m), 923 (m), 889 (m), 831 (s), 774 (s), 668 (m) cm^{-1}; ^1H NMR ($CDCl_3$, 400 MHz): δ 5.87 (1H, ddd, *J* = 17.2, 10.4, 6.4 Hz, *minor diast.*), 5.81 (1H, ddd, *J* = 17.2, 10.4, 6.0 Hz, *major diast.*), 5.64 (1H, dd, *J* = 11.2, 7.2 Hz, *minor diast.*), 5.52 (1H, ddd, *J* = 11.2, 9.2, 1.6 Hz, *minor diast.*), 5.49 (1H, Y of AXY, J_{XY} = 7.2 Hz, *major diast.*), 5.44 (1H, X of AXY, J_{XY} = 7.2 Hz, *major diast.*), 5.22 (1H, ddd, *J* = 17.2, 1.2, 1.2 Hz, *minor diast.*), 5.19 (1H, ddd, *J* = 17.2, 1.2, 1.2 Hz, *major diast.*), 5.17 (1H, ddd, *J* = 10.2, 1.2, 1.2 Hz, *minor diast.*), 5.12 (1H, ddd, *J* = 10.4, 1.2, 1.2 Hz, *major diast.*), 4.43-4.38 (1H, m, *major diast.*), 4.36 (1H, dd, *J* = 9.6, 7.2 Hz, *minor diast.*), 4.31 (1H, dd, *J* = 8.4, 5.6 Hz, *major diast.*), 3.94 (1H, dd, *J* = 5.6, 5.6 Hz, *major diast.*), 3.62 (1H, B of ABX, J_{AB} = 10.0 Hz, *major diast.*), 3.59 (2H, d, *J* = 6.0 Hz, *minor diast.*), 3.41 (1H, A of ABX, J_{AB} = 10.0 Hz, *major diast.*), 2.97 (1H, d, *J* = 2.4 Hz, *minor diast.*), 2.85 (1H, d, *J* = 2.0 Hz, *major diast.*), 0.91 (9H, s, *major diast.*), 0.90 (9H, s, *minor diast.*), 0.88 (9H, s, *minor diast.*), 0.88 (9H, s, *major diast.*), 0.87 (9H, s, *major diast.*), 0.85 (9H, s, *minor diast.*), 0.08 (6H, s, *major diast.*), 0.08 (6H, s, *minor diast.*), 0.07 (3H, s, *minor diast.*), 0.07 (3H, s, *minor diast.*), 0.06 (3H, s, *major diast.*), 0.05 (3H, s, *major diast.*), 0.04 (3H, s, *major diast.*), 0.02 (3H, s, *minor diast.*), 0.02 (3H, s, *major diast.*), 0.01 (3H, s, *minor diast.*); ^{13}C NMR ($CDCl_3$, 100 MHz): δ 139.2, 139.0, 135.7, 134.1, 130.9, 129.4, 116.7, 116.1, 78.1, 77.8, 73.3, 72.9, 69.2, 68.1, 67.2, 66.9, 26.2, 26.1, 26.1, 26.0, 26.0, 18.5, 18.5, 18.3, –4.09, –4.17, –4.27, –4.29, –4.41, –4.54, –5.14, –5.17; HRMS (ESI+): Calcd for $C_{26}H_{56}O_4Si_3Na$ $[M+Na]^+$: 539.3384. Found: 539.3396. Diastereomeric ratios were determined by HPLC analysis of the derived enones (below).

(5*S*,6*R*,*E*)-5,6-Bis(*t*-butyldimethylsilyloxy)-1-(*t*-butyldimethylsilyloxy)octa-3,7-dien-2-one (from 2.209). In an oven-dried 1-dram vial, under dry N_2 atmosphere, oxalyl chloride (0.010 mL, 0.12 mmol, 2.7 equiv) was dissolved in CH_2Cl_2 (0.30 mL), and the solution was allowed to cool to –78 °C; DMSO (0.010 mL, 0.14 mmol, 3.2 equiv) was added with vigorous stirring. After 5 min, the *E* alcohol isomer (23.0 mg, 0.0445 mmol, 1.00 equiv) was added in a drop-wise manner as a solution in CH_2Cl_2 (0.100 mL), and the resulting mixture was allowed to stir at –78 °C for 30 min, after which Et_3N (0.030 mL, 0.22 mmol, 4.8 equiv) was added (drop-wise). After the mixture was allowed to stir at –78 °C for 30 min, it was allowed to warm to 22 °C over 10-15 min. The resulting solution was diluted with H_2O (2.0 mL) and Et_2O (2.0 mL), layers were separated, and the aqueous layer was washed with Et_2O (2 x 10 mL). The combined organic layers were dried over anhydrous $MgSO_4$, filtered, and concentrated *in vacuo* to give light yellow oil. Purification by silica gel chromatography (50:1 hexanes:Et_2O) afforded the desired enone as colorless oil (16.0 mg, 0.0311 mmol, 70% yield). IR (neat): 2955 (m), 2929 (m), 2886 (w), 2857 (m), 1699 (w), 1631 (w), 1472 (m), 1463 (m), 1405 (w), 1390 (w), 1362 (w), 1293 (w), 1254 (s), 1105 (s), 1005 (w), 987 (m), 938 (m), 833 (s), 813 (m), 776 (s), 671 (m) cm^{-1}; ^1H-NMR ($CDCl_3$, 400 MHz): δ 6.98 (1H, dd, *J* = 16.0, 4.8 Hz), 6.54 (1H, dd, *J* = 16.0, 1.6 Hz), 5.83 (1H, ddd, *J* = 17.2, 10.8, 6.4 Hz), 5.21 (1H, ddd, *J* = 17.2, 1.6, 1.6 Hz), 5.15 (1H, ddd, *J* = 10.8, 1.2, 1.2 Hz), 4.36 (1H, B of AB, J_{AB} = 17.2 Hz), 4.32 (1H, A of AB, J_{AB} = 17.6 Hz), 4.17 (1H, ddd, *J* = 5.2, 1.6, 1.6 Hz), 4.01 (1H, dd, *J* = 6.4, 6.4 Hz), 0.93 (9H, s), 0.90 (9H, s), 0.87 (9H, s), 0.09 (3H, s), 0.09 (3H, s), 0.05 (3H, s), 0.02 (3H, s), 0.01 (3H, s), 0.00 (3H, s). Diastereomeric ratio for the *E*-isomer was established by HPLC analysis of the enone in comparison with authentic racemic material (90:10 er). Since cross partner is enantiomerically pure (>98%:<2 er), diastereomeric purity of the *E* isomer of the DROCM product is determined to be 90:10 dr. Daicel Chiralpak AD (99.5:0.5 hexanes:2-propanol, 0.5 mL/min, 230 nm) was used.

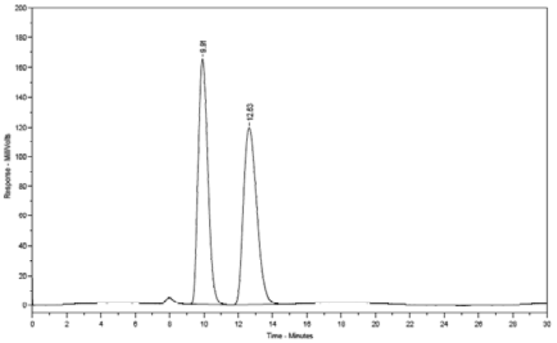

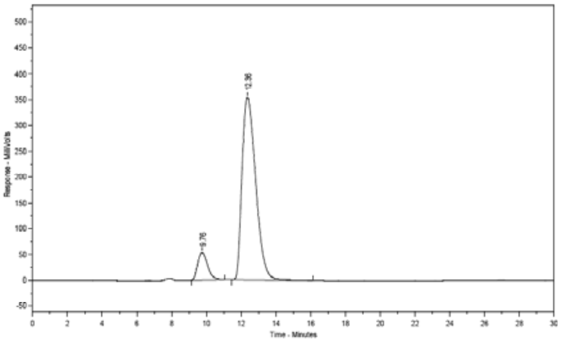

Peak #	Retention time (min)	Area	Area %	Peak #	Retention time (min)	Area	Area %
1	9.91	6442848	50.098	1	9.76	2099486	9.801
2	12.63	6417531	49.902	2	12.36	19322710	90.199

(5*R*,6*S*,*Z*)-5,6-Bis(*t*-butyldimethylsilyloxy)-1-(*t*-butyldimethylsilyloxy)octa-3,7-dien-2-one (from 2.210). This material was obtained through an identical procedure as described above. The desired enone was obtained in 78% yield as colorless oil. IR (neat): 2954 (m), 2929 (m), 2887 (w), 2857 (m), 1696 (w), 1623 (w), 1472 (m), 1463 (m), 1407 (w), 1389 (w), 1361 (w), 1252 (s), 1176 (w), 1102 (s), 1059 (s), 1004 (m), 958 (m), 938 (m), 921 (m), 832 (s), 774 (s), 669 (m), 477 (w) cm^{-1}; ^{1}H NMR (CDCl$_3$, 400 MHz): δ 6.36 (1H, dd, J = 11.6, 0.8 Hz), 6.03 (1H, dd, J = 11.6, 8.4 Hz), 5.85 (1H, ddd, J = 17.2, 10.4, 6.4 Hz), 5.29 (1H, ddd, J = 8.0, 3.2, 1.2 Hz), 5.11 (1H, ddd, J = 17.2, 1.6, 1.6 Hz), 5.06 (1H, ddd, J = 10.4, 1.2, 1.2 Hz), 4.24 (1H, B of AB, J_{AB} = 17.6 Hz), 4.17 (1H, A of AB, J_{AB} = 17.6 Hz), 4.14 (1H, dddd, J = 6.0, 3.2, 1.2, 1.2 Hz), 0.92 (9H, s), 0.89 (9H, s), 0.86 (9H, s), 0.11 (3H, s), 0.09 (6H, s), 0.04 (3H, s), 0.04 (3H, s), –0.02 (3H, s). At 22 °C, the resulting *Z* enone undergoes slow isomerization to the *E* enone, which is the *enantiomer* of the product obtained from oxidation of the corresponding *E* isomer; this process is accelerated in the presence of DMAP (0.2 equiv) in THF (0.5 M). The latter *E* enone isomer was subsequently separated from the enone of the *Z* isomer by silica gel chromatography, and was used to determine the diastereomeric purity of the *Z* isomer by HPLC analysis in comparison with authentic racemic material (82.5:17.5 er). Since enantiomeric purity of the starting allylic alcohol is >98:<2 er, the stereoselectivity of the DROCM reaction is measured to 82.5:17.5 dr. Daicel Chiralpak OD, 99.9:0.1 hexanes:2-propanol, 0.5 mL/min, 254 nm) used.

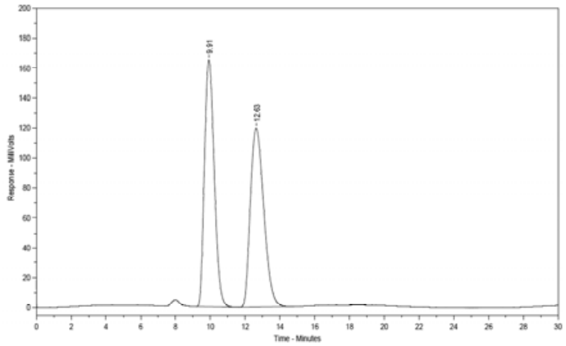

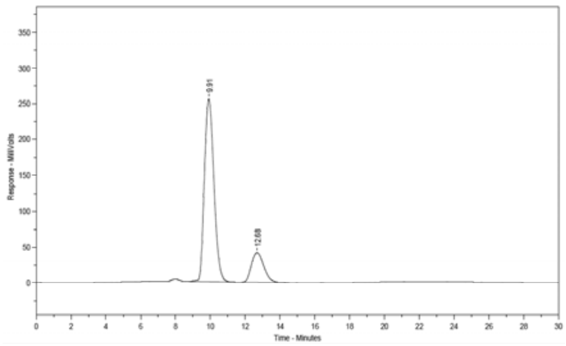

Peak #	Retention time (min)	Area	Area %	Peak #	Retention time (min)	Area	Area %
1	9.91	6442848	50.098	1	9.91	9736786	82.399
2	12.63	6417531	49.902	2	12.68	2079785	17.601

(2*S*,5*R*,6*S*,*E*)-5,6-Bis(*t*-butyldimethylsilyloxy)-2-phenylocta-3,7-diene (2.217) and (2*S*,5*S*,6R,*Z*)-5,6-bis(*t*-butyldimethylsilyloxy)-2-phenylocta-3,7-diene (2.218). This material was obtained through a similar procedure as described above; ~45% conversion is observed after 14 hours at 22 °C. The *E* isomer was isolated (15.4 mg, 0.0345 mmol, 21% yield) as colorless oil and the *Z* isomer (11.5 mg, 0.0257 mmol, 16% yield), also as colorless oil. In addition, *meso*-3,4-bis(*t*-butyldimethylsilyloxy)-hexa-1,5-diene (7.2 mg, 0.021 mmol, 13% yield) was isolated as a colorless oil. It should be noted that the *Z* isomer sample contains the dimer of (*S*)-3-phenyl-1-butene (13% wt); the yields shown are thus are corrected values.

***E* isomer.** IR (neat): 3028 (w), 2957 (m), 2928 (m), 2885 (w), 2856 (m), 1493 (w), 1472 (w), 1462 (w), 1404 (w), 1389 (w), 1251 (m), 1081 (m), 1031 (m), 1005 (m), 970 (m), 939 (m), 922 (m), 831 (s), 813 (m), 774 (s), 697 (s), 671 (m), 590 (w), 537 (w) cm^{-1}; ^{1}H NMR ($CDCl_3$, 400 MHz): δ 7.30-7.26 (2H, m), 7.21-7.16 (3H, m), 5.88-5.80 (1H, m), 5.76 (1H, dd, *J* = 15.6, 6.8 Hz), 5.47 (1H, ddd, *J* = 15.6, 6.4, 1.2 Hz), 5.18 (1H, dd, *J* = 17.2, 0.8 Hz), 5.10 (1H, dd, *J* = 10.4, 2.0 Hz), 3.92 (2H, m), 3.47 (1H, ddd, *J* = 6.4, 6.4, 6.4 Hz), 1.36 (3H, d, *J* = 7.2 Hz), 0.89 (9H, s), 0.84 (9H, s), 0.02 (3H, s), 0.00 (3H, s), -0.01 (3H, s), -0.06 (3H, s). ^{13}C NMR ($CDCl_3$, 100 MHz): δ 145.8, 139.4, 136.8, 136.6, 133.9, 129.9, 128.5, 128.4, 127.5, 127.4, 126.1, 115.6, 78.2, 77.6, 42.2, 26.1, 26.0, 21.7, 21.3, 18.4, –4.1, –4.2, –4.4; HRMS (ESI+): Calcd for $C_{26}H_{46}O_2Si_2Na$ $(M+Na)^+$: 469.2934. Found: 469.2917. *Meso* byproduct: ^{1}H NMR ($CDCl_3$, 400 MHz): δ 5.89-5.81

(2H, m), 5.19 (2H, ddd, *J* = 17.2, 1.6, 0.8 Hz), 5.11 (2H, ddd, *J* = 10.4, 2.0, 0.8 Hz), 3.96-3.92 (2H, m), 0.88 (18H, s), 0.04 (6H, s), 0.01 (6H, s).

***Z* isomer.** IR (neat): 3063 (w), 3027 (w), 2957 (m), 2928 (m), 2886 (w), 2856 (m), 1602 (w), 1493 (w), 1472 (w), 1462 (w), 1452 (w), 1405 (w), 1389 (w), 1361 (w), 1251 (m), 1076 (s), 1005 (m), 992 (m), 962 (w), 938 (m), 922 (m), 832 (s), 774 (s), 758 (m), 697 (s), 670 (s), 535 (w) cm^{-1}; ^{1}H NMR (CDCl$_3$, 400 MHz): δ 7.32-7.27 (3H, m, *Z* isomer + *dimer*), 7.24-7.26 (5H, m, *Z* isomer + dimer), 5.89 (1H, ddd, *J* = 16.8, 10.4, 6.4 Hz), 5.68 (0.58H, m, *dimer*), 5.64 (1H, ddd, *J* = 11.2, 10.4, 0.8 Hz), 5.32 (1H, ddd, *J* = 11.2, 9.2, 0.8 Hz), 5.21 (1H, ddd, *J* = 17.2, 1.6, 1.6 Hz), 5.15 (1H, ddd, *J* = 10.8, 2.0, 1.2 Hz), 4.39 (1H, ddd, *J* = 8.8, 4.4, 0.8 Hz), 4.00 (1H, dddd, *J* = 6.4, 4.8, 0.8, 0.8 Hz), 3.71 (1H, dq, *J* = 10.0, 2.8 Hz), 3.46 (0.54H, m, *dimer*), 1.35 (1.99H, d, *J* = 7.2 Hz, *dimer*), 1.33 (3H, d, *J* = 7.2 Hz), 0.92 (9H, s), 0.80 (9H, s), 0.08 (3H, s), 0.05 (3H, s), -0.10 (3H, s), -0.18 (3H, s); ^{13}C NMR (CDCl$_3$, 100 MHz): δ 146.3, 139.0, 135.2, 133.9, 130.1, 128.6, 128.5, 127.3, 127.1, 126.2, 115.9, 78.7, 73.0, 42.3, 38.1, 26.2, 26.0, 23.7, 21.7, 18.5, 18.3, –4.2, –4.3, –4.4, –4.6; HRMS (ESI+): Calcd for $C_{26}H_{46}O_2Si_2Na$ $[M+Na]^+$: 469.2934. Found: 469.2948. Diastereomeric ratios were determined by HPLC analysis of the derived mono-benzoate alcohols (below).

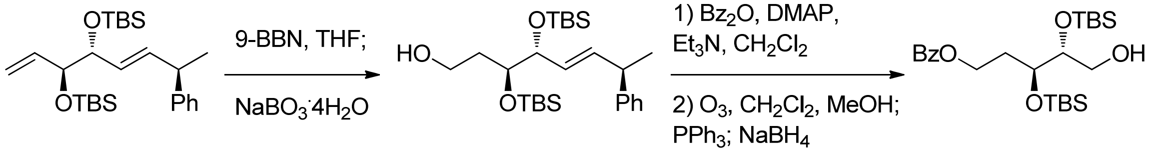

Preparation of the benzoate-alcohol derivative from DROCM *E* product isomer. Hydroboration with 9-BBN was performed under standard procedures to afford the desired primary alcohol as a colorless oil. ^{1}H NMR (CDCl$_3$, 400 MHz): δ 7.31-7.27 (2H, m), 7.21-7.17 (3H, m), 5.76 (1H, dd, *J* = 15.6, 6.4 Hz), 5.40 (1H, ddd, *J* = 15.6, 7.6, 1.6 Hz), 4.09 (1H, dd, *J* = 7.2, 4.4 Hz), 3.79-3.73 (3H, m), 3.50-3.43 (1H, m), 2.63 (1H, br s), 1.91-1.69 (2H, m), 0.89 (9H, s), 0.85 (9H, s), 0.07 (3H, s), 0.05 (3H, s), 0.02 (3H, s), –0.05 (3H, s). The derived benzoate was then obtained as colorless oil. ^{1}H NMR (CDCl$_3$, 400 MHz): δ 8.04-8.02 (2H, m), 7.56 (1H, dt, *J* = 7.2, 1.2 Hz), 7.46-7.42 (2H, m), 7.30-

7.25 (2H, m), 7.20-7.15 (3H, m), 5.76 (1H, ddd, *J* = 15.6, 6.4, 0.8 Hz), 5.44 (1H, ddd, *J* = 15.6, 6.8, 1.2 Hz), 4.47 (1H, ddd, *J* = 10.8, 6.8, 5.2 Hz), 4.34 (1H, ddd, *J* = 10.4, 8.0, 6.4 Hz), 4.04 (1H, dd, *J* = 6.4, 2.4 Hz), 3.83-3.80 (1H, m), 3.50-3.45 (1H, m), 1.98-1.84 (2H, m), 1.36 (3H, d, *J* = 7.2 Hz), 0.89 (9H, s), 0.86 (9H, s), 0.06 (3H, s), 0.05 (3H, s), 0.02 (3H, s), –0.05 (3H, s). Standard ozonolysis delivered the material to be used for determination of diastereoselectivity levels (benzoate-alcohol) as colorless oil. ^{1}H NMR ($CDCl_3$, 400 MHz): δ 8.05-8.02 (2H, m), 7.56 (1H, dt, *J* = 7.6, 1.2 Hz), 7.47-7.42 (2H, m), 4.46 (1H, ddd, *J* = 11.2, 7.2, 5.2 Hz), 4.37 (1H, ddd, *J* = 10.8, 8.0, 6.8 Hz), 3.97 (1H, ddd, *J* = 6.8, 4.4, 4.4 Hz), 3.73-3.68 (2H, m), 3.66-3.60 (1H, m), 2.09-1.93 (3H, m), 0.91 (9H, s), 0.91 (9H, s), 0.13 (3H, s), 0.12 (3H, s), 0.11 (3H, s), 0.09 (3H, s). Diastereomeric ratio for the DROCM *E* product isomer was established by HPLC analysis in comparison with authentic racemic material (74.5:25.5 er). After correction for enantiomeric purity of the cross partner (94:6 er), diastereoselectivity of DROCM reaction is determined to be 80:20 dr. Daicel Chiralpak OD (99.6:0.4 hexanes:2-propanol, 0.5 mL/min, 230 nm) was used.

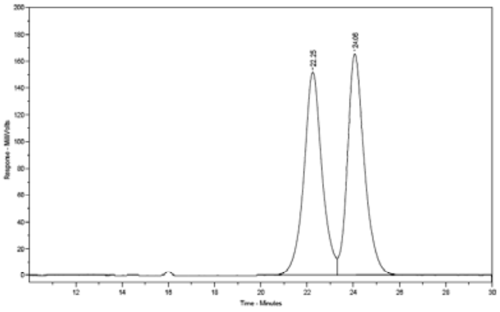

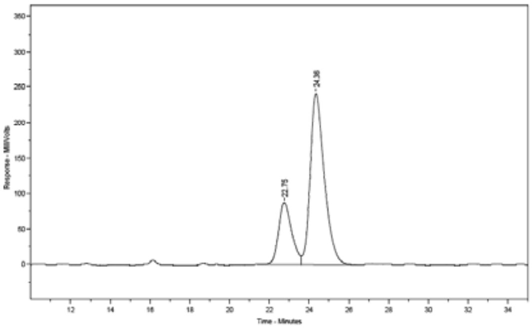

Peak #	Retention time (min)	Area	Area %	Peak #	Retention time (min)	Area	Area %
1	22.25	8277736	49.740	1	22.75	4036806	25.384
2	24.06	8364210	50.260	2	24.36	11866230	74.616

Preparation of the benzoate-alcohol derivative from DROCM *Z* product isomer. Hydroboration with 9-BBN was performed under standard procedures to afford the desired primary alcohol as a colorless oil. ^{1}H NMR ($CDCl_3$, 400 MHz): δ 7.32-7.27 (2H, m), 7.23-7.18 (3H, m), 5.63 (1H, ddd, *J* = 10.8, 10.8, 1.2 Hz), 5.37 (1H, ddd, *J* = 10.8, 8.4, 0.8 Hz), 4.59 (1H, ddd, *J* = 8.4, 3.6, 1.2 Hz), 3.86-3.80 (2H, m), 3.72-3.64 (1H, m), 3.06 (1H, dd, J = 7.6, 4.4 Hz), 1.97-1.73 (2H, m), 1.34 (3H, d, J = 7.2 Hz), 0.93 (9H, s), 0.82 (9H, s), 0.14 (3H, s), 0.12 (3H, s), -0.06 (3H, s), –0.13 (3H, s). The derived benzoate was obtained as colorless oil. ^{1}H NMR ($CDCl_3$, 400 MHz): δ 8.06-8.03 (2H, m), 7.56 (1H, tt, J = 8.0, 1.2 Hz), 7.47-7.42 (2H, m), 7.32-7.26 (2H, m), 7.23-7.19 (3H, m), 5.63 (1H, ddd, J = 11.2, 10.0, 1.2 Hz), 5.35 (1H, ddd, J = 11.2, 8.8, 1.2 Hz), 4.57-4.51 (2H, m), 4.42-4.36 (1H, m), 2.08-1.94 (2H, m), 1.33 (3H, d, J = 7.2 Hz), 0.93 (9H, s), 0.83 (9H, s), 0.14 (3H, s), 0.09 (3H, s), –0.08 (3H, s), –0.13 (3H, s). As before, ozonolysis delivered the benzoate-alcohol. ^{1}H NMR was identical to the material prepared starting with the corresponding *E* product isomer (see above). Diastereomeric ratio was established by HPLC analysis in comparison with authentic racemic material (89:11 er). After correction for enantiomeric purity of the cross partner (94:6 er) diastereoselectivity of the DROCM reaction was determined as 95:5 dr. Daicel Chiralpak OD, 99.6:0.4 hexanes:2-propanol, 0.5 mL/min, 230 nm) used.

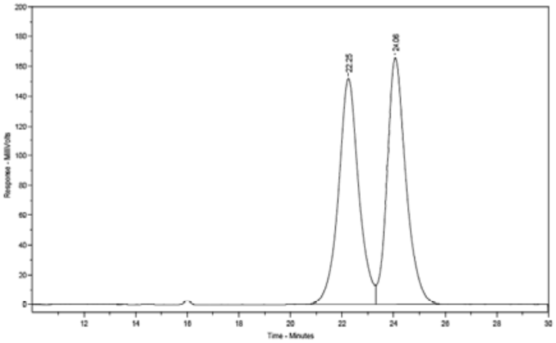

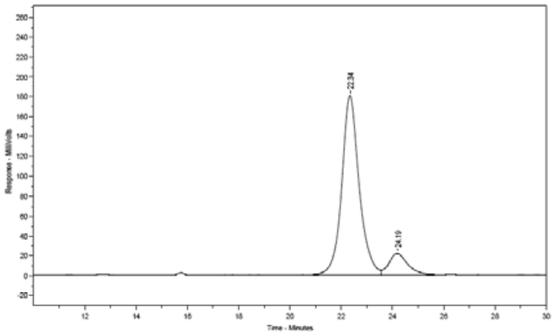

Peak #	Retention time (min)	Area	Area %	Peak #	Retention time (min)	Area	Area %
1	22.25	8277736	49.740	1	22.34	8451044	88.800
2	24.06	8364210	50.260	2	24.19	1065920	11.200

■ Reaction of a Diazabicyclic alkene

(3*S*,5*R*)-Diethyl 3-((*R*,*E*)-3-hydroxy-3-phenylprop-1-enyl)-5-vinylpyrazolidine-1,2-dicarboxylate (2.211) and (3*R*,5*S*)-diethyl 3-((*R*,*Z*)-3-hydroxy-3-phenylprop-1-enyl)-5-vinylpyrazolidine-1,2-dicarboxylate (2.212). The same procedure as used for reactions of cyclobutenes (Part 2) was used, except the reaction was allowed to proceed for 2.5 h. Silica gel chromatography (15% EtOAc in hexanes) of the unpurified tan oily residue afforded **2.211** (pale yellow oil, 17.1 mg, 0.046 mmol, 46% yield) and **2.212** (pale yellow oil, 9.9 mg, 0.024 mmol, 27% yield). It should be noted that **2.212** was isolated as an inseparable mixture of the desired product and small amount of cross partner dimer (~7%, yields shown above are corrected for the presence of dimer).

***E* isomer (2.211).** IR(neat): 3442 (br w), 2982 (w), 2933 (w), 2871 (w), 1706 (s), 1467 (m), 1450 (m), 1411 (m), 1378 (m), 1303 (m), 1277 (m), 1176 (m), 1130 (m), 1071 (m), 1032 (m), 926 (m), 754 (m), 701 (m) cm^{-1}; ^1H NMR ($CDCl_3$, 400 MHz): δ 7.35-7.22 (5H, m), 5.94-5.91 (1H, m), 5.84-5.76 (2H, m), 5.30 (1H, br d, J = 17.6 Hz), 5.20 (1H, d, J = 6.0 Hz), 5.11 (1H, d, J = 10.4 Hz), 4.55 (2H, br s), 4.20-4.12 (4H, m), 2.50 (1H, apparent ddd, J = 12.8, 8.8, 8.4 Hz), 1.86 (1H, apparent ddd, J = 12.8, 4.0, 3.6 Hz), 1.26-1.20 (6H, m); ^{13}C NMR ($CDCl_3$, 100 MHz): δ 156.1 (br), 142.7, 136.8, 134.0, 129.5, 128.7, 127.9, 126.4, 116.1, 74.3, 62.4, 60.9, 59.9, 40.2, 14.6, 14.6; HRMS (ESI+): Calcd for $C_{20}H_{25}N_2O_4$ $[M\text{-}OH]^+$: 357.18143; Found: 357.18211.

***Z* isomer (2.212).** IR (neat): 3431 (br m), 3063 (w), 2982 (m), 2933 (m), 1801 (w), 1685 (s), 1603 (w), 1467 (m), 1425 (m), 1379 (m), 1346 (m), 1301 (s), 1274 (s), 1176 (m), 1130 (m), 1032 (m), 749 (m), 700 (m) cm^{-1}; ^1H NMR ($CDCl_3$, 400 MHz): δ 7.42-7.24 (5H, m), 5.86 (1H, br s), 5.80-5.75 (1H, m), 5.70-5.68 (1H, m), 5.48-5.39 (2H, m), 5.20 (1H, dd, J = 10.4, 1.6 Hz), 5.07 (1H, app t, J = 8.8 Hz), 4.76 (1H, br s), 4.27-4.18 (4H, m), 2.51 (1H, apparent ddd, J = 12.8, 8.8, 8.4 Hz), 1.89 (1H, apparent ddd, J = 13.2, 2.4, 2.8 Hz), 1.31-1.27 (6H, m). ^{13}C NMR ($CDCl_3$, 100 MHz): δ 157.6 (br), 143.0, 135.8, 133.3, 129.5, 128.7, 128.6, 127.9, 126.2, 116.41, 74.5, 63.1, 62.5, 61.2, 54.4, 39.2, 14.7, 14.6;□ HRMS (ESI+): Calcd for $C_{20}H_{25}N_2O_4$ $[M\text{-}OH]^+$: 357.18143; Found: 357.18268. Diastereomeric ratios were determined by HPLC analysis of the derived enones (below).

(3*S*,5*R*)-Diethyl 3-((*E*)-3-oxo-3-phenylprop-1-enyl)-5-vinylpyrazolidine-1,2-dicarboxylate (enone derived from 2.211). This material was obtained through oxidation with MnO_2 as described above. The desired a,*b*-unsaturated ketone was isolated in 87% yield (pale yellow oil). IR (neat): 2958 (w), 2924 (w), 2853 (w), 1708 (s), 1672 (m), 1626 (m), 1597 (w), 1579 (w), 1465 (w), 1458 (w), 1408 (m), 1375 (m), 1287 (s), 1271 (s), 1217 (m), 1176 (m), 1132 (m), 1016 (w), 929 (m), 755 (w), 699 (m) cm^{-1}; ^{1}H NMR (CDCl$_3$, 400 MHz): δ 8.01-7.96 (2H, m), 7.78-7.10 (4H, m), 6.93 (1H, dd, *J* = 15.2, 5.6 Hz), 5.78 (1H, ddd, *J* = 16.9, 10.2, 7.2 Hz), 5.33-5.21 (1H, m), 5.15 (1H, d, *J* = 10.4 Hz), 4.88 (1H, app s), 4.60 (1H, app s), 4.22 (4H, q, *J* = 7.2 Hz), 2.65 (1H, apparent ddd, *J* = 12.8, 8.8, 8.8 Hz), 2.01 (1H, apparent ddd, *J* = 12.8, 3.6, 3.6 Hz), 1.30-1.25 (6H, m). Diastereomeric ratio was established by HPLC analysis of the enone in comparison with authentic racemic material (95:5 er). After correction for enantiomeric purity of the allylic alcohol substrate (95.5:4.5 er), stereoselectivity of the DROCM process was determined to be >98:<2 dr. Daicel Chiralpak OD (95:5 hexanes:2-propanol, 0.8 mL/min, 220 nm) was used.

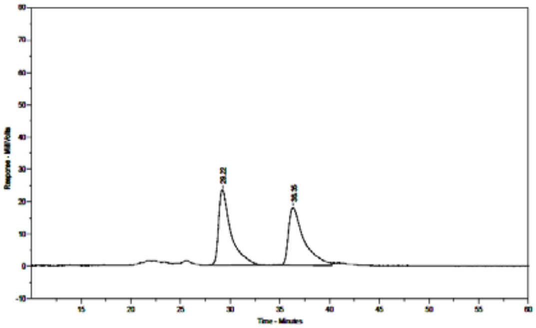

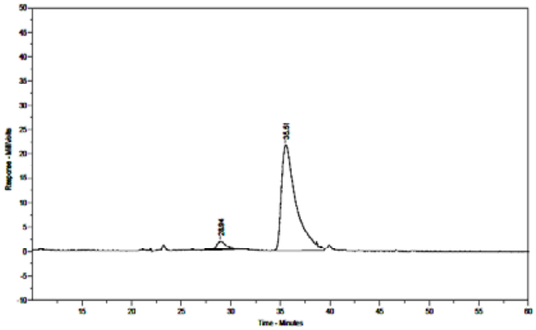

Peak #	Retention time (min)	Area	Area %	Peak #	Retention time (min)	Area	Area %
1	29.22	2001516	50.932	1	28.94	114952	4.921
2	36.35	1928243	49.068	2	35.51	2220889	95.079

(3*R*,5*S*)-Diethyl 3-((*Z*)-3-oxo-3-phenylprop-1-enyl)-5-vinylpyrazolidine-1,2-dicarboxylate (enone derived from 2.212). This material was obtained through oxidation with MnO$_2$ as described above. The desired a,*b*-unsaturated ketone was isolated in 53% yield (pale yellow oil). IR (neat): 2981 (w), 2959 (w), 2924 (w), 2854 (w), 1699 (s), 1665 (m), 1610 (m), 1579 (w), 1466 (m), 1448 (m), 1410 (m), 1376 (m), 1346 (m), 1298 (m), 1269 (m), 1230 (s), 1175 (m), 1133 (m), 1052 (m), 744 (m), 692 (m) cm^{-1}; ^{1}H NMR (CDCl$_3$, 400 MHz): δ 7.95-7.93 (2H, m), 7.59-7.55 (1H m), 7.49-7.46

(2H, m), 6.88 (1H, d, *J* = 11.6 Hz), 6.48 (1H, dd, *J* = 11.6, 8.0 Hz), 5.85-5.77 (1H, m), 5.43-5.40 (2H, m), 5.19 (1H, d, *J* = 10.8 Hz), 4.76 (1H, app s), 4.26-4.16 (4H, m), 2.89 (1H, apparent ddd, *J* = 13.2, 9.6, 8.0 Hz), 1.99 (1H, apparent ddd, *J* = 13.2, 3.0, 3.0 Hz), 1.30-1.23 (6H, m). Diastereomeric ratio was established by HPLC analysis of the corresponding enone in comparison with authentic racemic material (95.5:4.5 er). After correction for enantiomeric purity of the allylic alcohol substrate (95.5:4.5 er), diastereoselectivity of the DROCM reaction was determined to be >98:<2 dr. Chiralpak OD (95:5 hexanes:2-propanol, 0.8 mL/min, 220 nm) was used.

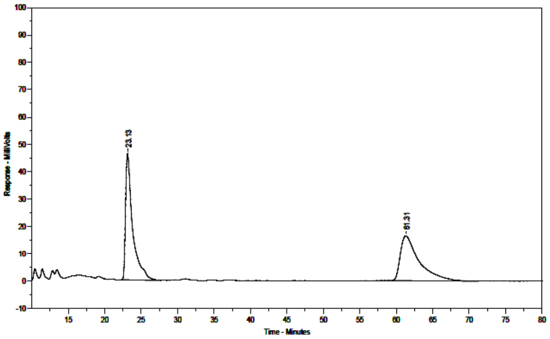

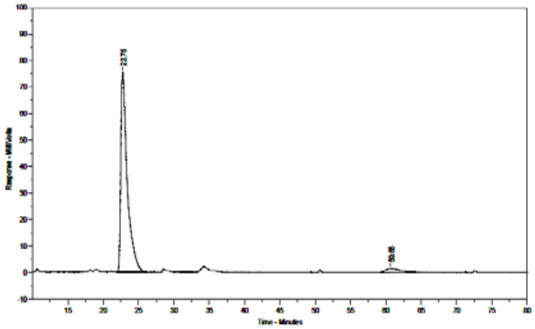

Peak #	Retention time (min)	Area	Area %	Peak #	Retention time (min)	Area	Area %
1	23.13	3145523	51.658	1	22.75	4800593	95.594
2	61.31	2943654	48.342	2	60.68	221260	4.406

■ Proof of Stereochemical Identities of Products

Please note: The stereochemical identities suggested for products other than those explicitly discussed in this section, are by inference.

Stereochemical identities of Ru-catalyzed DROCM reactions with Cyclopropenes

A. Synthesis of authentic materials for comparison with DROCM products. To determine the absolute stereochemistry of the DROCM products involving cyclopropenes, first a number of authentic materials with established stereochemical identity were prepared.

a. Synthesis of enantiomerically enriched ketone a

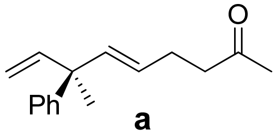

a

(7*S*,*E*)-7-Methyl-7-phenylnona-5,8-dien-2-one (a). This material, formed in 7:1 *E*:*Z* selectivity and 88:12 er (***S* enantiomer is major**; see below for X-ray analysis), was prepared through enantioselective Ru-catalyzed ROCM reaction of *g*,*d*-unsaturated ketone and cyclopropene **2.182**.[125] ^{1}H-NMR ($CDCl_3$, 400 MHz): δ 7.37-7.28 (*E*/*Z*, 4H, m), 7.24-7.17 (*E*/*Z*, 1H, m), 6.20 (*Z*, 1H, dd, *J* = 17.2, 10.4 Hz), 6.05 (*E*, 1H, dd, *J* = 17.2, 10.4 Hz), 5.66 (*Z*, 1H, dt, *J* = 11.6, 1.6 Hz) 5.71 (*E*, 1H, d, *J* = 16 Hz), 5.44-5.36 (*E*, 1H, m), 5.38-5.33(*Z*, 1H, overlapping m), 5.13 (*Z*, 1H, d, *J* = 10.4 Hz), 5.11 (*E*, 1H, dd, *J* = 10.6, 1.0 Hz), 5.06 (*Z*, 1H, d, *J* = 17.2), 4.99 (*E*, 1H, dd, *J* = 17.2, 1.2 Hz), 2.54 (*E*/*Z*, 2H, t, *J* = 7.4 Hz), 2.36 (*E*/*Z*, 2H, q, *J* = 7.2 Hz), 2.14 (*E*, 3H, s), 1.97 (*Z*, 3H, s), 1.46 (*E*, 3H, s), 1.51 (*Z*, 3H, s).

b. Synthesis of enantiomerically enriched hydrazone b. Hydrazone **b** (Scheme S-1) was synthesized from ketone **a**, as illustrated in Scheme S-1.[126] Ketone **a** (5.0 mg, 0.023 mmol) and *p*-toluenesulfonylhydrazide (5.0 mg, 0.027 mmol, 1.2 equiv) in 1.0 mL anhydrous THF. Purification of the resulting yellow solid by silica gel chromatography (100 % CH_2Cl_2), afforded **b** (9.2 mg, 0.023 mmol, >98% yield) as a yellow crystalline solid. The material was recrystallized from CH_2Cl_2/pentane, affording clear, colorless crystals, which were analyzed by X-ray crystallography (see Scheme S-1). ^{1}H-NMR ($CDCl_3$, 400 MHz): δ 7.86-7.80 (*E*/*Z*, 2H, m), 7.24-7.17 (*E*/*Z*, 8H, m), 6.13 (*Z*, 1H, dd, *J* = 17.2, 10.8 Hz), 5.87 (*E*, 1H, dd, *J* = 17.6, 10.8 Hz), 5.59 (*E*, 1H, d, *J* = 15.6 Hz), 5.53

---

[125] Details to be presented in a separate account. See: Giudici, R. E.; Hoveyda, A. H. *J. Am. Chem. Soc.* **2007**, *129*, 3824–3825.

[126] Bertz, S. H.; Dabbagh, G. *J. Org. Chem.* **1983**, *48*, 116–119.

(Z, 1H, dt, J = 11.2, 1.2 Hz), 5.35-5.28 (E, 1H, m), 5.27-5.20 (Z, 1H, m), 5.11 (Z, 1H, dd, J = 10.8, 1.2 Hz), 5.08 (E, 1H, dd, J = 10.4, 1.2 Hz), 5.00 (Z, 1H, dd, J = 17.6, 1.2 Hz), 4.94 (E, 1H, dd, J = 17.2, 1.2 Hz), 2.43 (Z, 3H, s), 2.39 (E, 3H, s), 2.27-2.21 (E/Z, 2H, m) 1.90 (Z, 3H, s), 1.75 (E, 3H, s), 1.47-1.43 (E/Z, 2H, m), 1.40 (Z, 3H, s), 1.38 (E, 3H, s).

Scheme S-1

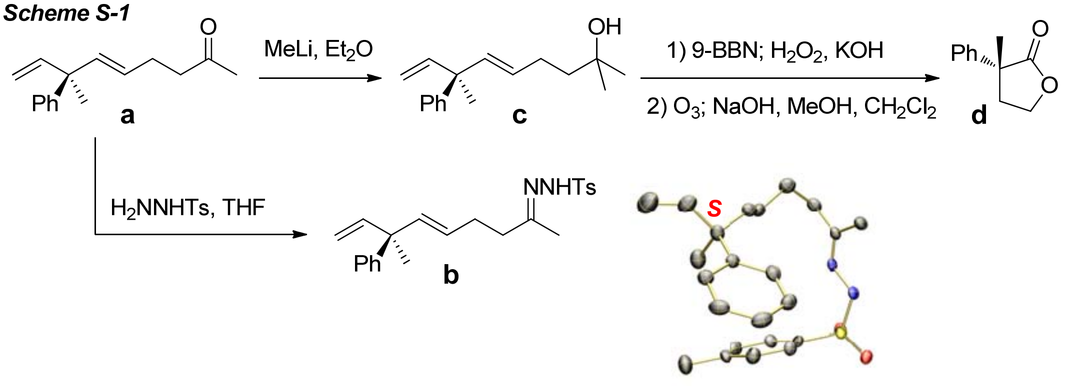

*X-ray of **b***

As illustrated in Scheme S-1, ketone **a** was also converted to lactone **d**. Thus, ketone **a** (25.7 mg, 0.113 mmol) was placed in an oven-dried vial containing a stir bar, and 2.0 mL anhydrous Et$_2$O was added, followed by 0.150 mL of a 1.6 M solution of MeLi (in Et$_2$O, 0.226 mmol). The resulting mixture was allowed to stir for 12 h at 22 °C. The reaction was quenched by addition of water at 0 °C. After addition of 1M solution of HCl (20 mL), the mixture was washed with CH$_2$Cl$_2$ (5 x 20mL). The combined organic layers were dried over anhydrous MgSO$_4$, and the volatiles were removed *in vacuo*. The resulting yellow oil was purified by silica gel chromatography (20% Et$_2$O in hexanes), affording alcohol **c** (21.8 mg, 0.089 mmol, 79% yield) as a yellow oil as a 4:1 E:Z mixture of alkene isomers. ^{1}H NMR (CDCl$_3$, 400 MHz): δ 7.40-7.27 (E/Z, 4H, m), 7.22-7.16 (E/Z, 1H, m), 6.22 (Z, 1H, dd, J = 17.6, 10.4 Hz), 6.06 (E, 1H, dd, J = 17.2, 10.4 Hz), 5.72 (E, 1H, dt, J = 15.6, 1.4 Hz) 5.65 (Z, 1H, dt, J = 11.2, 1.2 Hz), 5.44 (E, 1H, overlapping dt, J = 15.6, 6.8 Hz), 5.44-5.37 (Z, 1H, overlapping m), 5.12 (E/Z, 1H, d, J = 10.4, 1.2 Hz), 5.06 (Z, 1H, dd, J = 17.6, 1.2 Hz), 5.01 (E, 1H, d, J = 17.6, 1.2 Hz), 2.21-2.15 (E/Z, 2H, m), 1.72 (Z, 2H, q, J = 8.6 Hz), 1.61-1.56 (E, 2H, m), 1.51 (Z, 3H, s), 1.47 (E, 3H, s), 1.23 (E, 6H, s), 0.96 (Z, 6H, s). Alcohol **c** was converted to **d** following a standard hydroboration/oxidative ozonolysis procedure. The spectral data for **d** match the values reported previously.**Error! Bookmark not defined.**

c. Synthesis of enantiomerically enriched alcohol f. Enantiomerically enriched DROCM product **2.186** was converted to terminal carbinol **f**, as illustrated in Scheme S-2.

Scheme S-2

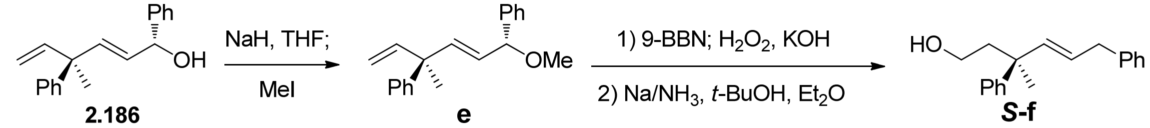

B. Determination of the absolute stereochemical identity of DROCM products with cyclopropene substrates. With the required authentic materials in hand, we determined the absolute stereochemistry of the products of Ru-catalyzed DROM reactions with cyclopropenes in the manner described below.

a. Absolute stereochemical identities of DROCM products 2.186 and 2.188. As detailed in Scheme S-3, the absolute stereochemical identity of DROCM products **2.186** and **2.188** was determined by comparison of the HPLC retention times for the lactones **d** (see Scheme S-1) derived from enantiomerically enriched **2.186** and **2.188** (obtained from catalytic DROCM reactions). The authentic enantiomerically enriched lactone **d** is that obtained from ketone **a** (Scheme S-1); the absolute stereochemistry of this material was established by X-ray crystallography (*S* enantiomer; Scheme S-1). Accordingly, the absolute configuration of **2.186** is (1*R*,4*S*), and that of **2.188** is (1*S*,4*S*).

Scheme S-3. Determination of Absolute Stereochemistry of Products **2.186** and **2.188**

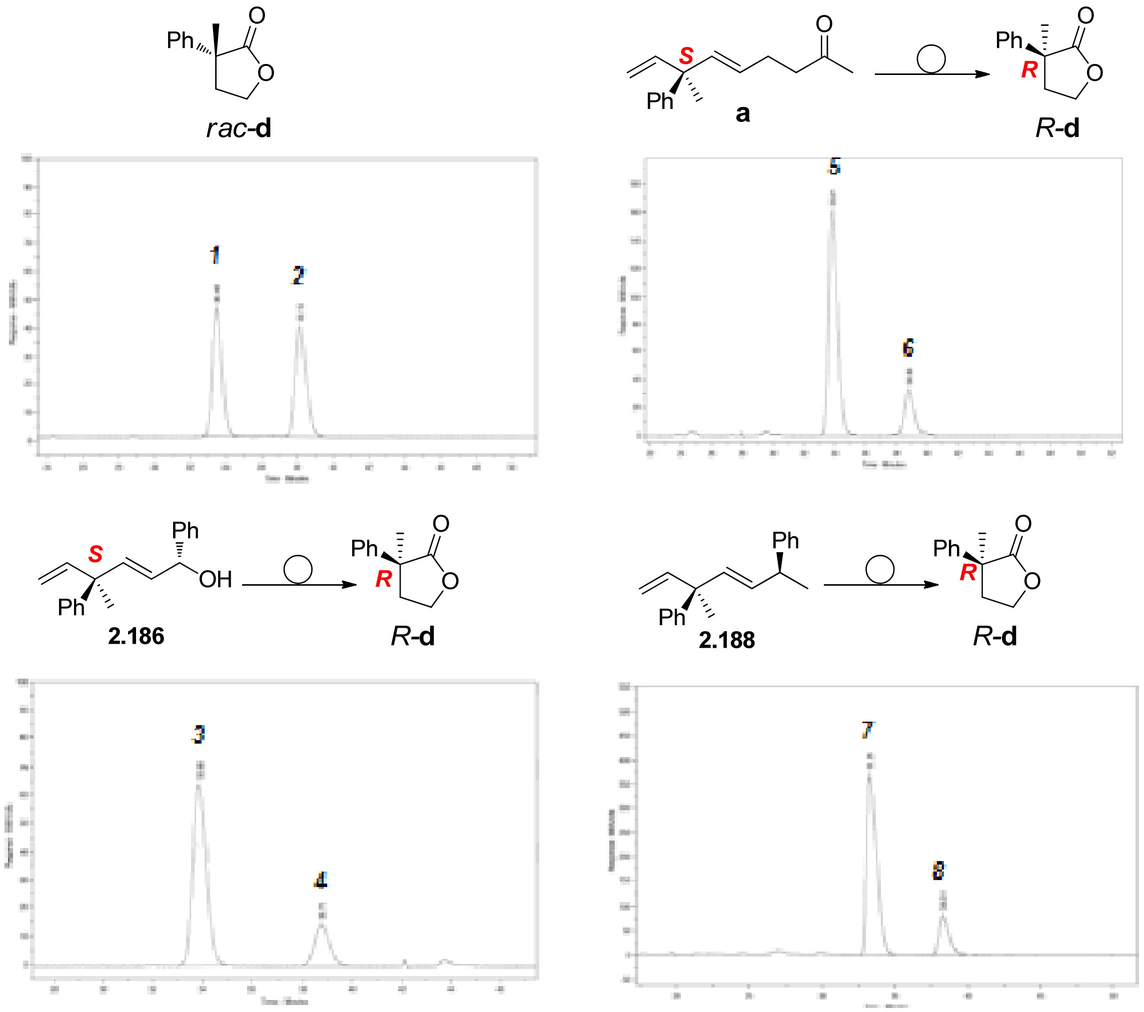

Peak #	Retention time (min)	Area	Area %	Peak #	Retention time (min)	Area	Area %
1 (*rac*-**d)**	33.48	1695685	50.009	5 (*R*-**d**)	33.86	2427155	80.206
2 (*rac*-**d)**	38.15	1695055	49.991	6 (*R*-**d**)	38.75	598990	19.794
3 (*R*-**d**)	33.81	6490434	81.695	7 (*R*-**d**)	33.25	17985270	82.328
4 (*R*-**d**)	38.80	1454327	18.305	8 (*R*-**d**)	38.31	3860550	17.672

Please note: Whereas the *R* enantiomer of allylic alcohol **2.185** was used, it was the *S* enantiomer of 3-phenyl-1-butene that was utilized. Thus, although the analysis presented herein points to formation of identical lactone enantiomers, the sense of stereochemical induction in the DROCM reactions of these two cross partners with cyclopropene **2.182** is *opposite*.

b. Absolute stereochemical identity of DROCM product 2.187. As detailed in Scheme S-4, the absolute stereochemical identity of methyl ether **2.187** was determined by comparison of the HPLC retention times for alcohol **f** derived from **2.187** with the same derivative derived from **2.186**. Accordingly, the absolute configuration for methyl ether **2.187** is (1*R*, 4*R*) [vs (1*R*, 4*S*) for **2.186**].

Scheme S-4. Determination of Absolute Stereochemistry of Product **2.187**

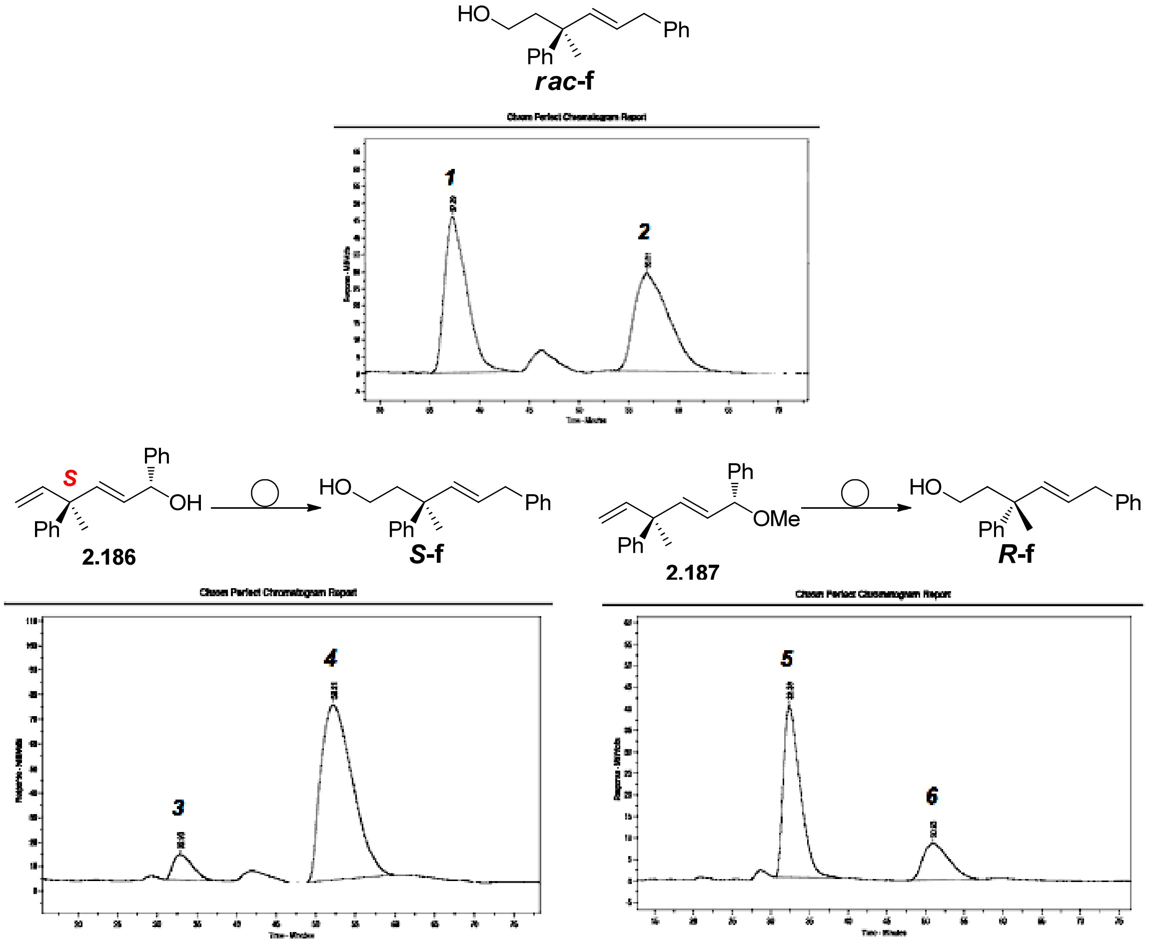

Peak #	Retention time (min)	Area	Area %	Peak #	Retention time (min)	Area	Area %
1 (*rac*-**f**)	37.29	7085191	50.395	3 (*S*-**f**)	32.93	1700050	7.829

2 (*rac*-**f**)	56.81	6974189	49.605	4 (*S*-**f**)	52.21	20015280	92.171
				5 (*R*-**f**)	32.38	6015720	75.473
				6 (*R*-**f**)	50.93	1954920	24.527

■ Stereochemical identities of Ru-catalyzed DROCM reactions with Cyclobutenes

Absolute stereochemical identity of **2.205** was established by X-ray crystallography (CuKα radiation source); see below for all details.

The stereochemical identity of DROM product **2.206** was established, as illustrated in Scheme S-5, through correlation with the enone and a carbinol derived from **2.205**.

Scheme S-4. Determination of Absolute Stereochemistry of Products **14** and **15**

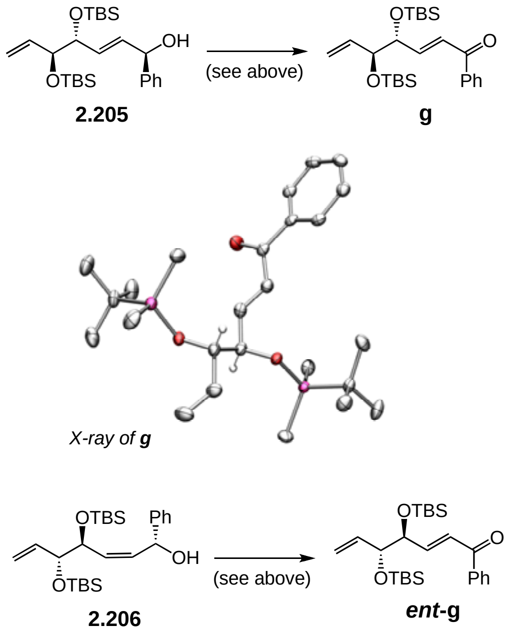

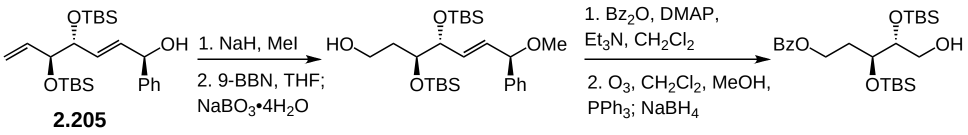

Determination of the identity of major diastereomers formed in DROCM reaction of cyclobutene 2.203 with *(S)*-3-phenyl-1-butene. The sequence illustrated above was carried out, starting from DROCM product **2.205**, the stereochemical identity of which is established by X-ray crystallography. Comparison of the stereochemical identity of the benzoate-alcohol obtained from **2.205** to that derived from the product of the reaction of cyclobutene and 3-phenyl-1-butene allowed us to establish that the latter process proceeds with *opposite* sense of stereochemical control. Methyl ether obtained as colorless oil. ^{1}H NMR (CDCl$_3$, 400 MHz): δ 7.35-7.30 (4H, m), 7.27-7.24 (1H, m), 5.81 (1H, ddd, J = 16.8, 10.4, 6.0 Hz), 5.81-5.69 (2H, m), 5.16 (1H, ddd, J = 17.2, 1.2, 1.2 Hz), 5.09 (1H, ddd, J = 10.4, 1.6, 0.4 Hz), 4.62 (1H, d, J = 6.0 Hz), 4.01-3.96 (2H, m), 3.34 (3H, s), 0.89 (9H, s), 0.86 (9H, s), 0.02 (3H, s), 0.00 (6H, s), –0.04 (3H, s); ^{13}C NMR (CDCl$_3$, 100 MHz): δ 141.4, 139.0, 133.0, 131.8, 128.4, 127.6, 127.0, 115.9, 84.1, 78.3, 76.9, 56.6, 26.0, 18.4, –4.2, –4.3, –4.48, –4.53. The hydroboration product was obtained as colorless oil. ^{1}H NMR (CDCl$_3$, 400 MHz): δ 7.36-7.24 (5H, m), 5.77-5.66 (2H, m), 4.62 (1H, d, J = 5.6 Hz), 4.14 (1H, dd, J = 5.6, 3.6 Hz), 3.80-3.65 (3H, m), 3.32 (3H, s), 1.91-1.52 (3H, m), 0.88 (9H, s), 0.87 (9H, s), 0.06 (3H, s), 0.05 (3H, s), 0.04 (3H, s), 0.00 (3H, s). The desired benzoate was obtained as a light yellow oil. ^{1}H NMR (CDCl$_3$, 400 MHz): δ 8.18-8.16 (1H, m), 8.03-8.01 (2H, m), 7.58-7.52 (2H, m), 7.46-7.42 (2H, m), 7.32-7.23 (3H, m), 5.74-5.73 (2H, m), 4.65-4.64 (1H, m), 4.44 (1H, ddd, J = 11.2, 6.8, 5.2 Hz), 4.32 (1H, ddd, J = 11.2, 8.4, 6.4 Hz), 4.12-4.10 (1H, m), 3.87-3.83 (1H, m), 3.33 (3H, s), 1.92-1.81 (2H, m), 0.88 (9H, s), 0.88 (9H, s), 0.06 (3H, s), 0.05 (3H, s), 0.04 (3H, s), –0.01 (3H, s). The final alcohol was isolated as colorless oil. Spectral data are identical to the material prepared before (see above).

The stereochemical identity was established by HPLC analysis in comparison with authentic racemic material (96:4 er). After correction for enantiomeric purity of the allylic alcohol substrate (97:3 er) diastereoselectivity was determined as >98:<2 dr. Daicel Chiralpak OD, 99.6:0.4 hexanes:2-propanol, 0.5 mL/min, 230 nm) used.

Please note: Whereas the *R* enantiomer of allylic alcohol **2.185** was used, it was (*S)*-3-phenyl-1-butene that was utilized. Thus, although the analysis presented herein points to formation of identical benzoate-alcohol enantiomers, the sense of stereochemical induction in the DROCM reactions of these two cross partners with cyclobutene **2.203** is *opposite*.

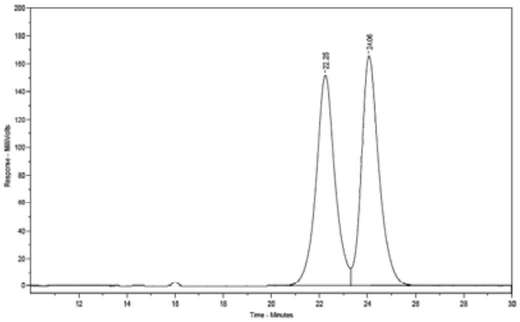

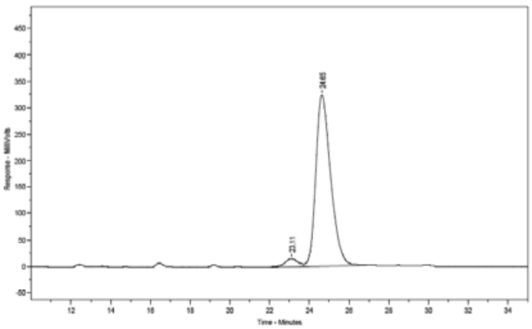

Peak #	Retention time (min)	Area	Area %	Peak #	Retention time (min)	Area	Area %
1	22.25	8277736	49.740	1	23.11	714829	4.075
2	24.06	8364210	50.260	2	24.65	16827120	95.925

2.5.5. *X-Ray Crystal Structures*

■ Crystal structure of 2.54

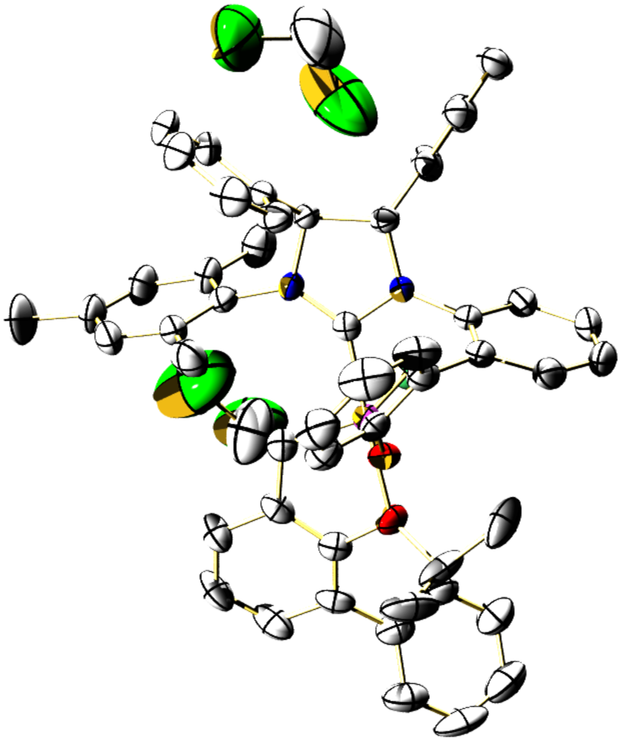

Identification code	az01	
Empirical formula	C54 H51 Cl4 I N2 O2 Ru	
Formula weight	1129.74	
Temperature	193(2) K	
Wavelength	0.71073 Å	
Crystal system	Monoclinic	
Space group	P2(1)	
Unit cell dimensions	a = 12.6693(18) Å	a= 90°.
	b = 15.589(2) Å	b= 90.318(2)°.
	c = 12.7899(18) Å	g = 90°.
Volume	2526.0(6) Å^3	
Z	2	

Density (calculated)	1.485 Mg/m^3
Absorption coefficient	1.175 mm^{-1}
F(000)	1140
Crystal size	0.10 x 0.10 x 0.05 mm^3
Theta range for data collection	1.59 to 28.38°.
Index ranges	-14<=h<=16, -20<=k<=16, -15<=l<=17
Reflections collected	19260
Independent reflections	10888 [R(int) = 0.0274]
Completeness to theta = 28.38°	99.7 %
Absorption correction	Empirical
Max. and min. transmission	0.9436 and 0.8916
Refinement method	Full-matrix least-squares on F^2
Data / restraints / parameters	10888 / 1 / 582
Goodness-of-fit on F^2	1.044
Final R indices [I>2sigma(I)]	R1 = 0.0504, wR2 = 0.1223
R indices (all data)	R1 = 0.0641, wR2 = 0.1328
Absolute structure parameter	0.02(2)
Largest diff. peak and hole	1.020 and -0.777 e.Å^{-3}

Table 2. Atomic coordinates (x 10^4) and equivalent isotropic displacement parameters (Å^{2}x 10^3) for AZ01. U(eq) is defined as one third of the trace of the orthogonalized U^{ij} tensor.

	x	y	z	U(eq)
Cl(3S)	4770(5)	8596(5)	283(6)	243(3)
C(29)	10597(4)	7823(4)	3716(5)	40(1)
Ru(1)	8077(1)	8785(1)	2800(1)	31(1)
I(2)	6182(1)	8762(1)	3667(1)	49(1)
C(103)	8186(4)	7533(4)	2825(4)	31(1)
O(2)	7914(3)	10229(3)	2831(3)	40(1)
C(27)	7642(4)	6932(4)	1080(4)	36(1)

O(1)	9607(3)	8950(2)	2908(3)	36(1)
N(2)	8049(3)	6890(3)	2136(3)	31(1)
C(2)	8172(4)	6029(3)	2603(4)	29(1)
C(9)	8198(4)	5191(4)	5204(4)	39(1)
C(17)	9738(6)	8344(4)	6440(5)	59(2)
C(10)	7788(4)	5800(3)	4551(4)	32(1)
C(19)	8232(5)	7743(4)	5524(4)	43(1)
C(3)	8489(4)	6238(3)	3745(4)	31(1)
C(18)	8668(6)	8121(5)	6411(4)	52(2)
C(14)	6732(4)	6008(4)	4629(4)	42(1)
C(22)	8316(5)	7034(4)	236(4)	40(1)
C(23)	7903(6)	7025(5)	-762(5)	53(2)
C(16)	10330(6)	8226(4)	5573(5)	53(2)
C(15)	9916(5)	7879(4)	4654(4)	38(1)
C(5)	8580(6)	4822(4)	1377(4)	49(2)
C(33)	7457(4)	9849(4)	1145(4)	39(1)
C(13)	6106(5)	5592(5)	5338(5)	49(2)
C(35)	7511(4)	10513(4)	1884(5)	37(1)
C(12)	6526(5)	4977(5)	5991(4)	49(2)
C(28)	5805(5)	6745(6)	1801(5)	60(2)
C(4)	8944(4)	5459(3)	2017(4)	36(1)
C(38)	6324(5)	11754(5)	3374(5)	51(2)
C(21)	9472(5)	7179(5)	391(5)	60(2)
C(36)	7125(4)	11324(4)	1695(5)	45(1)
C(34)	8677(5)	10822(5)	3393(7)	62(2)
N(1)	8429(3)	7173(3)	3763(3)	30(1)
C(20)	8855(5)	7631(4)	4637(4)	36(1)
C(30)	10385(4)	8361(4)	2863(4)	36(1)
C(31)	11083(5)	8372(4)	2023(5)	47(1)
C(24)	6825(6)	6904(5)	-953(5)	59(2)
C(8)	10715(6)	5062(5)	1558(6)	60(2)
C(6)	9292(7)	4315(4)	839(5)	59(2)
C(26)	6548(5)	6823(4)	926(4)	44(1)
C(32)	7693(4)	8979(4)	1439(4)	40(1)

C(11)	7565(5)	4784(4)	5928(5)	50(2)
C(25)	6180(6)	6827(5)	-108(5)	55(2)
C(37)	6923(4)	11967(4)	2513(5)	46(1)
C(7)	10352(6)	4432(5)	943(6)	60(2)
C(42)	7123(5)	10068(5)	119(5)	50(2)
C(44)	6831(5)	11507(5)	654(5)	55(2)
C(43)	6842(6)	10908(5)	-106(5)	58(2)
C(49)	7004(6)	13396(5)	3202(8)	78(3)
C(45)	10030(5)	5573(4)	2117(5)	47(1)
C(48)	7265(6)	12815(5)	2426(7)	64(2)
C(47)	11933(6)	7851(5)	2011(6)	65(2)
C(46)	11511(5)	7312(5)	3674(6)	57(2)
C(53)	12155(5)	7328(6)	2866(8)	71(2)
C(51)	6094(6)	12344(5)	4142(6)	64(2)
C(54)	8797(6)	10378(6)	4472(6)	71(2)
C(50)	6457(7)	13175(6)	4055(8)	71(2)
C(52)	6393(8)	6852(8)	-2076(6)	95(3)
C(55)	9652(6)	10947(5)	2767(8)	82(3)
Cl(2S)	3625(5)	5485(5)	3596(4)	226(3)
Cl(1S)	4430(7)	4246(4)	2202(4)	237(3)
C(124)	4443(9)	9489(10)	985(11)	133(5)
C(123)	4244(14)	4519(11)	3471(11)	164(7)
Cl(4S)	3197(4)	9693(3)	998(5)	179(2)

Table 3. Bond lengths [Å] and angles [°] for AZ01.

Cl(3S)-C(124)	1.709(14)
C(29)-C(30)	1.400(8)
C(29)-C(46)	1.407(9)
C(29)-C(15)	1.484(8)
Ru(1)-C(32)	1.830(6)
Ru(1)-C(103)	1.957(6)
Ru(1)-O(1)	1.960(3)

Ru(1)-O(2)	2.261(4)
Ru(1)-I(2)	2.6504(5)
C(103)-N(2)	1.346(7)
C(103)-N(1)	1.358(7)
O(2)-C(35)	1.384(7)
O(2)-C(34)	1.517(7)
C(27)-C(22)	1.390(7)
C(27)-C(26)	1.409(8)
C(27)-N(2)	1.444(7)
O(1)-C(30)	1.348(7)
N(2)-C(2)	1.476(7)
C(2)-C(4)	1.522(7)
C(2)-C(3)	1.548(7)
C(2)-H(2)	1.0000
C(9)-C(10)	1.366(8)
C(9)-C(11)	1.382(8)
C(9)-H(9)	0.9500
C(17)-C(16)	1.355(10)
C(17)-C(18)	1.400(10)
C(17)-H(17)	0.9500
C(10)-C(14)	1.381(7)
C(10)-C(3)	1.525(7)
C(19)-C(18)	1.390(8)
C(19)-C(20)	1.396(8)
C(19)-H(19)	0.9500
C(3)-N(1)	1.460(7)
C(3)-H(3)	1.0000
C(18)-H(18)	0.9500
C(14)-C(13)	1.372(8)
C(14)-H(14)	0.9500
C(22)-C(23)	1.377(8)
C(22)-C(21)	1.494(9)
C(23)-C(24)	1.399(10)
C(23)-H(23)	0.9500

C(16)-C(15)	1.394(8)
C(16)-H(16)	0.9500
C(15)-C(20)	1.398(8)
C(5)-C(4)	1.365(8)
C(5)-C(6)	1.385(10)
C(5)-H(5)	0.9500
C(33)-C(35)	1.403(9)
C(33)-C(42)	1.417(8)
C(33)-C(32)	1.439(8)
C(13)-C(12)	1.377(10)
C(13)-H(13)	0.9500
C(35)-C(36)	1.376(8)
C(12)-C(11)	1.352(9)
C(12)-H(12)	0.9500
C(28)-C(26)	1.472(9)
C(28)-H(28A)	0.9800
C(28)-H(28B)	0.9800
C(28)-H(28C)	0.9800
C(4)-C(45)	1.393(8)
C(38)-C(51)	1.378(10)
C(38)-C(37)	1.382(9)
C(38)-H(38)	0.9500
C(21)-H(21A)	0.9800
C(21)-H(21B)	0.9800
C(21)-H(21C)	0.9800
C(36)-C(44)	1.410(9)
C(36)-C(37)	1.472(9)
C(34)-C(55)	1.489(12)
C(34)-C(54)	1.551(12)
C(34)-H(34)	1.0000
N(1)-C(20)	1.430(7)
C(30)-C(31)	1.396(8)
C(31)-C(47)	1.350(10)
C(31)-H(31)	0.9500

C(24)-C(25)	1.364(10)
C(24)-C(52)	1.536(9)
C(8)-C(7)	1.339(10)
C(8)-C(45)	1.380(9)
C(8)-H(8)	0.9500
C(6)-C(7)	1.362(11)
C(6)-H(6)	0.9500
C(26)-C(25)	1.400(8)
C(32)-H(32)	0.9500
C(11)-H(11)	0.9500
C(25)-H(25)	0.9500
C(37)-C(48)	1.395(9)
C(7)-H(7)	0.9500
C(42)-C(43)	1.388(10)
C(42)-H(42)	0.9500
C(44)-C(43)	1.347(11)
C(44)-H(44)	0.9500
C(43)-H(43)	0.9500
C(49)-C(50)	1.341(12)
C(49)-C(48)	1.385(12)
C(49)-H(49)	0.9500
C(45)-H(45)	0.9500
C(48)-H(48)	0.9500
C(47)-C(53)	1.391(12)
C(47)-H(47)	0.9500
C(46)-C(53)	1.322(11)
C(46)-H(46)	0.9500
C(53)-H(53)	0.9500
C(51)-C(50)	1.380(12)
C(51)-H(51)	0.9500
C(54)-H(54A)	0.9800
C(54)-H(54B)	0.9800
C(54)-H(54C)	0.9800
C(50)-H(50)	0.9500

C(52)-H(52A)	0.9800
C(52)-H(52B)	0.9800
C(52)-H(52C)	0.9800
C(55)-H(55A)	0.9800
C(55)-H(55B)	0.9800
C(55)-H(55C)	0.9800
Cl(2S)-C(123)	1.706(17)
Cl(1S)-C(123)	1.696(16)
C(124)-Cl(4S)	1.610(12)
C(124)-H(12A)	0.9900
C(124)-H(12B)	0.9900
C(123)-H(12C)	0.9900
C(123)-H(12D)	0.9900
C(30)-C(29)-C(46)	117.7(6)
C(30)-C(29)-C(15)	119.0(5)
C(46)-C(29)-C(15)	123.1(6)
C(32)-Ru(1)-C(103)	101.5(2)
C(32)-Ru(1)-O(1)	107.7(2)
C(103)-Ru(1)-O(1)	93.46(18)
C(32)-Ru(1)-O(2)	80.1(2)
C(103)-Ru(1)-O(2)	177.69(17)
O(1)-Ru(1)-O(2)	87.64(15)
C(32)-Ru(1)-I(2)	99.41(16)
C(103)-Ru(1)-I(2)	92.50(15)
O(1)-Ru(1)-I(2)	150.47(11)
O(2)-Ru(1)-I(2)	85.56(11)
N(2)-C(103)-N(1)	107.4(5)
N(2)-C(103)-Ru(1)	136.4(4)
N(1)-C(103)-Ru(1)	116.2(4)
C(35)-O(2)-C(34)	116.7(5)
C(35)-O(2)-Ru(1)	109.7(3)
C(34)-O(2)-Ru(1)	123.9(3)
C(22)-C(27)-C(26)	120.9(5)

C(22)-C(27)-N(2)	120.9(5)
C(26)-C(27)-N(2)	118.2(5)
C(30)-O(1)-Ru(1)	129.1(3)
C(103)-N(2)-C(27)	128.5(5)
C(103)-N(2)-C(2)	113.5(4)
C(27)-N(2)-C(2)	117.1(4)
N(2)-C(2)-C(4)	113.5(4)
N(2)-C(2)-C(3)	102.5(4)
C(4)-C(2)-C(3)	115.1(4)
N(2)-C(2)-H(2)	108.5
C(4)-C(2)-H(2)	108.5
C(3)-C(2)-H(2)	108.5
C(10)-C(9)-C(11)	120.6(5)
C(10)-C(9)-H(9)	119.7
C(11)-C(9)-H(9)	119.7
C(16)-C(17)-C(18)	118.9(6)
C(16)-C(17)-H(17)	120.5
C(18)-C(17)-H(17)	120.5
C(9)-C(10)-C(14)	119.0(5)
C(9)-C(10)-C(3)	120.2(5)
C(14)-C(10)-C(3)	120.8(5)
C(18)-C(19)-C(20)	119.5(6)
C(18)-C(19)-H(19)	120.3
C(20)-C(19)-H(19)	120.3
N(1)-C(3)-C(10)	114.0(4)
N(1)-C(3)-C(2)	102.2(4)
C(10)-C(3)-C(2)	113.2(4)
N(1)-C(3)-H(3)	109.1
C(10)-C(3)-H(3)	109.1
C(2)-C(3)-H(3)	109.1
C(19)-C(18)-C(17)	120.5(6)
C(19)-C(18)-H(18)	119.7
C(17)-C(18)-H(18)	119.7
C(13)-C(14)-C(10)	120.0(6)

C(13)-C(14)-H(14)	120.0
C(10)-C(14)-H(14)	120.0
C(23)-C(22)-C(27)	119.1(6)
C(23)-C(22)-C(21)	119.5(6)
C(27)-C(22)-C(21)	121.4(5)
C(22)-C(23)-C(24)	122.0(6)
C(22)-C(23)-H(23)	119.0
C(24)-C(23)-H(23)	119.0
C(17)-C(16)-C(15)	122.5(6)
C(17)-C(16)-H(16)	118.8
C(15)-C(16)-H(16)	118.8
C(16)-C(15)-C(20)	118.4(6)
C(16)-C(15)-C(29)	119.1(5)
C(20)-C(15)-C(29)	122.3(5)
C(4)-C(5)-C(6)	119.6(6)
C(4)-C(5)-H(5)	120.2
C(6)-C(5)-H(5)	120.2
C(35)-C(33)-C(42)	117.4(6)
C(35)-C(33)-C(32)	120.6(5)
C(42)-C(33)-C(32)	122.0(6)
C(14)-C(13)-C(12)	120.5(6)
C(14)-C(13)-H(13)	119.8
C(12)-C(13)-H(13)	119.8
C(36)-C(35)-O(2)	125.2(6)
C(36)-C(35)-C(33)	122.9(6)
O(2)-C(35)-C(33)	111.7(5)
C(11)-C(12)-C(13)	119.5(6)
C(11)-C(12)-H(12)	120.3
C(13)-C(12)-H(12)	120.3
C(26)-C(28)-H(28A)	109.5
C(26)-C(28)-H(28B)	109.5
H(28A)-C(28)-H(28B)	109.5
C(26)-C(28)-H(28C)	109.5
H(28A)-C(28)-H(28C)	109.5

H(28B)-C(28)-H(28C)	109.5
C(5)-C(4)-C(45)	118.5(5)
C(5)-C(4)-C(2)	120.3(5)
C(45)-C(4)-C(2)	121.1(5)
C(51)-C(38)-C(37)	121.9(7)
C(51)-C(38)-H(38)	119.1
C(37)-C(38)-H(38)	119.1
C(22)-C(21)-H(21A)	109.5
C(22)-C(21)-H(21B)	109.5
H(21A)-C(21)-H(21B)	109.5
C(22)-C(21)-H(21C)	109.5
H(21A)-C(21)-H(21C)	109.5
H(21B)-C(21)-H(21C)	109.5
C(35)-C(36)-C(44)	116.3(6)
C(35)-C(36)-C(37)	124.4(6)
C(44)-C(36)-C(37)	119.2(6)
C(55)-C(34)-O(2)	110.7(6)
C(55)-C(34)-C(54)	117.4(6)
O(2)-C(34)-C(54)	102.0(6)
C(55)-C(34)-H(34)	108.8
O(2)-C(34)-H(34)	108.8
C(54)-C(34)-H(34)	108.8
C(103)-N(1)-C(20)	124.6(5)
C(103)-N(1)-C(3)	114.2(4)
C(20)-N(1)-C(3)	119.4(4)
C(19)-C(20)-C(15)	120.1(5)
C(19)-C(20)-N(1)	119.0(5)
C(15)-C(20)-N(1)	120.5(5)
O(1)-C(30)-C(31)	119.4(5)
O(1)-C(30)-C(29)	120.8(5)
C(31)-C(30)-C(29)	119.1(5)
C(47)-C(31)-C(30)	120.7(7)
C(47)-C(31)-H(31)	119.6
C(30)-C(31)-H(31)	119.6

C(25)-C(24)-C(23)	117.5(6)
C(25)-C(24)-C(52)	121.6(7)
C(23)-C(24)-C(52)	120.9(7)
C(7)-C(8)-C(45)	120.9(7)
C(7)-C(8)-H(8)	119.6
C(45)-C(8)-H(8)	119.6
C(7)-C(6)-C(5)	121.3(6)
C(7)-C(6)-H(6)	119.3
C(5)-C(6)-H(6)	119.3
C(25)-C(26)-C(27)	117.0(6)
C(25)-C(26)-C(28)	120.5(6)
C(27)-C(26)-C(28)	122.4(5)
C(33)-C(32)-Ru(1)	117.3(4)
C(33)-C(32)-H(32)	121.3
Ru(1)-C(32)-H(32)	121.3
C(12)-C(11)-C(9)	120.4(6)
C(12)-C(11)-H(11)	119.8
C(9)-C(11)-H(11)	119.8
C(24)-C(25)-C(26)	123.4(6)
C(24)-C(25)-H(25)	118.3
C(26)-C(25)-H(25)	118.3
C(38)-C(37)-C(48)	117.6(7)
C(38)-C(37)-C(36)	120.1(6)
C(48)-C(37)-C(36)	122.2(7)
C(8)-C(7)-C(6)	119.4(6)
C(8)-C(7)-H(7)	120.3
C(6)-C(7)-H(7)	120.3
C(43)-C(42)-C(33)	119.6(7)
C(43)-C(42)-H(42)	120.2
C(33)-C(42)-H(42)	120.2
C(43)-C(44)-C(36)	122.6(6)
C(43)-C(44)-H(44)	118.7
C(36)-C(44)-H(44)	118.7
C(44)-C(43)-C(42)	120.5(6)

C(44)-C(43)-H(43)	119.7
C(42)-C(43)-H(43)	119.7
C(50)-C(49)-C(48)	122.7(8)
C(50)-C(49)-H(49)	118.6
C(48)-C(49)-H(49)	118.6
C(8)-C(45)-C(4)	120.2(6)
C(8)-C(45)-H(45)	119.9
C(4)-C(45)-H(45)	119.9
C(49)-C(48)-C(37)	119.2(8)
C(49)-C(48)-H(48)	120.4
C(37)-C(48)-H(48)	120.4
C(31)-C(47)-C(53)	120.1(7)
C(31)-C(47)-H(47)	119.9
C(53)-C(47)-H(47)	119.9
C(53)-C(46)-C(29)	122.1(7)
C(53)-C(46)-H(46)	119.0
C(29)-C(46)-H(46)	118.9
C(46)-C(53)-C(47)	120.1(7)
C(46)-C(53)-H(53)	119.9
C(47)-C(53)-H(53)	119.9
C(38)-C(51)-C(50)	119.7(8)
C(38)-C(51)-H(51)	120.1
C(50)-C(51)-H(51)	120.1
C(34)-C(54)-H(54A)	109.5
C(34)-C(54)-H(54B)	109.5
H(54A)-C(54)-H(54B)	109.5
C(34)-C(54)-H(54C)	109.5
H(54A)-C(54)-H(54C)	109.5
H(54B)-C(54)-H(54C)	109.5
C(49)-C(50)-C(51)	118.8(8)
C(49)-C(50)-H(50)	120.6
C(51)-C(50)-H(50)	120.6
C(24)-C(52)-H(52A)	109.5
C(24)-C(52)-H(52B)	109.5

H(52A)-C(52)-H(52B)	109.5
C(24)-C(52)-H(52C)	109.5
H(52A)-C(52)-H(52C)	109.5
H(52B)-C(52)-H(52C)	109.5
C(34)-C(55)-H(55A)	109.5
C(34)-C(55)-H(55B)	109.5
H(55A)-C(55)-H(55B)	109.5
C(34)-C(55)-H(55C)	109.5
H(55A)-C(55)-H(55C)	109.5
H(55B)-C(55)-H(55C)	109.5
Cl(4S)-C(124)-Cl(3S)	114.0(8)
Cl(4S)-C(124)-H(12A)	108.7
Cl(3S)-C(124)-H(12A)	108.8
Cl(4S)-C(124)-H(12B)	108.7
Cl(3S)-C(124)-H(12B)	108.7
H(12A)-C(124)-H(12B)	107.6
Cl(1S)-C(123)-Cl(2S)	112.1(8)
Cl(1S)-C(123)-H(12C)	109.2
Cl(2S)-C(123)-H(12C)	109.2
Cl(1S)-C(123)-H(12D)	109.2
Cl(2S)-C(123)-H(12D)	109.2
H(12C)-C(123)-H(12D)	107.9

Symmetry transformations used to generate equivalent atoms:

Table 4. Anisotropic displacement parameters (Å^{2}x 10^3) for AZ01. The anisotropic displacement factor exponent takes the form: $-2\pi^2[h^2 a^{*2}U^{11} + ... + 2 h k a^* b^* U^{12}]$

	U^{11}	U^{22}	U^{33}	U^{23}	U^{13}	U^{12}
Cl(3S)	226(5)	178(6)	326(7)	-90(5)	122(5)	-14(4)
C(29)	37(3)	36(3)	45(3)	0(2)	-7(2)	-7(2)
Ru(1)	31(1)	29(1)	31(1)	0(1)	-2(1)	1(1)
I(2)	38(1)	56(1)	52(1)	-9(1)	8(1)	3(1)

C(103)	22(2)	38(3)	31(3)	0(2)	3(2)	-2(2)
O(2)	38(2)	35(2)	46(2)	-2(2)	-14(2)	-1(2)
C(27)	43(3)	29(3)	34(3)	-2(2)	-2(2)	2(2)
O(1)	35(2)	29(3)	43(2)	4(1)	-5(1)	-3(1)
N(2)	33(2)	32(2)	28(2)	-5(2)	-4(2)	-2(2)
C(2)	33(2)	26(3)	29(2)	-2(2)	3(2)	-3(2)
C(9)	36(3)	38(3)	43(3)	6(2)	-7(2)	-2(2)
C(17)	93(5)	47(4)	37(3)	-2(3)	-22(3)	-11(4)
C(10)	37(3)	28(3)	32(3)	-4(2)	7(2)	-1(2)
C(19)	59(4)	36(3)	35(3)	1(2)	6(3)	-1(3)
C(3)	32(2)	27(3)	34(3)	-1(2)	4(2)	0(2)
C(18)	81(5)	46(4)	28(3)	-1(2)	1(3)	-3(3)
C(14)	36(3)	52(4)	39(3)	4(3)	5(2)	9(3)
C(22)	53(3)	36(3)	30(3)	0(2)	4(2)	-3(3)
C(23)	78(5)	51(4)	30(3)	3(3)	7(3)	2(3)
C(16)	68(4)	43(4)	47(4)	9(3)	-20(3)	-13(3)
C(15)	49(3)	30(3)	35(3)	4(2)	-4(2)	-4(2)
C(5)	72(4)	45(4)	30(3)	-5(2)	7(3)	-9(3)
C(33)	30(2)	43(3)	43(3)	12(2)	0(2)	6(2)
C(13)	40(3)	61(4)	46(3)	-6(3)	11(3)	-2(3)
C(35)	27(2)	37(3)	46(3)	5(2)	0(2)	1(2)
C(12)	60(4)	58(4)	30(3)	2(3)	8(3)	-20(3)
C(28)	39(3)	82(6)	59(4)	-14(4)	-6(3)	-2(3)
C(4)	49(3)	26(3)	33(3)	3(2)	12(2)	0(2)
C(38)	52(3)	43(4)	58(4)	1(3)	-7(3)	-10(3)
C(21)	59(4)	70(5)	51(4)	10(3)	11(3)	-11(3)
C(36)	34(3)	40(3)	61(4)	12(3)	8(3)	-1(2)
C(34)	53(4)	31(4)	102(6)	-20(4)	-39(4)	9(3)
N(1)	35(2)	30(2)	24(2)	1(2)	-1(2)	-5(2)
C(20)	52(3)	25(3)	31(3)	3(2)	-3(2)	-2(2)
C(30)	32(3)	36(3)	40(3)	-6(2)	-6(2)	-8(2)
C(31)	38(3)	47(4)	55(4)	-6(3)	7(3)	-9(3)
C(24)	84(5)	59(5)	35(3)	-7(3)	-19(3)	-4(4)
C(8)	61(4)	55(5)	63(4)	-1(3)	26(3)	9(3)

C(6)	99(6)	41(4)	38(3)	-16(3)	11(3)	-6(4)
C(26)	43(3)	51(4)	37(3)	-8(3)	-5(2)	-1(3)
C(32)	39(3)	43(4)	39(3)	-1(2)	-1(2)	5(2)
C(11)	56(4)	46(4)	49(4)	15(3)	-4(3)	-13(3)
C(25)	53(4)	66(5)	45(4)	-8(3)	-17(3)	-3(3)
C(37)	33(3)	37(3)	67(4)	2(3)	-9(3)	8(2)
C(7)	82(5)	45(4)	53(4)	-11(3)	25(4)	11(4)
C(42)	52(4)	61(4)	37(3)	10(3)	4(3)	16(3)
C(44)	50(4)	58(4)	58(4)	23(3)	13(3)	21(3)
C(43)	62(4)	69(5)	43(4)	23(3)	3(3)	20(4)
C(49)	67(5)	26(4)	141(9)	-3(4)	-26(6)	3(3)
C(45)	52(3)	36(3)	52(4)	-1(3)	15(3)	0(3)
C(48)	60(4)	41(4)	92(6)	16(4)	-14(4)	-4(3)
C(47)	60(4)	59(5)	77(5)	-12(4)	20(4)	-3(4)
C(46)	41(3)	43(4)	86(5)	7(3)	-5(3)	0(3)
C(53)	39(4)	60(5)	115(7)	-4(5)	19(4)	12(3)
C(51)	64(4)	55(5)	73(5)	-18(4)	2(4)	7(4)
C(54)	64(4)	71(6)	78(5)	-35(4)	-37(4)	27(4)
C(50)	70(5)	50(4)	93(6)	-23(4)	-27(5)	11(4)
C(52)	132(8)	110(8)	43(4)	-1(4)	-36(5)	-14(7)
C(55)	57(4)	49(5)	139(8)	24(5)	-31(5)	-22(4)
Cl(2S)	213(5)	258(7)	207(5)	98(5)	48(4)	139(5)
Cl(1S)	396(9)	173(5)	139(4)	12(3)	-111(5)	29(5)
C(124)	107(9)	167(15)	125(10)	-44(10)	-5(8)	30(9)
C(123)	210(16)	170(17)	113(10)	33(10)	-48(11)	56(13)
Cl(4S)	142(3)	143(4)	251(6)	5(4)	22(3)	-16(3)

Table 5. Hydrogen coordinates (x 10^4) and isotropic displacement parameters ($Å^2$x 10 ^{3}) for AZ01.

	x	y	z	U(eq)
H(2)	7467	5742	2606	35
H(9)	8924	5046	5161	47
H(17)	10045	8576	7059	71
H(19)	7516	7563	5521	52
H(3)	9238	6059	3865	37
H(18)	8237	8228	7002	62
H(14)	6439	6440	4191	51
H(23)	8364	7103	-1338	63
H(16)	11053	8385	5592	63
H(5)	7843	4726	1302	59
H(13)	5376	5729	5379	59
H(12)	6091	4690	6482	59
H(28A)	5082	6824	1542	90
H(28B)	5965	7184	2327	90
H(28C)	5873	6175	2117	90
H(38)	6063	11186	3438	61
H(21A)	9822	6630	527	90
H(21B)	9584	7564	988	90
H(21C)	9769	7440	-239	90
H(34)	8328	11392	3494	74
H(31)	10958	8751	1454	56
H(8)	11454	5160	1611	72
H(6)	9035	3877	388	71
H(32)	7651	8524	947	48
H(11)	7861	4367	6385	61
H(25)	5442	6774	-228	66
H(7)	10831	4069	582	72
H(42)	7092	9641	-411	60

H(44)	6617	12073	482	66
H(43)	6655	11063	-801	69
H(49)	7221	13976	3126	94
H(45)	10300	6004	2570	56
H(48)	7672	12991	1842	77
H(47)	12381	7841	1418	78
H(46)	11669	6944	4245	68
H(53)	12772	6981	2868	85
H(51)	5686	12178	4730	77
H(54A)	9164	9829	4386	107
H(54B)	8097	10276	4769	107
H(54C)	9205	10748	4944	107
H(50)	6323	13583	4590	86
H(52A)	5672	6624	-2066	143
H(52B)	6843	6472	-2491	143
H(52C)	6389	7426	-2388	143
H(55A)	9897	10391	2505	122
H(55B)	10202	11205	3207	122
H(55C)	9499	11328	2175	122
H(12A)	4692	9414	1714	160
H(12B)	4818	9989	688	160
H(12C)	4937	4544	3832	197
H(12D)	3816	4070	3816	197

Table 6. Torsion angles [°] for AZ01.

C(32)-Ru(1)-C(103)-N(2)	-0.2(6)
O(1)-Ru(1)-C(103)-N(2)	-109.0(5)
O(2)-Ru(1)-C(103)-N(2)	133(4)
I(2)-Ru(1)-C(103)-N(2)	100.0(5)
C(32)-Ru(1)-C(103)-N(1)	-177.7(4)
O(1)-Ru(1)-C(103)-N(1)	73.5(4)
O(2)-Ru(1)-C(103)-N(1)	-45(5)

I(2)-Ru(1)-C(103)-N(1)	-77.6(4)
C(32)-Ru(1)-O(2)-C(35)	6.3(4)
C(103)-Ru(1)-O(2)-C(35)	-127(4)
O(1)-Ru(1)-O(2)-C(35)	114.7(4)
I(2)-Ru(1)-O(2)-C(35)	-94.1(3)
C(32)-Ru(1)-O(2)-C(34)	-138.4(5)
C(103)-Ru(1)-O(2)-C(34)	89(4)
O(1)-Ru(1)-O(2)-C(34)	-30.0(5)
I(2)-Ru(1)-O(2)-C(34)	121.3(5)
C(32)-Ru(1)-O(1)-C(30)	-95.6(4)
C(103)-Ru(1)-O(1)-C(30)	7.6(4)
O(2)-Ru(1)-O(1)-C(30)	-174.4(4)
I(2)-Ru(1)-O(1)-C(30)	108.9(4)
N(1)-C(103)-N(2)-C(27)	170.5(5)
Ru(1)-C(103)-N(2)-C(27)	-7.2(9)
N(1)-C(103)-N(2)-C(2)	1.5(6)
Ru(1)-C(103)-N(2)-C(2)	-176.1(4)
C(22)-C(27)-N(2)-C(103)	92.3(7)
C(26)-C(27)-N(2)-C(103)	-90.9(7)
C(22)-C(27)-N(2)-C(2)	-99.1(6)
C(26)-C(27)-N(2)-C(2)	77.8(6)
C(103)-N(2)-C(2)-C(4)	-128.1(5)
C(27)-N(2)-C(2)-C(4)	61.6(6)
C(103)-N(2)-C(2)-C(3)	-3.3(5)
C(27)-N(2)-C(2)-C(3)	-173.6(4)
C(11)-C(9)-C(10)-C(14)	0.5(9)
C(11)-C(9)-C(10)-C(3)	-179.3(5)
C(9)-C(10)-C(3)-N(1)	-129.3(5)
C(14)-C(10)-C(3)-N(1)	51.0(7)
C(9)-C(10)-C(3)-C(2)	114.4(6)
C(14)-C(10)-C(3)-C(2)	-65.3(7)
N(2)-C(2)-C(3)-N(1)	3.5(5)
C(4)-C(2)-C(3)-N(1)	127.2(4)
N(2)-C(2)-C(3)-C(10)	126.5(4)

C(4)-C(2)-C(3)-C(10)	-109.8(5)
C(20)-C(19)-C(18)-C(17)	-3.6(10)
C(16)-C(17)-C(18)-C(19)	3.2(10)
C(9)-C(10)-C(14)-C(13)	-1.5(9)
C(3)-C(10)-C(14)-C(13)	178.2(5)
C(26)-C(27)-C(22)-C(23)	-0.3(9)
N(2)-C(27)-C(22)-C(23)	176.5(6)
C(26)-C(27)-C(22)-C(21)	177.9(6)
N(2)-C(27)-C(22)-C(21)	-5.3(9)
C(27)-C(22)-C(23)-C(24)	-0.9(10)
C(21)-C(22)-C(23)-C(24)	-179.1(7)
C(18)-C(17)-C(16)-C(15)	-0.8(11)
C(17)-C(16)-C(15)-C(20)	-1.2(9)
C(17)-C(16)-C(15)-C(29)	175.9(6)
C(30)-C(29)-C(15)-C(16)	-109.8(6)
C(46)-C(29)-C(15)-C(16)	64.1(8)
C(30)-C(29)-C(15)-C(20)	67.2(8)
C(46)-C(29)-C(15)-C(20)	-118.9(7)
C(10)-C(14)-C(13)-C(12)	1.3(10)
C(34)-O(2)-C(35)-C(36)	-45.5(8)
Ru(1)-O(2)-C(35)-C(36)	167.0(5)
C(34)-O(2)-C(35)-C(33)	139.6(5)
Ru(1)-O(2)-C(35)-C(33)	-7.9(6)
C(42)-C(33)-C(35)-C(36)	8.9(8)
C(32)-C(33)-C(35)-C(36)	-168.6(5)
C(42)-C(33)-C(35)-O(2)	-176.0(5)
C(32)-C(33)-C(35)-O(2)	6.4(7)
C(14)-C(13)-C(12)-C(11)	-0.1(10)
C(6)-C(5)-C(4)-C(45)	-0.6(9)
C(6)-C(5)-C(4)-C(2)	179.2(6)
N(2)-C(2)-C(4)-C(5)	-103.3(6)
C(3)-C(2)-C(4)-C(5)	139.0(5)
N(2)-C(2)-C(4)-C(45)	76.5(6)
C(3)-C(2)-C(4)-C(45)	-41.2(7)

O(2)-C(35)-C(36)-C(44)	175.0(5)
C(33)-C(35)-C(36)-C(44)	-10.6(8)
O(2)-C(35)-C(36)-C(37)	-10.4(9)
C(33)-C(35)-C(36)-C(37)	164.0(6)
C(35)-O(2)-C(34)-C(55)	-63.8(7)
Ru(1)-O(2)-C(34)-C(55)	78.6(7)
C(35)-O(2)-C(34)-C(54)	170.6(5)
Ru(1)-O(2)-C(34)-C(54)	-47.0(7)
N(2)-C(103)-N(1)-C(20)	165.6(5)
Ru(1)-C(103)-N(1)-C(20)	-16.1(7)
N(2)-C(103)-N(1)-C(3)	1.1(6)
Ru(1)-C(103)-N(1)-C(3)	179.3(3)
C(10)-C(3)-N(1)-C(103)	-125.6(5)
C(2)-C(3)-N(1)-C(103)	-3.0(5)
C(10)-C(3)-N(1)-C(20)	69.0(6)
C(2)-C(3)-N(1)-C(20)	-168.4(4)
C(18)-C(19)-C(20)-C(15)	1.5(9)
C(18)-C(19)-C(20)-N(1)	174.4(6)
C(16)-C(15)-C(20)-C(19)	0.8(9)
C(29)-C(15)-C(20)-C(19)	-176.2(5)
C(16)-C(15)-C(20)-N(1)	-172.0(5)
C(29)-C(15)-C(20)-N(1)	11.0(8)
C(103)-N(1)-C(20)-C(19)	111.5(6)
C(3)-N(1)-C(20)-C(19)	-84.7(6)
C(103)-N(1)-C(20)-C(15)	-75.6(7)
C(3)-N(1)-C(20)-C(15)	88.2(6)
Ru(1)-O(1)-C(30)-C(31)	113.4(5)
Ru(1)-O(1)-C(30)-C(29)	-76.1(6)
C(46)-C(29)-C(30)-O(1)	-171.0(5)
C(15)-C(29)-C(30)-O(1)	3.2(8)
C(46)-C(29)-C(30)-C(31)	-0.5(8)
C(15)-C(29)-C(30)-C(31)	173.7(5)
O(1)-C(30)-C(31)-C(47)	173.0(6)
C(29)-C(30)-C(31)-C(47)	2.3(9)

C(22)-C(23)-C(24)-C(25)	2.5(11)
C(22)-C(23)-C(24)-C(52)	-176.9(8)
C(4)-C(5)-C(6)-C(7)	0.7(11)
C(22)-C(27)-C(26)-C(25)	-0.3(9)
N(2)-C(27)-C(26)-C(25)	-177.1(6)
C(22)-C(27)-C(26)-C(28)	-177.7(6)
N(2)-C(27)-C(26)-C(28)	5.4(9)
C(35)-C(33)-C(32)-Ru(1)	-0.7(7)
C(42)-C(33)-C(32)-Ru(1)	-178.2(4)
C(103)-Ru(1)-C(32)-C(33)	175.3(4)
O(1)-Ru(1)-C(32)-C(33)	-87.3(4)
O(2)-Ru(1)-C(32)-C(33)	-3.0(4)
I(2)-Ru(1)-C(32)-C(33)	80.8(4)
C(13)-C(12)-C(11)-C(9)	-1.0(10)
C(10)-C(9)-C(11)-C(12)	0.8(10)
C(23)-C(24)-C(25)-C(26)	-3.1(12)
C(52)-C(24)-C(25)-C(26)	176.3(8)
C(27)-C(26)-C(25)-C(24)	2.0(11)
C(28)-C(26)-C(25)-C(24)	179.5(7)
C(51)-C(38)-C(37)-C(48)	-2.0(10)
C(51)-C(38)-C(37)-C(36)	-178.3(6)
C(35)-C(36)-C(37)-C(38)	-51.3(8)
C(44)-C(36)-C(37)-C(38)	123.2(6)
C(35)-C(36)-C(37)-C(48)	132.6(7)
C(44)-C(36)-C(37)-C(48)	-52.9(8)
C(45)-C(8)-C(7)-C(6)	2.4(12)
C(5)-C(6)-C(7)-C(8)	-1.6(11)
C(35)-C(33)-C(42)-C(43)	-1.6(9)
C(32)-C(33)-C(42)-C(43)	176.0(6)
C(35)-C(36)-C(44)-C(43)	5.2(9)
C(37)-C(36)-C(44)-C(43)	-169.7(6)
C(36)-C(44)-C(43)-C(42)	1.7(11)
C(33)-C(42)-C(43)-C(44)	-3.5(10)
C(7)-C(8)-C(45)-C(4)	-2.4(11)

C(5)-C(4)-C(45)-C(8)	1.5(9)
C(2)-C(4)-C(45)-C(8)	-178.4(6)
C(50)-C(49)-C(48)-C(37)	1.9(11)
C(38)-C(37)-C(48)-C(49)	0.8(9)
C(36)-C(37)-C(48)-C(49)	176.9(6)
C(30)-C(31)-C(47)-C(53)	-3.5(11)
C(30)-C(29)-C(46)-C(53)	-0.1(10)
C(15)-C(29)-C(46)-C(53)	-174.1(7)
C(29)-C(46)-C(53)-C(47)	-1.0(12)
C(31)-C(47)-C(53)-C(46)	2.9(12)
C(37)-C(38)-C(51)-C(50)	0.7(11)
C(48)-C(49)-C(50)-C(51)	-3.3(12)
C(38)-C(51)-C(50)-C(49)	2.0(12)

Symmetry transformations used to generate equivalent atoms:

■ Crystal Structure 2.111

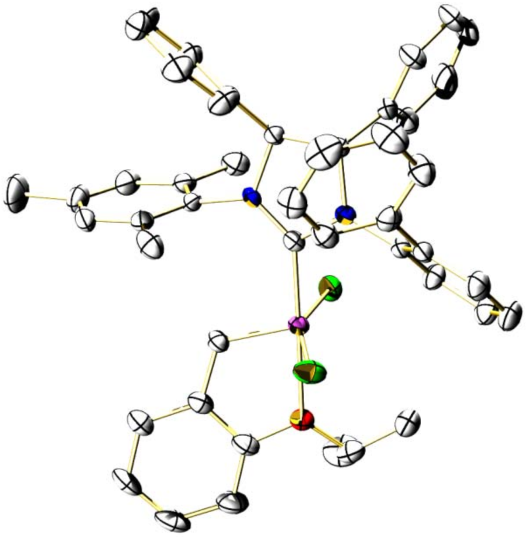

Identification code	az02	
Empirical formula	C46 H44 Cl2 N2 O Ru	
Formula weight	812.80	
Temperature	193(2) K	
Wavelength	0.71073 Å	
Crystal system	Orthorhombic	
Space group	P2(1)2(1)2(1)	
Unit cell dimensions	a = 9.7111(11) Å	□= 90°.
	b = 9.8468(12) Å	□= 90°.
	c = 40.586(5) Å	□ = 90°.
Volume	3880.9(8) Å^3	
Z	4	
Density (calculated)	1.391 Mg/m^3	
Absorption coefficient	0.580 mm^{-1}	
F(000)	1680	
Crystal size	0.10 x 0.10 x 0.05 mm^3	
Theta range for data collection	1.00 to 28.37°.	
Index ranges	-12<=h<=8, -12<=k<=13, -49<=l<=54	
Reflections collected	28077	
Independent reflections	9675 [R(int) = 0.0381]	

Completeness to theta = 28.37°	99.8 %
Absorption correction	Empirical
Max. and min. transmission	0.9716 and 0.9443
Refinement method	Full-matrix least-squares on F^2
Data / restraints / parameters	9675 / 0 / 474
Goodness-of-fit on F^2	1.105
Final R indices [I>2sigma(I)]	R1 = 0.0417, wR2 = 0.0916
R indices (all data)	R1 = 0.0477, wR2 = 0.1006
Absolute structure parameter	-0.01(3)
Largest diff. peak and hole	0.854 and -0.792 e.Å^{-3}

Table 2. Atomic coordinates (x 10^4) and equivalent isotropic displacement parameters (Å^{2}x 10^3) for AZ01. U(eq) is defined as one third of the trace of the orthogonalized U^{ij} tensor.

	x	y	z	U(eq)
Cl(1)	7818(1)	8838(1)	8497(1)	37(1)
Ru(1)	6286(1)	7041(1)	8445(1)	22(1)
Cl(2)	4248(1)	5815(1)	8545(1)	31(1)
O(1)	5085(2)	8366(3)	8082(1)	33(1)
C(39)	6904(3)	6395(3)	8049(1)	26(1)
C(3)	9588(4)	3274(3)	9038(1)	25(1)
C(22)	9363(3)	7937(4)	9412(1)	29(1)
C(1)	8191(3)	3944(3)	9034(1)	23(1)
C(20)	7289(3)	5848(3)	8750(1)	21(1)

C(32)	6934(4)	7458(3)	9212(1)	23(1)
C(38)	7222(4)	6918(4)	7449(1)	33(1)
C(31)	5571(3)	7859(4)	9188(1)	29(1)
C(12)	8479(4)	2111(4)	7893(1)	41(1)
N(2)	7341(3)	6174(3)	9077(1)	22(1)
C(33)	6580(3)	7161(4)	7753(1)	29(1)
C(13)	7346(4)	1945(4)	8087(1)	36(1)
C(15)	5845(4)	2542(4)	8571(1)	36(1)
C(14)	7082(3)	2786(3)	8356(1)	28(1)
C(4)	9693(4)	1903(4)	8973(1)	37(1)
C(23)	9916(4)	7816(4)	9726(1)	39(1)
C(10)	8025(3)	3830(3)	8421(1)	23(1)
C(18)	5677(5)	4413(4)	9527(1)	44(1)
C(24)	11274(4)	7471(4)	9771(1)	47(1)
N(1)	7861(3)	4625(3)	8717(1)	22(1)
C(9)	9177(3)	4044(3)	8225(1)	28(1)
C(34)	5611(4)	8213(4)	7771(1)	33(1)
C(2)	7960(3)	5106(3)	9289(1)	24(1)
C(25)	12109(4)	7231(4)	9502(1)	45(1)
C(35)	5284(5)	8998(4)	7503(1)	43(1)
C(28)	7426(4)	9532(4)	9491(1)	34(1)
C(30)	5149(4)	9106(4)	9305(1)	35(1)
C(7)	12047(4)	3397(5)	9071(1)	43(1)
C(8)	7060(4)	4650(4)	9565(1)	32(1)
C(27)	7891(4)	8302(3)	9371(1)	26(1)
C(41)	3866(4)	9201(4)	8129(1)	38(1)
C(6)	12146(4)	2027(5)	9008(1)	44(1)
C(36)	5953(4)	8732(4)	7206(1)	46(1)

C(11)	9366(4)	3170(4)	7960(1)	36(1)
C(17)	10166(4)	5188(4)	8291(1)	40(1)
C(21)	10235(4)	7733(4)	9144(1)	32(1)
C(40)	10778(4)	4005(4)	9086(1)	38(1)
C(29)	6079(4)	9947(4)	9462(1)	40(1)
C(26)	11591(4)	7384(4)	9191(1)	37(1)
C(16)	8778(6)	1108(5)	7613(1)	64(1)
C(42)	2629(4)	8521(5)	7979(1)	59(1)
C(37)	6908(4)	7713(4)	7177(1)	39(1)
C(5)	10962(5)	1288(4)	8963(1)	50(1)
C(19)	4900(6)	3866(5)	9785(1)	60(1)
C(46)	3724(5)	9454(4)	8488(1)	44(1)
C(43)	7670(5)	4374(5)	9873(1)	54(1)
C(44)	6862(8)	3808(7)	10118(1)	80(2)
C(45)	5528(8)	3565(5)	10077(1)	76(2)

Table 3. Bond lengths [Å] and angles [°] for AZ01.

Cl(1)-Ru(1)	2.3219(9)
Ru(1)-C(39)	1.828(3)
Ru(1)-C(20)	1.965(3)
Ru(1)-O(1)	2.288(2)
Ru(1)-Cl(2)	2.3536(9)
O(1)-C(34)	1.368(4)
O(1)-C(41)	1.454(4)
C(39)-C(33)	1.456(4)
C(39)-H(39)	0.9500

C(3)-C(40)	1.375(5)
C(3)-C(4)	1.379(5)
C(3)-C(1)	1.509(5)
C(22)-C(23)	1.385(5)
C(22)-C(21)	1.396(5)
C(22)-C(27)	1.484(5)
C(1)-N(1)	1.486(4)
C(1)-C(2)	1.557(4)
C(1)-H(1)	1.0000
C(20)-N(1)	1.333(4)
C(20)-N(2)	1.364(4)
C(32)-C(31)	1.385(5)
C(32)-C(27)	1.403(5)
C(32)-N(2)	1.435(4)
C(38)-C(37)	1.387(5)
C(38)-C(33)	1.401(5)
C(38)-H(38)	0.9500
C(31)-C(30)	1.379(5)
C(31)-H(31)	0.9500
C(12)-C(13)	1.361(6)
C(12)-C(11)	1.379(6)
C(12)-C(16)	1.534(5)
N(2)-C(2)	1.486(4)
C(33)-C(34)	1.401(5)
C(13)-C(14)	1.395(5)
C(13)-H(13)	0.9500
C(15)-C(14)	1.504(5)
C(15)-H(15A)	0.9800

C(15)-H(15B)	0.9800
C(15)-H(15C)	0.9800
C(14)-C(10)	1.402(4)
C(4)-C(5)	1.374(6)
C(4)-H(4)	0.9500
C(23)-C(24)	1.374(6)
C(23)-H(23)	0.9500
C(10)-C(9)	1.390(5)
C(10)-N(1)	1.443(4)
C(18)-C(8)	1.372(6)
C(18)-C(19)	1.396(6)
C(18)-H(18)	0.9500
C(24)-C(25)	1.379(6)
C(24)-H(24)	0.9500
C(9)-C(11)	1.387(5)
C(9)-C(17)	1.504(5)
C(34)-C(35)	1.375(5)
C(2)-C(8)	1.492(5)
C(2)-H(2)	1.0000
C(25)-C(26)	1.369(6)
C(25)-H(25)	0.9500
C(35)-C(36)	1.393(6)
C(35)-H(35)	0.9500
C(28)-C(29)	1.376(6)
C(28)-C(27)	1.381(5)
C(28)-H(28)	0.9500
C(30)-C(29)	1.381(5)
C(30)-H(30)	0.9500

C(7)-C(40)	1.371(5)
C(7)-C(6)	1.377(6)
C(7)-H(7)	0.9500
C(8)-C(43)	1.409(5)
C(41)-C(46)	1.484(5)
C(41)-C(42)	1.505(6)
C(41)-H(41)	1.0000
C(6)-C(5)	1.372(6)
C(6)-H(6)	0.9500
C(36)-C(37)	1.371(6)
C(36)-H(36)	0.9500
C(11)-H(11)	0.9500
C(17)-H(17A)	0.9800
C(17)-H(17B)	0.9800
C(17)-H(17C)	0.9800
C(21)-C(26)	1.375(5)
C(21)-H(21)	0.9500
C(40)-H(40)	0.9500
C(29)-H(29)	0.9500
C(26)-H(26)	0.9500
C(16)-H(16A)	0.9800
C(16)-H(16B)	0.9800
C(16)-H(16C)	0.9800
C(42)-H(42A)	0.9800
C(42)-H(42B)	0.9800
C(42)-H(42C)	0.9800
C(37)-H(37)	0.9500
C(5)-H(5)	0.9500

C(19)-C(45)	1.365(8)
C(19)-H(19)	0.9500
C(46)-H(46A)	0.9800
C(46)-H(46B)	0.9800
C(46)-H(46C)	0.9800
C(43)-C(44)	1.384(7)
C(43)-H(43)	0.9500
C(44)-C(45)	1.328(9)
C(44)-H(44)	0.9500
C(45)-H(45)	0.9500
C(39)-Ru(1)-C(20)	100.57(14)
C(39)-Ru(1)-O(1)	78.48(12)
C(20)-Ru(1)-O(1)	178.08(11)
C(39)-Ru(1)-Cl(1)	97.75(11)
C(20)-Ru(1)-Cl(1)	94.65(9)
O(1)-Ru(1)-Cl(1)	87.15(7)
C(39)-Ru(1)-Cl(2)	104.46(11)
C(20)-Ru(1)-Cl(2)	90.05(9)
O(1)-Ru(1)-Cl(2)	88.58(7)
Cl(1)-Ru(1)-Cl(2)	156.05(3)
C(34)-O(1)-C(41)	119.2(3)
C(34)-O(1)-Ru(1)	109.9(2)
C(41)-O(1)-Ru(1)	130.8(2)
C(33)-C(39)-Ru(1)	118.4(2)
C(33)-C(39)-H(39)	120.8
Ru(1)-C(39)-H(39)	120.8
C(40)-C(3)-C(4)	118.5(3)
C(40)-C(3)-C(1)	121.8(3)

C(4)-C(3)-C(1)	119.5(3)
C(23)-C(22)-C(21)	118.0(3)
C(23)-C(22)-C(27)	119.9(3)
C(21)-C(22)-C(27)	122.0(3)
N(1)-C(1)-C(3)	113.6(3)
N(1)-C(1)-C(2)	102.2(2)
C(3)-C(1)-C(2)	116.3(3)
N(1)-C(1)-H(1)	108.1
C(3)-C(1)-H(1)	108.1
C(2)-C(1)-H(1)	108.1
N(1)-C(20)-N(2)	107.2(3)
N(1)-C(20)-Ru(1)	133.1(2)
N(2)-C(20)-Ru(1)	119.3(2)
C(31)-C(32)-C(27)	119.8(3)
C(31)-C(32)-N(2)	119.1(3)
C(27)-C(32)-N(2)	121.0(3)
C(37)-C(38)-C(33)	120.4(4)
C(37)-C(38)-H(38)	119.8
C(33)-C(38)-H(38)	119.8
C(30)-C(31)-C(32)	120.8(3)
C(30)-C(31)-H(31)	119.6
C(32)-C(31)-H(31)	119.6
C(13)-C(12)-C(11)	118.8(3)
C(13)-C(12)-C(16)	120.2(4)
C(11)-C(12)-C(16)	121.0(4)
C(20)-N(2)-C(32)	124.7(3)
C(20)-N(2)-C(2)	114.3(3)
C(32)-N(2)-C(2)	120.9(3)

C(38)-C(33)-C(34)	118.2(3)
C(38)-C(33)-C(39)	122.9(3)
C(34)-C(33)-C(39)	118.9(3)
C(12)-C(13)-C(14)	121.9(4)
C(12)-C(13)-H(13)	119.1
C(14)-C(13)-H(13)	119.1
C(14)-C(15)-H(15A)	109.5
C(14)-C(15)-H(15B)	109.5
H(15A)-C(15)-H(15B)	109.5
C(14)-C(15)-H(15C)	109.5
H(15A)-C(15)-H(15C)	109.5
H(15B)-C(15)-H(15C)	109.5
C(13)-C(14)-C(10)	117.6(3)
C(13)-C(14)-C(15)	120.4(3)
C(10)-C(14)-C(15)	122.0(3)
C(5)-C(4)-C(3)	120.2(4)
C(5)-C(4)-H(4)	119.9
C(3)-C(4)-H(4)	119.9
C(24)-C(23)-C(22)	121.0(4)
C(24)-C(23)-H(23)	119.5
C(22)-C(23)-H(23)	119.5
C(9)-C(10)-C(14)	121.9(3)
C(9)-C(10)-N(1)	119.0(3)
C(14)-C(10)-N(1)	118.9(3)
C(8)-C(18)-C(19)	120.7(5)
C(8)-C(18)-H(18)	119.7
C(19)-C(18)-H(18)	119.7
C(23)-C(24)-C(25)	120.1(4)

C(23)-C(24)-H(24)	120.0
C(25)-C(24)-H(24)	120.0
C(20)-N(1)-C(10)	128.3(3)
C(20)-N(1)-C(1)	114.2(2)
C(10)-N(1)-C(1)	116.9(2)
C(11)-C(9)-C(10)	117.1(3)
C(11)-C(9)-C(17)	121.3(3)
C(10)-C(9)-C(17)	121.6(3)
O(1)-C(34)-C(35)	125.7(4)
O(1)-C(34)-C(33)	112.5(3)
C(35)-C(34)-C(33)	121.8(3)
N(2)-C(2)-C(8)	114.3(3)
N(2)-C(2)-C(1)	101.2(2)
C(8)-C(2)-C(1)	111.2(3)
N(2)-C(2)-H(2)	109.9
C(8)-C(2)-H(2)	109.9
C(1)-C(2)-H(2)	109.9
C(26)-C(25)-C(24)	119.7(4)
C(26)-C(25)-H(25)	120.1
C(24)-C(25)-H(25)	120.1
C(34)-C(35)-C(36)	118.2(4)
C(34)-C(35)-H(35)	120.9
C(36)-C(35)-H(35)	120.9
C(29)-C(28)-C(27)	122.8(3)
C(29)-C(28)-H(28)	118.6
C(27)-C(28)-H(28)	118.6
C(31)-C(30)-C(29)	119.9(3)
C(31)-C(30)-H(30)	120.0

C(29)-C(30)-H(30)	120.0
C(40)-C(7)-C(6)	120.0(4)
C(40)-C(7)-H(7)	120.0
C(6)-C(7)-H(7)	120.0
C(18)-C(8)-C(43)	118.6(4)
C(18)-C(8)-C(2)	122.7(4)
C(43)-C(8)-C(2)	118.6(4)
C(28)-C(27)-C(32)	117.7(3)
C(28)-C(27)-C(22)	119.1(3)
C(32)-C(27)-C(22)	123.2(3)
O(1)-C(41)-C(46)	107.5(3)
O(1)-C(41)-C(42)	110.2(3)
C(46)-C(41)-C(42)	113.5(4)
O(1)-C(41)-H(41)	108.5
C(46)-C(41)-H(41)	108.5
C(42)-C(41)-H(41)	108.5
C(5)-C(6)-C(7)	119.1(4)
C(5)-C(6)-H(6)	120.5
C(7)-C(6)-H(6)	120.5
C(37)-C(36)-C(35)	121.9(3)
C(37)-C(36)-H(36)	119.1
C(35)-C(36)-H(36)	119.1
C(12)-C(11)-C(9)	122.6(3)
C(12)-C(11)-H(11)	118.7
C(9)-C(11)-H(11)	118.7
C(9)-C(17)-H(17A)	109.5
C(9)-C(17)-H(17B)	109.5
H(17A)-C(17)-H(17B)	109.5

C(9)-C(17)-H(17C)	109.5
H(17A)-C(17)-H(17C)	109.5
H(17B)-C(17)-H(17C)	109.5
C(26)-C(21)-C(22)	120.6(3)
C(26)-C(21)-H(21)	119.7
C(22)-C(21)-H(21)	119.7
C(7)-C(40)-C(3)	121.3(4)
C(7)-C(40)-H(40)	119.4
C(3)-C(40)-H(40)	119.4
C(28)-C(29)-C(30)	118.9(3)
C(28)-C(29)-H(29)	120.5
C(30)-C(29)-H(29)	120.5
C(25)-C(26)-C(21)	120.5(4)
C(25)-C(26)-H(26)	119.7
C(21)-C(26)-H(26)	119.7
C(12)-C(16)-H(16A)	109.5
C(12)-C(16)-H(16B)	109.5
H(16A)-C(16)-H(16B)	109.5
C(12)-C(16)-H(16C)	109.5
H(16A)-C(16)-H(16C)	109.5
H(16B)-C(16)-H(16C)	109.5
C(41)-C(42)-H(42A)	109.5
C(41)-C(42)-H(42B)	109.5
H(42A)-C(42)-H(42B)	109.5
C(41)-C(42)-H(42C)	109.5
H(42A)-C(42)-H(42C)	109.5
H(42B)-C(42)-H(42C)	109.5
C(36)-C(37)-C(38)	119.5(4)

C(36)-C(37)-H(37)	120.3
C(38)-C(37)-H(37)	120.3
C(4)-C(5)-C(6)	120.9(4)
C(4)-C(5)-H(5)	119.5
C(6)-C(5)-H(5)	119.6
C(45)-C(19)-C(18)	119.4(5)
C(45)-C(19)-H(19)	120.3
C(18)-C(19)-H(19)	120.3
C(41)-C(46)-H(46A)	109.5
C(41)-C(46)-H(46B)	109.5
H(46A)-C(46)-H(46B)	109.5
C(41)-C(46)-H(46C)	109.5
H(46A)-C(46)-H(46C)	109.5
H(46B)-C(46)-H(46C)	109.5
C(44)-C(43)-C(8)	118.5(5)
C(44)-C(43)-H(43)	120.8
C(8)-C(43)-H(43)	120.8
C(45)-C(44)-C(43)	122.2(5)
C(45)-C(44)-H(44)	118.9
C(43)-C(44)-H(44)	118.9
C(44)-C(45)-C(19)	120.5(5)
C(44)-C(45)-H(45)	119.7
C(19)-C(45)-H(45)	119.7

Symmetry transformations used to generate equivalent atoms:

Table 4. Anisotropic displacement parameters ($Å^2 x 10^3$) for AZ01. The anisotropic displacement factor exponent takes the form: $-2\pi^2[h^2 a^{*2}U^{11} + ... + 2 h k a^* b^* U^{12}]$

	U^{11}	U^{22}	U^{33}	U^{23}	U^{13}	U^{12}
Cl(1)	46(1)	29(1)	37(1)	7(1)	-8(1)	-10(1)
Ru(1)	27(1)	21(1)	19(1)	1(1)	-2(1)	0(1)
Cl(2)	32(1)	32(1)	29(1)	-3(1)	-1(1)	-6(1)
O(1)	38(1)	35(1)	25(1)	4(1)	-3(1)	10(1)
C(39)	32(2)	29(2)	19(2)	0(1)	-1(1)	0(1)
C(3)	34(2)	25(2)	18(2)	2(1)	1(1)	4(1)
C(22)	33(2)	21(1)	32(2)	-4(2)	-2(1)	-4(2)
C(1)	27(2)	22(2)	20(2)	0(1)	1(1)	-1(1)
C(20)	23(2)	22(2)	19(1)	0(1)	-1(1)	-5(1)
C(32)	31(2)	19(1)	18(2)	0(1)	2(1)	0(1)
C(38)	37(2)	39(2)	24(2)	1(2)	1(1)	-8(2)
C(31)	28(2)	27(2)	32(2)	-6(2)	-3(1)	2(2)
C(12)	54(2)	39(2)	28(2)	-11(2)	-5(2)	17(2)
N(2)	27(1)	21(1)	18(1)	1(1)	-2(1)	1(1)
C(33)	33(2)	28(2)	25(2)	4(1)	-3(1)	-7(1)
C(13)	47(2)	31(2)	31(2)	-7(2)	-11(2)	3(2)
C(15)	39(2)	32(2)	37(2)	2(2)	-2(2)	-8(2)
C(14)	39(2)	21(2)	24(2)	1(1)	-5(1)	1(1)
C(4)	40(2)	31(2)	40(2)	1(2)	8(2)	1(2)
C(23)	35(2)	50(2)	32(2)	-4(2)	-2(2)	-1(2)
C(10)	30(2)	20(1)	19(1)	-1(1)	-3(1)	5(1)
C(18)	54(3)	41(2)	35(2)	3(2)	10(2)	-4(2)
C(24)	38(2)	64(3)	38(2)	2(2)	-13(2)	-9(2)

N(1)	29(1)	24(1)	12(1)	0(1)	0(1)	0(1)
C(9)	30(2)	30(2)	25(2)	2(1)	-1(1)	8(1)
C(34)	39(2)	34(2)	25(2)	3(1)	-5(2)	-7(2)
C(2)	27(2)	26(2)	19(2)	-1(1)	-2(1)	4(1)
C(25)	26(2)	45(2)	65(3)	1(2)	-5(2)	-6(2)
C(35)	53(2)	41(2)	33(2)	9(2)	-14(2)	4(2)
C(28)	42(2)	31(2)	30(2)	-9(2)	-1(2)	-5(2)
C(30)	30(2)	36(2)	38(2)	-4(2)	1(2)	7(2)
C(7)	34(2)	53(3)	44(2)	2(2)	-5(2)	3(2)
C(8)	49(2)	26(2)	22(2)	1(1)	6(2)	8(2)
C(27)	32(2)	28(2)	19(2)	0(1)	3(1)	-1(1)
C(41)	38(2)	32(2)	44(2)	6(2)	-3(2)	6(2)
C(6)	40(2)	53(2)	38(2)	4(2)	8(2)	19(2)
C(36)	62(3)	50(2)	27(2)	14(2)	-14(2)	-11(2)
C(11)	37(2)	50(2)	20(2)	1(2)	4(1)	13(2)
C(17)	35(2)	49(2)	34(2)	4(2)	8(2)	-6(2)
C(21)	35(2)	32(2)	30(2)	2(1)	1(2)	-6(2)
C(40)	40(2)	29(2)	46(2)	-3(2)	-7(2)	4(2)
C(29)	49(3)	28(2)	41(2)	-11(2)	6(2)	5(2)
C(26)	31(2)	37(2)	43(2)	0(2)	8(2)	-9(1)
C(16)	85(3)	65(3)	43(2)	-29(2)	2(3)	15(3)
C(42)	36(2)	69(3)	71(3)	11(3)	-14(2)	-3(2)
C(37)	47(2)	52(3)	18(2)	5(2)	0(2)	-14(2)
C(5)	65(3)	29(2)	57(3)	-1(2)	14(2)	17(2)
C(19)	72(3)	46(2)	62(3)	-2(2)	38(3)	-5(2)
C(46)	53(2)	35(2)	44(2)	-2(2)	9(2)	9(2)
C(43)	72(3)	66(3)	24(2)	10(2)	6(2)	26(3)
C(44)	127(5)	86(4)	28(2)	23(3)	31(3)	52(4)

C(45)	130(5)	51(3)	46(3)	20(2)	58(3)	21(3)

Table 5. Hydrogen coordinates (x 10^4) and isotropic displacement parameters ($Å^2$x 10^{3}) for AZ02.

	x	y	z	U(eq)
H(39)	7424	5580	8038	32
H(1)	7480	3228	9074	28
H(38)	7876	6205	7430	40
H(31)	4918	7267	9089	35
H(13)	6716	1236	8037	44
H(15A)	6058	1832	8732	54
H(15B)	5067	2253	8434	54
H(15C)	5605	3384	8686	54
H(4)	8885	1382	8935	45
H(23)	9348	7974	9912	47
H(18)	5244	4622	9324	52
H(24)	11638	7398	9987	56
H(2)	8866	5424	9377	29
H(25)	13039	6962	9533	54
H(35)	4620	9704	7519	51
H(28)	8064	10117	9597	41
H(30)	4220	9386	9277	42
H(7)	12856	3920	9105	52
H(41)	4014	10091	8016	45

H(6)	13021	1599	8996	52
H(36)	5742	9271	7019	55
H(11)	10136	3307	7820	43
H(17A)	9651	6002	8354	59
H(17B)	10704	5375	8092	59
H(17C)	10789	4930	8470	59
H(21)	9888	7836	8926	39
H(40)	10720	4951	9131	46
H(29)	5794	10798	9548	47
H(26)	12174	7247	9006	45
H(16A)	9178	276	7705	97
H(16B)	9429	1519	7458	97
H(16C)	7919	890	7498	97
H(42A)	2813	8323	7746	88
H(42B)	1830	9124	7996	88
H(42C)	2438	7672	8096	88
H(37)	7352	7552	6972	47
H(5)	11022	339	8924	61
H(19)	3942	3706	9757	72
H(46A)	3527	8597	8601	66
H(46B)	2967	10094	8526	66
H(46C)	4583	9840	8574	66
H(43)	8614	4570	9911	65
H(44)	7275	3587	10324	96
H(45)	5007	3179	10251	91

Table 6. Torsion angles [°] for AZ01.

C(39)-Ru(1)-O(1)-C(34)	-11.8(2)
C(20)-Ru(1)-O(1)-C(34)	-72(3)
Cl(1)-Ru(1)-O(1)-C(34)	86.7(2)
Cl(2)-Ru(1)-O(1)-C(34)	-116.9(2)
C(39)-Ru(1)-O(1)-C(41)	163.0(3)
C(20)-Ru(1)-O(1)-C(41)	103(3)
Cl(1)-Ru(1)-O(1)-C(41)	-98.5(3)
Cl(2)-Ru(1)-O(1)-C(41)	58.0(3)
C(20)-Ru(1)-C(39)-C(33)	-169.9(3)
O(1)-Ru(1)-C(39)-C(33)	11.8(2)
Cl(1)-Ru(1)-C(39)-C(33)	-73.7(3)
Cl(2)-Ru(1)-C(39)-C(33)	97.3(3)
C(40)-C(3)-C(1)-N(1)	79.4(4)
C(4)-C(3)-C(1)-N(1)	-96.8(4)
C(40)-C(3)-C(1)-C(2)	-38.9(4)
C(4)-C(3)-C(1)-C(2)	144.9(3)
C(39)-Ru(1)-C(20)-N(1)	-22.2(3)
O(1)-Ru(1)-C(20)-N(1)	38(4)
Cl(1)-Ru(1)-C(20)-N(1)	-121.0(3)
Cl(2)-Ru(1)-C(20)-N(1)	82.5(3)
C(39)-Ru(1)-C(20)-N(2)	166.4(2)
O(1)-Ru(1)-C(20)-N(2)	-134(3)
Cl(1)-Ru(1)-C(20)-N(2)	67.6(2)
Cl(2)-Ru(1)-C(20)-N(2)	-88.9(2)
C(27)-C(32)-C(31)-C(30)	2.9(5)
N(2)-C(32)-C(31)-C(30)	-177.7(3)

N(1)-C(20)-N(2)-C(32)	174.5(3)
Ru(1)-C(20)-N(2)-C(32)	-12.0(4)
N(1)-C(20)-N(2)-C(2)	-1.3(4)
Ru(1)-C(20)-N(2)-C(2)	172.1(2)
C(31)-C(32)-N(2)-C(20)	64.0(4)
C(27)-C(32)-N(2)-C(20)	-116.7(4)
C(31)-C(32)-N(2)-C(2)	-120.5(4)
C(27)-C(32)-N(2)-C(2)	58.9(4)
C(37)-C(38)-C(33)-C(34)	0.6(5)
C(37)-C(38)-C(33)-C(39)	-177.6(3)
Ru(1)-C(39)-C(33)-C(38)	166.8(3)
Ru(1)-C(39)-C(33)-C(34)	-11.4(4)
C(11)-C(12)-C(13)-C(14)	-2.2(6)
C(16)-C(12)-C(13)-C(14)	176.1(4)
C(12)-C(13)-C(14)-C(10)	0.6(5)
C(12)-C(13)-C(14)-C(15)	-177.9(3)
C(40)-C(3)-C(4)-C(5)	1.1(6)
C(1)-C(3)-C(4)-C(5)	177.4(3)
C(21)-C(22)-C(23)-C(24)	-1.7(6)
C(27)-C(22)-C(23)-C(24)	179.6(4)
C(13)-C(14)-C(10)-C(9)	0.8(5)
C(15)-C(14)-C(10)-C(9)	179.2(3)
C(13)-C(14)-C(10)-N(1)	-173.5(3)
C(15)-C(14)-C(10)-N(1)	4.9(4)
C(22)-C(23)-C(24)-C(25)	-0.4(7)
N(2)-C(20)-N(1)-C(10)	178.6(3)
Ru(1)-C(20)-N(1)-C(10)	6.5(5)
N(2)-C(20)-N(1)-C(1)	7.6(4)

Ru(1)-C(20)-N(1)-C(1)	-164.6(2)
C(9)-C(10)-N(1)-C(20)	86.3(4)
C(14)-C(10)-N(1)-C(20)	-99.2(4)
C(9)-C(10)-N(1)-C(1)	-102.8(3)
C(14)-C(10)-N(1)-C(1)	71.7(4)
C(3)-C(1)-N(1)-C(20)	-136.4(3)
C(2)-C(1)-N(1)-C(20)	-10.2(3)
C(3)-C(1)-N(1)-C(10)	51.5(4)
C(2)-C(1)-N(1)-C(10)	177.6(3)
C(14)-C(10)-C(9)-C(11)	-0.5(5)
N(1)-C(10)-C(9)-C(11)	173.8(3)
C(14)-C(10)-C(9)-C(17)	178.5(3)
N(1)-C(10)-C(9)-C(17)	-7.2(5)
C(41)-O(1)-C(34)-C(35)	14.9(5)
Ru(1)-O(1)-C(34)-C(35)	-169.6(3)
C(41)-O(1)-C(34)-C(33)	-166.8(3)
Ru(1)-O(1)-C(34)-C(33)	8.8(3)
C(38)-C(33)-C(34)-O(1)	-178.5(3)
C(39)-C(33)-C(34)-O(1)	-0.2(5)
C(38)-C(33)-C(34)-C(35)	-0.1(5)
C(39)-C(33)-C(34)-C(35)	178.3(3)
C(20)-N(2)-C(2)-C(8)	-124.4(3)
C(32)-N(2)-C(2)-C(8)	59.6(4)
C(20)-N(2)-C(2)-C(1)	-4.7(3)
C(32)-N(2)-C(2)-C(1)	179.2(3)
N(1)-C(1)-C(2)-N(2)	8.1(3)
C(3)-C(1)-C(2)-N(2)	132.5(3)
N(1)-C(1)-C(2)-C(8)	129.9(3)

C(3)-C(1)-C(2)-C(8)	-105.7(3)
C(23)-C(24)-C(25)-C(26)	2.2(7)
O(1)-C(34)-C(35)-C(36)	177.8(4)
C(33)-C(34)-C(35)-C(36)	-0.4(6)
C(32)-C(31)-C(30)-C(29)	-2.9(6)
C(19)-C(18)-C(8)-C(43)	-2.1(6)
C(19)-C(18)-C(8)-C(2)	174.0(4)
N(2)-C(2)-C(8)-C(18)	42.8(5)
C(1)-C(2)-C(8)-C(18)	-71.0(4)
N(2)-C(2)-C(8)-C(43)	-141.2(3)
C(1)-C(2)-C(8)-C(43)	105.0(4)
C(29)-C(28)-C(27)-C(32)	0.4(6)
C(29)-C(28)-C(27)-C(22)	179.9(4)
C(31)-C(32)-C(27)-C(28)	-1.6(5)
N(2)-C(32)-C(27)-C(28)	179.0(3)
C(31)-C(32)-C(27)-C(22)	178.9(3)
N(2)-C(32)-C(27)-C(22)	-0.4(5)
C(23)-C(22)-C(27)-C(28)	61.3(5)
C(21)-C(22)-C(27)-C(28)	-117.4(4)
C(23)-C(22)-C(27)-C(32)	-119.3(4)
C(21)-C(22)-C(27)-C(32)	62.0(5)
C(34)-O(1)-C(41)-C(46)	-166.9(3)
Ru(1)-O(1)-C(41)-C(46)	18.7(4)
C(34)-O(1)-C(41)-C(42)	69.0(4)
Ru(1)-O(1)-C(41)-C(42)	-105.4(3)
C(40)-C(7)-C(6)-C(5)	-0.4(7)
C(34)-C(35)-C(36)-C(37)	0.4(6)
C(13)-C(12)-C(11)-C(9)	2.5(6)

C(16)-C(12)-C(11)-C(9)	-175.7(4)
C(10)-C(9)-C(11)-C(12)	-1.2(5)
C(17)-C(9)-C(11)-C(12)	179.8(3)
C(23)-C(22)-C(21)-C(26)	1.9(5)
C(27)-C(22)-C(21)-C(26)	-179.4(3)
C(6)-C(7)-C(40)-C(3)	-0.2(7)
C(4)-C(3)-C(40)-C(7)	-0.2(6)
C(1)-C(3)-C(40)-C(7)	-176.3(4)
C(27)-C(28)-C(29)-C(30)	-0.4(6)
C(31)-C(30)-C(29)-C(28)	1.6(6)
C(24)-C(25)-C(26)-C(21)	-2.0(6)
C(22)-C(21)-C(26)-C(25)	0.0(6)
C(35)-C(36)-C(37)-C(38)	0.1(6)
C(33)-C(38)-C(37)-C(36)	-0.7(6)
C(3)-C(4)-C(5)-C(6)	-1.7(6)
C(7)-C(6)-C(5)-C(4)	1.4(7)
C(8)-C(18)-C(19)-C(45)	-0.1(7)
C(18)-C(8)-C(43)-C(44)	3.3(7)
C(2)-C(8)-C(43)-C(44)	-172.9(4)
C(8)-C(43)-C(44)-C(45)	-2.4(9)
C(43)-C(44)-C(45)-C(19)	0.2(9)
C(18)-C(19)-C(45)-C(44)	1.1(8)

Symmetry transformations used to generate equivalent atoms:

■ Crystal Structure 2.113

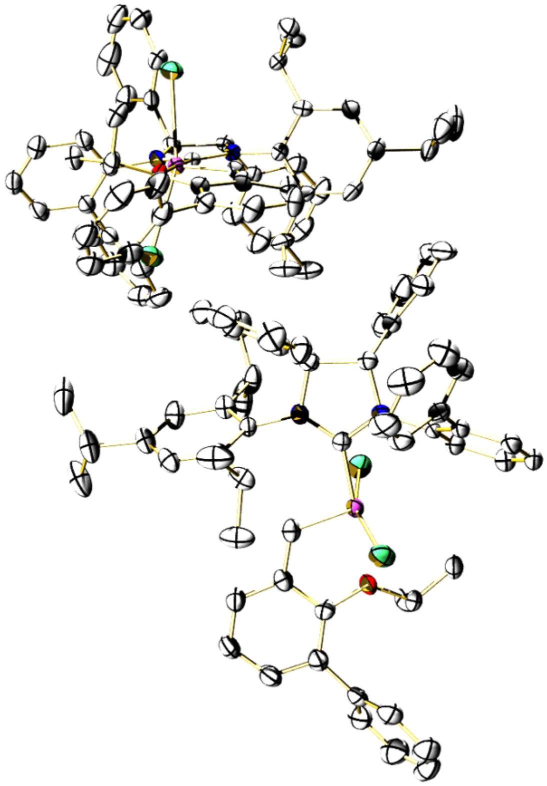

Identification code	az04mono	
Empirical formula	C58 H60 I2 N2 O Ru	
Formula weight	1155.95	
Temperature	193(2) K	
Wavelength	0.71073 Å	
Crystal system	Monoclinic	
Space group	P2(1)	
Unit cell dimensions	a = 12.751(2) Å	a= 90°.
	b = 19.648(3) Å	b= 90.153(3)°.
	c = 20.240(3) Å	g = 90°.
Volume	5071.0(14) Å^3	
Z	4	
Density (calculated)	1.514 Mg/m^3	

Absorption coefficient	1.568 mm^{-1}
F(000)	2320
Crystal size	0.10 x 0.10 x 0.08 mm^3
Theta range for data collection	1.01 to 28.40°.
Index ranges	-7<=h<=16, -25<=k<=26, -26<=l<=27
Reflections collected	38430
Independent reflections	24724 [R(int) = 0.0235]
Completeness to theta = 28.40°	99.0 %
Absorption correction	Empirical
Max. and min. transmission	0.8848 and 0.8590
Refinement method	Full-matrix least-squares on F^2
Data / restraints / parameters	24724 / 1 / 1169
Goodness-of-fit on F^2	1.032
Final R indices [I>2sigma(I)]	R1 = 0.0420, wR2 = 0.0954
R indices (all data)	R1 = 0.0511, wR2 = 0.1007
Absolute structure parameter	-0.032(11)
Largest diff. peak and hole	1.150 and -0.572 e.Å^{-3}

Table 2. Atomic coordinates (x 10^4) and equivalent isotropic displacement parameters (Å^{2}x 10^3) for AZ04mono. U(eq) is defined as one third of the trace of the orthogonalized U^{ij} tensor.

	x	y	z	U(eq)
Ru(1)	4473(1)	7532(1)	3426(1)	26(1)
I(2)	4509(1)	6723(1)	2377(1)	44(1)
Ru(2)	526(1)	8116(1)	8427(1)	26(1)
I(4)	493(1)	8925(1)	7379(1)	45(1)
I(3)	-115(1)	7385(1)	9465(1)	40(1)
I(1)	5113(1)	8264(1)	4465(1)	40(1)
C(19)	1203(4)	7302(2)	3650(2)	29(1)

C(41)	3801(4)	8346(2)	8652(2)	31(1)
O(2)	5339(2)	8276(2)	2726(2)	32(1)
O(1)	-336(2)	7373(2)	7728(2)	32(1)
C(18)	331(4)	7720(3)	3620(3)	39(1)
C(42)	4681(4)	7927(3)	8621(3)	39(1)
C(30)	1303(3)	8756(2)	9013(2)	24(1)
C(27)	3434(4)	8137(2)	3205(2)	32(1)
C(49)	1562(4)	7512(2)	8205(2)	31(1)
C(3)	3702(3)	6892(2)	4015(2)	25(1)
C(2)	3618(4)	5972(2)	4771(2)	30(1)
C(23)	5213(4)	6098(2)	4047(2)	28(1)
C(24)	5339(4)	5440(3)	3772(2)	30(1)
C(26)	6059(4)	6505(3)	4143(2)	36(1)
C(31)	811(4)	9655(3)	10441(2)	33(1)
C(34)	-334(4)	10205(3)	8775(2)	31(1)
N(4)	807(3)	9321(2)	9246(2)	29(1)
N(2)	4192(3)	6328(2)	4244(2)	29(1)
C(28)	2440(4)	9295(2)	9778(2)	29(1)
C(37)	-219(4)	9549(2)	9047(2)	27(1)
C(50)	1390(4)	6997(2)	7713(2)	32(1)
C(54)	3613(4)	8654(2)	2710(2)	33(1)
C(29)	1373(4)	9676(2)	9774(2)	31(1)
C(52)	357(4)	6943(2)	7435(2)	32(1)
C(53)	-1487(4)	7271(3)	7678(2)	35(1)
C(11)	634(4)	6124(3)	4891(3)	44(1)
C(35)	-1066(4)	9143(3)	9139(2)	35(1)
C(47)	3613(4)	8848(3)	8096(2)	39(1)
C(39)	4371(5)	9515(3)	9887(3)	45(1)
C(57)	6490(4)	8376(3)	2678(2)	34(1)
C(4)	4188(4)	5992(3)	5439(2)	36(1)
C(13)	1881(3)	7373(2)	4191(2)	27(1)
C(45)	3325(4)	7780(2)	9681(2)	33(1)
C(56)	4640(4)	8708(2)	2434(2)	31(1)
C(38)	3410(4)	9726(3)	9653(2)	34(1)

C(58)	6989(4)	7764(3)	2995(3)	38(1)
N(1)	2735(3)	6903(2)	4283(2)	27(1)
C(22)	1383(4)	6799(3)	3093(2)	39(1)
C(16)	771(4)	8262(3)	4612(3)	40(1)
C(40)	3118(3)	8277(2)	9194(2)	29(1)
C(1)	2559(4)	6355(2)	4782(2)	29(1)
C(10)	1589(4)	5918(3)	4648(2)	33(1)
C(44)	4229(4)	7388(3)	9610(3)	39(1)
C(7)	4902(5)	6607(5)	6365(3)	65(2)
C(5)	4447(5)	5387(4)	5751(3)	51(2)
N(3)	2263(3)	8742(2)	9289(2)	29(1)
C(43)	4915(4)	7458(3)	9089(3)	41(1)
C(14)	1670(4)	7869(2)	4684(2)	32(1)
C(9)	4935(6)	5402(5)	6366(3)	69(2)
C(17)	79(4)	8184(3)	4089(3)	39(1)
C(51)	2184(4)	6573(3)	7497(3)	39(1)
C(59)	6794(4)	9036(3)	2997(3)	41(1)
C(25)	6357(4)	5245(3)	3613(2)	38(1)
C(55)	2817(4)	9077(3)	2492(3)	39(1)
C(46)	2620(4)	7658(3)	10277(3)	43(1)
C(36)	-2072(4)	9349(3)	8958(3)	40(1)
C(6)	4438(5)	6610(4)	5751(3)	50(2)
C(12)	-268(5)	5751(4)	4781(3)	55(2)
C(33)	-1354(4)	10404(3)	8612(2)	41(1)
C(32)	565(4)	9051(3)	10745(3)	48(1)
C(15)	2366(4)	7995(3)	5274(3)	44(1)
C(8)	5126(5)	6009(5)	6669(3)	69(2)
C(60)	4471(4)	4945(3)	3655(2)	34(1)
C(65)	5804(4)	9243(3)	1517(2)	41(1)
C(64)	4812(4)	9164(3)	1900(3)	39(1)
C(62)	-220(5)	5163(4)	4428(3)	56(2)
C(61)	7216(4)	5669(3)	3699(2)	42(1)
C(63)	456(6)	6299(3)	3034(3)	56(2)
C(67)	3435(5)	8481(3)	7430(2)	49(2)

C(66)	1999(4)	6105(3)	7008(3)	45(1)
C(68)	-2215(4)	9988(3)	8700(2)	41(1)
C(75)	4464(5)	4326(3)	3990(3)	45(1)
C(76)	6324(5)	9871(3)	1521(3)	50(1)
C(74)	3688(5)	5050(3)	3184(2)	44(1)
C(72)	-683(6)	9352(3)	3933(4)	68(2)
C(71)	-924(5)	8609(3)	4050(3)	50(2)
C(70)	1552(5)	7170(3)	2430(2)	49(2)
C(69)	3001(5)	9540(3)	2007(3)	47(1)
C(73)	1623(5)	5319(3)	4304(3)	47(1)
C(79)	-814(4)	6409(3)	6516(2)	42(1)
C(82)	-1797(4)	6607(3)	7998(3)	43(1)
C(92)	528(4)	10703(3)	8653(2)	35(1)
C(77)	192(4)	6487(3)	6897(2)	36(1)
C(88)	5215(5)	10488(4)	9428(3)	52(2)
C(100)	6187(5)	8731(4)	1122(3)	52(2)
C(91)	1315(5)	10598(3)	8189(3)	44(1)
C(83)	-1991(4)	7888(3)	7993(3)	40(1)
C(95)	2968(6)	3945(4)	3394(3)	61(2)
C(78)	1020(5)	6075(3)	6718(3)	46(1)
C(81)	-1331(5)	5781(4)	6526(3)	51(2)
C(101)	3979(5)	9574(3)	1724(3)	46(1)
C(102)	7232(5)	9973(4)	1159(3)	62(2)
C(86)	4550(6)	9350(3)	8035(3)	55(2)
C(93)	2045(5)	11094(4)	8057(3)	56(2)
C(97)	732(5)	4946(3)	4184(3)	57(2)
C(85)	3139(6)	7901(4)	10916(3)	64(2)
C(84)	5920(5)	7039(3)	9046(3)	50(2)
C(99)	2645(5)	8747(4)	5346(4)	68(2)
C(98)	1853(5)	7753(4)	5910(3)	63(2)
C(89)	554(5)	10260(4)	10750(3)	52(2)
C(94)	2954(5)	4548(4)	3059(3)	57(2)
C(80)	-1183(5)	6927(4)	6123(3)	51(2)
C(96)	3725(6)	3838(3)	3868(3)	58(2)

C(90)	94(5)	9034(5)	11361(3)	66(2)
C(87)	5267(5)	9896(4)	9781(3)	57(2)
C(107)	2028(6)	11706(4)	8400(3)	62(2)
C(117)	7124(6)	8836(5)	746(3)	66(2)
C(118)	7072(4)	6302(3)	3961(3)	42(1)
C(109)	4274(5)	10698(3)	9190(4)	59(2)
C(113)	-2128(6)	6811(5)	5743(3)	66(2)
C(108)	3377(5)	10326(3)	9301(3)	49(1)
C(114)	-2622(5)	6191(5)	5773(3)	66(2)
C(110)	6614(5)	7138(4)	9653(4)	77(2)
C(115)	-2227(5)	5673(4)	6160(3)	64(2)
C(116)	7617(5)	9458(5)	778(3)	65(2)
C(105)	538(5)	11324(3)	8986(3)	48(1)
C(106)	1276(6)	11808(3)	8869(3)	58(2)
C(112)	2346(5)	6898(3)	10344(4)	64(2)
C(119)	-1613(5)	8505(4)	4653(4)	76(2)
C(104)	-127(5)	9640(5)	11672(3)	70(2)
C(103)	70(5)	10246(5)	11367(4)	69(2)
C(111)	5680(6)	6294(3)	8928(4)	67(2)

Table 3. Bond lengths [Å] and angles [°] for AZ04mono.

Ru(1)-C(27)	1.835(5)
Ru(1)-C(3)	1.995(5)
Ru(1)-O(2)	2.316(3)
Ru(1)-I(2)	2.6521(6)
Ru(1)-I(1)	2.6727(5)
Ru(2)-C(49)	1.834(5)
Ru(2)-C(30)	1.991(4)
Ru(2)-O(1)	2.310(3)
Ru(2)-I(4)	2.6509(6)
Ru(2)-I(3)	2.6756(5)
C(19)-C(18)	1.382(7)

C(19)-C(13)	1.400(6)
C(19)-C(22)	1.517(7)
C(41)-C(42)	1.393(7)
C(41)-C(40)	1.411(6)
C(41)-C(47)	1.515(7)
O(2)-C(56)	1.365(6)
O(2)-C(57)	1.484(6)
O(1)-C(52)	1.360(6)
O(1)-C(53)	1.484(6)
C(18)-C(17)	1.356(8)
C(18)-H(18)	0.9500
C(42)-C(43)	1.356(8)
C(42)-H(42)	0.9500
C(30)-N(3)	1.344(6)
C(30)-N(4)	1.362(6)
C(27)-C(54)	1.444(7)
C(27)-H(27)	0.9500
C(49)-C(50)	1.437(7)
C(49)-H(49)	0.9500
C(3)-N(1)	1.347(6)
C(3)-N(2)	1.353(6)
C(2)-N(2)	1.473(6)
C(2)-C(4)	1.534(7)
C(2)-C(1)	1.546(7)
C(2)-H(2)	1.0000
C(23)-C(26)	1.356(7)
C(23)-C(24)	1.416(7)
C(23)-N(2)	1.435(6)
C(24)-C(25)	1.392(7)
C(24)-C(60)	1.493(7)
C(26)-C(118)	1.401(7)
C(26)-H(26)	0.9500
C(31)-C(32)	1.374(8)
C(31)-C(89)	1.383(8)

C(31)-C(29)	1.530(7)
C(34)-C(33)	1.396(7)
C(34)-C(37)	1.408(7)
C(34)-C(92)	1.493(8)
N(4)-C(37)	1.439(6)
N(4)-C(29)	1.465(6)
C(28)-N(3)	1.486(6)
C(28)-C(38)	1.522(7)
C(28)-C(29)	1.553(7)
C(28)-H(28)	1.0000
C(37)-C(35)	1.356(7)
C(50)-C(51)	1.383(7)
C(50)-C(52)	1.434(7)
C(54)-C(55)	1.383(7)
C(54)-C(56)	1.430(7)
C(29)-H(29)	1.0000
C(52)-C(77)	1.426(7)
C(53)-C(82)	1.510(8)
C(53)-C(83)	1.514(7)
C(53)-H(53)	1.0000
C(11)-C(10)	1.376(8)
C(11)-C(12)	1.381(9)
C(11)-H(11)	0.9500
C(35)-C(36)	1.394(7)
C(35)-H(35)	0.9500
C(47)-C(67)	1.547(7)
C(47)-C(86)	1.553(8)
C(47)-H(47)	1.0000
C(39)-C(38)	1.377(8)
C(39)-C(87)	1.382(9)
C(39)-H(39)	0.9500
C(57)-C(59)	1.500(7)
C(57)-C(58)	1.503(7)
C(57)-H(57)	1.0000

C(4)-C(5)	1.386(8)
C(4)-C(6)	1.404(8)
C(13)-C(14)	1.422(6)
C(13)-N(1)	1.440(6)
C(45)-C(44)	1.395(7)
C(45)-C(40)	1.411(6)
C(45)-C(46)	1.525(7)
C(56)-C(64)	1.422(7)
C(38)-C(108)	1.377(8)
C(58)-H(58A)	0.9800
C(58)-H(58B)	0.9800
C(58)-H(58C)	0.9800
N(1)-C(1)	1.493(6)
C(22)-C(70)	1.542(7)
C(22)-C(63)	1.542(8)
C(22)-H(22)	1.0000
C(16)-C(17)	1.385(7)
C(16)-C(14)	1.390(7)
C(16)-H(16)	0.9500
C(40)-N(3)	1.436(6)
C(1)-C(10)	1.529(7)
C(1)-H(1)	1.0000
C(10)-C(73)	1.367(8)
C(44)-C(43)	1.378(7)
C(44)-H(44)	0.9500
C(7)-C(8)	1.356(12)
C(7)-C(6)	1.375(8)
C(7)-H(7)	0.9500
C(5)-C(9)	1.391(9)
C(5)-H(5)	0.9500
C(43)-C(84)	1.525(7)
C(14)-C(15)	1.506(7)
C(9)-C(8)	1.362(12)
C(9)-H(9)	0.9500

C(17)-C(71)	1.530(7)
C(51)-C(66)	1.372(8)
C(51)-H(51)	0.9500
C(59)-H(59A)	0.9800
C(59)-H(59B)	0.9800
C(59)-H(59C)	0.9800
C(25)-C(61)	1.386(8)
C(25)-H(25)	0.9500
C(55)-C(69)	1.359(8)
C(55)-H(55)	0.9500
C(46)-C(85)	1.529(9)
C(46)-C(112)	1.539(9)
C(46)-H(46)	1.0000
C(36)-C(68)	1.372(8)
C(36)-H(36)	0.9500
C(6)-H(6)	0.9500
C(12)-C(62)	1.359(10)
C(12)-H(12)	0.9500
C(33)-C(68)	1.381(8)
C(33)-H(33)	0.9500
C(32)-C(90)	1.386(8)
C(32)-H(32)	0.9500
C(15)-C(99)	1.527(9)
C(15)-C(98)	1.522(9)
C(15)-H(15)	1.0000
C(8)-H(8)	0.9500
C(60)-C(75)	1.392(8)
C(60)-C(74)	1.393(7)
C(65)-C(100)	1.376(9)
C(65)-C(76)	1.401(9)
C(65)-C(64)	1.493(8)
C(64)-C(101)	1.380(8)
C(62)-C(97)	1.379(10)
C(62)-H(62)	0.9500

C(61)-C(118)	1.366(8)
C(61)-H(61)	0.9500
C(63)-H(63A)	0.9800
C(63)-H(63B)	0.9800
C(63)-H(63C)	0.9800
C(67)-H(67A)	0.9800
C(67)-H(67B)	0.9800
C(67)-H(67C)	0.9800
C(66)-C(78)	1.379(8)
C(66)-H(66)	0.9500
C(68)-H(68)	0.9500
C(75)-C(96)	1.366(9)
C(75)-H(75)	0.9500
C(76)-C(102)	1.385(9)
C(76)-H(76)	0.9500
C(74)-C(94)	1.382(9)
C(74)-H(74)	0.9500
C(72)-C(71)	1.512(9)
C(72)-H(72A)	0.9800
C(72)-H(72B)	0.9800
C(72)-H(72C)	0.9800
C(71)-C(119)	1.519(10)
C(71)-H(71)	1.0000
C(70)-H(70A)	0.9800
C(70)-H(70B)	0.9800
C(70)-H(70C)	0.9800
C(69)-C(101)	1.375(8)
C(69)-H(69)	0.9500
C(73)-C(97)	1.374(8)
C(73)-H(73)	0.9500
C(79)-C(80)	1.374(8)
C(79)-C(81)	1.399(9)
C(79)-C(77)	1.504(7)
C(82)-H(82A)	0.9800

C(82)-H(82B)	0.9800
C(82)-H(82C)	0.9800
C(92)-C(105)	1.394(8)
C(92)-C(91)	1.392(8)
C(77)-C(78)	1.379(8)
C(88)-C(109)	1.355(10)
C(88)-C(87)	1.367(10)
C(88)-H(88)	0.9500
C(100)-C(117)	1.433(9)
C(100)-H(100)	0.9500
C(91)-C(93)	1.374(9)
C(91)-H(91)	0.9500
C(83)-H(83A)	0.9800
C(83)-H(83B)	0.9800
C(83)-H(83C)	0.9800
C(95)-C(94)	1.366(10)
C(95)-C(96)	1.375(9)
C(95)-H(95)	0.9500
C(78)-H(78)	0.9500
C(81)-C(115)	1.376(9)
C(81)-H(81)	0.9500
C(101)-H(101)	0.9500
C(102)-C(116)	1.366(11)
C(102)-H(102)	0.9500
C(86)-H(86A)	0.9800
C(86)-H(86B)	0.9800
C(86)-H(86C)	0.9800
C(93)-C(107)	1.389(10)
C(93)-H(93)	0.9500
C(97)-H(97)	0.9500
C(85)-H(85A)	0.9800
C(85)-H(85B)	0.9800
C(85)-H(85C)	0.9800
C(84)-C(111)	1.515(9)

C(84)-C(110)	1.524(10)
C(84)-H(84)	1.0000
C(99)-H(99A)	0.9800
C(99)-H(99B)	0.9800
C(99)-H(99C)	0.9800
C(98)-H(98A)	0.9800
C(98)-H(98B)	0.9800
C(98)-H(98C)	0.9800
C(89)-C(103)	1.394(10)
C(89)-H(89)	0.9500
C(94)-H(94)	0.9500
C(80)-C(113)	1.446(9)
C(80)-H(80)	0.9500
C(96)-H(96)	0.9500
C(90)-C(104)	1.377(12)
C(90)-H(90)	0.9500
C(87)-H(87)	0.9500
C(107)-C(106)	1.367(9)
C(107)-H(107)	0.9500
C(117)-C(116)	1.375(11)
C(117)-H(117)	0.9500
C(118)-H(118)	0.9500
C(109)-C(108)	1.377(9)
C(109)-H(109)	0.9500
C(113)-C(114)	1.371(11)
C(113)-H(113)	0.9500
C(108)-H(108)	0.9500
C(114)-C(115)	1.378(11)
C(114)-H(114)	0.9500
C(110)-H(11A)	0.9800
C(110)-H(11B)	0.9800
C(110)-H(11C)	0.9800
C(115)-H(115)	0.9500
C(116)-H(116)	0.9500

C(105)-C(106)	1.358(9)
C(105)-H(105)	0.9500
C(106)-H(106)	0.9500
C(112)-H(11D)	0.9800
C(112)-H(11E)	0.9800
C(112)-H(11F)	0.9800
C(119)-H(11G)	0.9800
C(119)-H(11H)	0.9800
C(119)-H(11I)	0.9800
C(104)-C(103)	1.366(13)
C(104)-H(104)	0.9500
C(103)-H(103)	0.9500
C(111)-H(11J)	0.9800
C(111)-H(11K)	0.9800
C(111)-H(11L)	0.9800

C(27)-Ru(1)-C(3)	101.4(2)
C(27)-Ru(1)-O(2)	77.71(17)
C(3)-Ru(1)-O(2)	178.79(14)
C(27)-Ru(1)-I(2)	101.95(14)
C(3)-Ru(1)-I(2)	96.33(11)
O(2)-Ru(1)-I(2)	83.09(9)
C(27)-Ru(1)-I(1)	93.56(14)
C(3)-Ru(1)-I(1)	91.05(11)
O(2)-Ru(1)-I(1)	89.82(8)
I(2)-Ru(1)-I(1)	161.11(2)
C(49)-Ru(2)-C(30)	101.4(2)
C(49)-Ru(2)-O(1)	77.43(17)
C(30)-Ru(2)-O(1)	178.44(15)
C(49)-Ru(2)-I(4)	101.69(14)
C(30)-Ru(2)-I(4)	96.06(11)
O(1)-Ru(2)-I(4)	83.25(9)
C(49)-Ru(2)-I(3)	93.80(14)
C(30)-Ru(2)-I(3)	91.33(12)

O(1)-Ru(2)-I(3)	89.74(8)
I(4)-Ru(2)-I(3)	161.13(2)
C(18)-C(19)-C(13)	118.1(4)
C(18)-C(19)-C(22)	118.5(4)
C(13)-C(19)-C(22)	123.4(4)
C(42)-C(41)-C(40)	118.5(4)
C(42)-C(41)-C(47)	118.5(4)
C(40)-C(41)-C(47)	122.9(4)
C(56)-O(2)-C(57)	122.3(4)
C(56)-O(2)-Ru(1)	110.2(3)
C(57)-O(2)-Ru(1)	126.6(3)
C(52)-O(1)-C(53)	122.0(4)
C(52)-O(1)-Ru(2)	110.6(3)
C(53)-O(1)-Ru(2)	126.6(3)
C(17)-C(18)-C(19)	124.1(5)
C(17)-C(18)-H(18)	118.0
C(19)-C(18)-H(18)	118.0
C(43)-C(42)-C(41)	123.1(5)
C(43)-C(42)-H(42)	118.4
C(41)-C(42)-H(42)	118.4
N(3)-C(30)-N(4)	107.3(4)
N(3)-C(30)-Ru(2)	133.3(3)
N(4)-C(30)-Ru(2)	119.3(3)
C(54)-C(27)-Ru(1)	120.6(4)
C(54)-C(27)-H(27)	119.7
Ru(1)-C(27)-H(27)	119.7
C(50)-C(49)-Ru(2)	121.1(4)
C(50)-C(49)-H(49)	119.4
Ru(2)-C(49)-H(49)	119.4
N(1)-C(3)-N(2)	107.3(4)
N(1)-C(3)-Ru(1)	133.1(3)
N(2)-C(3)-Ru(1)	119.5(3)
N(2)-C(2)-C(4)	113.0(4)
N(2)-C(2)-C(1)	102.4(3)

C(4)-C(2)-C(1)	112.7(4)
N(2)-C(2)-H(2)	109.5
C(4)-C(2)-H(2)	109.5
C(1)-C(2)-H(2)	109.5
C(26)-C(23)-C(24)	120.2(4)
C(26)-C(23)-N(2)	119.7(4)
C(24)-C(23)-N(2)	120.1(4)
C(25)-C(24)-C(23)	116.7(5)
C(25)-C(24)-C(60)	118.4(5)
C(23)-C(24)-C(60)	124.9(4)
C(23)-C(26)-C(118)	121.9(5)
C(23)-C(26)-H(26)	119.1
C(118)-C(26)-H(26)	119.1
C(32)-C(31)-C(89)	118.9(5)
C(32)-C(31)-C(29)	121.8(5)
C(89)-C(31)-C(29)	119.2(5)
C(33)-C(34)-C(37)	116.5(5)
C(33)-C(34)-C(92)	117.6(5)
C(37)-C(34)-C(92)	126.0(4)
C(30)-N(4)-C(37)	125.5(4)
C(30)-N(4)-C(29)	114.3(4)
C(37)-N(4)-C(29)	120.1(4)
C(3)-N(2)-C(23)	125.6(4)
C(3)-N(2)-C(2)	114.0(4)
C(23)-N(2)-C(2)	120.3(4)
N(3)-C(28)-C(38)	114.7(4)
N(3)-C(28)-C(29)	102.5(4)
C(38)-C(28)-C(29)	116.3(4)
N(3)-C(28)-H(28)	107.6
C(38)-C(28)-H(28)	107.6
C(29)-C(28)-H(28)	107.6
C(35)-C(37)-C(34)	120.6(4)
C(35)-C(37)-N(4)	120.1(4)
C(34)-C(37)-N(4)	119.2(4)

C(51)-C(50)-C(52)	120.3(5)
C(51)-C(50)-C(49)	122.1(5)
C(52)-C(50)-C(49)	117.5(4)
C(55)-C(54)-C(56)	120.2(5)
C(55)-C(54)-C(27)	121.8(5)
C(56)-C(54)-C(27)	118.0(4)
N(4)-C(29)-C(31)	113.5(4)
N(4)-C(29)-C(28)	101.8(3)
C(31)-C(29)-C(28)	113.2(4)
N(4)-C(29)-H(29)	109.3
C(31)-C(29)-H(29)	109.3
C(28)-C(29)-H(29)	109.3
O(1)-C(52)-C(77)	129.0(4)
O(1)-C(52)-C(50)	112.4(4)
C(77)-C(52)-C(50)	118.6(5)
O(1)-C(53)-C(82)	110.3(4)
O(1)-C(53)-C(83)	106.5(4)
C(82)-C(53)-C(83)	113.6(4)
O(1)-C(53)-H(53)	108.8
C(82)-C(53)-H(53)	108.8
C(83)-C(53)-H(53)	108.8
C(10)-C(11)-C(12)	121.6(6)
C(10)-C(11)-H(11)	119.2
C(12)-C(11)-H(11)	119.2
C(37)-C(35)-C(36)	121.8(5)
C(37)-C(35)-H(35)	119.1
C(36)-C(35)-H(35)	119.1
C(41)-C(47)-C(67)	111.4(4)
C(41)-C(47)-C(86)	110.7(5)
C(67)-C(47)-C(86)	109.7(4)
C(41)-C(47)-H(47)	108.3
C(67)-C(47)-H(47)	108.3
C(86)-C(47)-H(47)	108.3
C(38)-C(39)-C(87)	121.3(6)

C(38)-C(39)-H(39)	119.4
C(87)-C(39)-H(39)	119.4
O(2)-C(57)-C(59)	110.0(4)
O(2)-C(57)-C(58)	106.5(4)
C(59)-C(57)-C(58)	113.5(4)
O(2)-C(57)-H(57)	108.9
C(59)-C(57)-H(57)	108.9
C(58)-C(57)-H(57)	108.9
C(5)-C(4)-C(6)	118.9(5)
C(5)-C(4)-C(2)	119.4(5)
C(6)-C(4)-C(2)	121.7(5)
C(19)-C(13)-C(14)	120.0(4)
C(19)-C(13)-N(1)	120.2(4)
C(14)-C(13)-N(1)	119.6(4)
C(44)-C(45)-C(40)	117.6(4)
C(44)-C(45)-C(46)	118.9(4)
C(40)-C(45)-C(46)	123.4(4)
O(2)-C(56)-C(64)	128.3(4)
O(2)-C(56)-C(54)	112.5(4)
C(64)-C(56)-C(54)	119.2(5)
C(39)-C(38)-C(108)	117.5(5)
C(39)-C(38)-C(28)	119.8(5)
C(108)-C(38)-C(28)	122.6(5)
C(57)-C(58)-H(58A)	109.5
C(57)-C(58)-H(58B)	109.5
H(58A)-C(58)-H(58B)	109.5
C(57)-C(58)-H(58C)	109.5
H(58A)-C(58)-H(58C)	109.5
H(58B)-C(58)-H(58C)	109.5
C(3)-N(1)-C(13)	130.6(4)
C(3)-N(1)-C(1)	113.6(4)
C(13)-N(1)-C(1)	115.7(4)
C(19)-C(22)-C(70)	111.1(4)
C(19)-C(22)-C(63)	110.8(5)

C(70)-C(22)-C(63)	110.0(4)
C(19)-C(22)-H(22)	108.3
C(70)-C(22)-H(22)	108.3
C(63)-C(22)-H(22)	108.3
C(17)-C(16)-C(14)	122.8(5)
C(17)-C(16)-H(16)	118.6
C(14)-C(16)-H(16)	118.6
C(41)-C(40)-C(45)	119.7(4)
C(41)-C(40)-N(3)	120.9(4)
C(45)-C(40)-N(3)	119.2(4)
N(1)-C(1)-C(10)	114.1(4)
N(1)-C(1)-C(2)	102.1(4)
C(10)-C(1)-C(2)	115.4(4)
N(1)-C(1)-H(1)	108.3
C(10)-C(1)-H(1)	108.3
C(2)-C(1)-H(1)	108.3
C(73)-C(10)-C(11)	117.6(5)
C(73)-C(10)-C(1)	123.1(5)
C(11)-C(10)-C(1)	119.2(5)
C(43)-C(44)-C(45)	123.4(5)
C(43)-C(44)-H(44)	118.3
C(45)-C(44)-H(44)	118.3
C(8)-C(7)-C(6)	120.3(8)
C(8)-C(7)-H(7)	119.9
C(6)-C(7)-H(7)	119.9
C(4)-C(5)-C(9)	119.7(7)
C(4)-C(5)-H(5)	120.2
C(9)-C(5)-H(5)	120.2
C(30)-N(3)-C(40)	130.4(4)
C(30)-N(3)-C(28)	113.5(4)
C(40)-N(3)-C(28)	116.1(4)
C(42)-C(43)-C(44)	117.6(5)
C(42)-C(43)-C(84)	120.7(5)
C(44)-C(43)-C(84)	121.7(5)

C(16)-C(14)-C(13)	117.7(4)
C(16)-C(14)-C(15)	118.4(4)
C(13)-C(14)-C(15)	123.9(4)
C(8)-C(9)-C(5)	120.0(7)
C(8)-C(9)-H(9)	120.0
C(5)-C(9)-H(9)	120.0
C(18)-C(17)-C(16)	117.3(5)
C(18)-C(17)-C(71)	122.0(5)
C(16)-C(17)-C(71)	120.7(5)
C(66)-C(51)-C(50)	120.5(5)
C(66)-C(51)-H(51)	119.8
C(50)-C(51)-H(51)	119.8
C(57)-C(59)-H(59A)	109.5
C(57)-C(59)-H(59B)	109.5
H(59A)-C(59)-H(59B)	109.5
C(57)-C(59)-H(59C)	109.5
H(59A)-C(59)-H(59C)	109.5
H(59B)-C(59)-H(59C)	109.5
C(61)-C(25)-C(24)	122.9(5)
C(61)-C(25)-H(25)	118.6
C(24)-C(25)-H(25)	118.6
C(69)-C(55)-C(54)	120.4(5)
C(69)-C(55)-H(55)	119.8
C(54)-C(55)-H(55)	119.8
C(45)-C(46)-C(85)	111.4(5)
C(45)-C(46)-C(112)	110.9(5)
C(85)-C(46)-C(112)	109.1(5)
C(45)-C(46)-H(46)	108.5
C(85)-C(46)-H(46)	108.5
C(112)-C(46)-H(46)	108.5
C(68)-C(36)-C(35)	119.1(5)
C(68)-C(36)-H(36)	120.4
C(35)-C(36)-H(36)	120.4
C(7)-C(6)-C(4)	119.9(6)

C(7)-C(6)-H(6)	120.1
C(4)-C(6)-H(6)	120.0
C(62)-C(12)-C(11)	119.8(6)
C(62)-C(12)-H(12)	120.1
C(11)-C(12)-H(12)	120.1
C(68)-C(33)-C(34)	122.9(5)
C(68)-C(33)-H(33)	118.5
C(34)-C(33)-H(33)	118.5
C(31)-C(32)-C(90)	121.7(6)
C(31)-C(32)-H(32)	119.2
C(90)-C(32)-H(32)	119.2
C(14)-C(15)-C(99)	111.8(5)
C(14)-C(15)-C(98)	111.4(5)
C(99)-C(15)-C(98)	108.8(5)
C(14)-C(15)-H(15)	108.2
C(99)-C(15)-H(15)	108.2
C(98)-C(15)-H(15)	108.2
C(7)-C(8)-C(9)	121.1(6)
C(7)-C(8)-H(8)	119.4
C(9)-C(8)-H(8)	119.4
C(75)-C(60)-C(74)	117.2(5)
C(75)-C(60)-C(24)	119.9(5)
C(74)-C(60)-C(24)	122.8(5)
C(100)-C(65)-C(76)	118.6(6)
C(100)-C(65)-C(64)	121.9(6)
C(76)-C(65)-C(64)	119.4(5)
C(101)-C(64)-C(56)	116.4(5)
C(101)-C(64)-C(65)	117.3(5)
C(56)-C(64)-C(65)	126.3(5)
C(12)-C(62)-C(97)	119.5(6)
C(12)-C(62)-H(62)	120.2
C(97)-C(62)-H(62)	120.2
C(118)-C(61)-C(25)	119.3(5)
C(118)-C(61)-H(61)	120.4

C(25)-C(61)-H(61)	120.4
C(22)-C(63)-H(63A)	109.5
C(22)-C(63)-H(63B)	109.5
H(63A)-C(63)-H(63B)	109.5
C(22)-C(63)-H(63C)	109.5
H(63A)-C(63)-H(63C)	109.5
H(63B)-C(63)-H(63C)	109.5
C(47)-C(67)-H(67A)	109.5
C(47)-C(67)-H(67B)	109.5
H(67A)-C(67)-H(67B)	109.5
C(47)-C(67)-H(67C)	109.5
H(67A)-C(67)-H(67C)	109.5
H(67B)-C(67)-H(67C)	109.5
C(51)-C(66)-C(78)	119.3(5)
C(51)-C(66)-H(66)	120.4
C(78)-C(66)-H(66)	120.4
C(36)-C(68)-C(33)	119.1(5)
C(36)-C(68)-H(68)	120.4
C(33)-C(68)-H(68)	120.4
C(96)-C(75)-C(60)	122.0(6)
C(96)-C(75)-H(75)	119.0
C(60)-C(75)-H(75)	119.0
C(102)-C(76)-C(65)	121.4(7)
C(102)-C(76)-H(76)	119.3
C(65)-C(76)-H(76)	119.3
C(94)-C(74)-C(60)	120.2(5)
C(94)-C(74)-H(74)	119.9
C(60)-C(74)-H(74)	119.9
C(71)-C(72)-H(72A)	109.5
C(71)-C(72)-H(72B)	109.5
H(72A)-C(72)-H(72B)	109.5
C(71)-C(72)-H(72C)	109.5
H(72A)-C(72)-H(72C)	109.5
H(72B)-C(72)-H(72C)	109.5

C(72)-C(71)-C(119)	111.9(6)
C(72)-C(71)-C(17)	111.4(5)
C(119)-C(71)-C(17)	111.7(5)
C(72)-C(71)-H(71)	107.2
C(119)-C(71)-H(71)	107.2
C(17)-C(71)-H(71)	107.2
C(22)-C(70)-H(70A)	109.5
C(22)-C(70)-H(70B)	109.5
H(70A)-C(70)-H(70B)	109.5
C(22)-C(70)-H(70C)	109.5
H(70A)-C(70)-H(70C)	109.5
H(70B)-C(70)-H(70C)	109.5
C(55)-C(69)-C(101)	119.4(5)
C(55)-C(69)-H(69)	120.3
C(101)-C(69)-H(69)	120.3
C(10)-C(73)-C(97)	121.5(6)
C(10)-C(73)-H(73)	119.2
C(97)-C(73)-H(73)	119.2
C(80)-C(79)-C(81)	120.1(6)
C(80)-C(79)-C(77)	120.8(6)
C(81)-C(79)-C(77)	118.9(5)
C(53)-C(82)-H(82A)	109.5
C(53)-C(82)-H(82B)	109.5
H(82A)-C(82)-H(82B)	109.5
C(53)-C(82)-H(82C)	109.5
H(82A)-C(82)-H(82C)	109.5
H(82B)-C(82)-H(82C)	109.5
C(105)-C(92)-C(91)	116.8(6)
C(105)-C(92)-C(34)	120.0(5)
C(91)-C(92)-C(34)	123.2(5)
C(78)-C(77)-C(52)	117.2(5)
C(78)-C(77)-C(79)	117.4(5)
C(52)-C(77)-C(79)	125.4(5)
C(109)-C(88)-C(87)	119.1(6)

C(109)-C(88)-H(88)	120.4
C(87)-C(88)-H(88)	120.4
C(65)-C(100)-C(117)	120.1(7)
C(65)-C(100)-H(100)	120.0
C(117)-C(100)-H(100)	120.0
C(93)-C(91)-C(92)	121.1(5)
C(93)-C(91)-H(91)	119.5
C(92)-C(91)-H(91)	119.5
C(53)-C(83)-H(83A)	109.5
C(53)-C(83)-H(83B)	109.5
H(83A)-C(83)-H(83B)	109.5
C(53)-C(83)-H(83C)	109.5
H(83A)-C(83)-H(83C)	109.5
H(83B)-C(83)-H(83C)	109.5
C(94)-C(95)-C(96)	119.1(6)
C(94)-C(95)-H(95)	120.4
C(96)-C(95)-H(95)	120.4
C(66)-C(78)-C(77)	123.8(5)
C(66)-C(78)-H(78)	118.1
C(77)-C(78)-H(78)	118.1
C(115)-C(81)-C(79)	121.2(7)
C(115)-C(81)-H(81)	119.4
C(79)-C(81)-H(81)	119.4
C(69)-C(101)-C(64)	124.2(5)
C(69)-C(101)-H(101)	117.9
C(64)-C(101)-H(101)	117.9
C(116)-C(102)-C(76)	119.6(7)
C(116)-C(102)-H(102)	120.2
C(76)-C(102)-H(102)	120.2
C(47)-C(86)-H(86A)	109.5
C(47)-C(86)-H(86B)	109.5
H(86A)-C(86)-H(86B)	109.5
C(47)-C(86)-H(86C)	109.5
H(86A)-C(86)-H(86C)	109.5

H(86B)-C(86)-H(86C)	109.5
C(91)-C(93)-C(107)	120.4(6)
C(91)-C(93)-H(93)	119.8
C(107)-C(93)-H(93)	119.8
C(73)-C(97)-C(62)	119.9(7)
C(73)-C(97)-H(97)	120.1
C(62)-C(97)-H(97)	120.1
C(46)-C(85)-H(85A)	109.5
C(46)-C(85)-H(85B)	109.5
H(85A)-C(85)-H(85B)	109.5
C(46)-C(85)-H(85C)	109.5
H(85A)-C(85)-H(85C)	109.5
H(85B)-C(85)-H(85C)	109.5
C(111)-C(84)-C(110)	111.6(6)
C(111)-C(84)-C(43)	111.2(5)
C(110)-C(84)-C(43)	111.8(5)
C(111)-C(84)-H(84)	107.3
C(110)-C(84)-H(84)	107.3
C(43)-C(84)-H(84)	107.3
C(15)-C(99)-H(99A)	109.5
C(15)-C(99)-H(99B)	109.5
H(99A)-C(99)-H(99B)	109.5
C(15)-C(99)-H(99C)	109.5
H(99A)-C(99)-H(99C)	109.5
H(99B)-C(99)-H(99C)	109.5
C(15)-C(98)-H(98A)	109.5
C(15)-C(98)-H(98B)	109.5
H(98A)-C(98)-H(98B)	109.5
C(15)-C(98)-H(98C)	109.5
H(98A)-C(98)-H(98C)	109.5
H(98B)-C(98)-H(98C)	109.5
C(31)-C(89)-C(103)	119.6(7)
C(31)-C(89)-H(89)	120.2
C(103)-C(89)-H(89)	120.2

C(95)-C(94)-C(74)	121.3(6)
C(95)-C(94)-H(94)	119.3
C(74)-C(94)-H(94)	119.3
C(79)-C(80)-C(113)	118.2(7)
C(79)-C(80)-H(80)	120.9
C(113)-C(80)-H(80)	120.9
C(75)-C(96)-C(95)	120.1(6)
C(75)-C(96)-H(96)	119.9
C(95)-C(96)-H(96)	119.9
C(104)-C(90)-C(32)	118.7(8)
C(104)-C(90)-H(90)	120.7
C(32)-C(90)-H(90)	120.7
C(88)-C(87)-C(39)	120.1(6)
C(88)-C(87)-H(87)	119.9
C(39)-C(87)-H(87)	119.9
C(106)-C(107)-C(93)	119.1(6)
C(106)-C(107)-H(107)	120.4
C(93)-C(107)-H(107)	120.4
C(116)-C(117)-C(100)	119.0(7)
C(116)-C(117)-H(117)	120.5
C(100)-C(117)-H(117)	120.5
C(61)-C(118)-C(26)	119.1(5)
C(61)-C(118)-H(118)	120.5
C(26)-C(118)-H(118)	120.5
C(88)-C(109)-C(108)	121.1(7)
C(88)-C(109)-H(109)	119.5
C(108)-C(109)-H(109)	119.5
C(114)-C(113)-C(80)	120.0(7)
C(114)-C(113)-H(113)	120.0
C(80)-C(113)-H(113)	120.0
C(109)-C(108)-C(38)	120.9(6)
C(109)-C(108)-H(108)	119.5
C(38)-C(108)-H(108)	119.5
C(113)-C(114)-C(115)	120.9(6)

C(113)-C(114)-H(114)	119.6
C(115)-C(114)-H(114)	119.6
C(84)-C(110)-H(11A)	109.5
C(84)-C(110)-H(11B)	109.5
H(11A)-C(110)-H(11B)	109.5
C(84)-C(110)-H(11C)	109.5
H(11A)-C(110)-H(11C)	109.5
H(11B)-C(110)-H(11C)	109.5
C(81)-C(115)-C(114)	119.5(7)
C(81)-C(115)-H(115)	120.2
C(114)-C(115)-H(115)	120.2
C(102)-C(116)-C(117)	121.3(6)
C(102)-C(116)-H(116)	119.3
C(117)-C(116)-H(116)	119.4
C(106)-C(105)-C(92)	122.3(6)
C(106)-C(105)-H(105)	118.9
C(92)-C(105)-H(105)	118.9
C(105)-C(106)-C(107)	120.4(6)
C(105)-C(106)-H(106)	119.8
C(107)-C(106)-H(106)	119.8
C(46)-C(112)-H(11D)	109.5
C(46)-C(112)-H(11E)	109.5
H(11D)-C(112)-H(11E)	109.5
C(46)-C(112)-H(11F)	109.5
H(11D)-C(112)-H(11F)	109.5
H(11E)-C(112)-H(11F)	109.5
C(71)-C(119)-H(11G)	109.5
C(71)-C(119)-H(11H)	109.5
H(11G)-C(119)-H(11H)	109.5
C(71)-C(119)-H(11I)	109.5
H(11G)-C(119)-H(11I)	109.5
H(11H)-C(119)-H(11I)	109.5
C(103)-C(104)-C(90)	120.6(7)
C(103)-C(104)-H(104)	119.7

C(90)-C(104)-H(104)	119.7
C(104)-C(103)-C(89)	120.4(7)
C(104)-C(103)-H(103)	119.8
C(89)-C(103)-H(103)	119.8
C(84)-C(111)-H(11J)	109.5
C(84)-C(111)-H(11K)	109.5
H(11J)-C(111)-H(11K)	109.5
C(84)-C(111)-H(11L)	109.5
H(11J)-C(111)-H(11L)	109.5
H(11K)-C(111)-H(11L)	109.5

Symmetry transformations used to generate equivalent atoms:

Table 4. Anisotropic displacement parameters (Å^{2}x 10^3) for AZ04mono. The anisotropic displacement factor exponent takes the form: $-2\pi^2$[h^2 a*^{2}U^{11} + ... + 2 h k a* b* U^{12}]

	U^{11}	U^{22}	U^{33}	U^{23}	U^{13}	U^{12}
Ru(1)	27(1)	27(1)	25(1)	-2(1)	-2(1)	4(1)
I(2)	59(1)	41(1)	32(1)	-2(1)	0(1)	5(1)
Ru(2)	27(1)	27(1)	25(1)	2(1)	1(1)	4(1)
I(4)	59(1)	42(1)	33(1)	2(1)	0(1)	5(1)
I(3)	45(1)	39(1)	37(1)	11(1)	0(1)	-2(1)
I(1)	45(1)	39(1)	37(1)	-11(1)	-1(1)	-2(1)
C(19)	26(2)	29(2)	33(2)	1(2)	-4(2)	-5(2)
C(41)	31(2)	34(2)	30(2)	3(2)	5(2)	-5(2)
O(2)	26(2)	34(2)	35(2)	6(2)	-5(1)	4(1)
O(1)	25(2)	36(2)	36(2)	-4(2)	6(1)	5(2)
C(18)	34(3)	39(3)	44(3)	2(2)	-13(2)	-1(2)
C(42)	32(3)	42(3)	42(3)	-3(2)	17(2)	-3(2)
C(30)	24(2)	27(2)	21(2)	6(2)	3(2)	2(2)
C(27)	30(2)	28(2)	37(2)	-6(2)	-2(2)	2(2)
C(49)	30(2)	26(2)	36(2)	4(2)	1(2)	5(2)
C(3)	27(2)	27(2)	21(2)	-8(2)	-1(2)	1(2)

C(2)	33(3)	32(2)	25(2)	2(2)	1(2)	1(2)
C(23)	29(2)	32(2)	23(2)	4(2)	0(2)	11(2)
C(24)	34(3)	35(2)	22(2)	2(2)	2(2)	11(2)
C(26)	39(3)	33(3)	36(3)	2(2)	7(2)	10(2)
C(31)	26(2)	43(3)	31(2)	-5(2)	-3(2)	10(2)
C(34)	36(3)	36(3)	22(2)	-5(2)	1(2)	11(2)
N(4)	31(2)	31(2)	24(2)	-1(2)	-2(2)	8(2)
N(2)	34(2)	32(2)	20(2)	1(2)	3(2)	7(2)
C(28)	30(2)	33(2)	24(2)	1(2)	-1(2)	2(2)
C(37)	33(3)	29(2)	18(2)	1(2)	0(2)	8(2)
C(50)	32(3)	25(2)	39(2)	0(2)	1(2)	0(2)
C(54)	34(3)	27(2)	38(2)	-1(2)	-3(2)	1(2)
C(29)	35(3)	33(2)	25(2)	-2(2)	-4(2)	5(2)
C(52)	31(3)	29(2)	34(2)	4(2)	2(2)	2(2)
C(53)	22(2)	45(3)	37(2)	-5(2)	-3(2)	2(2)
C(11)	40(3)	58(4)	33(3)	1(2)	-4(2)	0(3)
C(35)	36(3)	38(3)	32(2)	-2(2)	-3(2)	13(2)
C(47)	46(3)	39(3)	34(2)	5(2)	14(2)	-6(2)
C(39)	42(3)	62(4)	31(3)	-2(2)	1(2)	2(3)
C(57)	22(2)	43(3)	37(2)	5(2)	2(2)	3(2)
C(4)	28(3)	48(3)	30(2)	6(2)	2(2)	4(2)
C(13)	24(2)	31(2)	26(2)	-4(2)	-2(2)	4(2)
C(45)	36(3)	33(2)	28(2)	8(2)	2(2)	0(2)
C(56)	30(2)	28(2)	35(2)	-1(2)	1(2)	-3(2)
C(38)	35(3)	42(3)	27(2)	-3(2)	-1(2)	0(2)
C(58)	30(3)	42(3)	42(3)	-3(2)	-1(2)	10(2)
N(1)	28(2)	27(2)	26(2)	-3(2)	-3(2)	4(2)
C(22)	47(3)	38(3)	31(2)	-5(2)	-13(2)	-5(2)
C(16)	33(3)	31(3)	55(3)	-13(2)	-5(2)	3(2)
C(40)	24(2)	33(2)	30(2)	3(2)	4(2)	2(2)
C(1)	33(3)	29(2)	26(2)	-1(2)	0(2)	1(2)
C(10)	33(3)	38(3)	28(2)	5(2)	3(2)	2(2)
C(44)	30(3)	35(3)	53(3)	13(2)	1(2)	3(2)
C(7)	42(4)	104(6)	50(4)	-22(4)	-8(3)	12(4)

C(5)	39(3)	62(4)	52(3)	22(3)	2(3)	0(3)
N(3)	28(2)	31(2)	27(2)	3(2)	4(2)	3(2)
C(43)	32(3)	36(3)	54(3)	-1(2)	12(2)	5(2)
C(14)	30(3)	29(2)	36(2)	-8(2)	-5(2)	0(2)
C(9)	48(4)	105(6)	53(4)	47(4)	0(3)	-6(4)
C(17)	34(3)	34(3)	50(3)	1(2)	-9(2)	5(2)
C(51)	29(3)	37(3)	51(3)	-1(2)	-4(2)	6(2)
C(59)	36(3)	39(3)	48(3)	5(2)	-8(2)	1(2)
C(25)	45(3)	38(3)	30(2)	2(2)	2(2)	14(2)
C(55)	30(3)	35(3)	52(3)	2(2)	2(2)	4(2)
C(46)	28(3)	57(3)	43(3)	20(2)	12(2)	8(2)
C(36)	29(3)	46(3)	45(3)	-4(2)	0(2)	2(2)
C(6)	45(3)	65(4)	40(3)	-6(3)	-7(2)	17(3)
C(12)	32(3)	90(5)	44(3)	17(3)	-2(2)	-6(3)
C(33)	49(3)	38(3)	35(3)	0(2)	-3(2)	20(2)
C(32)	39(3)	65(4)	40(3)	8(3)	9(2)	15(3)
C(15)	31(3)	56(3)	45(3)	-22(2)	-8(2)	10(2)
C(8)	39(4)	129(7)	38(3)	19(4)	-4(3)	6(4)
C(60)	41(3)	38(3)	22(2)	-8(2)	2(2)	7(2)
C(65)	36(3)	56(3)	31(3)	13(2)	-6(2)	5(3)
C(64)	33(3)	42(3)	42(3)	7(2)	-2(2)	2(2)
C(62)	43(4)	66(4)	60(4)	25(3)	-13(3)	-25(3)
C(61)	32(3)	62(4)	33(3)	8(2)	4(2)	18(3)
C(63)	78(5)	55(4)	35(3)	-2(3)	-7(3)	-31(3)
C(67)	73(4)	50(3)	25(2)	7(2)	3(3)	-18(3)
C(66)	35(3)	41(3)	59(3)	-17(3)	2(3)	10(2)
C(68)	32(3)	56(3)	35(3)	-7(2)	-3(2)	16(2)
C(75)	59(4)	37(3)	39(3)	0(2)	-5(3)	4(3)
C(76)	38(3)	61(4)	51(3)	10(3)	-6(3)	-6(3)
C(74)	50(3)	52(3)	28(2)	4(2)	-2(2)	-2(3)
C(72)	61(4)	45(4)	98(5)	3(4)	-29(4)	13(3)
C(71)	36(3)	37(3)	77(4)	-7(3)	-18(3)	7(2)
C(70)	75(4)	44(3)	29(3)	-3(2)	-6(3)	-22(3)
C(69)	42(3)	44(3)	55(3)	18(3)	-2(3)	10(3)

C(73)	34(3)	50(3)	58(3)	0(3)	0(3)	-3(3)
C(79)	32(3)	63(4)	30(2)	-13(2)	3(2)	1(3)
C(82)	35(3)	46(3)	47(3)	-8(2)	11(2)	1(2)
C(92)	40(3)	37(3)	29(2)	4(2)	-5(2)	8(2)
C(77)	35(3)	38(3)	35(3)	-4(2)	3(2)	-1(2)
C(88)	38(3)	62(4)	58(4)	-20(3)	14(3)	-20(3)
C(100)	51(4)	74(4)	32(3)	2(3)	-5(3)	3(3)
C(91)	51(3)	50(3)	31(3)	-7(2)	2(2)	4(3)
C(83)	35(3)	39(3)	47(3)	2(2)	1(2)	12(2)
C(95)	76(5)	60(4)	46(3)	-11(3)	-1(3)	-22(4)
C(78)	44(3)	47(3)	48(3)	-16(3)	8(3)	3(3)
C(81)	35(3)	64(4)	52(3)	-9(3)	6(3)	-6(3)
C(101)	45(3)	46(3)	46(3)	15(3)	-5(3)	2(3)
C(102)	48(4)	76(5)	61(4)	10(4)	0(3)	-19(3)
C(86)	81(5)	49(4)	35(3)	3(3)	7(3)	-27(3)
C(93)	52(4)	83(5)	33(3)	2(3)	7(3)	-11(3)
C(97)	53(4)	49(4)	70(4)	0(3)	-7(3)	-10(3)
C(85)	63(4)	90(5)	38(3)	23(3)	5(3)	18(4)
C(84)	33(3)	45(3)	73(4)	5(3)	20(3)	8(2)
C(99)	38(3)	68(4)	99(5)	-43(4)	-17(3)	11(3)
C(98)	60(4)	95(5)	35(3)	-24(3)	-2(3)	16(4)
C(89)	42(3)	65(4)	49(3)	-22(3)	-5(3)	6(3)
C(94)	56(4)	87(5)	29(3)	-4(3)	-10(3)	-11(4)
C(80)	53(4)	67(4)	32(3)	-3(3)	6(2)	8(3)
C(96)	74(5)	45(3)	56(4)	-1(3)	-5(3)	-3(3)
C(90)	46(4)	101(6)	51(4)	21(4)	7(3)	14(4)
C(87)	34(3)	92(5)	45(3)	-20(3)	-2(3)	-2(3)
C(107)	71(5)	62(4)	51(3)	11(3)	2(3)	-21(4)
C(117)	57(4)	106(6)	34(3)	-11(3)	-3(3)	10(4)
C(118)	35(3)	47(3)	43(3)	6(2)	2(2)	6(2)
C(109)	52(4)	47(4)	79(5)	-2(3)	14(4)	-8(3)
C(113)	55(4)	105(6)	39(3)	15(4)	2(3)	8(4)
C(108)	46(3)	45(3)	57(4)	2(3)	1(3)	-4(3)
C(114)	35(3)	115(7)	48(4)	1(4)	1(3)	1(4)

C(110)	34(4)	78(5)	120(7)	-4(5)	0(4)	15(3)
C(115)	48(4)	77(5)	66(4)	-15(4)	8(3)	-21(4)
C(116)	38(3)	116(7)	42(3)	-3(4)	0(3)	-2(4)
C(105)	61(4)	40(3)	44(3)	-3(2)	7(3)	6(3)
C(106)	72(4)	46(3)	54(3)	-3(3)	4(3)	-4(3)
C(112)	46(4)	58(4)	89(5)	39(4)	15(3)	13(3)
C(119)	36(4)	74(5)	118(7)	-1(5)	-3(4)	18(3)
C(104)	37(4)	133(8)	41(3)	-17(4)	5(3)	10(4)
C(103)	43(4)	107(6)	58(4)	-48(4)	-1(3)	0(4)
C(111)	61(4)	40(3)	100(5)	-2(3)	28(4)	10(3)

Table 5. Hydrogen coordinates (x 10^4) and isotropic displacement parameters (Å^{2}x 10 ^{3}) for AZ04mono.

	x	y	z	U(eq)
H(18)	-119	7679	3247	47
H(42)	5138	7972	8253	46
H(27)	2772	8111	3417	38
H(49)	2225	7539	8420	37
H(2)	3498	5488	4638	36
H(26)	5962	6939	4339	43
H(28)	2524	9078	10222	35
H(29)	1489	10161	9642	37
H(53)	-1688	7256	7200	42
H(11)	593	6532	5141	52
H(35)	-970	8707	9332	42
H(47)	2969	9117	8202	47
H(39)	4420	9100	10126	54
H(57)	6691	8390	2201	41
H(58A)	6841	7765	3470	57
H(58B)	7749	7778	2925	57

H(58C)	6702	7349	2796	57
H(22)	2030	6531	3197	46
H(16)	624	8599	4936	48
H(1)	2478	6573	5225	35
H(44)	4380	7055	9937	47
H(7)	5067	7025	6577	78
H(5)	4291	4964	5546	61
H(9)	5136	4989	6575	82
H(51)	2863	6607	7688	47
H(59A)	6328	9399	2841	62
H(59B)	7520	9147	2881	62
H(59C)	6734	8994	3478	62
H(25)	6468	4803	3438	45
H(55)	2139	9044	2683	47
H(46)	1954	7919	10211	51
H(36)	-2652	9051	9012	48
H(6)	4286	7030	5538	60
H(12)	-919	5904	4952	66
H(33)	-1459	10846	8433	49
H(32)	720	8635	10528	58
H(15)	3031	7733	5211	52
H(8)	5420	6013	7101	82
H(62)	-837	4905	4350	68
H(61)	7897	5521	3576	51
H(63A)	312	6098	3467	84
H(63B)	633	5938	2719	84
H(63C)	-167	6544	2878	84
H(67A)	4012	8162	7350	74
H(67B)	3408	8817	7073	74
H(67C)	2771	8230	7445	74
H(66)	2539	5804	6870	54
H(68)	-2897	10142	8583	50
H(75)	4989	4240	4313	54
H(76)	6047	10235	1776	60

H(74)	3659	5468	2949	52
H(72A)	-258	9527	4299	102
H(72B)	-1341	9610	3906	102
H(72C)	-296	9402	3518	102
H(71)	-1330	8443	3658	60
H(70A)	949	7464	2338	74
H(70B)	1626	6834	2076	74
H(70C)	2190	7447	2457	74
H(69)	2458	9838	1865	57
H(73)	2277	5158	4144	57
H(82A)	-1377	6236	7811	64
H(82B)	-2542	6519	7915	64
H(82C)	-1672	6634	8475	64
H(88)	5830	10749	9349	63
H(100)	5830	8307	1098	63
H(91)	1348	10177	7959	53
H(83A)	-1813	7901	8464	60
H(83B)	-2754	7861	7941	60
H(83C)	-1731	8302	7778	60
H(95)	2460	3604	3302	73
H(78)	910	5752	6376	55
H(81)	-1058	5423	6790	61
H(101)	4088	9901	1385	55
H(102)	7584	10398	1177	74
H(86A)	4675	9571	8462	83
H(86B)	4387	9696	7701	83
H(86C)	5179	9099	7902	83
H(93)	2563	11017	7729	67
H(97)	771	4538	3933	69
H(85A)	3697	7584	11042	96
H(85B)	2614	7921	11268	96
H(85C)	3438	8355	10848	96
H(84)	6321	7207	8655	60
H(99A)	2866	8928	4916	102

H(99B)	3219	8797	5665	102
H(99C)	2030	8999	5501	102
H(98A)	1311	8078	6043	95
H(98B)	2385	7720	6259	95
H(98C)	1534	7305	5838	95
H(89)	705	10682	10543	62
H(94)	2429	4625	2733	69
H(80)	-826	7351	6101	61
H(96)	3735	3424	4110	70
H(90)	-72	8612	11565	79
H(87)	5921	9746	9955	68
H(107)	2532	12049	8309	74
H(117)	7400	8482	478	79
H(118)	7650	6602	4019	50
H(109)	4233	11109	8944	71
H(113)	-2406	7163	5473	80
H(108)	2725	10485	9132	59
H(114)	-3244	6119	5524	79
H(11A)	6847	7613	9674	116
H(11B)	7226	6839	9622	116
H(11C)	6215	7027	10051	116
H(115)	-2572	5245	6174	76
H(116)	8238	9530	529	78
H(105)	10	11413	9304	58
H(106)	1270	12219	9116	69
H(11D)	2124	6720	9913	97
H(11E)	1774	6844	10662	97
H(11F)	2964	6647	10498	97
H(11G)	-1220	8630	5051	114
H(11H)	-1824	8027	4680	114
H(11I)	-2238	8793	4615	114
H(104)	-420	9636	12103	84
H(103)	-123	10660	11575	83
H(11J)	5277	6114	9301	101

H(11K)	6338	6040	8886	101
H(11L)	5269	6246	8521	101

Table 6. Torsion angles [°] for AZ04mono.

C(27)-Ru(1)-O(2)-C(56)	-9.0(3)
C(3)-Ru(1)-O(2)-C(56)	33(7)
I(2)-Ru(1)-O(2)-C(56)	94.9(3)
I(1)-Ru(1)-O(2)-C(56)	-102.7(3)
C(27)-Ru(1)-O(2)-C(57)	160.4(4)
C(3)-Ru(1)-O(2)-C(57)	-157(7)
I(2)-Ru(1)-O(2)-C(57)	-95.7(3)
I(1)-Ru(1)-O(2)-C(57)	66.7(3)
C(49)-Ru(2)-O(1)-C(52)	-9.1(3)
C(30)-Ru(2)-O(1)-C(52)	31(6)
I(4)-Ru(2)-O(1)-C(52)	94.5(3)
I(3)-Ru(2)-O(1)-C(52)	-103.0(3)
C(49)-Ru(2)-O(1)-C(53)	160.5(4)
C(30)-Ru(2)-O(1)-C(53)	-160(5)
I(4)-Ru(2)-O(1)-C(53)	-95.9(3)
I(3)-Ru(2)-O(1)-C(53)	66.6(3)
C(13)-C(19)-C(18)-C(17)	-1.5(8)
C(22)-C(19)-C(18)-C(17)	179.3(5)
C(40)-C(41)-C(42)-C(43)	-0.3(8)
C(47)-C(41)-C(42)-C(43)	-179.6(5)
C(49)-Ru(2)-C(30)-N(3)	-10.0(4)
O(1)-Ru(2)-C(30)-N(3)	-50(6)
I(4)-Ru(2)-C(30)-N(3)	-113.3(4)
I(3)-Ru(2)-C(30)-N(3)	84.1(4)
C(49)-Ru(2)-C(30)-N(4)	175.1(3)
O(1)-Ru(2)-C(30)-N(4)	136(5)
I(4)-Ru(2)-C(30)-N(4)	71.9(3)
I(3)-Ru(2)-C(30)-N(4)	-90.7(3)

C(3)-Ru(1)-C(27)-C(54)	-172.4(4)
O(2)-Ru(1)-C(27)-C(54)	6.8(4)
I(2)-Ru(1)-C(27)-C(54)	-73.3(4)
I(1)-Ru(1)-C(27)-C(54)	95.8(4)
C(30)-Ru(2)-C(49)-C(50)	-172.1(4)
O(1)-Ru(2)-C(49)-C(50)	6.9(4)
I(4)-Ru(2)-C(49)-C(50)	-73.4(4)
I(3)-Ru(2)-C(49)-C(50)	95.8(4)
C(27)-Ru(1)-C(3)-N(1)	-8.5(4)
O(2)-Ru(1)-C(3)-N(1)	-51(7)
I(2)-Ru(1)-C(3)-N(1)	-112.1(4)
I(1)-Ru(1)-C(3)-N(1)	85.3(4)
C(27)-Ru(1)-C(3)-N(2)	174.7(3)
O(2)-Ru(1)-C(3)-N(2)	132(7)
I(2)-Ru(1)-C(3)-N(2)	71.1(3)
I(1)-Ru(1)-C(3)-N(2)	-91.5(3)
C(26)-C(23)-C(24)-C(25)	0.1(7)
N(2)-C(23)-C(24)-C(25)	-178.0(4)
C(26)-C(23)-C(24)-C(60)	178.9(4)
N(2)-C(23)-C(24)-C(60)	0.8(7)
C(24)-C(23)-C(26)-C(118)	1.7(7)
N(2)-C(23)-C(26)-C(118)	179.8(4)
N(3)-C(30)-N(4)-C(37)	176.4(4)
Ru(2)-C(30)-N(4)-C(37)	-7.5(6)
N(3)-C(30)-N(4)-C(29)	-8.0(5)
Ru(2)-C(30)-N(4)-C(29)	168.1(3)
N(1)-C(3)-N(2)-C(23)	175.5(4)
Ru(1)-C(3)-N(2)-C(23)	-6.9(6)
N(1)-C(3)-N(2)-C(2)	-8.8(5)
Ru(1)-C(3)-N(2)-C(2)	168.7(3)
C(26)-C(23)-N(2)-C(3)	59.8(6)
C(24)-C(23)-N(2)-C(3)	-122.1(5)
C(26)-C(23)-N(2)-C(2)	-115.6(5)
C(24)-C(23)-N(2)-C(2)	62.5(6)

C(4)-C(2)-N(2)-C(3)	-113.7(4)
C(1)-C(2)-N(2)-C(3)	7.8(5)
C(4)-C(2)-N(2)-C(23)	62.2(6)
C(1)-C(2)-N(2)-C(23)	-176.3(4)
C(33)-C(34)-C(37)-C(35)	0.1(7)
C(92)-C(34)-C(37)-C(35)	179.5(4)
C(33)-C(34)-C(37)-N(4)	-178.0(4)
C(92)-C(34)-C(37)-N(4)	1.5(7)
C(30)-N(4)-C(37)-C(35)	60.0(6)
C(29)-N(4)-C(37)-C(35)	-115.3(5)
C(30)-N(4)-C(37)-C(34)	-121.9(5)
C(29)-N(4)-C(37)-C(34)	62.8(6)
Ru(2)-C(49)-C(50)-C(51)	174.3(4)
Ru(2)-C(49)-C(50)-C(52)	-4.3(6)
Ru(1)-C(27)-C(54)-C(55)	174.2(4)
Ru(1)-C(27)-C(54)-C(56)	-4.1(6)
C(30)-N(4)-C(29)-C(31)	-113.9(4)
C(37)-N(4)-C(29)-C(31)	62.0(6)
C(30)-N(4)-C(29)-C(28)	8.2(5)
C(37)-N(4)-C(29)-C(28)	-176.0(4)
C(32)-C(31)-C(29)-N(4)	58.5(6)
C(89)-C(31)-C(29)-N(4)	-122.2(5)
C(32)-C(31)-C(29)-C(28)	-57.0(6)
C(89)-C(31)-C(29)-C(28)	122.3(5)
N(3)-C(28)-C(29)-N(4)	-5.0(4)
C(38)-C(28)-C(29)-N(4)	121.0(4)
N(3)-C(28)-C(29)-C(31)	117.3(4)
C(38)-C(28)-C(29)-C(31)	-116.7(5)
C(53)-O(1)-C(52)-C(77)	21.2(7)
Ru(2)-O(1)-C(52)-C(77)	-168.6(4)
C(53)-O(1)-C(52)-C(50)	-161.1(4)
Ru(2)-O(1)-C(52)-C(50)	9.1(5)
C(51)-C(50)-C(52)-O(1)	176.8(5)
C(49)-C(50)-C(52)-O(1)	-4.5(6)

C(51)-C(50)-C(52)-C(77)	-5.2(7)
C(49)-C(50)-C(52)-C(77)	173.4(4)
C(52)-O(1)-C(53)-C(82)	62.9(5)
Ru(2)-O(1)-C(53)-C(82)	-105.6(4)
C(52)-O(1)-C(53)-C(83)	-173.5(4)
Ru(2)-O(1)-C(53)-C(83)	18.0(5)
C(34)-C(37)-C(35)-C(36)	1.4(7)
N(4)-C(37)-C(35)-C(36)	179.4(4)
C(42)-C(41)-C(47)-C(67)	62.9(6)
C(40)-C(41)-C(47)-C(67)	-116.3(5)
C(42)-C(41)-C(47)-C(86)	-59.5(6)
C(40)-C(41)-C(47)-C(86)	121.3(5)
C(56)-O(2)-C(57)-C(59)	62.7(5)
Ru(1)-O(2)-C(57)-C(59)	-105.6(4)
C(56)-O(2)-C(57)-C(58)	-173.9(4)
Ru(1)-O(2)-C(57)-C(58)	17.9(5)
N(2)-C(2)-C(4)-C(5)	-122.3(5)
C(1)-C(2)-C(4)-C(5)	122.3(5)
N(2)-C(2)-C(4)-C(6)	59.0(6)
C(1)-C(2)-C(4)-C(6)	-56.5(6)
C(18)-C(19)-C(13)-C(14)	-0.8(7)
C(22)-C(19)-C(13)-C(14)	178.4(5)
C(18)-C(19)-C(13)-N(1)	173.3(4)
C(22)-C(19)-C(13)-N(1)	-7.5(7)
C(57)-O(2)-C(56)-C(64)	21.0(7)
Ru(1)-O(2)-C(56)-C(64)	-169.1(4)
C(57)-O(2)-C(56)-C(54)	-160.9(4)
Ru(1)-O(2)-C(56)-C(54)	9.0(5)
C(55)-C(54)-C(56)-O(2)	177.1(4)
C(27)-C(54)-C(56)-O(2)	-4.6(6)
C(55)-C(54)-C(56)-C(64)	-4.7(7)
C(27)-C(54)-C(56)-C(64)	173.7(5)
C(87)-C(39)-C(38)-C(108)	0.9(8)
C(87)-C(39)-C(38)-C(28)	180.0(5)

N(3)-C(28)-C(38)-C(39)	-85.3(5)
C(29)-C(28)-C(38)-C(39)	155.2(4)
N(3)-C(28)-C(38)-C(108)	93.8(6)
C(29)-C(28)-C(38)-C(108)	-25.8(7)
N(2)-C(3)-N(1)-C(13)	-177.7(4)
Ru(1)-C(3)-N(1)-C(13)	5.2(7)
N(2)-C(3)-N(1)-C(1)	6.0(5)
Ru(1)-C(3)-N(1)-C(1)	-171.1(3)
C(19)-C(13)-N(1)-C(3)	83.0(6)
C(14)-C(13)-N(1)-C(3)	-102.8(5)
C(19)-C(13)-N(1)-C(1)	-100.7(5)
C(14)-C(13)-N(1)-C(1)	73.4(5)
C(18)-C(19)-C(22)-C(70)	62.7(6)
C(13)-C(19)-C(22)-C(70)	-116.5(5)
C(18)-C(19)-C(22)-C(63)	-59.9(6)
C(13)-C(19)-C(22)-C(63)	120.9(5)
C(42)-C(41)-C(40)-C(45)	-1.5(7)
C(47)-C(41)-C(40)-C(45)	177.7(5)
C(42)-C(41)-C(40)-N(3)	173.3(4)
C(47)-C(41)-C(40)-N(3)	-7.5(7)
C(44)-C(45)-C(40)-C(41)	1.9(7)
C(46)-C(45)-C(40)-C(41)	-178.7(5)
C(44)-C(45)-C(40)-N(3)	-172.9(4)
C(46)-C(45)-C(40)-N(3)	6.5(7)
C(3)-N(1)-C(1)-C(10)	-126.4(4)
C(13)-N(1)-C(1)-C(10)	56.7(5)
C(3)-N(1)-C(1)-C(2)	-1.2(5)
C(13)-N(1)-C(1)-C(2)	-178.1(3)
N(2)-C(2)-C(1)-N(1)	-3.6(4)
C(4)-C(2)-C(1)-N(1)	118.1(4)
N(2)-C(2)-C(1)-C(10)	120.8(4)
C(4)-C(2)-C(1)-C(10)	-117.6(4)
C(12)-C(11)-C(10)-C(73)	-1.4(8)
C(12)-C(11)-C(10)-C(1)	179.5(5)

N(1)-C(1)-C(10)-C(73)	93.5(6)
C(2)-C(1)-C(10)-C(73)	-24.3(7)
N(1)-C(1)-C(10)-C(11)	-87.5(5)
C(2)-C(1)-C(10)-C(11)	154.7(4)
C(40)-C(45)-C(44)-C(43)	-0.7(8)
C(46)-C(45)-C(44)-C(43)	179.9(5)
C(6)-C(4)-C(5)-C(9)	0.7(9)
C(2)-C(4)-C(5)-C(9)	-178.1(5)
N(4)-C(30)-N(3)-C(40)	-177.1(4)
Ru(2)-C(30)-N(3)-C(40)	7.6(7)
N(4)-C(30)-N(3)-C(28)	4.2(5)
Ru(2)-C(30)-N(3)-C(28)	-171.2(3)
C(41)-C(40)-N(3)-C(30)	81.6(6)
C(45)-C(40)-N(3)-C(30)	-103.6(5)
C(41)-C(40)-N(3)-C(28)	-99.7(5)
C(45)-C(40)-N(3)-C(28)	75.1(5)
C(38)-C(28)-N(3)-C(30)	-126.2(4)
C(29)-C(28)-N(3)-C(30)	0.8(5)
C(38)-C(28)-N(3)-C(40)	54.9(5)
C(29)-C(28)-N(3)-C(40)	-178.2(4)
C(41)-C(42)-C(43)-C(44)	1.6(9)
C(41)-C(42)-C(43)-C(84)	-176.8(5)
C(45)-C(44)-C(43)-C(42)	-1.0(9)
C(45)-C(44)-C(43)-C(84)	177.3(5)
C(17)-C(16)-C(14)-C(13)	0.7(8)
C(17)-C(16)-C(14)-C(15)	-179.8(5)
C(19)-C(13)-C(14)-C(16)	1.2(7)
N(1)-C(13)-C(14)-C(16)	-173.0(4)
C(19)-C(13)-C(14)-C(15)	-178.4(5)
N(1)-C(13)-C(14)-C(15)	7.5(7)
C(4)-C(5)-C(9)-C(8)	2.2(10)
C(19)-C(18)-C(17)-C(16)	3.3(9)
C(19)-C(18)-C(17)-C(71)	-176.9(5)
C(14)-C(16)-C(17)-C(18)	-2.8(9)

C(14)-C(16)-C(17)-C(71)	177.3(5)
C(52)-C(50)-C(51)-C(66)	1.0(8)
C(49)-C(50)-C(51)-C(66)	-177.5(5)
C(23)-C(24)-C(25)-C(61)	-1.6(7)
C(60)-C(24)-C(25)-C(61)	179.6(4)
C(56)-C(54)-C(55)-C(69)	1.0(8)
C(27)-C(54)-C(55)-C(69)	-177.3(5)
C(44)-C(45)-C(46)-C(85)	70.4(7)
C(40)-C(45)-C(46)-C(85)	-109.0(6)
C(44)-C(45)-C(46)-C(112)	-51.3(7)
C(40)-C(45)-C(46)-C(112)	129.3(5)
C(37)-C(35)-C(36)-C(68)	-2.2(8)
C(8)-C(7)-C(6)-C(4)	0.4(10)
C(5)-C(4)-C(6)-C(7)	-2.0(9)
C(2)-C(4)-C(6)-C(7)	176.8(5)
C(10)-C(11)-C(12)-C(62)	0.3(9)
C(37)-C(34)-C(33)-C(68)	-0.7(7)
C(92)-C(34)-C(33)-C(68)	179.7(5)
C(89)-C(31)-C(32)-C(90)	-2.0(8)
C(29)-C(31)-C(32)-C(90)	177.3(5)
C(16)-C(14)-C(15)-C(99)	-51.1(7)
C(13)-C(14)-C(15)-C(99)	128.4(6)
C(16)-C(14)-C(15)-C(98)	70.9(7)
C(13)-C(14)-C(15)-C(98)	-109.5(6)
C(6)-C(7)-C(8)-C(9)	2.6(11)
C(5)-C(9)-C(8)-C(7)	-3.9(11)
C(25)-C(24)-C(60)-C(75)	62.0(6)
C(23)-C(24)-C(60)-C(75)	-116.7(6)
C(25)-C(24)-C(60)-C(74)	-113.3(6)
C(23)-C(24)-C(60)-C(74)	68.0(7)
O(2)-C(56)-C(64)-C(101)	-176.3(5)
C(54)-C(56)-C(64)-C(101)	5.7(7)
O(2)-C(56)-C(64)-C(65)	3.3(9)
C(54)-C(56)-C(64)-C(65)	-174.6(5)

C(100)-C(65)-C(64)-C(101)	-114.2(6)
C(76)-C(65)-C(64)-C(101)	61.1(7)
C(100)-C(65)-C(64)-C(56)	66.2(8)
C(76)-C(65)-C(64)-C(56)	-118.6(6)
C(11)-C(12)-C(62)-C(97)	0.1(9)
C(24)-C(25)-C(61)-C(118)	1.2(8)
C(50)-C(51)-C(66)-C(78)	2.1(9)
C(35)-C(36)-C(68)-C(33)	1.5(8)
C(34)-C(33)-C(68)-C(36)	-0.1(8)
C(74)-C(60)-C(75)-C(96)	-0.1(9)
C(24)-C(60)-C(75)-C(96)	-175.6(5)
C(100)-C(65)-C(76)-C(102)	-2.9(8)
C(64)-C(65)-C(76)-C(102)	-178.3(5)
C(75)-C(60)-C(74)-C(94)	-0.8(8)
C(24)-C(60)-C(74)-C(94)	174.6(5)
C(18)-C(17)-C(71)-C(72)	-112.2(7)
C(16)-C(17)-C(71)-C(72)	67.7(8)
C(18)-C(17)-C(71)-C(119)	121.8(6)
C(16)-C(17)-C(71)-C(119)	-58.3(7)
C(54)-C(55)-C(69)-C(101)	1.5(9)
C(11)-C(10)-C(73)-C(97)	2.1(9)
C(1)-C(10)-C(73)-C(97)	-178.8(5)
C(33)-C(34)-C(92)-C(105)	62.4(6)
C(37)-C(34)-C(92)-C(105)	-117.0(6)
C(33)-C(34)-C(92)-C(91)	-113.9(6)
C(37)-C(34)-C(92)-C(91)	66.6(7)
O(1)-C(52)-C(77)-C(78)	-176.3(5)
C(50)-C(52)-C(77)-C(78)	6.2(7)
O(1)-C(52)-C(77)-C(79)	2.6(9)
C(50)-C(52)-C(77)-C(79)	-174.9(5)
C(80)-C(79)-C(77)-C(78)	-113.8(6)
C(81)-C(79)-C(77)-C(78)	61.2(7)
C(80)-C(79)-C(77)-C(52)	67.2(7)
C(81)-C(79)-C(77)-C(52)	-117.7(6)

C(76)-C(65)-C(100)-C(117)	2.6(8)
C(64)-C(65)-C(100)-C(117)	177.9(5)
C(105)-C(92)-C(91)-C(93)	-1.6(8)
C(34)-C(92)-C(91)-C(93)	174.8(5)
C(51)-C(66)-C(78)-C(77)	-1.0(10)
C(52)-C(77)-C(78)-C(66)	-3.2(9)
C(79)-C(77)-C(78)-C(66)	177.7(6)
C(80)-C(79)-C(81)-C(115)	-1.8(9)
C(77)-C(79)-C(81)-C(115)	-176.8(5)
C(55)-C(69)-C(101)-C(64)	-0.2(10)
C(56)-C(64)-C(101)-C(69)	-3.5(9)
C(65)-C(64)-C(101)-C(69)	176.9(6)
C(65)-C(76)-C(102)-C(116)	1.8(10)
C(92)-C(91)-C(93)-C(107)	1.8(9)
C(10)-C(73)-C(97)-C(62)	-1.7(10)
C(12)-C(62)-C(97)-C(73)	0.6(10)
C(42)-C(43)-C(84)-C(111)	-113.4(7)
C(44)-C(43)-C(84)-C(111)	68.3(8)
C(42)-C(43)-C(84)-C(110)	121.2(7)
C(44)-C(43)-C(84)-C(110)	-57.1(8)
C(32)-C(31)-C(89)-C(103)	1.2(8)
C(29)-C(31)-C(89)-C(103)	-178.1(5)
C(96)-C(95)-C(94)-C(74)	0.3(11)
C(60)-C(74)-C(94)-C(95)	0.7(10)
C(81)-C(79)-C(80)-C(113)	2.0(8)
C(77)-C(79)-C(80)-C(113)	177.0(5)
C(60)-C(75)-C(96)-C(95)	1.1(10)
C(94)-C(95)-C(96)-C(75)	-1.2(10)
C(31)-C(32)-C(90)-C(104)	-0.1(9)
C(109)-C(88)-C(87)-C(39)	0.7(9)
C(38)-C(39)-C(87)-C(88)	-1.2(9)
C(91)-C(93)-C(107)-C(106)	0.0(10)
C(65)-C(100)-C(117)-C(116)	-1.2(9)
C(25)-C(61)-C(118)-C(26)	0.6(8)

C(23)-C(26)-C(118)-C(61)	-2.1(8)
C(87)-C(88)-C(109)-C(108)	0.1(10)
C(79)-C(80)-C(113)-C(114)	-1.0(9)
C(88)-C(109)-C(108)-C(38)	-0.4(10)
C(39)-C(38)-C(108)-C(109)	-0.1(9)
C(28)-C(38)-C(108)-C(109)	-179.2(5)
C(80)-C(113)-C(114)-C(115)	-0.3(10)
C(79)-C(81)-C(115)-C(114)	0.4(10)
C(113)-C(114)-C(115)-C(81)	0.6(11)
C(76)-C(102)-C(116)-C(117)	-0.3(10)
C(100)-C(117)-C(116)-C(102)	0.0(10)
C(91)-C(92)-C(105)-C(106)	-0.3(9)
C(34)-C(92)-C(105)-C(106)	-176.8(5)
C(92)-C(105)-C(106)-C(107)	2.0(10)
C(93)-C(107)-C(106)-C(105)	-1.8(10)
C(32)-C(90)-C(104)-C(103)	2.9(10)
C(90)-C(104)-C(103)-C(89)	-3.6(10)
C(31)-C(89)-C(103)-C(104)	1.5(9)

Symmetry transformations used to generate equivalent atoms:

■ Crystal Structure of b (Scheme S-1, page 289)

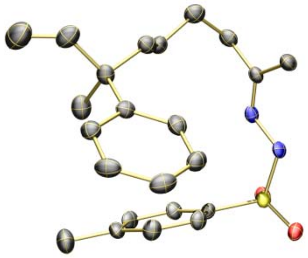

Identification code	rvo01x
Empirical formula	C23 H28 N2 O2 S
Formula weight	396.53

Temperature	100(2) K	
Wavelength	0.71073 Å	
Crystal system	Monoclinic	
Space group	P2(1)	
Unit cell dimensions	a = 10.8793(19) Å	a= 90°.
	b = 17.550(3) Å	b= 100.646(2)°.
	c = 11.456(2) Å	g = 90°.
Volume	2149.8(7) Å^3	
Z	4	
Density (calculated)	1.225 Mg/m^3	
Absorption coefficient	0.171 mm^{-1}	
F(000)	848	
Crystal size	0.10 x 0.05 x 0.04 mm^3	
Theta range for data collection	1.90 to 26.00°.	
Index ranges	-13<=h<=13, -21<=k<=21, -14<=l<=14	
Reflections collected	22790	
Independent reflections	8446 [R(int) = 0.0465]	
Completeness to theta = 26.00°	100.0 %	
Absorption correction	Semi-empirical from equivalents	
Max. and min. transmission	0.9932 and 0.9831	

Refinement method	Full-matrix least-squares on F^2
Data / restraints / parameters	8446 / 6 / 529
Goodness-of-fit on F^2	1.029
Final R indices [I>2sigma(I)]	R1 = 0.0488, wR2 = 0.1065
R indices (all data)	R1 = 0.0677, wR2 = 0.1156
Absolute structure parameter	0.03(6)
Largest diff. peak and hole	0.586 and -0.364 e.Å^{-3}

Table 2. Atomic coordinates ($x10^4$) and equivalent isotropic displacement parameters (Å^{2}x 10^3) for hydrazone **b**. U(eq) is defined as one third of the trace of the orthogonalized U^{ij} tensor

	x	y	z	U(eq)
S(1)	7528(1)	1084(1)	5810(1)	26(1)
S(2)	5592(1)	298(1)	2175(1)	28(1)
C(6)	10789(3)	1978(2)	1961(2)	29(1)
C(1)	10190(3)	1727(2)	2861(3)	35(1)
C(2)	9956(3)	2221(2)	3738(3)	37(1)
C(3)	10315(3)	2964(2)	3725(3)	40(1)
C(4)	10908(3)	3233(2)	2838(3)	38(1)
C(5)	11140(3)	2737(2)	1967(3)	33(1)
C(15)	8589(3)	-737(2)	2241(3)	27(1)
C(14)	9203(3)	-1123(2)	1332(3)	36(1)
C(8)	12291(3)	1624(2)	689(3)	44(1)
C(12)	10264(3)	70(2)	792(3)	35(1)
C(11)	11003(3)	625(2)	1316(3)	34(1)
C(13)	10397(4)	-744(2)	1151(3)	44(1)
C(7)	11010(3)	1454(2)	952(3)	32(1)

C(10)	9971(4)	1622(2)	-127(3)	45(1)
C(9)	12495(5)	1921(3)	-327(4)	74(1)
N(1)	7478(3)	-494(1)	1885(2)	28(1)
N(2)	6877(2)	-159(1)	2744(2)	28(1)
O(1)	5183(2)	615(1)	3202(2)	32(1)
O(2)	4789(2)	-207(1)	1419(2)	34(1)
C(16)	6013(3)	1056(2)	1328(2)	26(1)
C(21)	5647(3)	1042(2)	98(2)	33(1)
C(19)	7053(3)	2239(2)	1218(3)	38(1)
C(17)	6721(3)	1652(2)	1881(3)	32(1)
C(20)	5987(3)	1648(2)	-554(3)	38(1)
C(18)	6674(3)	2252(2)	-19(3)	33(1)
C(22)	7033(4)	2902(2)	-749(3)	51(1)
C(23)	9300(3)	-672(2)	3487(3)	35(1)
C(24)	2452(3)	-306(2)	5781(2)	26(1)
C(27)	2952(3)	-1366(2)	4106(3)	32(1)
C(31)	2823(3)	-69(2)	4749(2)	28(1)
C(28)	3078(3)	-597(2)	3920(3)	32(1)
C(25)	2352(3)	-1085(2)	5972(3)	28(1)
C(26)	2583(3)	-1607(2)	5142(3)	32(1)
C(33)	2946(3)	49(2)	7885(3)	33(1)
C(30)	742(3)	173(2)	6770(3)	42(1)
C(39)	4636(3)	2252(2)	5591(3)	31(1)
C(38)	4012(3)	2681(2)	6458(3)	42(1)
C(40)	4037(3)	2245(2)	4316(3)	38(1)
N(4)	6276(2)	1555(1)	5204(2)	28(1)
N(3)	5663(3)	1926(1)	6029(2)	30(1)
O(3)	7963(2)	770(1)	4804(2)	31(1)

O(4)	8324(2)	1575(1)	6599(2)	33(1)
C(41)	7022(3)	338(2)	6634(2)	23(1)
C(42)	7392(3)	313(2)	7854(2)	29(1)
C(46)	6205(3)	-204(2)	6044(2)	26(1)
C(45)	5754(3)	-772(2)	6687(3)	28(1)
C(43)	6942(3)	-255(2)	8485(3)	33(1)
C(44)	6116(3)	-801(2)	7925(3)	30(1)
C(47)	5589(3)	-1413(2)	8621(3)	43(1)
C(48)	2583(4)	-178(2)	8853(3)	47(1)
C(34)	2130(3)	255(2)	6726(2)	26(1)
C(35)	2134(8)	1073(4)	6276(6)	31(2)
C(36)	2772(7)	1621(3)	6892(6)	31(2)
C(37)	2675(4)	2453(2)	6459(3)	46(1)
C(34X)	2130(3)	255(2)	6726(2)	1000
C(35X)	2696(11)	1057(5)	6618(10)	27(3)
C(36X)	2041(9)	1685(4)	6411(7)	22(2)
C(37X)	2675(4)	2453(2)	6459(3)	1000

Table 3. Bond lengths [Å] and angles [°] for hydrazone **b**

S(1)-O(4)	1.422(2)
S(1)-O(3)	1.435(2)
S(1)-N(4)	1.634(2)
S(1)-C(41)	1.760(3)
S(2)-O(2)	1.421(2)
S(2)-O(1)	1.444(2)
S(2)-N(2)	1.639(3)
S(2)-C(16)	1.757(3)

C(6)-C(5)	1.385(4)
C(6)-C(1)	1.389(4)
C(6)-C(7)	1.530(4)
C(1)-C(2)	1.386(4)
C(2)-C(3)	1.361(5)
C(3)-C(4)	1.384(5)
C(4)-C(5)	1.382(4)
C(15)-N(1)	1.275(4)
C(15)-C(23)	1.497(4)
C(15)-C(14)	1.499(4)
C(14)-C(13)	1.507(5)
C(8)-C(9)	1.331(5)
C(8)-C(7)	1.510(5)
C(12)-C(11)	1.333(4)
C(12)-C(13)	1.485(5)
C(11)-C(7)	1.514(4)
C(7)-C(10)	1.541(5)
N(1)-N(2)	1.407(3)
C(16)-C(17)	1.381(4)
C(16)-C(21)	1.393(4)
C(21)-C(20)	1.389(5)
C(19)-C(17)	1.368(4)
C(19)-C(18)	1.401(4)
C(20)-C(18)	1.374(5)
C(18)-C(22)	1.509(5)
C(24)-C(31)	1.381(4)
C(24)-C(25)	1.392(4)
C(24)-C(34)	1.550(4)

C(27)-C(28)	1.378(5)
C(27)-C(26)	1.387(4)
C(31)-C(28)	1.391(4)
C(25)-C(26)	1.377(4)
C(33)-C(48)	1.307(5)
C(33)-C(34)	1.498(4)
C(30)-C(34)	1.527(4)
C(39)-N(3)	1.273(4)
C(39)-C(40)	1.486(4)
C(39)-C(38)	1.505(5)
C(38)-C(37)	1.509(5)
N(4)-N(3)	1.412(3)
C(41)-C(42)	1.382(4)
C(41)-C(46)	1.389(4)
C(42)-C(43)	1.373(4)
C(46)-C(45)	1.382(4)
C(45)-C(44)	1.401(4)
C(43)-C(44)	1.387(5)
C(44)-C(47)	1.512(4)
C(34)-C(35)	1.527(7)
C(35)-C(36)	1.313(9)
C(36)-C(37)	1.539(7)
C(35X)-C(36X)	1.311(11)
O(4)-S(1)-O(3)	119.36(13)
O(4)-S(1)-N(4)	108.97(13)
O(3)-S(1)-N(4)	103.04(12)
O(4)-S(1)-C(41)	108.93(13)
O(3)-S(1)-C(41)	109.16(13)

N(4)-S(1)-C(41)	106.59(13)
O(2)-S(2)-O(1)	119.33(13)
O(2)-S(2)-N(2)	108.69(14)
O(1)-S(2)-N(2)	103.43(12)
O(2)-S(2)-C(16)	109.28(13)
O(1)-S(2)-C(16)	108.01(14)
N(2)-S(2)-C(16)	107.44(13)
C(5)-C(6)-C(1)	117.9(3)
C(5)-C(6)-C(7)	120.0(3)
C(1)-C(6)-C(7)	122.1(3)
C(2)-C(1)-C(6)	120.9(3)
C(3)-C(2)-C(1)	120.0(3)
C(2)-C(3)-C(4)	120.6(3)
C(5)-C(4)-C(3)	119.1(3)
C(4)-C(5)-C(6)	121.5(3)
N(1)-C(15)-C(23)	124.9(3)
N(1)-C(15)-C(14)	116.5(3)
C(23)-C(15)-C(14)	118.6(3)
C(15)-C(14)-C(13)	113.7(3)
C(9)-C(8)-C(7)	124.1(4)
C(11)-C(12)-C(13)	124.0(3)
C(12)-C(11)-C(7)	127.7(3)
C(12)-C(13)-C(14)	114.9(3)
C(8)-C(7)-C(11)	107.2(3)
C(8)-C(7)-C(6)	108.2(3)
C(11)-C(7)-C(6)	111.1(3)
C(8)-C(7)-C(10)	111.7(3)
C(11)-C(7)-C(10)	111.3(3)

C(6)-C(7)-C(10)	107.3(3)
C(15)-N(1)-N(2)	116.8(2)
N(1)-N(2)-S(2)	113.47(18)
C(17)-C(16)-C(21)	120.6(3)
C(17)-C(16)-S(2)	120.0(2)
C(21)-C(16)-S(2)	119.3(3)
C(20)-C(21)-C(16)	118.4(3)
C(17)-C(19)-C(18)	121.0(3)
C(19)-C(17)-C(16)	119.9(3)
C(18)-C(20)-C(21)	121.8(3)
C(20)-C(18)-C(19)	118.3(3)
C(20)-C(18)-C(22)	120.7(3)
C(19)-C(18)-C(22)	120.9(3)
C(31)-C(24)-C(25)	118.3(3)
C(31)-C(24)-C(34)	123.1(3)
C(25)-C(24)-C(34)	118.6(3)
C(28)-C(27)-C(26)	118.9(3)
C(24)-C(31)-C(28)	120.8(3)
C(27)-C(28)-C(31)	120.6(3)
C(26)-C(25)-C(24)	121.0(3)
C(25)-C(26)-C(27)	120.4(3)
C(48)-C(33)-C(34)	127.1(3)
N(3)-C(39)-C(40)	125.2(3)
N(3)-C(39)-C(38)	115.8(3)
C(40)-C(39)-C(38)	119.0(3)
C(39)-C(38)-C(37)	114.8(3)
N(3)-N(4)-S(1)	114.13(19)
C(39)-N(3)-N(4)	115.6(2)

C(42)-C(41)-C(46)	120.8(3)
C(42)-C(41)-S(1)	120.3(2)
C(46)-C(41)-S(1)	118.9(2)
C(43)-C(42)-C(41)	119.3(3)
C(45)-C(46)-C(41)	119.5(3)
C(46)-C(45)-C(44)	120.4(3)
C(42)-C(43)-C(44)	121.4(3)
C(43)-C(44)-C(45)	118.6(3)
C(43)-C(44)-C(47)	121.6(3)
C(45)-C(44)-C(47)	119.8(3)
C(33)-C(34)-C(35)	119.1(4)
C(33)-C(34)-C(30)	112.1(3)
C(35)-C(34)-C(30)	99.4(4)
C(33)-C(34)-C(24)	107.1(2)
C(35)-C(34)-C(24)	110.2(3)
C(30)-C(34)-C(24)	108.4(2)
C(36)-C(35)-C(34)	122.8(7)
C(35)-C(36)-C(37)	121.6(7)
C(38)-C(37)-C(36)	104.0(4)

Symmetry transformations used to generate equivalent atoms:

Table 4. Anisotropic displacement parameters ($Å^2$x10^3) for hydrazone **b**. The anisotropic displacement factor exponent takes the form: $-2p^2[h^2a^{*2}U^{11} + ... + 2\ h\ k\ a^*\ b^*U^{12}]$

	U^{11}	U^{22}	U^{33}	U^{23}	U^{13}	U^{12}
S(1)	27(1)	24(1)	25(1)	2(1)	2(1)	-1(1)
S(2)	27(1)	34(1)	22(1)	1(1)	2(1)	-2(1)
C(6)	31(2)	31(2)	22(2)	-4(1)	-1(1)	4(1)
C(1)	36(2)	36(2)	32(2)	4(2)	1(2)	0(2)
C(2)	38(2)	46(2)	28(2)	-2(2)	9(2)	5(2)

C(3)	34(2)	48(2)	37(2)	-17(2)	1(2)	3(2)
C(4)	34(2)	29(2)	50(2)	-12(2)	3(2)	1(2)
C(5)	34(2)	31(2)	36(2)	-2(2)	7(1)	0(1)
C(15)	33(2)	22(2)	25(2)	2(1)	2(1)	-1(1)
C(14)	44(2)	25(2)	37(2)	-2(2)	4(2)	2(2)
C(8)	46(2)	42(2)	47(2)	-16(2)	16(2)	-7(2)
C(12)	39(2)	39(2)	29(2)	0(2)	12(2)	3(2)
C(11)	41(2)	34(2)	29(2)	-2(2)	7(2)	5(2)
C(13)	50(2)	41(2)	43(2)	-8(2)	13(2)	5(2)
C(7)	43(2)	25(2)	26(2)	-6(1)	6(1)	-6(2)
C(10)	63(2)	39(2)	33(2)	-7(2)	8(2)	-13(2)
C(9)	73(3)	64(3)	93(4)	-7(3)	39(3)	-9(2)
N(1)	38(2)	24(1)	21(1)	-1(1)	5(1)	-2(1)
N(2)	33(2)	33(2)	17(1)	4(1)	1(1)	2(1)
O(1)	28(1)	43(1)	25(1)	2(1)	6(1)	-1(1)
O(2)	35(1)	36(1)	30(1)	2(1)	-1(1)	-5(1)
C(16)	26(2)	33(2)	21(1)	-1(1)	5(1)	-1(2)
C(21)	36(2)	37(2)	24(2)	0(2)	-1(1)	0(2)
C(19)	44(2)	38(2)	31(2)	-6(2)	6(2)	-7(2)
C(17)	37(2)	37(2)	21(2)	-2(1)	3(1)	-3(2)
C(20)	44(2)	51(2)	17(2)	4(2)	1(1)	7(2)
C(18)	33(2)	34(2)	32(2)	10(2)	6(1)	6(2)
C(22)	58(2)	51(2)	45(2)	14(2)	9(2)	-7(2)
C(23)	39(2)	36(2)	31(2)	5(2)	5(1)	8(2)
C(24)	29(2)	24(2)	25(2)	-2(1)	4(1)	6(1)
C(27)	30(2)	35(2)	29(2)	-10(1)	3(1)	7(1)
C(31)	29(2)	28(2)	27(2)	-1(1)	3(1)	0(1)
C(28)	31(2)	40(2)	24(2)	0(2)	5(1)	-2(2)

C(25)	35(2)	24(2)	25(2)	-1(1)	7(1)	1(1)
C(26)	36(2)	22(2)	39(2)	1(1)	4(1)	2(1)
C(33)	32(2)	30(2)	34(2)	-15(1)	1(1)	3(1)
C(30)	35(2)	45(2)	43(2)	-16(2)	2(2)	11(2)
C(39)	36(2)	18(2)	37(2)	4(1)	1(2)	4(1)
C(38)	44(2)	30(2)	47(2)	-10(2)	-4(2)	10(2)
C(40)	40(2)	32(2)	40(2)	8(2)	1(2)	4(2)
N(4)	36(2)	23(1)	23(1)	9(1)	5(1)	7(1)
N(3)	39(2)	21(1)	29(1)	0(1)	7(1)	1(1)
O(3)	27(1)	40(1)	27(1)	2(1)	7(1)	0(1)
O(4)	33(1)	28(1)	35(1)	-2(1)	-1(1)	-6(1)
C(41)	24(1)	19(2)	26(1)	1(1)	3(1)	5(1)
C(42)	31(2)	31(2)	23(2)	-2(2)	-2(1)	-1(2)
C(46)	31(2)	25(2)	20(1)	0(1)	1(1)	4(1)
C(45)	26(2)	20(2)	35(2)	1(1)	1(1)	-1(1)
C(43)	39(2)	35(2)	22(2)	4(1)	2(1)	8(2)
C(44)	30(2)	28(2)	35(2)	11(1)	10(1)	15(1)
C(47)	43(2)	32(2)	56(2)	17(2)	14(2)	8(2)
C(48)	56(2)	53(2)	29(2)	-12(2)	-3(2)	8(2)
C(34)	32(2)	20(2)	26(2)	-3(1)	7(1)	4(1)
C(35)	34(4)	30(4)	28(4)	-2(3)	5(3)	10(3)
C(36)	32(4)	29(4)	33(3)	-7(3)	8(3)	6(3)
C(37)	57(2)	30(2)	55(2)	-11(2)	19(2)	2(2)
C(35X)	32(6)	26(6)	21(5)	-8(4)	-1(4)	9(5)
C(36X)	19(5)	21(5)	23(4)	-5(3)	-1(4)	7(3)

Table 5. Hydrogen coordinates (x10^4) and isotropic displacement parameters (Å^{2}x10) for hydrazone **b**

	x	y	z	U(eq)

H(1)	9938	1209	2876	42
H(2)	9545	2042	4347	44
H(3)	10158	3299	4332	48
H(4)	11151	3753	2828	46
H(5)	11550	2921	1359	40
H(14A)	8610	-1132	565	43
H(14B)	9389	-1657	1579	43
H(8)	12997	1510	1285	53
H(12)	9615	202	150	42
H(11)	11595	484	2000	41
H(13A)	11016	-781	1899	53
H(13B)	10735	-1029	534	53
H(10A)	9175	1417	19	67
H(10B)	10182	1382	-836	67
H(10C)	9895	2174	-249	67
H(9A)	11809	2041	-942	89
H(9B)	13326	2014	-438	89
H(2A)	7163	-192	3513	34
H(21)	5175	627	-287	39
H(19)	7548	2645	1602	45
H(17)	6977	1653	2720	39
H(20)	5738	1645	-1394	46
H(22A)	7239	2703	-1489	77
H(22B)	7762	3167	-298	77
H(22C)	6332	3259	-935	77
H(23A)	9536	-139	3658	53
H(23B)	10056	-987	3577	53
H(23C)	8774	-848	4042	53

H(27)	3114	-1726	3534	38
H(31)	2906	460	4605	34
H(28)	3341	-425	3219	38
H(25)	2120	-1259	6686	33
H(26)	2490	-2136	5280	39
H(33)	3823	89	7920	39
H(30A)	242	315	5999	62
H(30B)	530	508	7388	62
H(30C)	562	-357	6951	62
H(38A)	4033	3232	6276	50
H(38B)	4504	2604	7267	50
H(40A)	4671	2341	3827	57
H(40B)	3395	2642	4168	57
H(40C)	3651	1746	4111	57
H(4A)	6008	1575	4432	33
H(42)	7951	686	8252	35
H(46)	5957	-184	5204	31
H(45)	5197	-1144	6288	33
H(43)	7203	-274	9323	39
H(47A)	4679	-1438	8363	65
H(47B)	5787	-1291	9470	65
H(47C)	5959	-1906	8480	65
H(48A)	1716	-228	8867	57
H(48B)	3185	-294	9542	57
H(35)	1655	1191	5517	37
H(36)	3306	1502	7622	37
H(37A)	2163	2491	5651	55
H(37B)	2299	2780	7004	55

H(35X)	3580	1095	6709	33
H(36X)	1154	1657	6227	26

Table 6. Torsion angles [°] for hydrazone **b**

C(5)-C(6)-C(1)-C(2)	-0.2(4)
C(7)-C(6)-C(1)-C(2)	-177.3(3)
C(6)-C(1)-C(2)-C(3)	-0.1(5)
C(1)-C(2)-C(3)-C(4)	0.5(5)
C(2)-C(3)-C(4)-C(5)	-0.5(5)
C(3)-C(4)-C(5)-C(6)	0.3(5)
C(1)-C(6)-C(5)-C(4)	0.1(5)
C(7)-C(6)-C(5)-C(4)	177.3(3)
N(1)-C(15)-C(14)-C(13)	120.7(3)
C(23)-C(15)-C(14)-C(13)	-60.0(4)
C(13)-C(12)-C(11)-C(7)	174.5(3)
C(11)-C(12)-C(13)-C(14)	130.5(3)
C(15)-C(14)-C(13)-C(12)	-57.7(4)
C(9)-C(8)-C(7)-C(11)	125.8(4)
C(9)-C(8)-C(7)-C(6)	-114.3(4)
C(9)-C(8)-C(7)-C(10)	3.5(5)
C(12)-C(11)-C(7)-C(8)	-119.7(4)
C(12)-C(11)-C(7)-C(6)	122.3(3)
C(12)-C(11)-C(7)-C(10)	2.8(5)
C(5)-C(6)-C(7)-C(8)	42.3(4)
C(1)-C(6)-C(7)-C(8)	-140.6(3)
C(5)-C(6)-C(7)-C(11)	159.8(3)
C(1)-C(6)-C(7)-C(11)	-23.2(4)

C(5)-C(6)-C(7)-C(10)	-78.3(4)
C(1)-C(6)-C(7)-C(10)	98.7(3)
C(23)-C(15)-N(1)-N(2)	-1.8(4)
C(14)-C(15)-N(1)-N(2)	177.5(2)
C(15)-N(1)-N(2)-S(2)	167.6(2)
O(2)-S(2)-N(2)-N(1)	54.7(2)
O(1)-S(2)-N(2)-N(1)	-177.50(19)
C(16)-S(2)-N(2)-N(1)	-63.4(2)
O(2)-S(2)-C(16)-C(17)	175.4(2)
O(1)-S(2)-C(16)-C(17)	44.1(3)
N(2)-S(2)-C(16)-C(17)	-66.8(3)
O(2)-S(2)-C(16)-C(21)	-5.8(3)
O(1)-S(2)-C(16)-C(21)	-137.1(2)
N(2)-S(2)-C(16)-C(21)	112.0(3)
C(17)-C(16)-C(21)-C(20)	-1.4(5)
S(2)-C(16)-C(21)-C(20)	179.8(2)
C(18)-C(19)-C(17)-C(16)	0.7(5)
C(21)-C(16)-C(17)-C(19)	0.9(5)
S(2)-C(16)-C(17)-C(19)	179.7(2)
C(16)-C(21)-C(20)-C(18)	0.3(5)
C(21)-C(20)-C(18)-C(19)	1.2(5)
C(21)-C(20)-C(18)-C(22)	179.9(3)
C(17)-C(19)-C(18)-C(20)	-1.7(5)
C(17)-C(19)-C(18)-C(22)	179.6(3)
C(25)-C(24)-C(31)-C(28)	0.7(4)
C(34)-C(24)-C(31)-C(28)	-178.8(3)
C(26)-C(27)-C(28)-C(31)	-0.9(5)
C(24)-C(31)-C(28)-C(27)	0.7(5)

C(31)-C(24)-C(25)-C(26)	-1.8(5)
C(34)-C(24)-C(25)-C(26)	177.7(3)
C(24)-C(25)-C(26)-C(27)	1.5(5)
C(28)-C(27)-C(26)-C(25)	-0.2(5)
N(3)-C(39)-C(38)-C(37)	-125.4(3)
C(40)-C(39)-C(38)-C(37)	55.2(4)
O(4)-S(1)-N(4)-N(3)	-52.1(2)
O(3)-S(1)-N(4)-N(3)	-179.85(19)
C(41)-S(1)-N(4)-N(3)	65.3(2)
C(40)-C(39)-N(3)-N(4)	2.3(4)
C(38)-C(39)-N(3)-N(4)	-177.1(3)
S(1)-N(4)-N(3)-C(39)	-175.2(2)
O(4)-S(1)-C(41)-C(42)	1.2(3)
O(3)-S(1)-C(41)-C(42)	133.1(2)
N(4)-S(1)-C(41)-C(42)	-116.2(2)
O(4)-S(1)-C(41)-C(46)	178.4(2)
O(3)-S(1)-C(41)-C(46)	-49.6(3)
N(4)-S(1)-C(41)-C(46)	61.0(3)
C(46)-C(41)-C(42)-C(43)	0.0(4)
S(1)-C(41)-C(42)-C(43)	177.2(2)
C(42)-C(41)-C(46)-C(45)	0.2(4)
S(1)-C(41)-C(46)-C(45)	-177.0(2)
C(41)-C(46)-C(45)-C(44)	0.2(4)
C(41)-C(42)-C(43)-C(44)	-0.6(5)
C(42)-C(43)-C(44)-C(45)	1.0(5)
C(42)-C(43)-C(44)-C(47)	-178.1(3)
C(46)-C(45)-C(44)-C(43)	-0.7(4)
C(46)-C(45)-C(44)-C(47)	178.4(3)

C(48)-C(33)-C(34)-C(35)	115.6(5)
C(48)-C(33)-C(34)-C(30)	0.2(5)
C(48)-C(33)-C(34)-C(24)	-118.6(3)
C(31)-C(24)-C(34)-C(33)	-124.2(3)
C(25)-C(24)-C(34)-C(33)	56.3(4)
C(31)-C(24)-C(34)-C(35)	6.8(5)
C(25)-C(24)-C(34)-C(35)	-172.7(4)
C(31)-C(24)-C(34)-C(30)	114.6(3)
C(25)-C(24)-C(34)-C(30)	-64.8(4)
C(33)-C(34)-C(35)-C(36)	-3.9(9)
C(30)-C(34)-C(35)-C(36)	118.0(7)
C(24)-C(34)-C(35)-C(36)	-128.2(6)
C(34)-C(35)-C(36)-C(37)	-175.0(4)
C(39)-C(38)-C(37)-C(36)	64.7(4)
C(35)-C(36)-C(37)-C(38)	-125.6(6)

Symmetry transformations used to generate equivalent atoms:

Table 7. Hydrogen bonds for hydrazone **b** [Å and °]

D-H...A	d(D-H)	d(H...A)	d(D...A)	<(DHA)
N(2)-H(2A)...O(3)	0.88	2.31	2.931(3)	128.0
N(4)-H(4A)...O(1)	0.88	2.27	2.896(3)	127.8

Symmetry transformations used to generate equivalent atoms:

■ Crystal Structure of Enone Derived from 2.205

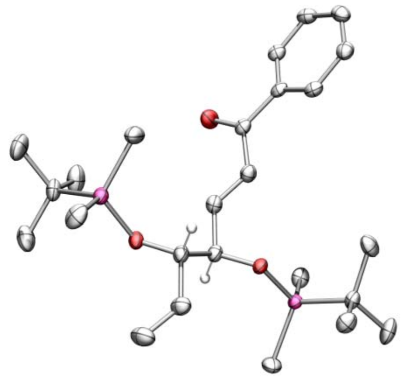

Identification code	d08038	
Empirical formula	C25 H42 O3 Si2	
Formula weight	446.77	
Temperature	100(2) K	
Wavelength	1.54178 Å	
Crystal system	Orthorhombic	
Space group	P2(1)2(1)2(1)	
Unit cell dimensions	a = 7.4780(3) Å	a= 90°.
	b = 15.0069(5) Å	b= 90°.
	c = 24.6083(9) Å	g = 90°.
Volume	2761.58(18) Å^3	
Z	4	
Density (calculated)	1.075 Mg/m^3	
Absorption coefficient	1.322 mm^{-1}	

F(000)	976
Crystal size	0.48 x 0.35 x 0.30 mm^3
Theta range for data collection	3.45 to 67.68°.
Index ranges	-8<=h<=8, -17<=k<=17, -28<=l<=29
Reflections collected	38328
Independent reflections	4964 [R(int) = 0.0296]
Completeness to theta = 67.68°	100.0 %
Absorption correction	Semi-empirical from equivalents
Max. and min. transmission	0.6925 and 0.5694
Refinement method	Full-matrix least-squares on F^2
Data / restraints / parameters	4964 / 0 / 281
Goodness-of-fit on F^2	1.100
Final R indices [I>2sigma(I)]	R1 = 0.0308, wR2 = 0.0809
R indices (all data)	R1 = 0.0309, wR2 = 0.0810
Absolute structure parameter	0.052(19)
Largest diff. peak and hole	0.291 and -0.208 e.Å^{-3}

Table 2. Atomic coordinates ($x10^4$) and equivalent isotropic displacement parameters (Å^2$x10^3$) for enone derived from **14**. U(eq) is defined as one third of the trace of the orthogonalized U^{ij} tensor

	x	y	z	U(eq)
Si(1)	5579(1)	6649(1)	1175(1)	19(1)
Si(2)	1544(1)	2830(1)	1264(1)	23(1)

O(1)	5268(2)	5561(1)	1258(1)	22(1)
O(2)	1824(2)	3891(1)	1090(1)	24(1)
O(3)	2282(2)	4647(1)	2999(1)	36(1)
C(1)	2846(3)	4276(1)	10(1)	41(1)
C(2)	3927(3)	4458(1)	415(1)	30(1)
C(3)	3527(2)	4292(1)	1006(1)	24(1)
C(4)	3557(2)	5172(1)	1333(1)	24(1)
C(5)	3168(2)	4980(1)	1919(1)	24(1)
C(6)	4329(2)	5068(1)	2321(1)	26(1)
C(7)	3837(2)	4825(1)	2886(1)	23(1)
C(8)	5255(2)	4787(1)	3314(1)	22(1)
C(9)	7078(2)	4742(1)	3194(1)	24(1)
C(10)	8325(2)	4633(1)	3607(1)	28(1)
C(11)	7753(3)	4582(1)	4143(1)	31(1)
C(12)	5945(3)	4648(1)	4267(1)	30(1)
C(13)	4707(2)	4742(1)	3855(1)	26(1)
C(21)	4515(2)	7287(1)	1739(1)	29(1)
C(22)	4580(3)	7020(1)	518(1)	34(1)
C(23)	8087(2)	6759(1)	1174(1)	23(1)
C(24)	8615(3)	7742(1)	1102(1)	38(1)
C(25)	8854(3)	6216(1)	697(1)	31(1)
C(26)	8862(2)	6400(1)	1707(1)	33(1)
C(31)	2871(3)	2570(1)	1884(1)	36(1)
C(32)	2294(3)	2093(1)	700(1)	36(1)
C(33)	-928(2)	2734(1)	1404(1)	28(1)
C(34)	-1358(3)	1788(1)	1608(1)	42(1)
C(35)	-1970(3)	2908(2)	878(1)	41(1)
C(36)	-1491(3)	3420(2)	1836(1)	44(1)

Table 3. Bond lengths [Å] and angles [°] for enone derived from **14**

Si(1)-O(1)	1.6617(11)
Si(1)-C(21)	1.8643(17)
Si(1)-C(22)	1.8663(18)
Si(1)-C(23)	1.8828(17)
Si(2)-O(2)	1.6629(11)
Si(2)-C(31)	1.8599(18)
Si(2)-C(32)	1.8601(19)
Si(2)-C(33)	1.8859(17)
O(1)-C(4)	1.4180(19)
O(2)-C(3)	1.424(2)
O(3)-C(7)	1.225(2)
C(1)-C(2)	1.311(3)
C(2)-C(3)	1.505(2)
C(3)-C(4)	1.547(2)
C(4)-C(5)	1.499(2)
C(5)-C(6)	1.323(2)
C(6)-C(7)	1.485(2)
C(7)-C(8)	1.496(2)
C(8)-C(13)	1.393(2)
C(8)-C(9)	1.396(2)
C(9)-C(10)	1.388(3)
C(10)-C(11)	1.389(3)
C(11)-C(12)	1.390(3)
C(12)-C(13)	1.381(3)
C(23)-C(26)	1.531(2)
C(23)-C(24)	1.537(2)

C(23)-C(25)	1.541(2)
C(33)-C(35)	1.533(3)
C(33)-C(36)	1.538(3)
C(33)-C(34)	1.540(3)
O(1)-Si(1)-C(21)	110.68(7)
O(1)-Si(1)-C(22)	110.12(8)
C(21)-Si(1)-C(22)	108.71(9)
O(1)-Si(1)-C(23)	103.06(7)
C(21)-Si(1)-C(23)	112.36(8)
C(22)-Si(1)-C(23)	111.82(9)
O(2)-Si(2)-C(31)	110.14(8)
O(2)-Si(2)-C(32)	109.83(8)
C(31)-Si(2)-C(32)	109.03(10)
O(2)-Si(2)-C(33)	104.09(7)
C(31)-Si(2)-C(33)	110.94(9)
C(32)-Si(2)-C(33)	112.73(9)
C(4)-O(1)-Si(1)	123.10(10)
C(3)-O(2)-Si(2)	123.73(10)
C(1)-C(2)-C(3)	125.18(19)
O(2)-C(3)-C(2)	112.87(14)
O(2)-C(3)-C(4)	107.32(13)
C(2)-C(3)-C(4)	111.04(14)
O(1)-C(4)-C(5)	112.29(13)
O(1)-C(4)-C(3)	107.24(13)
C(5)-C(4)-C(3)	109.50(13)
C(6)-C(5)-C(4)	124.89(16)
C(5)-C(6)-C(7)	120.87(16)
O(3)-C(7)-C(6)	120.08(16)

O(3)-C(7)-C(8)	120.35(15)
C(6)-C(7)-C(8)	119.57(14)
C(13)-C(8)-C(9)	119.14(16)
C(13)-C(8)-C(7)	117.73(15)
C(9)-C(8)-C(7)	123.02(15)
C(10)-C(9)-C(8)	120.46(16)
C(9)-C(10)-C(11)	119.61(17)
C(10)-C(11)-C(12)	120.31(17)
C(13)-C(12)-C(11)	119.84(17)
C(12)-C(13)-C(8)	120.61(17)
C(26)-C(23)-C(24)	109.91(16)
C(26)-C(23)-C(25)	108.99(14)
C(24)-C(23)-C(25)	108.87(14)
C(26)-C(23)-Si(1)	110.19(12)
C(24)-C(23)-Si(1)	109.92(12)
C(25)-C(23)-Si(1)	108.94(12)
C(35)-C(33)-C(36)	109.27(16)
C(35)-C(33)-C(34)	109.02(16)
C(36)-C(33)-C(34)	109.56(17)
C(35)-C(33)-Si(2)	109.34(13)
C(36)-C(33)-Si(2)	110.08(12)
C(34)-C(33)-Si(2)	109.55(12)

Symmetry transformations used to generate equivalent atoms:

Table 4. Anisotropic displacement parameters ($Å^2x10^3$) for enone derived from **14**. The anisotropic displacement factor exponent takes the form: $-2p^2[h^2 a^{*2}U^{11} + ... + 2 h k a^* b^* U^{12}]$

	U^{11}	U^{22}	U^{33}	U^{23}	U^{13}	U^{12}
Si(1)	22(1)	17(1)	19(1)	2(1)	0(1)	-1(1)

Si(2)	22(1)	19(1)	26(1)	1(1)	-1(1)	-1(1)
O(1)	22(1)	19(1)	24(1)	3(1)	0(1)	-2(1)
O(2)	24(1)	20(1)	30(1)	0(1)	-4(1)	-2(1)
O(3)	26(1)	54(1)	27(1)	4(1)	5(1)	-5(1)
C(1)	61(1)	35(1)	26(1)	1(1)	-6(1)	2(1)
C(2)	43(1)	24(1)	25(1)	0(1)	1(1)	0(1)
C(3)	24(1)	20(1)	27(1)	1(1)	0(1)	-2(1)
C(4)	23(1)	20(1)	28(1)	2(1)	0(1)	-1(1)
C(5)	24(1)	24(1)	25(1)	-4(1)	3(1)	0(1)
C(6)	24(1)	28(1)	26(1)	0(1)	3(1)	-1(1)
C(7)	27(1)	18(1)	24(1)	0(1)	4(1)	0(1)
C(8)	30(1)	13(1)	24(1)	1(1)	4(1)	-1(1)
C(9)	32(1)	19(1)	22(1)	2(1)	5(1)	1(1)
C(10)	28(1)	23(1)	35(1)	3(1)	0(1)	1(1)
C(11)	37(1)	26(1)	29(1)	2(1)	-7(1)	5(1)
C(12)	42(1)	26(1)	22(1)	3(1)	2(1)	4(1)
C(13)	30(1)	21(1)	26(1)	1(1)	4(1)	3(1)
C(21)	27(1)	26(1)	35(1)	-4(1)	5(1)	3(1)
C(22)	40(1)	32(1)	31(1)	10(1)	-10(1)	0(1)
C(23)	22(1)	21(1)	25(1)	-2(1)	4(1)	-2(1)
C(24)	32(1)	26(1)	56(1)	-4(1)	9(1)	-9(1)
C(25)	33(1)	31(1)	29(1)	-3(1)	9(1)	0(1)
C(26)	23(1)	46(1)	30(1)	-5(1)	-2(1)	4(1)
C(31)	29(1)	42(1)	37(1)	16(1)	-4(1)	-3(1)
C(32)	45(1)	21(1)	43(1)	-5(1)	11(1)	0(1)
C(33)	22(1)	23(1)	39(1)	-6(1)	0(1)	-3(1)
C(34)	28(1)	36(1)	64(1)	3(1)	4(1)	-8(1)
C(35)	28(1)	38(1)	56(1)	-6(1)	-12(1)	2(1)

C(36)	32(1)	46(1)	56(1)	-18(1)	12(1)	-6(1)

Table 5. Hydrogen coordinates (x10^4) and isotropic displacement parameters (Å^{2}x 10^3) for enone derived from **14**

	x	y	z	U(eq)
H(1A)	1709	4018	80	49
H(1B)	3199	4402	-352	49
H(2)	5051	4716	328	37
H(3)	4467	3887	1155	29
H(4)	2623	5584	1187	28
H(5)	1999	4779	2008	29
H(6)	5494	5290	2247	31
H(9)	7467	4788	2828	29
H(10)	9562	4593	3523	34
H(11)	8602	4501	4426	37
H(12)	5562	4629	4635	36
H(13)	3470	4777	3940	31
H(21A)	3237	7144	1754	44
H(21B)	4667	7927	1674	44
H(21C)	5081	7125	2084	44
H(22A)	5113	6681	219	51
H(22B)	4816	7656	465	51
H(22C)	3286	6917	525	51
H(24A)	8158	8091	1408	57
H(24B)	8103	7970	762	57
H(24C)	9921	7792	1088	57
H(25A)	10157	6283	687	47

H(25B)	8342	6433	355	47
H(25C)	8550	5585	744	47
H(26A)	10166	6465	1703	49
H(26B)	8550	5769	1745	49
H(26C)	8365	6736	2013	49
H(31A)	4138	2694	1814	54
H(31B)	2722	1940	1977	54
H(31C)	2453	2941	2186	54
H(32A)	1575	2213	376	55
H(32B)	2146	1469	808	55
H(32C)	3557	2210	621	55
H(34A)	-2649	1732	1667	64
H(34B)	-726	1679	1951	64
H(34C)	-972	1351	1336	64
H(35A)	-1644	2459	606	61
H(35B)	-1675	3502	740	61
H(35C)	-3256	2873	952	61
H(36A)	-2769	3354	1913	67
H(36B)	-1257	4023	1700	67
H(36C)	-804	3320	2169	67

2.5.6. Details of Computational Studies Described in Figure 2.11

All calculations were performed in Gaussian 03, Rev. E01.[127] All structures were optimized with tight convergence criteria (opt=tight and SCF=tight) on ultrafine grid

---

(127) Gaussian 03, Revision E.01, Frisch, M. J.; Trucks, G. W.; Schlegel, H. B.; Scuseria, G. E.; Robb, M. A.; Cheeseman, J. R.; Montgomery, Jr., J. A.; Vreven, T.; Kudin, K. N.; Burant, J. C.; Millam, J. M.; Iyengar, S. S.; Tomasi, J.; Barone, V.; Mennucci, B.; Cossi, M.; Scalmani, G.; Rega, N.; Petersson, G. A.; Nakatsuji, H.; Hada, M.; Ehara, M.; Toyota, K.; Fukuda, R.; Hasegawa, J.; Ishida, M.; Nakajima, T.; Honda, Y.; Kitao, O.; Nakai, H.; Klene, M.; Li, X.; Knox, J. E.; Hratchian, H. P.; Cross, J. B.; Bakken, V.;

(99,590). The stationary points minimum nature was assured by frequency calculations, where no imaginary frequencies were found. Throughout these studies BP86 GGA was employed as implemented in Gaussian 03, with Stuttgart-Dresden RECP on Ru (MWB28), 6-31G (d,p) on the rest of atoms with the exception of Cl atoms, where 6-31G(3df) was employed. N, O, and Cl atom basis sets were augmented with diffuse functions.

Please note: All basis sets are as implemented in Gaussian 03. APT charges were calculated as part of frequency calculations on the fully optimized structures at the same level of theory as above. The output was visualized with GaussView 3.09.[128]

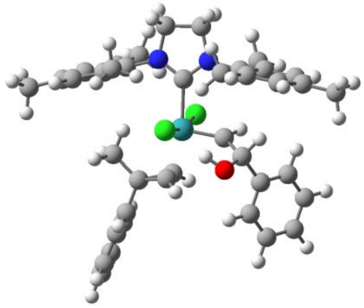

Cartesian Coordinates

C	0.000000000000	0.000000000000	0.000000000000
Ru	0.000000000000	0.000000000000	1.837471370000
H	7.811444201699	0.000000000000	4.489089271779
Cl	-0.262227885947	-2.408353946741	1.733551819428

Adamo, C.; Jaramillo, J.; Gomperts, R.; Stratmann, R. E.; Yazyev, O.; Austin, A. J.; Cammi, R.; Pomelli, C.; Ochterski, J. W.; Ayala, P. Y.; Morokuma, K.; Voth, G. A.; Salvador, P.; Dannenberg, J. J.; Zakrzewski, V. G.; Dapprich, S.; Daniels, A. D.; Strain, M. C.; Farkas, O.; Malick, D. K.; Rabuck, A. D.; Raghavachari, K.; Foresman, J. B.; Ortiz, J. V.; Cui, Q.; Baboul, A. G.; Clifford, S.; Cioslowski, J.; Stefanov, B. B.; Liu, G.; Liashenko, A.; Piskorz, P.; Komaromi, I.; Martin, R. L.; Fox, D. J.; Keith, T.; Al-Laham, M. A.; Peng, C. Y.; Nanayakkara, A.; Challacombe, M.; Gill, P. M. W.; Johnson, B.; Chen, W.; Wong, M. W.; Gonzalez, C.; and Pople, J. A.; Gaussian, Inc., Wallingford CT, 2004.

(128) GaussView, Version 3.09, Dennington II, Roy; Keith, Todd; Millam, John; Eppinnett, Ken; Hovell, W. Lee; and Gilliland, Ray; Semichem, Inc., Shawnee Mission, KS, 2003.

Cl	-0.296377030390	2.397697570715	2.190523352733
C	-2.133214732445	-0.052958399064	2.139943411962
N	-2.733247077269	-0.178751259216	3.356599742814
N	-3.116611477203	-0.000682053837	1.197784036430
C	-2.131871984206	-0.211371283200	4.670985433869
C	-4.217902424658	-0.135459262043	3.282564291684
C	-4.479434929016	-0.179764987464	1.770348646347
C	-3.026962785911	0.184027272550	-0.230249100561
H	-4.648435169500	-0.993589102052	3.824069788839
H	-5.145782110476	0.625320500234	1.419790734742
H	-4.583963575456	0.793761837796	3.755062222694
H	-4.897660599556	-1.146136077190	1.436301795919
C	-3.045257378521	0.564662265924	-3.030235437123
C	-3.122346179403	1.500638682392	-0.752546443022
C	-3.019344644858	-0.948949416365	-1.084145541643
C	-3.012132129601	-0.727774854729	-2.475327701728
C	-3.113788425666	1.661821495968	-2.150377996999
C	-3.254575605824	2.704978541019	0.150754191285
C	-3.043090938661	-2.358646413925	-0.539645462468
H	-2.997587545326	-1.598457776926	-3.142157599771
H	-3.173512430636	2.676961088515	-2.560451554468
C	-3.004137320087	0.773220348018	-4.528683711919
C	-1.067435417471	-0.294286421207	7.286094138999
C	-1.972935699470	0.998802630210	5.395385034834
C	-1.875766318437	-1.470262008410	5.278011032004
C	-1.328372886675	-1.479097989098	6.573364904508
C	-1.417692357206	0.927803821242	6.687122429075
C	-2.449722820581	2.332709520132	4.865135836956

C	-2.215628413533	-2.771456457757	4.590806828944
H	-1.112896122108	-2.446754313853	7.042221114233
H	-1.270375706464	1.861201487938	7.243842986701
C	-0.433395401095	-0.336540423679	8.659493659571
H	-4.182744771536	2.660698180939	0.750618173614
H	-3.289525525264	3.631841820431	-0.442926434439
H	-2.410220623646	2.775890427263	0.858115617572
H	-4.020984526819	-2.594234892835	-0.079055674385
H	-2.267000284009	-2.513934266868	0.230509541119
H	-2.881961339689	-3.089012604817	-1.348314189984
H	-3.297216893721	-2.839865709744	4.370211443981
H	-1.955567418193	-3.626606078842	5.234533473226
H	-1.675957081938	-2.873541640745	3.633486659542
H	-3.511527170305	2.497600959656	5.132293065191
H	-2.344464224572	2.410012446320	3.773602957348
H	-1.873171475435	3.158070688291	5.312239593995
H	-0.725485092359	0.535115307282	9.268006553241
H	0.669552472298	-0.328783707243	8.584997979164
H	-0.715701102866	-1.250612875881	9.207831319656
H	-3.617023099874	1.637949716435	-4.833008700828
H	-3.367396931700	-0.114874152293	-5.071122078490
H	-1.972194937945	0.970345956576	-4.872172818132
C	0.442427257715	1.013205315717	-1.041081469650
H	-0.303839225994	-0.948114841323	-0.487572802223
H	-0.463551324108	1.142495790241	-1.684890315052
C	1.514858625137	0.325014589705	-1.900076491735
O	0.908525355910	2.268935822092	-0.592823179036
H	0.464716981982	2.469194102389	0.273003649691

C	3.479727305557	-0.991075152798	-3.438230373556
C	2.877137490018	0.632488859300	-1.724088155331
C	1.143797970619	-0.641746643995	-2.856354420375
C	2.120564173758	-1.297769887650	-3.619827881207
C	3.852768478365	-0.021759012775	-2.493277748618
H	3.154055393437	1.403334884526	-1.000304448942
H	0.082194893935	-0.871850351446	-3.007914989844
H	1.819708647103	-2.044218514965	-4.362826227679
H	4.909542912585	0.230153852751	-2.353891905719
H	4.242897272511	-1.499786441277	-4.036588552483
C	2.067873232569	-0.682418071024	2.032003887219
H	2.412341363501	-1.520934107704	1.427463833050
C	2.497208731454	0.006925259560	3.320019455196
C	2.064558191014	0.701099201707	2.039331694303
H	2.399701818031	1.544651920657	1.436031925812
C	3.984128045814	0.006664676796	3.621523118874
C	1.625261625579	-0.009365715432	4.575198637704
H	1.832083485680	-0.904003905859	5.187948987454
H	0.545457257123	-0.024094253340	4.331937506088
H	1.805553303988	0.887085686910	5.193755363639
C	6.742713380227	0.002018833224	4.249536780209
C	4.664192676709	-1.204413423822	3.867751812852
C	4.706316522427	1.215307851565	3.698410079321
C	6.075406631242	1.214203190448	4.009475514125
C	6.032977228951	-1.208090930963	4.178300508210
H	4.112054419544	-2.149610815455	3.810062928854
H	4.187012985053	2.162227131213	3.511410942091
H	6.622345359620	2.161940423537	4.062783885701

```
H        6.547325868934     -2.157825005924      4.361777698443
```

Convergence

```
     Item                        Value      Threshold Converged?
 Maximum Force              0.000000    0.000015         YES
 RMS Force                  0.000000    0.000010         YES
 Maximum Displacement  0.000006    0.000060         YES
 RMS Displacement         0.000001    0.000040         YES
 Predicted change in Energy=-2.964756D-13
 Optimization completed.
    -- Stationary point found.
```

APT charges

APT atomic charges:

```
     1 C 0.407611
     2 Ru -0.225019
     3 H 0.002983
     4 Cl -0.457809
     5 Cl -0.473063
     6 C 0.983008
     7 N -0.654005
     8 N -0.629596
     9 C 0.136529
    10 C 0.153815
    11 C 0.167726
    12 C 0.136950
    13 H -0.015289
    14 H -0.016867
```

15 H -0.023154

16 H -0.025045

17 C 0.169830

18 C 0.067688

19 C 0.077746

20 C -0.158928

21 C -0.152764

22 C -0.003537

23 C -0.016657

24 H 0.014393

25 H 0.014744

26 C 0.056404

27 C 0.178689

28 C 0.063222

29 C 0.079625

30 C -0.141354

31 C -0.142200

32 C 0.013887

33 C -0.024113

34 H 0.009344

35 H 0.009255

36 C 0.061088

37 H -0.018389

38 H -0.009112

39 H 0.081685

40 H -0.017971

41 H 0.091690

42 H -0.006002

43 H -0.019919
44 H -0.015086
45 H 0.111460
46 H -0.030878
47 H 0.050347
48 H 0.006933
49 H -0.016901
50 H -0.021680
51 H -0.017906
52 H -0.017657
53 H -0.013700
54 H -0.015803
55 C 0.220305
56 H -0.016423
57 H -0.029005
58 C 0.028216
59 O -0.586643
60 H 0.341115
61 C -0.027178
62 C -0.093361
63 C -0.049881
64 C 0.006373
65 C 0.016130
66 H 0.065598
67 H 0.027613
68 H 0.006471
69 H 0.009637
70 H 0.005443

71 C 0.128204

72 H 0.008939

73 C 0.171234

74 C 0.131236

75 H 0.023814

76 C 0.061391

77 C -0.019483

78 H -0.012664

79 H -0.049783

80 H -0.011892

81 C -0.035680

82 C -0.085062

83 C -0.084517

84 C 0.007598

85 C 0.008309

86 H 0.033856

87 H 0.036620

88 H -0.001067

89 H -0.001713

Sum of APT charges= 0.00000

O-H Stretching Frequency

$$\tilde{v}(O-H) = 3349\,cm^{-1} \quad Intensity = 423.0$$

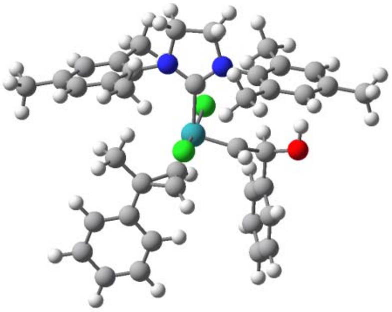

Cartesian Coordinates

C	0.000000000000	0.000000000000	0.000000000000
Ru	0.000000000000	0.000000000000	1.837985780000
H	7.957332165598	0.000000000000	3.969544228983
Cl	-0.342836176637	-2.407668601202	1.958937873870
Cl	-0.187514051367	2.421153862274	1.781973907545
C	-2.110265975890	0.067517097904	2.249650607979
N	-2.625608871876	0.119212028203	3.509674868922
N	-3.156857166021	0.048132743851	1.376891135463
C	-1.949773625669	0.208180653472	4.785387202113
C	-4.111895879027	0.073773177914	3.538934986639
C	-4.481826942157	0.139359256427	2.051419719175
C	-3.191103374747	-0.001825652828	-0.063687153341
H	-4.444656727537	-0.860422759800	4.024733389625
H	-4.976731044364	1.086080300784	1.770705568843
H	-4.502501037474	0.924084130834	4.121944236477
H	-5.126108525448	-0.694834399423	1.727944395677
C	-3.573987521945	-0.096492947561	-2.865374861831
C	-3.262044109234	1.210948179399	-0.798806011722
C	-3.370259340200	-1.259455626009	-0.696845801747
C	-3.540388695671	-1.278509175813	-2.097153462038

C	-3.439226796639	1.131794287090	-2.193282891951
C	-3.179489572103	2.557849610705	-0.121493214479
C	-3.411838181041	-2.548002652775	0.091727882574
H	-3.670489059529	-2.246600554386	-2.595364877441
H	-3.482288520724	2.064423694999	-2.767879585337
C	-3.727741217770	-0.150650178912	-4.369591107415
C	-0.805518720916	0.407589030380	7.359233382455
C	-1.745719023855	1.492257214510	5.358065810149
C	-1.686314679889	-0.977237374448	5.521133992590
C	-1.095716328647	-0.845675488037	6.792026617830
C	-1.157386076279	1.560215874929	6.634039259247
C	-2.167593912997	2.759319912792	4.651851468558
C	-2.061864884428	-2.346752667356	5.005282548035
H	-0.873703192238	-1.757040451966	7.360136233600
H	-0.983077633454	2.548297745151	7.076608537926
C	-0.138576065841	0.513983074131	8.713519854348
H	-4.040385313701	2.724925050100	0.552449768156
H	-3.186108984890	3.367236822880	-0.868297827692
H	-2.263659511082	2.649212195057	0.489692251188
H	-4.317922490585	-2.601433552286	0.724343212227
H	-2.537943228032	-2.645004869893	0.759464367969
H	-3.436839849585	-3.416298518133	-0.585560995719
H	-3.160159999869	-2.465783436959	4.944836362089
H	-1.687668357918	-3.129243463595	5.684228562560
H	-1.648263852429	-2.532952706047	3.999650896277
H	-3.257898469418	2.778572569985	4.467267001439
H	-1.663037385260	2.860822426170	3.675042203379
H	-1.922852228739	3.641209787686	5.264654625963

H	-0.374531234178	-0.354201444278	9.350762359245
H	-0.448199956989	1.428031046815	9.246819575402
H	0.961419320902	0.553912007710	8.610265225191
H	-4.230902202611	0.751062658700	-4.755345973600
H	-4.307795881825	-1.033211853501	-4.685583953064
H	-2.740540089198	-0.212163148555	-4.862569342678
C	0.265609918738	-1.113292027916	-1.007211536824
H	-0.100621798696	0.989521656809	-0.497821576633
H	-0.101887530271	-2.079912408026	-0.619096252243
C	1.768444093015	-1.207391847198	-1.247140688591
O	-0.345726401121	-0.779058291229	-2.268178164978
H	-1.318798777504	-0.834116690690	-2.150240704349
C	4.542926820158	-1.383738713492	-1.722959463270
C	2.444837261013	-0.162762122342	-1.912520694839
C	2.492551461041	-2.338828989876	-0.823381142959
C	3.873452794853	-2.427309696820	-1.061983881641
C	3.824867373203	-0.253291083804	-2.149435481598
H	1.877427072281	0.702791006772	-2.268028286728
H	1.964932316531	-3.152745833404	-0.313470993710
H	4.424872756593	-3.316412225686	-0.738239537150
H	4.340279519768	0.558226054382	-2.674124774756
H	5.618823416022	-1.455604392007	-1.914436348984
C	2.012242321463	-0.724903967639	2.185097594740
H	2.333802963331	-1.670564176080	1.750225919804
C	2.545634536148	0.160578048891	3.317229571640
C	2.088164838721	0.638085333237	1.947901232189
H	2.478738172377	1.344917879999	1.214714977140
C	4.046434898185	0.112809364797	3.501254401905

C	1.718894921633	0.428817098387	4.566673561483
H	1.857188950341	-0.360339707204	5.326221571018
H	0.642658531346	0.464303351226	4.327259111102
H	1.972049913718	1.404622815833	5.017538247559
C	6.870469217434	0.031020203322	3.839233339182
C	4.637849124632	0.321941542871	4.767825219279
C	4.908000299753	-0.142123338134	2.406493005700
C	6.299264913823	-0.181500110929	2.574299840629
C	6.030571795935	0.282333250451	4.934742710134
H	4.005378349033	0.519694984707	5.637787568312
H	4.486895813049	-0.315636314658	1.410960727778
H	6.940528515662	-0.380712717032	1.708696039890
H	6.459270103318	0.449474623987	5.929049236256

Convergence

Item	Value	Threshold	Converged?
Maximum Force	0.000001	0.000015	YES
RMS Force	0.000000	0.000010	YES
Maximum Displacement	0.000054	0.000060	YES
RMS Displacement	0.000010	0.000040	YES

Predicted change in Energy=-1.310851D-11

Optimization completed.

-- Stationary point found.

APT charges

APT atomic charges:

1

1 C 0.323900

2 Ru -0.254250

3 H 0.000478

4 Cl -0.483616

5 Cl -0.471015

6 C 1.030572

7 N -0.657416

8 N -0.649508

9 C 0.126419

10 C 0.159940

11 C 0.163471

12 C 0.150674

13 H -0.023533

14 H -0.025972

15 H -0.017953

16 H -0.019389

17 C 0.181079

18 C 0.090027

19 C 0.054395

20 C -0.170957

21 C -0.136112

22 C -0.028774

23 C -0.016336

24 H 0.018169

25 H 0.012508

26 C 0.048354

27 C 0.180901

28 C 0.073342

29 C 0.072854

30 C -0.143505

31 C -0.143827

32 C -0.019773

33 C -0.021329

34 H 0.008347

35 H 0.008592

36 C 0.062545

37 H -0.014039

38 H -0.011483

39 H 0.110823

40 H -0.016003

41 H 0.097027

42 H -0.008035

43 H -0.021419

44 H -0.010569

45 H 0.108069

46 H -0.021217

47 H 0.106455

48 H -0.013139

49 H -0.016856

50 H -0.017744

51 H -0.022452

52 H -0.014540

53 H -0.015319

54 H -0.007657

55 C 0.398877

56 H -0.001248

57 H 0.008083

58 C -0.024780

59 O -0.673394

60 H 0.265947

61 C -0.027408

62 C -0.061932

63 C -0.058290

64 C -0.021604

65 C 0.014852

66 H 0.054518

67 H 0.050379

68 H 0.018116

69 H 0.010770

70 H 0.016276

71 C 0.145043

72 H 0.013433

73 C 0.030719

74 C 0.229314

75 H 0.003179

76 C 0.100667

77 C -0.001855

78 H -0.014771

79 H -0.012040

80 H -0.015172

81 C -0.068241

82 C -0.088701

83 C -0.111557

84 C 0.034443

85 C 0.006028

86 H 0.039330

87 H 0.043448

88 H 0.007434

89 H -0.005070

Sum of APT charges= 0.00000

O-H Stretching Frequency

$\tilde{v} = 3582\,cm^{-1} \quad Intensity = 240.5$

2.5.7. ^{1}H NMR Spectra

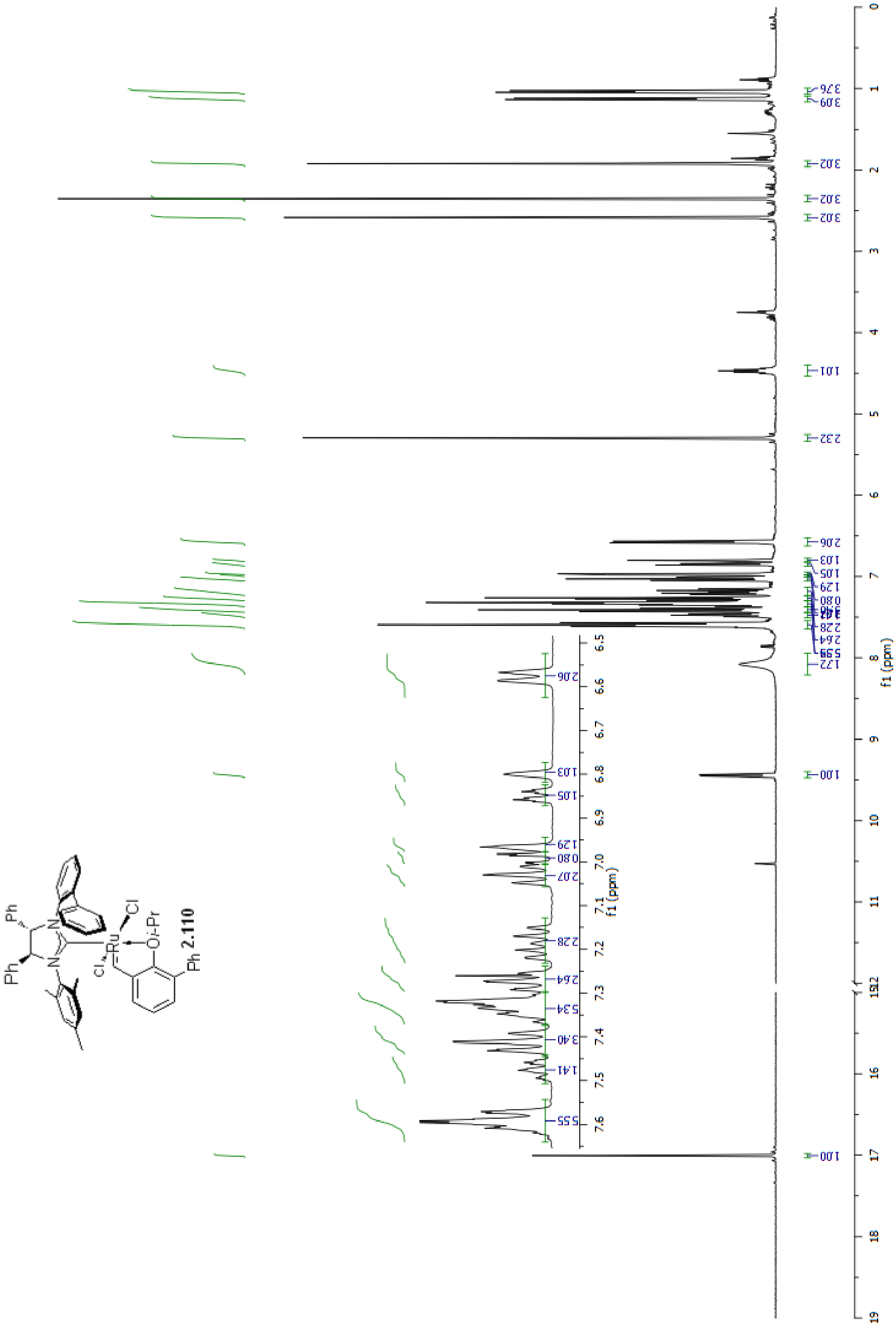
2.110

Ph
Ph
N
N
Cl
Ru
Cl
Oi-Pr
Ph
f1 (ppm)
0
1
2
3
4
5
6
7
8
9
10
11
12
15
16
17
18
19
3.76
3.09
3.02
3.02
3.02
1.01
2.32
2.06
1.03
1.05
1.29
0.80
2.07
2.28
2.64
5.34
3.40
1.41
5.55
1.72
1.00
1.00
6.5
6.6
6.7
6.8
6.9
7.0
7.1
7.2
7.3
7.4
7.5
7.6

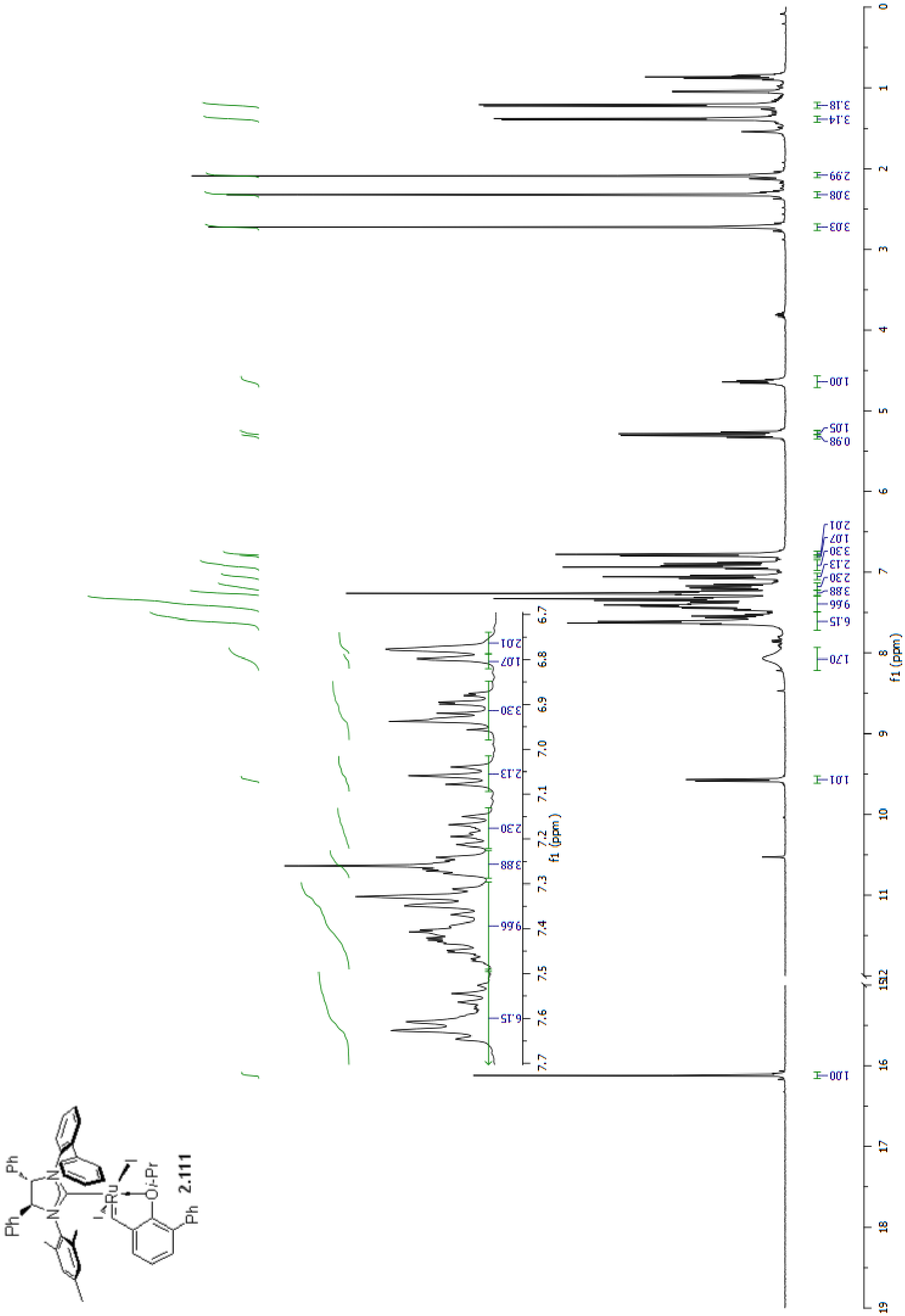
Ph
Ph
N
N
Ru
I
I
Oi-Pr
Ph
3.18
3.14
2.99
3.08
3.03
1.00
1.05
0.98
2.01
1.07
3.30
2.13
2.30
3.88
9.66
6.15
1.70
1.01
1.00
0
1
2
3
4
5
6
7
8
9
10
11
12
15
16
17
18
19
f1 (ppm)
6.7
6.8
6.9
7.0
7.1
7.2
7.3
7.4
7.5
7.6
7.7
f1 (ppm)

2.111

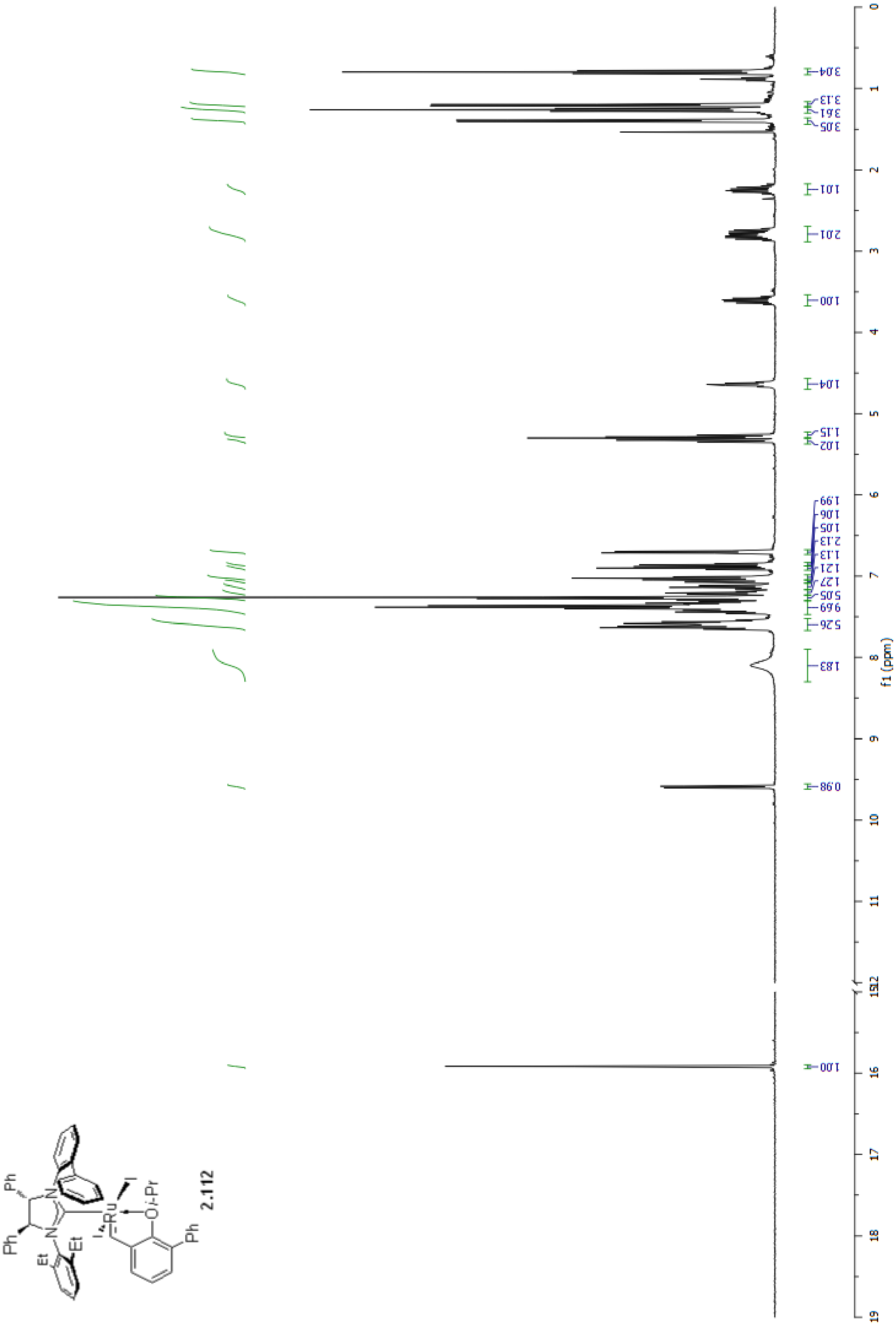

2.112
Ph
Ph
N
N
Et
Et
Ru
I
I
O-i-Pr
Ph
3.04
3.13
3.61
3.05
1.01
2.01
1.00
1.04
1.15
1.02
1.99
1.06
1.05
2.13
1.13
1.21
1.27
5.05
9.69
5.26
1.83
0.98
1.00
0
1
2
3
4
5
6
7
8
9
10
11
12
15
16
17
18
19
f1 (ppm)

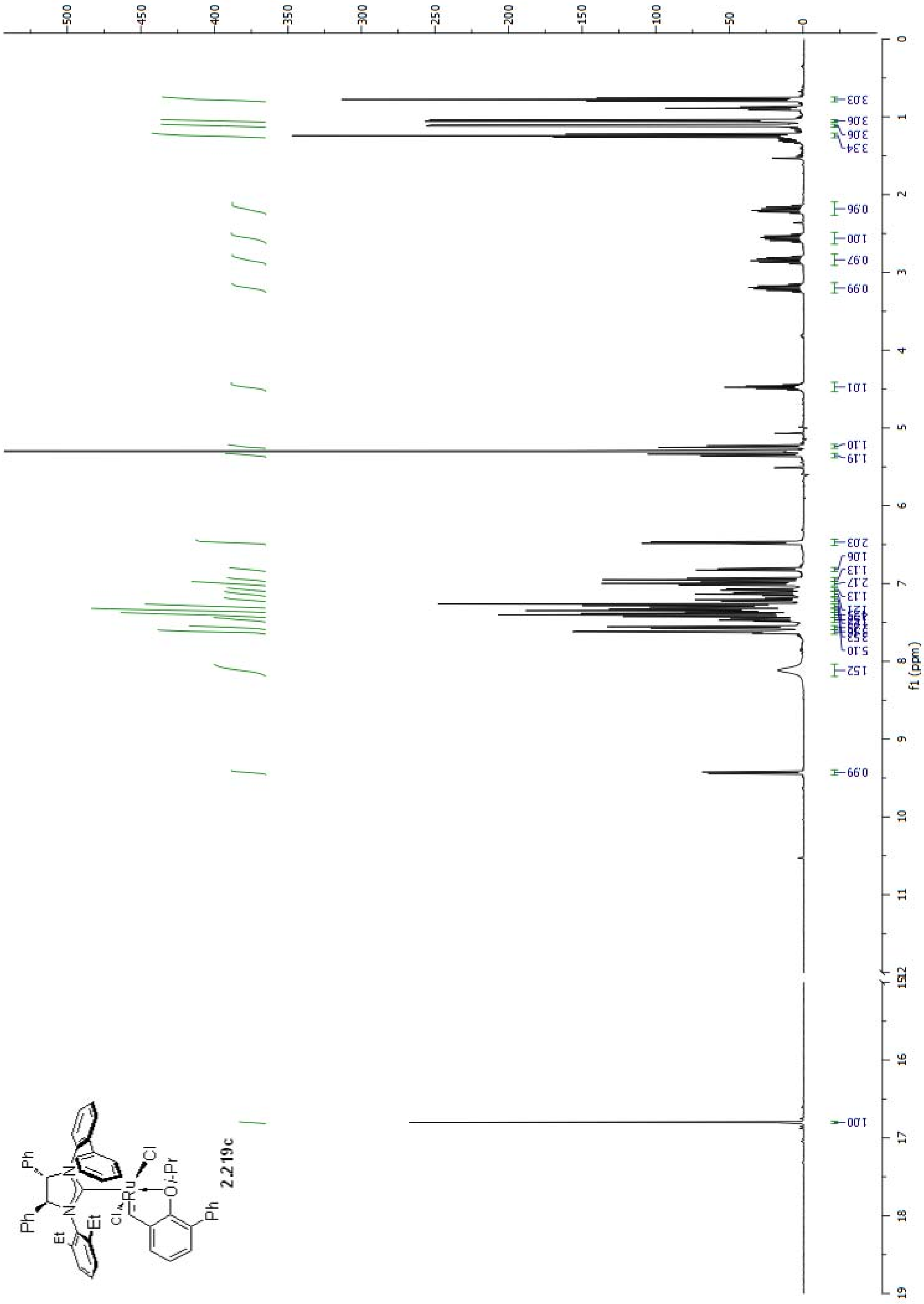
2.219c
Ph
Ph
N
N
Et
Et
Cl
Cl
Ru
O
i-Pr
Ph
3.03
3.06
3.06
3.34
0.96
1.00
0.97
0.99
1.01
1.10
1.19
2.03
1.06
1.13
2.17
1.13
5.10
1.52
0.99
1.00
f1 (ppm)
0
1
2
3
4
5
6
7
8
9
10
11
12
15
16
17
18
19
500
450
400
350
300
250
200
150
100
50
0

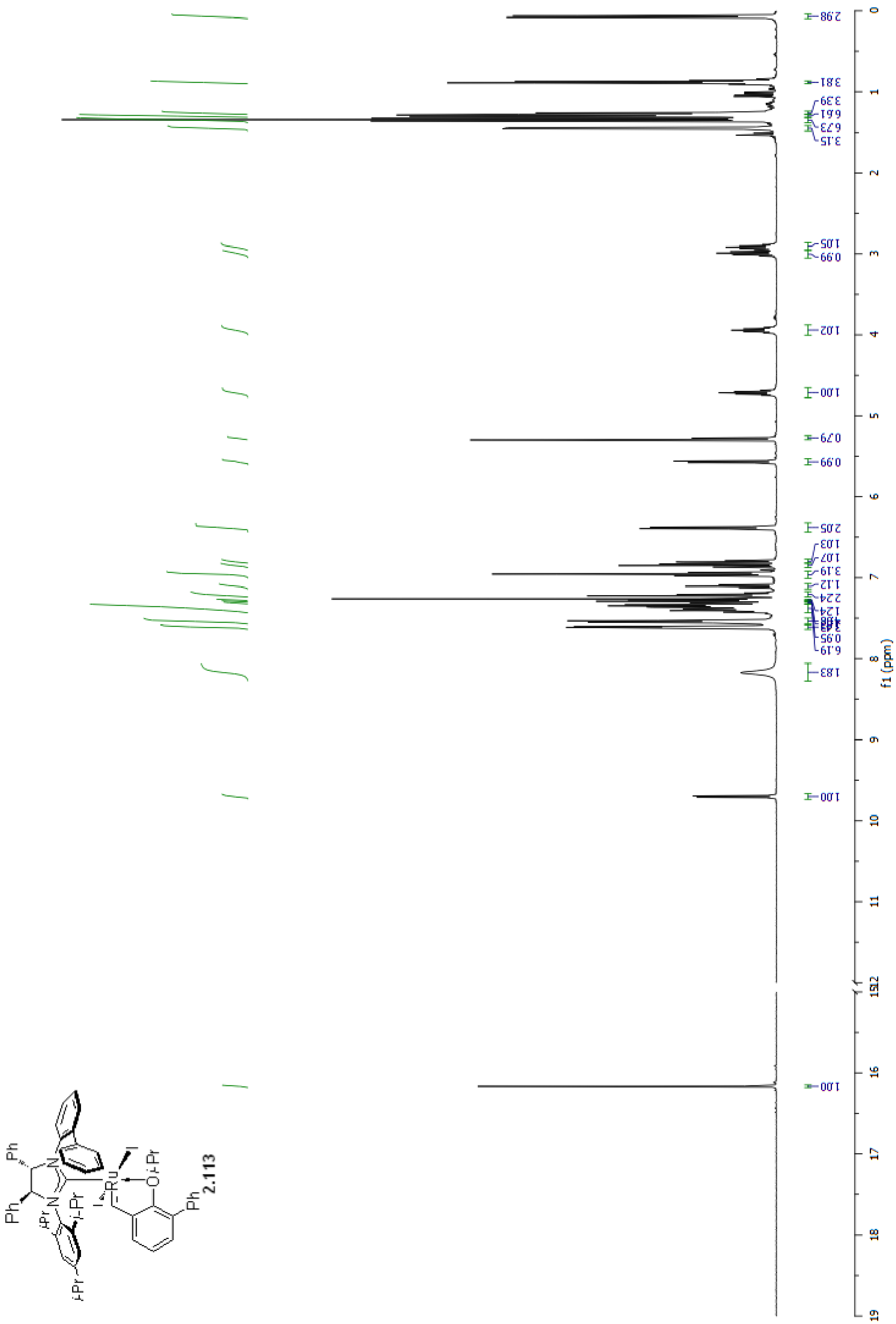
2.113

f1 (ppm)
0
1
2
3
4
5
6
7
8
9
10
11
12
15
16
17
18
19
2.98
3.81
3.39
6.61
6.73
3.15
1.05
0.99
1.02
1.00
0.79
0.99
2.05
1.03
1.07
3.19
1.12
2.24
1.24
0.95
6.19
1.83
1.00
1.00
Ph
Ph
N
N
i-Pr
i-Pr
i-Pr
I
I
Ru
O
i-Pr
Ph

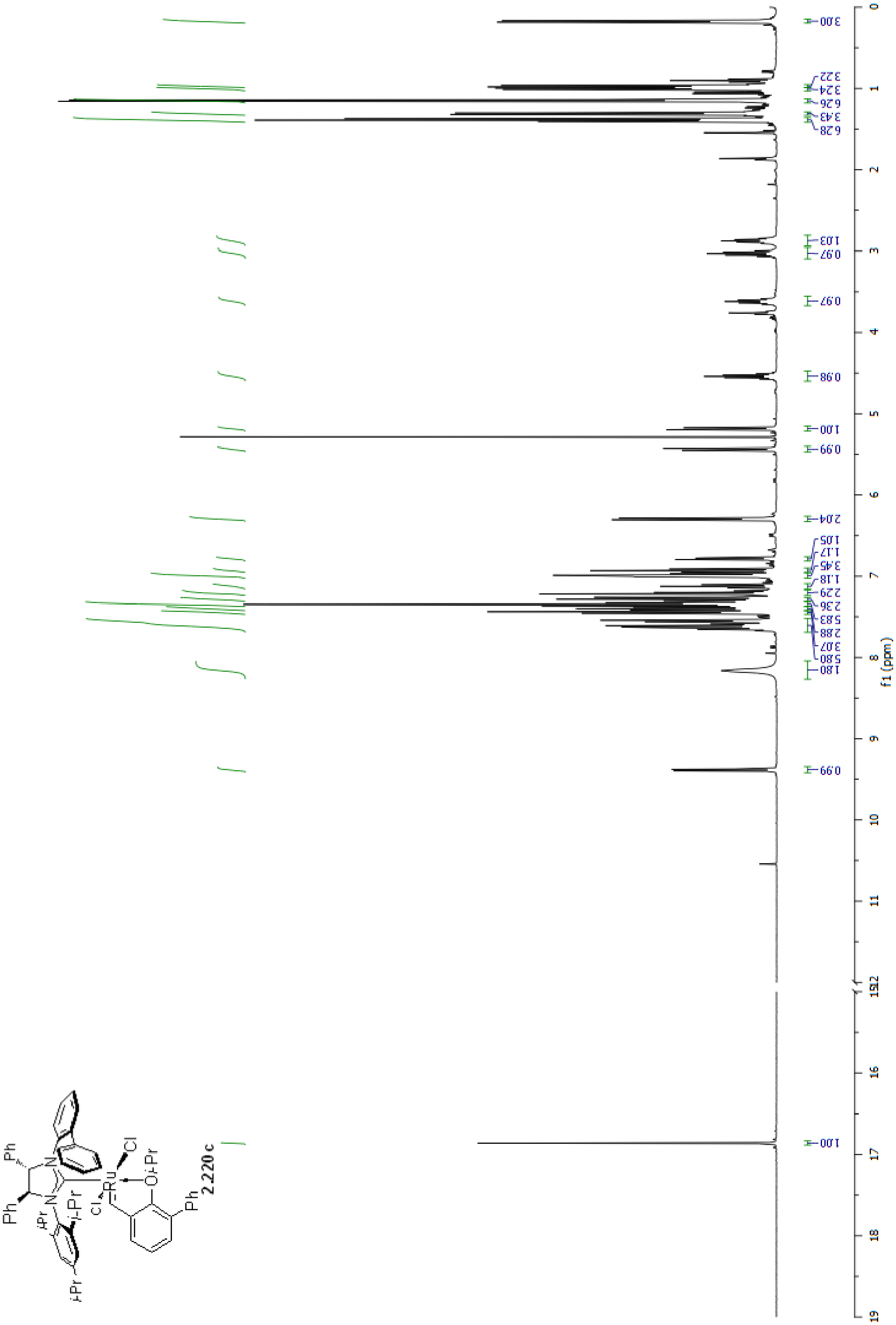

Ph
Ph
N
N
i-Pr
i-Pr
i-Pr
Cl
Ru
Cl
O
i-Pr
Ph
3.00
3.22
3.24
6.26
3.43
6.28
1.03
0.97
0.97
0.98
1.00
0.99
2.04
1.05
1.17
3.45
1.18
2.29
2.36
5.83
2.88
3.07
5.80
1.80
0.99
1.00
0
1
2
3
4
5
6
7
8
9
10
11
12
15
16
17
18
19
f1 (ppm)

2.220 c

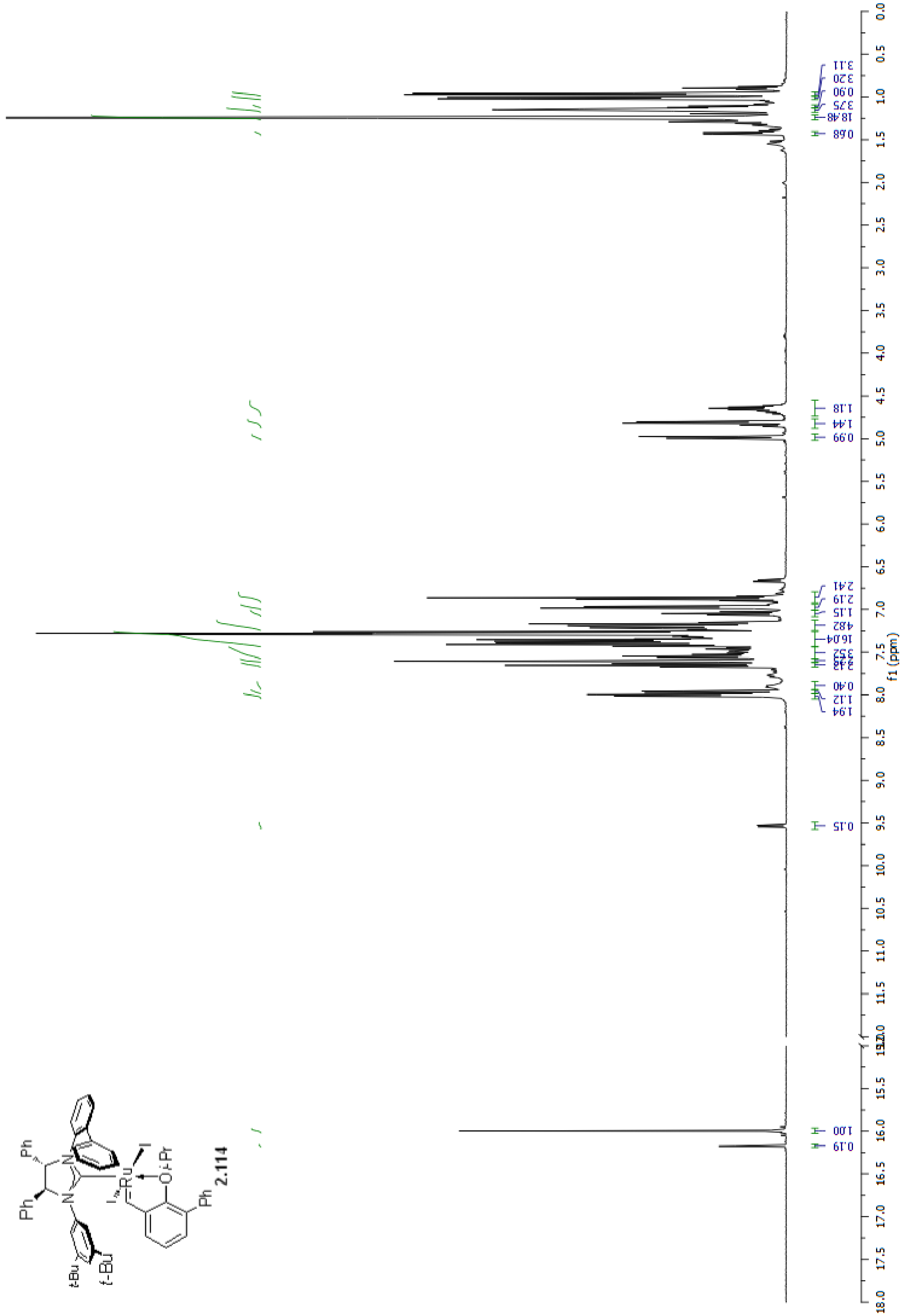
Ph
Ph
N
N
Ru
I
I
O-i-Pr
Ph
t-Bu
t-Bu
3.11
3.20
0.90
3.75
18.48
0.68
1.18
1.44
0.99
2.41
2.19
1.15
4.82
16.04
3.52
3.43
0.40
1.12
1.94
0.15
1.00
0.19
0.0
0.5
1.0
1.5
2.0
2.5
3.0
3.5
4.0
4.5
5.0
5.5
6.0
6.5
7.0
7.5
8.0
8.5
9.0
9.5
10.0
10.5
11.0
11.5
12.0
15.0
15.5
16.0
16.5
17.0
17.5
18.0
f1 (ppm)

2.114

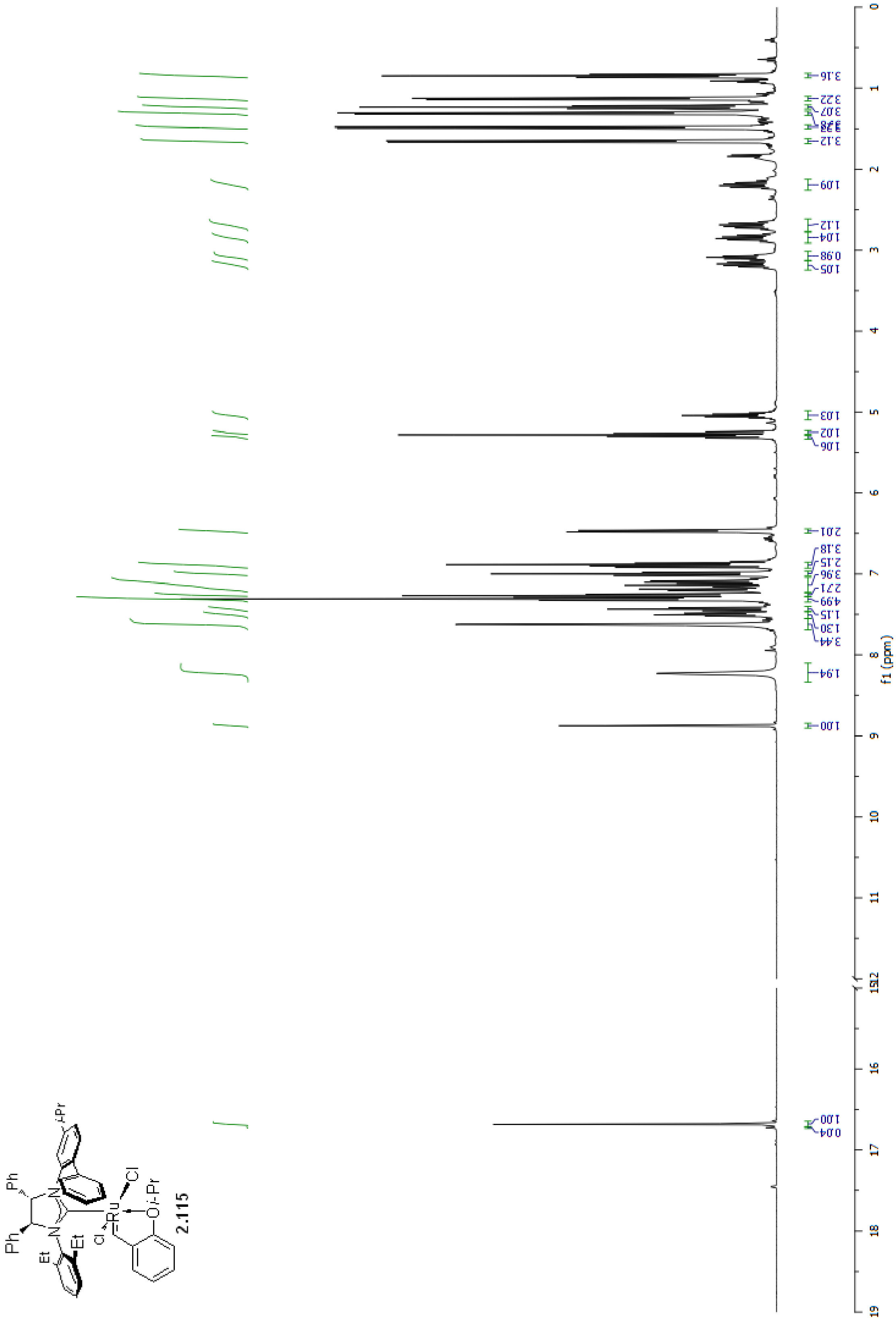
Ph
Ph
Et
Et
N
N
i-Pr
Cl
Cl
Ru
O
i-Pr
3.16
3.22
3.07
3.12
1.09
1.12
1.04
0.98
1.05
1.03
1.02
1.06
2.01
3.18
2.15
3.96
2.71
4.99
1.15
1.30
3.44
1.94
1.00
1.00
0.04
0
1
2
3
4
5
6
7
8
9
10
11
12
15
16
17
18
19
f1 (ppm)

2.115

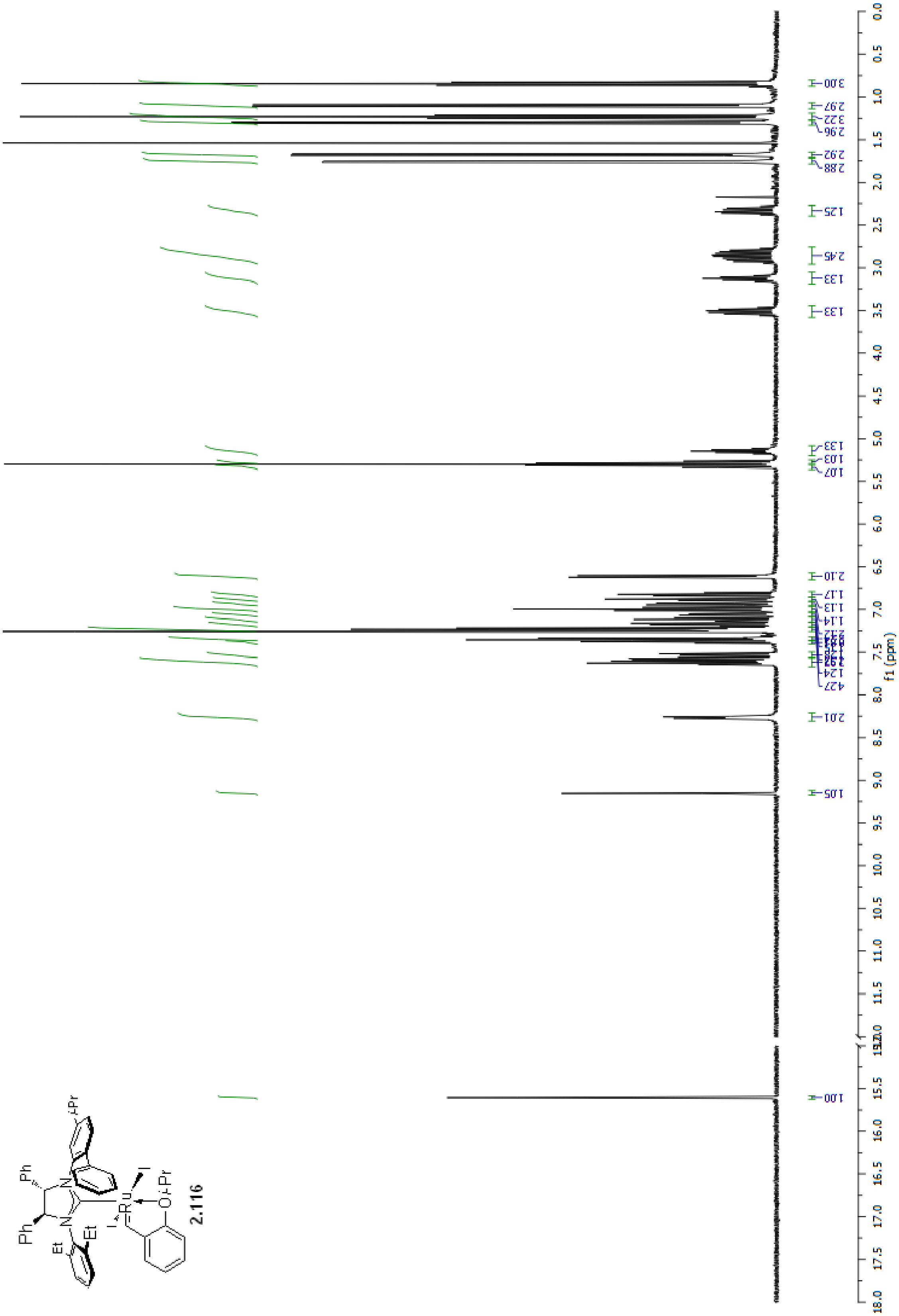

0.0
0.5
1.0
1.5
2.0
2.5
3.0
3.5
4.0
4.5
5.0
5.5
6.0
6.5
7.0
7.5
8.0
8.5
9.0
9.5
10.0
10.5
11.0
11.5
12.0
15.5
16.0
16.5
17.0
17.5
18.0
f1 (ppm)
3.00
2.97
3.22
2.96
2.92
2.88
1.25
2.45
1.33
1.33
1.33
1.03
1.07
2.10
1.17
1.13
1.14
1.24
4.27
2.01
1.05
1.00
Ph
Ph
N
N
Et
Et
i-Pr
Ru
I
I
O-i-Pr

2.116

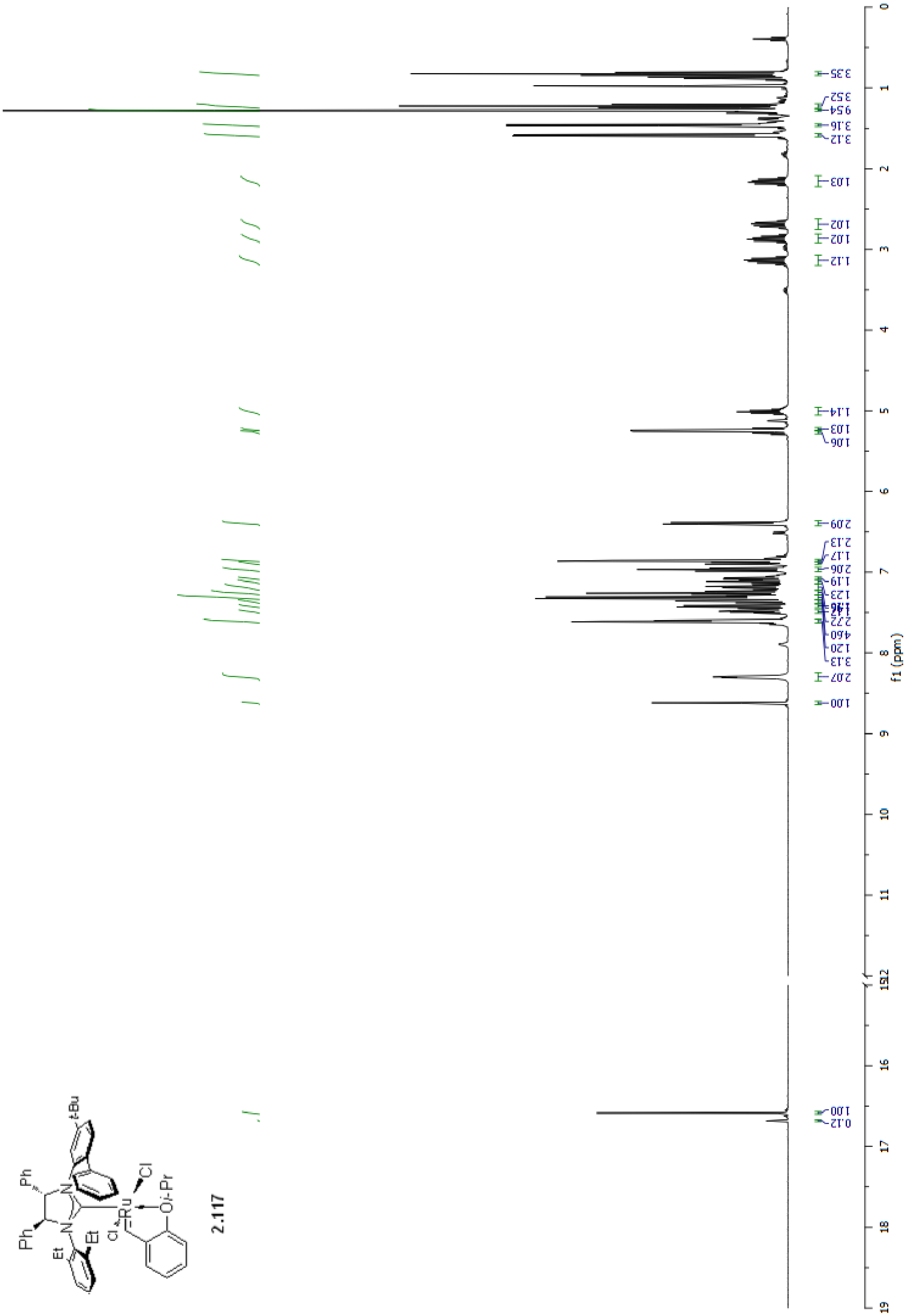
Ph
Ph
N
N
Et
Et
t-Bu
Cl
Ru
Cl
Oi-Pr
f1 (ppm)
0
1
2
3
4
5
6
7
8
9
10
11
12
15
16
17
18
19
3.35
3.52
9.54
3.16
3.12
1.03
1.02
1.02
1.12
1.14
1.03
1.06
2.09
2.13
1.17
2.06
1.19
1.23
1.46
1.47
2.22
4.60
1.20
3.13
2.07
1.00
1.00
0.12

2.117

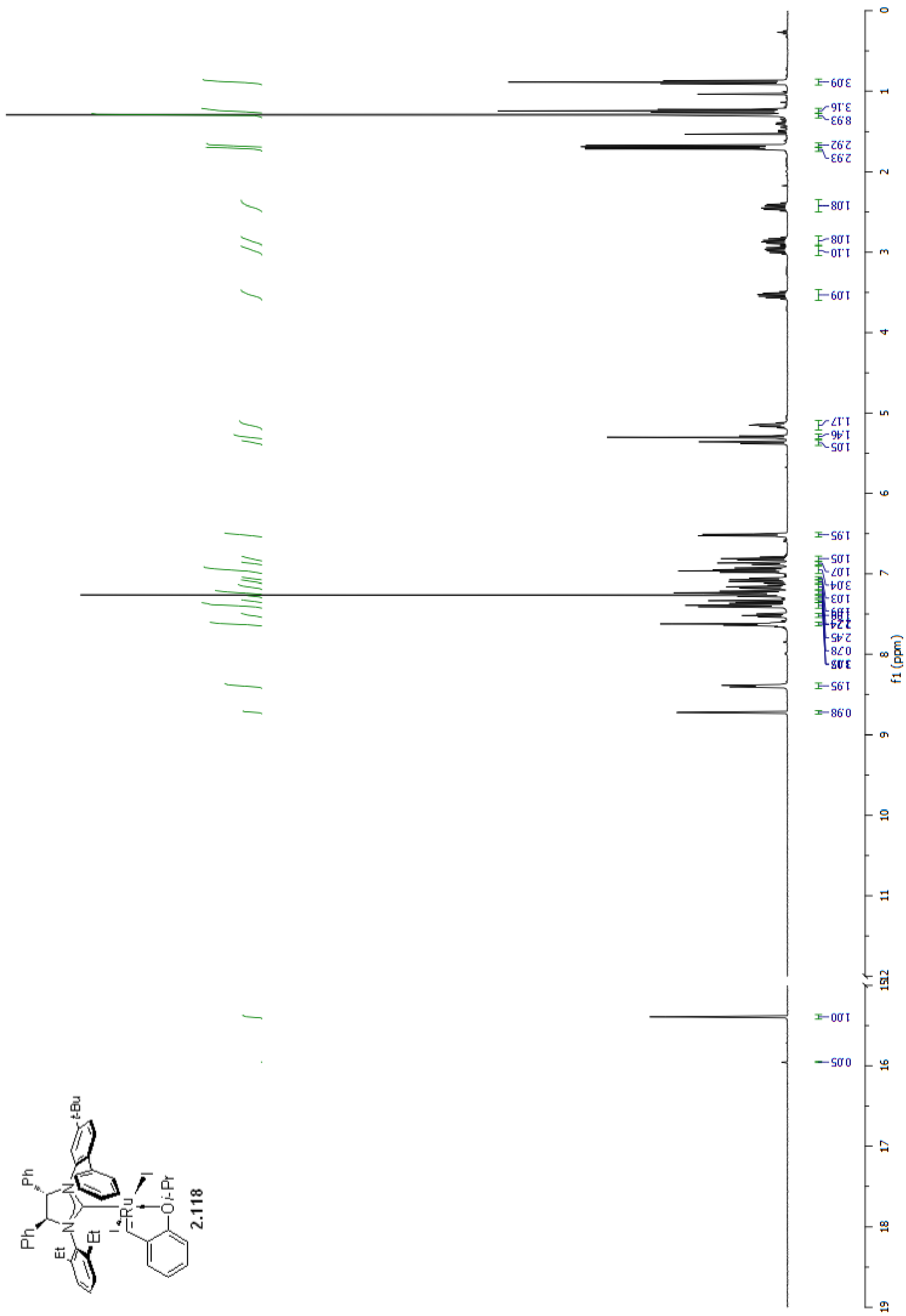
Ph
Ph
N
N
Et
Et
t-Bu
I
I
Ru
O
i-Pr
2.118
3.09
3.16
8.93
2.92
2.93
1.08
1.08
1.10
1.09
1.17
1.46
1.05
1.95
1.05
1.07
3.04
1.03
2.45
0.78
1.95
0.98
1.00
0.05
0
1
2
3
4
5
6
7
8
9
10
11
12
15
16
17
18
19
f1 (ppm)

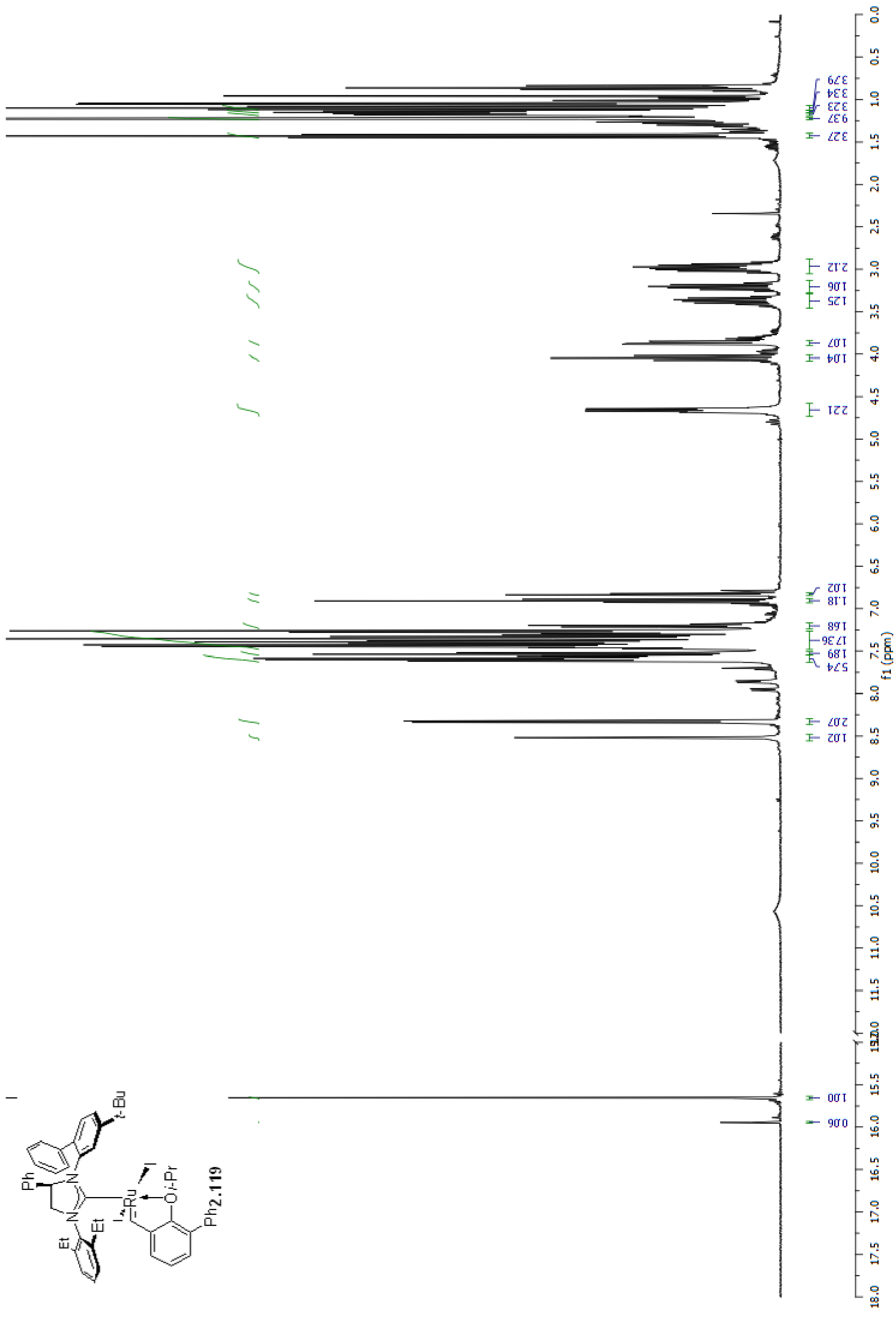
Ph
N
N
t-Bu
Et
Et
I
I
Ru
O*i*-Pr
Ph
3.79
3.34
3.23
9.37
3.27
2.12
1.06
1.25
1.07
1.04
2.21
1.02
1.18
1.68
17.36
1.89
5.74
2.07
1.02
1.00
0.06
0.0
0.5
1.0
1.5
2.0
2.5
3.0
3.5
4.0
4.5
5.0
5.5
6.0
6.5
7.0
7.5
8.0
8.5
9.0
9.5
10.0
10.5
11.0
11.5
12.0
15.5
16.0
16.5
17.0
17.5
18.0
f1 (ppm)

2.119

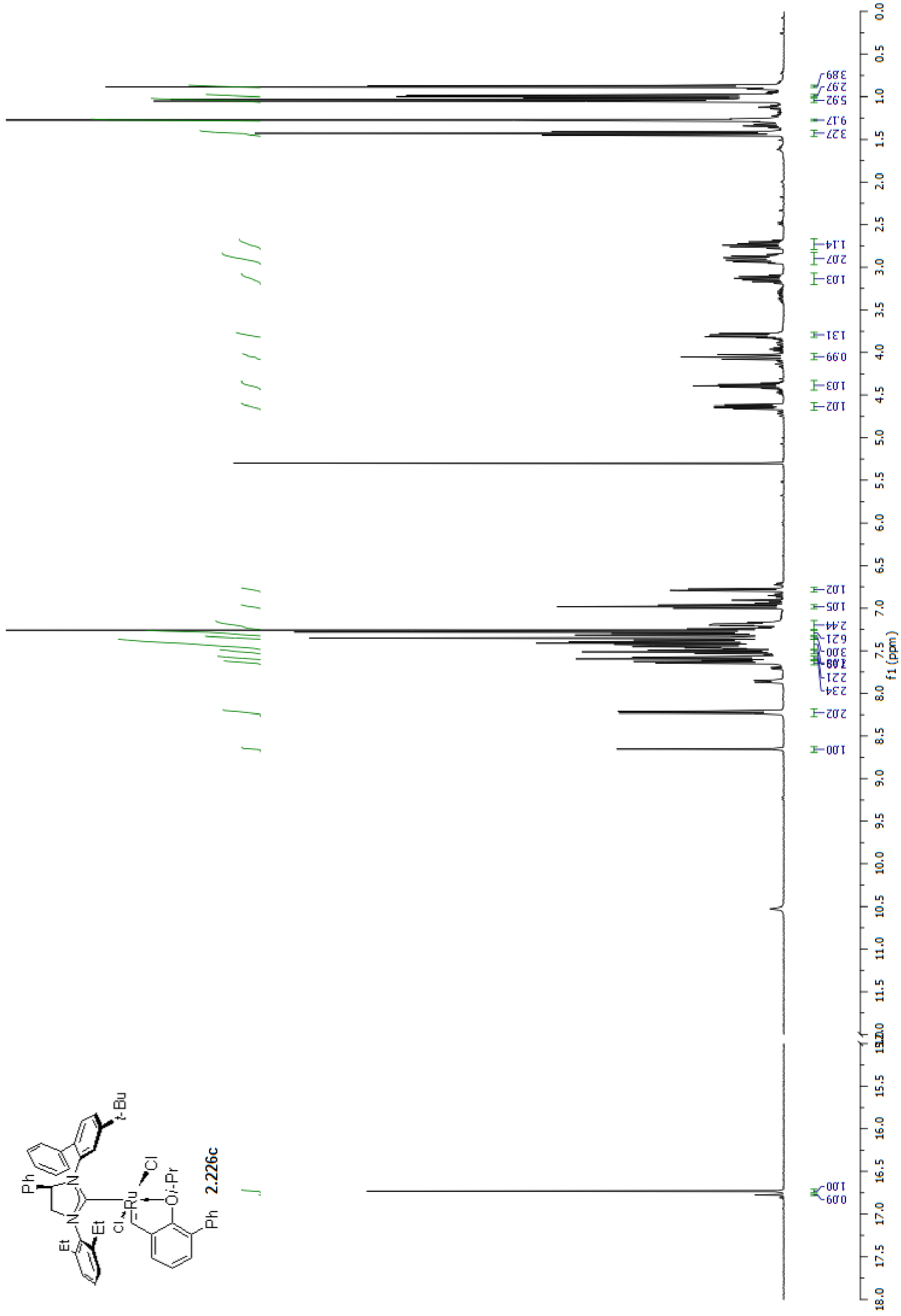
2.226c

t-Bu
Ph
N
N
Et
Et
Cl
Ru
Cl
Oi-Pr
Ph
f1 (ppm)
0.0
0.5
1.0
1.5
2.0
2.5
3.0
3.5
4.0
4.5
5.0
5.5
6.0
6.5
7.0
7.5
8.0
8.5
9.0
9.5
10.0
10.5
11.0
11.5
12.0
15.0
15.5
16.0
16.5
17.0
17.5
18.0
3.89
2.97
5.92
9.17
3.27
1.14
2.07
1.03
1.31
0.99
1.03
1.02
1.02
1.05
2.44
6.21
3.00
2.21
2.34
2.02
1.00
1.00
0.09

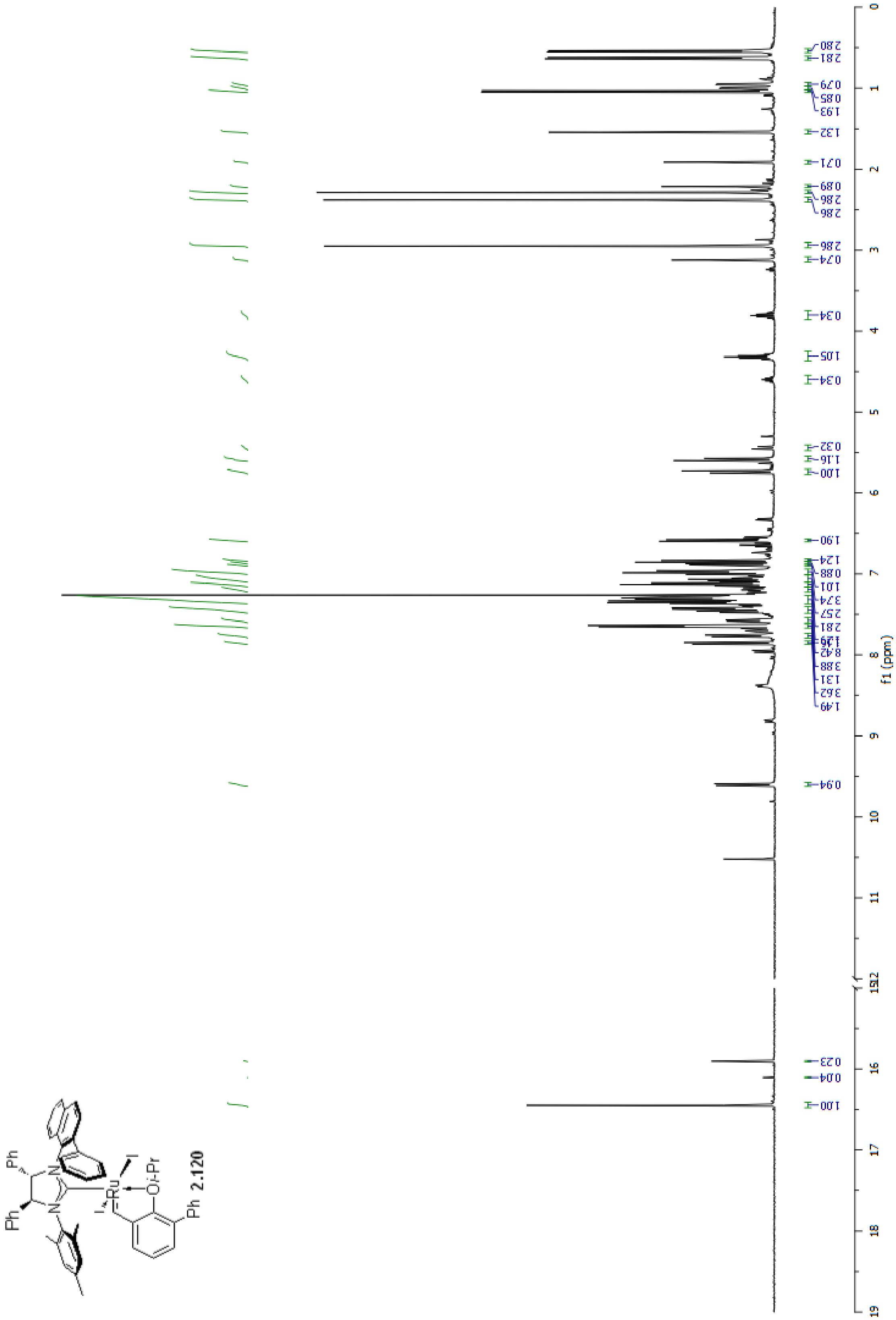

Ph
Ph
N
N
Ru
I
I
Oi-Pr
Ph
f1 (ppm)
0
1
2
3
4
5
6
7
8
9
10
11
12
15
16
17
18
19
2.80
2.81
0.79
0.85
1.93
1.32
0.71
0.89
2.86
2.86
2.86
0.74
0.34
1.05
0.34
0.32
1.16
1.00
1.90
1.24
0.88
1.01
3.74
2.57
2.81
1.46
8.42
3.88
1.31
3.62
1.49
0.94
0.23
0.04
1.00

2.120

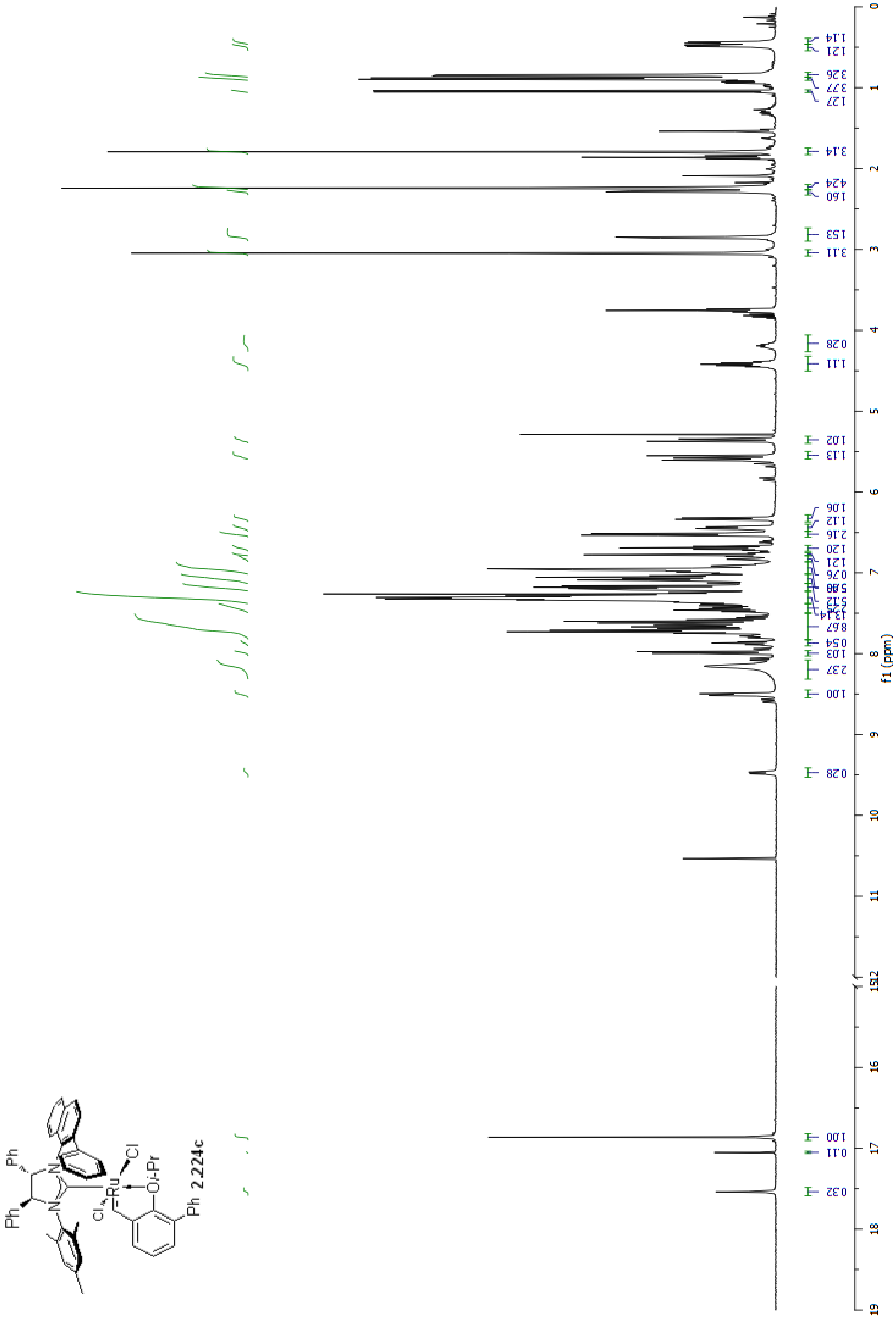
2.224c

Ph
Ph
N
N
Ru
Cl
Cl
Oi-Pr
Ph
f1 (ppm)
0
1
2
3
4
5
6
7
8
9
10
11
12
15
16
17
18
19
1.14
1.21
3.26
3.77
1.27
3.14
4.24
1.60
1.53
3.11
0.28
1.11
1.02
1.13
1.06
1.12
2.16
1.20
1.21
0.76
5.08
5.12
13.14
8.67
0.54
1.03
2.37
1.00
0.28
1.00
0.11
0.32

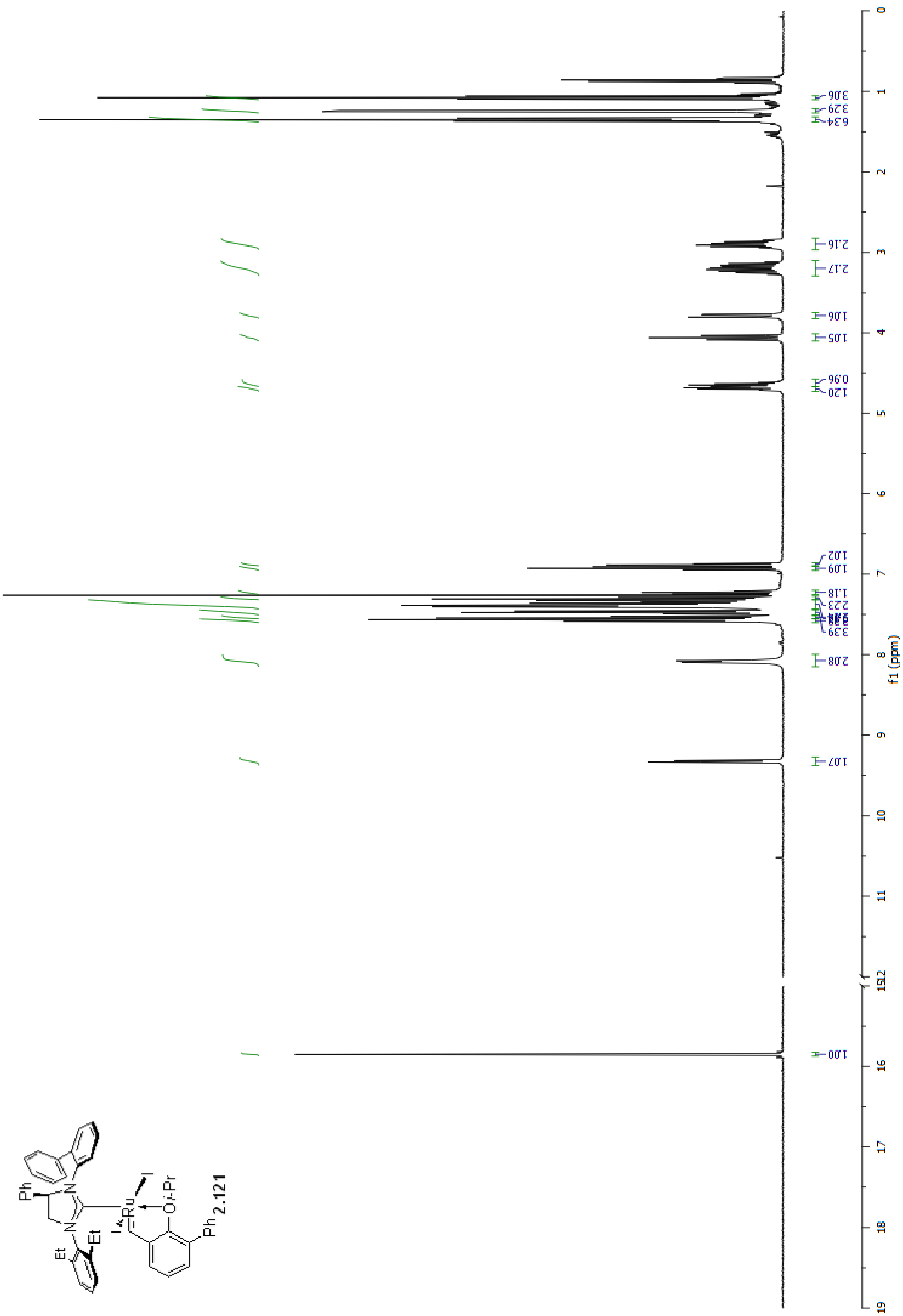

f1 (ppm)
0
1
2
3
4
5
6
7
8
9
10
11
12
15
16
17
18
19
3.06
3.29
6.34
2.16
2.17
1.06
1.05
0.96
1.20
1.02
1.09
1.18
2.23
3.39
2.08
1.07
1.00
Ph
N
Et
Ru
I
Oi-Pr
Ph

2.121

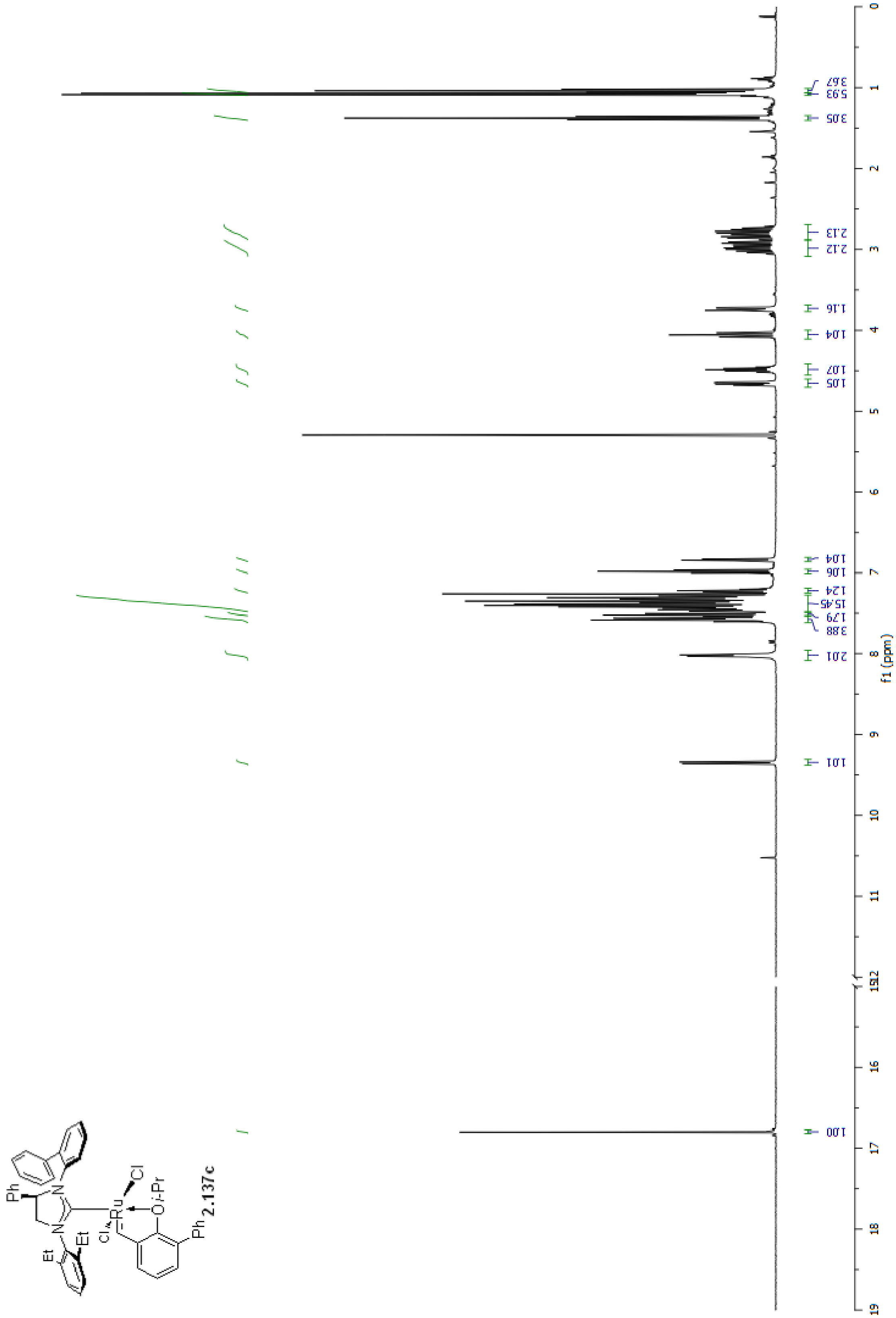

Ph
N
N
Et
Et
Cl
Ru
Cl
Oi-Pr
Ph
3.67
5.93
3.05
2.13
2.12
1.16
1.04
1.07
1.05
1.04
1.06
1.24
15.45
1.79
3.88
2.01
1.01
1.00
0
1
2
3
4
5
6
7
8
9
10
11
12
15
16
17
18
19
f1 (ppm)

2.137c

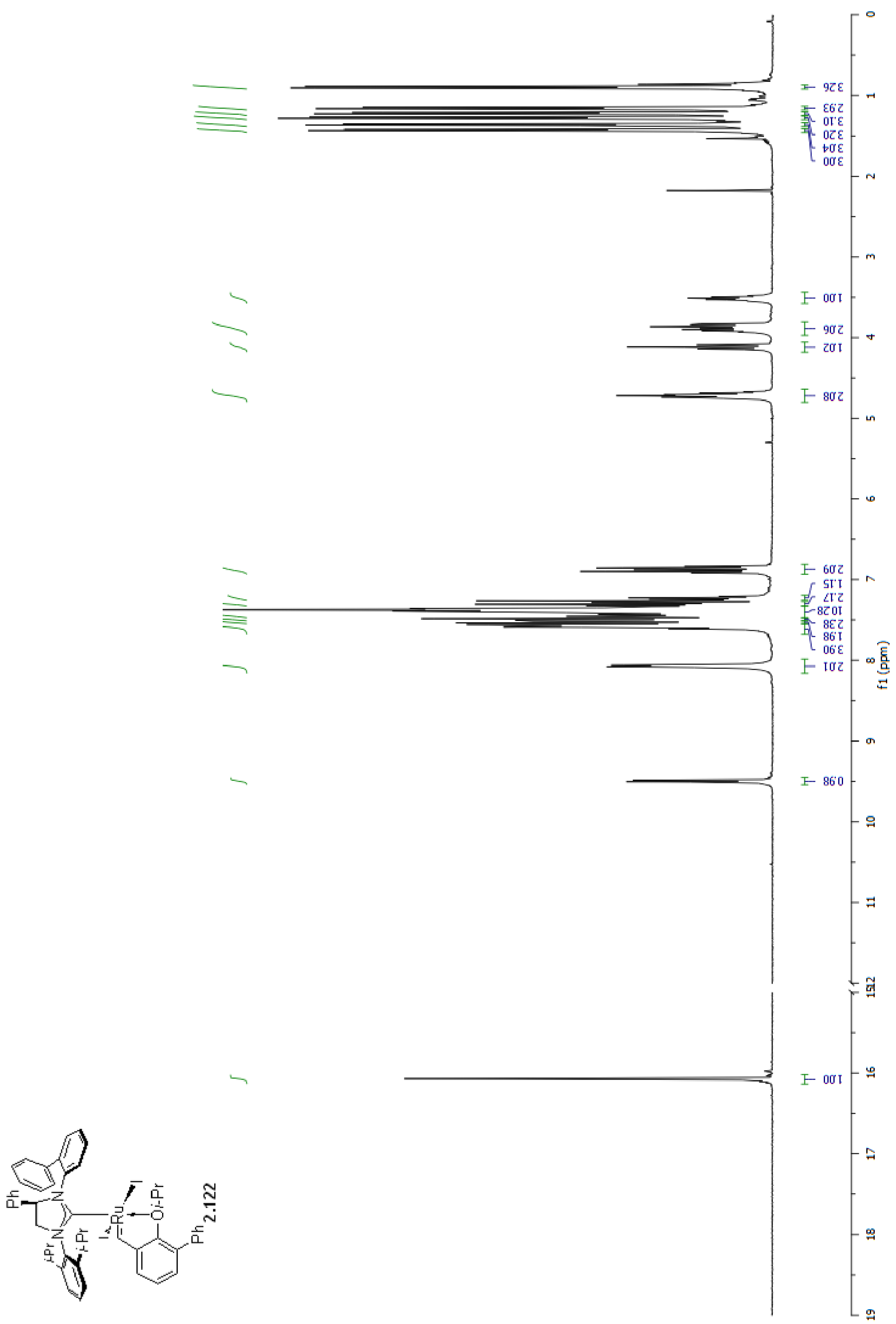
f1 (ppm)
0
1
2
3
4
5
6
7
8
9
10
11
12
15
16
17
18
19
3.26
2.93
3.10
3.20
3.04
3.00
1.00
2.06
1.02
2.08
2.09
1.15
2.17
10.28
2.38
1.98
3.90
2.01
0.98
1.00
Ph
N
N
i-Pr
i-Pr
Ru
I
I
Oi-Pr
Ph

2.122

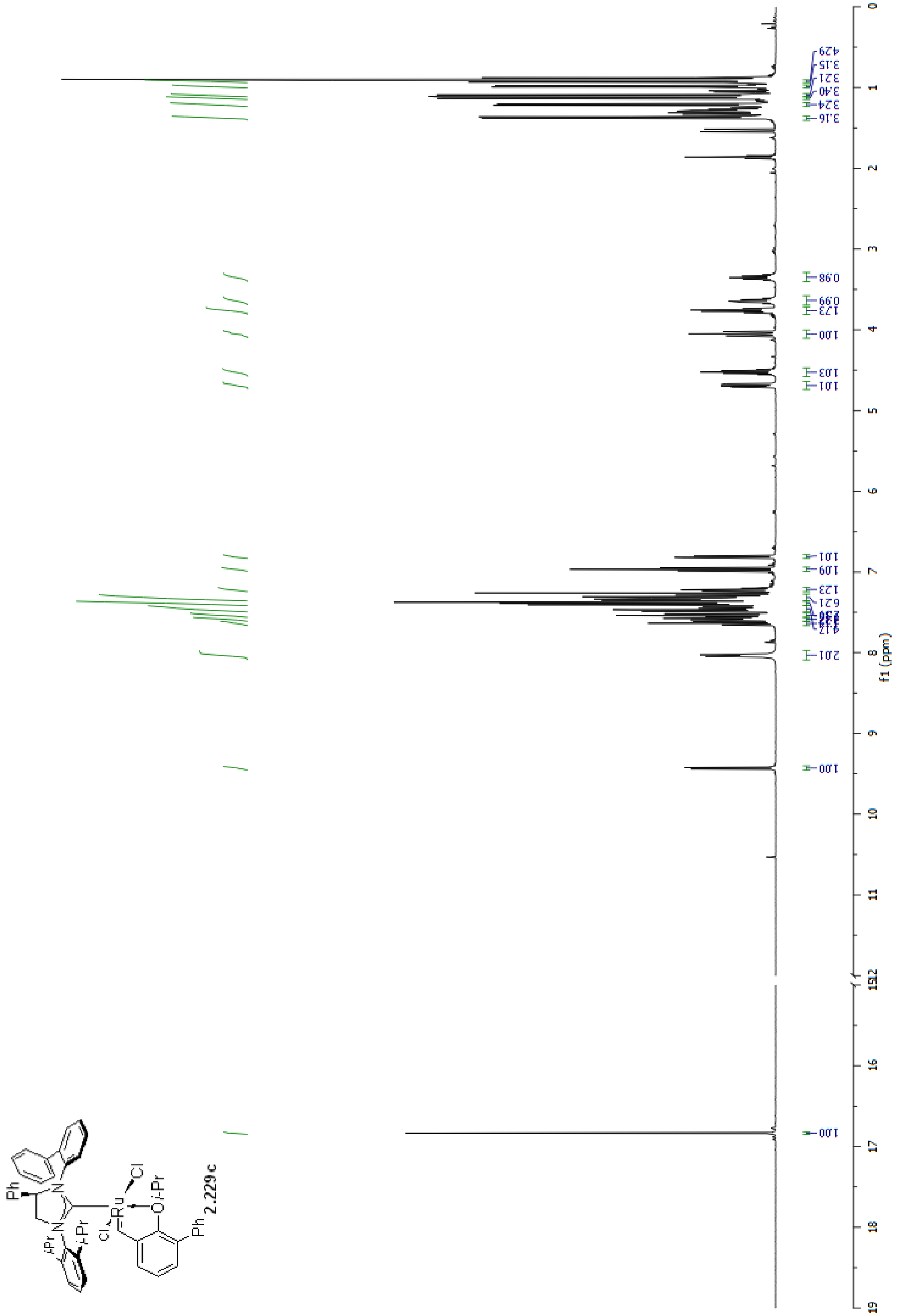

4.29
3.15
3.21
3.40
3.24
3.16
0.98
0.99
1.73
1.00
1.03
1.01
1.01
1.09
1.23
1.21
2.01
1.00
1.00
0
1
2
3
4
5
6
7
8
9
10
11
12
15
16
17
18
19
f1 (ppm)
Ph
N
N
i-Pr
i-Pr
Cl
Ru
Cl
O i-Pr
Ph

2.229c

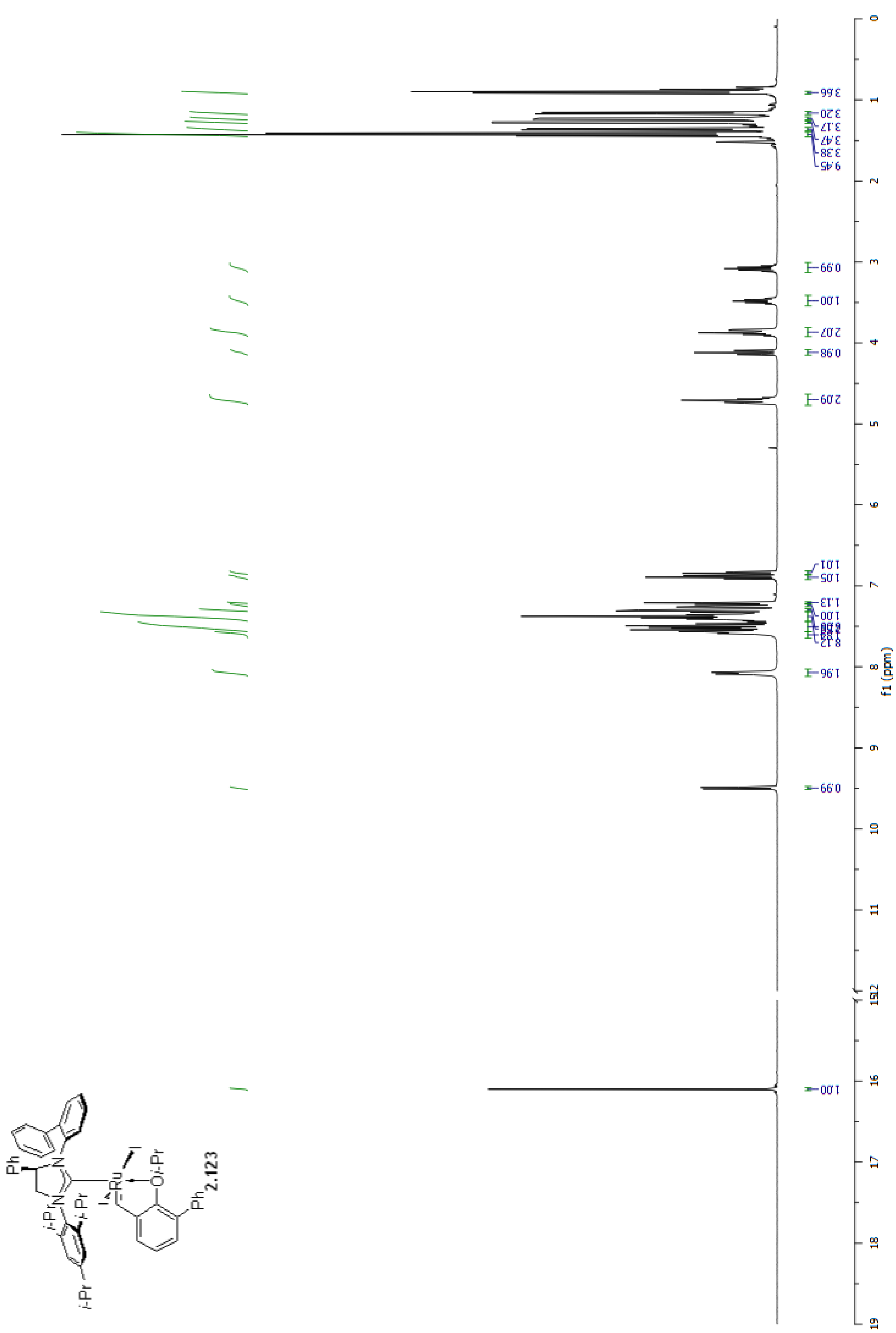
2.123
i-Pr
i-Pr
i-Pr
N
N
Ph
Ru
I
I
Oi-Pr
Ph
3.66
3.20
3.17
3.47
3.38
9.45
0.99
1.00
2.07
0.98
2.09
1.01
1.05
1.13
1.00
8.12
1.96
0.99
1.00
0
1
2
3
4
5
6
7
8
9
10
11
12
15
16
17
18
19
f1 (ppm)

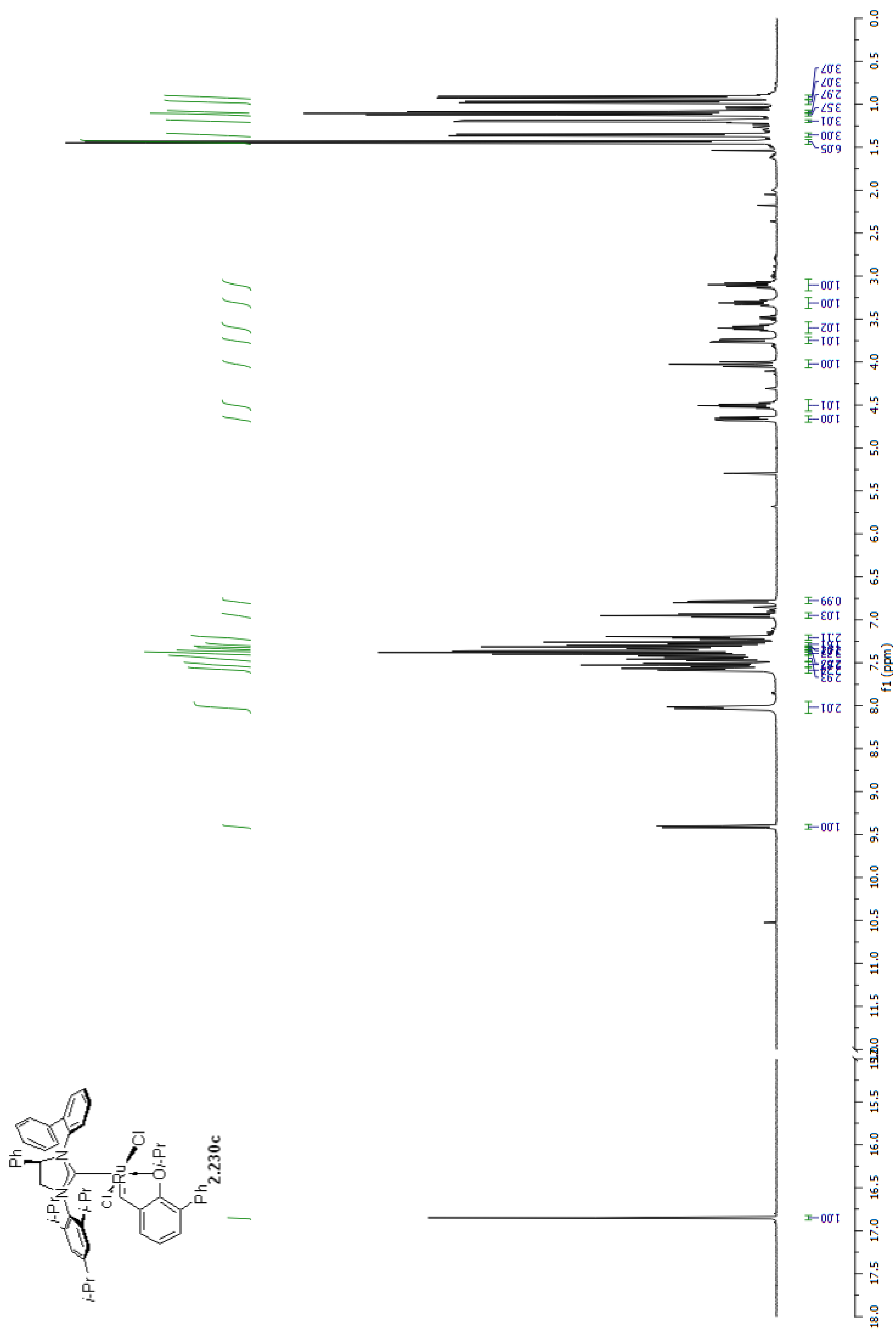
f1 (ppm)
0.0
0.5
1.0
1.5
2.0
2.5
3.0
3.5
4.0
4.5
5.0
5.5
6.0
6.5
7.0
7.5
8.0
8.5
9.0
9.5
10.0
10.5
11.0
11.5
12.0
15.5
16.0
16.5
17.0
17.5
18.0
3.07
3.07
2.97
3.57
3.01
3.00
6.05
1.00
1.00
1.02
1.01
1.00
1.01
1.00
0.99
1.03
2.11
2.01
1.00
1.00
Ph
N
i-Pr
i-Pr
i-Pr
Cl
Ru
Cl
O i-Pr
Ph

2.230c

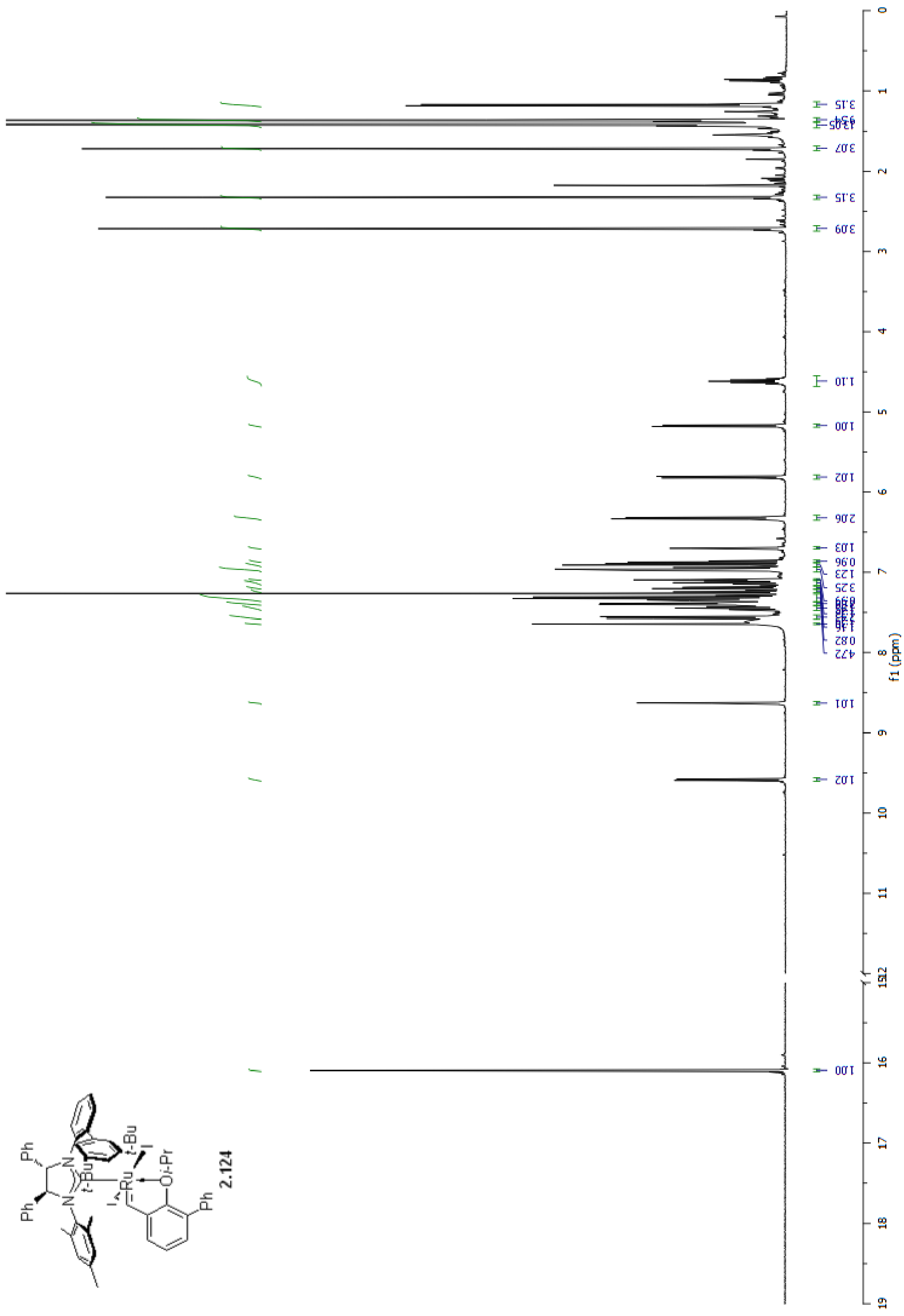
Ph
Ph
N
N
t-Bu
t-Bu
I
I
Ru
Oi-Pr
Ph
3.15
4.54
13.05
3.07
3.15
3.09
1.10
1.00
1.02
2.06
1.03
0.96
1.23
3.25
0.82
4.72
1.01
1.02
1.00
0
1
2
3
4
5
6
7
8
9
10
11
12
15
16
17
18
19
f1 (ppm)

2.124

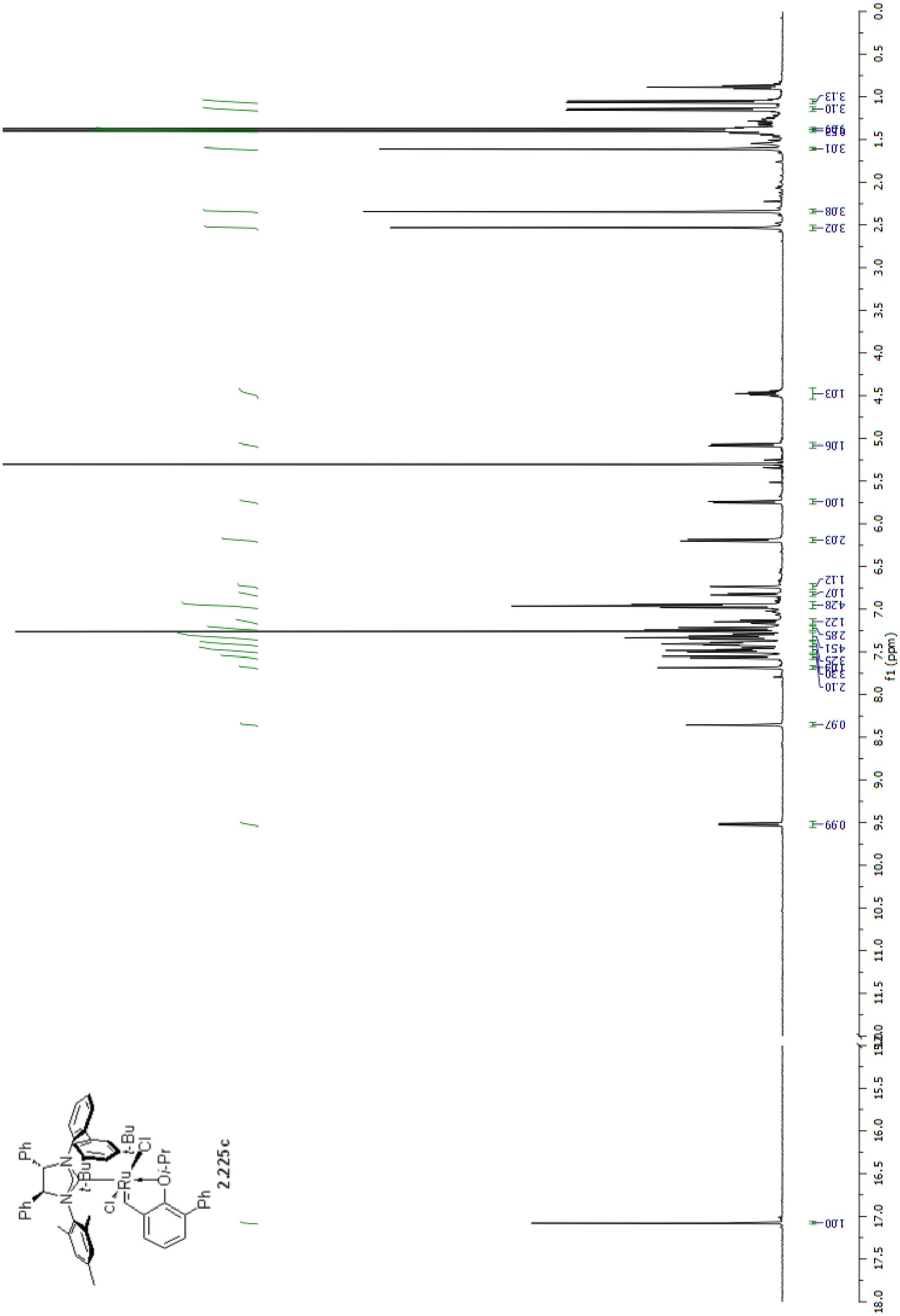
Ph
Ph
N
N
t-Bu
t-Bu
Cl
Ru
Cl
O-i-Pr
Ph
3.13
3.10
3.01
3.08
3.02
1.03
1.06
1.00
2.03
1.12
1.07
4.28
1.22
2.85
4.51
3.25
3.30
2.10
0.97
0.99
1.00
0.0
0.5
1.0
1.5
2.0
2.5
3.0
3.5
4.0
4.5
5.0
5.5
6.0
6.5
7.0
7.5
8.0
8.5
9.0
9.5
10.0
10.5
11.0
11.5
12.0
15.5
16.0
16.5
17.0
17.5
18.0
f1 (ppm)

2.225c

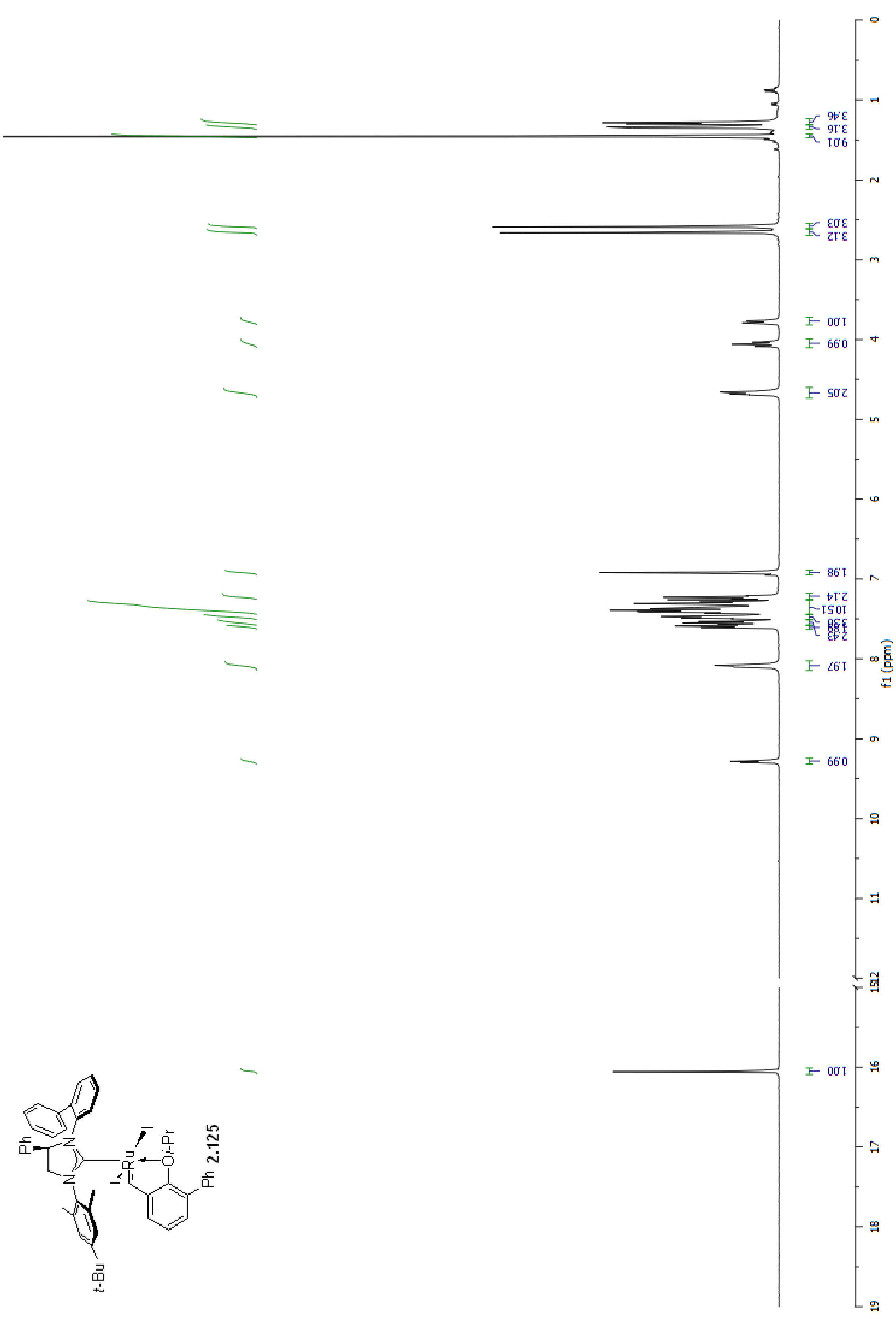
t-Bu
N
Ph
I
Ru
Oi-Pr
Ph
3.46
3.16
9.01
3.03
3.12
1.00
0.99
2.05
1.98
2.14
10.51
2.43
1.97
0.99
1.00
f1 (ppm)
0
1
2
3
4
5
6
7
8
9
10
11
12
15
16
17
18
19

2.125

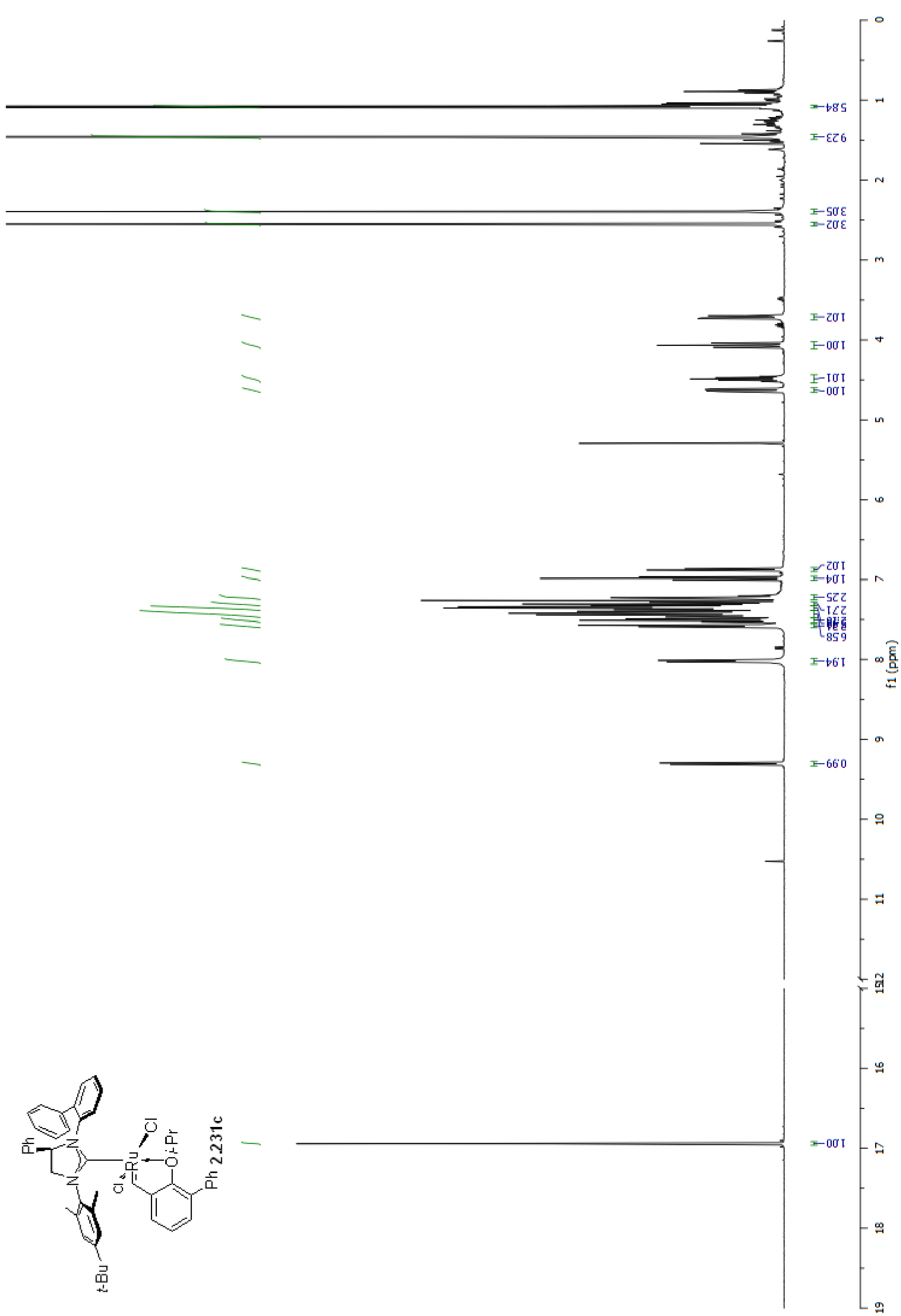

2.231c

Ph
N
N
t-Bu
Cl
Ru
Cl
Oi-Pr
Ph
f1 (ppm)
0
1
2
3
4
5
6
7
8
9
10
11
12
15
16
17
18
19
5.84
9.23
3.05
3.02
1.02
1.00
1.01
1.00
1.02
1.04
2.25
2.71
6.58
1.94
0.99
1.00

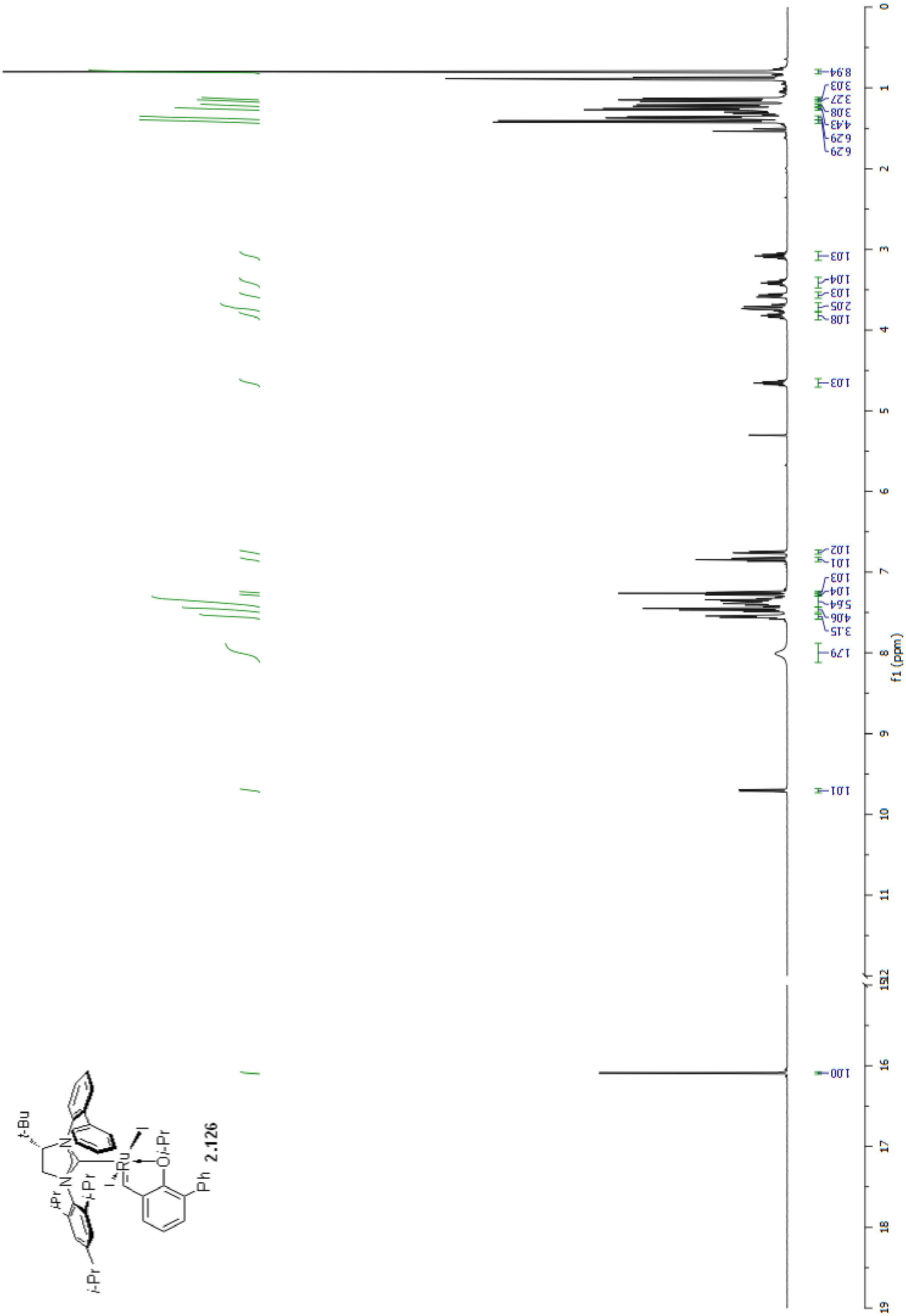
t-Bu
N
N
i-Pr
i-Pr
i-Pr
Ru
I
I
O-i-Pr
Ph
8.94
3.03
3.27
3.08
4.43
6.29
6.29
1.03
1.04
1.03
2.05
1.08
1.03
1.02
1.01
1.03
1.04
5.64
4.06
3.15
1.79
1.01
1.00
0
1
2
3
4
5
6
7
8
9
10
11
12
15
16
17
18
19
f1 (ppm)

2.126

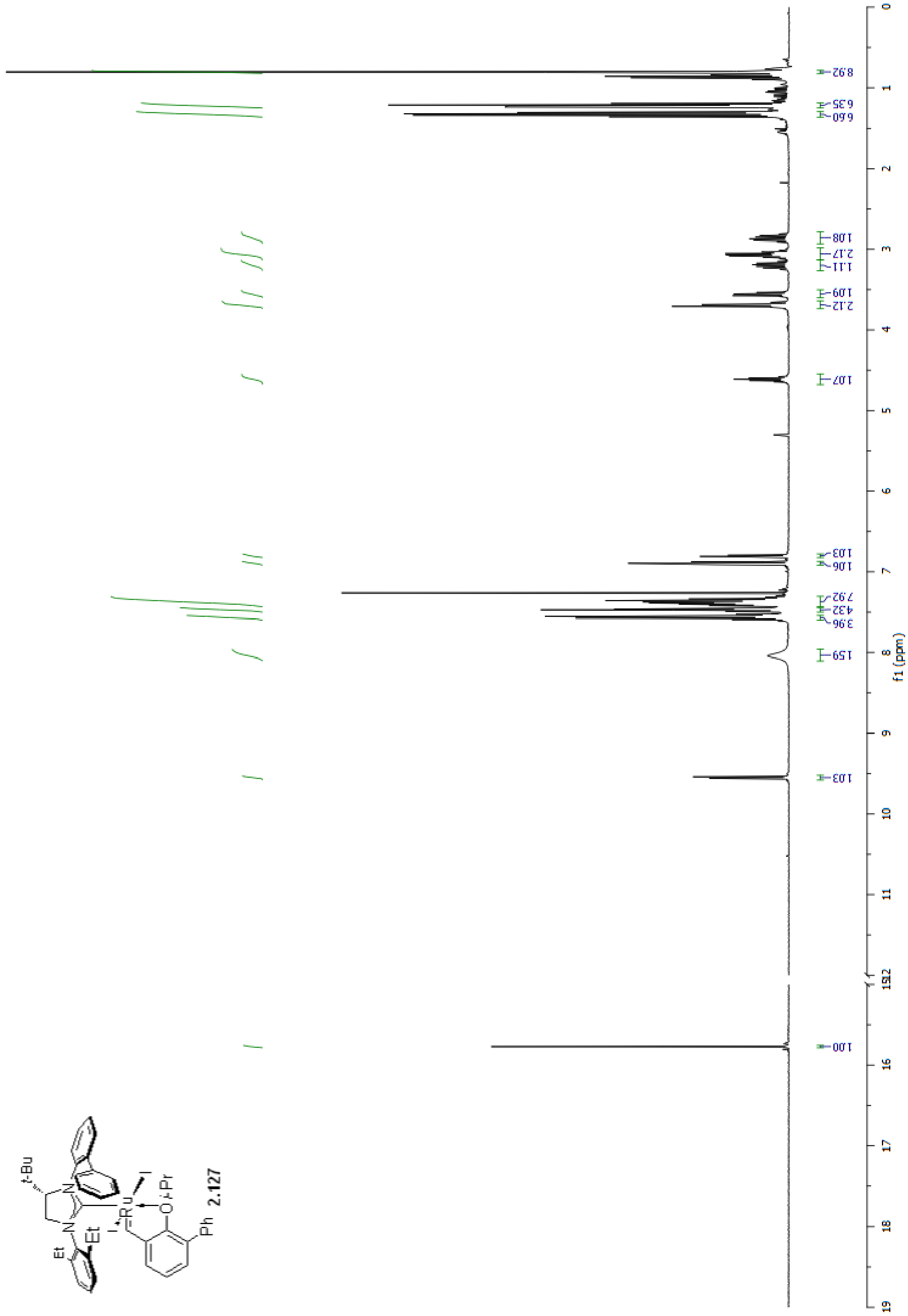
t-Bu
N
N
Et
Et
I
Ru
I
O-i-Pr
Ph
8.92
6.35
6.60
1.08
2.17
1.11
1.09
2.12
1.07
1.03
1.06
7.92
4.32
3.96
1.59
1.03
1.00
0
1
2
3
4
5
6
7
8
9
10
11
15|12
16
17
18
19
f1 (ppm)

2.127

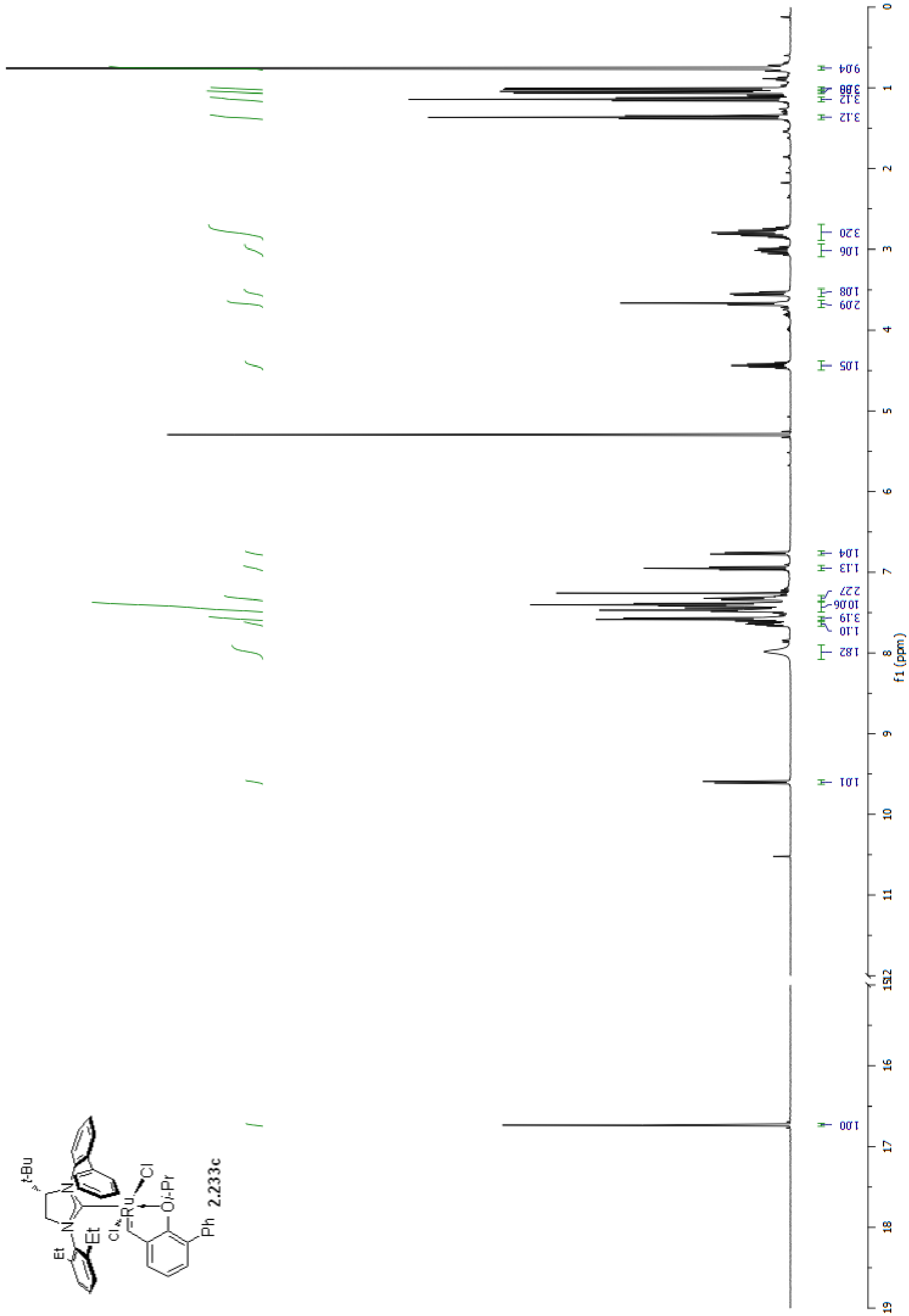
t-Bu
N
N
Et
Et
Cl
Ru
Cl
Oi-Pr
Ph
9.04
3.08
3.12
3.12
3.20
1.06
1.08
2.09
1.05
1.04
1.13
2.27
10.06
3.19
1.10
1.82
1.01
1.00
0
1
2
3
4
5
6
7
8
9
10
11
12
15
16
17
18
19
f1 (ppm)

2.233c

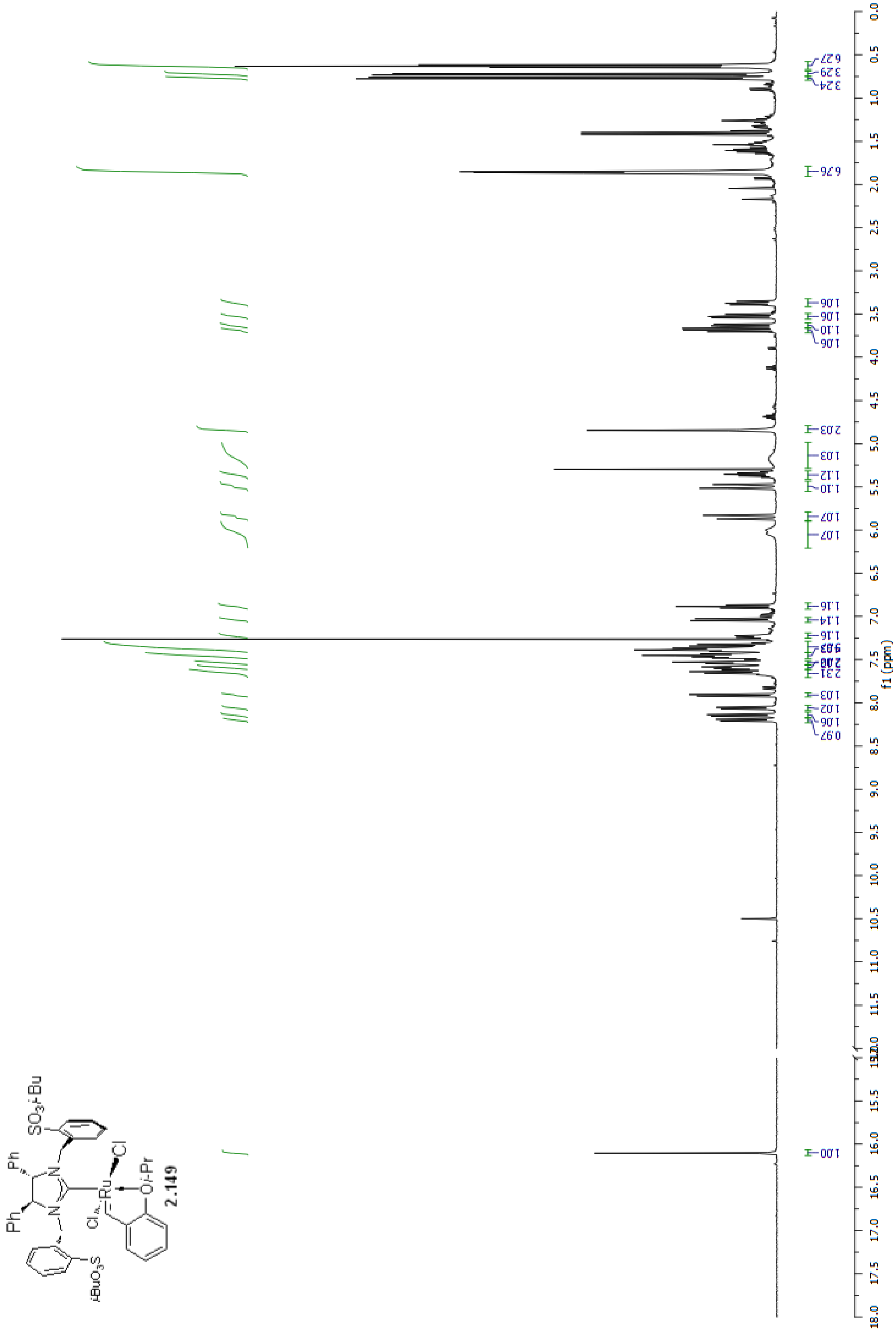
Ph
Ph
N
N
SO3i-Bu
iBuO3S
Cl
Cl
Ru
Oi-Pr
f1 (ppm)
0.0
0.5
1.0
1.5
2.0
2.5
3.0
3.5
4.0
4.5
5.0
5.5
6.0
6.5
7.0
7.5
8.0
8.5
9.0
9.5
10.0
10.5
11.0
11.5
12.0
15.5
16.0
16.5
17.0
17.5
18.0
6.27
3.29
3.24
6.76
1.06
1.06
1.10
1.06
2.03
1.03
1.12
1.10
1.07
1.07
1.16
1.14
1.16
2.31
1.03
1.02
1.06
0.97
1.00

2.149

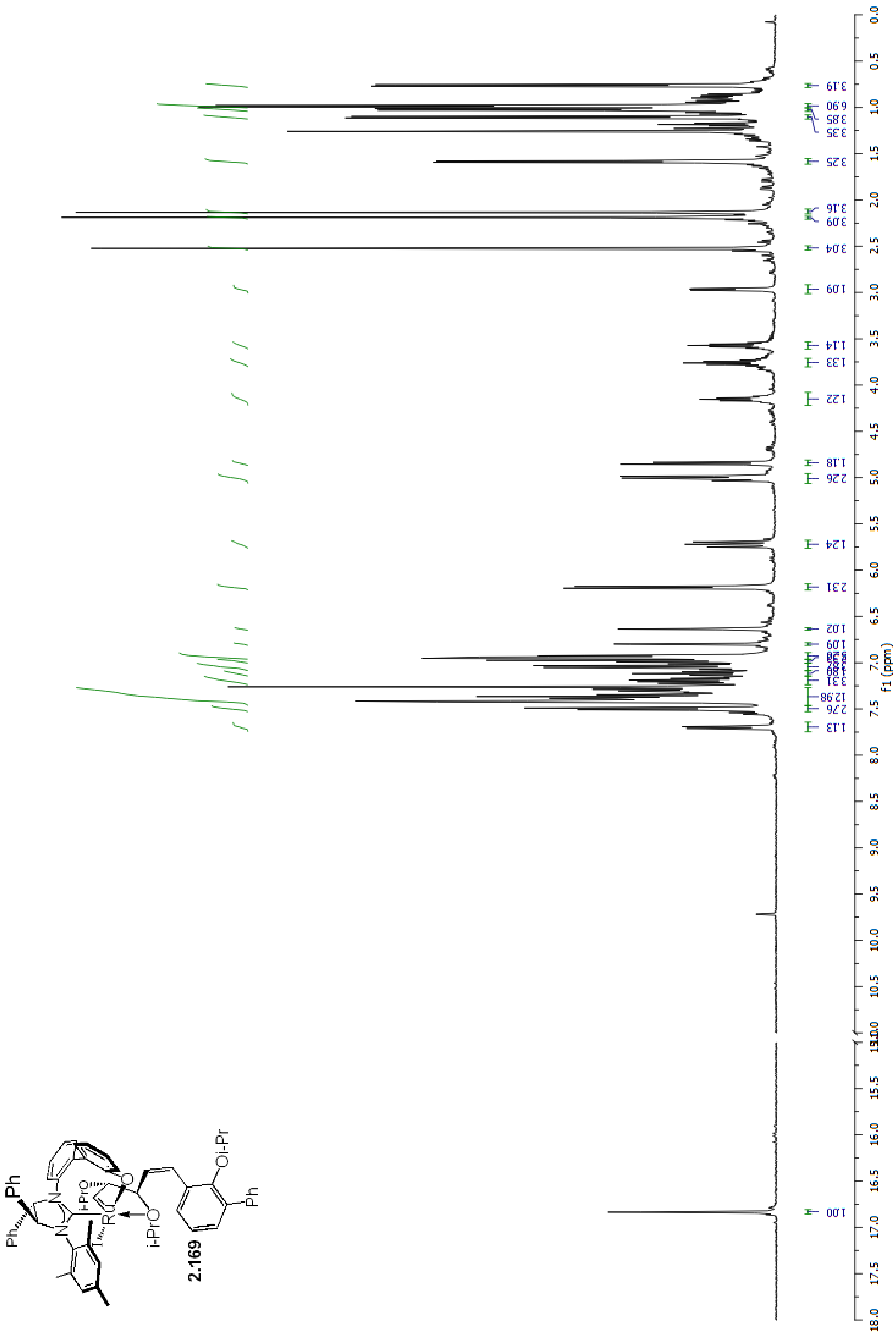
Ph
Ph
N
N
i-PrO
Ru
O
i-PrO
Oi-Pr
Ph
f1 (ppm)
0.0
0.5
1.0
1.5
2.0
2.5
3.0
3.5
4.0
4.5
5.0
5.5
6.0
6.5
7.0
7.5
8.0
8.5
9.0
9.5
10.0
10.5
11.0
15.0
15.5
16.0
16.5
17.0
17.5
18.0
3.19
6.90
3.85
3.35
3.25
3.16
3.09
3.04
1.09
1.14
1.33
1.22
1.18
2.26
1.24
2.31
1.02
1.09
3.31
12.98
2.76
1.13
1.00

2.169

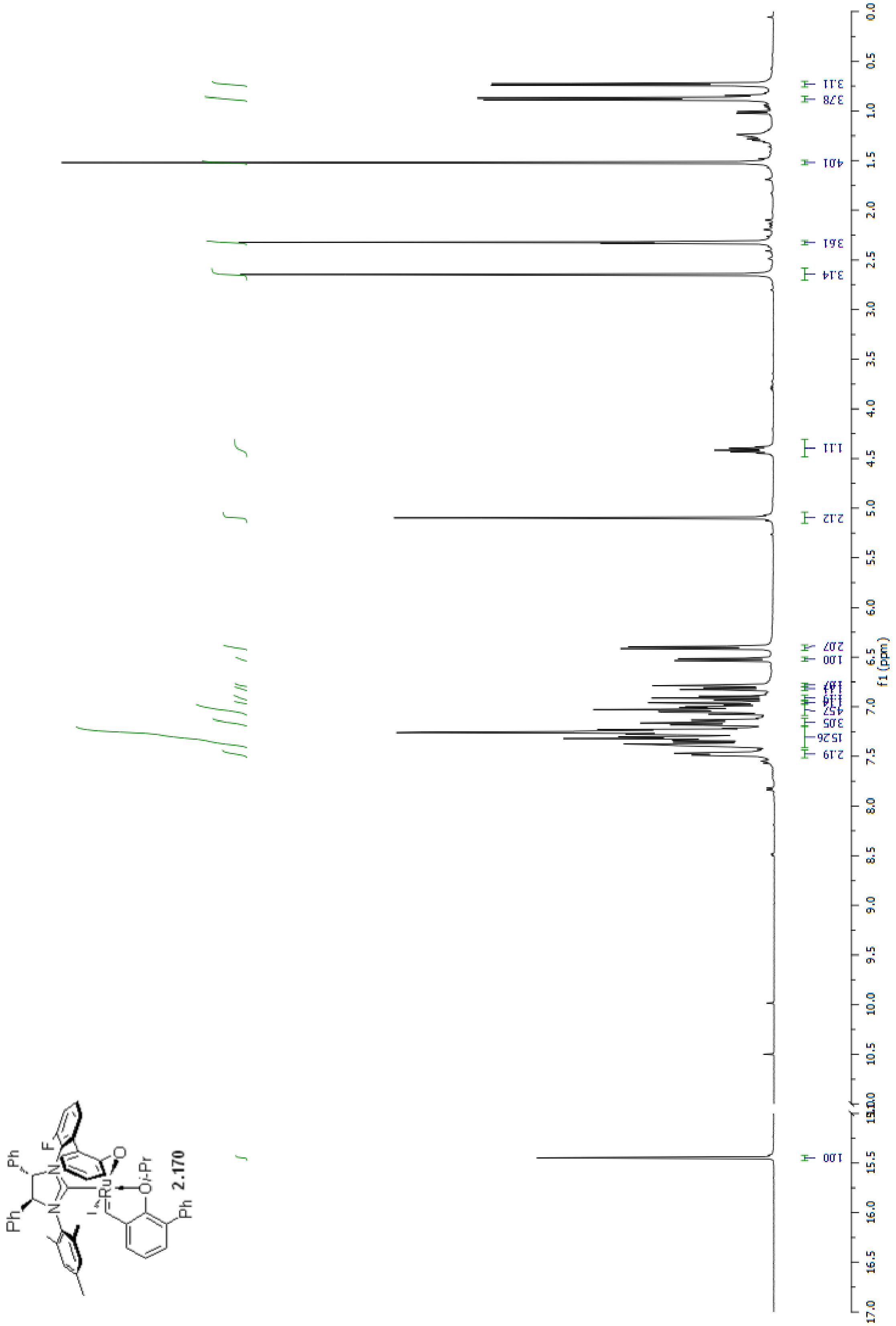

Ph
Ph
N
N
F
O
I
Ru
Oi-Pr
Ph
3.11
3.78
4.01
3.61
3.14
1.11
2.12
2.07
1.00
1.07
1.14
1.19
1.14
4.57
3.05
15.26
2.19
1.00
0.0
0.5
1.0
1.5
2.0
2.5
3.0
3.5
4.0
4.5
5.0
5.5
6.0
6.5
7.0
7.5
8.0
8.5
9.0
9.5
10.0
10.5
11.0
15.0
15.5
16.0
16.5
17.0
f1 (ppm)

2.170

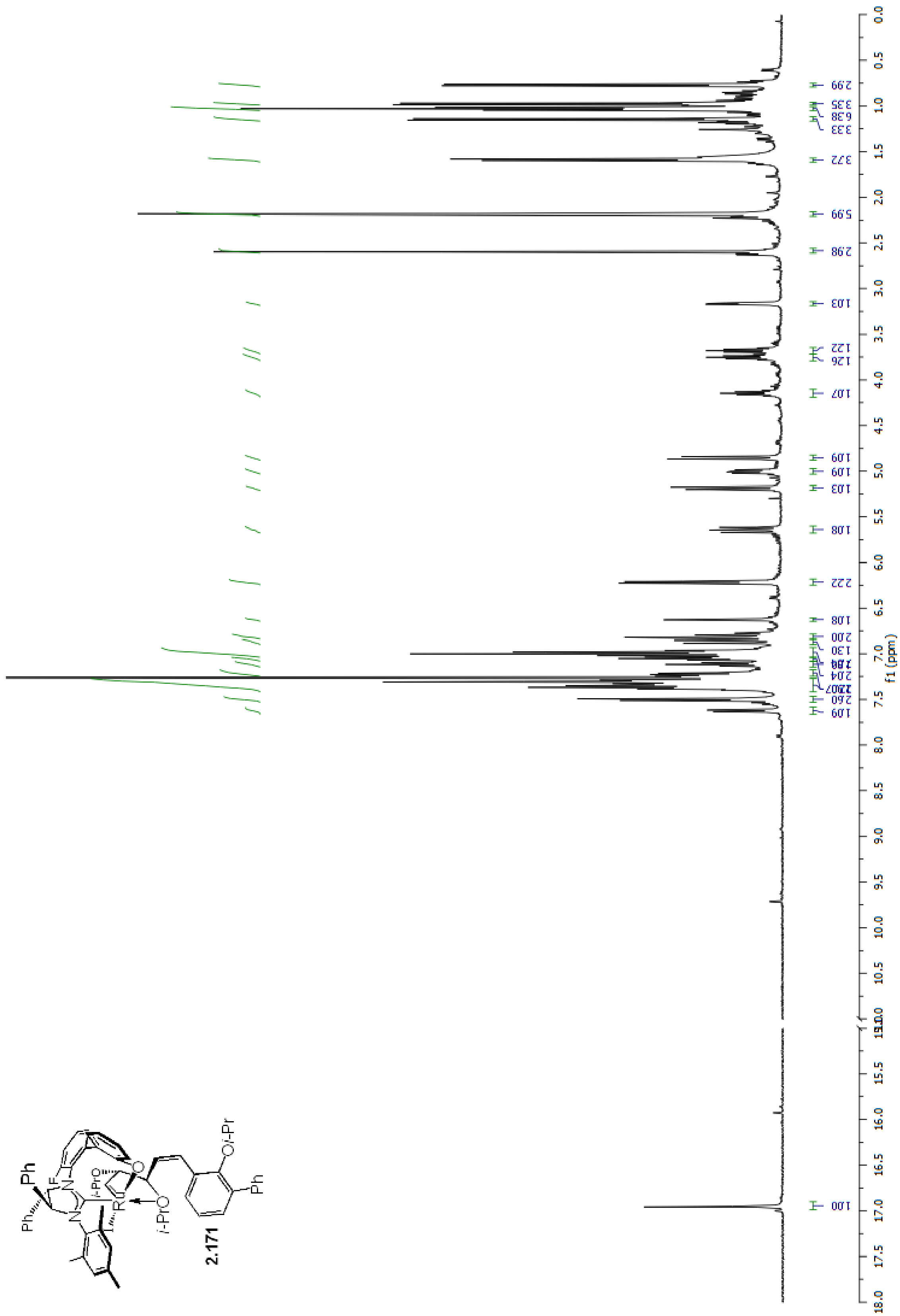
2.99
3.35
6.38
3.33
3.72
5.99
2.98
1.03
1.22
1.26
1.07
1.09
1.09
1.03
1.08
2.22
1.08
2.00
1.30
2.04
2.60
1.09
1.00
0.0
0.5
1.0
1.5
2.0
2.5
3.0
3.5
4.0
4.5
5.0
5.5
6.0
6.5
7.0
7.5
8.0
8.5
9.0
9.5
10.0
10.5
15.5
16.0
16.5
17.0
17.5
18.0
f1 (ppm)
Ph
Ph
F
N
N
i-PrO
Ru
O
i-PrO
O-i-Pr
Ph

2.171

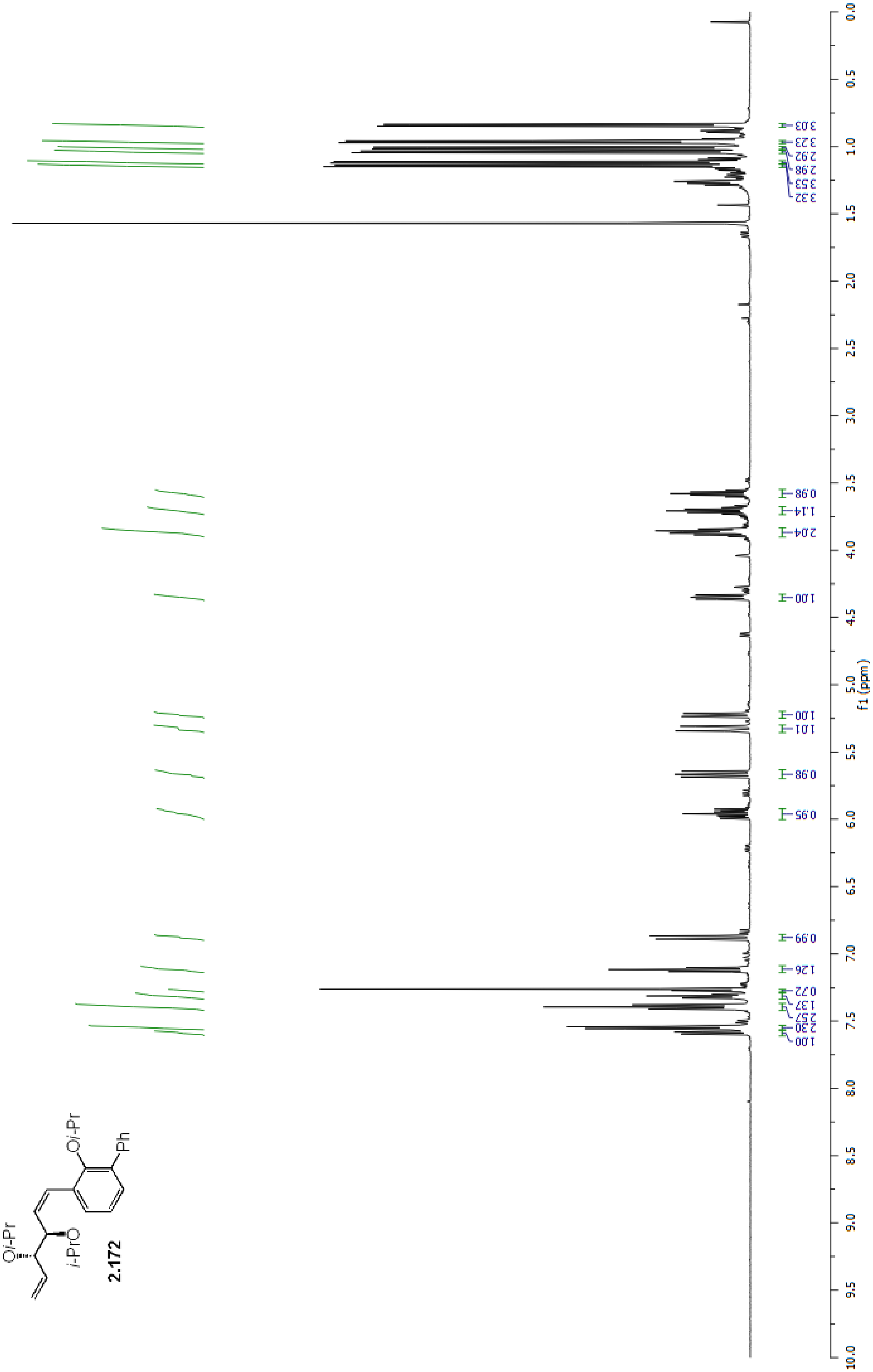
Oi-Pr
i-PrO
Oi-Pr
Ph
3.03
3.23
2.92
2.98
3.53
3.32
0.98
1.14
2.04
1.00
1.00
1.01
0.98
0.95
0.99
1.26
0.72
1.37
2.57
2.30
1.00
0.0
0.5
1.0
1.5
2.0
2.5
3.0
3.5
4.0
4.5
5.0
5.5
6.0
6.5
7.0
7.5
8.0
8.5
9.0
9.5
10.0
f1 (ppm)

2.172

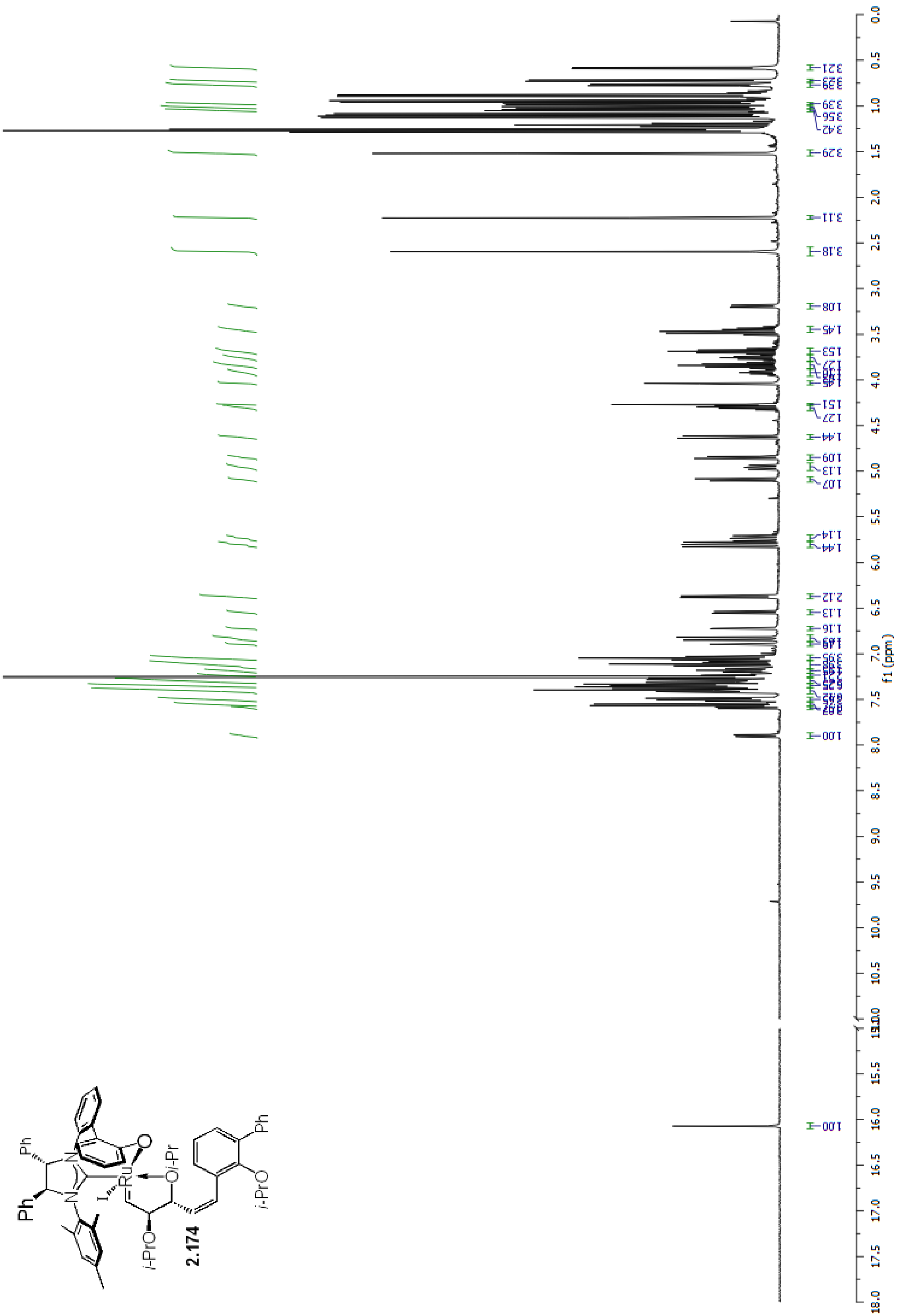
Ph
Ph
N
N
Ru
I
Oi-Pr
i-PrO
i-PrO
Ph
3.21
3.29
3.39
3.39
3.56
3.42
3.29
3.11
3.18
1.08
1.45
1.53
1.51
1.27
1.44
1.09
1.13
1.07
1.14
1.44
2.12
1.13
1.16
1.49
1.00
1.00
0.0
0.5
1.0
1.5
2.0
2.5
3.0
3.5
4.0
4.5
5.0
5.5
6.0
6.5
7.0
7.5
8.0
8.5
9.0
9.5
10.0
10.5
15.0
15.5
16.0
16.5
17.0
17.5
18.0
f1 (ppm)

2.174

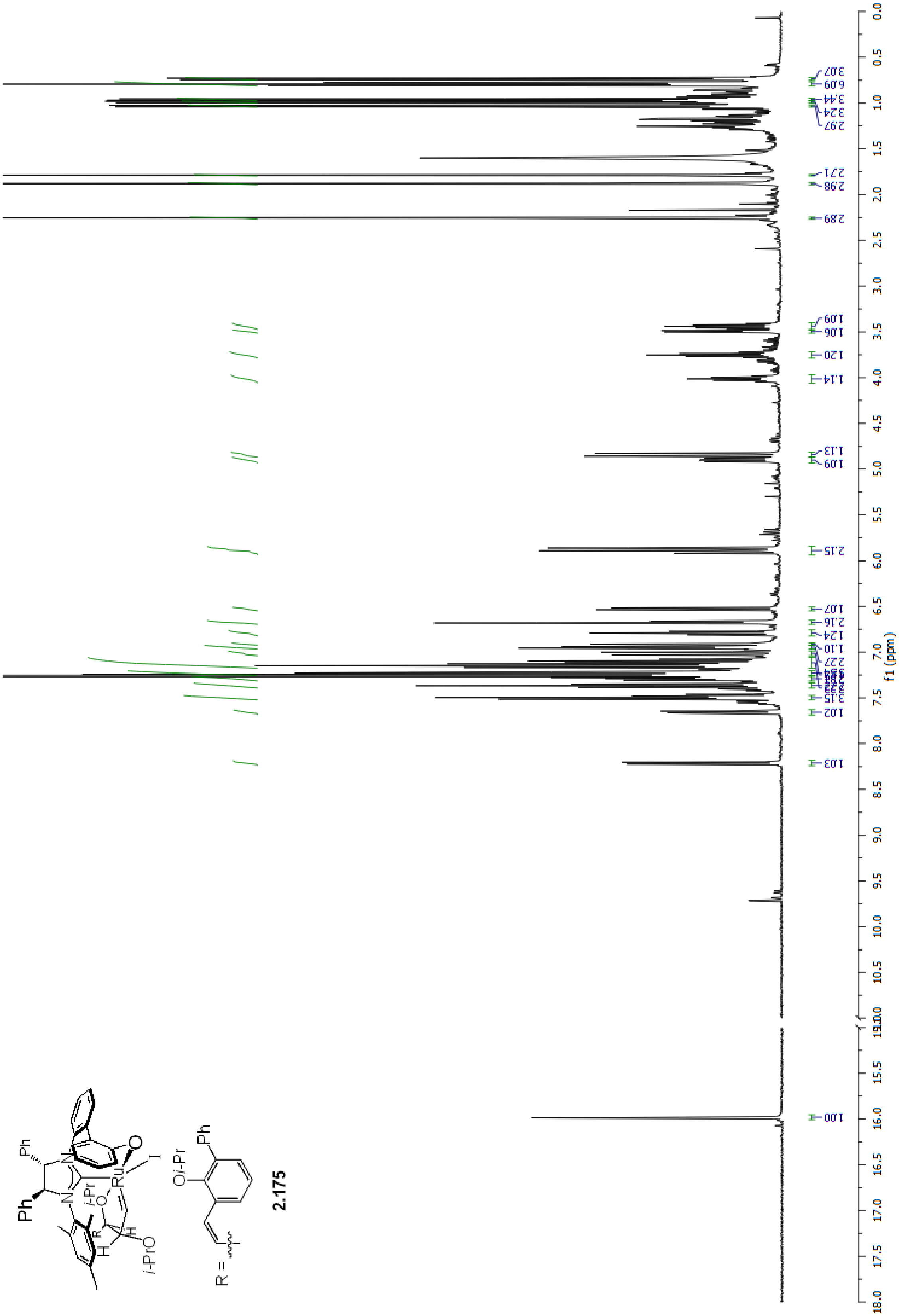

f1 (ppm)
0.0
0.5
1.0
1.5
2.0
2.5
3.0
3.5
4.0
4.5
5.0
5.5
6.0
6.5
7.0
7.5
8.0
8.5
9.0
9.5
10.0
10.5
11.0
15.0
15.5
16.0
16.5
17.0
17.5
18.0
3.07
6.09
3.44
3.24
2.97
2.71
2.98
2.89
1.09
1.06
1.20
1.14
1.13
1.09
2.15
1.07
2.16
1.24
1.10
2.27
3.15
1.02
1.03
1.00
Ph
Ph
N
N
Ru
O
I
i-Pr
O
R
H
H
i-PrO
Oi-Pr
Ph
R =
I

2.175

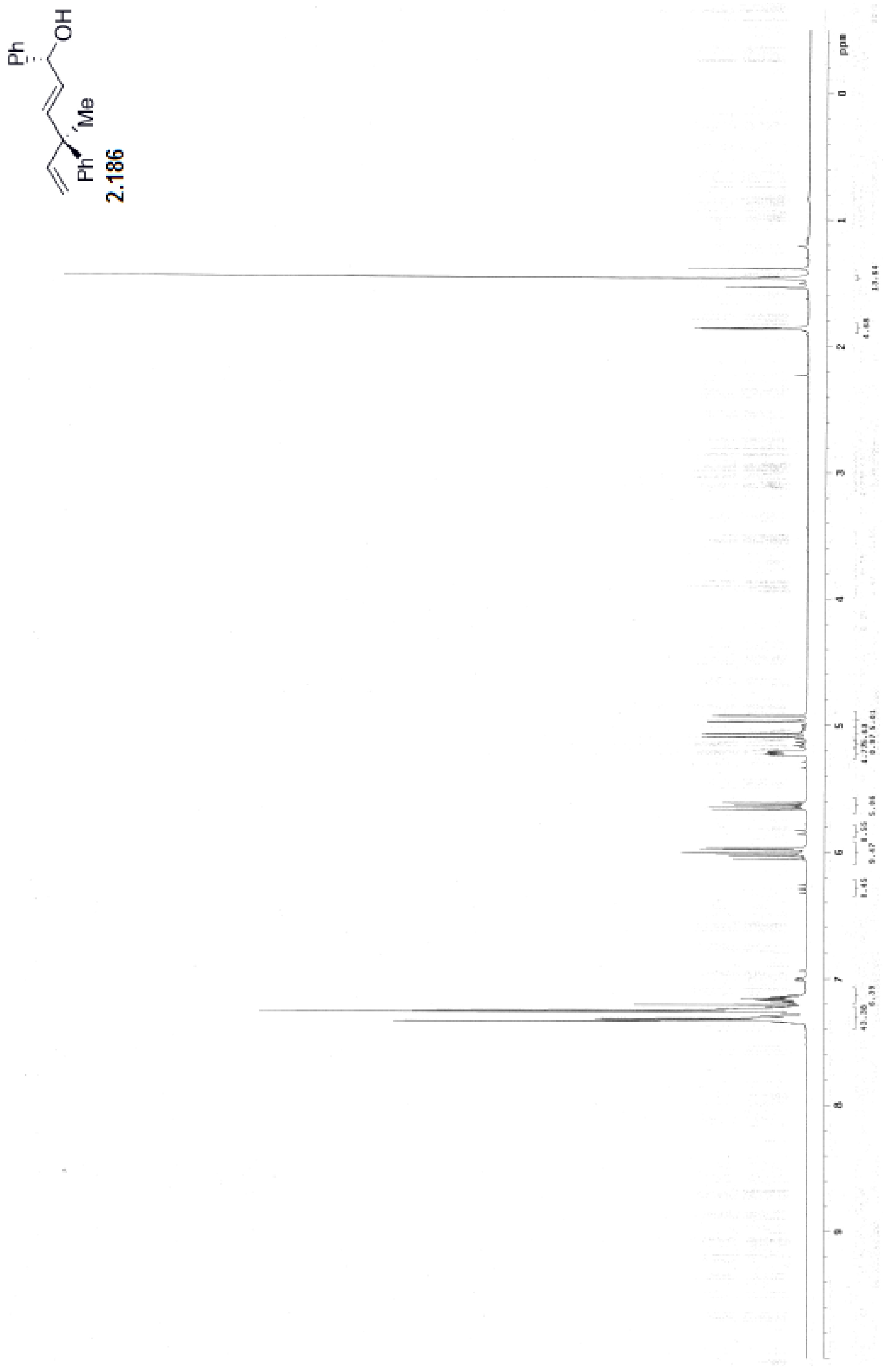

2.186

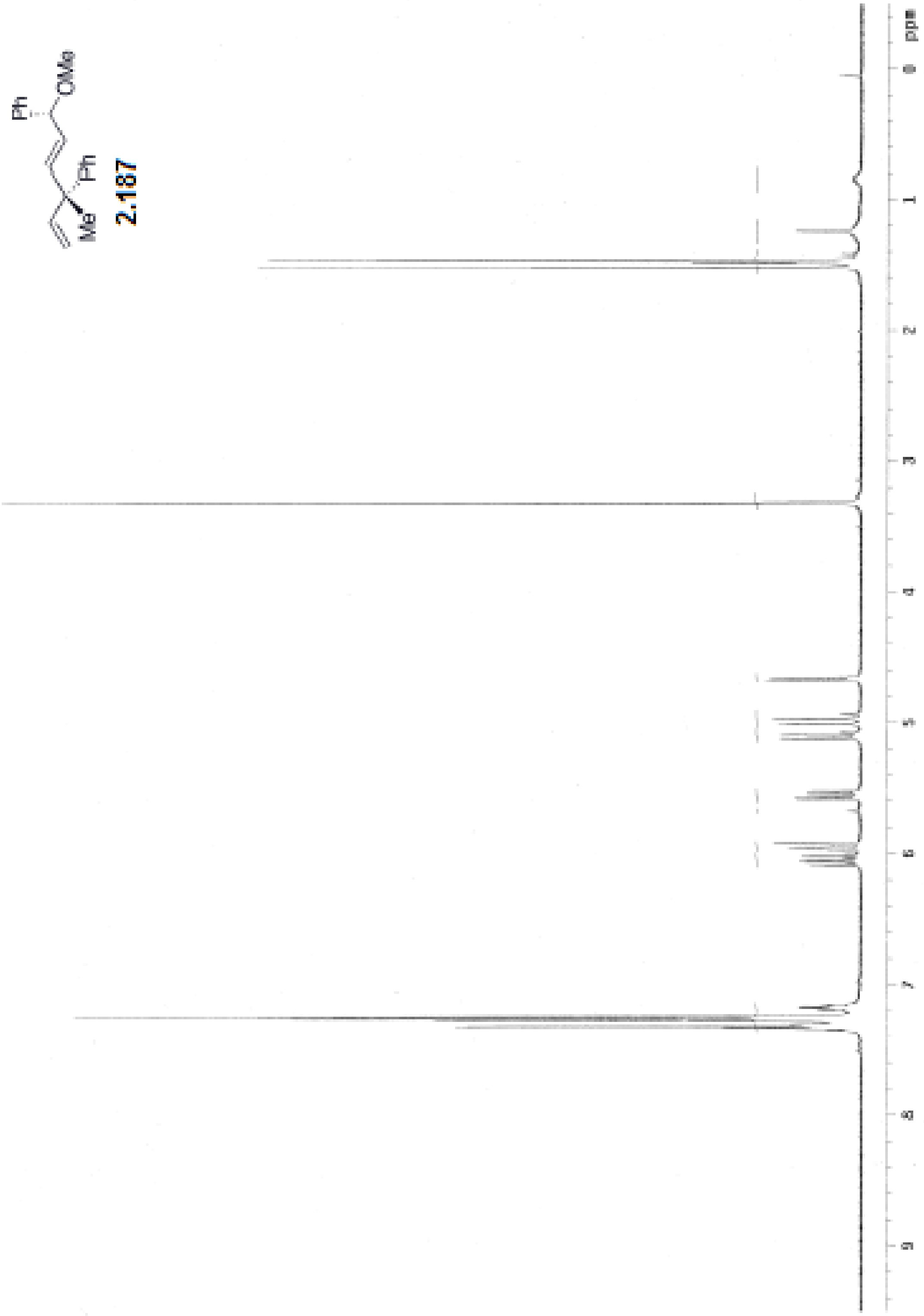

2.187

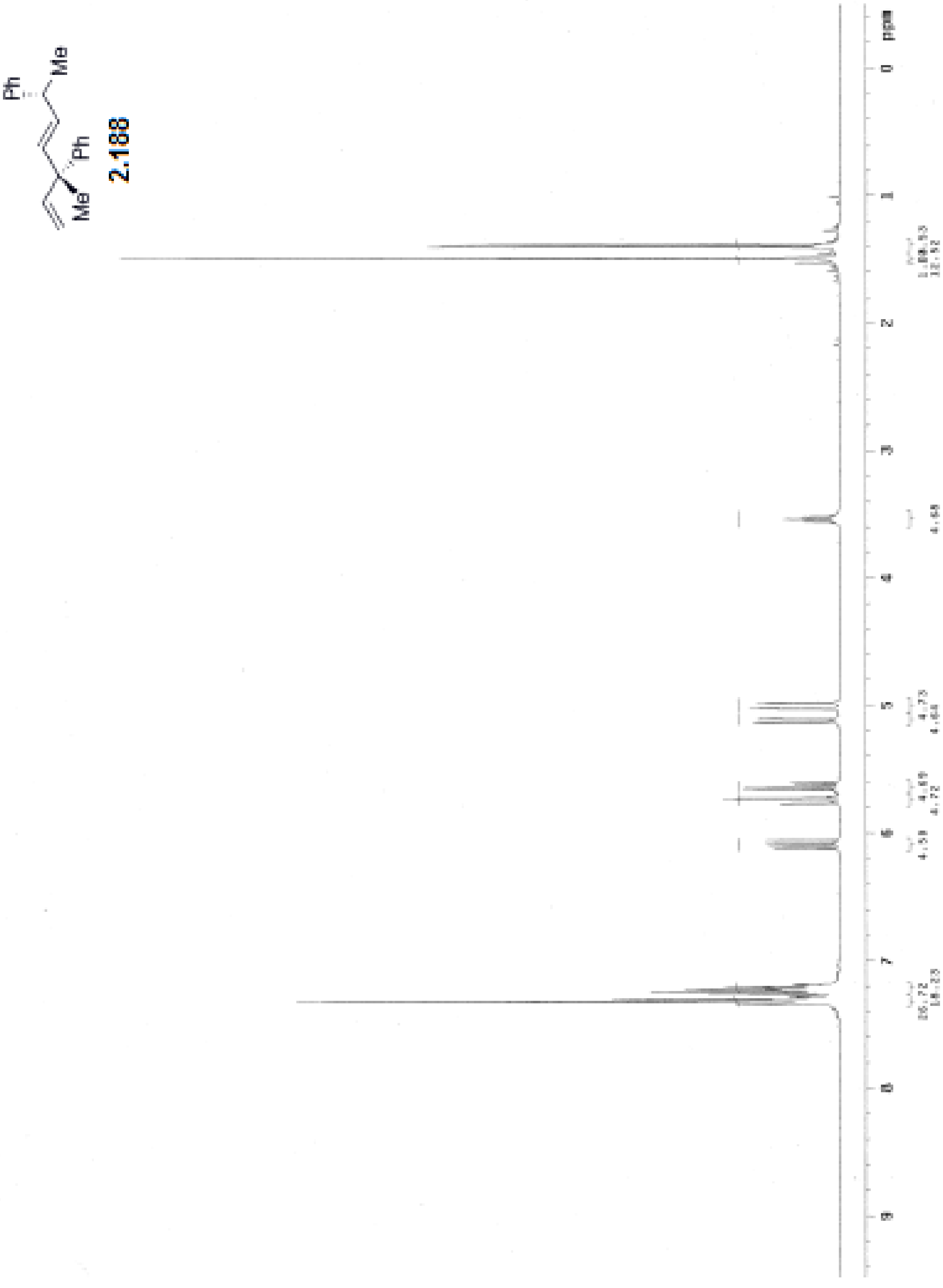

2.188

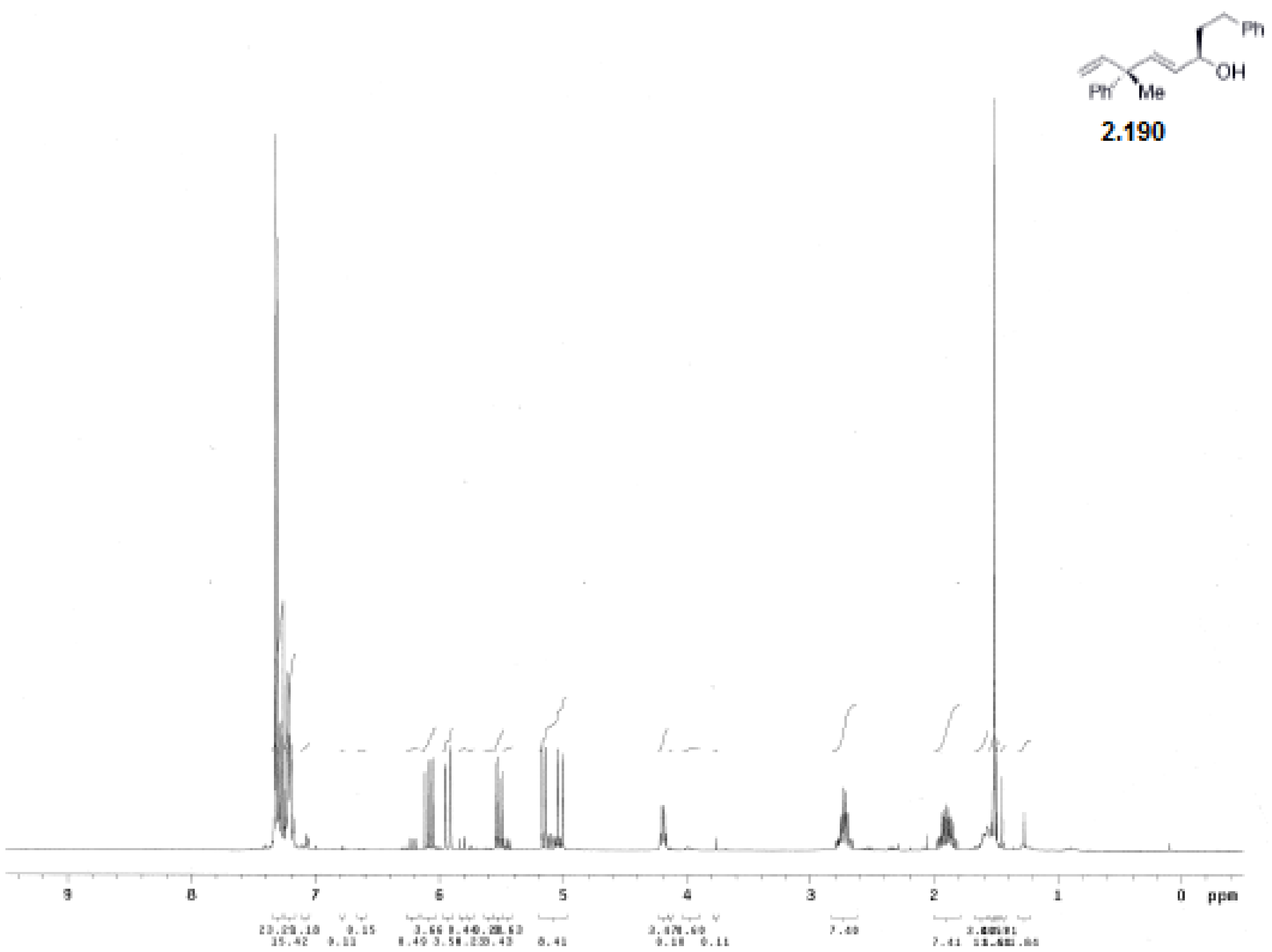

2.190

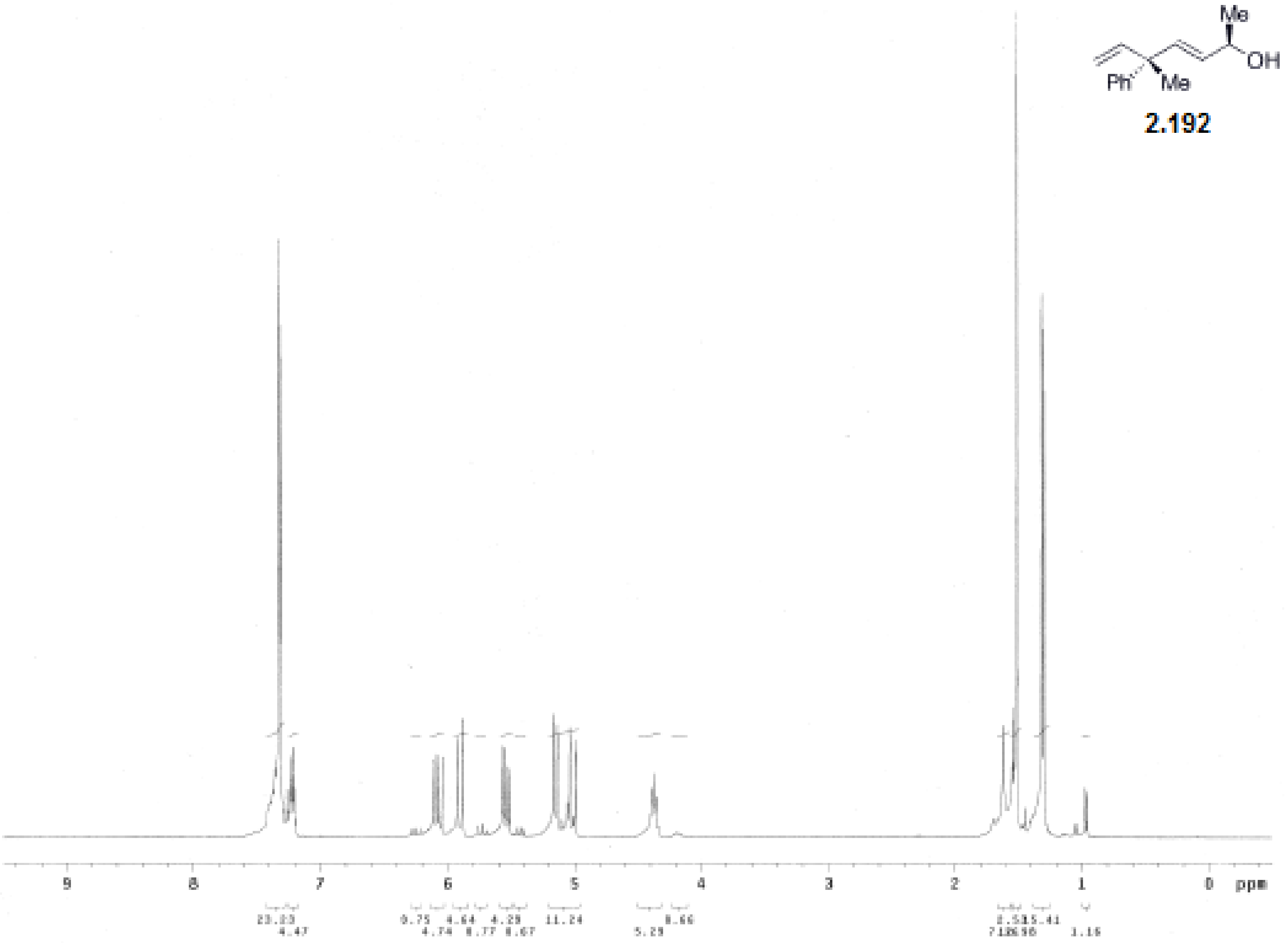

2.192

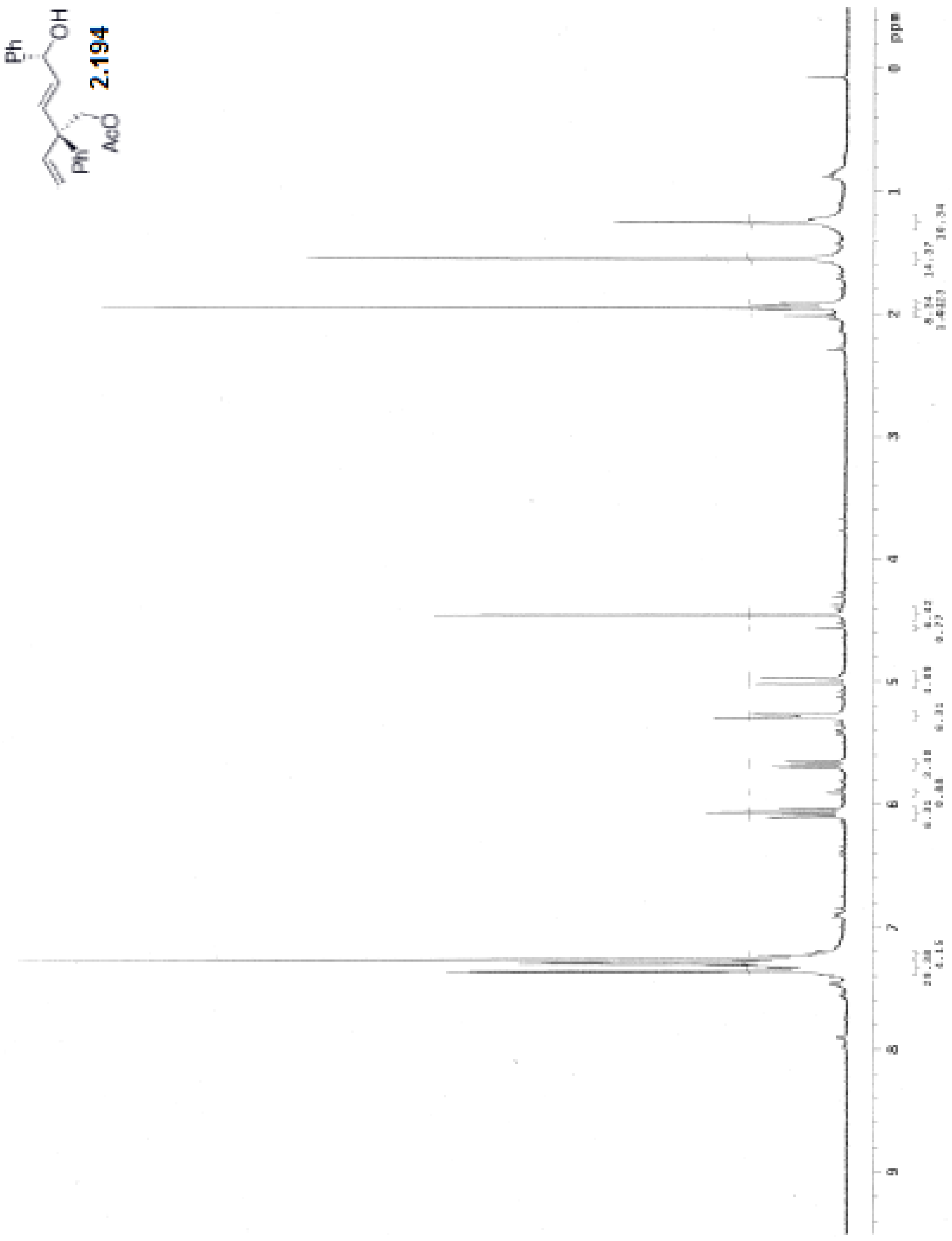

2.194

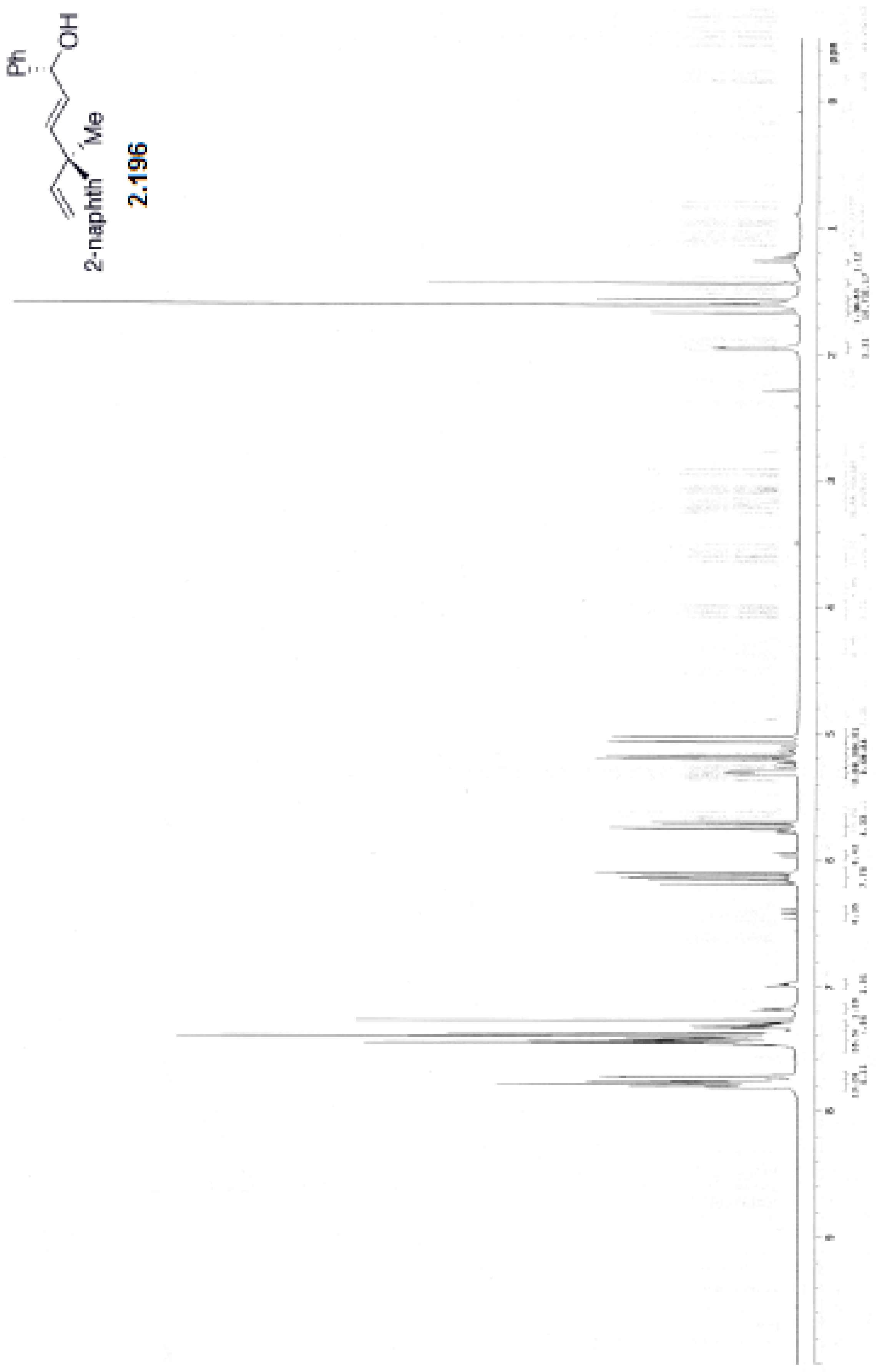

2.196

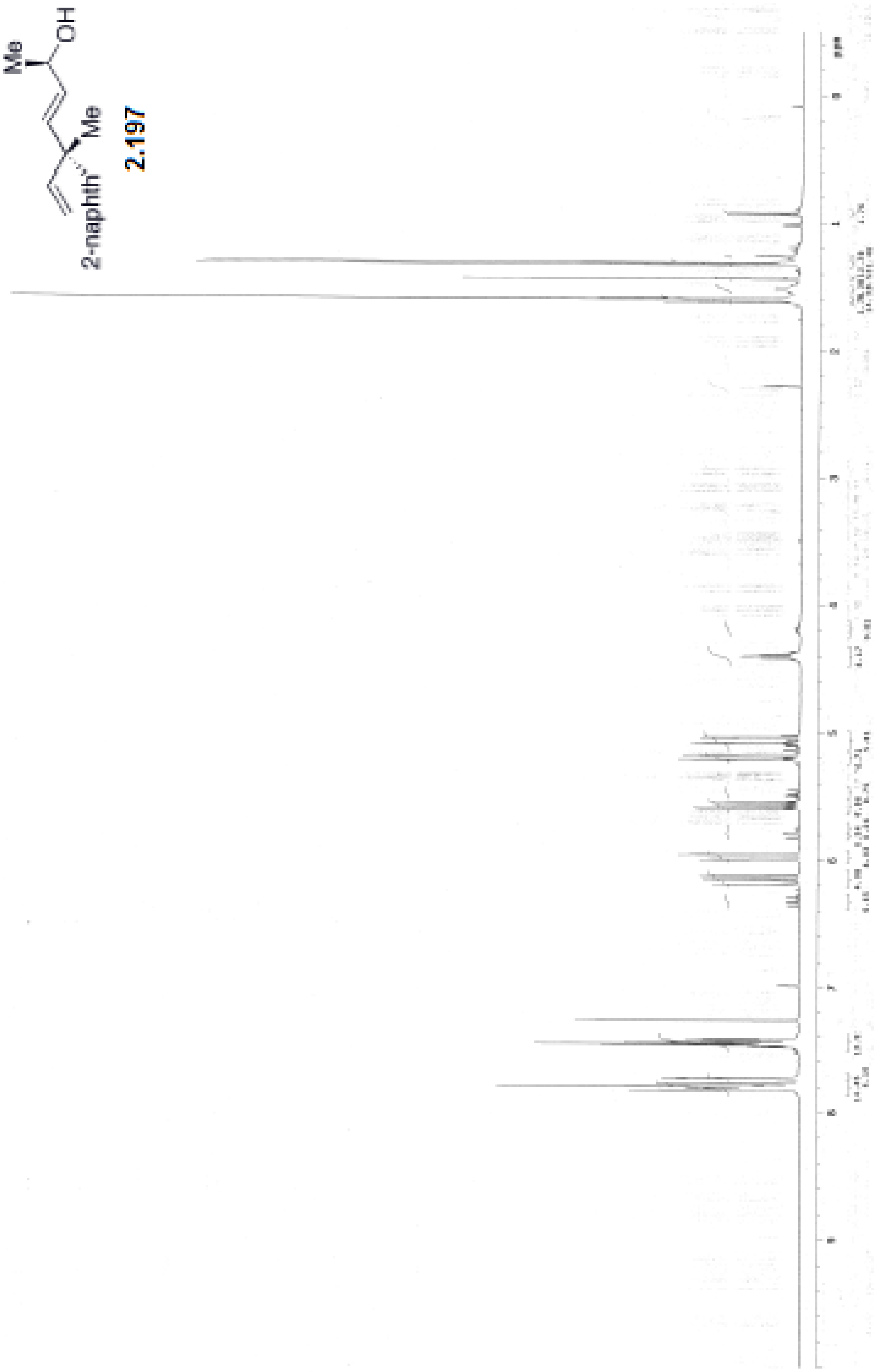

2.197

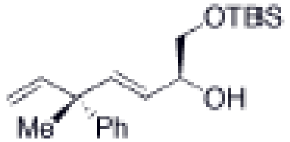

2.198

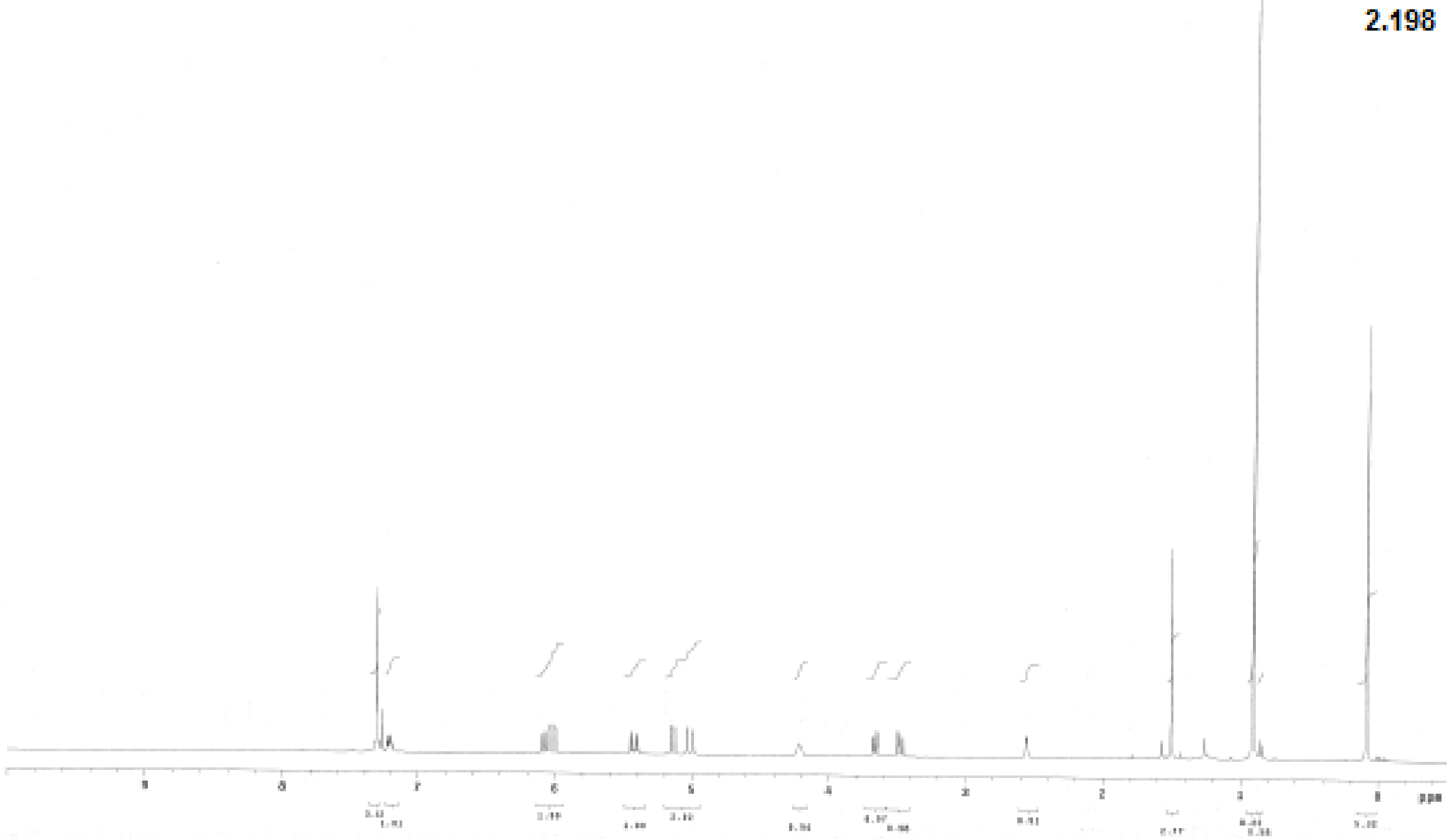

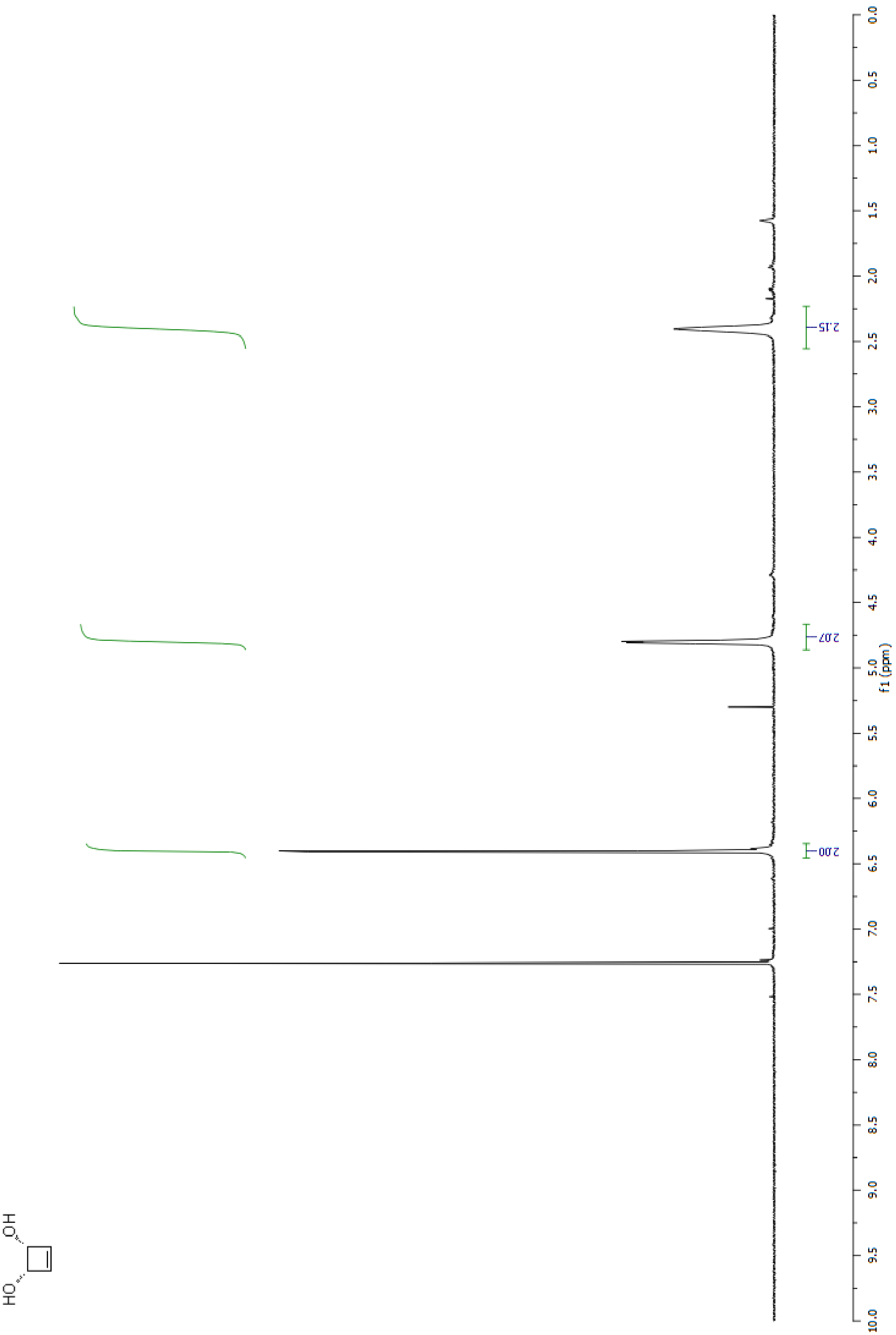
HO
OH
2.15
2.07
2.00
0.0
0.5
1.0
1.5
2.0
2.5
3.0
3.5
4.0
4.5
5.0
5.5
6.0
6.5
7.0
7.5
8.0
8.5
9.0
9.5
10.0
f1 (ppm)

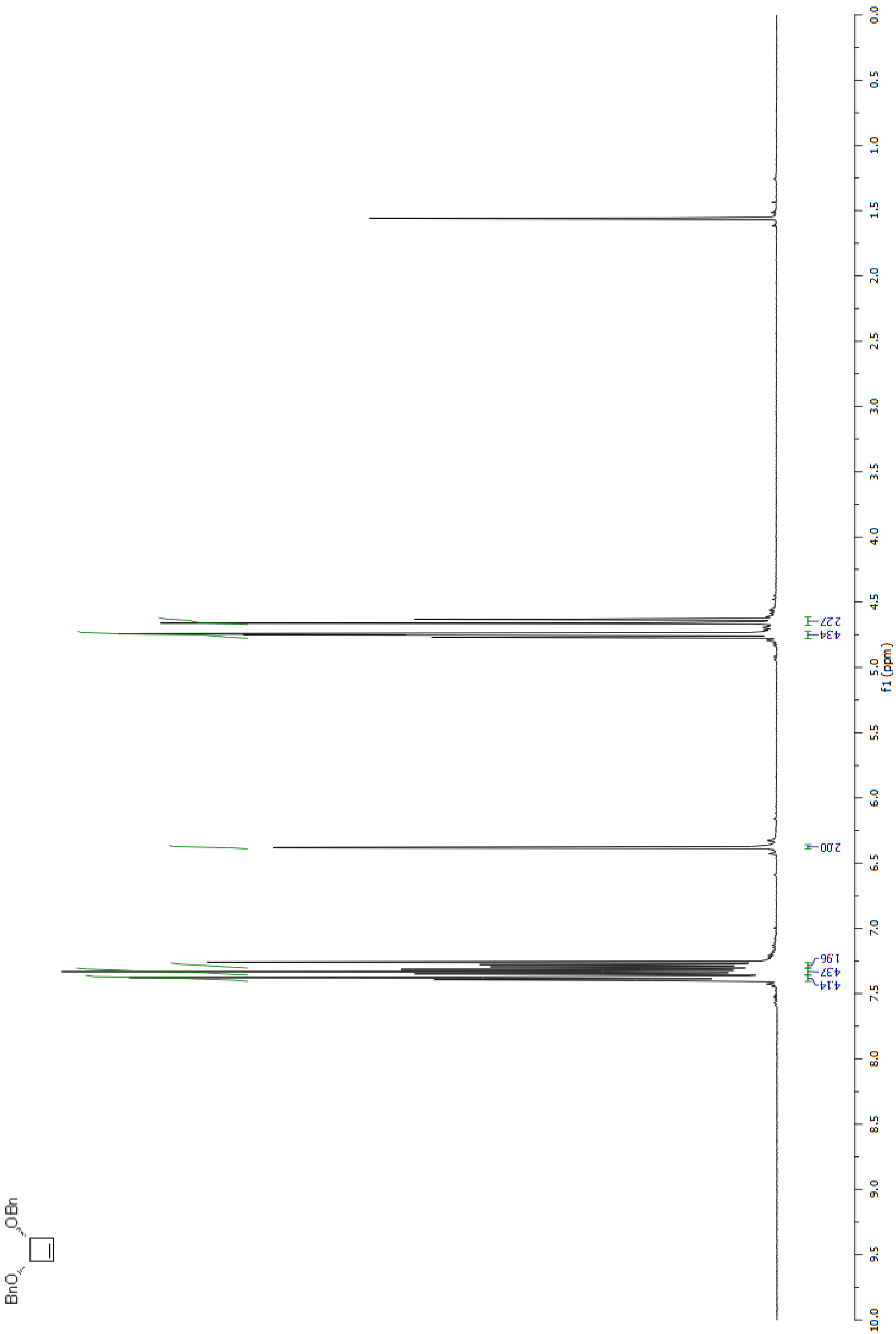
BnO
OBn
2.27
4.34
2.00
1.96
4.37
4.14
0.0
0.5
1.0
1.5
2.0
2.5
3.0
3.5
4.0
4.5
5.0
f1 (ppm)
5.5
6.0
6.5
7.0
7.5
8.0
8.5
9.0
9.5
10.0

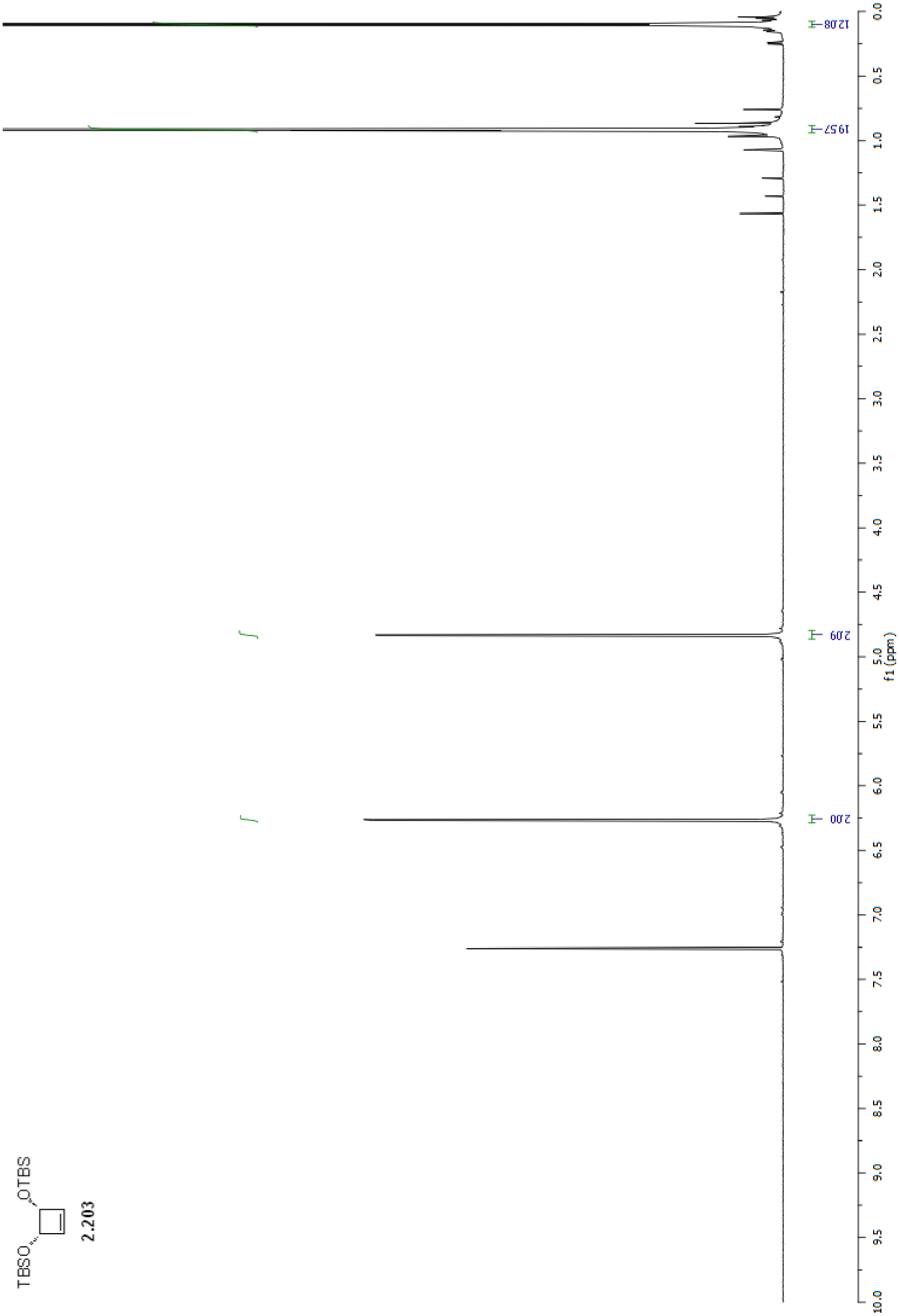
TBSO
OTBS
12.08
19.57
2.09
2.00
0.0
0.5
1.0
1.5
2.0
2.5
3.0
3.5
4.0
4.5
5.0
f1 (ppm)
5.5
6.0
6.5
7.0
7.5
8.0
8.5
9.0
9.5
10.0

2.203

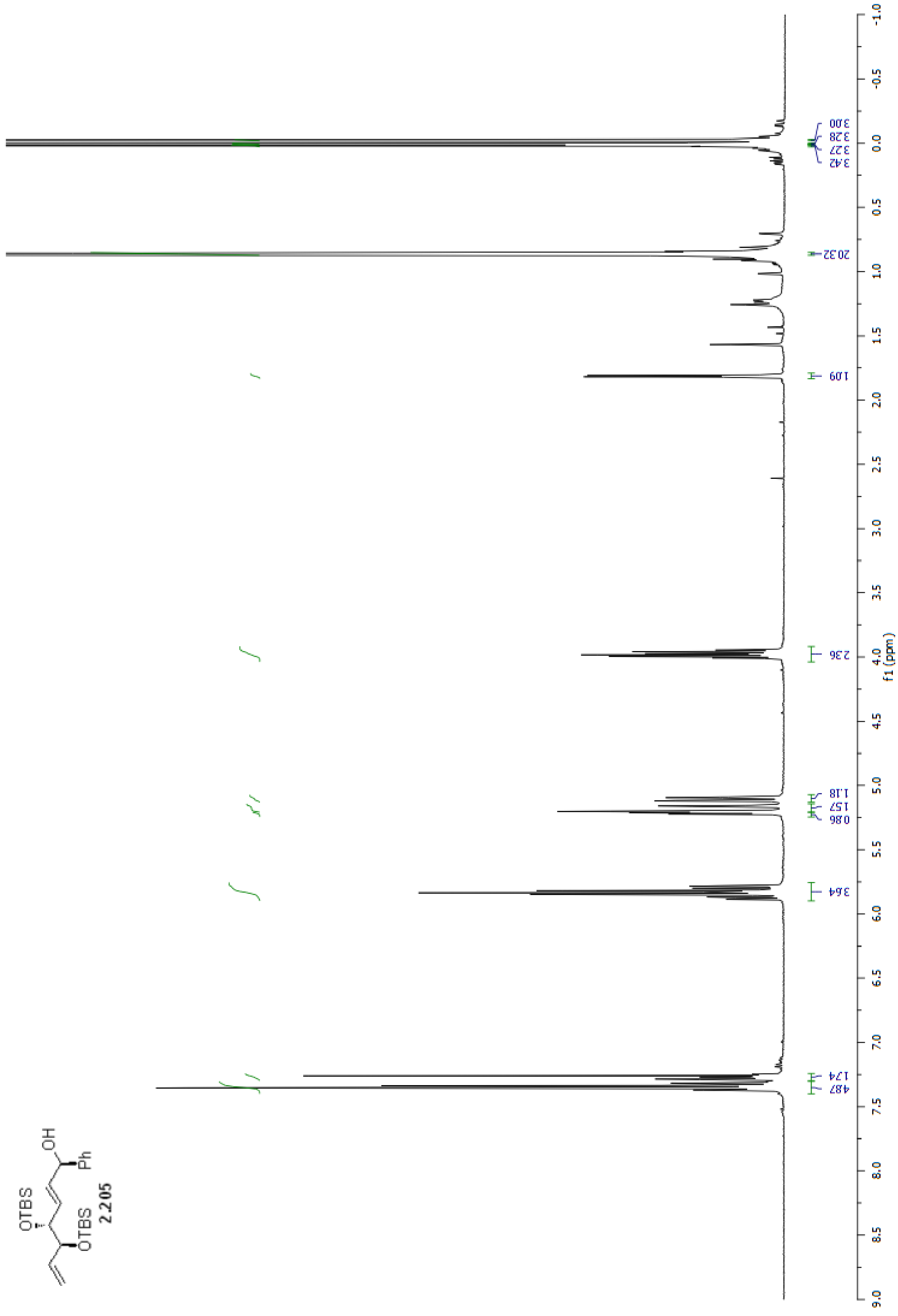

OTBS
OTBS
OH
Ph
2.205
3.42
3.27
3.28
3.00
20.32
1.09
2.36
1.18
1.57
0.86
3.64
1.74
4.87
9.0
8.5
8.0
7.5
7.0
6.5
6.0
5.5
5.0
4.5
4.0
3.5
3.0
2.5
2.0
1.5
1.0
0.5
0.0
-0.5
-1.0
f1 (ppm)

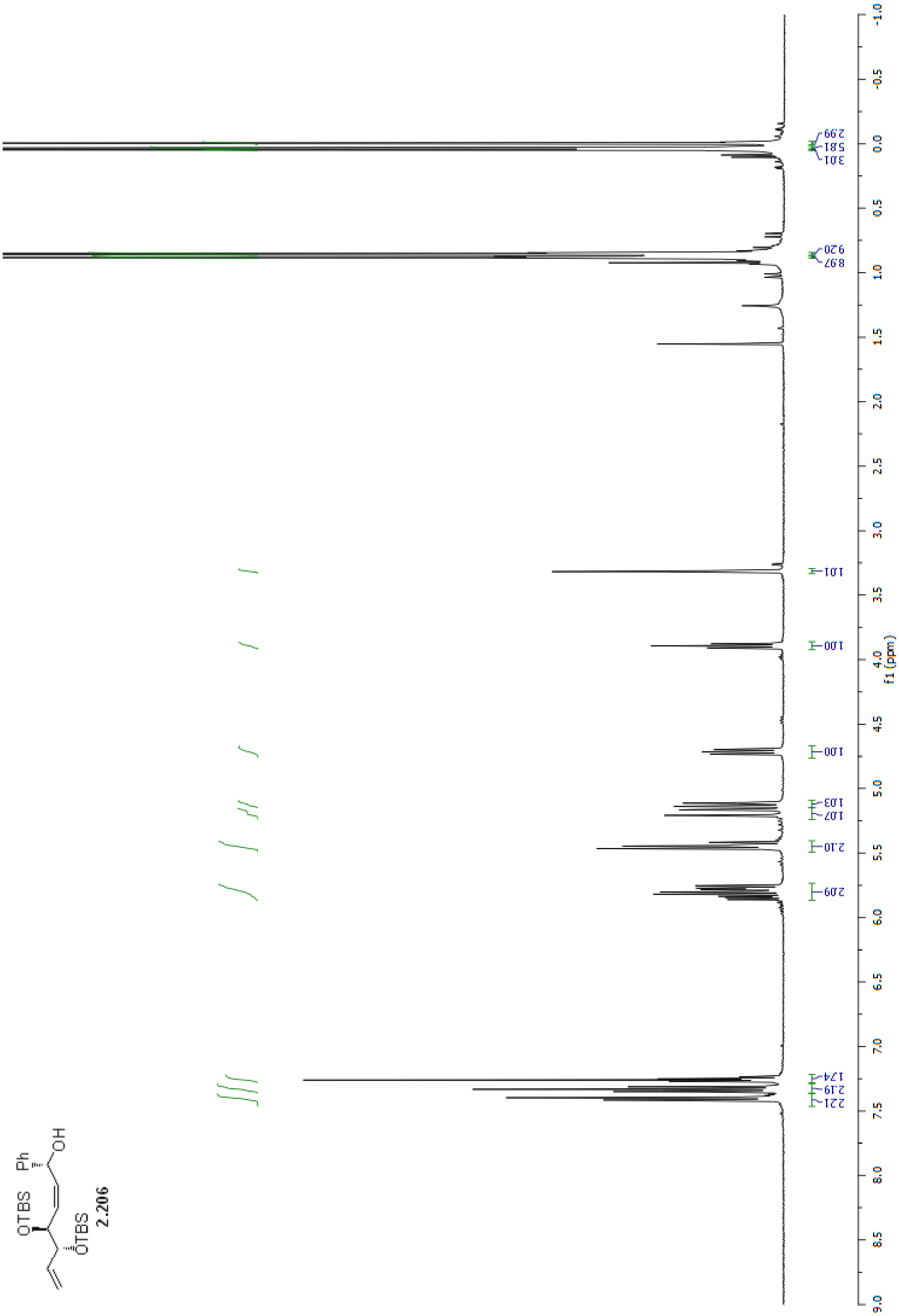

OTBS
Ph
OH
OTBS
2.99
5.81
3.01
9.20
8.97
1.01
1.00
1.00
1.03
1.07
2.10
2.09
1.74
2.19
2.21
-1.0
-0.5
0.0
0.5
1.0
1.5
2.0
2.5
3.0
3.5
4.0
f1 (ppm)
4.5
5.0
5.5
6.0
6.5
7.0
7.5
8.0
8.5
9.0

2.206

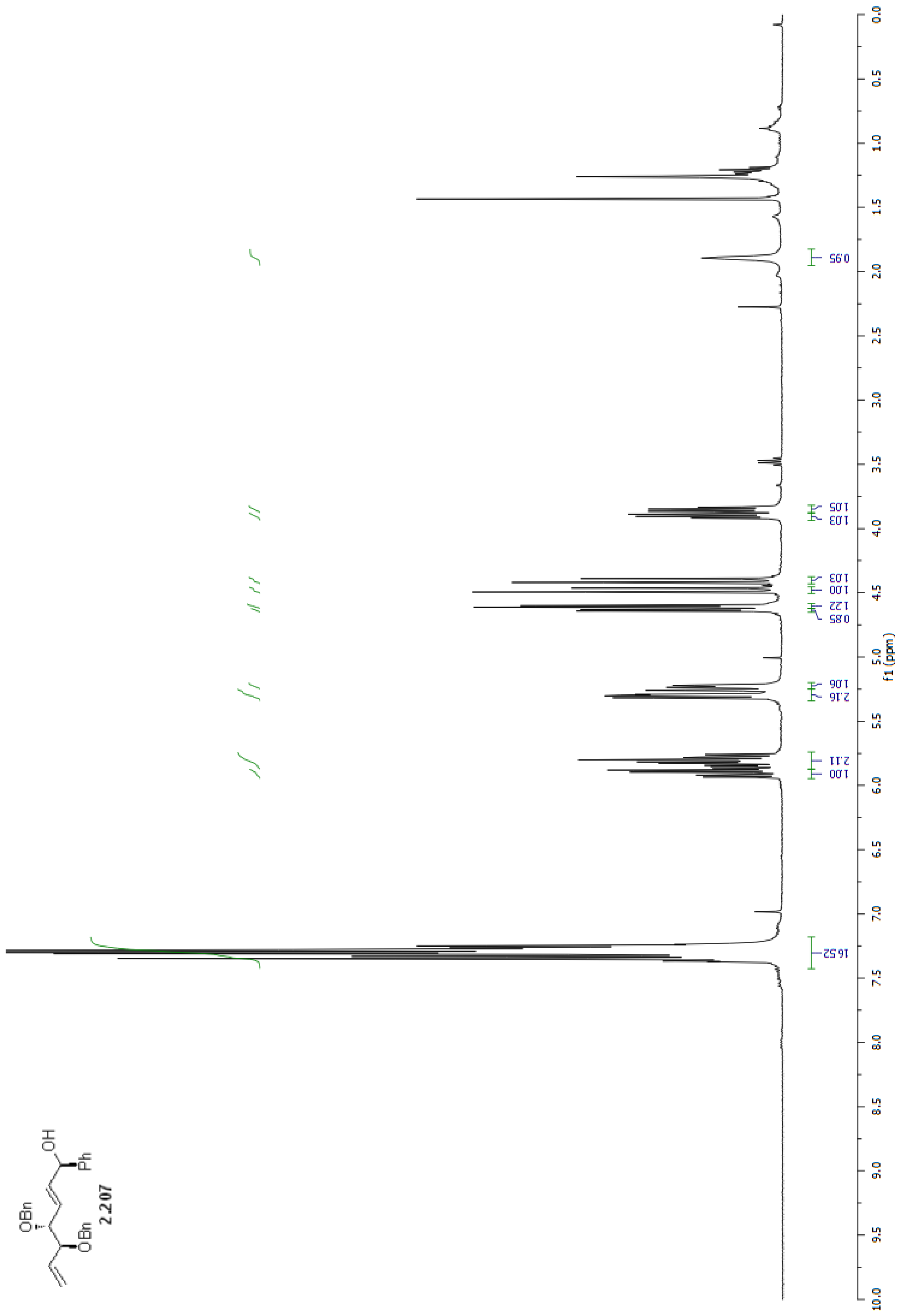
OBn
OBn
OH
Ph
0.95
1.05
1.03
1.03
1.00
1.22
0.85
1.06
2.16
2.11
1.00
16.52
0.0
0.5
1.0
1.5
2.0
2.5
3.0
3.5
4.0
4.5
5.0
5.5
6.0
6.5
7.0
7.5
8.0
8.5
9.0
9.5
10.0
f1 (ppm)

2.207

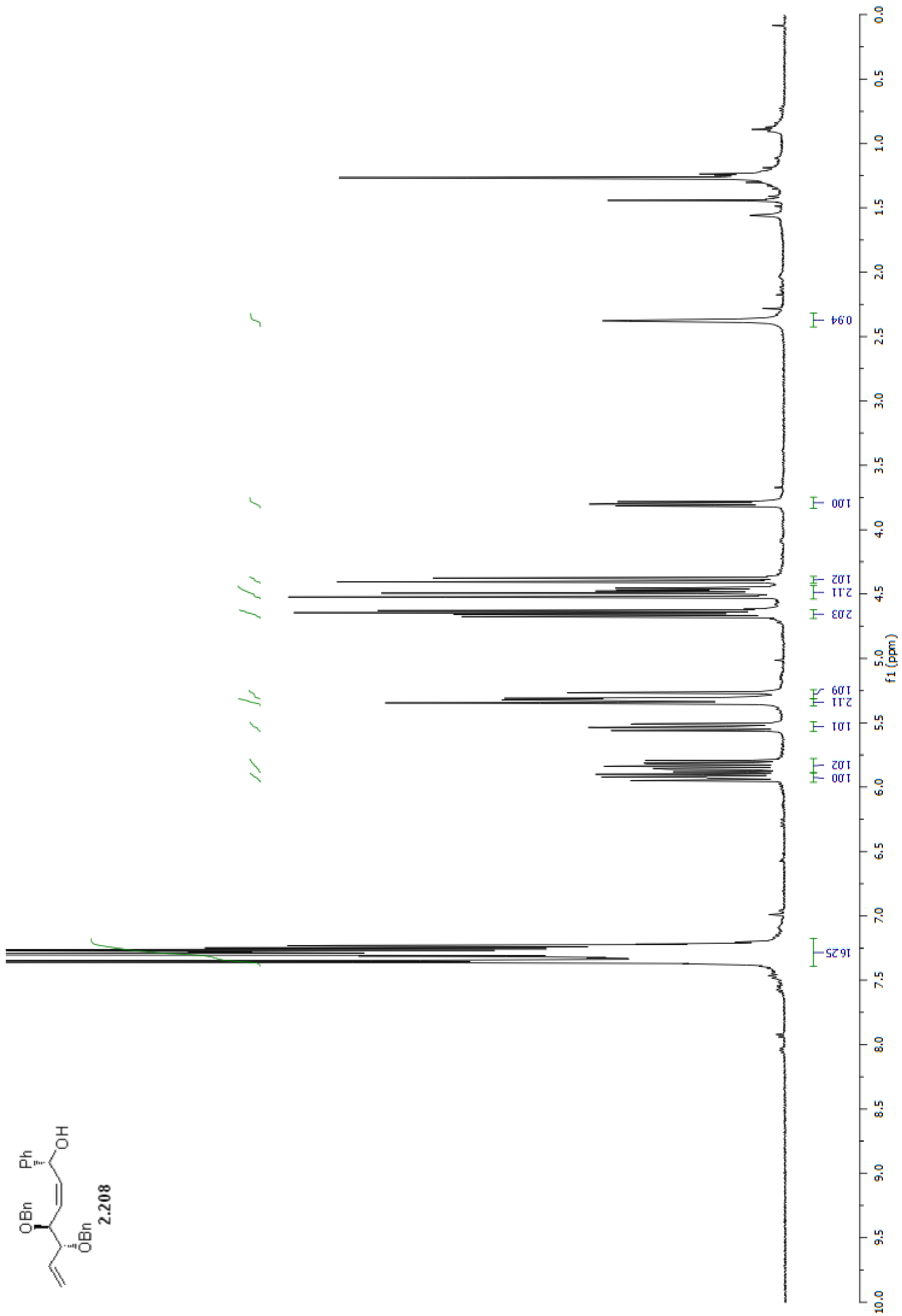
OBn
Ph
OH
OBn
16.25
1.00
1.02
1.01
2.11
1.09
2.03
2.11
1.02
1.00
0.94
10.0
9.5
9.0
8.5
8.0
7.5
7.0
6.5
6.0
5.5
5.0
4.5
4.0
3.5
3.0
2.5
2.0
1.5
1.0
0.5
0.0
f1 (ppm)

2.208

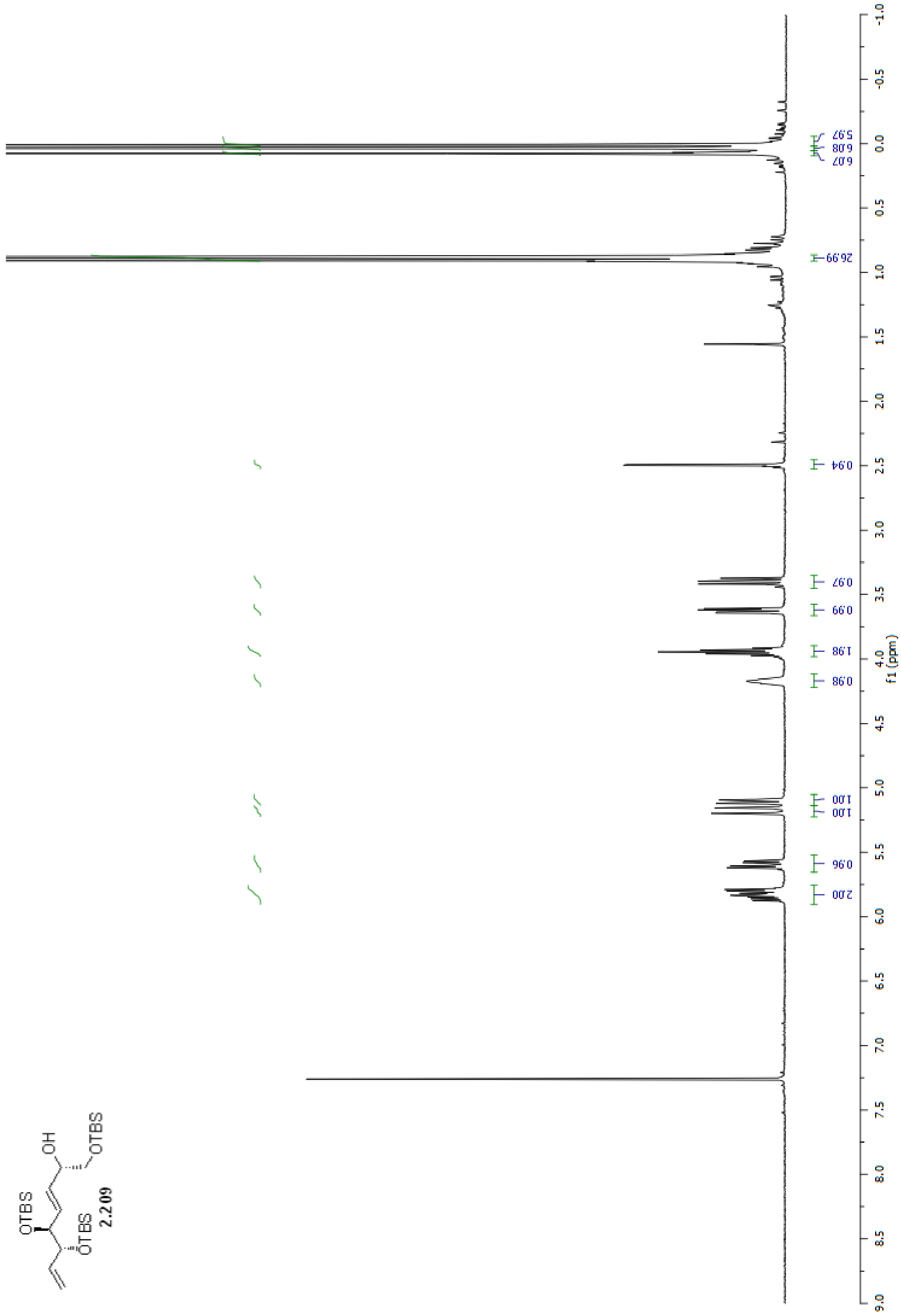
OTBS
OTBS
OH
OTBS
5.97
6.08
6.07
26.99
0.94
0.97
0.99
1.98
0.98
1.00
1.00
0.96
2.00
-1.0
-0.5
0.0
0.5
1.0
1.5
2.0
2.5
3.0
3.5
4.0
4.5
5.0
5.5
6.0
6.5
7.0
7.5
8.0
8.5
9.0
f1 (ppm)

2.209

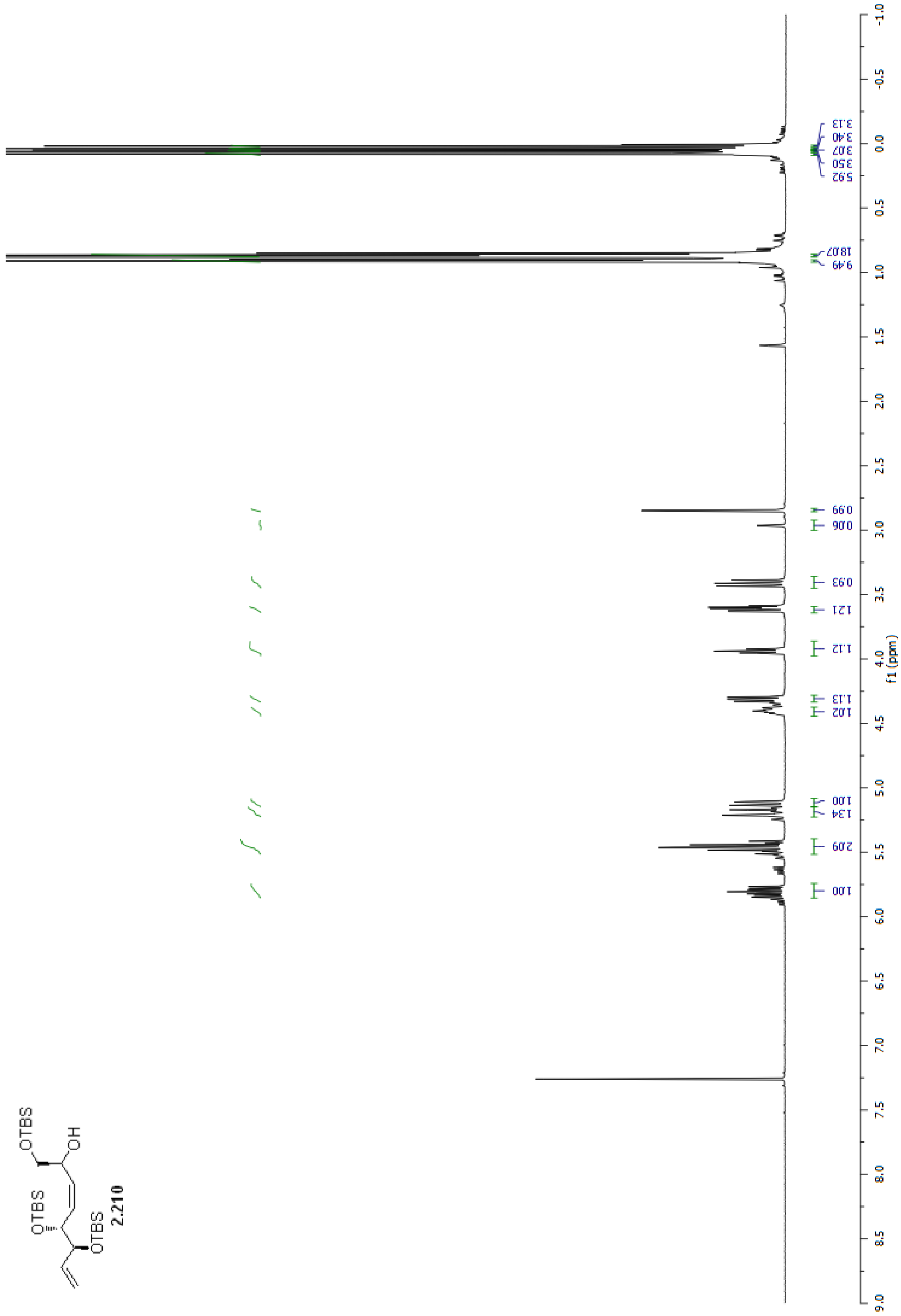
OTBS
OTBS
OTBS
OH
3.13
3.40
3.07
3.50
5.92
18.07
9.49
0.99
0.06
0.93
1.21
1.12
1.13
1.02
1.00
1.34
2.09
1.00
-1.0
-0.5
0.0
0.5
1.0
1.5
2.0
2.5
3.0
3.5
4.0
4.5
5.0
5.5
6.0
6.5
7.0
7.5
8.0
8.5
9.0
f1 (ppm)

2.210

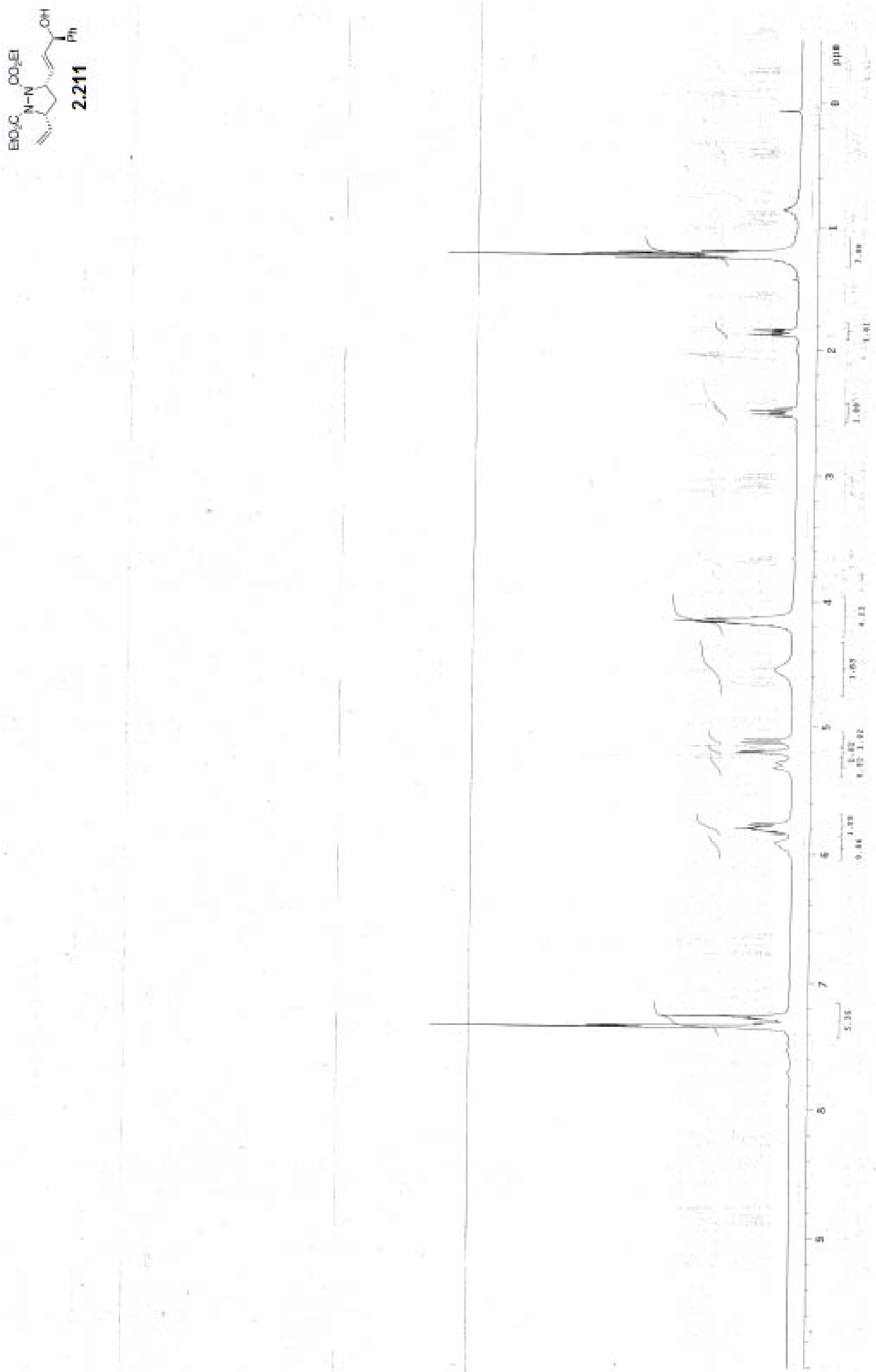

2.211

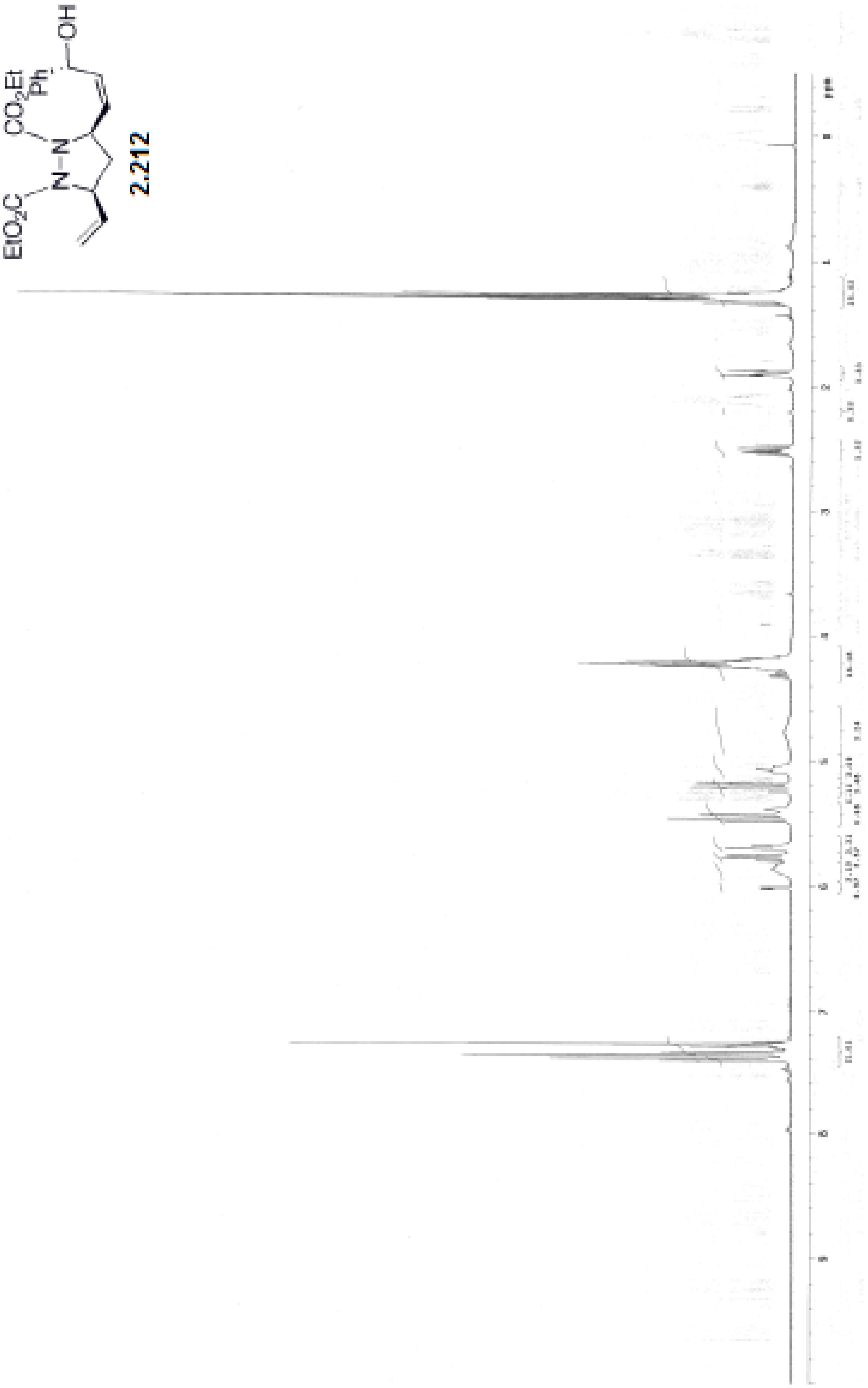

2.212

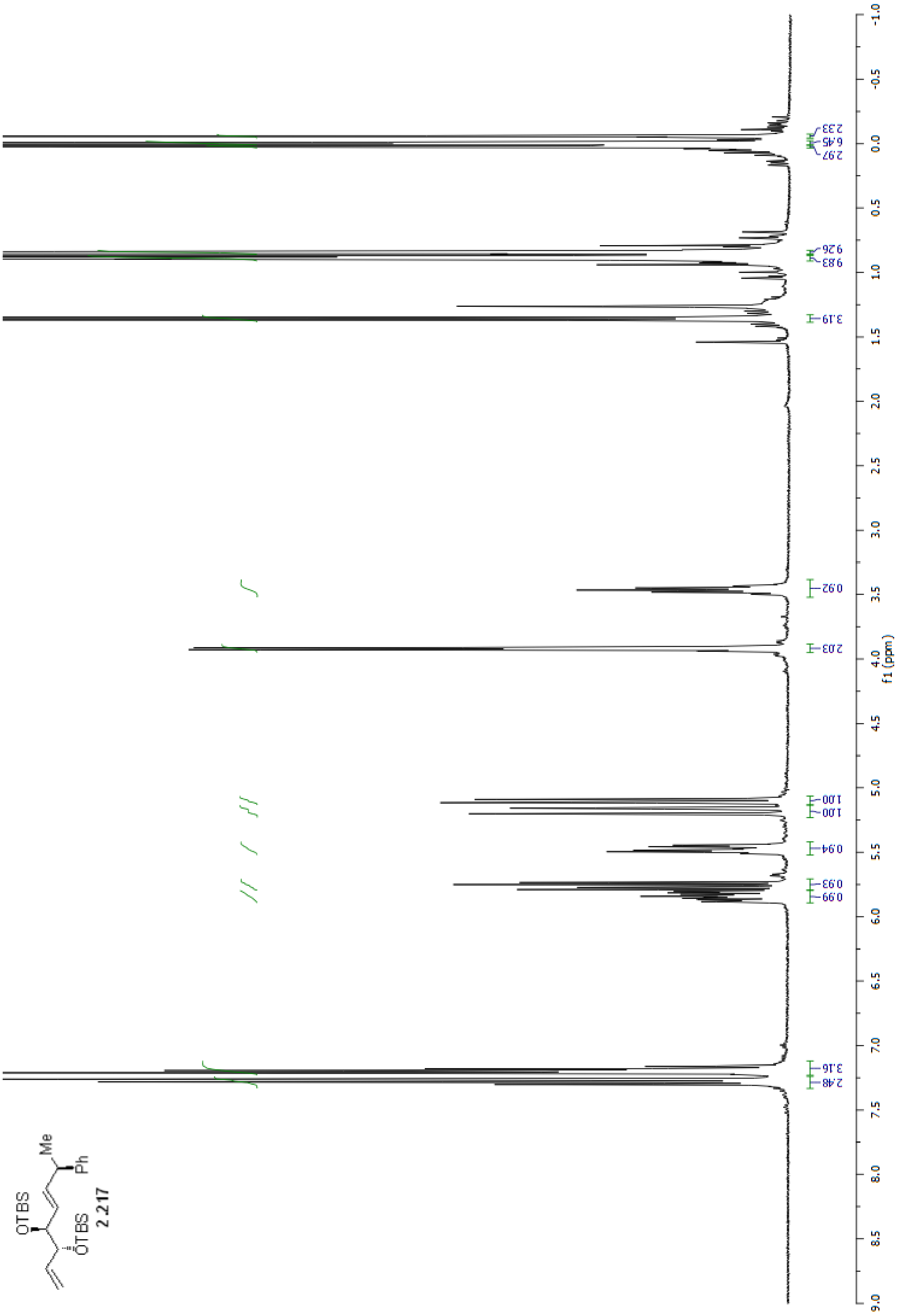
OTBS
Me
Ph
OTBS
2.33
6.45
2.97
9.26
9.83
3.19
0.92
2.03
1.00
1.00
0.94
0.93
0.99
3.16
2.48
-1.0
-0.5
0.0
0.5
1.0
1.5
2.0
2.5
3.0
3.5
4.0
4.5
5.0
5.5
6.0
6.5
7.0
7.5
8.0
8.5
9.0
f1 (ppm)

2.217

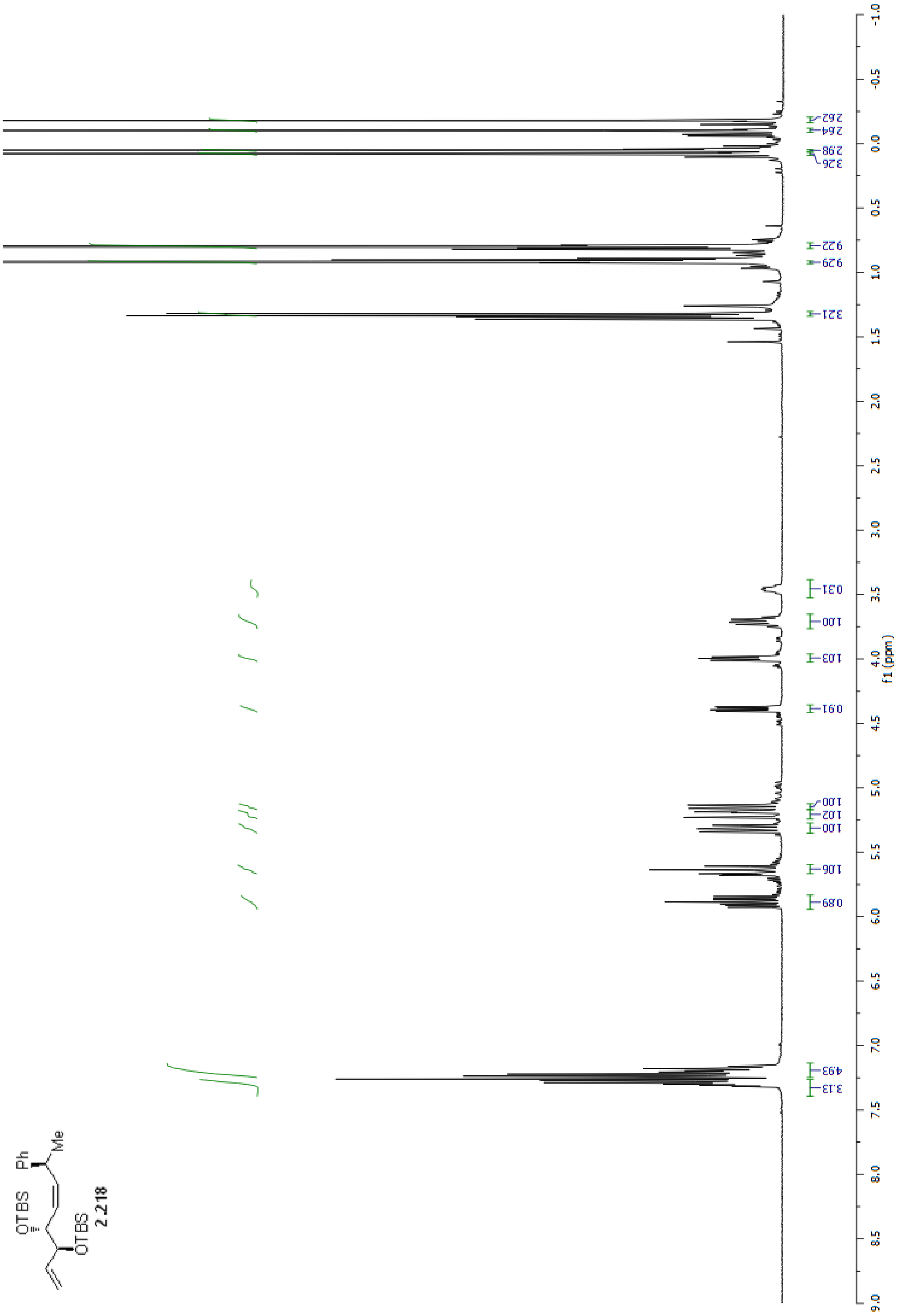
OTBS
OTBS
Ph
Me
2.62
2.64
2.98
3.26
9.22
9.29
3.21
0.31
1.00
1.03
0.91
1.00
1.02
1.00
1.06
0.89
4.93
3.13
-1.0
-0.5
0.0
0.5
1.0
1.5
2.0
2.5
3.0
3.5
4.0
4.5
5.0
5.5
6.0
6.5
7.0
7.5
8.0
8.5
9.0
f1 (ppm)

2.218

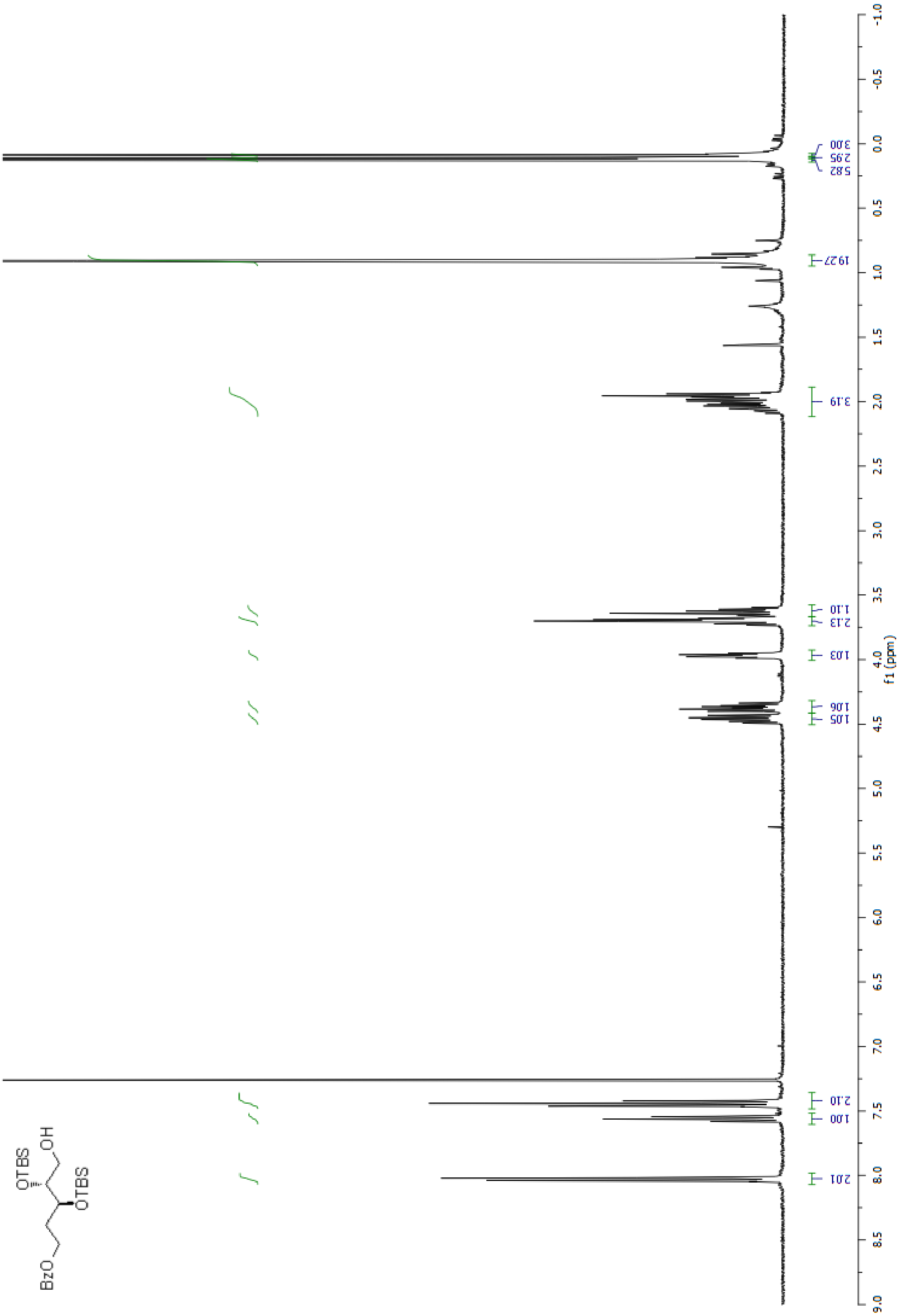
BzO
OTBS
OTBS
OH
2.01
1.00
2.10
1.05
1.06
1.03
2.13
1.10
3.19
19.27
5.82
2.95
3.00
9.0
8.5
8.0
7.5
7.0
6.5
6.0
5.5
5.0
4.5
4.0
3.5
3.0
2.5
2.0
1.5
1.0
0.5
0.0
-0.5
-1.0
f1 (ppm)

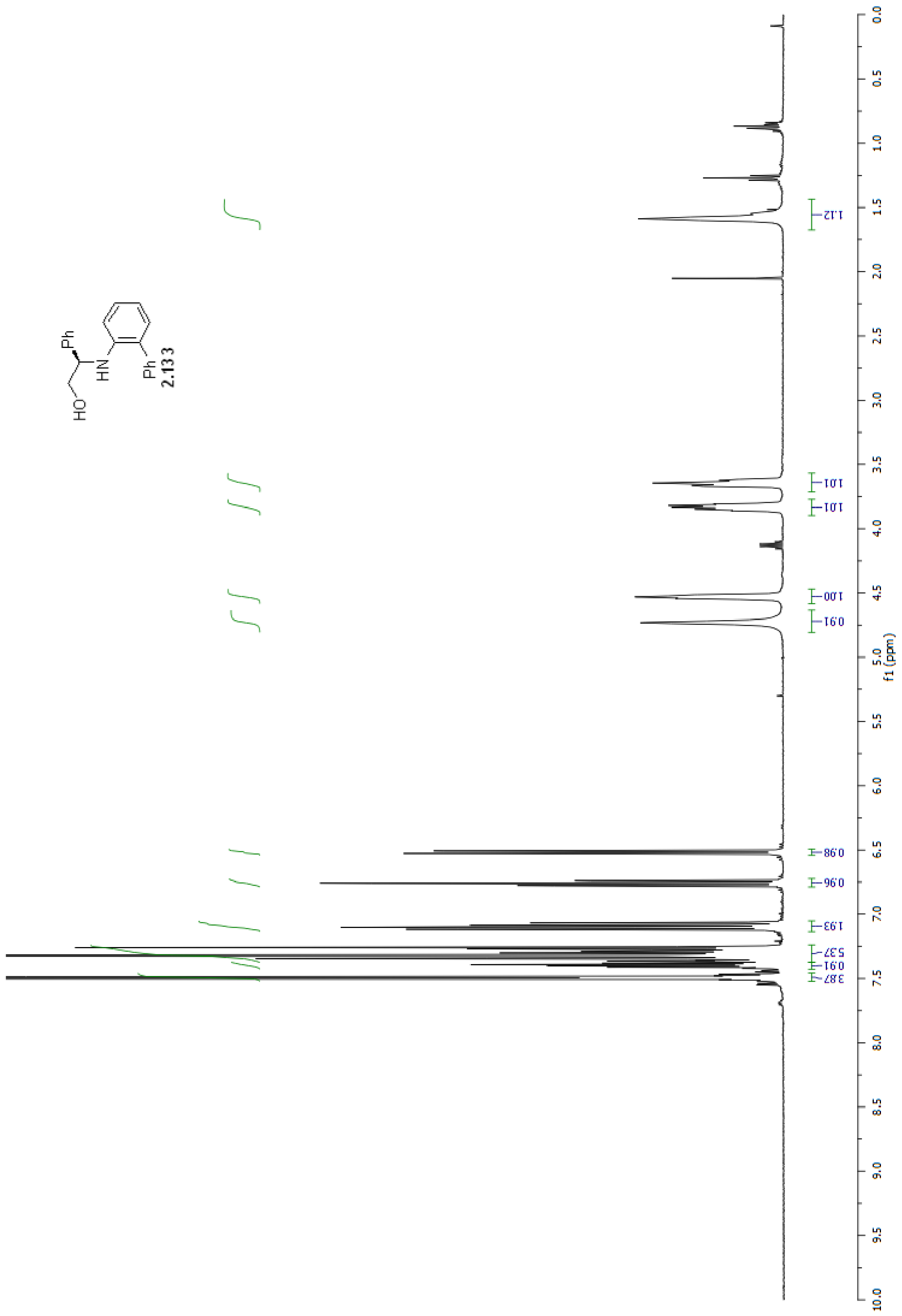
HO
HN
Ph
Ph
2.133
1.12
1.01
1.01
1.00
0.91
0.98
0.96
1.93
5.37
0.91
3.87
0.0
0.5
1.0
1.5
2.0
2.5
3.0
3.5
4.0
4.5
5.0
5.5
6.0
6.5
7.0
7.5
8.0
8.5
9.0
9.5
10.0
f1 (ppm)

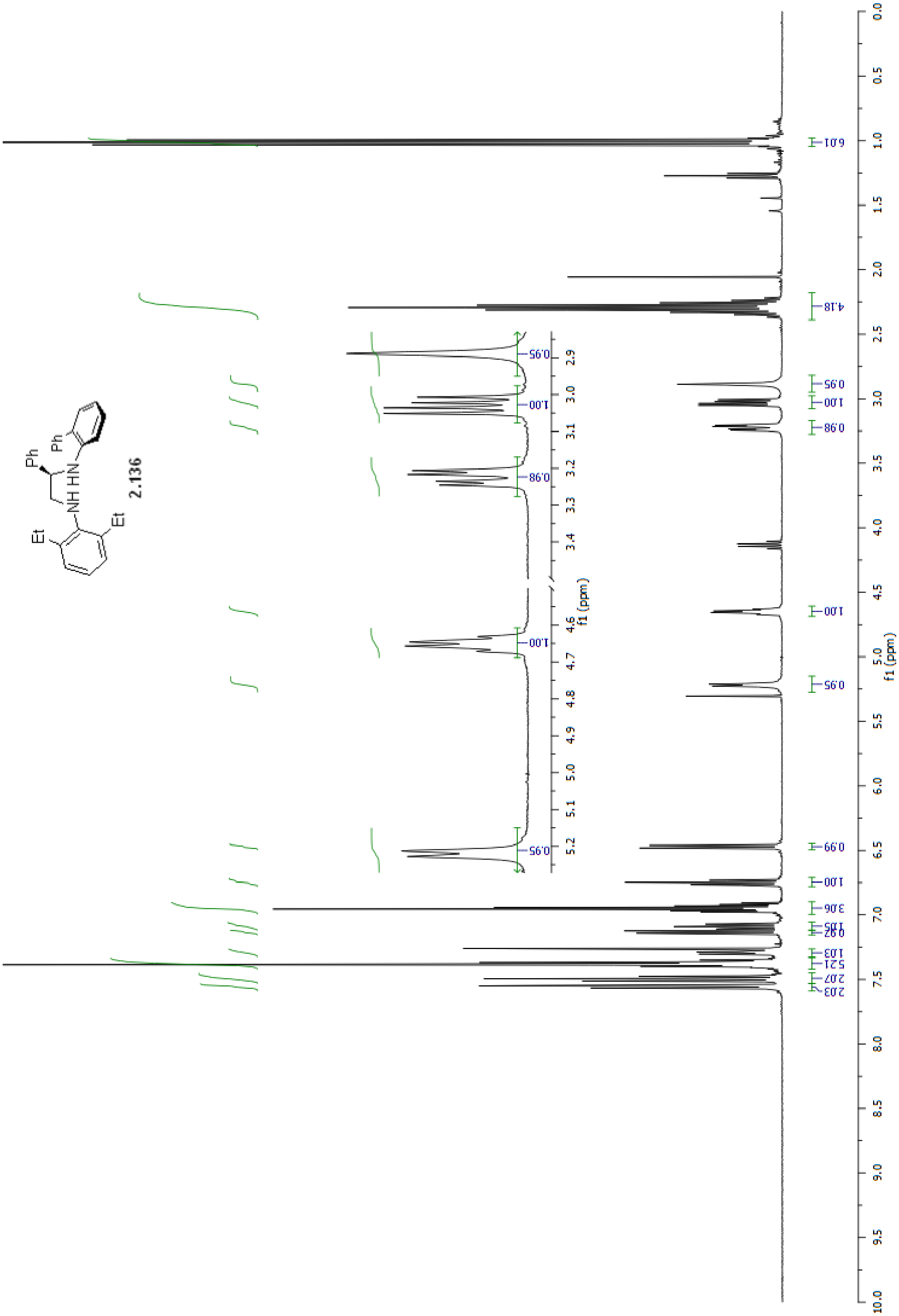

Et
Et
NH HN
Ph
Ph
6.01
4.18
0.95
1.00
0.98
1.00
0.95
0.99
1.00
3.06
1.05
0.92
1.03
5.21
2.07
2.03
0.0
0.5
1.0
1.5
2.0
2.5
3.0
3.5
4.0
4.5
5.0
5.5
6.0
6.5
7.0
7.5
8.0
8.5
9.0
9.5
10.0
f1 (ppm)
2.9
3.0
3.1
3.2
3.3
3.4
4.6
4.7
4.8
4.9
5.0
5.1
5.2
f1 (ppm)

2.136

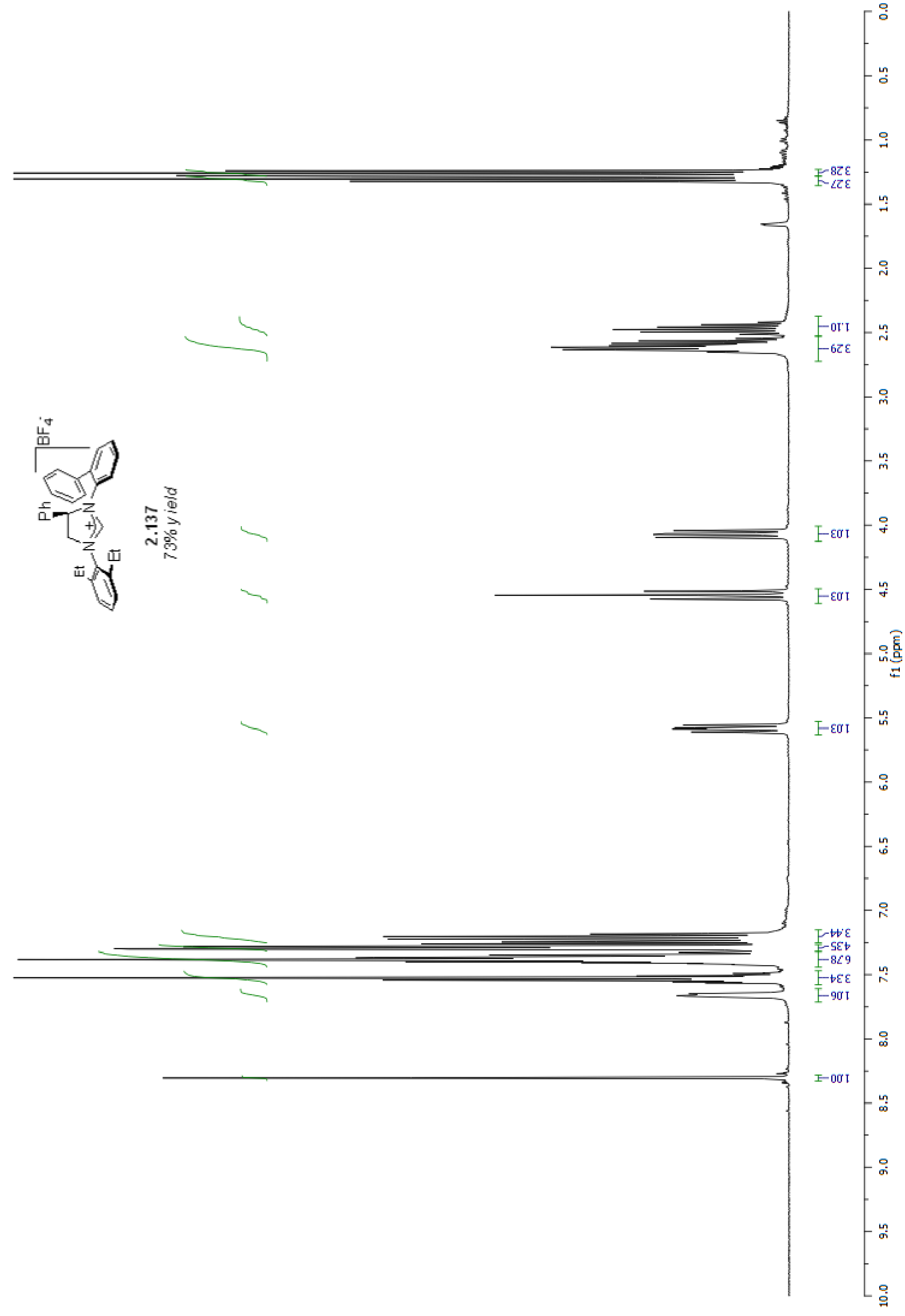

2.137

73% yield

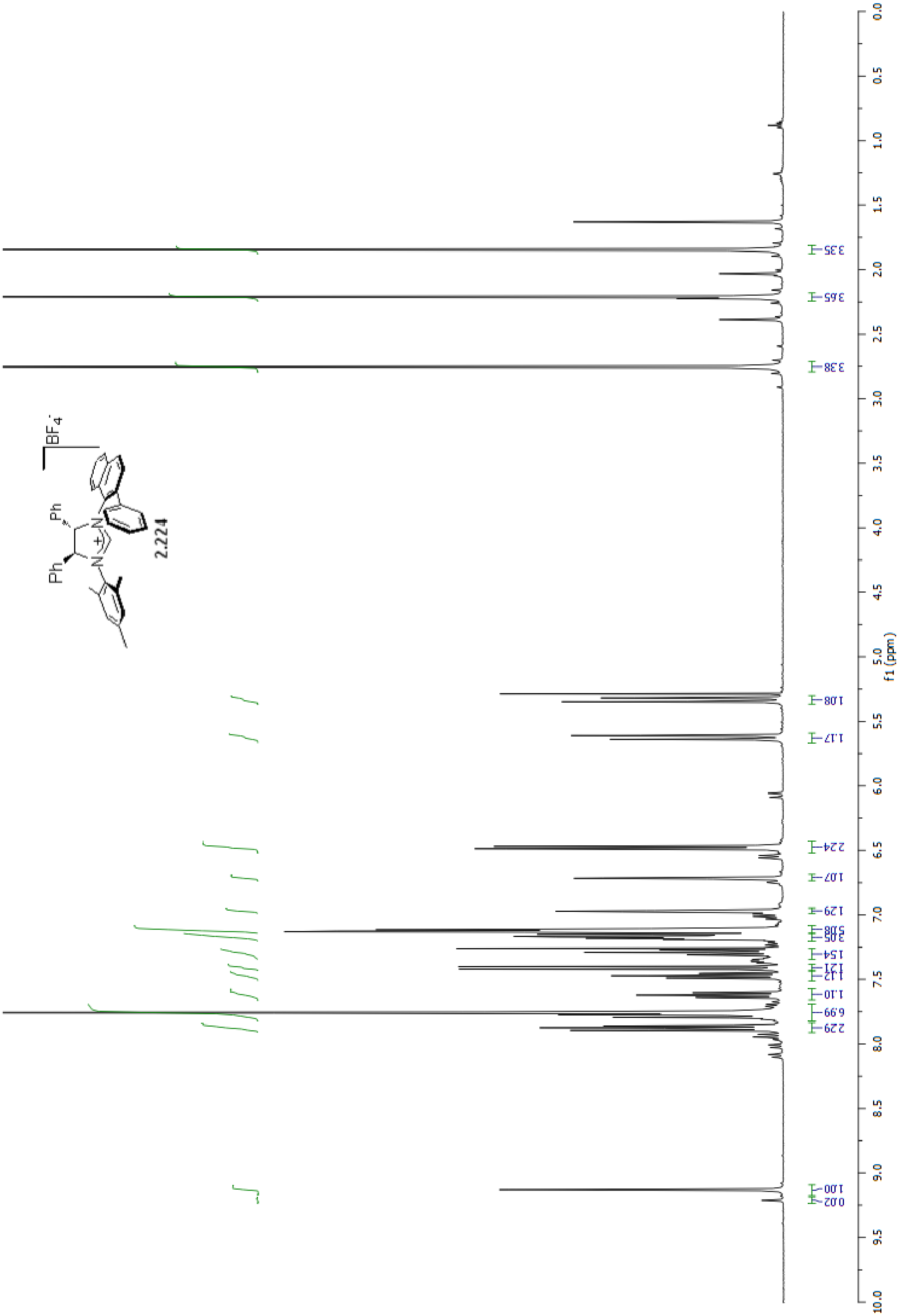
2.224

Ph
Ph
N
N
+
BF4-
f1 (ppm)
0.0
0.5
1.0
1.5
2.0
2.5
3.0
3.5
4.0
4.5
5.0
5.5
6.0
6.5
7.0
7.5
8.0
8.5
9.0
9.5
10.0
3.35
3.65
3.38
1.08
1.17
2.24
1.07
1.29
5.08
3.05
1.54
1.21
1.12
1.10
6.99
2.29
1.00
0.02

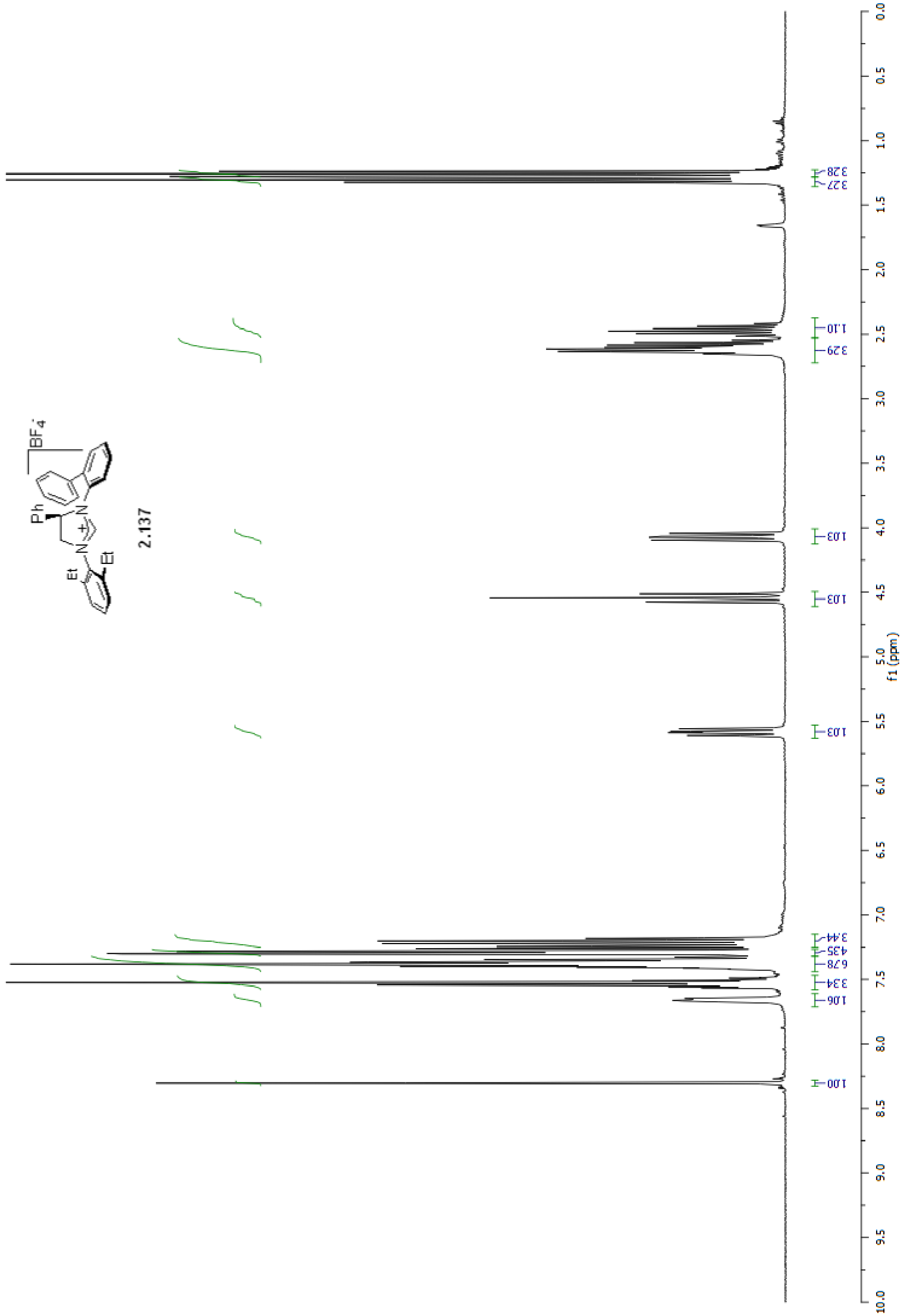
Ph
BF$_4^-$
N
N
+
Et
Et
3.28
3.27
1.10
3.29
1.03
1.03
1.03
3.44
4.35
6.78
3.34
1.06
1.00
0.0
0.5
1.0
1.5
2.0
2.5
3.0
3.5
4.0
4.5
5.0
5.5
6.0
6.5
7.0
7.5
8.0
8.5
9.0
9.5
10.0
f1 (ppm)

2.137

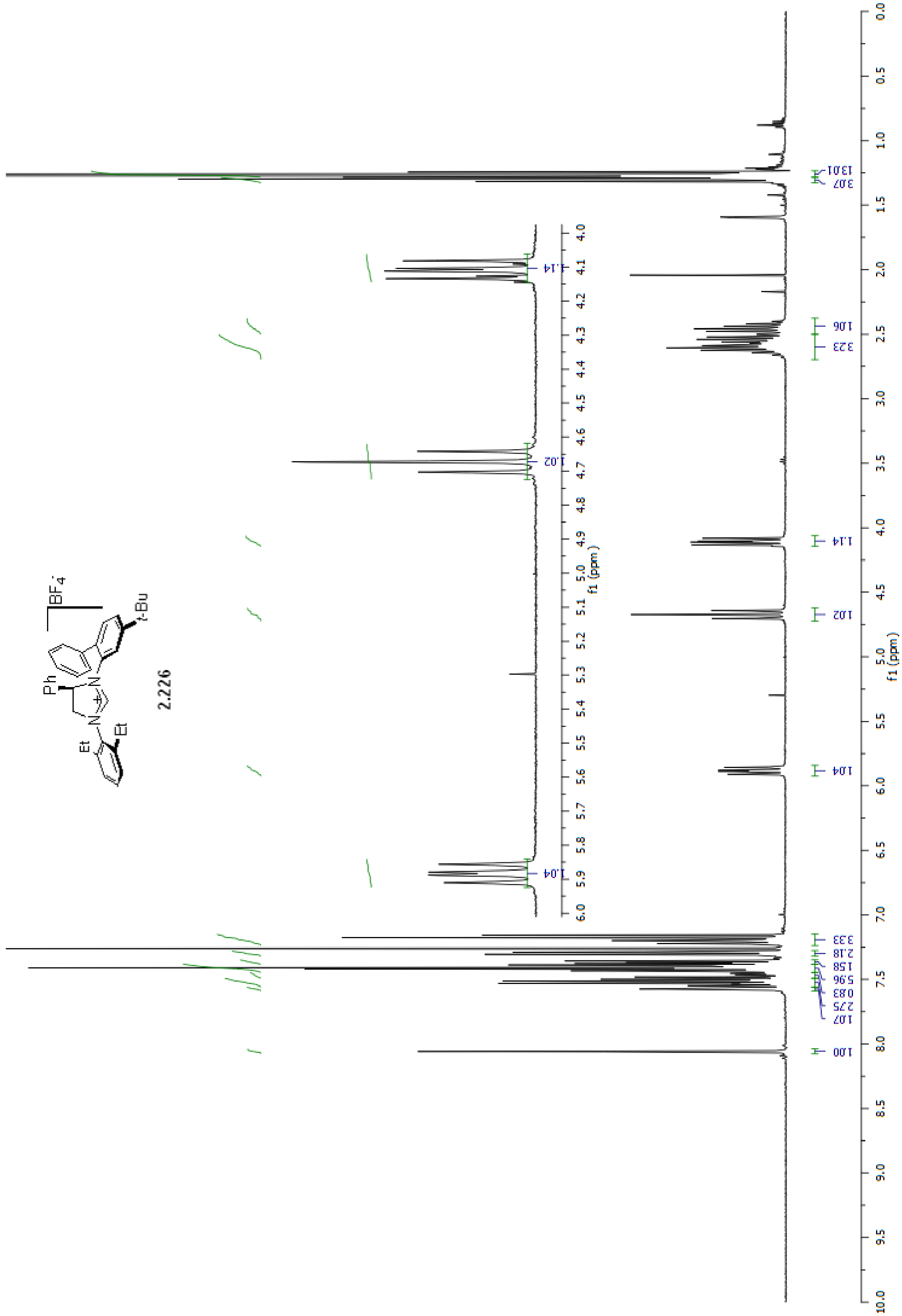
BF4-
Ph
Et
Et
t-Bu
f1 (ppm)
13.01
3.07
1.06
3.23
1.14
1.02
1.04
3.33
2.18
1.58
5.96
0.83
2.75
1.07
1.00

2.226

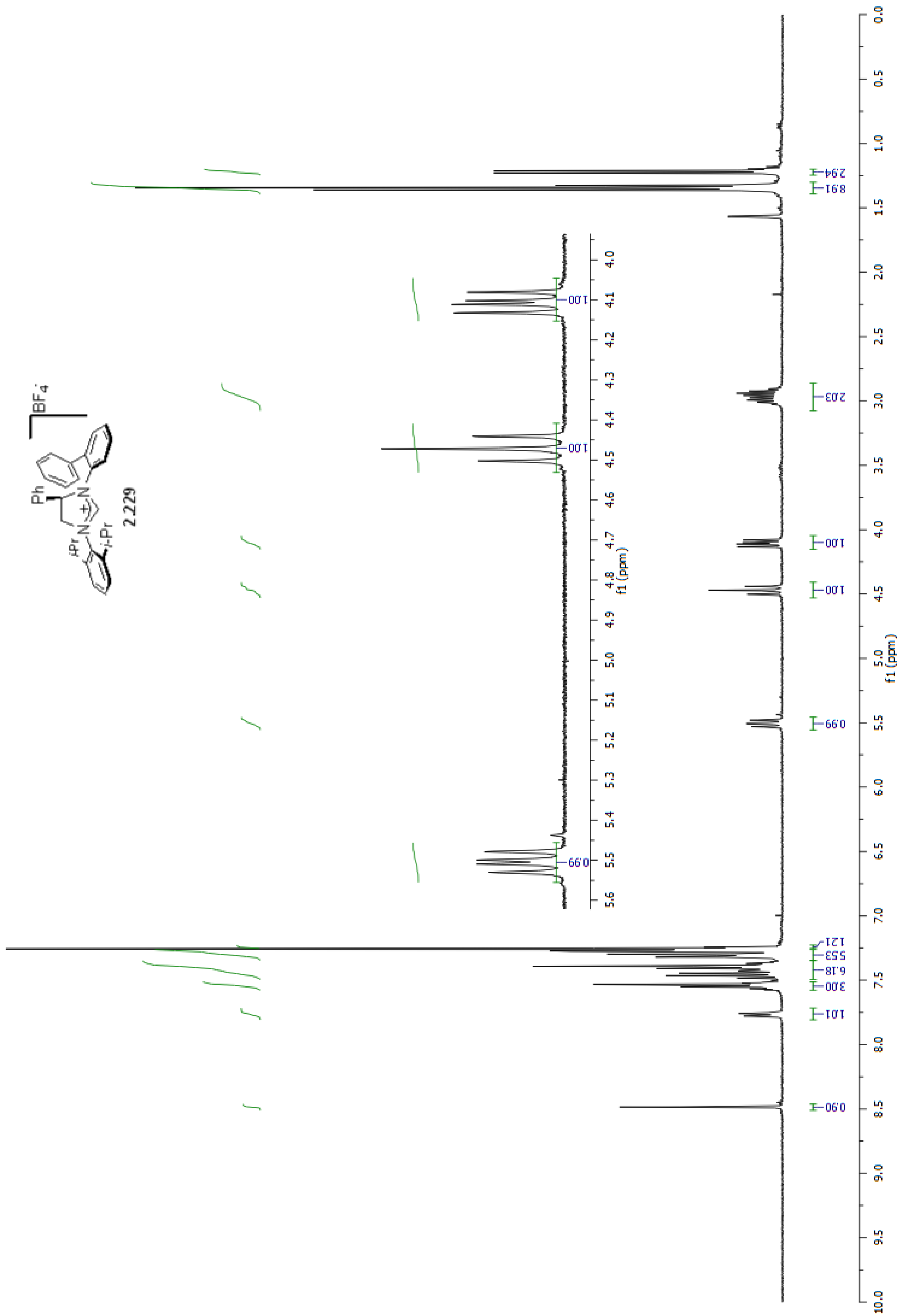
BF4⁻
Ph
i-Pr
i-Pr
N
N
+
2.94
8.91
2.03
1.00
1.00
0.99
1.21
5.53
6.18
3.00
1.01
0.90
1.00
1.00
0.99
f1 (ppm)
0.0
0.5
1.0
1.5
2.0
2.5
3.0
3.5
4.0
4.5
5.0
5.5
6.0
6.5
7.0
7.5
8.0
8.5
9.0
9.5
10.0
f1 (ppm)
4.0
4.1
4.2
4.3
4.4
4.5
4.6
4.7
4.8
4.9
5.0
5.1
5.2
5.3
5.4
5.5
5.6

2.229

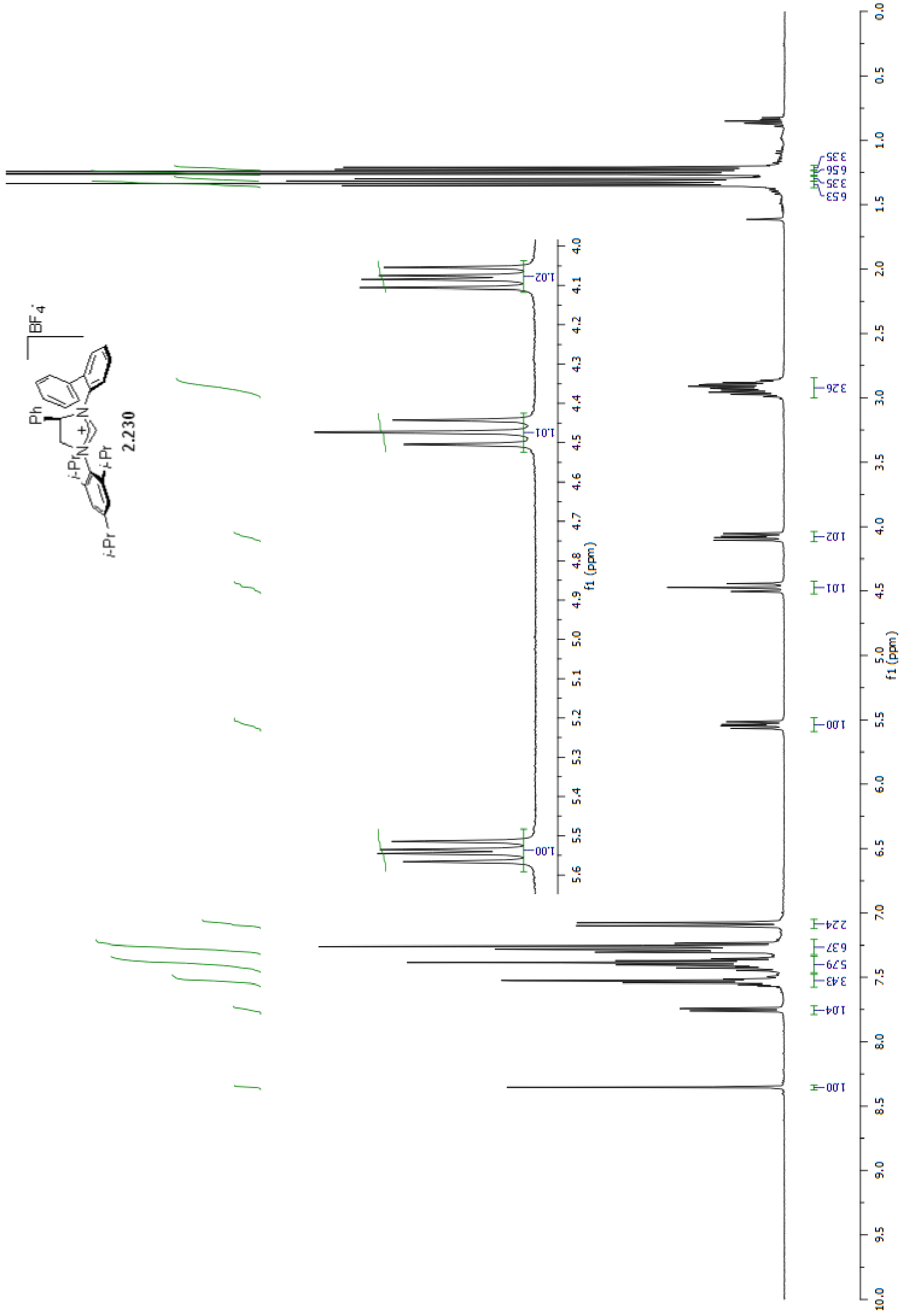
i-Pr
i-Pr
i-Pr
N
N
+
Ph
BF4-
1.02
1.01
1.00
4.0
4.1
4.2
4.3
4.4
4.5
4.6
4.7
4.8
4.9
5.0
5.1
5.2
5.3
5.4
5.5
5.6
f1 (ppm)
3.35
6.56
3.35
6.53
3.26
1.02
1.01
1.00
2.24
6.37
5.79
3.43
1.04
1.00
0.0
0.5
1.0
1.5
2.0
2.5
3.0
3.5
4.0
4.5
5.0
5.5
6.0
6.5
7.0
7.5
8.0
8.5
9.0
9.5
10.0
f1 (ppm)

2.230

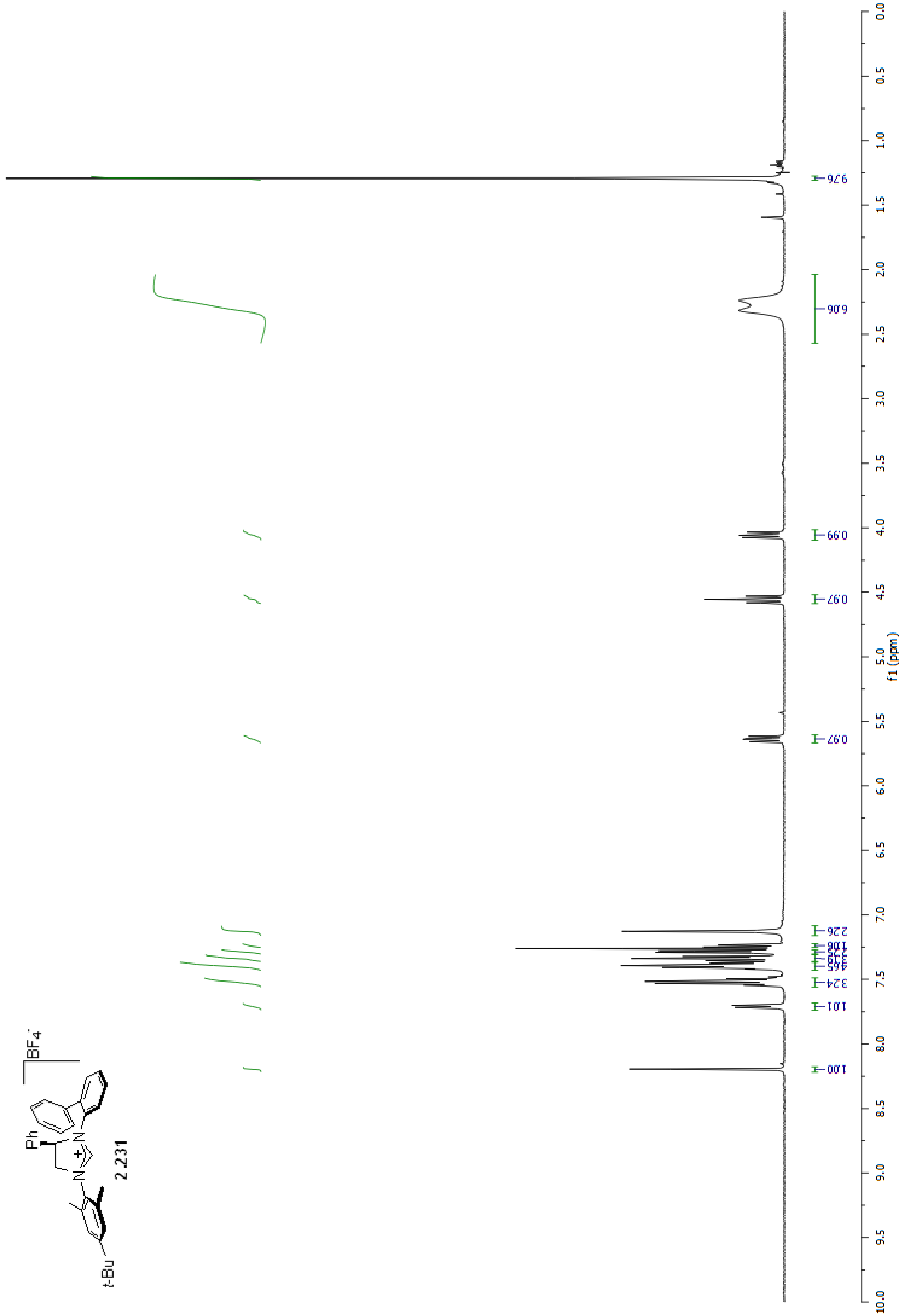

BF4-
Ph
N
+
N
t-Bu
9.76
6.06
0.99
0.97
0.97
2.26
1.06
1.25
3.19
4.65
3.24
1.01
1.00
0.0
0.5
1.0
1.5
2.0
2.5
3.0
3.5
4.0
4.5
5.0
f1 (ppm)
5.5
6.0
6.5
7.0
7.5
8.0
8.5
9.0
9.5
10.0

2.231

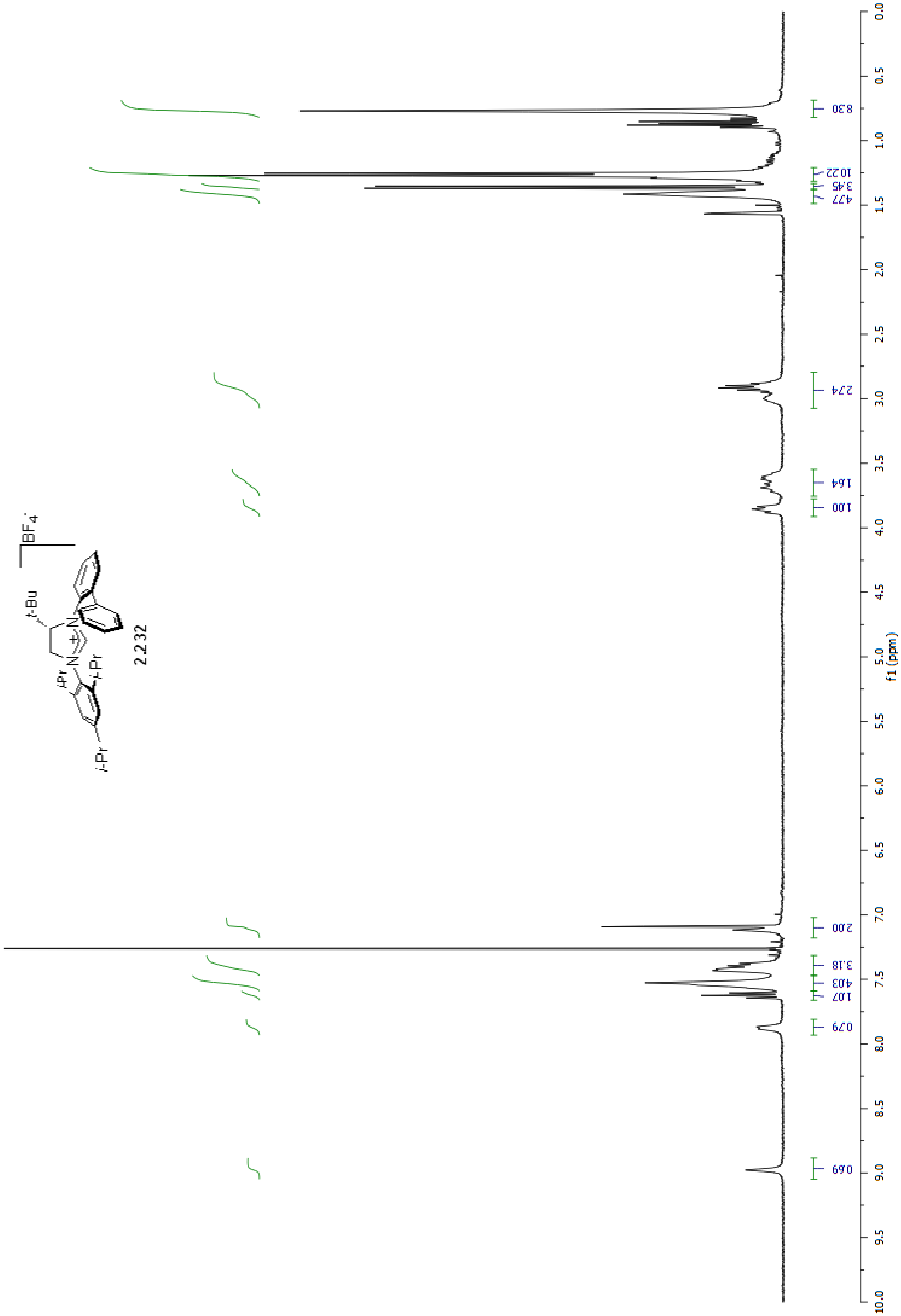
t-Bu
BF$_4^-$
N
N
+
i-Pr
i-Pr
i-Pr
8.30
10.22
3.45
4.27
2.74
1.64
1.00
2.00
3.18
4.03
1.07
0.79
0.69
0.0
0.5
1.0
1.5
2.0
2.5
3.0
3.5
4.0
4.5
5.0
5.5
6.0
6.5
7.0
7.5
8.0
8.5
9.0
9.5
10.0
f1 (ppm)

2.232

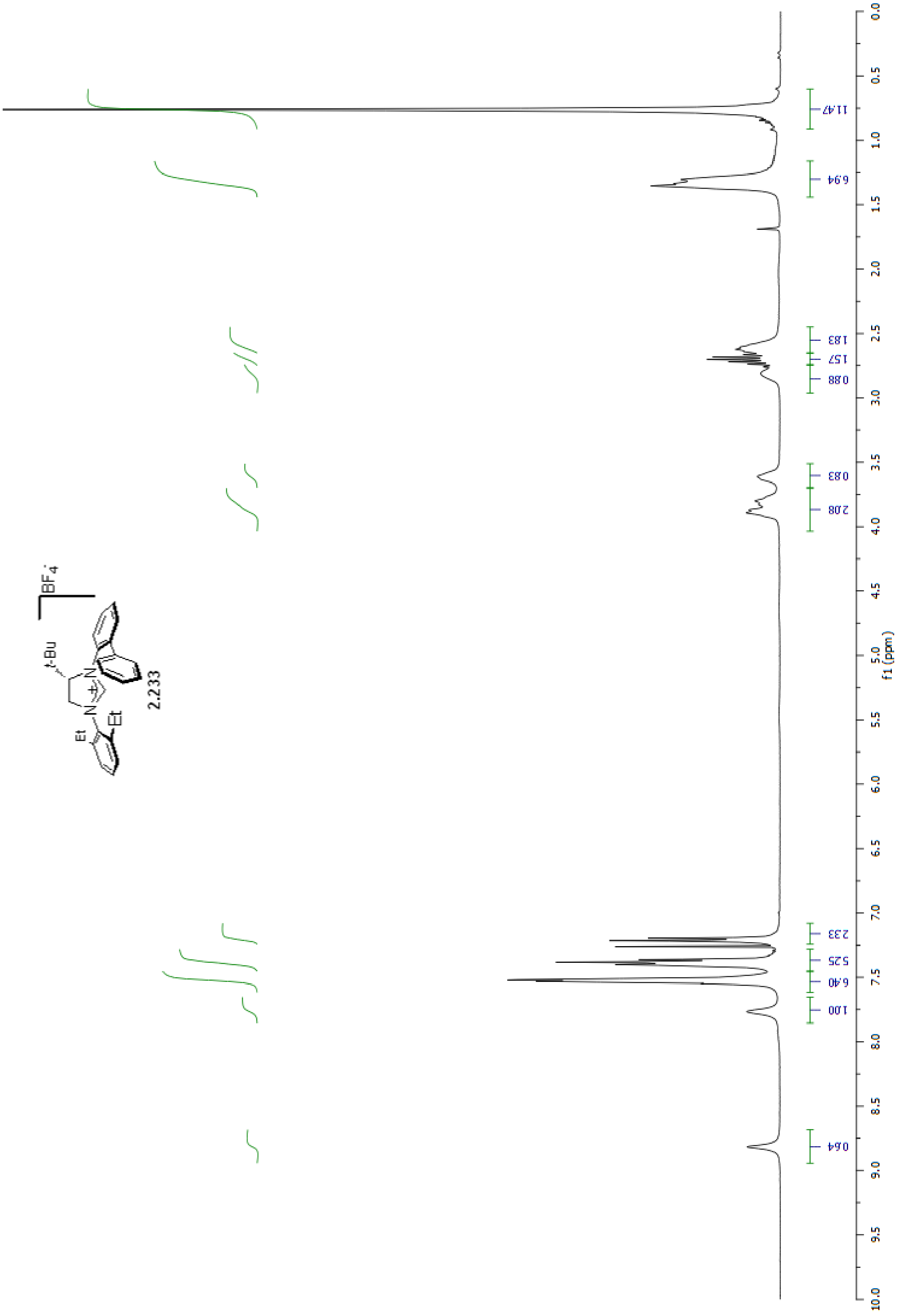

t-Bu
Et
Et
N
N
+
BF4-
11.47
6.94
1.83
1.57
0.88
0.83
2.08
2.33
5.25
6.40
1.00
0.64
0.0
0.5
1.0
1.5
2.0
2.5
3.0
3.5
4.0
4.5
5.0
5.5
6.0
6.5
7.0
7.5
8.0
8.5
9.0
9.5
10.0
f1 (ppm)

2.233

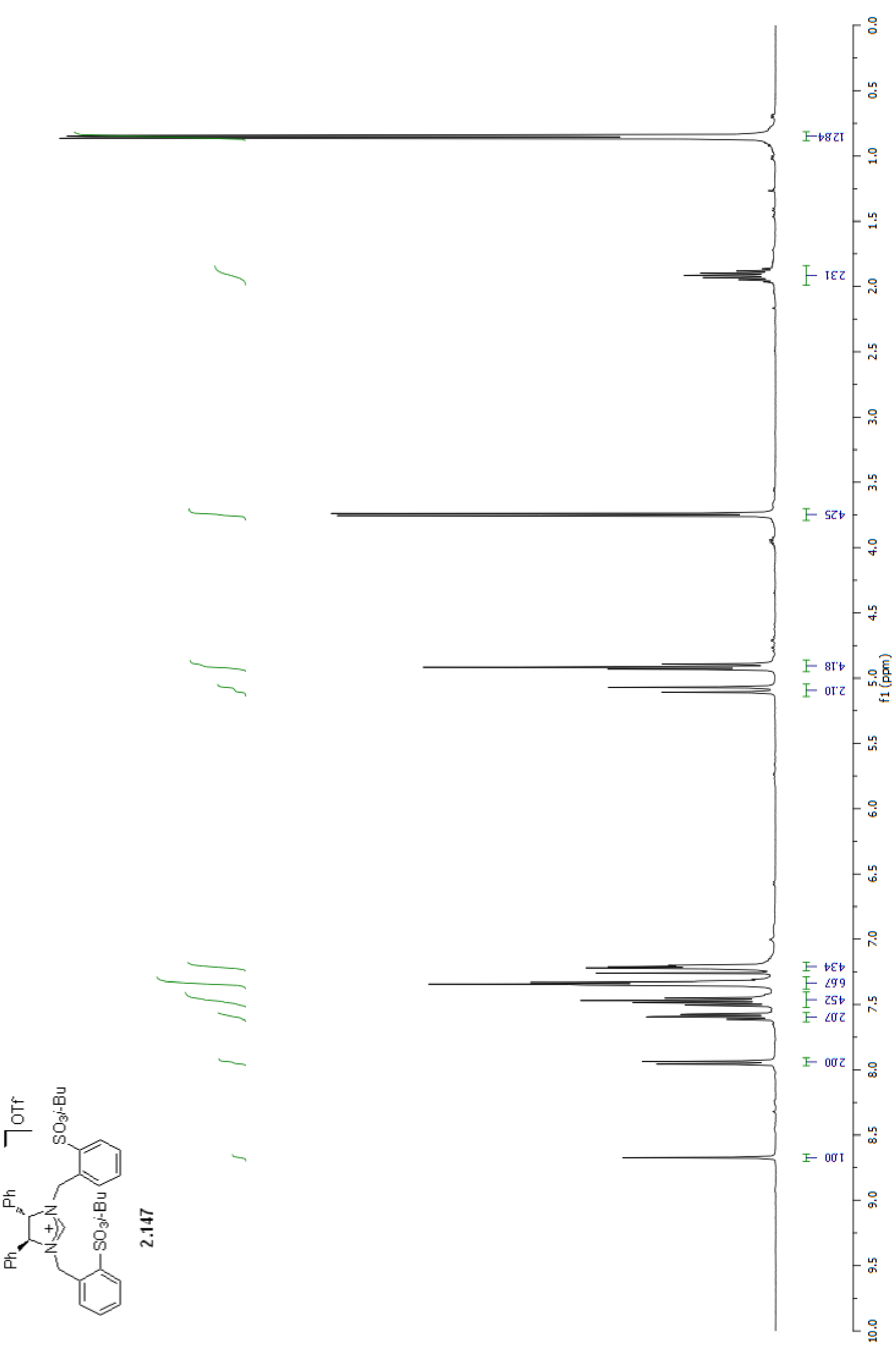
Ph
Ph
N
N
+
SO$_3$i-Bu
SO$_3$i-Bu
OTf$^-$
12.84
2.31
4.25
4.18
2.10
4.34
6.67
4.52
2.07
2.00
1.00
0.0
0.5
1.0
1.5
2.0
2.5
3.0
3.5
4.0
4.5
5.0
5.5
6.0
6.5
7.0
7.5
8.0
8.5
9.0
9.5
10.0
f1 (ppm)

2.147

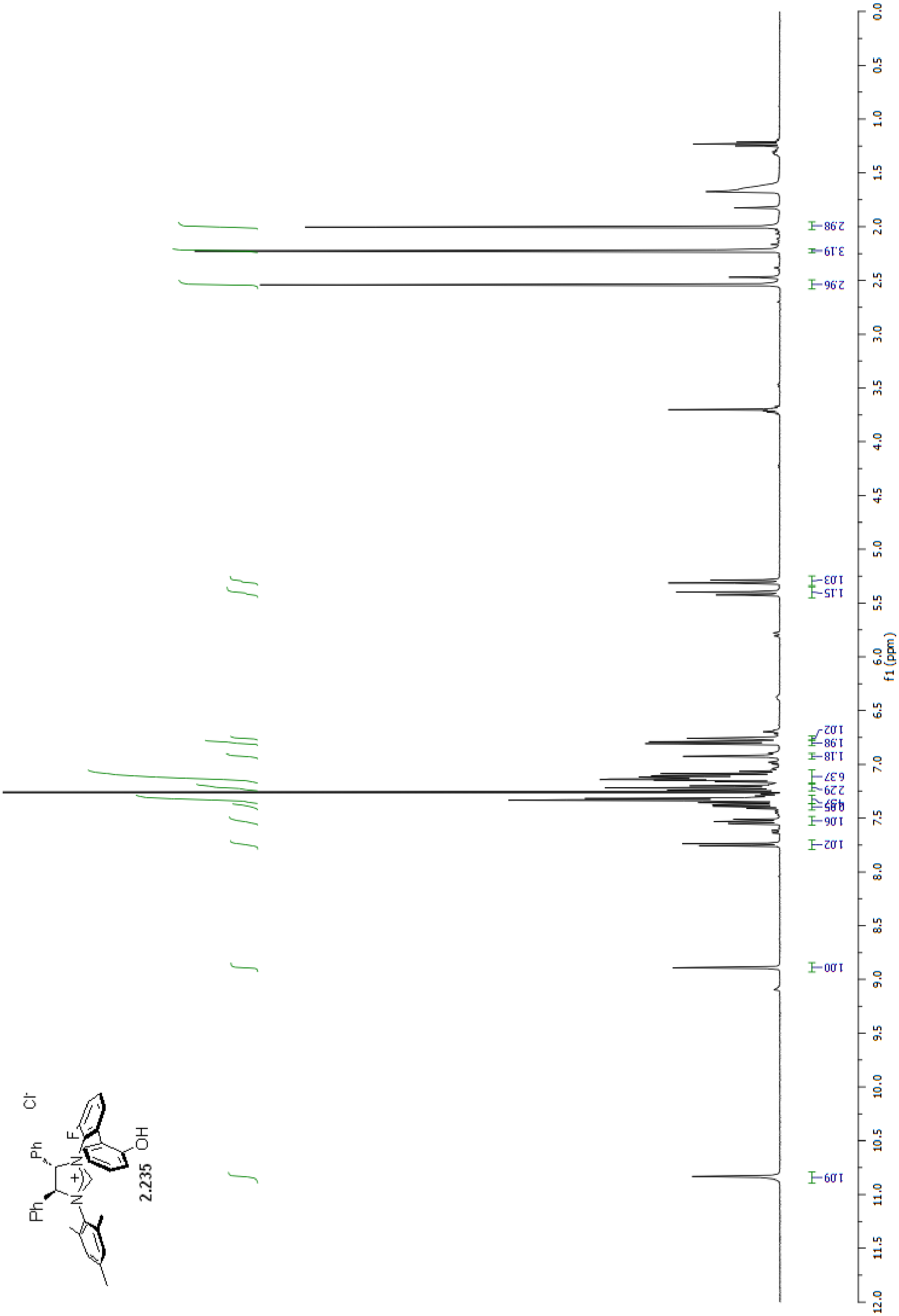
Cl⁻
Ph
Ph
N
N
+
F
OH
2.235
2.98
3.19
2.96
1.03
1.15
1.02
1.98
1.18
6.37
2.29
1.06
1.02
1.00
1.09
0.0
0.5
1.0
1.5
2.0
2.5
3.0
3.5
4.0
4.5
5.0
5.5
6.0
6.5
7.0
7.5
8.0
8.5
9.0
9.5
10.0
10.5
11.0
11.5
12.0
f1 (ppm)